

Microplastic pollution in composts, digestates and soils

Developing detection methods to identify input
pathways, local extent and fate of terrestrial
microplastic pollution

by
Julia Naima Möller
from Tübingen

DOCTORAL DISSERTATION

This dissertation is submitted to obtain the degree of
Doctor of Natural Sciences (Dr. rer. nat.)

at the
Bayreuth Graduate School of Mathematical and Natural Sciences
(BayNAT)
University of Bayreuth
2022

This doctoral thesis was prepared at the department of Animal Ecology I at the University of Bayreuth from June/2018 until June/2022 and was supervised by Prof. Dr. Christian Laforsch.

This is a full reprint of the thesis submitted to obtain the academic degree of Doctor of Natural Sciences (Dr. rer. nat.) and approved by the Bayreuth Graduate School of Mathematical and Natural Sciences (BayNAT) of the University of Bayreuth.

Date of submission: 29.08.2022

Date of defense: 13.07.2023

Acting director: Prof. Dr. Hans Keppler

Doctoral committee:

Prof. Dr. Christian Laforsch (reviewer)

Prof. Dr. Efsthathios Diamantopoulos (reviewer)

Prof. Dr. Holger Kress (chairman)

Prof. Dr. Eva Lehndorff (examiner)



“All truths are easy to understand once they are discovered; the point is to discover them.”

Galileo Galilei (1564-1642)

Content

Summary	3
Zusammenfassung	5
Figures	8
Abbreviations	9
1. Introduction	10
<i>A brief history of plastics</i>	10
<i>Plastics – a solution or a problem?</i>	11
<i>Defining microplastics</i>	13
<i>Microplastic sources and their input pathways to soils</i>	14
<i>The extent of microplastic pollution in soils</i>	16
<i>Detecting microplastics</i>	17
2. Knowledge gaps & objectives	21
3. Method development	23
<i>Article 1 - Finding Microplastics in Soils - A Review of Analytical Methods.</i>	23
<i>Article 2 - Microplastic sample purification methods - assessing detrimental effects of purification procedures on specific plastic types</i>	24
<i>Article 3 - Tackling the challenge of extracting microplastics from soils: A protocol to purify soil samples for spectroscopic analysis.</i>	24
<i>Conclusions – Method development</i>	25
4. Microplastic pollution and fate in soils	27
<i>Article 4 - Microplastics persist in an arable soil but do not affect soil microbial biomass, enzyme activities, and crop yield</i>	27
<i>Article 5 - Flooding frequency and floodplain topography determine abundance of microplastics in an alluvial Rhine soil</i>	27
<i>Conclusions - Microplastic pollution and fate in soils</i>	28
5. Assessment of organic fertilizers as microplastic input pathways	30
<i>Article 6 - Organic fertilizer as a vehicle for the entry of microplastic into the environment.</i>	30
<i>Article 7 - Microplastic contamination of composts and liquid fertilizers from municipal biowaste treatment plants — effects of the operating conditions</i>	30
<i>Article 8 – Municipal biowaste treatment plants contribute to the contamination of the environment with residues of biodegradable plastics with putative higher persistence potential</i>	31
<i>Conclusions – Organic fertilizers as microplastic input pathways</i>	32

6. General discussion and outlook	34
7. Bibliography	39
8. Articles	47
9. Author contributions	231
10. List of publications	236
11. Acknowledgements	239
Statutory Declaration and Statement	240

Summary

Although plastics have only been invented in the first half of the 20th century, they are possibly the most abundantly used materials in the history of human innovations. However, an estimated 60% of all plastics ever produced have been disposed of in landfills or the natural environment. Here, they may fragment into ever smaller pieces due to e.g. UV-radiation or mechanical abrasion. These microscopic plastic fragments are called microplastics. While microplastic contamination of aquatic ecosystems has been studied extensively, the focus has only recently shifted to terrestrial ecosystems, where data is still scarce and often not comparable. Due to a lack of appropriate analytical methods for complex solid matrices such as soils, the direct assessment of microplastic pollution is challenging. Therefore, hardly anything is known about the fate, degradation and fragmentation behavior in natural soils. Also, not all microplastic input pathways are recognized or fully understood. Therefore, I aimed to

- 1) develop a suitable method to identify and quantify microplastics in soils
- 2) use the developed methods to identify the contamination extent and fate of microplastics in agricultural and floodplain soils
- 3) observe the fate of plastics and microplastics in organic waste treatment plants, to assess the role of composts/digestates as input pathways for microplastics into arable soils.

Following the order of these research aims, the first part of my dissertation covers the development of an appropriate method to quantify microplastics in soils. In a literature review considering advantages and limitations of various methods used for other environmental matrices, I evaluated potentially suitable sample preparation and analysis methods for a particle-quantitative analysis with reliable polymer identification in soils (Article 1). In a direct comparison of the effects of sample purification protocols on different types of plastics, my second study showed that protocols using high temperatures and strong acids or bases are detrimental to certain types of plastics. This may lead to distorted analytical results. Although some of the effects were already known, my study gave a systematic overview on which protocols may be detrimental to certain plastics, while also showing non-detrimental alternatives for sample purification: Fenton's reagent, sequential oxidative-enzymatic-digestion and the treatment with a ZnCl₂ brine (Article 2). Based on this knowledge I developed a method to purify soil samples for micro-FTIR spectroscopy. This is the first protocol that allows the particle-quantitative analysis of microplastics <500 µm of a relatively large sample without destroying conventional plastics (Article 3).

In part two of this thesis, I applied the newly-developed methods to determine the abundance and fate of microplastics in specific soils. To study the fate of conventional and biodegradable plastics in soil, I analyzed spiked PE and PLA-PBAT-blend particles on an operating agricultural field after 0, 1, and 17 months. This experiment showed that both plastic types remained unaltered in the soil for nearly one and a half years. Therefore, even the biodegradable plastic seems to persist for some time in the soil environment (Article 4). My method was also used in a collaboration with the Institute of Geography, University of Cologne, on the soil of a Rhine River floodplain. In a first step towards understanding the complex dynamics of microplastic transport between environmental compartments, it showed that flooding events are a significant input pathway of microplastics into adjacent soils. Furthermore, the local topography and vegetation cover significantly influence the deposition and retention of microplastics in soils (Article 5).

Part three focuses on organic fertilizers from biowaste treatment (BWT) plants as potential microplastic input pathways into soils. In collaboration with the Chair for Process Biotechnology, I was able to show for the very first time that composts/digestates derived from household organic waste contained significant amounts of microplastics. These fertilizers are commonly applied to agricultural fields (Article 6). In a follow-up study the comparative analysis of organic fertilizers from different plants gave insight on how processing equipment influences the on-site generation of microplastics. Here, I was able to detect microplastics <math><500\ \mu\text{m}</math> in liquid digestate for the first time. The results showed a surprisingly high proportion of microplastics with a PBAT signature, possibly caused by the use of compostable organic waste collection bags (Article 7). Theoretically, these bags should be 100% compostable. Unfortunately, the certification norms for compostability do not represent realistic conditions in municipal BWT plants and I demonstrated that small microplastic fragments of the biodegradable PLA, PBAT or a PLA-PBAT-blend were present in liquid digestate. As composted fragments showed a tendency to a higher crystallinity and a shift towards a higher PBAT/PLA ratio than tested reference bags, it has become questionable if the bags are biodegradable, or simply fragment into very small microplastics (Article 8).

Zusammenfassung

Obwohl Kunststoffe erst in der ersten Hälfte des 20. Jahrhunderts erfunden wurden, sind sie wahrscheinlich die am häufigsten verwendete Materialgruppe in der Geschichte menschlicher Innovationen. Doch schätzungsweise 60% aller jemals hergestellten Kunststoffe wurden auf Mülldeponien oder in der Umwelt entsorgt, wo sie zu immer kleineren Teilchen zerfallen - z. B. durch UV-Strahlung oder mechanischen Abrieb. Diese mikroskopisch kleinen Kunststofffragmente werden als Mikroplastik bezeichnet. Während die Belastung aquatischer Ökosysteme durch Mikroplastik bereits ausgiebig untersucht wurde, hat sich erst seit kurzem der Schwerpunkt auf terrestrische Ökosysteme verlagert. In diesem Bereich gibt es noch immer nur wenige Daten, die oft untereinander nicht vergleichbar sind. Da es für komplexe feste Matrices wie Böden kaum geeignete Mikroplastikanalysenmethoden gibt, bleibt die direkte Erfassung der Mikroplastikkontamination von Böden eine Herausforderung. Außerdem sind nicht alle Eintragspfade von Mikroplastik in Böden bekannt. Daher war es mein Ziel:

- 1) eine geeignete Methode zur Identifizierung und Quantifizierung von Mikroplastik in Böden zu entwickeln,
- 2) diese Methode zu nutzen um das Ausmaß der Verschmutzung und den Verbleib von Mikroplastik in Ackerböden und Auenböden zu untersuchen,
- 3) den Verbleib von Kunststoffen und Mikroplastik in Bioabfallbehandlungsanlagen zu prüfen, um die Rolle von Komposten/Gärprodukten als Eintragspfad für Mikroplastik in Ackerböden besser beurteilen zu können.

Der Ordnung meiner Ziele folgend, befasst sich der erste Teil dieser Dissertation mit der Entwicklung einer geeigneten Methode zur Partikel-basierten Quantifizierung von Mikroplastik in Böden mit zuverlässiger Polymeridentifikation. In einem Literaturvergleich der Vor- und Nachteile verschiedener Methoden, die zur Analyse anderer Umweltmatrices eingesetzt werden, stellte ich fest, dass für eine partikelquantitative Analyse von kleinem Mikroplastik (<500 µm) nur die Mikro-Raman oder Mikro-FTIR-Spektroskopie in Frage kommen. Voraussetzung dafür ist eine geeignete Probenaufbereitung (Artikel 1). In einer Untersuchung der Effekte von Probenaufbereitungsprotokollen auf verschiedene Arten von Kunststofffolien zeigte meine zweite Studie, dass Protokolle, die hohe Temperaturen und starke Säuren oder starke Basen verwenden, die Zersetzung bestimmter Kunststoffarten verursachen. Dies

kann zu verzerrten analytischen Ergebnissen führen. Obwohl einige der Auswirkungen bereits bekannt waren, gab diese Studie erstmals einen systematischen Überblick darüber, welche Protokolle nicht geeignet sind und bot gleichzeitig Alternativen für die Probenaufbereitung, wie z. B. das Fenton-Reagenz, der sequentielle oxidativ-enzymatische Verdau oder die Behandlung mit einer ZnCl_2 -Lösung (Artikel 2). In Anbetracht dieser Erkenntnisse entwickelte ich eine Methode zur Aufbereitung von Bodenproben für die Mikro-FTIR-Spektroskopie. Dies ist das erste Protokoll, das eine partikelquantitative Analyse von Mikroplastik $<500 \mu\text{m}$ aus einer relativ großen Probe ermöglicht, ohne herkömmliche Kunststoffe zu zerstören (Artikel 3).

Im zweiten Teil dieser Arbeit habe ich die neu entwickelten Methoden angewandt, um das Vorkommen und den Verbleib von Mikroplastik in Böden zu untersuchen. Um das Verhalten von konventionellen und biologisch abbaubaren Kunststoffen in Ackerböden zu untersuchen, analysierte ich auf einem konventionell bearbeiteten Acker eingebrachte PE- und PLA-PBAT Partikel nach 0, 1 und 17 Monaten. Dieses Experiment zeigte, dass beide Kunststofftypen fast eineinhalb Jahre lang unverändert im Boden verblieben. Dies demonstrierte, dass sogar der biologisch abbaubare Kunststoff im Ackerboden über längere Zeiträume nicht abgebaut wird (Artikel 4). Die zweite Bodenuntersuchung wurde in Zusammenarbeit mit dem Geographischen Institut der Universität zu Köln in einer Rheinaue bei Köln durchgeführt. Hier zeigte sich, dass Überschwemmungsereignisse ein wichtiger Eintragspfad für Mikroplastik in angrenzende Böden sind. Darüber hinaus haben die Topographie und Vegetationsdecke einen erheblichen Einfluss auf die Deposition und Retention von Mikroplastik in Böden. Dies ist ein erster Schritt zum Verständnis der komplexen Transportwege zwischen Umweltkompartimenten (Artikel 5).

Der dritte Teil dieser Arbeit befasst sich mit organischen Düngemitteln aus Bioabfallbehandlungsanlagen als potenzielle Eintragspfade für Mikroplastik in Böden. In Zusammenarbeit mit dem Lehrstuhl für Bioprozesstechnik gelang es mir erstmals zu zeigen, dass eine erhebliche Menge an Mikroplastik in Komposten/Gärresten enthalten ist, wenn diese aus organischen Haushaltsabfällen generiert werden. Solche organischen Düngemittel werden dann direkt auf landwirtschaftliche Felder ausgebracht (Artikel 6). In einer Folgestudie habe ich eine vergleichende Analyse von Komposten und flüssigen Gärresten durchgeführt, die Aufschluss darüber gibt, wie die Anlagentechnik die Entstehung von Mikroplastik beeinflusst. Im Rahmen dieser Studie gelang es mir erstmals, Mikroplastik $<500 \mu\text{m}$ in flüssigen Gärresten nachzuweisen, wobei ein überraschend hoher Anteil an Mikroplastikpartikeln aus PBAT bestand. Dies wurde möglicherweise durch die Verwendung kompostierbarer

Zusammenfassung

Bioabfallsammelbeutel verursacht (Artikel 7). Theoretisch sollten diese Beutel zu 100% kompostierbar sein. Leider entsprechen die Zertifizierungsnormen für Kompostierbarkeit nicht den realen Bedingungen in kommunalen Bioabfallbehandlungsanlagen. In der neuesten Studie konnte ich kleine Mikroplastikfragmente aus biologisch abbaubarem PLA, PBAT oder PLA-PBAT-Blends in flüssigem Gärrest aus Bioabfallbehandlungsanlagen nachweisen. Da kompostierte Fragmente zusätzlich eine Tendenz zu einer höheren Kristallinität und eine Verschiebung hin zu einem höheren PBAT-PLA-Verhältnis als bei den getesteten Referenzbeuteln aufwiesen, ist es fraglich, ob die Beutel tatsächlich biologisch abbaubar sind oder ob sie einfach dazu neigen, in sehr kleine Mikroplastikpartikel zu zerfallen (Artikel 8).

Figures

Figure 1: Timeline of the beginning of the Plastic Age	11
Figure 2: Potential microplastic sources and input pathways to the environment*	14
Figure 3: Workflow of the sample purification and analysis protocol	25
Figure 4: Steps from development and research towards change in society*	34

Abbreviations

ATR-FTIR	–	Attenuated total reflectance Fourier-transform infrared spectroscopy
BWT	–	Biowaste treatment
DW	–	Dry weight
EPS	–	Expanded polystyrene
FPA	–	Focal plane array
FTIR	–	Fourier-transform infrared spectroscopy
GPC	–	Gel permeation chromatography
¹ H-NMR	–	Proton nuclear magnetic resonance spectroscopy
MP	–	Microplastics
PA	–	Polyamide
PAN	–	Polyacrylonitrile
PBT	–	Polybutylene terephthalate
PBAT	–	Polybutylene adipate terephthalate
PC	–	Polycarbonate
PE	–	Polyethylene
PET	–	Polyethylene terephthalate
PLA	–	Poly(lactic acid)
PMMA	–	Poly(methyl methacrylate)
PP	–	Polypropylene
PS	–	Polystyrene
PU	–	Polyurethane
PVC	–	Polyvinyl chloride
Pyr-GCMS	–	Pyrolysis gas chromatography mass Spectrometry
TED-GCMS	–	Thermal extraction desorption gas chromatography mass spectrometry

1. Introduction

A brief history of plastics

Stages in human history are often defined by the material of the tools that were used during this period – the stone age, the bronze age and the iron age. Arguably, we have now arrived in the plastic age, as nearly all of the tools we use today are at least in part made of plastic. However, this new age has developed in a very short time indeed. The first fully synthetic plastic was developed in 1907 by Leo Hendrik Baekeland and was called “Bakelite” (Baekeland, 1909). Its malleability, durability and insulating properties were quickly recognized and used industrially for telephones and household appliances. Shortly after Bakelite, a whole range of new synthetic polymers were invented: PVC (1912), Cellophane (1913), PMMA (1924), PE (1933), PU (1937), PA (1938), PS (1944), and PP (1954) (Chalmin, 2019). While all these synthetic polymers have different molecular structures and properties, their malleability coined their collective name: Plastic – a term used for an astoundingly wide range of substances. This also includes bio-based and biodegradable plastics, two denominations that are not interchangeable, as the former merely describes plastics that are made from biomass, but are not necessarily biodegradable, and the latter describes plastics that can be degraded by microorganisms, but could also be petrol-based (Filiciotto & Rothenberg, 2021). The uses for plastics are endless, as they can be molded into any form, used as a coating, extruded into a film, expanded into an insulating foam or spun into thread at a cheap price. This is why global plastic production increased exponentially from 1950, when the annual plastic production was at 1.5 million metric tons (Chalmin, 2019) to 368 million metric tons in 2019 (Plastics Europe, 2020).

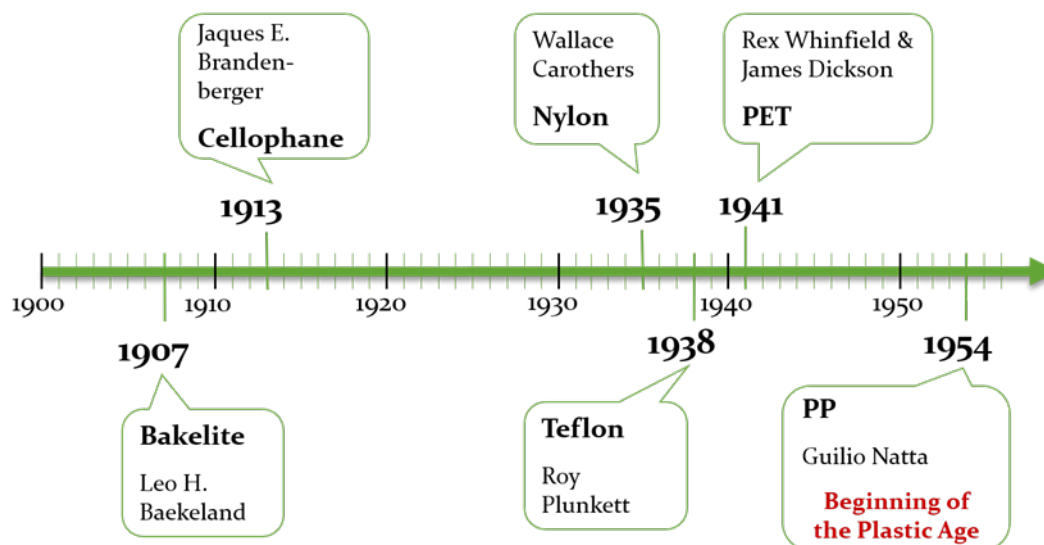


Figure 1: Timeline of the beginning of the Plastic Age

Plastics – a solution or a problem?

Due to their versatility, light weight, durability and low production costs, plastics have revolutionized our way of living. Lightweight packaging material reduces the amount of energy needed to transport goods, lowering costs. The shelf life of perishable goods can be increased, simply by packing them in sterile plastic. In the building sector, plastic pipes allow for a hygienic and safe water supply while their resistance to corrosion and impermeability are indispensable for modern plumbing systems. The medicine sector has also significantly profited from plastics, as single-use health care equipment such as gloves or syringes facilitate the fast treatment of patients and eliminates the risk of transferring diseases from one patient to another via contaminated appliances. These are just a few examples of how plastics have become essential in modern society (PlasticsEurope, 2021). However, with the emergence of single-use every-day products, plastic waste disposal has first become a logistical and then an environmental problem. The maxim to “reduce, reuse and recycle” waste does not seem to be feasible concerning plastics. Reducing plastic waste is near impossible considering how much plastic is used in everyday products, and avoiding plastic nowadays is a considerable challenge for individual consumers. Large scale reuse of plastic products is only practicable for a very small number of products (e.g. refilling hard-plastic bottles) and is essentially not done (Geyer, 2020). Therefore, recycling seems to be the last option of sustainability. However, recycling plastics comes with its own problems, as mechanical recycling is only possible for thermoplastics. Furthermore, recycled plastic cannot completely replace virgin material production, as contamination and mixing of plastic types - as happens when collecting plastics waste - often makes recycled plastic inferior

in its properties. Therefore, it must be acknowledged, that in this case “*recycling delays, rather than avoids, final disposal*” (Geyer, 2020, p. 23). Thus, incineration - as a form of energy recovery - is still the most common plastic waste management practice in Europe today (Plastics Europe, 2020). However, in a model-based estimation, Geyer et al. 2017 assume that the majority (around 60%) of all plastics ever produced globally were discarded directly into the natural environment or in landfills (Geyer et al., 2017). Controlled landfilling is a controversial but legal waste disposal method in many countries, unmanaged landfills are often illegal and equivalent to direct disposal into the environment. Here, conventional plastics either persist as they are, or fragment into so-called microplastics (i.e. plastic particles in the size range of 1 μm – 1000 μm). Fragmentation usually occurs due to physico-chemical degradation or mechanical abrasion (Cooper & Corcoran, 2010). Microplastics are seen as problematic, as they are persistent in the natural environment and will therefore accumulate over time. Their small size and sheer abundance in the natural environment make them bioavailable to a very wide range of organisms. Ample studies have shown in the field and in laboratory observations, that organisms exposed to plastic particles in the appropriate size range will ingest these particles (Botterell et al., 2019; R. R. Hurley et al., 2017; Schöpfer et al., 2020). Consequently, the uptake of plastic particles with no nutritional value is likely to have negative effects on the fitness of animals. Larger plastic debris have been shown to be ingested by a variety of bigger animals, reducing their fitness and often with fatal consequences (Derraik, 2002). However, in this section I will lay my focus on microplastics. A study by Schöpfer *et al.*, (2020), showed that the soil-dwelling nematode *Caenorhabditis elegans* produces less offspring when exposed to high levels of microplastics, independent of the microplastic type. Botterell et al., (2019) reviewed studies on the uptake and effects of microplastics on marine zooplankton, where negative effects of microplastic uptake on feeding behavior, reproduction, growth, development and lifespan were reported. The exact mechanisms of the detrimental effects on organisms (blockages of the gastrointestinal tract, inflammation, uptake into cells, leaching additives etc.) are still being investigated and cannot be generalized for all species or microplastic types (Laforsch et al., 2021). Also the long-term effects of microplastics on ecosystems are still not fully understood; but due to their persistence in the environment and indications that microplastics of a specific shape (e.g. fibers) can alter soil properties (De Souza Machado et al., 2019), as well as the soil microbiome (Sun et al., 2022), many scientists advocate to treat microplastics as potentially harmful on the precautionary principle.

Contrarily to the controversially discussed conventional plastics, biodegradable plastics are seen as a sustainable alternative due to their perceived low impact

after entering the natural environment. However, biodegradation only occurs if there is an interaction between microorganisms and the material, and this interaction is dependent on environmental factors such as temperature, oxygen availability, light, humidity and pH-value (Agarwal, 2020). Therefore studies in the laboratory often overestimate natural biodegradability rates; and partial degradation may lead to the formation of microplastics (Filiciotto & Rothenberg, 2021), of which the fate and effects in the environment are not yet clear.

Defining microplastics

The term microplastic was coined in 2004 by Thompson *et al.*, who alerted the public that beach sediments are contaminated with microscopic plastic fragments. In 2008 scientists at the International Research Workshop on the Occurrence, Effects and Fate of Microplastic Marine Debris defined microplastics as “*plastic particles smaller than 5 mm*” (Arthur *et al.*, 2009). This definition is most commonly used in literature, but it is ambiguous in its meaning. “Plastic particles smaller than 5 mm” has the drawback of not stating a lower cut-off size and does not define what is meant by plastic. For example, tire wear is considered a major microplastic pollutant, but is rubber-based, which is usually not considered as plastic in polymer sciences (Hartmann *et al.*, 2019). Without a consistent and universal definition of what is meant by “microplastics”, microplastic research to date is struggling to generate comparable data, as lower size limits and analyzed polymer types vary strongly. Furthermore, a constructive scientific and public debate on the occurrence and fate of microplastics in the environment is impossible if there is no comprehensive definition of what microplastics are. Therefore, Hartmann *et al.*, (2019) devised a new definition of plastic debris as “*objects consisting of synthetic or heavily modified natural polymers as an essential ingredient (criterion I) that, when present in natural environments without fulfilling an intended function, are solid (II) and insoluble (III) at 20 °C. [They] further recommend using the criteria size (IV), shape (V), color (VI), and origin (VII) to further categorize plastic debris*” (Hartmann *et al.*, 2019, p. 1045). They also propose the following size categorisation: nanoplastics (1 - < 1000 nm), microplastics (1 - < 1000 µm), mesoplastics (1 - < 10 mm), and macroplastics (> 1 cm) (Hartmann *et al.*, 2019, p. 1044).

A further, often used categorization is into primary microplastics – plastics that are manufactured in a small size (e.g. industrial scrubbers, plastic powders and micro-beads in cosmetics) and secondary microplastics that are the result of the fragmentation of larger plastic items (GESAMP, 2015). These categories may help

to identify potential sources and pathways for the microplastics entering the environment.

Microplastic sources and their input pathways to soils

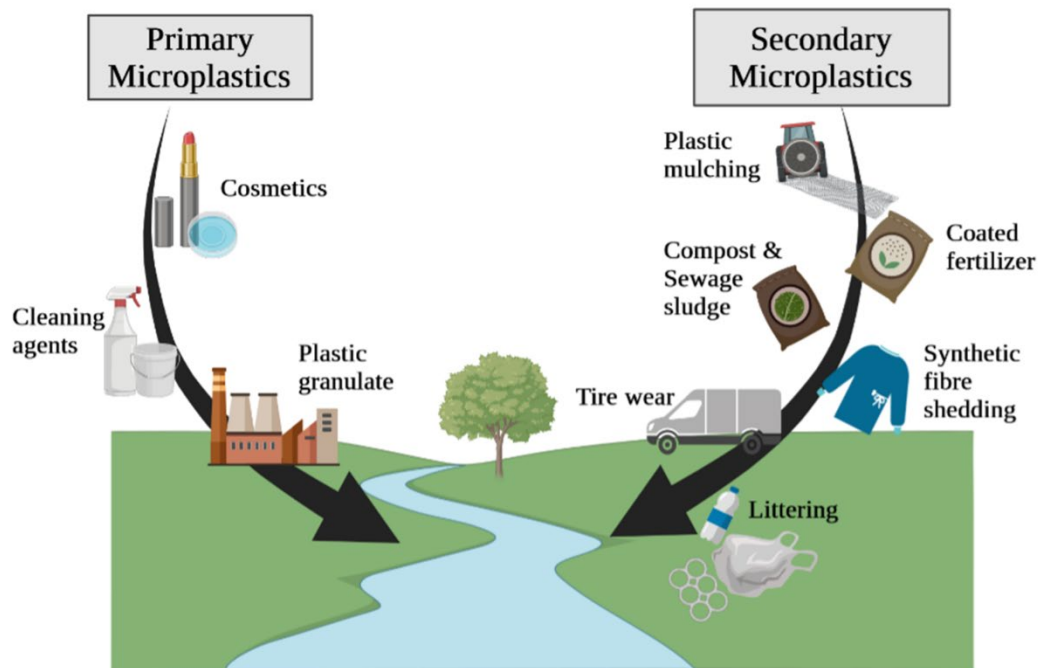


Figure 2: Potential microplastic sources and input pathways to the environment*

Microplastics can be found in all environmental compartments around the globe (Wang et al., 2021). Initially microplastic research was exclusively conducted in marine ecosystems, later expanding to freshwater systems, but only very recently the focus has shifted to include microplastics in the terrestrial environment. Sources and input pathways of microplastics into the environment are manifold, with human population being the root cause. Waldschläger *et al.*, (2020) made an effort to give a comprehensive overview over the sources, input pathways and transport of microplastics in the environment. They defined sources as “*the place, product or action that generates MP*” while “*entry paths are therefore defined as the particles' way from the source into the environment.*” (Waldschläger *et al.*, 2020, p.2). Sources can therefore be plastic production sites, synthetic textiles, landfills, construction sites, littering, tire abrasion and more, while the pathways can be loss (e.g. of virgin plastic pellets during transportation to a processing site), atmospheric drifting, surface runoff, wastewater effluent and sewage sludge application (Waldschläger *et al.*, 2020). As the atmosphere, hydrosphere, lithosphere and biosphere are all interconnected and microplastics can be

Introduction

transported via wind, water and biota, it is difficult to pinpoint the exact sources and pathways of microplastics into one specific environmental compartment. However, here I will try to give an overview over the most important sources and pathways that lead to a direct input of microplastics into soils.

Worldwide the most evident, albeit not easily quantifiable source of plastic pollution is littering and inappropriate waste management, i.e. uncontrolled landfills (Bläsing & Amelung, 2018). The larger plastic debris is likely to degrade over time due to UV-radiation and mechanical abrasion (Gabbott et al., 2020) and soils are assumed to be long-term sinks for these litter-derived secondary microplastics (R. R. Hurley & Nizzetto, 2018). Another very significant source of microplastics is tire wear from cars. Emissions are estimated at around 133 000 t/a in Germany alone, which can be transferred off the streets and into soils via surface water runoff or wind (Wagner et al., 2018). The normal daily handling of plastic products can also cause significant release of microplastics into the surroundings (Sobhani et al., 2020). Agricultural practices also contribute significantly to the input of microplastics into soils. Plastic mulching is often used to increase the harvest yield by increasing the soil temperature and reducing evaporation. However, the use of large plastic foils on fields that are worked with large machinery leads to the often unintentional incorporation of plastic into the soil (Bläsing & Amelung, 2018). In some countries, such as Japan, the use of plastic-coated fertilizer also contributes to the direct input of microplastics into soils (Katsumi et al., 2020). Also, the irrigation with untreated or partially treated wastewater, which is common practice in regions with water scarcity, is likely to be a major input pathway of microplastics into soils, as sewage often contains high amounts of small microplastics, such as fibers from synthetic textiles that were shed during washing. Where wastewater is treated, the amount of microplastics in the effluent is usually significantly reduced – up to 90% of the microplastics are removed from the water and retained in the sewage sludge (Bläsing & Amelung, 2018). However, due to the high nutrient content of sewage sludge, it is often used as a soil amendment, but has been shown to contain alarming amounts of microplastics that are then applied to agricultural fields where they accumulate over time due to recurring sludge application (Corradini et al., 2019; Crossman et al., 2020; Nizzetto et al., 2016; Van den Berg et al., 2020). Another input pathway is the atmospheric deposition of airborne microplastics into soils. Kernchen *et al.*, (2021) estimated an average airborne microplastic deposition of 0.05 ± 0.1 kg/ha in one year from measurements taken in the German Weser catchment area.

This section demonstrates how multifarious the microplastic sources and input pathways are, and I make no claim to completeness. Due to the infinite uses of

plastics in our daily lives, there may be some input pathways that have not yet been recognized. One example for such a pathway is indeed part of this dissertation: Only recently I was part of a research team that demonstrated for the first time that compost derived from household organic waste is a significant input pathway of microplastics to agricultural soils – a fact that was simply overlooked for years.

The extent of microplastic pollution in soils

Worldwide, only very few studies have conducted an assessment of microplastic pollution in soils. In a case study conducted by Fuller and Gautam (2016) the microplastic contamination of soil samples taken from an Australian industrial site ranged between 300 and 67500 mg/kg. Scheurer and Bigalke (2018) analyzed soils from 29 floodplains in Swiss nature reserves, stating that 90% of the floodplain soils were indeed contaminated with microplastics. They reported a mean concentration of 5 mg/kg and a maximum concentration of 55.5 mg/kg. Huerta Lwanga *et al.* (2017) studied home garden soils in Mexico and found a mean contamination of 0.87 particles/kg. Liu *et al.* (2018) observed an average of 78 particles/kg in the surface layer (0-3 cm) of 20 agricultural soils in Shanghai, China, while the deeper layers (3-6 cm) revealed an average abundance of 62.5 particles/kg. Zhang and Liu (2018) analyzed soils in southwestern China, where the use of plastic greenhouses is common practice. The study showed abundances of 7100 to 42960 particles/kg. These studies on the pollution of soils were revolutionary in the sense that they were among the very first to quantitatively analyze microplastics in soils. However, due to the different size ranges analyzed, the different analytical methods used, as well as the different concentration units reported (mass vs particles per kg dry weight), the results of these studies are not directly comparable. Furthermore, the data given is very location specific. Therefore, estimating the extent of microplastic pollution on a larger scale is extremely difficult, as the general data situation on microplastics in soils is still too thin. However, Büks and Kaupenjohann (2020) attempted to give an overview of global microplastics pollution in soils based on 23 studies that were published before August 2020. Of 223 sampling sites distributed unevenly across the globe (mainly in East Asia and Europe) the median of microplastics found in soils were 1167 particles/kg (n = 218; 25% – 89 items/kg; 75% – 2870 items/kg) and 0.6 mg/kg (n = 29; 0.004, 2.65 mg/kg), depending on which concentration unit was reported. Büks and Kaupenjohann, (2020) acknowledge the limitations of reporting absolute microplastics concentrations based on data sets that were collected with different and incomparable methods.

However, they managed to give a general overview of the relations of microplastic contamination to underlying entry pathways, land use and the vicinity to urban locations. Their review showed, that sites exposed to sewage sludge application exhibited microplastic loads one order of magnitude above the loads found on agricultural sites using plastic mulching. They further showed, that the microplastic concentration within soils is positively correlated to population density, as sites in the vicinity of urban areas were generally more heavily polluted than rural areas (Büks & Kaupenjohann, 2020).

While critically scrutinizing the methods used in previous literature, it became apparent that many methods could only reliably analyze for a very limited group of plastic types. Some protocols intrinsically eliminated high-density polymers due to the use of density separation procedures with pure water or a NaCl solution ($\rho = 1.2 \text{ g/cm}^3$) during sample processing. Others used solvent extraction, which is usually also limited to a handful of polymer types, dependent on the solvents used and again other protocols used high temperatures or strong acids and bases in an attempt to remove the residual organic matter, that may however also degrade certain plastic analytes. Therefore, the need for robust and reliable methods of sampling, sample processing, analysis and evaluation of a wide range of microplastics in soils is still given.

Detecting microplastics

Ever since the scientific community has been made aware of the microplastic pollution in the sea in 2004 (Thompson et al., 2004), microplastics research has emerged and evolved, and with it the methods to detect microplastics. Initially, microplastics were identified visually, assessing their color and structure under a light microscope (Day et al., 1990; Shaw & Day, 1994). However, this kind of assessment is extremely error prone (Hidalgo-Ruz et al., 2012) and should always be corroborated with a chemical analysis to verify if the particle in question is indeed plastic, and if yes, which type. In the following section, I will only mention the most commonly used and established instrumental detection methods for microplastics in environmental samples.

Pyrolysis gas chromatography mass spectrometry (Pyr-GCMS)

Pyr-GCMS is a thermal analytical technique, during which the analyte is thermally degraded under an inert atmosphere (pyrolysis) (Hermabessiere et al., 2018). Dependent on the pyrolysis temperature, the polymer is degraded to characteristic volatile components that, once separated in a gas chromatography

column and detected in a mass spectrometer, allow the fingerprint-like identification of the polymer due to the pyrolysis pattern (Käppler et al., 2018). For Polyesters and Polyethers, that have polar subunits and cannot appropriately be analyzed via a simple Pyr-GCMS can however be analyzed if pyrolyzed in the presence of a derivatization agent. This method is called Thermochemolysis and can improve the chromatographic data quality (Käppler et al., 2018). The Pyr-GCMS method has the advantage that it allows the mass quantification and identification of the polymer type as well as any contained organic additives that may be harmful to the environment while being robust against any inorganic components in the sample (Fries et al., 2013). However, it is a destructive method, and therefore not repeatable for the same sample. Furthermore, as a mass-quantitative method, data on the number, size, and shape of the microplastics contained in the sample is not given. This is in so far a major drawback as these parameters play a decisive role in the effects the particles have on organisms and soil properties (De Souza Machado et al., 2019), which in turn are important factors to consider in a comprehensive risk assessment. Additionally, the sample capsules, and therefore the sample amount per run is very small (0.5 mg), which perhaps impedes representativeness for the environment from which the sample was taken. Moreover, the setup is often prone to blockages (Dümichen et al., 2017).

Thermal extraction desorption gas chromatography mass spectrometry (TED-GCMS)

Another thermal analytical technique found in microplastic research is the TED-GCMS. This is a combination of a thermal extraction via thermogravimetric analysis (TGA), where the sample is pyrolyzed at temperatures up to 600°C and the volatile pyrolysis products are adsorbed on solid phase adsorbers, from where they are subsequently analysed via a thermal desorption gas chromatography mass spectrometry (Dümichen *et al.*, 2017). This method allows the identification of the most common plastic types in up to 100 mg of homogenized environmental samples, without much sample preparation (Eisentraut et al., 2018). However, as with all thermal mass-quantitative methods, the method is destructive and the number, size and shape of the microplastics cannot be identified via this technique, especially if the sample has to be homogenized (milled) before analysis.

Raman spectroscopy

Raman spectroscopy is based on the inelastic scattering of light that delivers a material specific pattern (Raman spectrum) dependent on the molecular vibrations of the material. Thus the material can be identified according to its fingerprint spectrum (Araujo et al., 2018). Raman micro-spectroscopy is commonly the tool of choice for the particle quantitative measurement of small microplastic particles (lower micrometer to nanometer range) (Anger et al., 2018; Gillibert et al., 2019; K appler et al., 2015). The technique is non-destructive, has an excellent spatial resolution and can be used to identify a very wide range of plastic types. However, Raman spectroscopy is prone to fluorescence interference – e.g. by natural organic matter and has an inherently low signal to noise ratio (Araujo et al., 2018), therefore environmental samples that are to be analysed need to undergo a thorough sample purification and preconcentration in order to obtain good spectra and allow a chemical point-by-point mapping of the particles in a relatively small area, as Raman imaging takes a lot of time (38 h for 1 mm² (K appler et al., 2016)).

Fourier-transform infrared spectroscopy (FTIR)

A complementary vibrational spectroscopy method to Raman spectroscopy is FTIR spectroscopy. It exploits the fact that infrared light is absorbed at specific wavelengths when it excites certain molecular vibrations. These excitable vibrations are dependent on the molecular structure of the sample – causing a fingerprint absorption IR-spectrum for specific substances (L oder & Gerdts, 2015). FTIR spectroscopy can be used in different techniques and modes. Attenuated total reflectance (ATR) FTIR spectroscopy is often used to identify the material of larger fragments (>500 m) that can easily be handled, e.g. using tweezers. The fragments are placed on a diamond crystal through which an infrared laser beam is directed. The beam is reflected at the interface between the crystal and the plastic fragment, whereby an interaction between the light and the plastic takes place, causing the absorption of specific regions of the infrared spectrum (Bruker, 2021). The attenuated spectrum is material specific, and in our case allows the identification of the plastic type. For smaller particles, that cannot be handled manually (10-500 m), the  -FTIR imaging method has become the most abundantly used method for particle quantitative microplastic analysis (Elert et al., 2017). Focal plane array (FPA) detectors are state of the art in  -FTIR imaging and allow faster imaging with higher resolution than single element- or line array detectors. For the  -FTIR spectroscopy, a purified sample is filtered onto an IR-transparent material and screened completely, giving a

chemical image with a resolution of 10 μm . Each pixel in the chemical image is represented by a spectrum, which can now be automatically identified and assigned to a certain plastic type - e.g. by using a random forest classifier (Hufnagl et al., 2019). In comparison to Raman mapping, the FPA detector based μ -FTIR imaging has a relatively short measurement time and reliably identifies most plastic types while also maintaining the information on particle number, shape and size (Löder et al., 2015). However, particles smaller than 10 μm cannot be detected via this technique and particles that are too thick (critical thickness is dependent on the material) will cause total absorption of the infrared beam in transmission mode, which leads to an unidentifiable spectrum, therefore the detectable size range for μ -FTIR imaging analysis has to be considered.

Comparability

In an international laboratory comparison for microplastic detection methods (μ -FTIR spectroscopy, μ -Raman spectroscopy, pyr-GCMS, TED-GCMS, scanning electron microscopy, light scattering particle counter and stereo microscopy) Müller *et al.* (2020) showed a “*Remarkable [] variance of results between the methods but also within the methods.*” (Müller *et al.*, 2020, p.1). This pinpointed the need for a standardization or harmonization and validation of methods for microplastic detection. This is not only true for the instrumental detection methods, but when dealing with environmental samples, this includes sampling techniques, sample processing, analysis and reporting.

The four techniques mentioned above are very different, but all are applied for the analysis of microplastic contamination of environmental samples. However, they all require some sort of sample pre-treatment, either to accommodate a representative sample amount and/or to remove any environmental matrix that may disturb the analysis. The methods used to pre-process environmental samples for microplastics analysis are as diverse as the samples themselves. As the analyte size ranges became smaller and the environmental matrices to be analyzed became more complex, ever new sample processing methods were developed, but to date, none of them has become standardized. And for the extremely complex environmental matrices of soils, only very few attempts at analyzing them for small microplastics have been pursued at all.

2. Knowledge gaps & objectives

1) Method development

Knowledge gaps:

Reliable particle-quantitative analysis of soil samples is an essential tool for the deeper understanding of the contamination extent, fate and potential impact of microplastics in the terrestrial environment. However, current analytical protocols have considerable limitations concerning the use of plastic-destructive purification protocols, analyzable sample sizes, lower size limits of the microplastic particles detected, and a limited spectrum of analyzed plastic types (e.g. only low-density plastics) that may hamper correct result-reporting.

Objectives:

- develop a robust and reliable sample purification and analysis method for soils and complex environmental matrices
- enable the microplastic analysis of relatively large, more representative sample sizes
- permit the identification of particles down to the lower micrometer range
- cover the analysis of a large spectrum of plastic types

2) Microplastic pollution and fate in soils

Knowledge gaps:

Previous reports on microplastics in soils were often limited to the finding of a certain amount of microplastics in samples at specific locations. However, next to nothing is known about the fate and fragmentation/degradation behavior of microplastics in agricultural and natural soils.

Objectives:

- apply the here developed methods in a field experiment to determine if biodegradable plastics degrade/fragment differently compared to conventional plastics in the agricultural soil environment
- use the here developed methods in collaboration with colleagues from the University of Cologne to gain deeper insight into the

mechanisms influencing flooding-related microplastic deposition and subsequent migration into floodplain soils.

3) Assessment of organic fertilizers as microplastic input pathways

Knowledge gaps:

Household organic waste is often very highly contaminated with plastic. This causes great problems for biowaste treatment (BWT) plants, whose aim it is to biologically process the organic waste into high quality composts, which are then used as fertilizers and soil amendments in agriculture. Most BWT plants take great pains to remove the plastic from their input material, but unfortunately it is not possible to remove everything. Furthermore, the extent of contamination of organic fertilizers with small microplastics and the influence of plant technology on the microplastic generation within BWT plants have not been examined in the past.

Objectives:

- determining if and how much microplastic is present in composts and digestates derived from BWT plants, which may thereby reach agricultural soil
- finding out if the respective technology or the technical processes in different BWT plant types influence the abundance and size of microplastics in the end-products.
- assessing the fate of biodegradable plastics in BWT plants and elucidate if biodegradable plastic bags contribute to the microplastic contamination in digestates derived from organic household waste.

3. Method development

Article 1 - Finding Microplastics in Soils - A Review of Analytical Methods.

In Article 1 I aimed to give a critical overview over methods reported in peer reviewed literature for sampling, extraction, sample purification and instrumental detection of microplastics in complex environmental samples. By assembling and critically assessing these methods, I focused on determining techniques that would potentially be suitable for a meaningful microplastics analysis of soils. I additionally compiled a comprehensive list of field sampling approaches suitable to the respective research objectives. Also dependent on the objective is the instrumental analysis method to determine the microplastics content in a sample. My research gave me insight to a wide variety of promising methods, of which many however are based on a mass-quantitative analysis. This means that ecologically relevant information on the particle number, shape and size is lost. If this information is not relevant for the research question, methods like Pyr-GCMS and TED-GCMS seem a valid option. However, for a comprehensive hazard and risk assessment, vibrational spectroscopy methods such as Raman and FTIR spectroscopy were deemed the most appropriate options, as they are the only methods currently available that allow the particle-quantitative analysis of microplastics with a reliable polymer identification. However, both methods require a thorough sample cleanup without changing the microplastics properties in any way. I found that a single step microplastics' extraction protocol for small microplastics is not practicable, as soils are made up of a complex mixture of minerals and organic matter that cannot be removed in one step without destroying the microplastics. Therefore, as a first step an oil-extraction or a density separation with a high-density brine using salts such as NaI ($\rho = 1.8 \text{ g/cm}^3$), $\text{Na}_6[\text{H}_2\text{W}_{12}\text{O}_6]$ ($\rho=1.4 \text{ g/cm}^3$), ZnCl_2 ($\rho = 1.6\text{--}1.7 \text{ g/cm}^3$) or NaBr ($\rho = 1.55 \text{ g/cm}^3$) is necessary. In a second step a digestion is required to remove the residual organic fraction. Fenton's reagent and a sequence of adapted enzymes were deemed the most appropriate methods presented in literature, but many other more controversial digestion methods using acidic or alkaline solutions were also presented.

Article 2 - Microplastic sample purification methods - assessing detrimental effects of purification procedures on specific plastic types

Article 2 is a systematic comparison of the effects of sample purification protocols on different types of plastic films. Seven purification protocols (with sodium hydroxide, hot nitric acid, peroxymonosulfuric acid, sequential enzymatic digestion, hydrogen peroxide, Fenton's reagent and zinc chloride brine) were compared in their effects on eight of the most common plastic types (PE, PP, PET, PVC, PU, PC, PS, PA). Visible and gravimetric changes, surface degradation via ATR-FTIR and bulk erosion on a molecular level via gel permeation chromatography (GPC) were analyzed. It became evident that strong acids and high temperatures, while very effective in removing environmental organic matter (ICES, 2015; Naidoo et al., 2017), cause a strong degradation of the polymers PA, PC, PET, PS, PUR and PVC. Strong alkaline solutions may cause damage to the polyesters PC and PET. Contrarily, Fenton's reagent, a sequential oxidative-enzymatic digestion including H_2O_2 and several technical grade enzymes as well as the treatment with a $ZnCl_2$ brine commonly used for density separation, did not degrade the eight plastic types tested in this experiment.

Article 3 - Tackling the challenge of extracting microplastics from soils: A protocol to purify soil samples for spectroscopic analysis.

In Article 3 I developed a protocol that allows the purification of up to 250 g soil sample in such a way that vibrational spectroscopic analyses such as micro-FTIR or micro-Raman spectroscopy become possible. A sequence of freeze drying, sieving, density separation with a $ZnCl_2$ brine and an enzymatic-oxidative digestion procedure allows the removal of over 99.9 % of the mineral mass and an average reduction of 77 % of the remaining organic fraction. In order to test the method for any negative effects on the microplastic particles, I surveyed microplastics (PA, PE, PET, PVC and PLA) in the size range of 100 μm to 400 μm and of different shapes. Visual integrity and analysis via ATR-FTIR, gel permeation chromatography (GPC) and differential scanning calorimetry (DSC) showed that none of the conventional microplastics were affected by this approach, however, PLA was shown to be slightly degraded by the enzyme protease. In an application of the protocol to a natural soil sample 160 microplastic particles down to a size of 10 μm (lower limit of detection for the micro-FTIR analysis used) were found. 85% were fragments and 15% were fibers.

Method development

The polymer types successfully identified were PP, PS, PE, PET, PBT and PAN. The protocol is effective, but time consuming and further research and development toward automated systems may be necessary to make the method feasible in larger microplastic monitoring schemes.

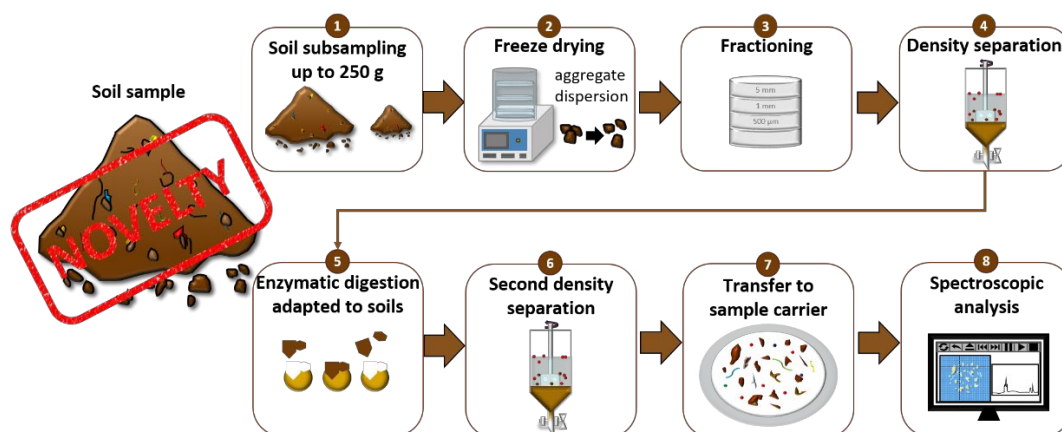


Figure 3: Workflow of the sample purification and analysis protocol

Conclusions – Method development

The results of a study are only ever as good as the methods used to produce them. In this chapter and during my PhD studies in general, I was mainly focused on finding methods to make a particle-quantitative analysis of microplastics in complex environmental matrices possible. During the process, I became aware of many issues that the microplastics research community needs to address in order to obtain reliable results. While writing Article 1, I was initially overwhelmed by the sheer abundance of methods used to analyze microplastics in environmental samples and the lack of any sort of standard that would allow a comparison of the studies. It is crucial for the scientific community to establish a unified, unambiguous definition of “microplastics” and to ensure that reporting is conducted in such a way that informed readers can easily evaluate the meaning of reported microplastic numbers or weight units. Furthermore, it is important to establish standardized validation methods (including the development of standard microplastics and standard samples with which to conduct the validation) that allow an objective evaluation of the method’s suitability. To date no such standardized validation procedures exist for microplastics analysis. Once the reliability of any method can be objectively confirmed, the choice between mass quantitative (Pyr-GCMS, TED GCMS) and particle quantitative (Raman and FTIR spectroscopy) analyses is heavily dependent on the research question at hand. Independent of the analytical instruments chosen, my research has shown

in Article 2 that if a sample purification procedure is necessary, future studies should refrain from using high temperatures, strong acids or bases, as these can degrade certain plastic types, which may lead to unreliable results. A density separation with a $ZnCl_2$ brine and an organic matter removal with Fenton's reagent and/or a sequential enzymatic digestion are on the other hand are fine for the detection of conventional plastics. This finding was corroborated in the additional analyses I conducted to test the sample purification method I developed in Article 3. The study in Article 3 however also showed, that the enzyme protease can degrade PLA and should therefore not be used if biodegradable polymers are on the analyte-spectrum. The protocol is effective and allows the analysis of up to 250 g of soil sample. However, in terms of time- and resource efficiency, an automation of the system would be necessary to make it eligible for any kind of broad scale monitoring. In general, I believe that the methods used for microplastic analysis in environmental samples are still in their infant stages. There is a necessity to invest time and resources into refining the currently available methods and most importantly establish a standard validation method to assess their accuracy. In a next step the methods themselves should be standardized and harmonized to make studies comparable which would give added value and enable meta-analyses that allow a more comprehensive understanding of the real environmental pollution with microplastics.

4. Microplastic pollution and fate in soils

Article 4 - Microplastics persist in an arable soil but do not affect soil microbial biomass, enzyme activities, and crop yield

In Article 4 the methods developed in chapter 3 were applied in a field experiment where I examined the background concentrations and the fate of conventional microplastics (PE) and biodegradable microplastics (a blend of PLA and PBAT here termed PLA/PBAT) over time. Additionally, the effects of microplastics in combination with organic fertilizers on the soil carbon turnover and crop yields were studied. The analysis for background contamination with microplastics showed an average loading of 296 ± 110 (mean \pm standard error) particles/kg soil, with nine different polymer types – of which PP (108 ± 36 particles/kg), PS (76 ± 34 particles/kg) and PE (60 ± 25 particles/kg) were by far the most abundant. Randomized plots in the field were treated with 2 g/m^2 of the following microplastic type – PE and PLA/PBAT. The average microplastics concentration at the start of the experiment was 1003 ± 76 PE particles/ kg and 134 ± 15 PLA/PBAT particles/kg. After one month as well as after 17 months the plots were sampled again, and no significant change in number or size distributions of the respective microplastics could be detected. This allows the assumption, that both the conventional and the so-called biodegradable plastics tested here persist in soils under field conditions. While persistence is a cause for concern, no direct negative effects on the agricultural performance of the field could be attributed to the addition of the microplastics to the soil in the given time-frame. The microbial carbon turnover and enzyme activities of treated plots showed no significant differences to the control. Also, the crop yields of silage maize and summer barley were not affected by the addition of the microplastics to the plots.

Article 5 - Flooding frequency and floodplain topography determine abundance of microplastics in an alluvial Rhine soil

Article 5 is a collaborative study with the Institute of Geography, University of Cologne, on the fate of microplastics in the dynamic interface of the Rhine River and an adjacent floodplain. The floodplain “Rheinaue Langel-Merkenich” near Cologne was analyzed for the abundance of microplastics in three locations along

the river. Due to the unique topography of the site, microplastic input via runoff from outside the floodplain is unlikely. Therefore, it is assumed that most of the microplastics found in the soil were deposited during flooding events. Using the methods described in chapter 3 (with an additional CaCl₂-brine density separation to remove the high amount of black carbon particles present in these samples) a very heavy general contamination (25502 - 84824 particles/kg) with microplastic particles was observed. The study here verified that topography and vegetation are key factors to the incorporation of suspended microplastic particles into the floodplain soil. In the location closest to the riverside vegetation is sparse and erosion is evident. Here, the least amount of microplastics was found, even though it is the most frequently flooded location. This is most probably due to recurrent erosive forces during flooding events, that prevent particles from settling and may re-suspend any deposited particles. In contrast, a grassy depression farthest from the riverside showed the highest microplastic contamination, even though flooding occurs less frequently. The depression is cut off from the main flow once the flood recedes. In the resulting ephemeral pool, all particles transported during the flood will settle and the grass coverage hinders re-suspension in the next flood, promoting microplastics accumulation in the soil and transport to deeper layers. A seldomly flooded grassy rise in between the former two locations contained an intermediate amount of microplastics, showing that flooding frequency is not necessarily correlated to microplastics accumulation.

Conclusions - Microplastic pollution and fate in soils

Soil systems are deemed to be one of the major sinks for microplastics; and although the number of studies concerned with microplastics contamination in soils is steadily rising, the scientific community still does not have a full understanding of the extent of microplastics pollution, the transport mechanisms or the fate of microplastics entering the soil system. In the agricultural field study (Article 4) we could show that even arable soils that are not treated with commonly known plastics input pathways (sewage sludge, compost, plastic mulching etc.) still had a noticeable background contamination with common plastic types. This may be due to the use of plastics in day-to day agricultural practices, atmospheric deposition, littering, or a combination of all, but is difficult to pinpoint. The study also showed that PE and the so-called biodegradable blend of PLA/PBAT used in this study did not degrade over the course of nearly one and a half years, highlighting that microplastics are a persistent pollutant. However, the study also showed that the soil system seemed quite resilient towards the relatively high loading with microplastics, as no

significant differences in crop yield, enzymatic activity or microbial carbon turnover could be detected. This is however not yet cause for relief, as a laboratory study conducted with the same types of polymers has shown that nematodes (*Caenorhabditis elegans*) can ingest the plastics and showed a decreased reproduction rate when exposed to the microplastics (Schöpfer et al., 2020). Article 5 on the other hand demonstrated that the soil-sample purification method developed in chapter 3 is inadequate when the soil is heavily loaded with black carbon particles. Here a third step to separately remove the carbon with a CaCl_2 -brine density separation was required. The data acquired in this study give indications to which factors of the natural riverbank-floodplain system are relevant to long-term microplastic deposition in soils during flooding events. It seems that topography and vegetation cover, which influence hydrological parameters such as flow-velocities and turbulences that in turn influence erosion or sedimentation, are more decisive concerning microplastic deposition than flooding frequency alone.

5. Assessment of organic fertilizers as microplastic input pathways

Article 6 - Organic fertilizer as a vehicle for the entry of microplastic into the environment.

Article 6 represents a first-time quantitative analysis of microplastics in organic fertilizers. The study was conducted in collaboration with the Chair for Process Biotechnology of the university of Bayreuth. As the research took place before methods were developed to allow the analysis of microplastics <1 mm in complex solid matrices, the analyzed sizes are in the range of 1 - 5 mm. It shows that not only do all products from the surveyed biowaste treatment (BWT) plants contain microplastics, but the amount between the plants varies strongly. This is due to the substrate pre-treatment, BWT plant type and type of organic waste used. The results (14 - 895 MPs/kg_{DW}), extrapolated to the amount of organic fertilizer that is applied to Germany's agricultural fields each year, let us assume that the amount of microplastics in the range of 1-5 mm introduced into the environment in Germany alone ranges between 35 billion and 2.2 trillion microplastic particles every year. Eleven polymer types were identified via ATR-FTIR spectroscopy, showing that plastic types conventionally used in packaging amongst others could also be found in the compost and digestate of BWT plants.

Article 7 - Microplastic contamination of composts and liquid fertilizers from municipal biowaste treatment plants — effects of the operating conditions

Article 7 represents a survey of the compost and digestate from several different biowaste treatment plants treating different types of organic waste (green clippings and household organic waste) as well as agricultural biogas plants using energy crops and manure for biogas production. The collaborative survey with the Chair for Process Biotechnology of the University of Bayreuth showed that while the fertilizers from the agricultural biogas plants were hardly contaminated at all, the composts and digestates deriving from organic waste treatment plants varied from extremely high to moderate contamination levels. While this is probably linked to the quality of the incoming organic waste, it appears that the operating conditions and equipment technology used also influence the amount of microplastics found in the final compost and digestate: Shredding of the incoming material, while potentially constructive to a better

processing of the organic matter, seems to significantly increase the amount of microplastics in the compost or digestate. On the other hand, sieving the compost at the end of the process is effective in removing a large proportion of the larger plastics fragments (>5 mm), but does not significantly reduce the amount of microplastics in the compost or digestate that is then applied to the agricultural fields. In a first-time analysis of liquid digestates from biowaste treatment plants for microplastic particles in the size range of 10 – 500 µm, I found a surprisingly high amount of microplastic particles (up to 10 000 particles per liter). In some cases, a large portion of the microplastics found in the liquid digestates contained the IR-signature of biodegradable plastics.

Article 8 – Municipal biowaste treatment plants contribute to the contamination of the environment with residues of biodegradable plastics with putative higher persistence potential

Article 8 aimed at determining if biodegradable plastic bags, commonly used for organic waste collection, can be completely degraded under the realistic conditions of municipal BWT plants. The goal was to see if residues of the biodegradable plastics can be found in the fertilizer products (compost and liquid digestate). The BWT plants in the study - analyzed in collaboration with the Chair for Process Biotechnology of the University of Bayreuth - conducted a two-stage treatment of the organic waste in form of an anaerobic digestion for biogas production and a subsequent composting of the solid residue. Varying amounts (0 - 50 particles/kg dry weight) of large microplastic fragments (1 mm - 5 mm) were found in the finished products, whereby 4 - 80 % of the particles that were found in the composts were derived from the biodegradable plastics PLA, PBAT or a blend of both. The chemical analysis via ATR-FTIR spectroscopy showed a very high similarity of the fragments found in the compost to the spectra of pristine commercially available composting bags made of biodegradable plastics. The analysis also showed, that biodegradable plastic fragments tended to be smaller than those of the non-biodegradable plastics, indicating a quicker fragmentation process due to a certain degree of partial degradation. In order to better assess if there were any chemical alterations to the biodegradable plastic fragments found, an ¹H-NMR analysis was conducted, confirming that the fragments and pristine bags are composed of PLA/PBAT blends of varied ratios. There seemed to be a shift in the composted fragments towards a higher PBAT ratio compared to the pristine bags tested in this study. This indicates a faster degradation of PLA than the PBAT. Furthermore, differential scanning calorimetry and wide-angle X-ray scattering showed that

the reference biodegradable polymers are semi-crystalline in their molecular structure, meaning that parts of the structure are amorphous (no systematic bound structure) and others are crystalline. The composted fragments showed a shift towards a higher crystallinity compared to the pristine bags, indicating that the crystalline structures within the co-polymer are less readily bioavailable than the amorphous structures. This may have negative implications for the continued biodegradation in the environment. This may mean that the fragments persist longer in the environment than anticipated based on data from laboratory tests (Napper & Thompson, 2019). At the time of the study the method to purify compost and do a meaningful analysis of microplastics via micro-FTIR had not yet been completely established, therefore an ¹H-NMR analysis was conducted for the < 1mm fraction, showing that the compost samples contained 0.5 - 1.5% (by dry weight) extractable material of which 6 - 30% were made up of the biodegradable polymers PLA and PBAT.

In two of the analyzed BWT plants the fermentation percolate is collected and used as liquid fertilizer that is directly applied to fields without further treatment. Here, no fragments > 1 mm were found (possibly due to the percolate being collected in a press filtration procedure, filtering out any larger particles). However, I adapted the enzymatic-oxidative purification protocol for this study in order to be able to analyze the percolate for small microplastic particles. In the smaller ranges approximately 20 000 microplastic particles per liter were found, of which 53 - 65% were biodegradable plastics. This shows that there is a higher abundance of biodegradable plastic fragments in the very small ranges compared to the abundance of any conventional plastic.

Conclusions – Organic fertilizers as microplastic input pathways

Concerning the assessment of fertilizers as microplastic input pathways, my research indicates that soil amendments derived from household organic waste not only introduce conventional microplastics in large amounts into the environment, but also fragments of so-called biodegradable plastics, that - in theory - are supposed to be degraded during the composting process itself. It is known that the conventional plastic will not degrade in the environment in a reasonable amount of time. However, the degradation kinetics of already composted biodegradable plastic fragments in soils under environmental conditions are still unknown. Therefore, in future research studies it should be investigated if fragments of the composted biodegradable plastics further degrade within the soil matrix under realistic conditions. It should also be

investigated if the degradation rates of biodegradable plastics are slower than the input rates via the compost, as this may lead to accumulation. I am also of the opinion, that the certification process for so-called compostable plastic products (e.g., EN 13432) does not represent realistic conditions in BWT plants. nor does it consider fragments smaller than 1 mm. Therefore the certification norm to call a product “compostable” should be revised in the face of this new scientific evidence. Research into the degradation of so-called biodegradable plastics under realistic composting and environmental conditions should be strongly driven forward, as many people see biodegradable plastics as a potential solution to our growing problem of macro- and microplastic pollution in the environment. My research so far indicates that biodegradable plastics fragment faster and into smaller pieces than conventional plastics, but still persist to a certain extent in the digestates that are applied to agricultural fields. If they are proven to persist in the soil over an unreasonable period of time, this would have major implications for the perception of the “environmentally friendly plastics”. The smaller the fragments are, the more likely they are to become bioavailable with to-date unknown consequences for organisms and environmental health. Therefore, the investigation into the fragmentation/degradation of biodegradable microplastics is not only of academic interest, but should also be an issue in a public debate, involving the plastics- and agricultural industries, policy makers and the general public.

6. General discussion and outlook

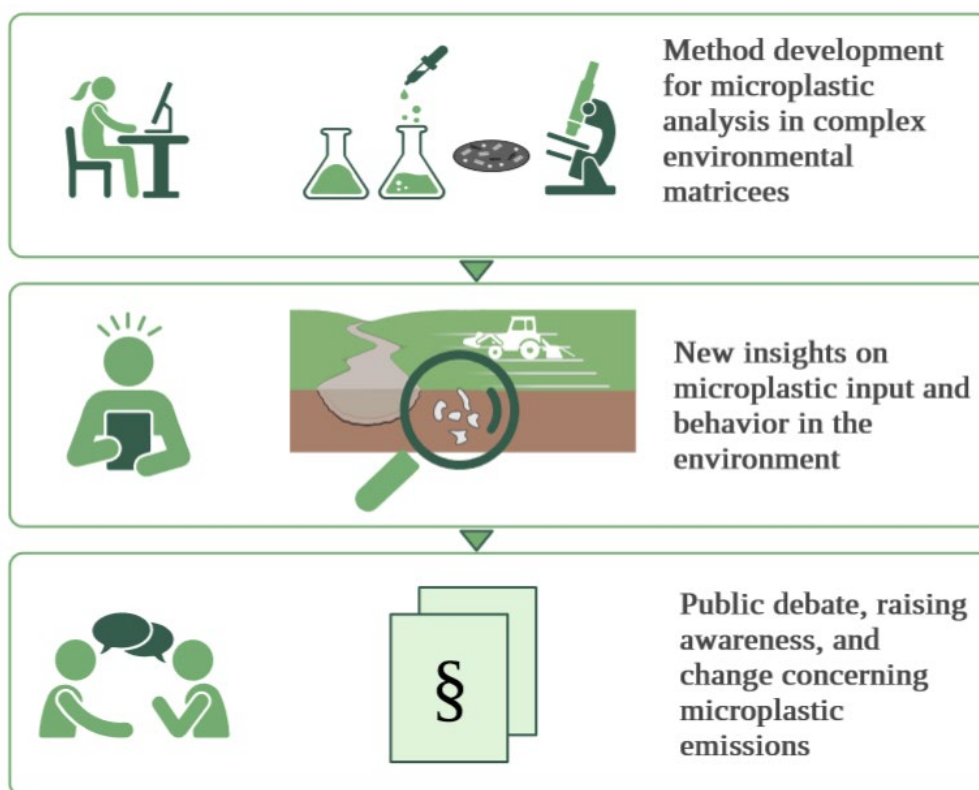


Figure 4: Steps from development and research towards change in society*

In the course of this PhD thesis, I developed a method that allows the reliable identification of conventional and biodegradable microplastics in soils down to a size of 10 μm . This method could also be adapted for smaller amounts of liquid digestate, allowing a first-time analysis of this complex matrix. The focus during the method development was to ensure that the sample purification preceding the $\mu\text{-FTIR}$ analysis is effective in removing complex environmental matrices, while not destroying or in any way affecting the microplastic composition in the sample.

Several surveys I discuss in my critical literature review and my own empirical study on the topic confirmed that the use of high temperatures and strong acids or bases lead to the destruction of certain polymer types (Nuelle et al., 2014; Roch & Brinker, 2017; Rocha-Santos & Duarte, 2015; Schrank et al., 2022). On the other hand Fenton's reagent, the use of zinc chloride and the use of technical enzymes are effective in removing mineral and biogenic matter, while retaining microplastic integrity (R. R. Hurley et al., 2018; Löder et al., 2017; Möller et al., 2021; Tagg et al., 2015). These then became the basis for my soil sample

purification protocol in Article 3. In parallel I contributed data to the machine-learning-based program for automated microplastic particle identification after μ -FTIR analysis. This specific program allows a faster and more extensive particle identification than previous more time-consuming database search algorithms (Pimpke et al., 2017). My work in method development and evaluation was the foundation for many of the findings published in the course of this PhD thesis concerning the fate of microplastics in soils, composts and digestates.

In the earliest application of the here developed analysis protocol, I was able to assess for the first time how relatively small microplastic particles (conventional PE and biodegradable PLA-PBAT-Blend) degrade/fragment over time in an agricultural field. The study showed that even though the field was worked with heavy machinery and the plastics were exposed to natural weather conditions for 17 months, no complete degradation or further fragmentation of the particles took place. Put into perspective, Sintim et al. (2020) reported that the degradation rate of biodegradable plastic mulch films in soils was initially slow and only started increasing after 1.5 years. After three years the degradation (assessed by surface area reduction) was reported to be between 26 – 83 %, dependent on climate and polymer types. Especially PLA-based mulches showed limited degradation in soils under ambient conditions, and the relatively long degradation periods raise concerns over the sustainability of continuous use of biodegradable plastic mulch foils (Sintim et al., 2020). In my study, the spiked plots showed no significant differences in crop yield and carbon turnover in comparison to the control plots. This may be seen as a confirmation of the findings of De Souza Machado et al. (2019), that stated microplastics with a similar shape to natural soil particles had less effects on the soil's biophysical properties (which impact plant performance) than particles with a completely different shape (such as fibers).

The second survey that applied my methods, showed that floodplain soils are contaminated with small microplastics. Scheurer & Bigalke, (2018) also found that soils of Swiss floodplains were contaminated with microplastics. Their numbers, however, were far less (max. 598 MPs/kg) from the ones found on the Rhine River floodplain near Cologne in a similar size range (7 619 – 21 048 MPs/kg). This difference may be due to the locations of the sampling spots, as the sampling site of our study was downriver and in close proximity to the City of Cologne with 1,08 Mio. inhabitants (Wollny, 2022) while the number of inhabitants in the catchment areas of the sampling sites in Switzerland were mostly less than 500 000 (Scheurer & Bigalke, 2018). Another likely reason for the discrepancy could be the different extraction methods of microplastics: Scheurer & Bigalke, (2018) centrifuged a slurry of soil and NaCl-solution with a density of

1.2 g/cm³, to separate the mineral from the organic fraction, followed by a treatment with 65% HNO₃ at 90°C. They therefore potentially lost high-density particles during the density separation and most polymers susceptible to degradation via acids and high temperatures, e.g PA and PET. The conspicuous lack of PA and PET (usually quite commonly found in the environment) in the microplastics composition of the found particles in Swiss-floodplains-study highlights the need for appropriate microplastic extraction methods from soils. The input of microplastics into floodplain soils is most probably due to floodwater of the river, as other studies indicate that flood events remobilize microplastics embedded in the river sediment, causing a generally higher load of microplastics in river water during flooding events than under normal flow conditions (R. Hurley et al., 2018; Woodward et al., 2021). The comparison of microplastic abundance at certain soil depths with hydrological, topographical and vegetation data gave indications that topography and vegetation cover influence the deposition and retention of microplastics more than flooding frequency alone. To my knowledge this is the first time this correlation has been made in the context of microplastic transport.

Investigating organic fertilizers as another input pathway for microplastics into soils, I was able to prove for the first time that composts or digestates derived from plastic-contaminated household organic waste contain a significant amount of microplastics. This was later corroborated by several other studies in different countries (Gui et al., 2021; van Schothorst et al., 2021). Van Schothorst et al. (2021) found similar numbers of microplastics in compost in the size range of 1 – 2 mm (21 MPs/kg) to the numbers we found in the size range of 1 - 5 mm (20 – 24 MPs/kg). This is insofar interesting, that van Schothorst et al., (2021) used a density separation step with distilled water, only allowing the extraction of low-density polymers, whereas our study also included high-density plastics such as PVC. However, one big drawback of the method used by van Schothorst et al. (2021) is the lack of information on the plastic types found: Only exemplary particles were measured via FTIR spectroscopy, while the identification plastic - non plastic was determined by visually assessing thermal effects (melting) of plastics on a hot plate according to the method of Zhang et al. (2018). Here a qualitative and quantitative assessment would benefit risk assessment for microplastics input into the environment. The microplastic extraction method development and adaptation to liquid digestate allowed me to do such a qualitative and particle-quantitative analysis of the percolate of biowaste digestion plants. I proved for the first time, that it contained a large amount of microplastic particles <500 µm, of which more than half had a PBAT signal. This indicates that the use of biodegradable plastic bags for organic waste collection may promote the generation of microplastics in the BWT plants, increasing

contamination levels in the end products. The exact effects of the different conventional microplastics and of so-called biodegradable microplastics in soils are not yet fully understood, therefore efforts should be made to reduce microplastic emissions to a minimum. Consequently, it is also necessary to know which equipment and technology in a BWT plant enhance microplastic generation and which ones help to reduce the output of microplastics in the end product. Once microplastics have entered the environment, they are impossible to remove again - at least not without causing severe damage to the environment during the cleanup process. Therefore, even if we cannot yet completely assess the extent of environmental pollution with microplastics, nor give a concise risk assessment concerning the various types of microplastics, I believe we should act after the precautionary principle and reduce the plastic and microplastic input into the environment as far as possible. Where possible, consumer awareness along the lines of “reduce, reuse, recycle” should be raised, but also the industry must be made accountable for their product designs to allow the realization of reuse and recycling, while the respective governmental policies need to be adapted and implemented. This approach should be seen as a holistic effort to reduce the waste of resources as well as reduce the plastic and microplastic emissions.

Based on experiences gained during my PhD studies, I believe there is hope for improvement. Especially after the publication of the study which showed for the first time that composts and digestates from BWT plants are considerably contaminated with microplastics, I saw the potential impact that science can have on political decisions: At the beginning of this PhD thesis (2018), the legal threshold for plastic contamination of composts and digestates used as soil amendments in Germany was 0.1% of the dry weight for particles >2 mm. At approximately 5 million tons of compost and digestate from BWT plants being distributed to fields in Germany each year (estimated from the annual biowaste input into biowaste treatment plants (Statistisches Bundesamt, 2022)), a legal annual output of 500 000 tons of plastic fragments >2 mm via the biowaste treatment plants is conceivable. The additional weight of fragments <2 mm is not considered in this scenario. Ever since, also in part due to the results of studies in this thesis, awareness for the role of biowaste-derived fertilizers as microplastic input pathways has risen. As a response, the size-threshold for the legal weight limit of plastic particles was reduced to >1 mm in October 2019 (Düngemittelverordnung (DüMV), 2012). While organic fertilizers are still likely to contain a high number of microplastics <1 mm, that are not yet considered in this new legal threshold, actions like this are small but consistent steps towards reducing the microplastic input into soils.

While I believe my research has allowed new insights into the fate and degradation/fragmentation behavior of microplastics in the terrestrial environment, there are still method improvements and several knowledge gaps that I would like to fill in my future research: The here developed method for microplastic extraction from soils and digestate is quite time consuming and warrants further development and automatization to allow high-throughput analyses in microplastic monitoring schemes. I am also of the opinion, that more effort and resources should be spent in harmonizing microplastic sampling, extraction, analysis and reporting, as currently the results of different research groups are hardly ever comparable. In the meantime, I will be further investigating the fate of biodegradable plastic bags in BWT plants – from the input to the output. I would like to know if the biodegradable bags fragment and degrade within the digestion- and composting process, or if residual small microplastics remain in the compost/digestate, with to date unknown consequences for soil health and effects on soil dwelling organisms.

7. Bibliography

- Agarwal, S. (2020). Biodegradable Polymers: Present Opportunities and Challenges in Providing a Microplastic-Free Environment. *Macromolecular Chemistry and Physics*, 221(6), 2000017. <https://doi.org/10.1002/macp.202000017>
- Anger, P. M., von der Esch, E., Baumann, T., Elsner, M., Niessner, R., & Ivleva, N. P. (2018). Raman microspectroscopy as a tool for microplastic particle analysis. *TrAC - Trends in Analytical Chemistry*, 109, 214–226. <https://doi.org/10.1016/j.trac.2018.10.010>
- Araujo, C. F., Nolasco, M. M., Ribeiro, A. M. P., & Ribeiro-Claro, P. J. A. (2018). Identification of microplastics using Raman spectroscopy: Latest developments and future prospects. *Water Research*, 142, 426–440. <https://doi.org/10.1016/j.watres.2018.05.060>
- Arthur, C., Baker, J., Bamford, H., & (eds.). (2009). Proceedings of the International Research Workshop on the Occurrence, Effects, and Fate of Microplastic Marine Debris. *September 9–11*.
- Baekeland, L. H. (1909). The synthesis, constitution, and uses of bakelite. *Industrial and Engineering Chemistry*, 1(3), 149–161. <https://doi.org/10.1021/ie50003a004>
- Bläsing, M., & Amelung, W. (2018). Plastics in soil: Analytical methods and possible sources. *Science of the Total Environment*, 612, 422–435. <https://doi.org/10.1016/j.scitotenv.2017.08.086>
- Botterell, Z. L. R., Beaumont, N., Dorrington, T., Steinke, M., Thompson, R. C., & Lindeque, P. K. (2019). Bioavailability and effects of microplastics on marine zooplankton: *Environmental Pollution*, 245, 98–110. <https://doi.org/10.1016/j.envpol.2018.10.065>
- Bruker. (2021). *Guide to Infrared Spectroscopy*. <https://www.bruker.com/en/products-and-solutions/infrared-and-raman/ft-ir-routine-spectrometer/what-is-ft-ir-spectroscopy.html>
- Büks, F., & Kaupenjohann, M. (2020). Global concentrations of microplastics in soils - A review. *Soil*, 6(2), 649–662. <https://doi.org/10.5194/soil-6-649-2020>
- Chalmin, P. (2019). The history of plastics: From the Capitol to the Tarpeian Rock. *Field Actions Science Report, Special Issue 19*, 6–11. <http://journals.openedition.org/factsreports/5071>
- Cooper, D. A., & Corcoran, P. L. (2010). Effects of mechanical and chemical processes on the degradation of plastic beach debris on the island of Kauai, Hawaii. *Marine Pollution Bulletin*, 60(5), 650–654. <https://doi.org/10.1016/j.marpolbul.2009.12.026>

- Corradini, F., Meza, P., Eguiluz, R., Casado, F., Huerta-Lwanga, E., & Geissen, V. (2019). Evidence of microplastic accumulation in agricultural soils from sewage sludge disposal. *Science of the Total Environment*, 671, 411–420. <https://doi.org/10.1016/j.scitotenv.2019.03.368>
- Crossman, J., Hurley, R. R., Futter, M., & Nizzetto, L. (2020). Transfer and transport of microplastics from biosolids to agricultural soils and the wider environment. *Science of the Total Environment*, 724(138334), 1–9. <https://doi.org/10.1016/j.scitotenv.2020.138334>
- Day, R. H., Shaw, D. G., & Ignell, S. E. (1990). the Quantitative Distribution and Characteristics of Neuston Plastic in the North Pacific Ocean, 1985-88. *Proceedings of the Second International Conference on Marine Debris, April 1989*, 247–263. <https://doi.org/10.1017/CBO9781107415324.004>
- De Souza Machado, A. A., Lau, C. W., Kloas, W., Bergmann, J., Bachelier, J. B., Faltin, E., Becker, R., Görlich, A. S., & Rillig, M. C. (2019). Microplastics Can Change Soil Properties and Affect Plant Performance. *Environmental Science and Technology*, 53(10), 6044–6052. <https://doi.org/10.1021/acs.est.9b01339>
- Derraik, J. G. B. (2002). The pollution of the marine environment by plastic debris: A review. *Marine Pollution Bulletin*, 44(9), 842–852. [https://doi.org/10.1016/S0025-326X\(02\)00220-5](https://doi.org/10.1016/S0025-326X(02)00220-5)
- Dümichen, E., Eisentraut, P., Bannick, C. G., Barthel, A. K., Senz, R., & Braun, U. (2017). Fast identification of microplastics in complex environmental samples by a thermal degradation method. *Chemosphere*, 174, 572–584. <https://doi.org/10.1016/j.chemosphere.2017.02.010>
- Düngemittelverordnung (DüMV), 117 (2012). https://www.gesetze-im-internet.de/bundesrecht/d_mv_2012/gesamt.pdf
- Eisentraut, P., Dümichen, E., Ruhl, A. S., Jekel, M., Albrecht, M., Gehde, M., & Braun, U. (2018). Two Birds with One Stone - Fast and Simultaneous Analysis of Microplastics: Microparticles Derived from Thermoplastics and Tire Wear. *Environmental Science and Technology Letters*, 5(10), 608–613. <https://doi.org/10.1021/acs.estlett.8b00446>
- Elert, A. M., Becker, R., Duemichen, E., Eisentraut, P., Falkenhagen, J., Sturm, H., & Braun, U. (2017). Comparison of different methods for MP detection: What can we learn from them, and why asking the right question before measurements matters? *Environmental Pollution*, 231, 1256–1264. <https://doi.org/10.1016/j.envpol.2017.08.074>
- Filiciotto, L., & Rothenberg, G. (2021). Biodegradable Plastics: Standards, Policies, and Impacts. *ChemSusChem*, 14(1), 56–72. <https://doi.org/10.1002/cssc.202002044>
- Fries, E., Dekiff, J. H., Willmeyer, J., Nuelle, M. T., Ebert, M., & Remy, D. (2013). Identification of polymer types and additives in marine microplastic particles using pyrolysis-GC/MS and scanning electron microscopy.

Bibliography

- Environmental Sciences: Processes and Impacts*, 15(10), 1949–1956.
<https://doi.org/10.1039/c3em00214d>
- Fuller, S., & Gautam, A. (2016). A Procedure for Measuring Microplastics using Pressurized Fluid Extraction. *Environmental Science and Technology*, 50(11), 5774–5780. <https://doi.org/10.1021/acs.est.6b00816>
- Gabbott, S., Key, S., Russell, C., Yohan, Y., & Zalasiewicz, J. (2020). The geography and geology of plastics: their environmental distribution and fate. In T. M. Letcher (Ed.), *Plastic Waste and Recycling* (pp. 33–63). <https://doi.org/10.1016/b978-0-12-817880-5.00003-7>
- GESAMP. (2015). Sources, fate and effects of microplastics in the marine environment: A global assessment. In *IMO/FAO/UNESCO-IOC/UNIDO/WMO/IAEA/UN/UNEP/UNDP Joint Group of Experts on the Scientific Aspects of Marine Environmental Protection*.
- Geyer, R. (2020). Production, use, and fate of synthetic polymers. In T. M. Letcher (Ed.), *Plastic Waste and Recycling - Environmental Impact, Societal issues, Prevention, and Solutions* (pp. 23–27). Elsevier. <https://doi.org/10.1016/C2018-0-01939-8>
- Geyer, R., Jambeck, J. R., & Law, K. L. (2017). Production, use, and fate of all plastics ever made. *Science Advances*, 3(7), 1–5. <https://doi.org/10.1126/sciadv.1700782>
- Gillibert, R., Balakrishnan, G., Deshoules, Q., Tardivel, M., Magazzù, A., Donato, M. G., Maragò, O. M., Lamy de La Chapelle, M., Colas, F., Lagarde, F., & Gucciardi, P. G. (2019). Raman Tweezers for Small Microplastics and Nanoplastics Identification in Seawater. *Environmental Science & Technology*, 53(15), 9003–9013. <https://doi.org/10.1021/acs.est.9b03105>
- Gui, J., Sun, Y., Wang, J., Chen, X., Zhang, S., & Wu, D. (2021). Microplastics in composting of rural domestic waste: abundance, characteristics, and release from the surface of macroplastics. *Environmental Pollution*, 274, 116553. <https://doi.org/10.1016/j.envpol.2021.116553>
- Hartmann, N. B., Hüffer, T., Thompson, R. C., Hassellöv, M., Verschoor, A., Dugaard, A. E., Rist, S., Karlsson, T., Brennholt, N., Cole, M., Herrling, M. P., Hess, M. C., Ivleva, N. P., Lusher, A. L., & Wagner, M. (2019). Are We Speaking the Same Language? Recommendations for a Definition and Categorization Framework for Plastic Debris. *Environmental Science and Technology*, 53(3), 1039–1047. <https://doi.org/10.1021/acs.est.8b05297>
- Hermabessiere, L., Hember, C., Boricaud, B., Kazour, M., Amara, R., Cassone, A. L., Laurentie, M., Paul-Pont, I., Soudant, P., Dehaut, A., & Duflos, G. (2018). Optimization, performance, and application of a pyrolysis-GC/MS method for the identification of microplastics. *Analytical and Bioanalytical Chemistry*, 410(25), 6663–6676. <https://doi.org/10.1007/s00216-018-1279-0>
- Hidalgo-Ruz, V., Gutow, L., Thompson, R. C., & Thiel, M. (2012). Microplastics in

- the Marine Environment: A Review of the Methods Used for Identification and Quantification. *Environmental Science and Technology*, 46(6), 3060–3075. <https://doi.org/10.1021/es2031505>
- Huerta Lwanga, E., Mendoza Vega, J., Ku Quej, V., Chi, J. de los A., Sanchez del Cid, L., Chi, C., Escalona Segura, G., Gertsen, H., Salánki, T., van der Ploeg, M., Koelmans, A. A., & Geissen, V. (2017). Field evidence for transfer of plastic debris along a terrestrial food chain. *Scientific Reports*, 7(1), 1–7. <https://doi.org/10.1038/s41598-017-14588-2>
- Hufnagl, B., Steiner, D., Renner, E., Löder, M. G. J., Laforsch, C., & Lohninger, H. (2019). A methodology for the fast identification and monitoring of microplastics in environmental samples using random decision forest classifiers. *Analytical Methods*, 11(17), 2277–2285. <https://doi.org/10.1039/c9ay00252a>
- Hufnagl, B., Stibi, M., Martirosyan, H., Wilczek, U., Möller, J. N., Löder, M. G. J., Laforsch, C., & Lohninger, H. (2022). Computer-Assisted Analysis of Microplastics in Environmental Samples Based on μ FTIR Imaging in Combination with Machine Learning. *Environmental Science & Technology Letters*, 9(1), 90–95. <https://doi.org/10.1021/acs.estlett.1c00851>
- Hurley, R. R., Lusher, A. L., Olsen, M., & Nizzetto, L. (2018). Validation of a Method for Extracting Microplastics from Complex, Organic-Rich, Environmental Matrices [Research-article]. *Environmental Science & Technology*, 52, 7409–7417. <https://doi.org/10.1021/acs.est.8b01517>
- Hurley, R. R., & Nizzetto, L. (2018). Fate and occurrence of micro(nano)plastics in soils: Knowledge gaps and possible risks. *Current Opinion in Environmental Science & Health*, 1, 6–11. <https://doi.org/10.1016/j.coesh.2017.10.006>
- Hurley, R. R., Woodward, J. C., & Rothwell, J. J. (2017). Ingestion of Microplastics by Freshwater Tubifex Worms. *Environmental Science and Technology*, 51(21), 12844–12851. <https://doi.org/10.1021/acs.est.7b03567>
- Hurley, R., Woodward, J., & Rothwell, J. J. (2018). Microplastic contamination of river beds significantly reduced by catchment-wide flooding. *Nature Geoscience*, 11(4), 251–257. <https://doi.org/10.1038/s41561-018-0080-1>
- ICES. (2015). *OSPAR request on development of a common monitoring protocol for plastic particles in fish stomachs and selected shellfish on the basis of existing fish disease surveys*. ICES Advice 2015, Book 1. [https://www.ices.dk/sites/pub/Publication Reports/Advice/2015/Special_Requests/OSPAR_PLAST_advice.pdf](https://www.ices.dk/sites/pub/Publication%20Reports/Advice/2015/Special_Requests/OSPAR_PLAST_advice.pdf)
- Käppler, A., Fischer, D., Oberbeckmann, S., Schernewski, G., Labrenz, M., Eichhorn, K. J., & Voit, B. (2016). Analysis of environmental microplastics by vibrational microspectroscopy: FTIR, Raman or both? *Analytical and Bioanalytical Chemistry*, 408(29), 8377–8391. <https://doi.org/10.1007/s00216->

Bibliography

016-9956-3

- Käppler, A., Fischer, M., Scholz-Böttcher, B. M., Oberbeckmann, S., Labrenz, M., Fischer, D., Eichhorn, K. J., & Voit, B. (2018). Comparison of μ -ATR-FTIR spectroscopy and py-GCMS as identification tools for microplastic particles and fibers isolated from river sediments. *Analytical and Bioanalytical Chemistry*, 410(21), 5313–5327. <https://doi.org/10.1007/s00216-018-1185-5>
- Käppler, A., Windrich, F., Löder, M. G. J., Malanin, M., Fischer, D., Labrenz, M., Eichhorn, K., & Voit, B. (2015). Identification of microplastics by FTIR and Raman microscopy: a novel silicon filter substrate opens the important spectral range below 1300 cm^{-1} for FTIR transmission measurements. *Analytical and Bioanalytical Chemistry*, 407(22), 6791–6801. <https://doi.org/10.1007/s00216-015-8850-8>
- Katsumi, N., Kusube, T., Nagao, S., & Okochi, H. (2020). The role of coated fertilizer used in paddy fields as a source of microplastics in the marine environment. *Marine Pollution Bulletin*, 161, 111727. <https://doi.org/https://doi.org/10.1016/j.marpolbul.2020.111727>
- Kernchen, S., Löder, M. G. J., Fischer, F., Fischer, D., Moses, S. R., Georgi, C., Nölscher, A. C., Held, A., & Laforsch, C. (2021). Airborne microplastic concentrations and deposition across the Weser River catchment. *Science of The Total Environment*, 151812. <https://doi.org/https://doi.org/10.1016/j.scitotenv.2021.151812>
- Laforsch, C., Ramsperger, A. F. R. M., Mondellini, S., & Galloway, T. S. (2021). Microplastics: A Novel Suite of Environmental Contaminants but Present for Decades. In *Regulatory Toxicology* (Issue November, pp. 1–26). https://doi.org/10.1007/978-3-642-36206-4_138-1
- Liu, M., Lu, S., Song, Y., Lei, L., Hu, J., Lv, W., Zhou, W., Cao, C., Shi, H., Yang, X., & He, D. (2018). Microplastic and mesoplastic pollution in farmland soils in suburbs of Shanghai, China. *Environmental Pollution*, 242(July), 855–862. <https://doi.org/10.1016/j.envpol.2018.07.051>
- Löder, M. G. J., & Gerdt, G. (2015). Methodology Used for the Detection and Identification of Microplastics - A Critical Appraisal. In M. Bergmann, L. Gutow, & M. Klages (Eds.), *Marine Anthropogenic Litter* (pp. 201–227). <https://doi.org/10.1007/978-3-319-16510-3>
- Löder, M. G. J., Imhof, H. K., Ladehoff, M., Löscher, L. A., Lorenz, C., Mintenig, S., Piehl, S., Primpke, S., Schrank, I., Laforsch, C., & Gerdt, G. (2017). Enzymatic Purification of Microplastics in Environmental Samples. *Environmental Science and Technology*, 51(24), 14283–14292. <https://doi.org/10.1021/acs.est.7b03055>
- Löder, M. G. J., Kuczera, M., Mintenig, S., Lorenz, C., & Gerdt, G. (2015). Focal plane array detector-based micro- Fourier-transform infrared imaging for the analysis of microplastics in environmental samples. *Environmental*

- Chemistry*, 12(5), 563–581. <https://doi.org/http://dx.doi.org/10.1071/EN14205>
- Möller, J. N., Heisel, I., Satzger, A., Vizsolyi, E. C., Oster, S. D. J., Agarwal, S., Laforsch, C., & Löder, M. G. J. (2021). Tackling the Challenge of Extracting Microplastics from Soils: A Protocol to Purify Soil Samples for Spectroscopic Analysis. *Environmental Toxicology and Chemistry*, 00, 1–14. <https://doi.org/10.1002/etc.5024>
- Müller, Y. K., Wernicke, T., Pittroff, M., Witzig, C. S., Storck, F. R., Klinger, J., & Zumbülte, N. (2020). Microplastic analysis—are we measuring the same? Results on the first global comparative study for microplastic analysis in a water sample. *Analytical and Bioanalytical Chemistry*, 412(3), 555–560. <https://doi.org/10.1007/s00216-019-02311-1>
- Naidoo, T., Goordiyal, K., & Glassom, D. (2017). Are Nitric Acid (HNO₃) Digestions Efficient in Isolating Microplastics from Juvenile Fish? *Water, Air, and Soil Pollution*, 228(12). <https://doi.org/10.1007/s11270-017-3654-4>
- Napper, I. E., & Thompson, R. C. (2019). Environmental Deterioration of Biodegradable, Oxo-biodegradable, Compostable, and Conventional Plastic Carrier Bags in the Sea, Soil, and Open-Air Over a 3-Year Period. *Environmental Science & Technology*, 53(9), 4775–4783. <https://doi.org/10.1021/acs.est.8bo6984>
- Nizzetto, L., Futter, M., & Langaas, S. (2016). Are Agricultural Soils Dumps for Microplastics of Urban Origin? *Environmental Science and Technology*, 50(20), 10777–10779. <https://doi.org/10.1021/acs.est.6bo4140>
- Nuelle, M. T., Dekiff, J. H., Remy, D., & Fries, E. (2014). A new analytical approach for monitoring microplastics in marine sediments. *Environmental Pollution*, 184, 161–169. <https://doi.org/10.1016/j.envpol.2013.07.027>
- Plastics Europe. (2020). Plastics – the Facts 2020. *PlasticsEurope*, 16. <https://www.plasticseurope.org/en/resources/market-data>
- PlasticsEurope. (2021). *What Are Plastics?* <https://www.plasticseurope.org/en/about-plastics/what-are-plastics>
- Primpke, S., Lorenz, C., Rascher-Friesenhausen, R., & Gerdts, G. (2017). An automated approach for microplastics analysis using focal plane array (FPA) FTIR microscopy and image analysis. *Analytical Methods*, 9(9), 1499–1511. <https://doi.org/10.1039/c6ay02476a>
- Roch, S., & Brinker, A. (2017). Rapid and Efficient Method for the Detection of Microplastic in the Gastrointestinal Tract of Fishes. *Environmental Science & Technology*, 51, 4522–4530. <https://doi.org/10.1021/acs.est.7b00364>
- Rocha-Santos, T., & Duarte, A. C. (2015). A critical overview of the analytical approaches to the occurrence, the fate and the behavior of microplastics in the environment. *TrAC - Trends in Analytical Chemistry*, 65, 47–53. <https://doi.org/10.1016/j.trac.2014.10.011>

Bibliography

- Scheurer, M., & Bigalke, M. (2018). Microplastics in Swiss Floodplain Soils. *Environmental Science and Technology*, 52(6), 3591–3598. <https://doi.org/10.1021/acs.est.7bo6003>
- Schöpfer, L., Menzel, R., Schnepf, U., Ruess, L., Marhan, S., Brümmer, F., Pagel, H., & Kandeler, E. (2020). Microplastics Effects on Reproduction and Body Length of the Soil-Dwelling Nematode *Caenorhabditis elegans*. *Frontiers in Environmental Science*, 8(April), 1–9. <https://doi.org/10.3389/fenvs.2020.00041>
- Schrank, I., Möller, J. N., Imhof, H. K., Hauenstein, O., Zielke, F., Agarwal, S., Löder, M. G. J., Greiner, A., & Laforsch, C. (2022). Microplastic sample purification methods - Assessing detrimental effects of purification procedures on specific plastic types. *Science of The Total Environment*, 833(November 2021). <https://doi.org/10.1016/j.scitotenv.2022.154824>
- Shaw, D. G., & Day, R. H. (1994). Colour- and form-dependent loss of plastic micro-debris from the North Pacific Ocean. *Marine Pollution Bulletin*, 28(1), 39–43. [https://doi.org/10.1016/0025-326X\(94\)90184-8](https://doi.org/10.1016/0025-326X(94)90184-8)
- Sintim, H. Y., Bary, A. I., Hayes, D. G., Wadsworth, L. C., Anunciado, M. B., English, M. E., Bandopadhyay, S., Schaeffer, S. M., DeBruyn, J. M., Miles, C. A., Reganold, J. P., & Flury, M. (2020). In situ degradation of biodegradable plastic mulch films in compost and agricultural soils. *Science of The Total Environment*, 727, 138668. <https://doi.org/10.1016/J.SCITOTENV.2020.138668>
- Sobhani, Z., Lei, Y., Tang, Y., Wu, L., Zhang, X., & Naidu, R. (2020). Microplastics generated when opening plastic packaging. *Scientific Reports*, 10(4841), 1–7. <https://doi.org/10.1038/s41598-020-61146-4>
- Statistisches Bundesamt. (2022). *Abfallwirtschaft*. Menge Des in Behandlungsanlagen Eingesetzten Biomülls in Deutschland in Den Jahren 2009 Bis 2019. <https://de.statista.com/statistik/daten/studie/257365/umfrage/biomuelleinsatz-in-behandlungsanlagen-in-deutschland/>
- Sun, Y., Duan, C., Cao, N., Li, X., Li, X., Chen, Y., Huang, Y., & Wang, J. (2022). Effects of microplastics on soil microbiome: The impacts of polymer type, shape, and concentration. *Science of The Total Environment*, 806, 150516. <https://doi.org/10.1016/J.SCITOTENV.2021.150516>
- Tagg, A. S., Sapp, M., Harrison, J. P., & Ojeda, J. J. (2015). Identification and Quantification of Microplastics in Wastewater Using Focal Plane Array-Based Reflectance Micro-FT-IR Imaging. *Analytical Chemistry*, 87(12), 6032–6040. <https://doi.org/10.1021/acs.analchem.5b00495>
- Thompson, R. C., Olsen, Y., Mitchell, R. P., Davis, A., Rowland, S. J., John, A. W. G., Mcgonigle, D., & Russell, A. E. (2004). Lost at sea: where is all the plastic? *Science*, 304, 838. <https://doi.org/doi:10.1126/science.1094559>

- Van den Berg, P., Huerta-Lwanga, E., Corradini, F., & Geissen, V. (2020). Sewage sludge application as a vehicle for microplastics in eastern Spanish agricultural soils. *Environmental Pollution*, 261, 114198. <https://doi.org/10.1016/j.envpol.2020.114198>
- van Schothorst, B., Beriot, N., Huerta Lwanga, E., & Geissen, V. (2021). Sources of light density microplastic related to two agricultural practices: The use of compost and plastic mulch. *Environments - MDPI*, 8(4), 1–12. <https://doi.org/10.3390/ENVIRONMENTS8040036>
- Wagner, S., Hüffer, T., Klöckner, P., Wehrhahn, M., Hofmann, T., & Reemtsma, T. (2018). Tire wear particles in the aquatic environment - A review on generation, analysis, occurrence, fate and effects. *Water Research*, 139, 83–100. <https://doi.org/10.1016/j.watres.2018.03.051>
- Waldschläger, K., Lechthaler, S., Stauch, G., & Schüttrumpf, H. (2020). The way of microplastic through the environment – Application of the source-pathway-receptor model (review). *Science of the Total Environment*, 713, 136584. <https://doi.org/10.1016/j.scitotenv.2020.136584>
- Wang, C., Zhao, J., & Xing, B. (2021). Environmental source, fate, and toxicity of microplastics. *Journal of Hazardous Materials*, 407, 124357. <https://doi.org/https://doi.org/10.1016/j.jhazmat.2020.124357>
- Wollny, B. (2022). *Statista*. Entwicklung Der Einwohnerzahl in Köln (Kreisfreie Stadt) von 1995 Bis 2020. <https://de.statista.com/statistik/daten/studie/322477/umfrage/entwicklung-der-gesamtbevoelkerung-in-koeln/#professional>
- Woodward, J., Li, J., Rothwell, J., & Hurley, R. (2021). Acute riverine microplastic contamination due to avoidable releases of untreated wastewater. *Nature Sustainability*, 4(9), 793–802. <https://doi.org/10.1038/s41893-021-00718-2>
- Zhang, G. S., & Liu, Y. F. (2018). The distribution of microplastics in soil aggregate fractions in southwestern China. *Science of the Total Environment*, 642, 12–20. <https://doi.org/10.1016/j.scitotenv.2018.06.004>
- Zhang, S., Yang, X., Gertsen, H., Peters, P., Salánki, T., & Geissen, V. (2018). A simple method for the extraction and identification of light density microplastics from soil. *Science of The Total Environment*, 616–617, 1056–1065. <https://doi.org/10.1016/j.scitotenv.2017.10.213>

* Illustrations with asterisk were created in BioRender.com (May 2022)

8. Articles

Article 1 - Finding Microplastics in Soils - A Review of Analytical Methods	48
Article 2 - Microplastic sample purification methods - assessing detrimental effects of purification procedures on specific plastic types	68
Article 3 - Tackling the challenge of extracting microplastics from soils: A protocol to purify soil samples for spectroscopic analysis	106
Article 4 - Microplastics persist in an arable soil but do not affect soil microbial biomass, enzyme activities, and crop yield	128
Article 5 - Flooding frequency and floodplain topography determine abundance of microplastics in an alluvial Rhine soil	156
Article 6 - Organic fertilizer as a vehicle for the entry of microplastic into the environment	178
Article 7 - Microplastic contamination of composts and liquid fertilizers from municipal biowaste treatment plants — effects of the operating conditions	188
Article 8 - Municipal biowaste treatment plants contribute to the contamination of the environment with residues of biodegradable plastics with putative higher persistence potential	208

Article 1

Finding Microplastics in Soils - A Review of Analytical Methods

Finding Microplastics in Soils: A Review of Analytical Methods

Julia N. Möller, Martin G. J. Löder, and Christian Laforsch*



Cite This: *Environ. Sci. Technol.* 2020, 54, 2078–2090



Read Online

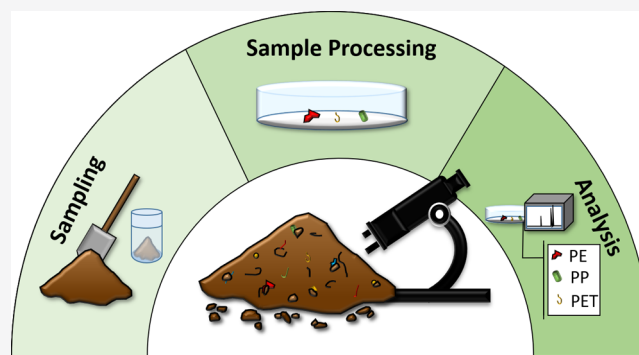
ACCESS |

Metrics & More

Article Recommendations

Supporting Information

ABSTRACT: Research on microplastics in soils is still uncommon, and the existing publications are often incomparable due to the use of different sampling, processing, and analytical methods. Given the complex nature of soils, a suitable and efficient method for standardized microplastic analysis in the soil matrix has yet to be found. This paper proposes a critical review on the different published methods for sampling, extraction, purification, and identification/quantification of microplastics in complex environmental matrices, with the main focus on their applicability for soil samples. While large microplastic particles can be manually sorted out and verified with chemical analysis, sample preparation for smaller microplastic analysis is usually more difficult. Of the analytical approaches proposed in the literature, some are established, whereas others are a proof of principle and have not yet been applied to environmental samples. For the sake of development, all approaches are discussed and assessed for their potential applicability for soil samples. So far, none of the published methods seems ideally suitable for the analysis of smaller microplastics in soil samples, but slight modifications and combinations of methods may prove promising and need to be explored.



1. INTRODUCTION

Microplastics have been defined as “plastic particles smaller than 5 mm”,¹ and while this upper size limit is widely accepted, the lower size limit is still under scientific debate. Some groups, such as the Joint Group of Experts on the Scientific Aspects of Marine Environmental Protection (GESAMP) include “particles in the nano-size range”.² Frias and Nash,³ proposed the following definition: “Microplastics are any synthetic solid particle or polymeric matrix, with regular or irregular shape and with size ranging from 1 μm to 5 mm, of either primary or secondary manufacturing origin, which are insoluble in water”. This is the definition that is also followed by the authors of this critical review. We also distinguish between “large” microplastics (>500 μm –5 mm) and “small” microplastics (1 μm –500 μm), as some analytical methods perform better when searching for larger microplastic particles.

Research on microplastics has shown that synthetic polymer particles can be found in all environmental compartments worldwide, ranging from the arctic sea ice,⁴ to the waters of remote mountain lakes,⁵ to agricultural soils.⁶ Initially, microplastic research mainly focused on the marine environment, where numerous studies analyzed the occurrence and abundance of microplastic particles in the ocean and along beaches, while many other studies showed the negative effects of microplastics on marine organisms.⁷ Later, researchers began to examine river and lake systems, which are also strongly affected by microplastic pollution and are considered to be significant microplastic transportation pathways.⁸

However, considering that the majority of plastic waste is generated and emitted on land, it is rather surprising that microplastic research has only recently expanded to terrestrial ecosystems, where soils may be a significant long-term sink for microplastic particles.^{9,10} Especially urban and agricultural soils are assumed to be prone to microplastic contamination, as they are most exposed to human activities and therefore microplastic input pathways.¹¹ Potential pathways are littering and street runoff,¹² often containing tire wear,¹³ atmospheric deposition,¹⁴ irrigation with wastewater, as well as applying soil amendments such as compost derived from biowaste¹⁵ or sewage sludge.¹⁶ Plastic mulching is also a potentially significant source of microplastic contamination in agricultural soils, where a long-term accumulation of the plastic fragments may have severe effects on the soil quality.^{17,18}

It has been stated, that microplastics are likely to be transported through the soil vertically, for example, due to biopores, cracking or plowing, and horizontally, due to soil biota or agricultural activities such as harvesting and plowing.¹⁹ De Souza Machado et al.²⁰ suspect that microplastic pollution may be a major stressor on the terrestrial environment, causing physicochemical changes to the soil ecosystem by impacting

Received: July 31, 2019

Revised: January 25, 2020

Accepted: January 30, 2020

Published: January 30, 2020

the soil structure and chemical composition (e.g., by leaching hazardous additives). Shifts in the microbial activity within the soil due to the presence of microplastic could also be observed.^{20,21} Further, introduced plastic particles can be transferred along the terrestrial food chain.^{22–24} Although model studies give a first estimation of the macro- and microplastic input into terrestrial and aquatic environments, estimating the terrestrial input to be significantly higher than the aquatic input,¹⁰ the actual extent of terrestrial and microplastic pollution is still unknown.^{25,26} This is mainly attributed to the lack of customized analytical tools to detect microplastics in soils. Due to the complexity of the soil matrix, containing variable proportions of mineral and organic matter in various grain sizes, and the added difficulty of tracing a solid analyte in a sample composed of solids, a comprehensive method for the effective microplastic analysis in soils is yet to be developed.^{27,28}

The following review aims to give a critical overview over the methods developed and used in scientific literature for sampling, extraction, purification, and detection of microplastics in complex environmental samples with a special focus on their applicability for the analysis of soil samples. While other recent reviews on the topic have already given an overview over the most commonly used analytical methods and their challenges,^{28,29} this review is more extensive. It includes novel innovations to analyze microplastics in other environmental compartments, that may inspire readers to think “out-of-the-box” to find new solutions to the challenging problem of finding solid analytes in a complex solid matrix. Furthermore, the often-neglected aspects of representative sampling of a nonhomogeneously distributed particulate contaminant and quality assurance during sample processing and analysis are also discussed in depth.

2. SAMPLING

Arguably, representative sampling is one of the most important steps during environmental analysis: Nonrepresentative sampling will lead to unreliable data, independent of the reliability the subsequent sample processing and analysis.³⁰ Naturally, each sampling design must be adapted to the respective research question. Especially when dealing with such an inhomogeneous matrix as soil, in combination with solid analytes such as microplastics, the sampling design must be very well planned in order to achieve reliable results.³¹ This means the research objective, the sampling area, as well as the sampling depths must be accurately defined beforehand. The history of utilization (e.g. agricultural farmland where plastic mulching has been applied) and possible discharge from point sources (e.g., bins, picnic sites, etc.) or diffuse sources such as nearby roads should be taken into account. Furthermore, potential accumulation zones such as hollows, where microplastics from surface runoff may be deposited or ridges and hedges where wind velocities are decelerated and deposition of windborne particulate matter increases, should be identified. Depending on the research objective, several different sampling approaches may be used. An overview of possible sampling approaches is given in Table 1.

After selecting a suitable sampling approach according to the respective research objective, the number of sampling points at each site must also be addressed.

Samples can be taken as single point samples, or composite samples (several discrete point samples of the same size within a spatial unit are combined and homogenized to a single

one).³³ As microplastic particles are particulate and vary strongly in their size, it is likely that the microplastic distribution within the soil varies significantly as well. To overcome this heterogeneity, using composite samples taken from defined subunits within a sampling site may prove beneficial to get a more representative image of the extent of microplastic contamination, without having to transport, store, and analyze too many samples. Zhang and Liu¹⁸ applied this method by defining five plots at each sampling site, taking six point samples randomly from each plot and combining these to a single composite sample. Scheurer and Bigalke³⁴ assumed a similar approach, compositing five samples taken along parallel transects with differing distances to the river.

The number of sampling points at each site (single point samples or composite samples) could be determined by a statistical power analysis. However, the ideal number of replicates and the sample volume is strongly restricted by sample processing and subsequent analysis methods, which are still the bottleneck of microplastic quantification in all environmental compartments.³⁵ Hence, at this point in time, no recommendation regarding the minimum amount of sampling points per spatial unit can be given.

As soils are a three-dimensional medium, the sampling depth is of utmost importance and should always be defined and documented. If, for instance, the deposition of microplastics on the surface of an undisturbed soil is in the focus of the study, bulk sampling of the predefined first few centimeters may be sufficient. If the vertical distribution of microplastics after plowing should be taken into account the sampling depth must be adapted accordingly. On the other hand, if the contamination at varying depths of the soil is to be determined, core sampling is required. To date, mainly the soil surface within the upper 10 cm has been analyzed,^{6,18,34,36,37} as this is the range where the bulk of microplastic particles is most probable to be. However, the downward transportation mechanisms of microplastic particles of various sizes in undisturbed soils have not yet been analyzed.³⁸ This should be done before defining a standard depth for soil surface analysis.

The resulting sample amount (mass/volume) for each sampling point should also be defined and documented. It should exceed the amount required for the microplastic quantification, allowing for additional aliquots of the sample to be used (after homogenization) for the determination of water content, as backup samples, and samples for recovery analysis (as a control for the suitability of the method for this specific soil).³⁰ Due to the heterogeneous nature of microplastic distribution, larger samples taken in the field are more representative than small amounts and can be reduced to a smaller laboratory sample by homogenization and splitting.³⁹ In the literature, sampling amounts were chosen arbitrarily, ranging from 50 g²² to 4 kg.³⁶ So far, too little is known for us to recommend the minimum amount for representative soil samples, but it should at least exceed the mass or volume of the reference unit to avoid unjustifiable extrapolation. A sensible reference unit would be items per kg(dw), (mean dry weight determined from aliquots of the sample using a standard procedure, e.g., ISO 11465⁴⁰). In this case, the samples taken from the field should exceed 1 kg significantly, taking into account their water content and additional aliquots that may be needed as mentioned above.

The sampling tools can vary, depending on the objective, a stainless-steel spoon, scoop, or shovel can be used for surface

samples, whereas a core sampler may be used if an analysis of deeper horizons is the objective. All samples should be transferred into clean and labeled metal or glass containers with (plastic free) lids for transportation and storage. Generally, measures should be taken to avoid the contamination of samples with microplastics from tools, clothing, or the ambient air of laboratories and storage facilities. Further information on this topic is given in section 5. For more information on which sampling methods were used by previous research groups, please refer to the Supporting Information (SI Table S1).

3. EXTRACTION

For an analysis of microplastic particles, it is usually necessary to remove the bulk of the sample matrix, preferably isolating the microplastic particles from the matrix and removing adhering substances. For inhomogeneous solid samples such as soils, microplastic isolation is challenging—and becomes even more so with decreasing grain size of the soil matrix—and particle sizes of the microplastic particles.⁴¹ Soil particles can form relatively stable aggregates, which may enclose microplastic particles and obscure them from analysis.^{18,42} Thus, finding a method for soil aggregate dispersion without risking the destruction or artificial fragmentation of microplastic particles is an important first step for the microplastic analysis of soils.

3.1. Manual Extraction. The simplest method for microplastic isolation is sieving and manual sorting, using a stereo microscope to exclude obviously mineral or biogenic matter, for example, particles with visible cell structures.⁴³ This method can be combined with the “hot needle test” to further confine the number of putative microplastic particles. However, manual sorting and visual identification is extremely time and labor intensive, restricted to sizes $>500\ \mu\text{m}$ and is highly prone to misidentification and bias, rendering a subsequent reliable polymer identification indispensable.^{44–47}

3.2. Electrostatic Separation. A rather novel methodology is the electrostatic separation of microplastic particles from solid matter. While experiments conducted by Hidalgo-Ruz et al.⁴⁶ in this direction failed, Felsing et al.⁴⁸ managed to modify a smaller fair demonstration device of an electrostatic separation unit commonly used in the recycling industry to isolate microplastics from sand and sediment samples. The method allows a relatively high sample throughput with a mass reduction of up to 99% and recovery rates of 90–100% for pristine microplastic particles ranging from $63\ \mu\text{m}$ to $5\ \text{mm}$. However, to achieve these high recovery rates, the samples underwent the procedure three times, with a temporal effort of 3–4 h per 150 g sample. Furthermore the authors claim that the method is independent of organic matter content, particle density, shape, age, or biofouling.⁴⁸ However, the method is not suitable for moist samples,⁴⁸ and its suitability for cohesive soil samples is questionable due to the unavoidable formation of aggregates. Furthermore, the applicability for very small particles must be verified, as the adhesive forces to the metal drum and scraper may be higher than the gravity-force, possibly leading to significant losses of the small microplastic fraction in the final sample.

3.3. Consecutive Matrix Removal, Removal of the Mineral Fraction. **3.3.1. Oil Extraction.** Crichton et al.⁴⁹ developed the oil extraction protocol, a simple approach for the extraction of microplastic from solid samples, taking advantage of the lipophilic surface properties of most plastics.

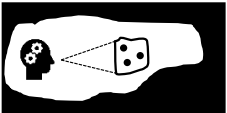
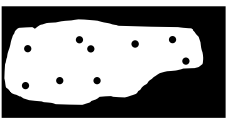
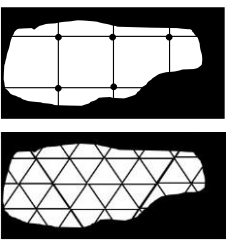
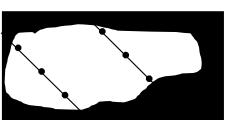
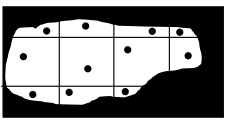
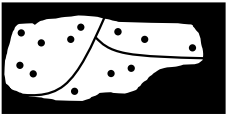
Dried sediment samples are mixed with water and canola oil, then agitated thoroughly and left to settle until the oil, water, and mineral fractions are completely separated, any microplastic particles coming into contact with the oil should thus be conveyed into the oil layer, which can easily be transferred onto a filter. According to Crichton et al.⁴⁹ recovery rates range from 90–100% for all seven tested pristine polymer types, showing better recovery results than two compared density separation methods with NaI and CaCl_2 . The procedure is simple, safe, cheap, and time efficient, but may require an additional step to remove organic substances from a sample.⁴⁹

A recent study conducted by Mani et al.⁵⁰ tested the oil extraction method using castor oil to separate microplastics ($0.3\text{--}1\ \text{mm}$) from four complex environmental matrices: Fluvial and marine suspended surface solids as well as marine beach sediments and agricultural soil. The method showed high recovery rates for the four pristine polymers (polypropylene PP, polystyrene PS, poly(methyl methacrylate) PMMA, and glycol modified polyethylene terephthalate PET-G) used in the spiking experiment, with an average recovery rate of $99\% \pm 4\%$ (mean \pm SD) and a mean matrix reduction of $95\% \pm 4\%$ (dry weight). For validation, nonspiked Rhine river suspended solids underwent the castor oil extraction protocol. Of 978 microplastic particles found in total in the five examined samples, 773 microplastic particles were recovered in the upper oil phase, whereas 205 microplastic particles were recovered from the lower aqueous and solid phase, resulting in a recovery rate of $74\% \pm 13\%$. For organic-rich sample matrices, an additional H_2O_2 digestion step was required to achieve an adequate sample purification.⁵⁰

3.3.2. Density Separation. For the separation of microplastics from sediment, density separation protocols are the most commonly applied using high density salt solutions as extraction media.⁵¹ In an early study by Thompson et al.⁵² a method was devised using a saturated NaCl solution to separate microplastic from sand. After stirring and sedimentation the plastic-containing supernatant is sucked into an extra flask from where it is transferred onto a filtering system.^{41,52} Losses may occur in the tubing or while decanting, which is why more sophisticated devices have been built since. Furthermore, saturated NaCl solution can only achieve a maximum density of $1.2\ \text{g cm}^{-3}$, and several synthetic polymers, such as polyethylene terephthalate (PET) and polyvinylchloride (PVC) have higher densities and are not extracted by saturated NaCl solutions. Thus, alternative salt solutions such as NaI ($\rho = 1.8\ \text{g cm}^{-3}$),^{41,53} $\text{Na}_6[\text{H}_2\text{W}_{12}\text{O}_6]$ ($\rho = 1.4\ \text{g cm}^{-3}$)⁵⁴ Zn_2Cl ($\rho = 1.6\text{--}1.7\ \text{g cm}^{-3}$),^{55,56} and NaBr ($\rho = 1.55\ \text{g cm}^{-3}$)³⁷ were recommended,⁵⁷ although costs and hazardousness of these solutions may impose a need for alternatives.

Imhof et al.⁵⁵ developed the Munich Plastic Sediment Separator (MPSS), to separate a diverse range of microplastics from a maximum of 6 L of sediments using a ZnCl_2 -solution. A removable sample chamber equipped with a filter holder allows for a direct transfer of the microplastic particles onto a filter, separating the sample from the density solution. As no decantation or repetitive extraction steps are required, losses and contamination can be avoided. According to Imhof et al.,⁵⁵ recovery rates of 95–100% can be achieved. However, Zobkov and Esiukova⁵⁸ evaluated the MPSS and found the recovery rates of pristine plastics to be similarly high as stated by Imhof et al., but the recovery of aged plastics was significantly lower at only 13–39%. Moreover, ZnCl_2 is hazardous and corrosive,

Table 1. Overview over Possible Sampling Approaches Dependent on the Research Objective^{30,32,33}

Sampling Approach		Objective	Description
Judgmental sampling		Verify a suspected contamination.	Judgmental sampling is a subjective choice of sampling points, based on expert information (e.g. historical utilisation, visual inspection etc.) This method is simple to implement, but biased and may only be suitable for studies focusing on specific sampling zones such as hollows.
Simple random sampling		Identify the contamination of a supposedly homogeneously contaminated site.	Random sampling is the random distribution of sampling points under the premise that each point has an equal chance of being selected and is selected independently of the positions of the other sampling points. It allows unbiased statistical analysis. Attention: Microplastics are often not distributed homogeneously.
Systematic grid sampling		Identify the contamination extent, delineate hot-spots or spatial concentration gradients.	Systematic grid sampling is the distribution of sampling points along the nodes of a regular pattern (e.g. squares or triangles). The initial point is selected at random and from here the coordinate axis is defined. Then the remaining sampling points are spaced in regular intervals from this initial point. This method provides an even coverage of the site and is simple to implement.
Transect sampling		Identify the contamination extent along linear features (e.g. roads, drainage ditches), define concentration gradients, identify the extent of contamination in an area.	Transect sampling is a one-dimensional systematic sampling method. Sampling points are collected in regular intervals along one or more straight lines. The transect lines can be, but do not have to be, parallel to each other. Defining and implementing transects in the field is easier than using a grid.
Unaligned grid sampling		Identify the contamination extent in a sampling area	Unaligned grid sampling combines the benefits of random sampling and systematic grid sampling. The grid is defined as above, but the sampling points are located randomly within the grid compartments. This allows for a good coverage while maintaining randomness.
Stratified sampling		Identify the contamination extent in defined sub-areas within the total sampling area	Stratified random sampling is the division of the initial sampling area into smaller compartments (strata). This is helpful if the strata differ from each other significantly, and it is assumed, that the contamination within each stratum is distributed more homogeneously than in the sampling site as a whole.

has a low pH value, and may react with natural components of sediment, especially carbonates, resulting in bubbling and a foam that significantly hampers the procedure.⁵⁸ It is also questionable if soil aggregates will be adequately dispersed in the MPSS, or if a previous dispersion is required, especially for cohesive soils. Furthermore, the large surface area which may corrode due to the nature of the $ZnCl_2$ may be problematic if

small particles get caught on the rough surface and cannot rise upward, possibly causing significant losses. Coppock et al.⁵⁹ saw the need for a cheaper and portable microplastic-sediment separator and devised the Sediment-Microplastic-Isolation unit consisting of PVC tubes, a PVC ball valve, and zinc chloride agitated by a magnetic stir bar. The principle mirrors that of the MPSS and shows similarly high recovery rates of 92–98%.

However, PVC must be excluded from the analysis as abrasion from the PVC tubing may contaminate the samples. This may compromise the value of the analytic results, as PVC is a relevant contaminant in environmental samples such as sediments and possibly soils, and excluding it from the analysis poses a significant loss of information. Also inspired by the MPSS is the so-called Bauta-separator developed by the Norwegian Technical Institute. Instead of a metal cone, a glass cylinder constricted at the top and fitted with a ball valve and separation chamber is used. The separation medium is a mixed solution of ZnCl_2 and CaCl_2 , and the stated recovery rate was between 82% for fibers and 100% for pellets.⁶⁰ The applicability of these methods for terrestrial soils has not yet been tested but may face similar constrictions as mentioned for the MPSS, especially concerning the dispersion of soil aggregates.

Claessens et al.⁵³ developed an elutriation step with water after the principle of Barnett's fluidized sand bath⁶¹ to reduce the sample bulk before density separation. The sediment sample is aerated and fluidized while an upward stream of water transports small and light particles toward the top, where they overflow and are retained on a 35 μm filter. Subsequently the reduced sample undergoes a density separation with a NaI solution. The extraction efficiency is stated to be higher than 98%.⁵³ However, for the fluidization method, loose sand is necessary, thus this protocol may be unsuitable for most soil samples.

Recently, Liu et al.³⁷ developed a device specifically designed for the extraction of microplastics from soil samples, using an acrylic glass cylinder constructed with an aeration disc at the bottom and two rows of holes (diameter 5 mm) at the top. A circumjacent tray with an inclination collects the floating particles and transports them toward a tube leading to a vacuum filtration system. Here, the particulate matter is retained and the liquid is recycled via a circulation pump back to the separator cylinder, in order to retain the constant overflow. The soil samples (50–200 g) are mixed with the separation medium and stirred manually for 5 min and then left to subsequently settle for 2 h. After settling, the aeration disc is turned on and separation medium continuously added until the system overflows into the tray leading to the collection filter. A NaBr solution (1.55 g cm^{-3}) was determined as the most suitable separation medium, due to its relatively high density and low viscosity. Recovery rates of over 90% were reported for 10 types of microplastics (PA, PC, PP, ABS, PE, PS, PMMA, POM, PET, and PVC). PE particles of different size ranges (100–500 μm , 500–1000 μm , 100–3000 μm) and shapes (particle, fiber, film) were tested with the device. The recovery rates only differed marginally for the different sizes, whereas the shape of "particles", that is, fragments, showed the highest recovery rate (98.3%), opposed to films, with the lowest recovery rate (85%).

This method appears promising for soil sample analysis for microplastic particles $>100 \mu\text{m}$, and although particles down to 32 μm were found in soil samples, the recovery rate (i.e., reliability) of the device for smaller particles (e.g., 1–100 μm) must first be systematically determined. One severe drawback of the described system is that the separation cylinder is made of Plexiglas (i.e., PMMA). Abrasion caused by the stirring of coarse soils may lead to overestimation of the PMMA contamination in the samples, thus, a nonplastic material should be used, or PMMA excluded from the analysis.

Reviewing the above-named publications, no upper or lower size limit for the extraction of microplastic particles using density separation has been established. In general, the recovery rates of the particles were established for size ranges between 40 μm ⁵⁵ and 5 mm.^{37,55} The applicability for smaller microplastics and nanoplastics have not yet been analyzed. However, according to the Stokes equation, small particles have very low settling velocities, that are further reduced by high drag coefficients which are dependent on the particle shape, thus, an in-depth empirical study of the minimum size of various microplastic particles in common density separation fluids is called for.

3.3.3. Froth Flotation. Another method, which is not only dependent on the density of the matter, but also on the hydrophobicity of its surface, is froth flotation, commonly used in the recycling industry.^{62–64} Air bubbles will selectively attach to the more hydrophobic particles and carry them upward, thus separating them from the less hydrophobic matrix. According to Imhof et al.⁵⁵ however, the mean efficiency of the froth flotation to separate microplastic from sediment is quite low ($55 \pm 28\%$), with high differences between polymer types.

3.3.4. Magnetic Extraction. Another method relying on the hydrophobic nature of microplastic surfaces is the method introduced by Grbic et al.⁶⁵ By functionalizing iron nanoparticles with hydrophobic hydrocarbon tails (using hexadecyltrimethoxysilane (HDTMS)), the iron nanoparticles will bind to the microplastic surfaces, and allow extraction with a magnet. In addition to water samples, the method was tested for sieved (mesh size 45 μm) benthic sediment spiked with microplastics (200 μm to 1 mm; PP, PVC, PU, PS, and PE). The recovery rates ranged from 49% (PP) to 90% (PE), albeit with high standard deviations within trials. This method is a proof of concept, that still has a few disadvantages: Lipophilic substances, that may very well be present in soil organic matter may result in nonspecific binding, reducing the effectiveness of the method. The authors suggest using the method for sediment samples after density separation or digestion, after which perhaps a further extraction method would no more be necessary. Furthermore, brittle microplastic particles were shown to fragment during the procedure. In environmental samples, where aged microplastics may be more brittle than pristine particles, this could distort the results significantly. Grbic et al.⁶⁵ propose that limiting microplastic contact with the magnet may reduce fragmentation. However, the question of the iron interfering with possible subsequent analytical characterization methods is not addressed, and should be further examined. While the authors describe that sonicating the magnet in a surfactant or acid solution can remove the iron nanoparticles from the microplastic surfaces, this method may lead to further fragmentation of microplastic particles,⁴⁵ and is thus undesirable.

3.3.5. Vertical Density Gradient Separation. A new methodology for density separation developed for the recycling industry uses a liquid containing colloidal ferromagnetic particles. A magnetic field around the liquid creates a vertical density gradient, with the highest density being at the bottom and the lowest density being at the top of the liquid container, thus a separation of a sample into different strata of various densities can be achieved.⁶⁶ This method may have potential concerning the isolation of microplastics from environmental samples; however, no research in this field has been conducted yet, and the costs may be unjustifiably high.

In general, density separation may be useful to remove the mineral fraction of soil samples, but methods developed for aquatic sediments must be adjusted to the new matrix “terrestrial soil” which can be extremely heterogeneous as stated above. Special care must be taken here that no microplastic losses occur due to enclosure in soil aggregates. Also, soil organic matter has a similar density ($\rho = 1\text{--}1.4 \text{ g cm}^{-3}$)⁴² to most plastics and needs to be removed separately, as organic compounds can impede microplastic analysis.

3.4. Consecutive Matrix Removal, Removal of the Organic Fraction. 3.4.1. Acidic and Alkaline Digestion.

Acidic and alkaline digestion methods are frequently reported in literature to remove the organic fraction of the sample matrix. Due to the fact that also soils contain organic matter, a digestive step is imperative for an undisturbed analysis. Claessens et al.⁵³ determined, that the most efficient chemical digestion of mussel tissue was obtained by treating the sample with 22.5 M HNO₃. Also the ICES (international council for the exploration of the sea) recommends an acid blend of HNO₃:HClO₄ (4:1) to digest marine animal tissue for microplastic analysis.⁶⁷ However, several studies state that certain strong acids may destroy specific polymers such as polystyrene and polyamide.^{68–71} Alkaline digestion is similarly discussed, especially for the digestion of animal tissue. However, treatment with NaOH was found to destroy polyamide and polyethylene (PE) fibers while leading to melting or discoloration of other polymers.^{72,73} Foekema et al.⁷⁴ digested fish intestines with 10% KOH solution at room temperature for 2–3 weeks. While apparently successful and nondestructive to synthetic polymers, the procedure is time-consuming and may not be applicable for plant material or stabilized soil organic matter.^{42,73} Generally, purification of samples with strong acidic or alkaline solutions will lead to uncontrolled bias in the resulting microplastic composition of the sample.⁷⁵

3.4.2. Oxidisation with Hydrogen Peroxide. Oxidization treatment with boiling hydrogen peroxide (30% H₂O₂) is commonly used in soil analysis to remove soil organic matter.⁷⁶ It has also been used, at lower temperatures, to destroy organic matter in the context of microplastic isolation from organic rich sediment matrices: Nuelle et al. (2014)⁶⁹ allowed samples to remain in 30% H₂O₂ for 7 days. Around 50% of the biogenic matter was dissolved completely, but polyamide (PA), polycarbonate (PC), and polypropylene (PP) pellets showed visible signs of degradation such as discoloration and size reduction. Liebezeit and Dubaish⁵⁶ claim that a 30% H₂O₂ treatment overnight does not affect plastic particles;⁵⁶ however, it is not stated if pristine or weathered plastic polymers were used, which can affect results. Zhao et al.⁷⁷ observed in a study concerning microplastics in marine snow, that 30% hydrogen peroxide treatment of organic-rich samples often results in the formation of a dense foam, which may suspend a significant portion of the sample above the reagent.⁷⁷ They therefore propose using 15% H₂O₂ at 75 °C for 24 h, instead, which is claimed to be just as effective as 30% H₂O₂; however, temperature sensitive polymers may be altered at such high temperatures. Instead of reducing the concentration in order to avoid the alteration of microplastic samples, Tagg et al.⁷⁸ propose reducing the exposure time. Fenton’s reagent uses ferrous cations to catalyze the oxidation of organic components with H₂O₂. It was successfully used in the isolation of microplastic particles in wastewater and shows no alteration of the surface of PE, PP, and PVC microplastics,

while differences in the PA particles are attributed to variations of the nylon fragment stock rather than the effect of Fenton’s reagent.⁷⁸ However, the effect on weathered plastics was not tested here, and may show different results than when using pristine particles. Hurley et al.,⁷⁹ conducted a test series for the removal of organic matter from complex, organic-rich environmental matrices with 30% H₂O₂ at 60 and 70 °C, with Fenton’s reagent at room temperature and 1 M NaOH as well as 10 M NaOH at 60 °C and 10% KOH at 60 °C. They found that oxidization with Fenton’s reagent at room temperature has the highest organic removal rate for soils and sewage sludge while having no effects on any of the tested microplastic granules. They also tested the effect of the order of digestion procedure combined with density separation by water and NaI: Organic matter removal followed by density separation *or* density separation followed by organic matter removal, and found the order to have no significant effect on the recovery rate.⁷⁹ To exclude any effects of the highly reactive H₂O₂ on weathered microplastics on environmental samples, it may be advisable to test weathered microplastics instead of pristine granules. Furthermore, care should be taken that organic-rich samples treated with Fenton’s reagent do not exceed temperatures above 60 °C due to the strong exothermal reaction to avoid thermal degradation.⁸⁰ Hurley et al.⁷⁹ recommend not to let reaction temperatures exceed 40 °C. Frei et al.⁸¹ successfully used Fenton’s reagent for the removal of organic matter in sediment samples from the hyporheic zone of rivers.

Hurley et al.⁷⁹ show that Fenton’s reagent can effectively reduce organic matter from soil samples, as this method is relatively cost and time-efficient, it shows potential to become an important step in the microplastic analysis of terrestrial samples. However, certain biogenic matter will not be removed, thus a complementary organic removal step may be necessary (personal observation).

3.4.3. Enzymatic Digestion. Organic matter within soils is one of the most difficult fractions to remove without destroying the microplastic particles. Thus, an adapted enzymatic digestion may be beneficial; however, most reports on enzymatic digestion procedures were developed for aquatic samples. Cole et al.⁷² developed one of the first enzymatic digestion protocols using Proteinase-K for plankton-rich seawater samples, resulting in digestion efficiencies >97% by weight. The enzymatic method was then compared to digestion protocols using HCl and NaOH and proved to have the highest efficiency with the additional benefit of not degrading the plastic particles. Other groups further developed the enzymatic digestion protocols for mussel tissue^{71,82,83} and fish guts,⁷² reporting good matrix removal rates and very high microplastic recovery rates, with no degradation of the polymer particles. However, all the above-named enzymatic protocols are aimed at removing animal soft tissue, and exclusively use proteolytic enzymes, that will not be able to remove the stabilized plant organic matter contained in soils. Thus, a more promising approach was derived by Löder et al.:⁷⁵ A sequential enzymatic digestion coupled with short-term reactions with H₂O₂. The used enzymes target specific organic compounds and using different enzymes may result in better digestion efficiencies than, for example, a single oxidization step using H₂O₂. The presented protocol by Löder et al.⁷⁵ is adequate for complex aquatic samples, but the removal of terrestrial plant matter and stabilized soil organic matter will probably require a different set of enzymes; thus, an adaptation of this protocol

may be necessary for terrestrial samples. In the authors' experience, (unpublished results) and as proposed by Löder et al.⁷⁵ a sequential combination of Fenton's reagent, SDS and specific enzymes can enhance the purification of soil organic matter compared to the use of Fenton's reagent alone.

4. IDENTIFICATION AND QUANTIFICATION

Since microplastic occurrence in the environment has become a scientific issue, a surprising amount of methods has been developed for the qualitative, quantitative, or combined analysis of microplastics in environmental samples. Some of these methods may be well applicable for soil samples, if the preceding sample purification is adequate.

4.1. Methods That Are Based on Visual Identification.

The earliest and simplest mode of microplastic analysis was visual identification under a light microscope,^{84,85} which however, is extremely prone to bias with error rates ranging from 20%⁸⁶ to 70%.⁴⁶ To reduce the shortcomings of the purely visual distinction between plastic and natural particles, some publications recommend the "hot needle test" which makes use of the thermoplastic properties of many synthetic polymers.^{67,87–91} Zhang et al.⁹² further developed this principle for a simple identification of low-density polymers in soils: After a density separation with water the residue in the supernatant is analyzed by comparing microscope-images taken prior and after heating the sample at 130 °C for 3–5 s. Melted particles are then identified as thermoplastic polymers. While simple and feasible in most field laboratories, this form of identification neglects high density and thermosetting plastics, does not consider that some natural substances such as wax also melt at certain temperatures, is destructive and lacks the possibility of identifying the exact type of polymer.

Similarly indiscriminate, but nondestructive is the use of polarized light microscopy under which certain synthetic particles appear vibrantly illuminated.^{16,93,94} Maes et al.⁹⁵ proposed the use of Nile Red—a lipophilic fluorescent dye—to specifically stain microplastic particles in environmental samples and make them fluoresce under a microscope by applying blue light and an orange filter.⁹⁵ This method has, however, not yet been tested for soil samples containing organic matter, where it may be possible that the dye unselectively adsorbs to other lipophilic compounds in the surrounding matrix.

4.2. Chromatography. More sophisticated methods, which allow the qualitative and quantitative identification of individual polymer types include various extraction methods coupled to a chromatographic unit. Suggested developments in the literature include high temperature gel-permeation chromatography (HT-GPC) for the identification of polyolefins in cosmetics,⁹⁶ liquid extraction with size-exclusion chromatography (SEC) for the identification and quantification of polystyrene (PS) and polyethylene terephthalate (PET) in soil samples,⁹⁷ and pyrolysis gas chromatography mass spectrometry (Pyr GC-MS). Pyr GC-MS is a sensitive and well-established method for the characterization and mass-quantification of many polymer types and their organic additives.^{69,98–102} Together with μ -ATR-FTIR spectroscopy, Pyr GC-MS has been shown to be well suitable for the detection of microplastics in environmental samples.¹⁰³ However, it also has several drawbacks. The size of the pyrolysis capsule and accordingly the sample amount per run is exceedingly small, 1.5 mm⁹⁹ and 0.5 mg,¹⁰⁴ respectively, which

requires an extensive sample cleanup for matrix-rich samples, making it rather unsuitable for bulk analysis. Additionally it is prone to contaminations or even blockages.¹⁰⁴ To overcome these shortcomings, Dümichen et al.¹⁰⁴ developed the thermal extraction desorption gas chromatography mass spectrometry (TED GC-MS) for microplastic detection. Each run can accommodate up to 100 mg of sample, which requires no pretreatment other than grinding and mixing in an attempt to homogenize the samples. The processing time requires 2–3 h, which is less than most of the current spectroscopic methods available.¹⁰⁴ This new analytical method may still need some refinement, but seems suitable for the fast analysis of many different environmental sample types, including soils. Eisen-traut et al.,¹⁰⁵ confirmed the possibility of identifying tire wear in environmental samples using TED GC-MS, an achievement that is very important to monitor the massive input of microplastic particles into the environment by traffic. However, if sample grinding is necessary, quality controls should take place, ensuring that the risk of microplastic losses and contamination remain at a minimum. One significant drawback of TED GC-MS is—as with all extraction-chromatography methods—that it is destructive. Hence, information on the number, size, and morphology of the plastic particles cannot be obtained, although this information may be crucial in the context of assessing the effects of microplastics on organisms and eco-systems: The bioavailability of polymer particles is dependent on its size and form and the environmental impact is most probably dependent on the concentration of bioavailable particles in the ecosystem. In addition, the morphology of the microplastics may also be important in the context of their influence on the soil structure and function.²⁰

4.3. Thermogravimetric Analysis. A different thermal analysis method is the thermogravimetric analysis (TGA). Majewsky et al.¹⁰⁶ coupled TGA with differential scanning calorimetry (DSC) for the microplastic analysis of wastewater. However, in that study, only polyethylene (PE) and polypropylene (PP) could clearly be identified. David et al.¹⁰⁷ attempted coupling TGA with mass spectrometry (MS) to quantitatively analyze polyethylene terephthalate (PET) in soil samples without sample pretreatment. While successful, the method still requires further development and is, to the best of the author's knowledge, still restricted to the analysis of PET only.

Thermogravimetric analysis and chromatography bear several promising approaches for fast mass-quantitative identification of microplastics in soils and other complex matrices.¹⁰⁸ However, they are limited insofar that subsequent analyses are impossible due to the destructive nature of the methods and number, size and form of the particles remain unknown, resulting in the drawbacks mentioned above in the chromatography section.

4.4. Vibrational Spectroscopy. Vibrational spectroscopy, such as Raman or Fourier transform infrared (FTIR) spectroscopy are the most commonly used state of the art analytical methods in microplastic research, because they enable the precise identification of polymer types, their abundance, shape, and size. Raman microspectroscopy allows chemical imaging of samples down to a pixel resolution of 500 nm,¹⁰⁹ while focal plane array (FPA) based micro-FTIR spectroscopy allows the identification of particles in a size range from 10 to 500 μ m.¹¹⁰ Larger particles (>500 μ m) can be analyzed by attenuated total reflectance (ATR)-FTIR

spectroscopy.¹¹¹ For further information on the function and application modes of FTIR and Raman spectroscopy, please refer to Renner et al.¹¹¹ and K ppler et al.¹¹² Information on the automatic software recognition of microplastics in samples measured with a micro-FTIR spectrometer can be found in the publications by Hufnagl et al.¹¹³ and Primpke et al.¹¹⁴ Raman- and FTIR-based chemical imaging complement each other and should be chosen in accordance with the specific research questions: The Raman imaging run time is significantly higher than FTIR imaging,¹¹² but is independent of the shape, size, or thickness of the measured particles, which can influence the results in micro-FTIR imaging. Black particles often result in unidentifiable FTIR-spectra, due to the high absorption of infrared radiation. Additionally, Raman is insensitive to water and atmospheric CO₂. However, background fluorescence of organic matter or pigments in the polymers may strongly interfere with the desired spectra, making them unidentifiable.¹¹² This may be especially problematic when dealing with soil samples with a high soil organic matter content. For both vibrational spectroscopy methods, a thorough sample purification is needed prior to the concentration on the filter surface on which the analysis takes place.⁷⁵ For solid samples, this fact significantly reduces the amount of sample that can realistically be processed. Thus, the need for an easy high-throughput technique for a representative amount of solid samples, such as soils, has been recognized and solutions have been proposed.

Fuller and Gautam¹¹⁵ used pressurized fluid extraction (PFE) to dissolve specific microplastics from a soil matrix, let the polymer-solvent-extract evaporate and measured the solid residue with ATR-FTIR spectroscopy.¹¹⁵ This method is fast, as it does not require sample purification and it is independent of particle size. However, similar to the chromatographic methods, it is also a destructive method and only allows mass-quantitative analysis, not providing information on number, size, and shape of the polymer particles. Additionally, multiple polymer types in one sample produce complex absorption spectra that may hamper identification.

A similar, novel method was introduced by Schmidt et al.¹¹⁶ who used short-wave infrared (SWIR) imaging spectroscopy to analyze surface water samples taken from the Teltow Canal in Berlin (Germany). The purified (using H₂O₂) samples were filtered onto several glass fiber filters each (diameter 47 mm) and scanned with a SWIR imaging spectrometer, measurement speed: 52 048 mm² per hour, resulting in the measurement of 10 filters within 20 min. The lower detection limit is for particles of a size of 560 μm by 280 μm (2 pixels). The evaluation of the spectroscopic images was done automatically by the "PlaMAPP" algorithm, yielding a 75% true detection efficiency. To achieve more reliable results, additional manual checking was required.¹¹⁶ While the SWIR imaging spectroscopy can process many sample filters in comparatively little time, its drawbacks are the rather large lower size limit and the need for improvement for correct particle detection in the automated analysis algorithm.

4.5. Proton Nuclear Magnetic Resonance Spectroscopy (¹H NMR). A completely new approach for size-independent microplastic analysis was recently described by Peez et al.¹¹⁷ Using quantitative ¹H NMR spectroscopy, model samples of polyethylene (PE) particles, polystyrene (PS) beads, and polyethylene terephthalate (PET) fibers could successfully be qualitatively and quantitatively analyzed with a calibration curve method. Each analyte was separately

dissolved in the corresponding deuterated solvent: Deuterated toluene for PE, deuterated chloroform for PS, and deuterated chloroform with trifluoroacetic acid for PET, and subsequently measured with an NMR spectrometer. Polymer mixtures were not tested. Although the method is described as cost-efficient and fast (approximately 1 min per measurement), there is the severe drawback of having to completely remove any organic matter from the environmental sample to avoid signal overlays.¹¹⁷ As a 100% removal of organic matter from soil samples without destroying the plastic as well is not possible at this point in time, the ¹H NMR method is deemed unsuitable for microplastic detection in soil samples.

4.6. In-Situ Identification. An approach for an in situ methodology was developed by Paul et al.,¹¹⁸ who attempted to combine near-infrared (NIR) spectroscopy (opposed to the mid-infrared range used in conventional FTIR spectroscopy) with chemometrics to identify microplastics in soils. Near-infrared radiation can penetrate deeper than mid-infrared radiation, enabling analysis of particles even when coated with a thick biofilm, and the method is generally not sensitive to water.¹¹⁸ Paul et al.¹¹⁸ were not able to achieve a sensitive quantification of the plastic content in soil samples. However, Corradini et al.¹¹⁹ developed a method to "rapidly assess microplastic concentrations in soils without extraction"¹¹⁹ using a portable visible NIR spectroscope. Here the microplastic concentration is to be estimated directly on the field, without time- and labor-consuming extraction and detection procedures. LDPE, PET, and PVC (0.5–1 mm) particles in artificially polluted soil samples were successfully detected, with an accuracy of 10 g kg⁻¹ and a detection limit of around 15 g kg⁻¹ in the predictive model. Current limitations to this method are the low accuracy and high detection limit (which may be much higher than realistic concentrations in natural soils) as well as the need for a training set to accurately predict the polymer concentrations, which has to be adapted to different soil types. Additionally, only the concentration is given, while no information is obtained on the size or shape of the polymer particles. As the method is nondestructive though, where necessary subsamples for plastic extraction and analysis could be taken after the NIR assessment.

Shan et al.¹²⁰ also addressed a method for in situ microplastic analysis on soil surfaces by hyperspectral imaging. Like FTIR or Raman spectroscopy, hyperspectral imaging is a nonbiased, nondestructive identification method, giving information on the spatial position, size, and specific reflectance spectrum of objects. However, the method is limited by the particle size and can only be applied to the soil surface, whereas polymer particles situated in deeper soil strata are neglected.¹²⁰ Hyperspectral imaging or visible NIR spectroscopy for microplastic analysis in environmental samples are methods in development and have the potential for rapid automated identification methods in soil samples in the future.^{119,121,122}

5. QUALITY ASSURANCE/QUALITY CONTROL

Synthetic polymers are ubiquitous, and the risk of contamination of environmental samples during sampling, sample processing, and analysis for microplastics is very high, for example, by contamination with abraded particles from plastic equipment, synthetic fibers from clothes, or airborne polymer particles and fibers.⁴⁵ Thus, precautions must be taken during each processing step: Generally, plastic material should be

avoided and replaced wherever possible by alternative materials like metal or glass.

Woodall et al.¹²³ comprehensively describe using a forensic science approach to minimize sample contamination. Recommended steps are all equipment and material should be thoroughly cleaned with prefiltered (0.2 μm) deionized water and 35% ethanol.^{6,75} Samples should be taken with clean metal tools and stored in clean glass or metal containers with a lid. While handling the samples or being in the laboratory, only clothing made of natural fibers should be worn and covered by a 100% cotton lab coat. To avoid cross contamination, all tools have to be thoroughly cleaned before coming into contact with the next sample. To control if the cleaning steps are sufficient, regular equipment (rinsate) blanks should be taken after “decontamination”, by rinsing the equipment with filtered water and collecting the rinsate for subsequent analysis. Any certified precleaned labware obtained from third parties should previously be tested for contamination. Furthermore, taking field blanks to assess the extent of unavoidable contamination on site is imperative. A field blank is prepared, treated, and kept with the actual samples throughout the sampling event to identify any ambient contamination of the samples during the sampling process. Thus the empty field blank jars are opened, rinsed, and if possible filled with, for example, sand that was previously treated in a muffle kiln at 550 °C to remove all plastics or any other microplastic-free particular matrix similar to the sample matrix before being closed, sealed, and transported the same way as the soil samples.¹²⁴

Processing in the laboratory should take place under a laminar flow box/clean box/clean lab to prevent airborne contamination. Furthermore, restricting access to the laboratory to a minimum of employees and covering vents with natural-fiber dustfilters will also help reduce ambient contamination.¹²³ All lab-equipment should be plastic-free; where this is not possible a polymer that seldom occurs in environmental samples should be used and characterized, for example, Teflon, which will be excluded from the analyte list. To monitor possible sample contaminations, it is essential to apply blank samples that undergo the same treatment as the environmental samples,⁶⁷ as well as monitoring used liquids and the ambient air (e.g., by laying out wet filter papers for a defined amount of time.¹²³ Finally, prior to and after working in a workspace all surfaces should be wiped clean.

Apart from reducing and monitoring any sample contamination, other QA/QC procedures have been widely lacking in past microplastic research, not only for soils, but also for the analysis of samples from other environmental compartments: The comprehensive validation of procedures and interlaboratory comparisons of protocols, even among similar analytical methods, are severely lacking in frequency and quality.¹²⁵ Regular internal quality control and external proficiency tests have never, to the best of the authors' knowledge, been conducted. This is mainly due to a lack of certified reference materials,⁹¹ that are urgently needed for such procedures. Hence, research efforts are currently being made on this topic on a national and international level. Validation processes must address standardized microplastic particles of different polymer types, sizes and forms. Also “aged” particles vs “pristine” particles is a factor that should be considered. This is a major task that has, to date, not been addressed appropriately. But not only the spiking material is lacking, but also a standard procedure for spiking with very small microplastic particles. The smaller the particle size, the more difficult the spiking of a

matrix becomes, as many small polymer particles tend to stick to walls, forceps or other equipment,¹²⁵ so counting and manually transferring them into the sample is near impossible for sizes smaller than 100 μm . Emulsifying an exact mass of particles for transfer is possible, but only applicable for mass-quantification analysis (e.g., Pyr GC-MS or TED GC-MS) as long as the losses during transfer are negligible (which may not be the case, depending on the adhering forces of the particles in the pipet). However, for number-quantification analysis (e.g., vibrational spectroscopy) determining the exact number of particles within any volume before transferring it completely to the sample may prove difficult. One possibility, (unpublished data) would be to emulsify a defined amount of microplastics in a liquid that hardens upon drying and is resolvable in water (e.g., gelatin), allowing the exact determination of particle number in each hardened gelatin platelet under a microscope before transferring it (loss free) to the sample, where it can be redissolved and homogenized in a mixture of soil and water, which can subsequently be dried again. This procedure not only allows the addition of an exactly defined number of very small standard particles to the sample, but also allows the particles to be incorporated into soil aggregates formed by the drying of moist soil, making the validation more representative of environmental soil samples.⁷⁹

During the research for this critical review, it has become apparent, that not only a standardized analytical process has to be found, but that beforehand, a consensus on how to validate any given analytical process for each environmental matrix must be determined.

6. PERSPECTIVES AND OUTLOOK

As with all analytical processes there is a trade-off between time- and effort reduction for sample preparation and analysis on one hand and on information quality of the generated data on the other hand. This also holds especially true with respect to the new research field of microplastic analysis in soil samples. Thus, researchers as well as readers should be cautious of large extrapolation factors when normalizing data to larger units (e.g., kg) as a consequence of the small sample amounts currently processable in microplastic analysis of soils. Authors of publications based on such data should be aware of the potential uncertainties related to such extrapolation and call attention of the readers.

Nevertheless, the research conducted in the frame of this critical review has shown, that several different analytical methods can be validly used for microplastic detection and quantification, depending on the research question at hand. In order to enhance the methods toward a standard protocol for soil-microplastic monitoring, several aspects need to be addressed in the near future:

- (1) Developing a framework of sampling procedures, in order to harmonize sample taking and to render projects with similar research questions comparable.
- (2) Automating currently labor-intensive purification protocols, to reduce bias and promote parallel processing of several samples at once.
- (3) Promoting in situ microplastic detection methods.
- (4) Establishing standard validation processes for microplastic detection methods and develop appropriate reference materials.
- (5) Developing methods that are capable of identifying nanoplastic particles in soil samples.

In the meantime, the currently available methods can not only be used to exemplarily analyze soil samples for microplastic contamination, but are often also suitable to analyze sources and input pathways of microplastic into the environment. Investigating the extent of microplastic input into soils through pathways such as sewage sludge, compost, road runoff, etc. may help find measures to reduce the entry of plastics and microplastics into the environment in the first place. This is important as precautionary principle in the face of the potential environmental risks and the thusly connected public pressure on policy makers, consumers and industry to take action. To correctly assess the risk of microplastics in the terrestrial environment and to form a scientific basis for regulatory action concerning microplastic input pathways, it is important that research institutions work closely together in terms of empirical research, method development, and quality control standards.

■ ASSOCIATED CONTENT

SI Supporting Information

The Supporting Information is available free of charge at <https://pubs.acs.org/doi/10.1021/acs.est.9b04618>.

A list of publications on microplastic analysis of soil samples is given in Table S1, summarizing the sampling methods and procedures for each publication (PDF)

■ AUTHOR INFORMATION

Corresponding Author

Christian Laforsch – Department of Animal Ecology I and BayCEER, University of Bayreuth, Bayreuth, Germany; Phone: +49-921-55-2650; Email: christian.laforsch@uni-bayreuth.de; Fax: +49-921-55-2784

Authors

Julia N. Möller – Department of Animal Ecology I and BayCEER, University of Bayreuth, Bayreuth, Germany; orcid.org/0000-0002-7390-3994

Martin G. J. Löder – Department of Animal Ecology I and BayCEER, University of Bayreuth, Bayreuth, Germany; orcid.org/0000-0001-9056-8254

Complete contact information is available at: <https://pubs.acs.org/doi/10.1021/acs.est.9b04618>

Notes

The authors declare no competing financial interest.

■ ACKNOWLEDGMENTS

This review was completed with the support of the Ministry for Environment, Climate Protection and Energy of Baden Württemberg, funding Julia N. Möller in the scope of the research programme MiKoBo (Mikrokunststoffe in Komposten und Gärprodukten aus Bioabfallverwertungsanlagen und deren Eintrag in landwirtschaftlich genutzte Böden - Erfassen, Bewerten, Vermeiden), reference number BMWK18007. Furthermore, we gratefully acknowledge the support of the German Research Foundation (DFG), reference number 391977956 - SFB 1357 and the Federal Ministry of Education and Research (BMBF), reference number 03F0789A for funding the microplastic research projects “SFB Mikroplastik” and “PLAWES”, respectively.

■ REFERENCES

- (1) *International Research Workshop on the Occurrence, Effects, and Fate of Microplastic Marine Debris*; Arthur, C.; Baker, J.; Bamford, H.; Eds.; NOAA Technical Memorandum NOS-OR&R-30: Tacoma, WA, 2009.
- (2) *Sources, Fate and Effects of Microplastics in the Marine Environment: Part 2 of a Global Assessment*; Kershaw, P. J.; Rochman, C. M.; Eds.; IMO/FAO/UNESCO-IOC/UNIDO/WMO/IAEA/UN/UNEP/UNDP. Joint Group of Experts on the Scientific Aspects of Marine Environmental Protection Rep. Stud. GESAMP No. 93, 2016.
- (3) Frias, J. P. G. L.; Nash, R. Microplastics: Finding a Consensus on the Definition. *Mar. Pollut. Bull.* **2019**, *138* (2019), 145–147.
- (4) Peeken, I.; Primpke, S.; Beyer, B.; Gütermann, J.; Kattlein, C.; Krumpfen, T.; Bergmann, M.; Hehemann, L.; Gerdt, G. Arctic Sea Ice Is an Important Temporal Sink and Means of Transport for Microplastic. *Nat. Commun.* **2018**, *9* (1), 1–12.
- (5) Free, C. M.; Jensen, O. P.; Mason, S. a.; Eriksen, M.; Williamson, N. J.; Boldgiv, B. High-Levels of Microplastic Pollution in a Large, Remote, Mountain Lake. *Mar. Pollut. Bull.* **2014**, *85* (2014), 156–163.
- (6) Piehl, S.; Leibner, A.; Löder, M. G. J.; Laforsch, C.; Bogner, C. Identification and Quantification of Macro- and Microplastics on an Agricultural Farmland. *Sci. Rep.* **2018**, *8* (17950), 1–9.
- (7) Li, W. C.; Tse, H. F.; Fok, L. Plastic Waste in the Marine Environment: A Review of Sources, Occurrence and Effects. *Sci. Total Environ.* **2016**, *566–567* (2016), 333–349.
- (8) Li, J.; Liu, H.; Chen, J. P. Microplastics in Freshwater Systems: A Review on Occurrence, Environmental Effects, and Methods for Microplastics Detection. *Water Res.* **2018**, *137* (2018), 362–374.
- (9) Rochman, C. M. Microplastics Research - from Sink to Source. *Science* **2018**, *360* (6384), 28–29.
- (10) Kawecki, D.; Nowack, B. Polymer-Specific Modeling of the Environmental Emissions of Seven Commodity Plastics As Macro- and Microplastics. *Environ. Sci. Technol.* **2019**, *53* (16), 9664–9676.
- (11) Horton, A. A.; Walton, A.; Spurgeon, D. J.; Lahive, E.; Svendsen, C. Microplastics in Freshwater and Terrestrial Environments: Evaluating the Current Understanding to Identify the Knowledge Gaps and Future Research Priorities. *Sci. Total Environ.* **2017**, *586*, 127–141.
- (12) Liu, F.; Vianello, A.; Vollertsen, J. Retention of Microplastics in Sediments of Urban and Highway Stormwater Retention Ponds. *Environ. Pollut.* **2019**, *255*, 1–8.
- (13) Lassen, C.; Hansen, S. F.; Magnusson, K.; Hartmann, N. B.; Rehne Jensen, P.; Nielsen, T. G.; Brinch, A. *Microplastics - Occurrence, Effects and Sources of Releases to the Environment in Denmark*; Danish Environmental Protection Agency: Copenhagen, 2015.
- (14) Dris, R.; Gasperi, J.; Rocher, V.; Saad, M.; Renault, N.; Tassin, B. Microplastic Contamination in an Urban Area: A Case Study in Greater Paris. *Environ. Chem.* **2015**, *12* (5), 592–599.
- (15) Weithmann, N.; Möller, J. N.; Löder, M. G. J.; Piehl, S.; Laforsch, C.; Freitag, R. Organic Fertilizer as a Vehicle for the Entry of Microplastic into the Environment. *Sci. Adv.* **2018**, *4* (4), 1–7.
- (16) Zubris, K. A. V.; Richards, B. K. Synthetic Fibers as an Indicator of Land Application of Sludge. *Environ. Pollut.* **2005**, *138*, 201–211.
- (17) Steinmetz, Z.; Wollmann, C.; Schaefer, M.; Buchmann, C.; David, J.; Tröger, J.; Muñoz, K.; Frör, O.; Schaumann, G. E. Plastic Mulching in Agriculture. Trading Short-Term Agronomic Benefits for Long-Term Soil Degradation? *Sci. Total Environ.* **2016**, *550*, 690–705.
- (18) Zhang, G. S.; Liu, Y. F. The Distribution of Microplastics in Soil Aggregate Fractions in Southwestern China. *Sci. Total Environ.* **2018**, *642*, 12–20.
- (19) Rillig, M. C.; Ziersch, L.; Hempel, S. Microplastic Transport in Soil by Earthworms. *Sci. Rep.* **2017**, *7* (1), 1–6.
- (20) De Souza Machado, A. A.; Lau, C. W.; Till, J.; Kloas, W.; Lehmann, A.; Becker, R.; Rillig, M. C. Impacts of Microplastics on the Soil Biophysical Environment. *Environ. Sci. Technol.* **2018**, *52* (17), 9656–9665.

- (21) De Souza Machado, A. A.; Kloas, W.; Zarfl, C.; Hempel, S.; Rillig, M. C. Microplastics as an Emerging Threat to Terrestrial Ecosystems. *Glob. Chang. Biol.* **2018**, *24* (4), 1405–1416.
- (22) Huerta Lwanga, E.; Mendoza Vega, J.; Ku Quej, V.; Chi, J. de los A.; Sanchez del Cid, L.; Chi, C.; Escalona Segura, G.; Gertsen, H.; Salánki, T.; van der Ploeg, M.; Koelmans, A. A.; Geissen, V. Field Evidence for Transfer of Plastic Debris along a Terrestrial Food Chain. *Sci. Rep.* **2017**, *7* (1), 1–7.
- (23) Ng, E. L.; Huerta Lwanga, E.; Eldridge, S. M.; Johnston, P.; Hu, H. W.; Geissen, V.; Chen, D. An Overview of Microplastic and Nanoplastic Pollution in Agroecosystems. *Sci. Total Environ.* **2018**, *627*, 1377–1388.
- (24) Zhao, S.; Zhu, L.; Li, D. Microscopic Anthropogenic Litter in Terrestrial Birds from Shanghai, China: Not Only Plastics but Also Natural Fibers. *Sci. Total Environ.* **2016**, *550*, 1110–1115.
- (25) Nizzetto, L.; Futter, M.; Langaas, S. Are Agricultural Soils Dumps for Microplastics of Urban Origin? *Environ. Sci. Technol.* **2016**, *50* (20), 10777–10779.
- (26) Hurley, R. R.; Nizzetto, L. Fate and Occurrence of Micro(Nano)Plastics in Soils: Knowledge Gaps and Possible Risks. *Curr. Opin. Environ. Sci. Heal.* **2018**, *1*, 6–11.
- (27) He, D.; Luo, Y.; Lu, S.; Liu, M.; Song, Y.; Lei, L. Microplastics in Soils: Analytical Methods, Pollution Characteristics and Ecological Risks. *TrAC, Trends Anal. Chem.* **2018**, *109*, 163–172.
- (28) Da Costa, J. P.; Paço, A.; Santos, P. S. M.; Duarte, A. C.; Rocha-Santos, T. Microplastics in Soils: Assessment, Analytics and Risks. *Environ. Chem.* **2019**, *16* (1), 18–30.
- (29) Chae, Y.; An, Y. Current Research Trends on Plastic Pollution and Ecological Impacts on the Soil Ecosystem: A Review. *Environ. Pollut.* **2018**, *240*, 387–395.
- (30) Zhang, C. C. *Fundamentals of Environmental Sampling and Analysis*; John Wiley & Sons, Inc.: Hoboken, NJ, 2007; DOI: 10.1002/0470120681.
- (31) Dümichen, E.; Barthel, A. K.; Braun, U.; Bannick, C. G.; Brand, K.; Jekel, M.; Senz, R. Analysis of Polyethylene Microplastics in Environmental Samples, Using a Thermal Decomposition Method. *Water Res.* **2015**, *85*, 451–457.
- (32) Environmental Protection Agency Oceans and Coastal Protection Division. *Plastic Pellets in the Aquatic Environment: Sources and Recommendations*, EPA 842-S-93-001; Duxbury, 1992.
- (33) International Atomic Energy Agency (IAEA). *Soil Sampling for Environmental Contaminants*; Vienna, 2004.
- (34) Scheurer, M.; Bigalke, M. Microplastics in Swiss Floodplain Soils. *Environ. Sci. Technol.* **2018**, *52* (6), 3591–3598.
- (35) Miller, M. E.; Kroon, F. J.; Motti, C. A. Recovering Microplastics from Marine Samples: A Review of Current Practices. *Mar. Pollut. Bull.* **2017**, *123* (1–2), 6–18.
- (36) Zhou, Q.; Zhang, H.; Fu, C.; Zhou, Y.; Dai, Z.; Li, Y.; Tu, C.; Luo, Y. The Distribution and Morphology of Microplastics in Coastal Soils Adjacent to the Bohai Sea and the Yellow Sea. *Geoderma* **2018**, *322*, 201–208.
- (37) Liu, M.; Song, Y.; Lu, S.; Qiu, R.; Hu, J.; Li, X.; Bigalke, M.; Shi, H.; He, D. A Method for Extracting Soil Microplastics through Circulation of Sodium Bromide Solutions. *Sci. Total Environ.* **2019**, *691*, 341–347.
- (38) Rillig, M. C.; Ingrassia, R.; De Souza Machado, A. A. Microplastic Incorporation into Soil in Agroecosystems. *Front. Plant Sci.* **2017**, *8* (1805), 1–4.
- (39) Länderarbeitsgemeinschaft Abfall (LAGA). *LAGA PN 98 Richtlinie Für Das Vorgehen Bei Physikalischen, Chemischen Und Biologischen Untersuchungen Im Zusammenhang Mit Der Verwertung/Beseitigung von Abfällen*; Ministerium für Umwelt und Forsten Rheinland Pfalz: Mainz, 2001.
- (40) ISO (International Organization for Standardization). ISO 11465, Soil quality - Determination of dry matter and water content on a mass basis - Gravimetric method, Technical corrigendum 1 <https://www.iso.org/standard/20886.html> (accessed October 25, 2019).
- (41) Crawford, C. B.; Quinn, B. Microplastic Separation Techniques. In *Microplastic Pollutants* **2017**, 203–218.
- (42) Bläsing, M.; Amelung, W. Plastics in Soil: Analytical Methods and Possible Sources. *Sci. Total Environ.* **2018**, *612*, 422–435.
- (43) Norén, F. Small Plastic Particles in Coastal Swedish Waters. In *N-Research Report commissioned by KIMO Sweden (Submitted to BDC)*; Lysekil, Sweden, 2007.
- (44) Lenz, R.; Enders, K.; Stedmon, C. A.; MacKenzie, D. M. A.; Nielsen, T. G. A Critical Assessment of Visual Identification of Marine Microplastic Using Raman Spectroscopy for Analysis Improvement. *Mar. Pollut. Bull.* **2015**, *100* (1), 82–91.
- (45) Löder, M. G. J.; Gerdt, G. Methodology Used for the Detection and Identification of Microplastics - A Critical Appraisal. In *Marine Anthropogenic Litter*; Bergmann, M., Gutow, L., Klages, M., Eds.; Springer, 2015; pp 201–227; DOI: 10.1007/978-3-319-16510-3.
- (46) Hidalgo-Ruz, V.; Gutow, L.; Thompson, R. C.; Thiel, M. Microplastics in the Marine Environment: A Review of the Methods Used for Identification and Quantification. *Environ. Sci. Technol.* **2012**, *46* (6), 3060–3075.
- (47) Shim, W. J.; Hong, S. H.; Eo, S. E. Identification Methods in Microplastic Analysis: A Review. *Anal. Methods* **2017**, *9* (9), 1384–1391.
- (48) Felsing, S.; Kochleus, C.; Buchinger, S.; Brennholt, N.; Stock, F.; Reifferscheid, G. A New Approach in Separating Microplastics from Environmental Samples Based on Their Electrostatic Behavior. *Environ. Pollut.* **2018**, *234*, 20–28.
- (49) Crichton, E. M.; Noël, M.; Gies, E. A.; Ross, P. S. A Novel, Density-Independent and FTIR-Compatible Approach for the Rapid Extraction of Microplastics from Aquatic Sediments. *Anal. Methods* **2017**, *9* (9), 1419–1428.
- (50) Mani, T.; Frehland, S.; Kalberer, A.; Burkhardt-Holm, P. Using Castor Oil to Separate Microplastics from Four Different Environmental Matrices. *Anal. Methods* **2019**, *11*, 1788–1794.
- (51) Hanvey, J. S.; Lewis, P. J.; Lavers, J. L.; Crosbie, N. D.; Pozo, K.; Clarke, B. O. A Review of Analytical Techniques for Quantifying Microplastics in Sediments. *Anal. Methods* **2017**, *9*, 1369–1383.
- (52) Thompson, R. C.; Olsen, Y.; Mitchell, R. P.; Davis, A.; Rowland, S. J.; John, A. W. G.; Mcgonigle, D.; Russell, A. E. Lost at Sea: Where Is All the Plastic? *Science* **2004**, *304*, 838.
- (53) Claessens, M.; Van Cauwenberghe, L.; Vandegehuchte, M. B.; Janssen, C. R. New Techniques for the Detection of Microplastics in Sediments and Field Collected Organisms. *Mar. Pollut. Bull.* **2013**, *70* (1–2), 227–233.
- (54) Corcoran, P. L.; Biesinger, M. C.; Grifi, M. Plastics and Beaches: A Degrading Relationship. *Mar. Pollut. Bull.* **2009**, *58* (1), 80–84.
- (55) Imhof, H. K.; Schmid, J.; Niessner, R.; Ivleva, N. P.; Laforsch, C. A Novel, Highly Efficient Method for the Separation and Quantification of Plastic Particles in Sediments of Aquatic Environments. *Limnol. Oceanogr.: Methods* **2012**, *10* (7), S24–S37.
- (56) Liebezeit, G.; Dubaish, F. Microplastics in Beaches of the East Frisian Islands Spiekeroog and Kachelotplate. *Bull. Environ. Contam. Toxicol.* **2012**, *89* (1), 213–217.
- (57) Filella, M. Questions of Size and Numbers in Environmental Research on Microplastics: Methodological and Conceptual Aspects. *Environ. Chem.* **2015**, *12* (5), 527–538.
- (58) Zobkov, M. B.; Esiukova, E. E. Evaluation of the Munich Plastic Sediment Separator Efficiency in Extraction of Microplastics from Natural Marine Bottom Sediments. *Limnol. Oceanogr.: Methods* **2017**, *15* (11), 967–978.
- (59) Coppock, R. L.; Cole, M.; Lindeque, P. K.; Queirós, A. M.; Galloway, T. S. A Small-Scale, Portable Method for Extracting Microplastics from Marine Sediments. *Environ. Pollut.* **2017**, *230*, 829–837.
- (60) Mahat, S. Separation and Quantification of Microplastics from Beach and Sediment Samples Using the Bauta Microplastic-Sediment Separator Separation and Quantification of Microplastics from Beach and Sediment Samples Using the Bauta Microplastic-Sediment

Separator, Masters Thesis, Norwegian University of Life Sciences, 2017.

(61) Southwood, T. R. E.; Henderson, P. A. *Ecological Methods*, 3rd ed., Blackwell Science: Oxford, 2000.

(62) Alter, H. The Recovery of Plastics from Waste with Reference to Froth Flotation. *Resour. Conserv. Recycl.* **2005**, *43* (2), 119–132.

(63) Fraunholz, N. Separation of Waste Plastics by Froth Flotation - A Review, Part I. *Miner. Eng.* **2004**, *17*, 261–268.

(64) Marques, G. A.; Tenório, J. A. S. Use of Froth Flotation to Separate PVC/PET Mixtures. *Waste Manage.* **2000**, *20* (4), 265–269.

(65) Grbic, J.; Nguyen, B.; Guo, E.; You, J. B.; Sinton, D.; Rochman, C. M. Magnetic Extraction of Microplastics from Environmental Samples. *Environ. Sci. Technol. Lett.* **2019**, *6* (2), 68–72.

(66) Hu, B. *Magnetic Density Separation of Polyolefin Wastes*; **2014**; DOI: 10.4233/uuid:0c3717fa-8000-4de0-a938-d65605bf2a96.

(67) International Council for the Exploration of the Sea (ICES). OSPAR request on development of a common monitoring protocol for plastic particles in fish stomachs and selected shellfish on the basis of existing fish disease surveys. https://www.ices.dk/sites/pub/Publication%20Reports/Advice/2015/Special_Requests/OSPAR_PLAST_advice.pdf (accessed January 23, 2020).

(68) Rocha-Santos, T.; Duarte, A. C. A Critical Overview of the Analytical Approaches to the Occurrence, the Fate and the Behavior of Microplastics in the Environment. *TrAC, Trends Anal. Chem.* **2015**, *65*, 47–53.

(69) Nuelle, M. T.; Dekiff, J. H.; Remy, D.; Fries, E. A New Analytical Approach for Monitoring Microplastics in Marine Sediments. *Environ. Pollut.* **2014**, *184*, 161–169.

(70) Avio, C. G.; Gorbi, S.; Regoli, F. Experimental Development of a New Protocol for Extraction and Characterization of Microplastics in Fish Tissues: First Observations in Commercial Species from Adriatic Sea. *Mar. Environ. Res.* **2015**, *111*, 18–26.

(71) Catarino, A. I.; Thompson, R.; Sanderson, W.; Henry, T. B. Development and Optimization of a Standard Method for Extraction of Microplastics in Mussels by Enzyme Digestion of Soft Tissues. *Environ. Toxicol. Chem.* **2017**, *36* (4), 947–951.

(72) Cole, M.; Webb, H.; Lindeque, P. K.; Fileman, E. S.; Halsband, C.; Galloway, T. S. Isolation of Microplastics in Biota-Rich Seawater Samples and Marine Organisms. *Sci. Rep.* **2015**, *4* (4528), 1–8.

(73) Herrera, A.; Garrido-Amador, P.; Martínez, I.; Samper, M. D.; López-Martínez, J.; Gómez, M.; Packard, T. T. Novel Methodology to Isolate Microplastics from Vegetal-Rich Samples. *Mar. Pollut. Bull.* **2018**, *129*, 61–69.

(74) Foekema, E. M.; De Gruijter, C.; Mergia, M. T.; Van Franeker, J. A.; Murk, A. J.; Koelmans, A. A. Plastic in North Sea Fish. *Environ. Sci. Technol.* **2013**, *47*, 8818–8824.

(75) Löder, M. G. J.; Imhof, H. K.; Ladehoff, M.; Löschel, L. A.; Lorenz, C.; Mintenig, S.; Piehl, S.; Primpke, S.; Schrank, I.; Laforsch, C.; Gerdt, G. Enzymatic Purification of Microplastics in Environmental Samples. *Environ. Sci. Technol.* **2017**, *51* (24), 14283–14292.

(76) Pansu, M.; Gautheryou, J. *Handbook of Soil Analysis: Mineralogical, Organic and Inorganic Methods*; Springer Berlin Heidelberg, 2006; DOI: 10.1007/978-3-540-31211-6.

(77) Zhao, S.; Danley, M.; Ward, J. E.; Li, D.; Mincer, T. J. An Approach for Extraction, Characterization and Quantitation of Microplastic in Natural Marine Snow Using Raman Microscopy. *Anal. Methods* **2017**, *9* (9), 1470–1478.

(78) Tagg, A. S.; Harrison, J. P.; Ju-Nam, Y.; Sapp, M.; Bradley, E. L.; Sinclair, C. J.; Ojeda, J. J. Fenton's Reagent for the Rapid and Efficient Isolation of Microplastics from Wastewater. *Chem. Commun.* **2017**, *53* (2), 372–375.

(79) Hurley, R. R.; Lusher, A. L.; Olsen, M.; Nizzetto, L. Validation of a Method for Extracting Microplastics from Complex, Organic-Rich, Environmental Matrices. *Environ. Sci. Technol.* **2018**, *52*, 7409–7417.

(80) Munno, K.; Helm, P. A.; Jackson, D. A.; Rochman, C.; Sims, A. Impacts of Temperature and Selected Chemical Digestion Methods on Microplastic Particles. *Environ. Toxicol. Chem.* **2018**, *37* (1), 91–98.

(81) Frei, S.; Piehl, S.; Gilfedder, B. S.; Löder, M. G. J.; Krutzke, J.; Wilhelm, L.; Laforsch, C. Occurrence of Microplastics in the Hyporheic Zone of Rivers. *Sci. Rep.* **2019**, *9* (1), 1–11.

(82) Karlsson, T. M.; Vethaak, A. D.; Almroth, B. C.; Ariese, F.; van Velzen, M.; Hassellöv, M.; Leslie, H. A. Screening for Microplastics in Sediment, Water, Marine Invertebrates and Fish: Method Development and Microplastic Accumulation. *Mar. Pollut. Bull.* **2017**, *122* (1–2), 403–408.

(83) Courtene-Jones, W.; Quinn, B.; Murphy, F.; Gary, S. F.; Narayanaswamy, B. E. Optimisation of Enzymatic Digestion and Validation of Specimen Preservation Methods for the Analysis of Ingested Microplastics. *Anal. Methods* **2017**, *9* (9), 1437–1445.

(84) Shaw, D. G.; Day, R. H. Colour- and Form-Dependent Loss of Plastic Micro-Debris from the North Pacific Ocean. *Mar. Pollut. Bull.* **1994**, *28* (1), 39–43.

(85) Day, R. H.; Shaw, D. G.; Ignell, S. E. The Quantitative Distribution and Characteristics of Neuston Plastic in the North Pacific Ocean, 1985–88. *Proceedings of the Second International Conference on Marine Debris* **1990**, 247–263 No. April 1989.

(86) Eriksen, M.; Mason, S.; Wilson, S.; Box, C.; Zellers, A.; Edwards, W.; Farley, H.; Amato, S. Microplastic Pollution in the Surface Waters of the Laurentian Great Lakes. *Mar. Pollut. Bull.* **2013**, *77* (1–2), 177–182.

(87) Galgani, F.; Hanke, G.; Werner, S.; Oosterbaan, L.; Nilsson, P.; Fleet, D.; Kinsey, S.; RC, T.; Van Franeker, J.; Vlachogianni, T.; Scoullou, M.; Mira Veiga, J.; Palatinus, A. *Guidance on Monitoring of Marine Litter in European Seas*; **2013**; DOI: 10.2788/99475.

(88) Campbell, S. H.; Williamson, P. R.; Hall, B. D. Microplastics in the Gastrointestinal Tracts of Fish and the Water from an Urban Prairie Creek. *Facets* **2017**, *2*, 395–409.

(89) Lusher, A. L.; Welden, N. A.; Sobral, P.; Cole, M. Sampling, Isolating and Identifying Microplastics Ingested by Fish and Invertebrates. *Anal. Methods* **2017**, *9* (9), 1346–1360.

(90) Roch, S.; Brinker, A. Rapid and Efficient Method for the Detection of Microplastic in the Gastrointestinal Tract of Fishes. *Environ. Sci. Technol.* **2017**, *51* (8), 4522–4530.

(91) Silva, A. B.; Bastos, A. S.; Justino, C. I. L.; da Costa, J. P.; Duarte, A. C.; Rocha-Santos, T. A. P. Microplastics in the Environment: Challenges in Analytical Chemistry - A Review. *Anal. Chim. Acta* **2018**, *1017*, 1–19.

(92) Zhang, S.; Yang, X.; Gertsen, H.; Peters, P.; Salánki, T.; Geissen, V. A Simple Method for the Extraction and Identification of Light Density Microplastics from Soil. *Sci. Total Environ.* **2018**, *616–617*, 1056–1065.

(93) Habib, D.; Locke, D. C.; Cannone, L. J. Synthetic Fibers As Indicators of Municipal Sewage Sludge, Sludge Products, and Sewage Treatment Plant Effluents. *Water, Air, Soil Pollut.* **1996**, *103*, 1–8.

(94) von Moos, N.; Burkhardt-Holm, P.; Koehler, A. Uptake and Effects of Microplastics on Cells and Tissue of the Blue Mussel *Mytilus Edulis* L. after an Experimental Exposure. *Environ. Sci. Technol.* **2012**, *46* (20), 11327–11335.

(95) Maes, T.; Jessop, R.; Wellner, N.; Haupt, K.; Mayes, A. G. A Rapid-Screening Approach to Detect and Quantify Microplastics Based on Fluorescent Tagging with Nile Red. *Sci. Rep.* **2017**, *7* (44501), 1–10.

(96) Hintersteiner, I.; Himmelsbach, M.; Buchberger, W. W. Characterization and Quantitation of Polyolefin Microplastics in Personal-Care Products Using High-Temperature Gel-Permeation Chromatography. *Anal. Bioanal. Chem.* **2015**, *407* (4), 1253–1259.

(97) Elert, A. M.; Becker, R.; Duemichen, E.; Eisentraut, P.; Falkenhagen, J.; Sturm, H.; Braun, U. Comparison of Different Methods for MP Detection: What Can We Learn from Them, and Why Asking the Right Question before Measurements Matters? *Environ. Pollut.* **2017**, *231*, 1256–1264.

(98) Li, J.; Liu, H.; Paul Chen, J. Microplastics in Freshwater Systems: A Review on Occurrence, Environmental Effects, and Methods for Microplastics Detection. *Water Res.* **2018**; 137362.

(99) Fries, E.; Dekiff, J. H.; Willmeyer, J.; Nuelle, M. T.; Ebert, M.; Remy, D. Identification of Polymer Types and Additives in Marine

Microplastic Particles Using Pyrolysis-GC/MS and Scanning Electron Microscopy. *Environ. Sci. Process. Impacts* **2013**, *15* (10), 1949–1956.

(100) Hendrickson, E.; Minor, E. C.; Schreiner, K. Microplastic Abundance and Composition in Western Lake Superior As Determined via Microscopy, Pyr-GC/MS, and FTIR. *Environ. Sci. Technol.* **2018**, *52* (4), 1787–1796.

(101) Crawford, C. B.; Quinn, B. Microplastic Identification Techniques. In *Microplastic Pollutants*; Elsevier, 2017; pp 219–267; .

(102) Fischer, M.; Scholz-Böttcher, B. M. Simultaneous Trace Identification and Quantification of Common Types of Microplastics in Environmental Samples by Pyrolysis-Gas Chromatography-Mass Spectrometry. *Environ. Sci. Technol.* **2017**, *51* (9), 5052–5060.

(103) Käßler, A.; Fischer, M.; Scholz-Böttcher, B. M.; Oberbeckmann, S.; Labrenz, M.; Fischer, D.; Eichhorn, K. J.; Voit, B. Comparison of μ -ATR-FTIR Spectroscopy and Py-GCMS as Identification Tools for Microplastic Particles and Fibers Isolated from River Sediments. *Anal. Bioanal. Chem.* **2018**, *410* (21), 5313–5327.

(104) Dümichen, E.; Eisentraut, P.; Bannick, C. G.; Barthel, A. K.; Senz, R.; Braun, U. Fast Identification of Microplastics in Complex Environmental Samples by a Thermal Degradation Method. *Chemosphere* **2017**, *174*, 572–584.

(105) Eisentraut, P.; Dümichen, E.; Ruhl, A. S.; Jekel, M.; Albrecht, M.; Gehde, M.; Braun, U. Two Birds with One Stone - Fast and Simultaneous Analysis of Microplastics: Microparticles Derived from Thermoplastics and Tire Wear. *Environ. Sci. Technol. Lett.* **2018**, *5* (10), 608–613.

(106) Majewsky, M.; Bitter, H.; Eiche, E.; Horn, H. Determination of Microplastic Polyethylene (PE) and Polypropylene (PP) in Environmental Samples Using Thermal Analysis (TGA-DSC). *Sci. Total Environ.* **2016**, *568*, 507–511.

(107) David, J.; Steinmetz, Z.; Kucerik, J.; Schaumann, G. E. Quantitative Analysis of Poly(Ethylene Terephthalate) Microplastics in Soil via Thermogravimetry-Mass Spectrometry. *Anal. Chem.* **2018**, *90*, 8793–8799.

(108) Huppertsberg, S.; Knepper, T. P. Instrumental Analysis of Microplastics—Benefits and Challenges. *Anal. Bioanal. Chem.* **2018**, *410* (25), 6343–6352.

(109) Käßler, A.; Windrich, F.; Löder, M. G. J.; Malanin, M.; Fischer, D.; Labrenz, M.; Eichhorn, K.; Voit, B. Identification of Microplastics by FTIR and Raman Microscopy: A Novel Silicon Filter Substrate Opens the Important Spectral Range below 1300 cm^{-1} for FTIR Transmission Measurements. *Anal. Bioanal. Chem.* **2015**, *407* (22), 6791–6801.

(110) Löder, M. G. J.; Kuczera, M.; Mintening, S.; Lorenz, C.; Gerdt, G. Focal Plane Array Detector-Based Micro-Fourier-Transform Infrared Imaging for the Analysis of Microplastics in Environmental Samples. *Environ. Chem.* **2015**, *12*, 563–581.

(111) Renner, G.; Schmidt, T. C.; Schram, J. Characterization and Quantification of Microplastics by Infrared Spectroscopy. *Compr. Anal. Chem.* **2017**, *75*, 67–118.

(112) Käßler, A.; Fischer, D.; Oberbeckmann, S.; Schernewski, G.; Labrenz, M.; Eichhorn, K. J.; Voit, B. Analysis of Environmental Microplastics by Vibrational Microspectroscopy: FTIR, Raman or Both? *Anal. Bioanal. Chem.* **2016**, *408* (29), 8377–8391.

(113) Hufnagl, B.; Steiner, D.; Renner, E.; Löder, M. G. J.; Laforsch, C.; Lohninger, H. A Methodology for the Fast Identification and Monitoring of Microplastics in Environmental Samples Using Random Decision Forest Classifiers. *Anal. Methods* **2019**, *11* (17), 2277–2285.

(114) Primpke, S.; Lorenz, C.; Rascher-Friesenhausen, R.; Gerdt, G. An Automated Approach for Microplastics Analysis Using Focal Plane Array (FPA) FTIR Microscopy and Image Analysis. *Anal. Methods* **2017**, *9* (9), 1499–1511.

(115) Fuller, S.; Gautam, A. A Procedure for Measuring Microplastics Using Pressurized Fluid Extraction. *Environ. Sci. Technol.* **2016**, *50* (11), 5774–5780.

(116) Schmidt, L. K.; Bochow, M.; Imhof, H. K.; Oswald, S. E. Multi-Temporal Surveys for Microplastic Particles Enabled by a Novel

and Fast Application of SWIR Imaging Spectroscopy – Study of an Urban Watercourse Traversing the City of Berlin, Germany. *Environ. Pollut.* **2018**, *239*, 579–589.

(117) Peez, N.; Janiska, M.; Imhof, W. The First Application of Quantitative ^1H NMR Spectroscopy as a Simple and Fast Method of Identification and Quantification of Microplastic Particles (PE, PET, and PS). *Anal. Bioanal. Chem.* **2019**, *411* (4), 823–833.

(118) Paul, A.; Wander, L.; Becker, R.; Goedecke, C.; Braun, U. High-Throughput NIR Spectroscopic (NIRS) Detection of Microplastics in Soil. *Environ. Sci. Pollut. Res.* **2018**, 1–11.

(119) Corradini, F.; Bartholomeus, H.; Lwanga, E. H.; Gertsen, H.; Geissen, V. Predicting Soil Microplastic Concentration Using Vis-NIR Spectroscopy. *Sci. Total Environ.* **2019**, *650*, 922–932.

(120) Shan, J.; Zhao, J.; Liu, L.; Zhang, Y.; Wang, X.; Wu, F. A Novel Way to Rapidly Monitor Microplastics in Soil by Hyperspectral Imaging Technology and Chemometrics. *Environ. Pollut.* **2018**, *238*, 121–129.

(121) Karlsson, T. M.; Grahn, H.; Van Bavel, B.; Geladi, P. Hyperspectral Imaging and Data Analysis for Detecting and Determining Plastic Contamination in Seawater Filtrates. *J. Near Infrared Spectrosc.* **2016**, *24* (2), 141–149.

(122) Serranti, S.; Palmieri, R.; Bonifazi, G.; Cózar, A. Characterization of Microplastic Litter from Oceans by an Innovative Approach Based on Hyperspectral Imaging. *Waste Manage.* **2018**, *76* (March), 117–125.

(123) Woodall, L. C.; Gwinnett, C.; Packer, M.; Thompson, R. C.; Robinson, L. F.; Paterson, G. L. J. Using a Forensic Science Approach to Minimize Environmental Contamination and to Identify Microfibres in Marine Sediments. *Mar. Pollut. Bull.* **2015**, *95* (1), 40–46.

(124) Carter, M. R.; Gregorich, E. G. *Soil Sampling and Methods of Analysis*; CRC Press, 2007.

(125) Duis, K.; Coors, A. Microplastics in the Aquatic and Terrestrial Environment: Sources (with a Specific Focus on Personal Care Products), Fate and Effects. *Environ. Sci. Eur.* **2016**, *28* (1), 1–25.

Cover Sheet: Supporting Information

Manuscript: Finding Microplastics in Soils - A Review of Analytical Methods

Authors: Julia N. Möller¹, Martin G.J. Löder¹ and Christian Laforsch^{1*}

Affiliations

1. Department of Animal Ecology I and BayCEER, University of Bayreuth, Bayreuth, Germany.

* Corresponding author:

Name: Christian Laforsch

Address: Department of Animal Ecology I
University of Bayreuth
Universitätsstraße 30, 95447 Bayreuth

Phone: +49-921-55-2650

Fax: +49-921-55-2784

E-mail: christian.laforsch@uni-bayreuth.de

The supporting Information consists of a single table (Table S1) that ranges over three pages from S1-S3. On page S1 there is an additional short description of the table and how readers can interpret its contents. On page S4 the respective references are given. In total, there are four pages (S1-S4).

1 Supporting Information

2 Table S1 summarizes sampling strategies used in the few published studies analysing
 3 microplastic contamination in terrestrial soils. To date, no sampling standard has been
 4 derived for monitoring microplastic abundance in soils ^{1,2}, therefore laboratories around
 5 the globe have individually developed their own sampling method, rendering the results
 6 of the studies incomparable to each other. The following table gives examples of
 7 possible sampling techniques used in recent literature.

8 *Table S1: Sampling methods used for MP analysis in soils in recent scientific literature*

Research question	Matrix	Sampling Method	Reference
Quantifying the extent of MP pollution along the Shandong (China) coastline and identify a correlation between the occurrence of MP and different intensive human activities	Coastal soils	Nr. of samples: 120 Mass per sample: 4 kg Nr. of sites: 53 along >3000 km coastline Sample point Area: n.d. Soil depth: 0-2 cm Method: Simple random sampling 2-3 replicates per site, taken randomly using multipoint mixed method along intertidal zone using a stainless steel shovel.	³
Developing a method of identifying, quantifying and measuring MPs in soil and evaluating the extent of MP contamination in Swiss floodplain soils	Floodplain soils	Nr. of samples: 87 Mass per sample: n.d. Nr. of sites: 29 Sample point area: 8 cm x 8 cm Soil depth: 0-5 cm Method: Transect sampling 0,5-1 m above max. waterline, 3 composite samples per site composed of 5	⁴

of protected areas (no evident anthropogenic pollution)		subsamples collected in intervals of 4m parallel to the river. The three parallel lines were distanced 1 m apart (i.e. 1 m, 2 m, 3 m away from the high water line). Steel tools.	
Investigation of microplastic pollution in agricultural (vegetable-crop) soils around Shanghai's suburbs	Agricultural soil	<p>Nr. of samples: 120 duplicate samples</p> <p>Mass per sample: 1 kg</p> <p>Nr. of sites: 20</p> <p>Sample point area: 50 cm x 50 cm</p> <p>Soil depth: 0-3 cm & 3-6 cm</p> <p>Method: n.d.</p> <p>At each of the 20 sites 3 duplicate samples were taken with a depth up to 3 cm and 3 duplicate samples were taken with a depth from 3-6 cm in a sample point of 0,5 x 0,5 m².</p>	5
Investigation of the abundance and distribution of MPs in soil aggregate fractions	Agricultural soil and soil of a riparian forest	<p>Nr. of samples: 50</p> <p>Mass per sample: n.d.</p> <p>Nr. of sites: 5</p> <p>Sample point area: 30 m x 5 m</p> <p>Soil depth: 0-5 cm & 5-10 cm</p> <p>Method: Random sampling</p> <p>At each site 30 m x 5 m plots were set, in which randomly 6 subsamples per sample were taken with a spade. 5 samples for each depth.</p>	6
Investigation of plastic pollution in home gardens in Mexico, with a specific focus	Garden soil in small agroforestry land-use	<p>Nr. of samples: 100</p> <p>Mass per sample: 50 g</p> <p>Nr. of sites: 10</p> <p>Sample point area: n.d.</p>	7

on the transfer of low-density polymers through a terrestrial food web (soil, earthworms, chickens)	systems of Mexican homesteads	Soil depth:0-10 cm & 10-20 cm Method: n.d. 5 samples per garden at a depth of 0-10 cm and 5 samples per garden at a depth of 10-20 cm were taken	
Analysing different soil conditioners for the abundance, form and type of MP contamination	Compost, (liquid agricultural digestate not included here)	Nr. of samples: 6 Vol. per sample: 3 litres Nr. of sites: 2 Sample point area: n.d. Soil depth: n.d. Method: Transect sampling 4 x 0,75 litre subsamples at a constant height of each processing heap in the plants were taken and pooled	8
Assessing microplastic contamination of a conventionally treated field in southern Germany	Agricultural soil	Nr. of samples: 14 Vol. per sample: 5 litres Nr. of sites: 1 Sample point area: 32 cm x 32 cm Soil depth: 0-5 cm Method: Transect sampling Each sample was taken from an area of 32 cm x 32 cm with a depth of 5 cm along one of two transects in the field	9

References:

- (1) Chae, Y.; An, Y. Current Research Trends on Plastic Pollution and Ecological Impacts on the Soil Ecosystem: A Review. *Environ. Pollut.* **2018**, *240*, 387–395; DOI S0269749117348637.
- (2) Costa, M. F.; Pinto da Costa, J.; Duarte, A. C. “Sampling of Micro(Nano)Plastics in Environmental Compartments: How to Define Standard Procedures?” *Curr. Opin. Environ. Sci. Heal.* **2018**, *1*, 36–40; DOI 10.1016/j.coesh.2017.10.001.
- (3) Zhou, Q.; Zhang, H.; Fu, C.; Zhou, Y.; Dai, Z.; Li, Y.; Tu, C.; Luo, Y. The Distribution and Morphology of Microplastics in Coastal Soils Adjacent to the Bohai Sea and the Yellow Sea. *Geoderma* **2018**, *322*, 201–208; DOI 10.1016/j.geoderma.2018.02.015.
- (4) Scheurer, M.; Bigalke, M. Microplastics in Swiss Floodplain Soils. *Environ. Sci. Technol.* **2018**, *52* (6), 3591–3598; DOI 10.1021/acs.est.7b06003.
- (5) Liu, M.; Lu, S.; Song, Y.; Lei, L.; Hu, J.; Lv, W.; Zhou, W.; Cao, C.; Shi, H.; Yang, X.; He, D. Microplastic and Mesoplastic Pollution in Farmland Soils in Suburbs of Shanghai, China. *Environ. Pollut.* **2018**, *242* (July), 855–862; DOI 10.1016/j.envpol.2018.07.051.
- (6) Zhang, G. S.; Liu, Y. F. The Distribution of Microplastics in Soil Aggregate Fractions in Southwestern China. *Sci. Total Environ.* **2018**, *642*, 12–20; DOI 10.1016/j.scitotenv.2018.06.004.
- (7) Huerta Lwanga, E.; Mendoza Vega, J.; Ku Quej, V.; Chi, J. de los A.; Sanchez del Cid, L.; Chi, C.; Escalona Segura, G.; Gertsen, H.; Salánki, T.; van der Ploeg, M.; Koelmans A. A.; Geissen V. Field Evidence for Transfer of Plastic Debris along a Terrestrial Food Chain. *Sci. Rep.* **2017**, *7* (1), 1–7; DOI 10.1038/s41598-017-14588-2.
- (8) Weithmann, N.; Möller, J. N.; Löder, M. G. J.; Piehl, S.; Laforsch, C.; Freitag, R. Organic Fertilizer as a Vehicle for the Entry of Microplastic into the Environment. *Sci. Adv.* **2018**, *4* (4), 1–7; DOI 10.1126/sciadv.aap8060.
- (9) Piehl, S.; Leibner, A.; Löder, M. G. J.; Laforsch, C.; Bogner, C. Identification and Quantification of Macro- and Microplastics on an Agricultural Farmland. *Sci. Rep.* **2018**, *8* (17950), 1–9; DOI 10.1038/s41598-018-36172-y.

Article 2



Microplastic sample purification methods - assessing detrimental effects of purification procedures on specific plastic types



Microplastic sample purification methods - Assessing detrimental effects of purification procedures on specific plastic types



Isabella Schrank ^{a,1}, Julia N. Möller ^{a,1}, Hannes K. Imhof ^a, Oliver Hauenstein ^b, Franziska Zielke ^a, Seema Agarwal ^b, Martin G.J. Löder ^a, Andreas Greiner ^b, Christian Laforsch ^{a,*}

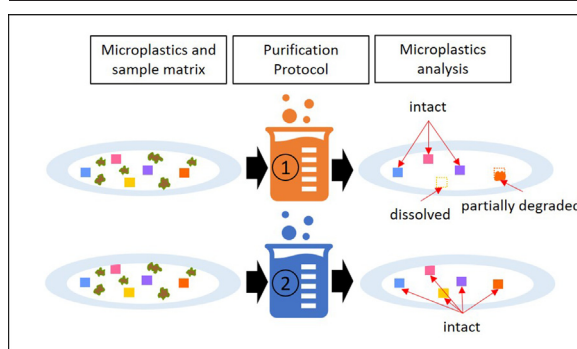
^a Department of Animal Ecology I and BayCEER, University of Bayreuth, Universitätsstr. 30, 95440 Bayreuth, Germany

^b Macromolecular Chemistry II, University of Bayreuth, Universitätsstr. 30, 95447 Bayreuth, Germany

HIGHLIGHTS

- Purification protocols tested for damage on eight plastic analytes
- Plastics affected by treatment with NaOH, HNO₃, H₂SO₅ and H₂O₂
- Fenton's reagent; ZnCl₂-brine and enzymatic digestion do not affect common plastics.
- Experimental results are corroborated by extensive literature review.

GRAPHICAL ABSTRACT



ARTICLE INFO

Editor: Kevin V Thomas

Keywords:

Microplastics analysis
Purification protocol
Plastic degradation
FTIR
GPC

ABSTRACT

In search of effective, fast, and cheap methods to purify environmental samples for microplastic analysis, scientific literature provides various purification protocols. However, while most of these protocols effectively purify the samples, some may also degrade the targeted polymers. This study was conducted to systematically compare the effects of purification protocols based on acidic, alkaline, oxidative, and enzymatic digestion and extraction via density separation on eight of the most relevant plastic types. It offers insights into how specific purification protocols may compromise microplastic detection by documenting visible and gravimetric effects, analyzing potential surface degradation using Fourier transform infrared spectroscopy (FTIR) and bulk erosion on a molecular level using gel permeation chromatography (GPC). For example, protocols using strong acids and high temperatures are likely to completely dissolve or cause strong degradation to a wide range of polymers (PA, PC, PET, PS, PUR & PVC), while strong alkaline solutions may damage PC and PET. Contrarily, Fenton's reagent, multiple enzymatic digestion steps, as well as treatment with a zinc chloride solution frequently used for density-separation, do not degrade the eight polymers tested here. Therefore, their implementation in microplastic sample processing may be considered an essential stepping-stone towards a standardized protocol for future microplastics analyses.

* Corresponding author.

E-mail address: christian.laforsch@uni-bayreuth.de (C. Laforsch).

¹ Shared first authorship.

1. Introduction

The contamination of the environment with plastic debris has become a ubiquitous issue. It is in the focus of many studies examining marine (See et al., 2020; Díaz-Mendoza et al., 2020; Barboza and Gimenez, 2015; Botterell et al., 2019; Browne et al., 2015), freshwater (Wagner and Lambert, 2018; Li et al., 2018a; Dris et al., 2018) as well as terrestrial ecosystems (Sarker et al., 2020; Piehl et al., 2018; He et al., 2018; Bläsing and Amelung, 2018). Microplastic has become the focal point of scientific and public interest (Li et al., 2018a; Crawford et al., 2017; Science Advice for Policy by European, 2019; Chae and An, 2018; Li, 2018). An often used and historical size definition defines microplastic as plastic particles smaller than 5 mm (Arthur et al., 2009). However, the authors here prefer the definition by Hartmann et al. (Hartmann et al., 2019) which specifically defines microplastic as particles between 1 μm and 1 mm.

Due to the omnipresence and longevity of the minuscule synthetic particles, microplastics accumulate in the environment and may pose potential hazards for ecosystems and organisms with widely unknown implications for human health. Thus, scientists and policymakers are showing increasing interest in monitoring the occurrence of microplastics to assess their potential risks. However, to enable comprehensive monitoring of microplastics in the environment, a standard operating procedure for the identification and quantification of microplastics is needed but does not – as of now – exist (Wagner and Lambert, 2018; Zhao et al., 2018; Braun et al., 2018; de Souza Machado et al., 2018; Müller et al., 2020). In the past few years, a general scientific consensus has been achieved that microplastic identification based on visual characteristics alone is highly prone to misidentification and should thus be superseded by more reliable chemical identification (Hidalgo-Ruz et al., 2012; Löder and Gerdt, 2015; Ivleva, 2021). Especially for particles below a certain size, usually 500 μm (Möller et al., 2020), chemical verification is indispensable. Additionally, the identification of polymer types may be of consequence for source identification and risk assessment. A wide range of analytical methods from vibrational spectroscopy (e.g., Fourier Transform Infrared (FTIR)-microspectroscopy, Raman microspectroscopy) to mass spectrometry (e.g., pyrolysis-gas chromatography–mass spectrometry (Pyr GC–MS) and thermal extraction desorption gas chromatography–mass spectrometry (TED-GC–MS)) are available. While mass spectrometric methods allow the quantification of the total mass content of synthetic polymers in a sample (Zarfl, 2019; Fischer and Scholz-Böttcher, 2019; Möller et al., 2021), vibrational spectroscopic methods provide the identification and enumeration of single particles down to the lower micrometer range (Möller et al., 2021; Primpke et al., 2020; Anger et al., 2018). The latter is important for risk assessment since particle properties such as size and shape may account for adverse effects (Wagner and Lambert, 2018; Dris et al., 2018; Ramsperger et al., 2020). However, both analytical strategies struggle with the high content of organic and inorganic matter in an environmental sample, disrupting the analysis by covering and shielding the analyte or causing interferences during measurements (Käppler et al., 2016; Löder et al., 2017). Additionally, biofouling can interfere with spectroscopic methods (Löder and Gerdt, 2015; Zhao et al., 2017). Therefore, a prerequisite for a reliable analysis of microplastic from environmental samples is removing the sample matrix by a purification procedure that does not negatively affect the microplastic particles themselves. An additional benefit of these purification procedures is the accompanying pre-concentration of the microplastic particles.

To date, various sample purification methods have been developed to remove the natural sample matrix, often combining a density separation to remove the bulk mineral fraction and a chemical digestion step to eliminate the remaining organic matter from the sample (Herrera et al., 2018; Hurley et al., 2018; Miller et al., 2017). A very different approach that will not be surveyed in this study but should be mentioned at this point is the solvent extraction of microplastics from environmental samples. Here, the objective is not to remove the surrounding matrix but to extract the analyte-plastics in an organic solvent, which is then separated from the matrix and later used in the analysis (Thomas et al., 2020). This approach

inherently destroys the solid-state of plastics and prevents the use of particle-quantitative analysis methods. As the information on microplastics' size and shape are ecologically relevant (de Souza Machado et al., 2019), this approach will not be addressed here. We will solely concentrate on methods that aim to purify samples without altering the microplastic particles' integrity.

Depending on the sample matrix and the aim of the research, several sample purification methods with different advantages and disadvantages are available: Strong acids (Imhof et al., 2016; Cole et al., 2014; Claessens et al., 2013), alkaline solutions (e.g. Karami et al., 2017; Dehaut et al., 2016), oxidation agents (e.g. hydroxide peroxide or Fenton's reagent, Zhao et al., 2017; Tagg et al., 2017) as well as enzymes (e.g., Löder et al., 2017; Cole et al., 2014; Courtene-Jones et al., 2017; Catarino et al., 2018) or combinations of the methods mentioned above (Möller et al., 2021). The main differences occur in the digestion efficiency of the matrix, aggressiveness against plastics, the complexity of the methods (number of steps involved), and the time necessary. Often the digestion efficiency and the time effort are the main drivers to choose a specific purification method. However, the effects on the different plastic materials are often not sufficiently tested, or validation experiments are often solely based on gravimetry and/or visual inspection of larger fragments, that may not represent small microplastics.

Hence, this study aims to overview the different currently used sample purification methods, their applicability for environmental samples, and already proven degenerative effects on synthetic polymers. Secondly, we seek to provide a comprehensive investigation of seven selected sample purification methods on standardized films of the eight most common plastic types with a large surface and a small thickness to resemble microplastic as well as possible while maintaining the possibility of using a wide variety of analytical methods: (I) the degradation of the films was analyzed by gravimetric and visual inspection as frequently used for validation in previous studies; (II) we additionally used measurements of bulk erosion and polymer fragmentation by gel permeation chromatography (GPC) which provides a direct measurement on polymer chain degradation, and can therefore give insights into the degradative effect of a sample purification method on small particles; (III) further, attenuated total reflection Fourier transform infrared (ATR-FTIR) spectroscopy was applied, to analyze molecular changes on the surface of a specific plastic material.

These analyses should discern which protocols are suitable for the purification of environmental samples and cause unwarrantable changes to the analyte plastics. The results of this study are accompanied by extensive literature research bringing together all currently available studies which evaluated sample processing and purification protocols. This integrative approach might be the first step towards developing a universally applicable standard operation procedure for the extraction and purification of samples during microplastic monitoring.

2. Materials and methods

2.1. Plastic film production

In order to assess visual integrity and to have enough cohering material for the experimental analyses, we decided to use relatively thin plastic films as reference material (100 μm). The large surface area allows simple handling and reduces the probability of accidental loss (e.g. by particles sticking to filtration funnels). At the same time, the thickness of just 100 μm will ensure that degrading processes become evident quickly (high surface area to volume ratio). The raw material (granulate) of the eight plastics, low density-polyethylene (LD-PE), polypropylene (PP), polyethylene terephthalate (PET), polyvinylchloride (PVC), polyurethane (PUR), polycarbonate (PC), polystyrene (PS), and polyamide (PA6) was pressed into films of 100 μm thickness using a hydraulic press (Carver Model #3925, Inc. Laboratory Equipment, USA). For a detailed description of the polymers, including trade name, density, mean film weight, glass transition temperature, and melting temperature, please see Table S1. These films were cut into squares of 10 \times 10 mm by a razor blade (Fig. S1). Each

quadratic film was stored in a pre-cleaned glass vial which was covered by aluminum foil.

2.2. Experimental procedure

To analyze the extent of chemical degradation caused by current sample purification methods, the films of the selected plastics underwent each of the eight treatments (including control) in triplicates. Before and after undergoing the treatments, the films were visually analyzed for apparent corrosion (higher transparency, jagged edges, change in color, change in shape). ATR-FTIR spectrometry was used to identify changes in surface chemistry, measurement of dry weight, and gel permeation chromatography (GPC) was used to assess changes in the molecular weight distribution. Due to a potential surface change when pressing the sample on the ATR-crystal during ATR-FTIR analysis, the ATR-FTIR pre-treatment examinations were performed on a separate set of blank films, which were then compared to the films that underwent the treatments. For all other analytical methods, pre-treatment and post-treatment examinations were carried out with the same set of films. An overview of the experimental procedure is given in Fig. 1.

In order to document the pre-treatment conditions, the films were rinsed with filtered de-ionized water and dried in their respective reaction vials covered with aluminum foil at 50 °C under vacuum (10^{-2} mbar) for at least 24 h (Heraeus Instruments Vacutherm, Thermo Fisher Scientific Inc., USA). Before weighing with a set of precision scales (Ohaus Discovery DV215CD, Ohaus Corporation, USA), one edge (0.5–0.8 mg) was removed from each film with a razor blade for GPC analysis. Here the edges of the three replicates per treatment were pooled to gain enough material for the analysis. Subsequently, the films underwent their respective treatments. After that, they were removed from the reaction vials, examined visually and thoroughly rinsed with ultrapure water, then dried at 50 °C under vacuum (10^{-2} mbar) for 24 h. After determining the dry weight, a second edge per film was cut off and pooled for GPC analysis to compare the results with the pre-treatment condition. The remaining film was then analyzed by ATR-FTIR spectroscopy. A detailed description of the analytical methods and treatments is given below. The classification of the disintegration level was based on a classification established by Enders et al. (2017) but was adapted to include not only the recognizable visual changes but also the weight, GPC, and ATR-FTIR measurements (Table 1). The assignment of the disintegration levels to the purification protocols is based on the respective analytical measurement showing the highest effect.

2.2.1. Loss of mass and visual degradation

Chemically induced surface- and bulk erosion is expected to lead to a reduction in mass. Thus the dry weight of each film was determined before and after the treatment. The mass measurements of the vacuum-dried films were performed by a Semi-Micro Analytical Balance (Ohaus Discovery DV215CD, Ohaus Corporation, USA) with $d = 0.01$ mg. We are aware that dry plastic films can carry a static charge that may increase the measuring error, therefore we chose a relatively large deviation margin of 5% of the original film weights as an effect threshold in our reporting. First, each of the three replicate films were weighed individually before and after treatment (original weights ranged from 7.3 mg to 39 mg, dependent on plastic type). Then, the difference in mass was calculated individually and converted to the percentage of the original film weight before treatment. Then the mean mass difference was calculated for each treatment. Additionally, any obvious macroscopic visually discernible degradation of the films (e.g., complete loss, partial loss, fragmentation, change of shape and change in color) was photo-documented under a stereomicroscope (Leica M50, Leica Microsystems, coupled with an Olympus DP 26 camera, Olympus Corporation).

2.2.2. Bulk erosion and polymer fragmentation: molecular weight and molecular weight distribution

The degree of bulk erosion (bulk erosion meaning the degradation occurs evenly throughout the entire polymer film) and polymer fragmentation at the molecular level was evaluated using the molecular weight and the molecular weight distribution, analyzed by gel permeation chromatography (GPC) on an Agilent 1200 system with a refractive index (RI) detector for PS, PC, PET, PA6, PVC, and PUR. PE and PP were analyzed by high-temperature gel permeation chromatography (HT-GPC) on an Agilent (Polymer Laboratories Ltd.) PL-GPC 220 high-temperature chromatographic unit equipped with DP (differential pressure) and RI detectors and four linear mixed bed columns (3 x PSS Polefin linear XL + 1 guard column). For a detailed description of the application and the used solvents, please refer to the Supplementary Information.

2.2.3. Surface alterations: attenuated total reflection Fourier transform infrared (ATR-FTIR) spectroscopy

Potential chemical changes on the surface of the films were analyzed by ATR-FTIR spectroscopy to visualize alterations of the plastic material, such as the formation of functional groups (e.g., hydroxyl groups). The films were probed using a “Tensor 27” FTIR spectrometer equipped with an ATR unit (Bruker Optik GmbH, Germany). To identify polymer alterations, we focused on the spectral region between 1800 and 1500 cm^{-1} (Fig. 3).

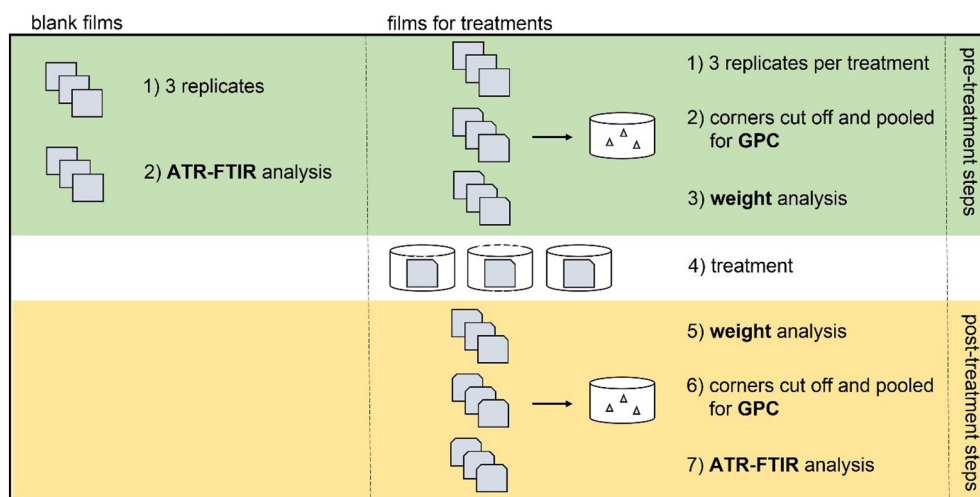


Fig. 1. Overview of the experimental procedure. For each polymer type, a triplicate of blank films was used for the pre-treatment ATR-FTIR analysis. Another triplicate of films for each polymer type underwent the treatments including control with ultrapure water and was used for all other pre- (GPC, weight) and post-treatment (weight, GPC, ATR-FTIR) analytical methods.

Table 1

The disintegration caused by different microplastic purification methods was classified based on disintegration levels introduced by Enders et al. (2017). The original levels were adopted to include weight, bulk changes (e.g., GPC, DSC), and surface alterations (spectroscopic methods like FTIR/Raman) besides noticeable visual changes. Thus, treatment classification is always based on the highest disintegration level. In addition, the adopted classification system was also used to classify the effects of purification approaches found in already published literature.

Disintegration level	Visually recognizable changes	Weight reduction/loss	Surface alterations (changes in FTIR/Raman spectra)	Bulk changes (changes in GPC chromatogram)
L0	No effect	0 – 5%	No effect	No effect
L1	Color changes, beginning surface erosion	6 - 25%	Weak changes: Increased or decreased peak intensity; reduced peak sharpness	Weak shift
L2	Morphological changes and early stage of disintegration	26 – 50%	Significant changes: Additional bands or reduction of bands	Significant shift
L3	Strong morphological changes, loss/change of bulk structure	51 – 75 %	Significant changes with gravimetric manifestation	Significant shift with gravimetric manifestation
L4	Complete dissolution/disintegration	76%-100%	Measurement not possible due to dissolution	Measurement not possible due to dissolution

For a detailed description of the ATR-FTIR spectrometer and measurement settings, please refer to the Supplementary Information.

2.3. Treatments

2.3.1. Control

15 ml ultrapure water was added to each replicate glass vial containing one respective plastic film as a control. The samples were incubated for 13 days, and 5 h in a climate chamber at 20 °C. The duration of this treatment is analogous to that of the enzymatic digestion protocol, the most prolonged treatment conducted in this study.

2.3.2. Alkaline: sodium hydroxide (NaOH)

Alkaline digestion is a hydrolytic process rendering solid biogenic matter (e.g., proteins, lipids, and some carbohydrates) into an aqueous solution of low molecular compounds and was therefore applied in several studies quantifying microplastic in environmental samples (e.g., Karami et al., 2017; Dehaut et al., 2016; Braun et al., 2021). Alkaline digestion is specifically suited for the maceration of animal tissue, as large carbohydrate molecules such as cellulose are resistant to alkaline hydrolysis (Thacker and Kastner, 2004). Furthermore, maceration can be performed with NaOH or KOH, whereas KOH is the more potent maceration agent (Gibb, 2015).

In this survey, 15 ml of sodium hydroxide solution (50%) was added to the glass vials containing the polymer films and incubated for 7 days at room temperature (~20.5 °C) based on a protocol introduced by Nuelle et al. (2014). However, there are other, more recent studies using high NaOH concentrations for the reduction of biogenic matter before microplastics analysis (Ibrahim et al., 2017).

2.3.3. Acidic: hot nitric acid (HNO₃) and peroxymonosulfuric acid (H₂SO₅)

Acids of different strengths have been used in microplastic research to treat environmental samples. Therefore, we selected two of them to cover the entire spectrum of available and applied acids.

Nitric acid, for example, is a strong mineral acid and, in higher concentrations, a strong oxidizing agent. Therefore, it is well suited for the relatively quick destruction of biogenic matter and is often the method of choice for pre-treating organic samples for diverse analytical examinations. To test the degradative potential of nitric acid, 10 ml of nitric acid (69%, 15,7 M, Sigma-Aldrich Co., USA) were added to each reaction vial

containing one film. Next, the reaction vials were heated in a heating block until boiling. After 2 h, the glass vials were filled with warm ultrapure water and filtered over a stainless-steel mesh to recover the film or its remains. Hot nitric acid treatment has been used in several protocols to digest biota (Claessens et al., 2013; Van Cauwenberghe and Janssen, 2014).

A much stronger acid than nitric acid is Peroxymonosulfuric acid, generated by mixing hydrogen peroxide with sulfuric acid. This strong oxidizing agent was used to efficiently remove the high amount of organic impurities in studies examining the contamination of lake sediments before Raman spectroscopy analysis (Imhof et al., 2016; Imhof et al., 2018; Imhof et al., 2013) and for river sediments before infrared spectroscopy and visual inspection (Klein et al., 2015). The H₂SO₅ was prepared directly before the application by mixing hydrogen peroxide (30%) with sulfuric acid (98%) dropwise to a ratio of 3:1 until bubbles were visible. Then, 15 ml of the stock solution were added into the replicate glass vials and incubated for 48 h at room temperature (~20.5 °C).

2.3.4. Enzymatic: sequential enzymatic digestion

The use of an enzyme for the gentle purification of organic-rich samples for microplastic analysis was first described by Cole et al. (2014), who used the proteolytic enzyme Proteinase-K to digest marine zooplankton samples. Due to increasing sample complexity and high costs for Proteinase-K, the idea of enzymatic digestion was taken up and further developed (Löder et al., 2017; Courtene-Jones et al., 2017; Catarino et al., 2018). In this survey, the enzymatic digestion protocol of Löder et al. (2017) was used, as adaptations of this method were already applied by several studies (Möller et al., 2021; Mintenig et al., 2017; Mani et al., 2015; Dris et al., 2015; Kumar et al., 2021) to remove organic material from environmental samples without the use of strong acidic or alkaline treatments. Using technical grade enzymes combined with intermittent oxidation steps with hydrogen peroxide provides sufficient purification of most aquatic samples to allow for subsequent analysis with vibrational spectroscopy methods. The individual reagents were added sequentially to the glass vials containing the respective films. Then they were incubated at the given temperature. After each incubation, the films were removed, and both the film and the vial were rinsed with ultrapure water. Finally, the reagent of the next step was added before the film was set back into the vial. The list of reagents, incubation time, temperature, and pH is given in Table S2 in the

Supplementary Information. Likewise, the protocols for the production of both buffers are available in the Supplementary Information.

2.3.5. Oxidative: hydrogen peroxide (H_2O_2)

Hydrogen peroxide (H_2O_2) is a strong oxidizing agent known to break down organic matter. It is often used as an oxidation agent to prepare various environmental samples (Zhao et al., 2017; Nuelle et al., 2014; Liu et al., 2018; Tagg et al., 2015). Hydrogen peroxide is also used in the enzymatic digestion protocol and may potentially degrade specific synthetic polymers (Bürkle GmbH, 2011). Therefore, hydrogen peroxide was tested on its own at a concentration of 30%. First, 15 ml were added to each replicate glass vial, covered by aluminum foil, and incubated for 24 h at 37 °C. Then the film was removed, rinsed with ultrapure water, the hydrogen peroxide was replaced by fresh hydrogen peroxide, and the film was placed back into the glass vial for another 24 h at 37 °C. This procedure was repeated a third time, but this time only for 5 h. This incubation procedure was applied to mimic the hydrogen peroxide steps used in the enzymatic purification protocol of Löder et al. (2017).

2.3.6. Oxidative: Fenton protocol

The Fenton reaction was suggested as a more efficient alternative to the sole application of hydrogen peroxide (Hurley et al., 2018; Tagg et al., 2017; Masura et al., 2015). This application of hydrogen peroxide accompanied by a ferric ion (Fe(III)) catalyst allows the quick decomposition of biogenic matter to carboxylic acids, aldehydes, carbon dioxide, and water under relatively mild conditions (Dyachenko et al., 2017).

The Fenton protocol was conducted as follows (Masura et al. (2015)): 20 ml of a 0.05 M $FeSO_4$ solution and 20 ml H_2O_2 (30%) were added to test tubes containing one film each. The mixture was amber in color. The test tubes were heated in a heating block at 75 °C. As soon as gas bubbles appeared at the surface, the heating block was turned off, but the exothermic reaction was allowed to continue in the warm block until the solution color turned from amber to yellow (1.5–2 h). Exothermic reactions of this kind can peak to temperatures of around 90 °C (Al-Azzawi et al., 2020).

2.3.7. Zinc chloride ($ZnCl_2$) solution

Density separation procedures with highly dense brines are often used as a sample preparation step before microplastic analysis, either to extract the microplastics from a sediment or soil sample (Möller et al., 2020; Quinn et al., 2017; Coppock et al., 2017) or to remove mineral suspended matter from water samples (Rodrigues et al., 2018).

Dense brines such as aqueous solutions of zinc chloride, sodium iodide, or calcium chloride are often used to achieve a density of 1.6–1.8 $g\ cm^{-3}$ (Zhao et al., 2017; Herrera et al., 2018; Hurley et al., 2018; Miller et al., 2017; Coppock et al., 2017; Hamm et al., 2018).

Zinc chloride was used exemplarily to verify the effects of common density separation fluids on the examined polymer types. Here, 15 ml of zinc chloride stock solution with a density of 1.8 $g\ cm^{-3}$ was added into 20 ml glass vials, covered with aluminum foil, and incubated for 48 h at room temperature (~20.5 °C).

3. Results

The effects of seven different purification approaches based on acidic, alkaline, oxidative, and enzymatic digestion and the extraction via density separation on eight of the most relevant plastic types evaluated with three different methods are compiled in Fig. 4. In the following paragraphs, results for each of the three parameters are given. To conclude, we present the results of an extensive literature review of currently published studies evaluating the effects of purification protocols on plastic particles.

3.1. Weight and visual degradation

The application of hot nitric acid, sodium hydroxide, and peroxymonosulfuric acid (H_2SO_5) resulted in a severe and visually apparent disintegration of specific polymer types (Fig. 4 & Fig. S2). For the other

treatments, no distinct visually identifiable effects were detected. The average mass losses were strongly associated with a visible disintegration – only those films that showed visible degradation also showed a significant loss in mass. For all other treatments, the mass loss was below 5% (Table 2).

The hot nitric acid protocol (69%, 15.7 M HNO_3 , ~85 °C) destroyed all PA6 and PUR films (Fig. S2), leaving a transparent, colorless or clear yellow liquid, respectively. PET was disintegrated into a white precipitate, and the PS and PC films were reduced to small yellowish beads with a mean mass loss of 35.5% and 67.5%, respectively (Table 2 & Fig. S2). In addition, a deformation of the LDPE films was observed, but with no significant loss of mass.

The sodium hydroxide treatment (50% NaOH, 7 days 20.5 °C) dissolved two PC replicates completely into a clear and colorless solution, while the third replicate was found swollen and fragmented. As a result of the alkaline treatment, the PET films became thinner, more transparent, and showed an average mass reduction of 68.3% (Table 2 & Fig. S2).

Peroxymonosulfuric acid led to the degradation of PUR to a yellowish residue (Fig. S2) and severe frothing and fragmentation of PA6.

3.2. Bulk erosion and polymer fragmentation: molecular weight and molecular weight distribution

The GPC analysis was only conducted for films that were not morphologically altered during the exposure to specific treatments. However, certain optically intact films exposed to specific treatments display an apparent negative shift in the average molecular weight distribution compared to the control, which is an indicator for the degradation of the polymer (Figs. 2 & 4).

Hot nitric acid caused significant molecular degradation of PE and PP, as evidenced by the shifting of GPC curves to the lower mass region. The GPC of PET after treatment with sodium hydroxide showed no significant change in the molecular weight and molecular weight distribution compared to the pristine PET despite a significant weight loss as seen by weighing the sample before and after treatment. The hydrogen peroxide treatment and the enzymatic digestion (which also utilizes intermittent hydrogen peroxide steps) caused a measurable degradation of PA, while the Fenton treatment showed no effect on any of the polymers.

The use of zinc chloride resulted in the broadening of GPC curves which might be due to the complexation of $ZnCl_2$ with PUR. On the other hand, treatments with peroxymonosulfuric acid and sodium hydroxide did not show any evident shift in the molecular masses of the respective plastic films that remained after the treatment.

3.3. ATR-FTIR

Additional functional groups were formed for PE and PP after the treatment with nitric acid (Figs. 3 & 4). For both plastics, additional peaks were visible between 1800 and 1500 cm^{-1} (Fig. 3, panels A and C), indicating carbonylated compounds formation (Bäckström et al., 2017). The treatment combinations of PA6- HNO_3 , PA6- H_2SO_5 , PC- HNO_3 , PC-NaOH, PET- HNO_3 , PS- HNO_3 , PUR- HNO_3 and PUR- H_2SO_5 led to a complete loss of the polymer films or the films were too damaged to allow a follow-up ATR-FTIR measurement. The polymer films in the treatment combinations PA6- H_2O_2 , PA6-Enzymatic digestion and PUR- $ZnCl_2$ showed weak changes in the GPC analysis, but none in the ATR-FTIR spectra (Fig. 3, panels E, F, G). PET-NaOH films on the other hand showed a significant reduction in weight, but no alterations in the GPC analysis, nor in the ATR-FTIR spectra (Fig. 3, panel H).

3.4. Overview of published purification protocols

The available literature was screened for papers evaluating sample purification methods, and the results were classified in the same degradation levels as described in Table 1 and compared to the evaluation of purification methods performed during this study. Although not all studies evaluated the assessed methods with comparable polymers, particles, size

Table 2

Average changes in the mass of examined polymers after being exposed to different sample purification protocols. Only changes in mass are represented when the effect threshold of 5% for L1 was exceeded. The level of degradation is depicted in the same color scale as shown in Table 1, where white represents no degradation (L0), and dark red depicts complete degradation (L4). Figures signify the average percentage change in mass \pm standard error. The asterisk * signifies complete disintegration.

	PA6	PC	PE	PET	PP	PS	PUR	PVC
ZnCl ₂	<5%	<5%	<5%	<5%	<5%	<5%	<5%	<5%
Enzymatic digestion	<5%	<5%	<5%	<5%	<5%	<5%	<5%	<5%
H ₂ O ₂	<5%	<5%	<5%	<5%	<5%	<5%	<5%	<5%
Fenton's reagent	<5%	<5%	<5%	<5%	<5%	<5%	<5%	<5%
HNO ₃	*-100%	-35.5 \pm 6.5%	<5%	*-100%	ns	-51.2 \pm 6.6%	*-100%	<5%
H ₂ SO ₅	*-100%	<5%	<5%	<5%	<5%	<5%	*-100%	<5%
NaOH	<5%	*-100%	<5%	-68.3 \pm 12.7%	<5%	<5%	<5%	<5%
Control	<5%	<5%	<5%	<5%	<5%	<5%	<5%	<5%

classes, and protocols, this additional and comprehensive information is designed to complement the results provided by this study (Tables S3–S9). In addition, our study is one of the very few studies that also included GPC in their analysis.

Between 2013 and 2021, 25 studies performed a purification of environmental samples to quantify microplastic and evaluated purification efficiency and the influence on the analyte itself. Some studies evaluated multiple purification protocols. Applied approaches were for example alkaline treatments with NaOH ($n = 7$) and KOH ($n = 11$), acid treatments with HNO₃ ($n = 6$), or HCl ($n = 1$), both in various concentrations. These are accompanied by oxidative protocols solely using hydrogen peroxide ($n = 5$) or the Fenton reaction ($n = 7$), as well as enzymatic approaches ($n = 5$). Also, combinations of different approaches like alkaline and oxidative ($n = 2$), acidic in combination with a second acid, oxidation agents or microwave digestion ($n = 7$), or alkaline, acidic and oxidative ($n = 1$) were applied. Effects of density separation was evaluated based on ZnCl₂ ($n = 4$), NaCl ($n = 1$), sucrose ($n = 1$) and canola oil ($n = 1$).

All observed effects of sample purification protocols were categorized according to the scheme presented in Table 1, summarized, and compared to the results found in our study (Fig. 5).

Considering the validation of the sequential enzymatic digestion in (B), we would like to note that this was performed by nine consecutive steps, where two steps involved hydrogen peroxide, which caused the L2 level degradation of PA6 only. This could be replaced by Fenton, which does not cause any alterations (Möller et al., 2021).

4. Discussion

Selecting a specific purification method to eliminate organic matter from environmental samples is crucial for reliable microplastic particle verification via chemical identification by different vibrational spectroscopic and mass spectrometric techniques. The importance increases if particles down to a few micrometers or the sub-micron range are analyzed. To facilitate the selection of an appropriate purification method, we evaluated six commonly used sample purification methods (alkaline, acidic, oxidative, enzymatic digestion, or combinations of the above) and one density separation extraction method (ZnCl₂) using gravimetry, visual inspection, measurement of surface modifications (ATR-FTIR), bulk erosion, and polymer fragmentation (GPC). In addition, we summarized the current published data, discussed the results accordingly, and gave recommendations for sample processing.

4.1. Alkaline sample purification methods

Both sodium hydroxide (NaOH) and potassium hydroxide (KOH) was shown to effectively digest environmental samples, especially animal tissue, in a short time (Karami et al., 2017; Li et al., 2018b; Prata et al., 2019). However, a drawback of the alkaline treatment is the degradation of specific plastic particles, which depends on the exposure duration,

temperature, and concentration of the alkaline solution. In this study, the exposure of the plastics to a 12 M/50% NaOH solution for 7 days at room temperature (20.5 °C) led to a complete dissolution of PC films and a significant loss of weight ($-68.3 \pm 22\%$) of the PET films. However, as no shift in the molecular weight distribution (via GPC) was observed, this indicates the degradation of PET by the surface erosion mechanism. In contrast to the bulk erosion mechanism, where degradation takes place homogeneously throughout the polymer, retaining size but reducing molecular mass, surface erosion is a heterogeneous process, in which the degradation only takes place at the surface, reducing size over time, but not affecting the polymer particle's core. PET is a hydrophobic polymer, and therefore sodium hydroxide first degrades the outer surfaces exposing newer surfaces for the degradation. Likewise, the exposure to 10 M NaOH at higher temperatures and a shorter exposure (60 °C for 24 h) similarly resulted in a significant decrease in size and weight for PC and PET (Hurley et al., 2018; Dehaut et al., 2016). PC and PET have carbonate and ester linkages, so they are susceptible to saponification - the alkaline hydrolysis of these organic functional groups - when exposed to concentrated alkaline solutions. When treated with a diluted alkaline solution, e.g., 1 M NaOH or 10% KOH (at 60 °C), the hydrolytic effect is less severe, but still significant as can be seen in the loss of mass of around 16% for PC particles exposed to 10% KOH for 24 h at 60 °C. Hurley et al. (2018) reported that exposure time and temperature are key factors when considering degenerative effects of alkaline treatments. Here, no visible effects and only slight alterations of the polymer surface were detected by Raman microspectroscopy for ABS, PA, PET, PC, PVC, and PMMA after treatment with highly concentrated (20 M/113%) KOH at 20 °C for 5 h followed by short-term exposure of 20 min at 80 °C. However, the authors did not record potential changes in weight during their experiments.

According to Cole et al. (2014), after the treatment with 10 M NaOH at 60 °C for 24 h PA, PE, and unplasticized PVC were visibly damaged or discolored. We could not confirm these findings, nor were mentions made to this effect by other literature sources (Herrera et al., 2018; Hurley et al., 2018; Dehaut et al., 2016). Nevertheless, the degenerative potential on polyesters in general (which also include polylactic acid (PLA) and cellulose acetate (CA), should always be taken into account before choosing a purification protocol based on alkaline solutions, especially if the goal is to analyze smaller microplastic particles (Kühn et al., 2017). Low temperatures and short exposure periods may reduce damage to microplastics (Munno et al., 2018), but this may also negatively impact the purification effectiveness.

4.2. Acidic sample purification methods

Organic material can be efficiently removed using various acidic sample purification methods. For example, nitric acid (22.5 M) digestion efficiency was described as higher than hypo-chloric acid, hydrogen peroxide, and sodium hydroxide when digesting mussel tissue (Claessens et al., 2013). In 2015 the International Council of the Exploration of the Sea (ICES)

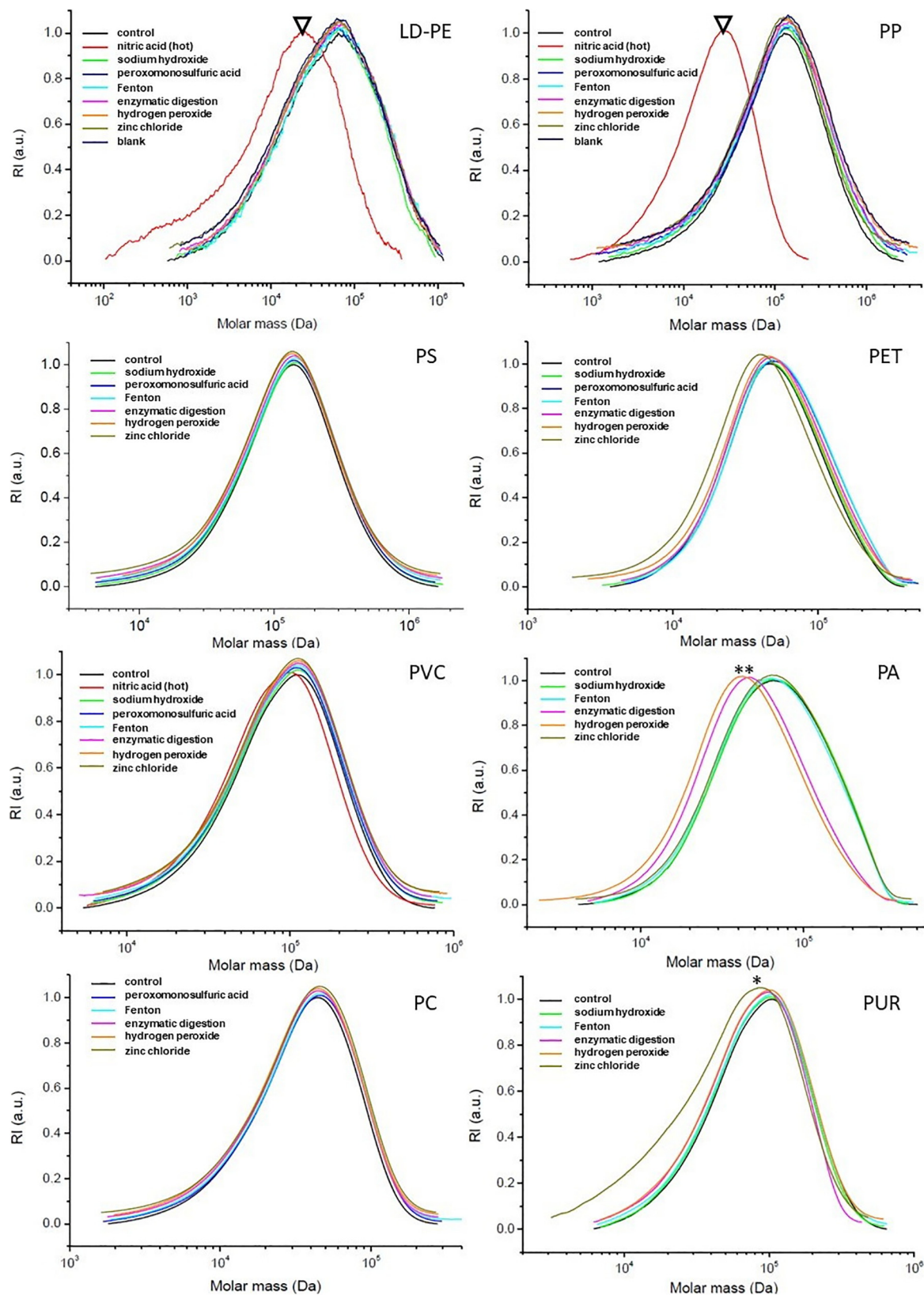


Fig. 2. Determination of the molecular weight distribution as a measurement of bulk erosion by high-temperature GPC for PE and PP and GPC for PC, PUR, PA, PVC, PS, and PET. Significant shifts of the molecular weight distribution are marked with an inverted triangle; weak shifts are marked with an *.

recommended the use of an acid mixture of $\text{HNO}_3:\text{HClO}_4$ (4:1 v:v) to digest organic matter at $>80^\circ\text{C}$ as purification protocol for the monitoring of plastic particles in fish and shellfish (ICES, 2015). However, while the organic matter destruction with acids may be very effective, our study, among

others, has shown that hot nitric acid (80°C , 15.7 M HNO_3 , 2 h) is exceptionally destructive to PA, PET, and PUR, which were entirely dissolved by the procedure. Furthermore, as verified by ATR-FTIR analysis, PE and PP showed a significant shift towards a lower molar mass in the GPC

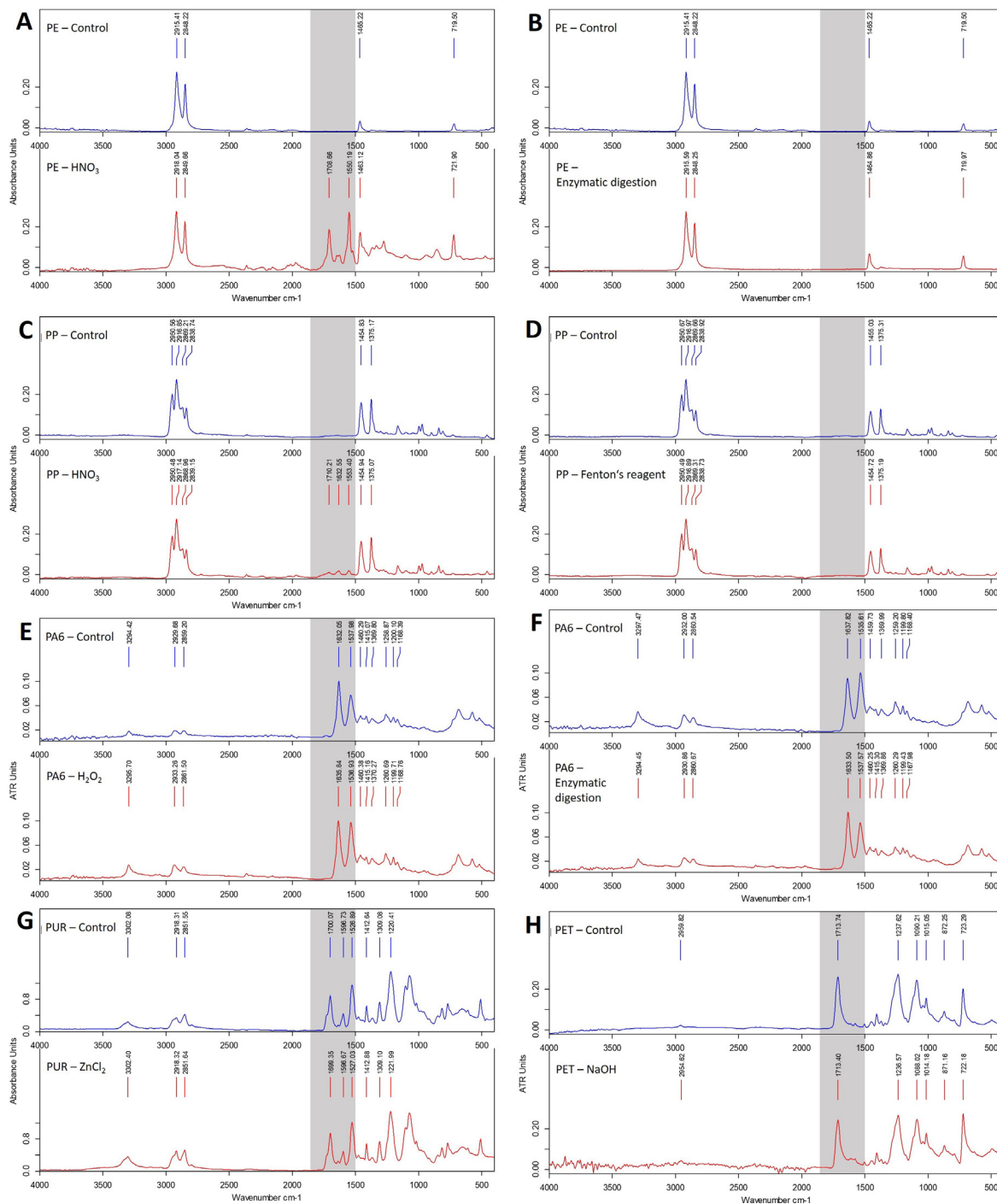


Fig. 3. Examples of ATR-FTIR spectra with visible effects compared to spectra with no visible effects. Blue spectra (upper spectra) represent the control treated with water, red spectra the respective treatment (lower spectra). (A) PE after treatment with HNO_3 . The formation of carbonylated compounds is visible after treatment with HNO_3 in the wavenumber range of $1800\text{--}1500\text{ cm}^{-1}$ (grey bars). (B) PE after treatment with enzymatic digestion. No changes are visible. (C) PP after treatment with HNO_3 . The formation of carbonylated compounds is visible after treatment with HNO_3 in the wavenumber range of $1800\text{--}1500\text{ cm}^{-1}$ (grey bars). (D) PP after treatment with Fenton. No changes are visible. (E) & (F) PA6 after H_2O_2 and enzymatic digestion, no alterations visible. (G) PUR after ZnCl_2 treatment, no visible effects. (H) PET after treatment with NaOH . Although significant weight loss occurred, the ATR-FTIR spectra show no visible changes. (For interpretation of the references to color in this figure legend, the reader is referred to the web version of this article.)

analysis and changes in their surface functional groups on a molecular level. Similar results were reported by Catarino et al. (2017; 65%/14 M HNO_3 ; 20 °C; overnight then 60 °C; 2 h), Karami et al. (2017; 69%/15.5 M HNO_3 ; 25 °C; 96 h), Dehaut et al. (2016; 65%/14 M HNO_3 ; 20 °C; overnight then 60 °C; 2 h) and Claessens et al. (2013; 22.5 M/95% HNO_3 ; 20 °C; overnight then 100 °C; 2 h). It became apparent that the combination of HNO_3 with HClO_4 as proposed by the ICES in 2015 causes severe

degradation of several common polymers (e.g., PA, PUR, ABS, PMMA, PVC, tire rubber). Additionally, surface alterations of ABS, PE, PVC, and PMMA were detected by Raman microspectroscopy, rendering the mixture equally unsuitable as the pure hot nitric acid procedure (Dehaut et al., 2016; Enders et al., 2017).

Another strong acid tested in our study was peroxymonosulfuric acid (H_2SO_5), which showed a good digestion efficiency and facilitated Raman

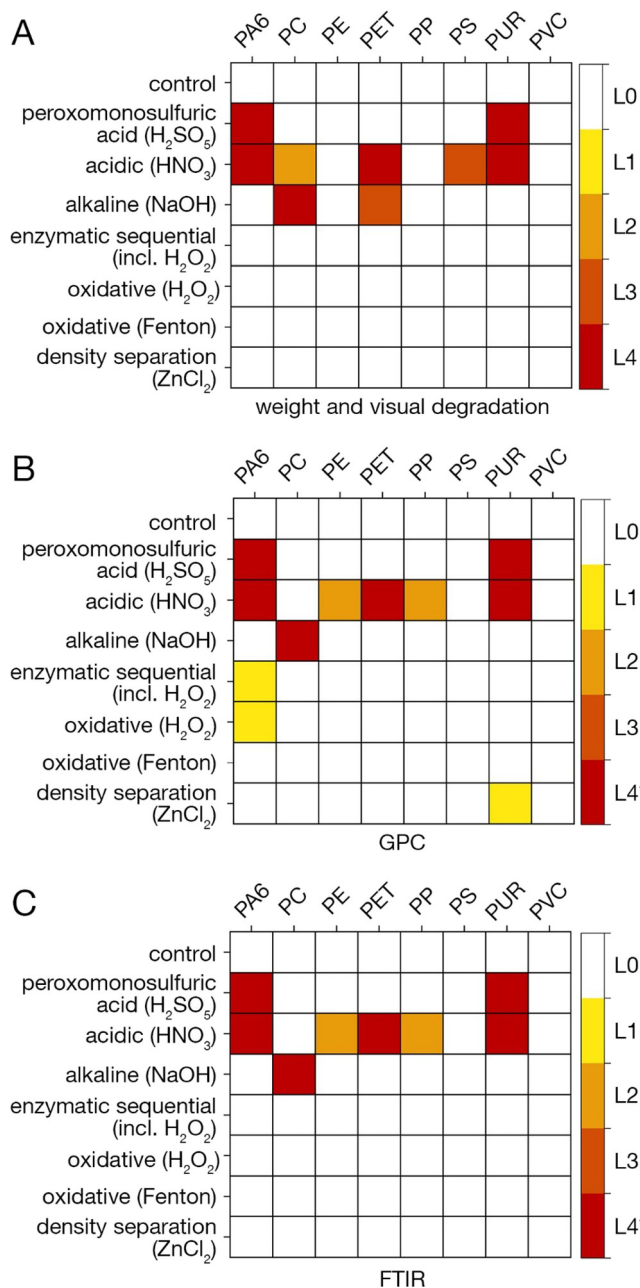


Fig. 4. Degradation-levels of the eight polymer types after the respective treatments displayed for each analytical method. L0–L4 (colored blocks) symbolize the level of degradation in correspondence to Table 1. *No GPC and FTIR measurements were performed for all L4 degradation levels.

microspectroscopy to identify microplastic in lake sediments (Imhof et al., 2016; Imhof et al., 2018; Imhof et al., 2013). However, after a 48 h exposure to H₂SO₅ at 20.5 °C, PA and PUR were severely degraded, confirming that these two polymers are not resilient to any stronger acid. Another strong acidic treatment frequently mentioned in microplastic literature but noted for its relatively low digestion efficiency of organic matter is hydrochloric acid (HCl). For example, Karami et al. (2017) reported that 37% HCl (25 °C, 96 h) disintegrated PA and led to the clumping of PET and caused surface modifications of PVC.

In general, it can be said that the use of strong acids to purify environmental samples for microplastics analysis is not recommendable, as many plastics are susceptible to acidic degradation (Fig. 5), which may lead to biased analytical results. Especially PA, PU, and PET undergo substantial degradation. Concerning the treatment of microplastic samples with weaker

acids (ascorbic acid, citric acid) in the context of use as enhancers or buffers, no detrimental effects on common polymer types have been reported (Weisser et al., 2021).

4.3. Oxidative sample purification methods

The oxidation of organic material is another efficient way for sample purification (Vandermeersch et al., 2014; Van Cauwenberghe et al., 2015). It is often performed using hydrogen peroxide (H₂O₂, 15%–35%), which was reported to be more efficient than alkaline (NaOH) or acidic (HCl) treatments (Zhao et al., 2017; Karami et al., 2017; Nuelle et al., 2014; Qiu et al., 2016). However, the treatment of large sample volumes or samples that have previously undergone a density separation step with ZnCl₂, NaI, or CaCl₂ should be performed carefully due to the exothermic reaction and the undesirable production of gases and the formation of HCl or HI (Nuelle et al., 2014). Furthermore, temperature regulation is an essential aspect of the oxidative purification procedure: Cooling may be necessary to prevent thermally induced damage to the microplastics during a highly exothermic reaction. At the same time, other samples may require heating to initiate the oxidation reaction and reduce the reaction time (Möller et al., 2020). In this study, the polymer types treated with 30% H₂O₂ at 37 °C for 24 h seemed to be unaffected by the treatment, except for PA, which showed changes in the molar mass by GPC analysis. The same pattern for PA was observed after the treatment with the sequential enzymatic purification, which includes two oxidative steps performed with hydrogen peroxide. Thus, we conclude that not the enzymatic treatment was responsible for this observation, and the effects on PA were linked to the H₂O₂ steps included in the sequential enzymatic purification approach.

While no surface changes could be determined via ATR spectroscopy in our study, Karami et al. (2017) showed that a 35% H₂O₂ treatment of PA66 at higher temperatures (60 °C, 96 h) alters peak intensity at 1435 cm⁻¹ (CH₂ bending mode) and 1118 cm⁻¹ in Raman spectra (Karami et al., 2017; Nagae and Nakamae, 2002). Such alterations can be a sign of polymer degradation at the particle surface through structural rearrangement or chemical decomposition (Mažeikiėnė et al., 2006). Similarly, PS and PVC did not show any signs of degradation by H₂O₂ in our study, but slight variations in their respective Raman spectra, indicating alterations in the polymer structure, were reported by Karami et al. (2017). However, these could be caused by a much longer exposure time and higher reaction temperature, allowing a more thorough matrix removal and affecting the targeted polymers.

The Fenton reaction is a modification of the hydrogen peroxide treatment by adding a ferrous ion catalyst, commonly a solution of Fe(II) sulfate. NOAA recommended the Fenton reaction at 75 °C as a protocol for removing organic material (Masura et al., 2015). However, in the last years, it has been increasingly used in microplastic sample treatment as it is more effective than hydrogen peroxide alone, and it seems to be less aggressive to polymers (Hurley et al., 2018; Tagg et al., 2017). No hydrolytic changes to the polymer surface or bulk erosion were detected in this study at 75 °C. Additionally, no other study reported color changes or other signs of degradation (Hurley et al., 2018; Al-Azzawi et al., 2020; Weisser et al., 2021).

In contrast to the original NOAA protocol (Masura et al., 2015), it is advised that the reaction temperature does not exceed 40–50 °C to avoid the reaction to moving from the formation of hydroxyl radicals into the direct degradation of hydrogen peroxide (Walling, 1975; Bishop et al., 1968). Such a temperature reduction results in a higher purification efficiency at lower, more polymer friendly temperatures. Möller et al., (2021) corroborated that treatment with Fenton's reagent at lower temperatures (2 × 1 h of Fenton's reagent at 30–40 °C in addition to several enzymatic digestion steps) show good purification results without affecting the tested polymers (100–400 µm of PA, PET, PE and PVC). They analyzed the plastics visually, via ATR-FTIR, GPC and DSC and found no signs of degradation for these conventional plastic types. Only biodegradable plastics like PLA-based blends might show changes if small particles are treated by the Fenton protocol as (Pfohl et al., (2021)) described. One limitation is the high

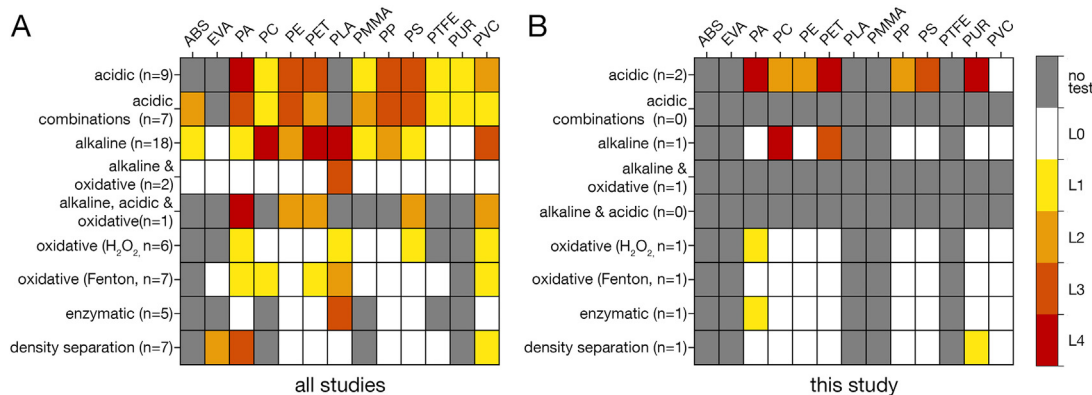


Fig. 5. Summarized results of polymer degradation after sample processing available in the current literature (A) and this study (B). The complete list of studies and their results is provided in the Supplementary Information (Table S3-S9). Strength of degradation was classified as L0 (no effect) to L4 (complete dissolution/disintegration), corresponding to the classification in Table 1. Grey boxes mark if no test was performed.

exothermic characteristic of the Fenton reaction, requiring careful thermo-regulation, e.g., via an ice bath (Munno et al., 2018). The addition of ascorbic acid has been shown to increase the effectiveness of the Fenton reaction (Weisser et al., 2021). In some cases, depending on the sample, the Fenton reaction can produce oxidized iron, leading to an orange precipitate that can be removed by adding citric acid alone or in combination with a density separation step, e.g., by ZnCl₂ (Weisser et al., 2021).

4.4. Combination of acidic and alkaline agents with/without oxidative treatments for sample purification

Roch and Brinker (2017) developed a rapid purification method for the extraction of microplastics from the gastrointestinal tracts of fishes as a sequence of 1 M NaOH (50 °C, 15 min), 10 M HNO₃ (50 °C, 15 min followed by 80 °C, 15 min) combined with a density separation with NaI. While effective in removing the fish tissue, the study also reported a complete loss of PA and visible changes to PET, PS, and PVC.

Several studies combined an acidic and/or alkaline treatment with oxidative agents to increase the digestion efficiency of organic material. For example, Enders et al. (2017) suggest a 1:1 combination of potassium hydroxide (KOH, 30%) and sodium hypochlorite (NaClO) at 20 °C for 5 h followed by 80 °C for 20 min which had a good digestion efficiency for biota. Although no substantial effects on PP, PE, PS, PET, PC, PVC, PMMA, and PTFE were observed, slight surface alterations for ABS were visible as alterations of Raman spectra. Nevertheless, potential changes in weight as a consequence of this treatment were not measured in this study.

A similar combination of sodium hypochlorite (NaClO, 9%), this time with nitric acid (HNO₃, 65%), was performed at 20 °C for 5 min by Collard et al. (2015). Herein no adverse effects on weight and Raman spectra were reported, however, if detrimental effects occur after longer exposure times was not tested. However, according to Correia & Loeschner (2018), the combination of nitric acid and hydrogen peroxide led to the generation of large agglomerates after treating PS nanoparticles.

4.5. Enzymatic sample purification methods

Effectively removing biogenic matter from samples while avoiding the use of strong acids or bases is a clear advantage of enzymatic purification protocols (Zhao et al., 2018). Proteinase K was the first enzyme used in the context of “gentle” sample purification of zooplankton samples described by (Cole et al., 2014). Several research groups further developed the approach (Löder et al., 2017; Courteney-Jones et al., 2017; Catarino et al., 2018). To cope with the complexity of different environmental matrices, a modular and sequential protocol of SDS, protease, cellulase, hydrogen peroxide, chitinase and again hydrogen peroxide was developed by Löder et al. (2017) and adapted by several other studies (Mintenig et al., 2017; Mani et al., 2015; Dris et al., 2015; Kumar et al., 2021; Alligant et al.,

2020). In this study, all tested plastics remained unaffected after the sequential enzymatic-oxidative treatment. This finding is confirmed by several other studies (Cole et al., 2014; Courteney-Jones et al., 2017; Catarino et al., 2017; Weisser et al., 2021). Furthermore, enzymatic purification of fish samples with Proteinase K did not affect PS nanoparticles in contrast to acid digestion, resulting in the large agglomerates of PS nanoparticles (Correia and Loeschner, 2018).

In our study, solely hydrogen peroxide as an intermediate step resulted in hydrolytic surface alterations of PA (as discussed above). However, the oxidative step can be substituted by the more efficient and less aggressive Fenton reaction (e.g., Löder et al., 2017; Weisser et al., 2021). Furthermore, the treatment with the enzyme protease will degrade the biodegradable polylactic acid (PLA), as described by Möller et al. (2021), and the use thereof should be critically considered if PLA is on the analyte spectrum.

While the high removal efficiency and the flexibility to adapt the sequence of enzymes to different sample matrices are advantageous, several drawbacks must be considered. On the one hand, long incubation times are necessary to perform enzymatic digestion effectively. Furthermore, the samples have to be handled and filtered in between each step of the protocol, increasing the risk of particle loss and/or sample contamination with each additional step.

However, the enzymatic-oxidative purification approach's high purification efficiency and broad adjustability for different sample matrices (compare: Möller et al., 2021; Löder et al., 2017; Kumar et al., 2021; Weisser et al., 2021) is a striking reason to nonetheless perform such a laborious sample purification method. Its application results in an excellent quality enhancement of the subsequent identification and quantification process when using vibrational spectroscopy (Möller et al., 2021; Löder et al., 2017; Kumar et al., 2021; Weisser et al., 2021) or mass spectrometric methods (Fischer and Scholz-Böttcher, 2017) and thus the generation of reliable data on the whole spectrum of microplastics present in a sample (Löder et al., 2017). Moreover, enzymes are more environmentally friendly than many other purification agents and should thus be favored (Zhao et al., 2018).

4.6. Density separation

Density separation is a commonly performed step for reducing the sample size before removing organic material by purification. Dense brines of zinc chloride, sodium iodide, or calcium chloride solutions with a density of 1.6–1.8 g cm⁻³ are used to remove minerals or other denser material (Herrera et al., 2018; Hurley et al., 2018; Miller et al., 2017; Coppock et al., 2017; Hamm et al., 2018). However, their corrosiveness and acidity may potentially be aggressive towards some plastics (Zobkov and Esiukova, 2017). Another drawback is their toxicity to the aquatic environment (Zobkov and Esiukova, 2017). Density separation with oil also

showed a good efficiency for sediment samples but the effectiveness depends on the amount of organic matter in the sample (Radford et al., 2021).

Concerning the validation of density separation procedures, the recovery rate of microplastics is often assessed from a spiked (artificial) sample. However, the microplastic particles' integrity after the treatment is not checked, even though some brines, like zinc chloride, are known for their corrosive properties (Zobkov and Esiukova, 2017). No degrading effects of density separation procedures on the microplastic particles were detected by four recent studies (Table S9, Möller, 2021; Radford, 2021; Rodrigues, 2018; Weisser, 2021). In this study, we exemplarily investigated the effects of zinc chloride solution (1.8 g cm^{-3} , 48 h, $\sim 20.5 \text{ }^\circ\text{C}$) on eight plastic types and found no visual degradation or reduction of weight during our experiments.

Furthermore, only GPC analysis showed a particular shift of the molecular mass distribution for PUR, indicating a complexation of zinc chloride with PUR. In contrast a heightened aggregation of PA as well as an agglomeration and melting of EvOH particles of 125–200 μm after the treatment with ZnCl_2 at 1.85 kg/l, whereas no changes of the FTIR spectra were observed (Weisser et al., 2021). Thus, it is generally recommended to extend the exposition time of microplastic samples to density separation solutions no longer than necessary to reduce potential effects to a minimum.

4.7. Purification protocols in the context of microplastic analyses

We emphasise the need to carefully select an appropriate sample purification protocol when targeting microplastic analysis of the whole spectrum of plastics potentially present in the samples. By evaluating several commonly used purification protocols, our study results accompanied by an extensive literature review (Fig. 5) may be a first step for recommendations of purification approaches for harmonizing microplastic analysis with particular respect to reducing the risk of biased research results due to the application of destructive purification protocols and the associated loss of sensitive plastics. Most of our own findings are corroborated by the until now published literature evaluating purification strategies. Differences are mainly due to differences in the analytical approach to assess degradation processes.

Dependent on the research question, the environmental matrix, and the microplastic-analyte spectrum, some methods may be appropriate, while others are not. Polyesters, for example, are susceptible to degradation by strong bases, while strong acids, especially at high temperatures, can degrade an extensive range of plastic species to various degrees (PA, PET, PUR, PS, PC, PE, PP). In this context, researchers must also always consider that the tested polymers were made from pristine plastics, which may be more resilient to degradation than aged and embrittled plastics that may occur in the environment. We cannot exclude the possibility that aged microplastics may degrade under conditions that do not degrade pristine particles, but we believe that we can say with confidence that treatments that degrade pristine (and relatively thick) films will also degrade aged microplastics and should therefore not be used. Readers must also consider that even though no visible or gravimetrically apparent changes may occur for relatively large particles used in many validation studies, the GPC analysis here, as in the example of the hydrogen peroxide treatment on PA, showed that degradation on a molecular level may still occur. This molecular degradation may translate to loss of mass and is especially relevant for smaller particles or thin fibers in the nano- and lower micrometer range, rendering molecular assays on degenerative effects of purification protocols essential before doing any micro-, or nanoplastic analysis. When choosing a validated protocol for a specific study goal, it is also necessary to consider and adhere to the given time and temperature of the given protocol. While higher temperatures and longer exposure times may increase the digestion efficiency of the sample matrix, the comparisons between studies have made it apparent that these factors may also lead to a degradation of microplastic that was not evident in the validation process adhering to the time and temperature of the tested protocol. Protocols including sonication in the purification process should be avoided. Especially in the case of

weathered and brittle microplastics, the introduced strong mechanical force can lead to the disintegration into smaller particles with increasing risk of fragmentation if combined with heat or one of the treatments mentioned above (e.g., potassium hydroxidem, Löder and Gerdts, 2015; von der Esch et al., 2020; Davranche et al., 2019). The same is true for the application of microwave digestion (Karlsson et al., 2017).

5. Conclusions

Comparing the results of degenerative effects of purification protocols on thin polymer films, we show that the use of strong acids and bases is destructive to many conventional plastic types. Given the even higher surface to volume ratio in microplastics and a higher porosity due to environmental aging, destructive effects of these purification protocols on microplastics is likely much higher. Therefore, such treatments are deemed unsuitable for most environmental microplastic analyses. Acknowledging this is especially important considering the fact that e.g. alkaline solutions are - to date still often advocated as purification protocols for certain matrices (Lee and Lee, 2021; Alfonso et al., 2021) without testing for negative effects on polyesters on a molecular level (e.g., via GPC analysis).

Treatment with hydrogen peroxide showed degradation on a molecular level for PA but can easily be substituted with Fenton's reagent, which is highly effective in a much shorter exposure time and showed no adverse effects on any of the tested plastic types. However, the treatment with Fenton's reagent for soil organic matter is often not enough to remove a considerable amount of the sample matrix (Möller et al., 2020). In that case, the combination of Fenton's reagent and sequential enzymatic digestion may lead to the required purification results, although this leads to higher time and resource expenditures.

CRedit authorship contribution statement

Isabella Schrank: Conceptualization, Methodology, Investigation, Writing – original draft,

Julia N. Möller: Conceptualization, Methodology, Investigation, Formal Analysis, Data Curation, Writing – original draft,

Hannes K. Imhof: Conceptualization, Methodology, Writing original Draft, Supervision, Project Administration

Oliver Hauenstein: Investigation,

Franziska Zielke: Investigation,

Seema Agarwal: Formal Analysis, Resources, Writing – original draft,

Martin G. J. Löder: Conceptualization, Supervision, Project Administration, Funding Acquisition

Andreas Greiner: Resources, Supervision

Christian Laforsch: Resources, Supervision, Funding Acquisition

Declaration of competing interest

The authors declare that they have no known competing financial interests or personal relationships that could have appeared to influence the work reported in this paper.

Acknowledgments

We thank the department for Macromolecular Chemistry I at the University of Bayreuth, who generously conducted the HT-GPC and mass analysis in their facilities.

Additionally, we are grateful for helpful discussions and the support by Elmar Sehl from the Macromolecular Chemistry II at the University of Bayreuth.

This study was funded by the Deutsche Forschungsgemeinschaft (DFG, German Research Foundation) - SFB 1357 - 391977956 and the Federal Ministry of Education and Research (BMBF), project number 03F0789A -

PLAWES. We furthermore thank the Ministry for Environment, Climate Protection and Energy of Baden Württemberg for funding J.N. Möller in the scope of the German research program MiKoBo (BWMK18007). The funding agencies had no influence on the study design, collection of data or reporting of results. This was the sole work of the listed authors.

Appendix A. Supplementary data

Supplementary data to this article can be found online at <https://doi.org/10.1016/j.scitotenv.2022.154824>.

References

- Al-Azzawi, M.S., et al., 2020. Validation of sample preparation methods for microplastic analysis in wastewater matrices—reproducibility and standardization. *Water* 12 (9), 2445.
- Alfonso, M.B., et al., 2021. Microplastics on plankton samples: multiple digestion techniques assessment based on weight, size, and FTIR spectroscopy analyses. *Mar. Pollut. Bull.* 173, 113027.
- Alligant, S., et al., 2020. Microplastic contamination of sediment and water column in the Seine River estuary. Proceedings of the 2nd International Conference on Microplastic Pollution in the Mediterranean Sea. Springer International Publishing, Cham.
- Anger, P.M., et al., 2018. Raman microspectroscopy as a tool for microplastic particle analysis. *TRAC Trends Anal. Chem.* 109, 214–226.
- Arthur, C., Baker, J., Bamford, H., 2009. Proceedings of the International Research Workshop on the Occurrence, Effects and Fate of Microplastic Marine Debris. U.S. Department of Commerce.
- Bäckström, E., Odélius, K., Hakkarainen, M., 2017. Trash to treasure: microwave-assisted conversion of polyethylene to functional chemicals. *Ind. Eng. Chem. Res.* 56 (50), 14814–14821.
- Barboza, L.G.A., Gimenez, B.C.G., 2015. Microplastics in the marine environment: current trends and future perspectives. *Mar. Pollut. Bull.* 97 (1–2), 5–12.
- Bishop, D.F., et al., 1968. Hydrogen peroxide catalytic oxidation of refractory organics in municipal waste waters. *Ind. Eng. Chem. Process. Des. Dev.* 7 (1), 110–117.
- Bläsing, M., Amelung, W., 2018. Plastics in soil: analytical methods and possible sources. *Sci. Total Environ.* 612, 422–435.
- Botterell, Z.L.R., et al., 2019. Bioavailability and effects of microplastics on marine zooplankton: a review. *Environ. Pollut.* 245, 98–110.
- Braun, U., et al., 2018. Diskussionspapier "Mikroplastik-Analytik" - Probenahme, Probenaufbereitung und Detektionsverfahren. BMBF Forschungsschwerpunkt "Plastik in der Umwelt", Querschnittsthema "Analytik und Referenzmaterialien".
- Braun, T., et al., 2021. Detection of microplastic in human placenta and meconium in a clinical setting. *Pharmaceutics* 13 (7), 921.
- Browne, M.A., et al., 2015. Spatial and temporal patterns of stranded intertidal marine debris: is there a picture of global change? *Environ. Sci. Technol.* 49 (12), 7082–7094.
- Bürkle GmbH, 2011. Chemische Beständigkeit von Kunststoffen. Bad Bellingen, Germany.
- Catarino, A.I., et al., 2017. Development and optimization of a standard method for extraction of microplastics in mussels by enzyme digestion of soft tissues. *Environ. Toxicol. Chem.* 36 (4), 947–951.
- Catarino, A.I., et al., 2018. Low levels of microplastics (MP) in wild mussels indicate that MP ingestion by humans is minimal compared to exposure via household fibres fallout during a meal. *Environ. Pollut.* 237, 675–684.
- Chae, Y., An, Y.-J., 2018. Current research trends on plastic pollution and ecological impacts on the soil ecosystem: a review. *Environ. Pollut.* 240, 387–395.
- Claessens, M., et al., 2013. New techniques for the detection of microplastics in sediments and field collected organisms. *Mar. Pollut. Bull.* 70 (1–2), 227–233.
- Cole, M., et al., 2014. Isolation of microplastics in biota-rich seawater samples and marine organisms. *Sci. Rep.* 4, 4528.
- <collab>Science Advice for Policy by European, A.collab, 2019. A Scientific Perspective on Microplastics in Nature and Society Berlin.
- Collard, F., et al., 2015. Detection of anthropogenic particles in fish stomachs: an isolation method adapted to identification by Raman spectroscopy. *Arch. Environ. Contam. Toxicol.* 69 (3), 331.
- Coppock, R.L., et al., 2017. A small-scale, portable method for extracting microplastics from marine sediments. *Environ. Pollut.* 230, 829–837.
- Correia, M., Loeschner, K., 2018. Detection of nanoplastics in food by asymmetric flow field-flow fractionation coupled to multi-angle light scattering: possibilities, challenges and analytical limitations. *Anal. Bioanal. Chem.* 410 (22), 5603–5615.
- Courtene-Jones, W., et al., 2017. Optimisation of enzymatic digestion and validation of specimen preservation methods for the analysis of ingested microplastics. *Anal. Methods* 9 (9), 1437–1445.
- Crawford, C.B., Quinn, B., Crawford, C.B., Quinn, B. (Eds.), 2017. *Microplastic Pollutants*. Microplastic Pollutants. Elsevier.
- Davranche, M., et al., 2019. Are nanoplastics able to bind significant amount of metals? The lead example. *Environ. Pollut.* 249, 940–948.
- de Souza Machado, A.A., et al., 2018. Microplastics as an emerging threat to terrestrial ecosystems. *Glob. Chang. Biol.* 24 (4), 1405–1416.
- de Souza Machado, A.A., et al., 2019. Microplastics can change soil properties and affect plant performance. *Environ. Sci. Technol.* 53 (10), 6044–6052.
- Dehaut, A., et al., 2016. Microplastics in seafood: benchmark protocol for their extraction and characterization. *Environ. Pollut.* 215, 223–233.
- Díaz-Mendoza, C., et al., 2020. Plastics and microplastics, effects on marine coastal areas: a review. *Environ. Sci. Pollut. Res.* 27 (32), 39913–39922.
- Dris, R., et al., 2015. Microplastic contamination in an urban area: a case study in Greater Paris. *Environ. Chem.* 12 (5), 592–599.
- Dris, R., et al., 2018. Chapter 3 - microplastic contamination in freshwater systems: methodological challenges, occurrence and sources. In: Zeng, E.Y. (Ed.), *Microplastic Contamination in Aquatic Environments*. Elsevier, pp. 51–93.
- Dyachenko, A., Mitchell, J., Arsem, N., 2017. Extraction and identification of microplastic particles from secondary wastewater treatment plant (WWTP) effluent. *Anal. Methods* 9 (9), 1412–1418.
- Enders, K., et al., 2017. Extraction of microplastic from biota: recommended acidic digestion destroys common plastic polymers. *ICES J. Mar. Sci.* 74 (1), 326–331.
- Fischer, M., Scholz-Böttcher, B.M., 2017. Simultaneous trace identification and quantification of common types of microplastics in environmental samples by pyrolysis-gas chromatography–mass spectrometry. *Environ. Sci. Technol.* 51 (9), 5052–5060.
- Fischer, M., Scholz-Böttcher, B.M., 2019. Microplastics analysis in environmental samples – recent pyrolysis-gas chromatography–mass spectrometry method improvements to increase the reliability of mass-related data. *Anal. Methods* 11 (18), 2489–2497.
- Gibb, T., 2015. Chapter 2 - equipping a diagnostic laboratory. In: Gibb, T. (Ed.), *Contemporary Insect Diagnostics*. Academic Press, San Diego, pp. 9–49.
- Hamm, T., Lorenz, C., Piehl, S., 2018. Microplastics in aquatic systems – monitoring methods and biological consequences. *YOUMARES 8 – Oceans Across Boundaries: Learning From Each Other*. Springer International Publishing, Cham.
- Hartmann, N.B., et al., 2019. Are we speaking the same language? Recommendations for a definition and categorization framework for plastic debris. *Environ. Sci. Technol.* 53 (3), 1039–1047.
- He, D., et al., 2018. Microplastics in soils: analytical methods, pollution characteristics and ecological risks. *TRAC Trends Anal. Chem.* 109, 163–172.
- Herrera, A., et al., 2018. Novel methodology to isolate microplastics from vegetal-rich samples. *Mar. Pollut. Bull.* 129 (1), 61–69.
- Hidalgo-Ruz, V., et al., 2012. Microplastics in the marine environment: a review of the methods used for identification and quantification. *Environ. Sci. Technol.* 6 (46), 3060–3075.
- Hurley, R., et al., 2018. Validation of a method for extracting microplastics from complex, organic-rich, environmental matrices. *Environ. Sci. Technol.* 52 (13), 7409–7417.
- Ibrahim, Y.S., et al., 2017. Isolation and characterisation of microplastic abundance in Lates calcarifer from Setiu wetlands, Malaysia. *Malays. J. Anal. Sci.* 21 (5), 1054–1064.
- ICES, 2015. OSPAR Request on Development of a Common Monitoring Protocol for Plastic Particles in Fish Stomachs and Selected Shellfish on the Basis of Existing Fish Disease Surveys. ICES Advice.
- Imhof, H.K., et al., 2013. Contamination of beach sediments of a subalpine lake with microplastic particles. *Curr. Biol.* 23 (19), R867–R868.
- Imhof, H.K., et al., 2016. Pigments and plastic in limnetic ecosystems: a qualitative and quantitative study on microparticles of different size classes. *Water Res.* 98, 64–74.
- Imhof, H.K., et al., 2018. Variation in plastic abundance at different lake beach zones - a case study. *Sci. Total Environ.* 613 (Supplement C), 530–537.
- Ivleva, N.P., 2021. Chemical analysis of microplastics and nanoplastics: challenges, advanced methods, and perspectives. *Chem. Rev.* 121 (19), 11886–11936.
- Käppler, A., et al., 2016. Analysis of environmental microplastics by vibrational microspectroscopy: FTIR, Raman or both? *Anal. Bioanal. Chem.* 408 (29), 8377–8391.
- Karami, A., et al., 2017. A high-performance protocol for extraction of microplastics in fish. *Sci. Total Environ.* 578, 485–494.
- Karlsson, T.M., et al., 2017. Screening for microplastics in sediment, water, marine invertebrates and fish: method development and microplastic accumulation. *Mar. Pollut. Bull.* 122 (1), 403–408.
- Klein, S., Worch, E., Knepper, T.P., 2015. Occurrence and spatial distribution of microplastics in river shore sediments of the Rhine-Main area in Germany. *Environ. Sci. Technol.* 49 (10), 6070–6076.
- Kühn, S., et al., 2017. The use of potassium hydroxide (KOH) solution as a suitable approach to isolate plastics ingested by marine organisms. *Mar. Pollut. Bull.* 115 (1), 86–90.
- Kumar, V.B.N., et al., 2021. Analysis of microplastics of a broad size range in commercially important mussels by combining FTIR and Raman spectroscopy approaches. *Environ. Pollut.* 269, 116147.
- Lee, S., Lee, T.G., 2021. A novel method for extraction, quantification, and identification of microplastics in CreamType of cosmetic products. *Sci. Rep.* 11 (1), 18074.
- Li, W.C., 2018. Chapter 5 - the occurrence, fate, and effects of microplastics in the marine environment. In: Zeng, E.Y. (Ed.), *Microplastic Contamination in Aquatic Environments*. Elsevier, pp. 133–173.
- Li, J., Liu, H., Paul Chen, J., 2018. Microplastics in freshwater systems: a review on occurrence, environmental effects, and methods for microplastics detection. *Water Res.* 137, 362–374.
- Li, F., et al., 2018. Comparison of six digestion methods on fluorescent intensity and morphology of the fluorescent polystyrene beads. *Mar. Pollut. Bull.* 131, 515–524.
- Liu, M., et al., 2018. Microplastic and mesoplastic pollution in farmland soils in suburbs of Shanghai, China. *Environ. Pollut.* 242, 855–862.
- Löder, M.G.J., Gerdts, G., 2015. Methodology used for the detection and identification of microplastics—a critical appraisal. In: Bergmann, Gutow, Klages (Eds.), *Marine Anthropogenic Litter*. Springer International Publishing, pp. 201–227.
- Löder, M.G.J., et al., 2017. Enzymatic purification of microplastics in environmental samples. *Environ. Sci. Technol.* 51 (24), 14283–14292.
- Mani, T., et al., 2015. Microplastics profile along the Rhine River. *Sci. Rep.* 5, 17988.
- Masura, J., et al., 2015. Laboratory methods for the analysis of microplastics in the marine environment: recommendations for quantifying synthetic particles in waters and sediments. *NOAA Tech. Memo.* 39.
- Mažeikienė, R., et al., 2006. In situ raman spectroelectrochemical study of self-doped polyaniline degradation kinetics. *Electrochem. Commun.* 8 (7), 1082–1086.
- Miller, M.E., Kroon, F.J., Motti, C.A., 2017. Recovering microplastics from marine samples: a review of current practices. *Mar. Pollut. Bull.* 123 (1), 6–18.

- Mintenig, S.M., et al., 2017. Identification of microplastic in effluents of waste water treatment plants using focal plane array-based micro-Fourier-transform infrared imaging. *Water Res.* 108, 365–372.
- Möller, J.N., Löder, M.G.J., Laforsch, C., 2020. Finding microplastics in soils: a review of analytical methods. *Environ. Sci. Technol.* 54 (4), 2078–2090.
- Möller, J.N., et al., 2021. Tackling the challenge of extracting microplastics from soils: a protocol to purify soil samples for spectroscopic analysis. *Environ. Toxicol. Chem.* 41 (4), 844–857.
- Müller, Y.K., et al., 2020. Microplastic analysis—are we measuring the same? Results on the first global comparative study for microplastic analysis in a water sample. *Anal. Bioanal. Chem.* 412 (3), 555–560.
- Munno, K., et al., 2018. Impacts of temperature and selected chemical digestion methods on microplastic particles. *Environ. Toxicol. Chem.* 37 (1), 91–98.
- Nagae, S., Nakamae, K., 2002. Characterization of glass fiber/nylon-6 interface by laser Raman spectroscopy. *Int. J. Adhes. Adhes.* 22 (2), 139–142.
- Nuelle, M.-T., et al., 2014. A new analytical approach for monitoring microplastics in marine sediments. *Environ. Pollut.* 184, 161–169.
- Pfohl, P., et al., 2021. Microplastic extraction protocols can impact the polymer structure. *Microplast. Nanoplast.* 1 (1), 8.
- Piehl, S., et al., 2018. Identification and quantification of macro- and microplastics on an agricultural farmland. *Sci. Rep.* 8 (1), 17950.
- Prata, J.C., et al., 2019. Methods for sampling and detection of microplastics in water and sediment: a critical review. *TrAC Trends Anal. Chem.* 110, 150–159.
- Primpe, S., et al., 2020. Toward the systematic identification of microplastics in the environment: evaluation of a new independent software tool (siMPLE) for spectroscopic analysis. *Appl. Spectrosc.* 74 (9), 1127–1138.
- Qiu, Q., et al., 2016. Extraction, enumeration and identification methods for monitoring microplastics in the environment. *Estuar. Coast. Shelf Sci.* 176, 102–109.
- Quinn, B., Murphy, F., Ewins, C., 2017. Validation of density separation for the rapid recovery of microplastics from sediment. *Anal. Methods* 9 (9), 1491–1498.
- Radford, F., et al., 2021. Developing a systematic method for extraction of microplastics in soils. *Anal. Methods* 13 (14), 1695–1705.
- Ramsperger, A.F.R.M., et al., 2020. Environmental exposure enhances the internalization of microplastic particles into cells. 6 (50), eabd1211.
- Roch, S., Brinker, A., 2017. Rapid and efficient method for the detection of microplastic in the gastrointestinal tract of fishes. *Environ. Sci. Technol.* 51 (8), 4522–4530.
- Rodrigues, M.O., et al., 2018. Effectiveness of a methodology of microplastics isolation for environmental monitoring in freshwater systems. *Ecol. Indic.* 89, 488–495.
- Sarker, A., et al., 2020. A review of microplastics pollution in the soil and terrestrial ecosystems: a global and Bangladesh perspective. *Sci. Total Environ.* 733, 139296.
- See, M., et al., 2020. Microplastics in the marine environment: a literature review and north-east England case study. *Water Environ. J.* 34 (3), 489–505.
- Tagg, A.S., et al., 2015. Identification and quantification of microplastics in wastewater using focal plane array-based reflectance micro-FT-IR imaging. *Anal. Chem.* 87 (12), 6032–6040.
- Tagg, A.S., et al., 2017. Fenton's reagent for the rapid and efficient isolation of microplastics from wastewater. *Chem. Commun.* 53 (2), 372–375.
- Thacker, H.L., Kastner, J., 2004. Chapter 6: alkaline hydrolysis. *Carcass Disposal: A Comprehensive Review*.
- Thomas, D., et al., 2020. Sample preparation techniques for the analysis of microplastics in soil—a review. *Sustainability* 12 (21).
- Van Cauwenberghe, L., Janssen, C.R., 2014. Microplastics in bivalves cultured for human consumption. *Environ. Pollut.* 193, 65–70.
- Van Cauwenberghe, L., et al., 2015. Microplastics in sediments: a review of techniques, occurrence and effects. *Mar. Environ. Res.* 111, 5–17.
- Vandermeersch, G., et al., 2014. A critical view on microplastic quantification in aquatic organisms. *Environ. Res.* 2015 (143), 46.
- von der Esch, E., et al., 2020. Simple generation of suspensible secondary microplastic reference particles via ultrasound treatment. *Front. Chem.* 8 (169).
- Freshwater microplastics - emerging environmental contaminants. In: Wagner, M., Lambert, S. (Eds.), *The Handbook of Environmental Chemistry. XIV*. Springer International Publishing, p. 303.
- Walling, C., 1975. Fenton's reagent revisited. *Acc. Chem. Res.* 8 (4), 125–131.
- Weisser, J., et al., 2021. From the well to the bottle: identifying sources of microplastics in mineral water. *Water* 13 (6).
- Zarfl, C., 2019. Promising techniques and open challenges for microplastic identification and quantification in environmental matrices. *Anal. Bioanal. Chem.* 411, 3743–3756.
- Zhao, S., et al., 2017. An approach for extraction, characterization and quantitation of microplastic in natural marine snow using Raman microscopy. *Anal. Methods* 9 (9), 1470–1478.
- Zhao, S., et al., 2018. Chapter 2 - limitations for microplastic quantification in the ocean and recommendations for improvement and standardization. In: Zeng, E.Y. (Ed.), *Microplastic Contamination in Aquatic Environments*. Elsevier, pp. 27–49.
- Zobkov, M.B., Esiukova, E.E., 2017. Evaluation of the Munich plastic sediment separator efficiency in extraction of microplastics from natural marine bottom sediments. *Limnol. Oceanogr. Methods* 15 (11), 967–978.

Supplementary Information: Microplastic sample purification methods - assessing detrimental effects of purification procedures on specific plastic types

Authors: Isabella Schrank^{1#}, Julia N. Möller^{1#}, Hannes K. Imhof¹, Oliver Hauenstein², Franziska Zielke¹, Seema Agarwal², Martin G. J. Löder¹, Andreas Greiner², Christian Laforsch^{1,*}

Affiliations:

¹Department of Animal Ecology I and BayCEER, University of Bayreuth, Universitätsstr. 30, 95440 Bayreuth, Germany

²Macromolecular Chemistry II, University of Bayreuth, Universitätsstr. 30, 95447 Bayreuth, Germany

shared first authorship

*Correspondence to: E-Mail: christian.laforsch@uni-bayreuth.de; Tel.: +49(0)921/552650,

Fax: +49(0)921/552784

Materials and methods

Film production

Table S1: Platelet specifications. Platelet material and trade name, density (ρ), mean platelet weight ($\bar{\varnothing} m_{\text{platelet}}$) \pm standard deviation, glass transition temperature (T_g) and melting temperature (T_m).

Material	Trade name	ρ [g/cm ³]	$\bar{\varnothing} m_{\text{platelet}}$ [mg]	T_g [°C]	T_m [°C]
PA6	Ultramid B3K	1.13	11.29 \pm 1.0	n.d.	220°C
PC	Makrolon 2800	1.20	14.2 \pm 1.2	145	280
PE (LD)	Purell 1840H (Lyondell Basell)	0.92	14.3 \pm 2.3	-100	110
PET	RT 32/49 (Invista)	1.39	14.4 \pm 1.1	n.d.	250
PP	Bormed HD810 MO	0.90	8.6 \pm 1.1	-10	164
PS	Vestyron 325 (Evonik)	1.04	11.5 \pm 1.0	89	n.d.
PUR	Thermoplast	1.10	13.3 \pm 1.0	n.d.	n.d.
PVC	Vinoflex 5715	1.20	30.1 \pm 6.0	n.d.	n.d.

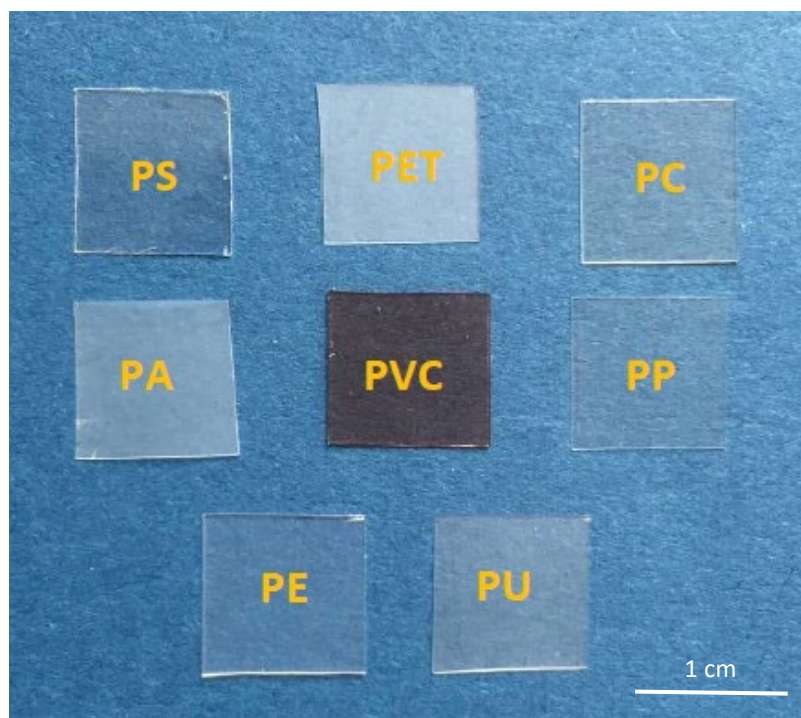


Figure S1: Photography of the 10 mm \times 10 mm \times 100 μ m films with corresponding polymer denomination

Enzymatic: Sequential enzymatic digestion

Table S2. List of chemicals used during the sequential steps of the enzymatic purification protocol. Adapted from Löder, Imhof [1]. Buffer for pH 9 was Tris-buffer* and for pH 5 Sodium acetate buffer*

Step	Reagents	Concentration	Volume	Incubation time	Incubation temperature	pH
1	Sodiumdodecylsulfate (SDS)*	10 %	15 ml	24 h	50 °C	
2	Protease A-01**	>1 000 U ml ⁻¹ 10 %	2.5 ml Protease 12.5 ml buffer	24 h	50 °C	9
3	Lipase FE-01**	>18 000 U ml ⁻¹ 10 %	0.5 ml Protease 12.5 ml buffer	24 h	50 °C	9
4	Amylase TXL**	>40 000 U ml ⁻¹ 10 %	2.5 ml Amylase 12.5 ml buffer	24 h	50 °C	5
5	Cellulase TXL**	>70 U ml ⁻¹ 10 %	2.5 ml Cellulase 12.5 ml buffer	72 h	50 °C	5
6	Hydrogen peroxide***	30%	15 ml	24 h	37 °C	
7	Hydrogen peroxide***	30%	15 ml	24 h	37 °C	
8	Chitinase**	>100 U ml ⁻¹ 10%	0.5 ml Chitinase 12.5 ml buffer	96 h	37 °C	5
9	Hydrogen peroxide***	30%	15 ml	5 h	37 °C	
10	Final rinsing with ultrapure water					

* Carl Roth GmbH & Co. KG, Germany

**ASA Spezialenzyme GmbH, Germany

*** VWR International GmbH, Germany

Buffer production

pH 9: Tris HCl 1 M buffer

For 1 L buffer solution 121.14 g Tris are dissolved in 800 mL ultrapure water and a pH value of 9 is adjusted with concentrated HCl. Afterwards the solution is filled up to 1 L.

pH 5: NaOAc (C₂H₃NaO₂) 1 M buffer

For 1 L buffer solution 82.03 g NaOAc (anhydrous) are dissolved in 800 mL ultrapure water and a pH value of 5 is set with concentrated acetic acid. The solution is filled up to 1 L.

Gel permeation chromatography settings

Gel permeation chromatography (GPC)

The GPC measurements for PS and PC were performed on an Agilent 1200 system equipped with a refractive index (RI) detector and a single column (SDV Linear XL 5 µm, PSS Polymer Standards Service GmbH, Germany). The analysis was performed at 23 °C using chloroform as the mobile phase. The molecular weights of the samples were referenced to

polystyrene standards (PSS Polymer Standards Service GmbH, Germany). PET and PA6 were analysed using an Agilent 1200 system equipped with an RI detector and four columns (PSS PFG 300 7 μm). The GPC analysis was performed at 23 °C using hexafluoroisopropanol as the mobile phase. The molecular weights of the samples were referenced to poly(methylmethacrylate) standards (PSS Polymer Standards Service GmbH, Germany). The analysis of PVC and PUR were carried out on an Agilent 1200 system equipped with an RI detector and one column (4x PSS SDV 5 μm 100 / 1000 / 10000 / 100000). The GPC analysis was performed at 40 °C using tetrahydrofuran as the mobile phase. The molecular weights of the samples were referenced to poly(methylmethacrylate) standards (PSS Polymer Standards Service GmbH, Germany).

High temperature gel permeation chromatography (HT-GPC).

For the polyolefins PP and PE the analysis of the average molecular weight and molecular weight distribution was conducted using a high temperature gel permeation chromatography (HT-GPC). The analysis was carried out on an Agilent (Polymer Laboratories Ltd.) PL-GPC 220 high temperature chromatographic unit equipped with DP and RI detectors and four linear mixed bed columns (3 x PSS Polefin linear XL + 1 gard column). The HT-GPC analysis was performed at 150 °C using 1,2,4-trichlorobenzene as the mobile phase. The samples were prepared by dissolving the polymer (0.1 wt-%) in the mobile phase solvent in an external oven and the solutions were run without filtration. The molecular weights of the samples were referenced to polystyrene standards ($M_w = 518\text{-}2,600,000 \text{ g mol}^{-1}$, $K = 12.100$ and $\text{Alpha} = 0.707$) and were corrected with K and Alpha values for the measured polymers (PE: $K = 40,600$ and $\text{Alpha} = 0,725$; PP: $K = 19,000$ and $\text{Alpha} = 0,725$).

Attenuated total reflection Fourier transform infrared (ATR-FTIR) spectroscopy settings

The platelets were analysed using a 'Tensor 27' FTIR spectrometer with ATR-unit (Bruker Optik GmbH, Germany). It was equipped with a silicon carbide Globar as M-IR source, an internal deuterated L-alanine doped triglycine sulfate (DLαTGS) single detector working at room temperature and a pure diamond 'attenuated total reflectance' (ATR) unit (Platinum-ATR-unit, Bruker Optik GmbH) used for sample measurements. The diamond has a sample interface of 2x2 mm, 45° single reflection and 1.66 μm penetration depth. The system was operated by the software OPUS 7.5 (Bruker Optik GmbH) during measurements and analyses. IR spectra were recorded in the wavenumber range 4000 - 400 cm⁻¹ with a resolution of 8 cm⁻¹ and 16 co-added scans. The background measurement against air was conducted prior to each sample measurement with the same settings. In order to identify polymer modifications, we focused on the spectral region between 1800-1500 cm⁻¹. No corrections were applied for the measured IR spectra.

Results

Weight and visual degradation

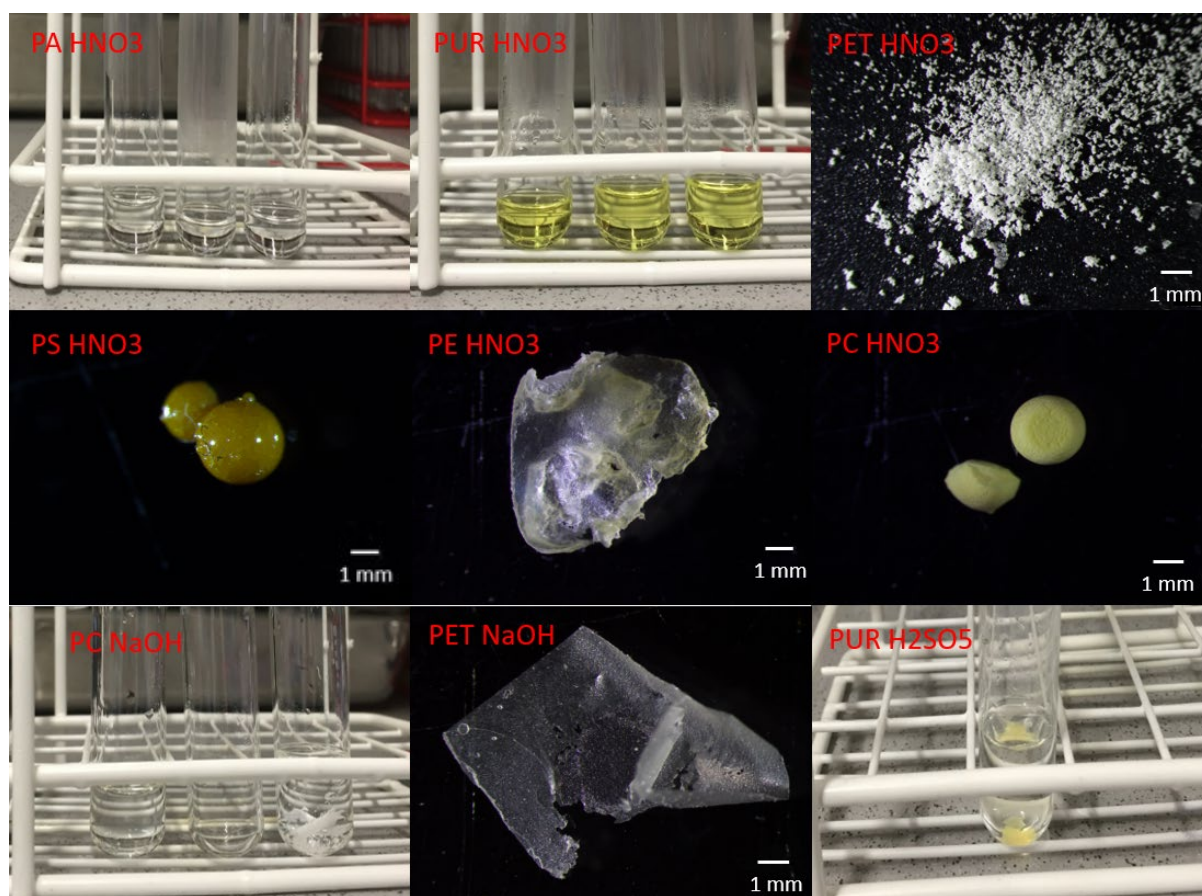


Figure S2: Optically visible degradation of PA, PUR, PET, PS, PE and PC films after the treatment with hot nitric acid (HNO₃) for 2 h. Alteration of PC and PET films after the treatment with sodium hydroxide (NaOH) for 7 days at room temperature (~20.5°C) and the degradation of PUR films after the treatment with peroxymonosulfuric acid (H₂SO₅) for 48h at room temperature (~20.5°C).

Overview of published purification protocols

Alkaline sample purification methods

Table S3: List of studies that evaluated sample purification methods on their potential to degrade common plastics based on alkaline solutions.

The degradation strength was classified according to the classification scheme in Table 1.

	Sample matrix	Protocol	Purification efficiency	Observed effect on synthetic polymers*	Size of assessed particles/fibers	Evaluation method	Reference
Alkaline (NaOH or KOH)	Organic rich sediment	40%/10M NaOH; 60°C; 24h	9%	L0: PA, PE, PP, PVC, PUR, PS L2: PET	pellets <5mm and fragments generated from commercial products	visually	[2]
	Zooplankton	10M/40% NaOH; 60°C; 24h	91%	L0: PS L1: PVC L2: PE, PA L3: PES	PS spheres (1.5 – 3.0 mm), PA fishing line (400 µm diameter, length 1mm), PES fibers (10 – 30 µm diameter, length 0.75 – 1.5 mm), PVC granules (60 – 120 µm), PE fragments (60 – 500 µm) from cosmetics	visually, weight, counts	[3]
	Mussel tissue	10M/40% NaOH; 60°C; 24h	n.d.	L0: ePS, LDPE, HDPE, PA12, PA6, PMMA, PP, PS, PSXL, PTFE, PUR L3: CA, PVC L4: PC	n.d.	weight, visually, Pyr-GC/MS, Raman	[4]
	Sludge, soil and no matrix	10M/40% NaOH; 60°C; 24h	sludge: mass loss 34.6 ± 3.01% organic matter removal 67.2% ± 5.84% soil: mass loss 4.38% ± 2.90%, organic matter removal 64.4% ± 42.7%	L0: PP, LDPE, HDPE, PS, PA, PMMA L2: PET L3: PC	Pellets: PP (3 - 6.3 mm) LDPE (3.4 – 4.5 mm) HDPE (3.6 - 5.0 mm) Granules: PS (3.1 - 4.0 mm) PA (2.9 - 4.4 mm) PC (3.1 - 3.8 mm) PMMA (2.8 - 4.3 mm) Beads: PET (2.9 - 3.6 mm)	weight, size, optical changes	[5]
	Sludge, soil and no matrix	1M/4% NaOH; 60°C; 24h	sludge: mass loss 31.4% ± 2.88%, organic matter removal 60.9% ± 5.60% soil: mass loss 4.59% ± 1.39%, organic matter removal 67.6% ± 20.5%	L0: PP, LDPE, HDPE, PS, PA, PMMA L1: PC L2: PET	Pellets: PP (3 - 6.3 mm) LDPE (3.4 – 4.5 mm) HDPE (3.6-5.0 mm) Granules: PS (3.1 - 4.0 mm) PA (2.9 - 4.4 mm) PC (3.1 - 3.8 mm) PMMA (2.8 - 4.3 mm) Beads: PET (2.9 - 3.6 mm)	weight, size, optical changes	[5]
	Mussel tissue (frozen)	1M NaOH, 1h, stirred	100%	L0 (94% recovery rate): PET, HDPE, PVC, PA	Fragments (125 – 500 µm): PET, HDPE, PVC Fibers (500 – 1000 µm): Nylon thread	recovery, rate, visual, FTIR	[6]

Alkaline (NaOH or KOH)	No matrix	50%/12.5M NaOH; 20°C, 7 days		L0: PE, PA PP, PS, PUR, PVC L3: PET L4: PC	Films: 10 mm x 10 mm x 100 µm	visual, gravimetry, bulk erosion (GPC), ATR-FTIR	this study
	Sludge, soil and no matrix	10%/2M KOH; 60°C; 24h	sludge: mass loss 29.2 ± 8.56%, organic matter removal 56.8% ± 16.6% soil: mass loss 2.34% ± 1.53%, organic matter removal 34.5% ± 22.5%	L0: PP, LDPE, HDPE, PS, PA, PMMA, PET L1: PC	Pellets: PP (3 - 6.3 mm) LDPE (3.4 – 4.5 mm) HDPE (3.6 - 5.0 mm) Granules: PS (3.1 - 4.0 mm) PA (2.9 - 4.4 mm) PC (3.1 - 3.8 mm) PMMA (2.8 - 4.3 mm) Beads: PET (2.9 - 3.6 mm)	weight, size, optical changes	[5]
	Mussel tissue	10%/2M KOH; 60°C; 24h	>99%	L2: PET L3: CA L0: LDPE, HDPE, PA-12, PA-6, PC, PMMA, PP, PS, PSXL, PTFE, PUR, uPVC, ePS	n.d.	weight, visually, PyroGC/MS, Raman	[4]
	Fish tissue	10%/2M KOH; 25°C; 96h	97%	L0: LDPE, HDPE, PP, PS, PET, PVC, PA-6; PA-6,6	fragments (<300 µm): LDPE, HDPE, PP, PS, PET, PVC, PA6, PA	recovery rate, SEM, Raman spectroscopy	[7]
	Fish tissue	10%/2M KOH; 40°C; 96h	99%	L0: LDPE, HDPE, PP, PS, PET, PVC, PA6, PA	fragments (<300 µm): LDPE, HDPE, PP, PS, PET, PVC, PA6, PA	recovery rate, SEM, Raman spectroscopy	[7]
	Fish tissue	6%/1M KOH; 20°C; 48h	good	L2: CA, Cradonyl L1: PA L4: PLA	Pristine and aged plastics from various sources: ABS, CA, EVA, PE, PS, PE, NBR, PA, PBT, PC, PET, PP, PUR, PVC, SAN, PHB, PLA	weight	[8]
	Fish tissue	saturated KOH solution (20M/113%) ; 20°C; 5h then 80°C; 20 min	good	L1: ABS, PA; PET; PC; PVC, PMMA L0: PP, LDPE, HDPE, PS, EPS, PU, EVA, Rubber	Cut fragments: 0.5 cm x 1 cm x 1mm: PP, PE, PS, ABS, PU, PA, EVA, PET, PC, Nitrile, PVC, PMMA, PTFE, Rubber	visually	[9]
	No matrix	KOH 56g/L		L0: PE	Spheres: cera microcrystallina, PE, EPS – 125µm – 1mm Fragments: PE – 125µm-1mm Fibers: Nylon – 125µm-1mm	recovery rate, FTIR	[10]

Alkaline (NaOH or KOH)	Fish tissue	KOH 10% 20°C 2-3		Previous tests confirmed the resistance of plastic particles against 10% KOH (Mergia, unpublished data)	particles >0.2 mm	visually	[11]
	no matrix, efficiency with zebrafish and D. magna mixed and ingested	KOH 10% (w/v), 60°C, 24h	>99% mixed >95% ingested	limited effect on fluorescence well dispersed after treatment L0: PS	3 fluorescent PS beads: A Thermo Fisher Scientific B Baseline ChromTech Research Centre C: Big Goose ChromTech Research Centre	fluorescence intensity, SEM ATR-FTIR	[12]
	no matrix	NaOH 10M, 60°C, 24h		limited effect on fluorescence aggregation after treatment L0: PS	3 fluorescent PS beads: A Thermo Fisher Scientific B Baseline ChromTech Research Centre C: Big Goose ChromTech Research Centre	fluorescence intensity, SEM ATR-FTIR	[12]
	activated sludge	KOH 10%, 60°C, 24h	not considered due to the L4 of 2 polymers	L4: PLA, PET L1: PS, PVC	PS, LDPE, PVC, PP, PET, PA, PLA size: 80 – 330 µm	size distribution (Malvern Mastersizer S long bed), spectral changes by µFTIR and TD-Pyr-GC/MS, effectivity by reduction of dry weight	[13]
	Soil organic matter	KOH 10%, 40°C and 50°C, 24h	20-70 %	L0: PET, PE, PVC, PP, PS fragments	250 – 500 µm fragments (PE, PVC, PS) 500 µm-1 mm fragments (PET, PE, PVC, PP, PS) 1-5 mm fibers (PET, PP)	ATR-FTIR	[14]

*Polymer abbreviations: Cellulose acetate (CA), high and low density polyethylene (HDPE & LDPE), poly(lauryl)lactam (PA12), polycaprolactam (PA6), polyamide (PA), polycarbonate (PC), polyethylene terephthalate (PET), poly(methyl-methacrylate) (PMMA), poly-propylene (PP), polystyrene (PS), cross-linked polystyrene (PSXL), polytetrafluoroethylene (PTFE), polyurethane (PUR) and polyvinyl chloride (PVC). expanded polystyrene (ePS), polyester (PEST).

Acidic sample purification methods (one acid e.g. HNO₃; HCl, H₂SO₄)

Table S3: List of studies that evaluated sample purification methods on their potential to degrade common plastics based on acidic solutions.

The degradation strength was classified according to the classification scheme in Table 1.

	Sample matrix	Protocol	Purification efficiency	Observed effect on synthetic polymers	Size of assessed particles/fibers	Evaluation method	Reference
Acidic (e.g., HNO₃, HCl, H₂SO₄)	Mussel tissue	22.5M/95% HNO ₃ ; 20°C; overnight then 100°C; 2h	n.d.	L4: PA L3 (without tissue): PS	Fragments: PVC, PE – 250µm Fibers of unknown origin with different sizes	recovery rate, visually	[15]
	Mussel tissue	Protocol 3: 65%/14M HNO ₃ ; 20°C; overnight then 60°C; 2h	n.d.	L3: PA-12 L1: CA, LDPE, HDPE, PA-12, PC, PET, PMMA, PP, PS, PSXL, PTFE, PUR, uPVC, ePS	n.d.	weight, visually, Pyr-GC/MS, Raman	[4]
	no matrix	HNO ₃ , 69% (w/w), 70°C, 2h		strong decrease of fluorescence aggregation after treatment L2: PS	3 fluorescent PS beads: A Thermo Fisher Scientific (5 µm) B Baseline ChromTech Research Centre C: Big Goose ChromTech Research Centre	fluorescence intensity, SEM ATR-FTIR	[12]
	Mussel tissue (frozen)	35%/6.5M HNO ₃ ; 60°C; >12h, stirred	100%	L3: PET, HDPE L4: PA L0: PVC	Fragments 125µm-500µm: PET, HDPE, PVC Nylon thread: 500µm-1000µm	recovery, rate, visual, FTIR	[6]
	Fish tissue and no matrix	55%/12M HNO ₃ ; room temperature 4 weeks	n.d.	L4: PA (24h) L0: HDPE (film, pellet & bead), PS, PVC, PES	Nylon (Polyhexamethylene nonanediamide) cylindrical HD PE pellet round 4 mm ² and film square 5 mm ² bead 0.3 mm diameter, PS foam round 5 mm ² , PES square 5 mm ² , PVC fragment irregular	Visually, recovery rate, weight	[16]

Acidic (e.g., HNO₃, HCl, H₂SO₄)	no matrix	HNO ₃ 69%/15,7 M, boiling, 2h	n.n	L4: PA, PET, PUR L3: PS, L2: PC, PE, PP L0: PVC		visual, gravimetry, bulk erosion (GPC), ATR-FTIR	this study
	Fish tissue	37% HCl; 25 °C; 96h	>95%	L4: PA, L3: PET L2: PVC	LDPE, HDPE, PP, PS, PET, PVC, PA-6; PA-6,6 fragments, <300µm LDPE, HDPE, PP, PS foil 0,25mm ² (derived from packaging products)	recovery rate, SEM, Raman spectroscopy recovery rate, weight	[7]
	Fish tissue	69%/15.5M HNO ₃ ; 25 °C; 96h	>95%	L4: PA-6, PA-6,6 L3: LDPE, HDPE, PP L2: PET, PVC L1: PS	LDPE, HDPE, PP, PS, PET, PVC, PA-6; PA-6,6 fragments, <300µm LDPE, HDPE, PP, PS foil 0,25mm ² (derived from packaging products)	recovery rate, SEM, Raman spectroscopy	[7]
	no matrix	ascorbic acid (25 mL, 100 g L-1) 1h		L0: PE, PP, PET(PEST), PVC, PS, PTFE, PA, PLA, EvOH	PE, PP, PET(PEST), PVC, PS, PTFE, PA, PLA, EvOH, size: 125 - 200 µm	visual, FTIR in reflection mode on gold-coated polycarbonate membranes	[17]
	no matrix	citric acid (30 mL, 0.55M) 24h		L0: PE, PP, PET(PEST), PVC, PS, PTFE, PA, PLA, EvOH	PE, PP, PET(PEST), PVC, PS, PTFE, PA, PLA, EvOH, size: 125 - 200 µm	visual, FTIR in reflection mode on gold-coated polycarbonate membranes	[17]
	no matrix	H ₂ SO ₅ Peroxymon osulfuric acid (3:1 H ₂ O ₂ & H ₂ SO ₄), 20.5°C, 48h	n.d.	L4: PA, PUR L0: PET, PUR, PC, PS, PE, PP	Films 10 mm x 10 mm x 100 µm	visual, gravimetry, bulk erosion (GPC), ATR-FTIR	this study

*Polymer abbreviations: Cellulose acetate (CA), high and low density polyethylene (HDPE & LDPE), poly(lauryl)lactam (PA12), polycaprolactam (PA6), polyamide (PA), polycarbonate (PC), polyethylene terephthalate (PET), poly(methyl-methacrylate) (PMMA), poly-propylene (PP), polystyrene (PS), cross-linked polystyrene (PSXL), polytetrafluoroethylene (PTFE), polyurethane (PUR) and polyvinyl chloride (PVC). expanded polystyrene (ePS), polyester (PEST).

Acidic sample purification methods in combination with a second acid, oxidation

agents or microwave digestion (e.g. HNO₃ & HClO₄, H₂SO₅, HNO₃ & NaClO)

Table S5: List of studies that evaluated sample purification methods on their potential to degrade common plastics based on acidic solutions in combination with a second acid, an oxidation agent or microwave digestion. The degradation strength was classified according to the classification scheme in Table 1.

	Sample matrix	Protocol	Purification efficiency	Observed effect on synthetic polymers	Size of assessed particles/fibers	Evaluation method	Reference
Acidic in combination with a second treatment	Mussel tissue	Protocol 4: 4:1 mixture 65%/14M HNO ₃ & 65% HClO ₄ ; 20°C; overnight then boiling 10 min	n.d.	L3: PA-12 L1: CA, LDPE, HDPE, PA- 12, PC, PET, PMMA, PP, PS, PSXL, PTFE, PUR, uPVC, ePS	n.d.	weight, visually, Pyr- GC/MS, Raman	[4]
	no matrix	HNO ₃ (69%) : HCL (37%), 1:1, 80°C, 1 & 2h		strong decrease of fluorescence aggregation after treatment L2: PS	3 fluorescent PS beads: A Thermo Fisher Scientific B Baseline ChromTech Research Centre C: Big Goose ChromTech Research Centre	fluorescence intensity, SEM ATR- FTIR	[12]
	no matrix	HNO ₃ (69%) : HCL (71%), 4:1, 20°C & 90°C, 1, 6 & 12h		strong decrease of fluorescence aggregation after treatment L2: PS	3 fluorescent PS beads: A Thermo Fisher Scientific B Baseline ChromTech Research Centre C: Big Goose ChromTech Research Centre	fluorescence intensity, SEM ATR- FTIR	[12]

Acidic in combination with a second treatment	Fish tissue	9% NaClO; 20°C; overnight then filtered; 65% HNO ₃ & 9% NaClO; 20°C; 5min; then filtered; 99% methanol; ultrasonicati on; 20°C, 5 min	very good	formaldehyde : none NaClO treatment: none Methanol: loss of mass for PVC (25%, L1)	PET, PVC, PE, PP, PS, PC, PA – 0.5-4 mm	visually, weight, Raman	[18]
	Marine biota	Microwave digestion with 65%/14M HNO ₃ and then H ₂ O ₂	n.d.	L3: plastic recovery <25% for PP, LDPE, PE and EPS P2: plastic recovery 50 – 75% for PET, PA	Reference: PP & PE (3 µm), Household samples: PA, EPS, PET and 2 type of LDPE (0.25 mm ²)	Recovery rate, weight	[19]
	Fish tissue	4:1 mixture 69% HNO ₃ & 70% HClO ₄ ; 20°C; 5h then 80°C; 20 min	n.d.	L3: PA, PU, tire rubber L2: ABS, PMMA, PVC L1: PS, EPS, PET, PC	LDPE, HDPE, PP, PS, PET, PVC, PA-6; PA-6,6 fragments, <300µm	Visually recovery rate, SEM, Raman spectroscopy	[9]
	Fish tissue	65% HNO ₃ & 9% NaClO; 20°C; 5min; then filtered;	very good	formaldehyde : L0 for all NaClO: L0 for all Methanol: L1 loss of mass for PVC (25%) HNO ₃ & NaClO: L0 for all	PET, PVC, PE, PP, PS, PC, PA – 0.5-4 mm	visually, weight, Raman	[18]

*Polymer abbreviations: Cellulose acetate (CA), high and low density polyethylene (HDPE & LDPE), poly(lauryl)lactam (PA12), polycaprolactam (PA6), polyamide (PA), polycarbonate (PC), polyethylene terephthalate (PET), poly(methyl-methacrylate) (PMMA), poly-propylene (PP), polystyrene (PS), cross-linked polystyrene (PSXL), polytetrafluoroethylene (PTFE), polyurethane (PUR) and polyvinyl chloride (PVC). expanded polystyrene (ePS), polyester (PEST).

Enzymatic sample purification methods

Table S6: List of studies that evaluated sample purification methods on their potential to degrade common plastics based on single enzymes or a sequential use of different enzymes and/or other agents. The degradation strength was classified according to the classification scheme in Table 1.

	Sample matrix	Protocol	Purification efficiency	Observed effect on synthetic polymers	Size of assessed particles/fibers	Evaluation method	Reference
Enzymatic	Zooplankton	Proteinase-K; 50°C; 2h	>97%	L0: PS, PA, PES, PE, PVC	PS spheres (1.5 – 3.0 mm), PA fishing line (400 µm diameter, length 1mm), PES fibers (10 – 30 µm diameter, length 0.75 – 1.5 mm), PVC granules (60 – 120 µm), PE fragments (60 – 500 µm) from cosmetics	visually, weight, counts	[3]
	Mussel tissue	0.3125% Trypsin digestion; 38-42°C; 30 min	88%	L0: PET, HDPE, PVC, PP, PS, PA	< 0.5 mm and 0.5-5.0 mm	Visually, recovery rate, SEM	[20]
	Mussel tissue	Corolase 7086; 60°C; >12h	100%	L0 (93% recovery rate): PET, HDPE, PVC, PA	Fragments: PET, HDPE, PVC – 125µm-500µm Nylon thread: 500µm-1000µm	recovery, rate, visual, FTIR	[6]
	no matrix	sequence of SDS, 5 enzymes and hydrogen peroxide	very good according to Löder, Imhof [1]	L0: PET, PUR, PC, PS, PE, PP, PVC L1: PA (due to hydrogen peroxide)	Films 10 mm x 10 mm x 100 µm	visual, gravimetry, bulk erosion (GPC), ATR-FTIR	this study
	Marine biota	sequence of SDS, proteinase-K, H2O2 (30%) filtration until dry.	n.d.	L0: PP, PE, LDPE, PET, PA, EPS	Reference: PP & PE (3 µm), Household samples: PA, EPS, PET and 2 type of LDPE (0.25 mm ²)	Recovery rate, weight	[19]
	Soil organic matter	10% SDS 48 h 50°C; Fenton's reagent: 1:1 0.05M FeSO ₄ solution H ₂ O ₂ (30%), 1h, 40°C; Protease 12 h 50°C; Pectinase 48 h 50°C; Viscozyme 48 h 50°C; Cellulase 24 h 40°C; Fenton's reagent 1 h 40°C	77.2 ± 6.6% (SD)	L0: PET, PE, PVC, PA L3: PLA due to Protease treatment	100-400 µm	Visual, ATR-FTIR, Bulk erosion (GPC), thermal transition characteristics via differential scanning calorimetry (DSC)	[21]

*Polymer abbreviations: Cellulose acetate (CA), high and low density polyethylene (HDPE & LDPE), polylauryllactam (PA12), polycaprolactam (PA6), polyamide (PA), polycarbonate (PC), polyethylene terephthalate (PET), poly(methyl-methacrylate) (PMMA), poly-propylene (PP), polystyrene (PS), cross-linked polystyrene (PSXL), polytetrafluoroethylene (PTFE), polyurethane (PUR) and polyvinyl chloride (PVC). expanded polystyrene (ePS), polyester (PEST).

Oxidative sample purification methods

Table S7: List of studies that evaluated sample purification methods on their potential to degrade common plastics based on oxidative agents.

The degradation strength was classified according to the classification scheme in Table 1.

	Sample matrix	Protocol	Purification efficiency	Observed effect on synthetic polymers	Size of assessed particles/fibers	Evaluation method	Reference
oxidative	Sludge, soil and no matrix	30% H ₂ O ₂ ; 60°C; 24h	sludge: mass loss 41.3% ± 2.16%, organic matter removal 80.2% ± 4.20% soil: mass loss 41 6.54% ± 1.01%, organic matter removal 96.3% ± 14.9%	L1: PS, PA66, PVC L0: PP, LDPE, HDPE, PMMA, PC, PET	Pellets: PP - 3-6.3 mm LDPE - 3.4 - 4.5 mm HDPE - 3.6-5.0 mm Granules: PS - 3.1-4.0 mm PA-6,6 - 2.9-4.4 mm PC - 3.1-3.8 mm PMMA - 2.8-4.3 mm Beads: PET - 2.9-3.6 mm	weight, size, optical changes	[5]
	no matrix	H ₂ O ₂ 30% (w/w), 65°C, 24h		limited effect on fluorescence well dispersed after treatment L0: PS	3 fluorescent PS beads: A Thermo Fisher Scientific B Baseline ChromTech Research Centre C: Big Goose ChromTech Research Centre	fluorescence intensity, SEM ATR-FTIR	[12]
	Fish tissue	9% NaClO ₂ ; 20°C; overnight then filtered;	very good	L0: formaldehyde & PET, PVC, PE, PP, PS, PC, PA L0: NaClO & PET, PVC, PE, PP, PS, PC, PA L1: Methanol & PVC	Fragments: 0.5-4 mm: PET, PVC, PE, PP, PS, PC, PA	visually, weight, Raman	[18]
	organic matter from marine snow	H ₂ O ₂ 15%, 30% 24h, 75°C	n.d.	L0: PE, PS	Cospheric polyethylene microspheres (500–600 mm), polystyrene powder (PS, 250 µm, Goodfellow Cambridge Ltd., Huntingdon, England), and polyethylene powder (PE, Alfa Aesar, Ward Hill MA, US)	Raman	[22]
	no matrix	H ₂ O ₂ 30%, 37°C, 24h	n.d.	L0: PET, PUR, PC, PS, PE, PP, PVC L1: PA	Films 10 mm x 10 mm x 100 µm	visual, gravimetry, bulk erosion (GPC), ATR-FTIR	this study

oxidative	Soil organic matter	H ₂ O ₂ 30%, 50°C, 24h	~80-90%	L0: PET, PE, PVC, PP, PS	250 – 500 µm fragments: PE, PVC, PS 500 µm-1 mm fragments: PET, PE, PVC, PP, PS 1-5 mm fibers: PET, PP	ATR-FTIR	[14]
	activated sludge	20 ml H ₂ O ₂ (30%), 60°C, 24H	71.3% ± 1.2%	L1: PLA, PVC L0: PS, LDPE, PVC, PP, PET, PA	PS, LDPE, PVC, PP, PET, PA, PLA size: 80 – 330 µm	size distribution (Malvern Mastersizer S long bed), spectral changes by µFTIR and TD-Pyr-GC/MS, effectivity by reduction of dry weight	[13]
Fenton	no matrix	Fenton's reagent; pH3, 21°C, 2h	n.d	L0: TPU_ester, TPU_ether, PA6, LD-PE L2: PLA-based, PBAT-based, PBS-based L3: tire rubber	particle obtained by cryo-milling: size 80 µm, 250 µm, 315 µm, 1 mm) Biodegradable polymer blends: PLA-based, PBAT-based and PBS-based, thermoplastic polyurethane (TPU_ester, TPU_ether), PA6, tire rubber, LD-PE	Scanning Electron Microscopy, ATR-FTIR, Size distribution, GPC, µ-CT	[23]
	Sludge, soil and no matrix	Fenton's reagent; 20-40°C; 24h	sludge: mass loss 43.8% ± 6.61%, organic matter removal 86.9% ± 9.87% soil: mass loss 6.81% ± 1.56%, organic matter removal 106% ± 13.8%	L0: PP, LDPE, HDPE, PS, PA-6,6, PMMA, PC, PET	Pellets: PP - 3-6.3 mm LDPE – 3.4 – 4.5 mm HDPE – 3.6-5.0 mm Granules: PS – 3.1-4.0 mm PA-6,6 – 2.9-4.4 mm PC – 3.1-3.8 mm PMMA – 2.8-4.3 mm Beads: PET – 2.9-3.6 mm	weight, size, optical changes	[5]
	Wastewater	Fenton's reagent; 20°C; 10 min & 10 min cooling phase	good	L0: PE, PP, PVC, PA (at low catalyst concentrations) L1: PA (at high catalyst concentrations)	PE – 7mm ² PP – 85mm ² PVC – 13mm ² Nylon – 12mm ²	Visually (surface area) , ATR-FTIR	[24]
	no matrix	Fenton's reagent 1:1 0.05M FeSO ₄ solution H ₂ O ₂ (30%), 75 °C,m 24h	n.d.	L0: PET, PUR, PC, PS, PE, PP, PVC, PA	Films 10 mm x 10 mm x 100 µm	visual, gravimetry, bulk erosion (GPC), ATR-FTIR	this study

Fenton	activated sludge	Fenton: 10 ml FeSO ₄ 7H ₂ O (20g/L) with ph3, add 20 ml H ₂ O 30% + additional 50 ml at 90°C, 2x 10 min, addition of H ₂ SO ₄ 98% in drops to dissolve FeO for 30s	83.5% ± 1.8%	L1: PLA, PVC, PET L0: PS, LDPE, PP, PA	PS, LDPE, PVC, PP, PET, PA, PLA size: 80 – 330 μm	size distribution (Malvern Mastersizer S long bed), spectral changes by μFTIR and TD-Pyr-GC/MS, effectivity by reduction of dry weight	[13]
	no matrix	Fenton: (100 mL 30% H ₂ O ₂ , 12.5 mL 0.5 M FeSO ₄). 1h		L0: PE, PP, PET(PEST), PVC, PS, PTFE, PA, PLA, EvOH	125 - 200 μm: PE, PP, PET(PEST), PVC, PS, PTFE, PA, PLA, EvOH,	visual, FTIR in reflection mode on gold-coated polycarbonate membranes	[17]
	Soil organic matter	Fenton: 25 mL H ₂ O ₂ (30%), 25 mL 0.05M FeSO ₄ solution; 50°C	~50-90%	L0: PET, PE, PVC, PP, PS	250 – 500 μm fragments (PE, PVC, PS) 500 μm-1 mm fragments (PET, PE, PVC, PP, PS) 1-5 mm fibers (PET, PP)	ATR-FTIR	[14]
	Treated wastewater effluent, sewage sludge, raw wastewater	Fenton: 100 mL 0.05 M FeSO ₄ , 100 mL 30% H ₂ O ₂ , sequence of up o 3 cycles	n.d.	n.d.	38-50 μm: PMMA particles 100 μm: PS beads	μ-FTIR	(Cunsolo et al. 2021)

*Polymer abbreviations: Cellulose acetate (CA), high and low density polyethylene (HDPE & LDPE), poly(lauryl)lactam (PA12), polycaprolactam (PA6), polyamide (PA), polycarbonate (PC), polyethylene terephthalate (PET), poly(methyl-methacrylate) (PMMA), poly-propylene (PP), polystyrene (PS), cross-linked polystyrene (PSXL), polytetrafluoroethylene (PTFE), polyurethane (PUR) and polyvinyl chloride (PVC). expanded polystyrene (ePS), polyester (PEST).

Other combinations for sample purification

Table S8: List of studies that evaluated sample purification methods on their potential to degrade common plastics based on combinations of different treatment agents.

The degradation strength was classified according to the classification scheme in Table 1.

	Sample matrix	Protocol	Purification efficiency	Observed effect on synthetic polymers	Size of assessed particles/fibers	Evaluation method	Reference
alkaline and oxidative	no matrix	Basic Piranha (H ₂ O ₂ and NH ₃); 21°C, 2h		L0: TPU_ester, TPU_ether, PA6, LD-PE L3: PLA-based PBAT-based, PBS-based, L4: tire rubber,	particles obtained by cryo-milling: size 80 µm, 250 µm, 315 µm, 1 mm) Biodegradable polymer blends: PLA-based, PBAT-based and PBS-based, thermoplastic polyurethane (TPU_ester, TPU_ether), PA6, tire rubber, LD-PE	Scanning Electron Microscopy, ATR-FTIR, Size distribution, GPC, µ-CT	[23]
	Fish tissue	1:1 (KOH:NaCl O); 20°C; 5h then 80°C; 20 min	very good	L0: PP, LDPE, HDPE, PS, EPS, ABS, PU, PA, EVA, PET, PC, Nitrile, PVC, PMMA, PTFE, Rubber	0.5cm x 1cm x 1mm	visually	[9]
alkaline, acidic and oxidative	Fish tissue	1M/4% NaOH; 50°C; 15 min then add 65%/14M HNO ₃ & H ₂ O; 50°C; 15 min; then 80°C; 15 min	100%	L4: PA L2: EPS, LDPE, PVC-soft and rigid L1: PET	HDPE, LDPE, PP PET, PA, PVC – 1-2 mm EPS – 1-5 mm	Weight, visual, ATR-FTIR	[25]

*Polymer abbreviations: Cellulose acetate (CA), high and low density polyethylene (HDPE & LDPE), polylaurylactam (PA12), polycaprolactam (PA6), polyamide (PA), polycarbonate (PC), polyethylene terephthalate (PET), poly(methyl-methacrylate) (PMMA), poly-propylene (PP), polystyrene (PS), cross-linked polystyrene (PSXL), polytetrafluoroethylene (PTFE), polyurethane (PUR) and polyvinyl chloride (PVC). expanded polystyrene (ePS), polyester (PEST).

Density separation

Table S9: List of studies that evaluated sample purification methods on their potential to degrade common plastics based on density separation agents.

The degradation strength was classified according to the classification scheme in Table 1

	Sample matrix	Protocol	Purification efficiency	Observed effect on synthetic polymers	Size of assessed particles/fibres	Evaluation method	Reference
Zinc chloride	no matrix		n.d.	L1: PUR L0: PET, PA, PC, PS, PE, PP	Films 10 mm x 10 mm x 100 μ m	visual, gravimetry, bulk erosion (GPC), ATR-FTIR	this study
	Freshwater	Density separation with zinc chloride	n.d.	L0: LDPE, HDPE, PP, PS, PVC, PET	LDPE, HDPE, PP, PS, PVC, PET – 0.2 mm -5 mm	Visually, FTIR	[26]
	no matrix	ZnCl ₂ density 1.75 kg/L, 24h		L2: EvOH L3: PA L0: PE, PP, PET(PEST), PVC, PS, PTFE, PA, PLA, EvOH	PE, PP, PET(PEST), PVC, PS, PTFE, PA, PLA, EvOH, size: 125 - 200 μ m	visual, FTIR in reflection mode on gold-coated polycarbonate membranes	[17]
	Soil	ZnCl ₂ solution density 1.8 g/cm ³ , 24 h	>99% (dry wt)	L0: PE, PET, PVC, PA, PLA	100-400 μ m (all)	Visual, ATR-FTIR	[21]
	Soil	ZnCl ₂ density 1.7 g/cm ³ , overnight	n.d.	L0: PET, PE, PVC, PP, PS	250 – 500 μ m fragments (PE, PVC, PS) 500 μ m-1 mm fragments (PET, PE, PVC, PP, PS) 1-5 mm fibers (PET, PP)	ATR-FTIR	[14]
Sodium chloride	Soil	NaCl solution density 1.2 g/cm ³ , overnight	n.d.	L0: PET, PE, PVC, PP, PS	250 – 500 μ m fragments (PE, PVC, PS) 500 μ m-1 mm fragments (PET, PE, PVC, PP, PS) 1-5 mm fibers (PET, PP)	ATR-FTIR	[14]
Canola oil	Soil	5 mL Canola oil in 300 mL distilled water in an orbital shaker, 2 h at 100 rpm, settling overnight	n.d.	L0: PET, PE, PP, PS L1: PVC (oil residue may change the IR spectra)	250 – 500 μ m fragments (PE, PVC, PS) 500 μ m-1 mm fragments (PET, PE, PVC, PP, PS) 1-5 mm fibers (PET, PP)	ATR-FTIR	[14]

Sucrose	Freshwater	Density separation with a sucrose solution	n.d.	L0: LDPE, HDPE, PP, PS, PVC, PET	LDPE, HDPE, PP, PS, PVC, PET – 0.2 mm -5 mm	Visually, FTIR	[26]
----------------	------------	--	------	----------------------------------	---	----------------	------

*Polymer abbreviations: Cellulose acetate (CA), high and low density polyethylene (HDPE & LDPE), poly(lauryl)lactam (PA12), polycaprolactam (PA6), polyamide (PA), polycarbonate (PC), polyethylene terephthalate (PET), poly(methyl-methacrylate) (PMMA), poly-propylene (PP), polystyrene (PS), cross-linked polystyrene (PSXL), polytetrafluoroethylene (PTFE), polyurethane (PUR) and polyvinyl chloride (PVC). expanded polystyrene (ePS), polyester (PEST).

References

1. Löder, M.G.J., et al., *Enzymatic purification of microplastics in environmental samples*. Environmental Science & Technology, 2017.
2. Herrera, A., et al., *Novel methodology to isolate microplastics from vegetal-rich samples*. Marine Pollution Bulletin, 2018. **129**(1): p. 61-69.
3. Cole, M., et al., *Isolation of microplastics in biota-rich seawater samples and marine organisms*. Scientific Reports, 2014. **4**: p. Article number: 4528.
4. Dehaut, A., et al., *Microplastics in seafood: Benchmark protocol for their extraction and characterization*. Environmental Pollution, 2016. **215**: p. 223-233.
5. Hurley, R., et al., *Validation of a method for extracting microplastics from complex, organic-rich, environmental matrices*. Environmental Science & Technology, 2018. **52**(13): p. 7409-7417.
6. Catarino, A.I., et al., *Development and optimization of a standard method for extraction of microplastics in mussels by enzyme digestion of soft tissues*. Environmental Toxicology and Chemistry, 2017. **36**(4): p. 947-951.
7. Karami, A., et al., *A high-performance protocol for extraction of microplastics in fish*. Science of The Total Environment, 2017. **578**: p. 485-494.
8. Kühn, S., et al., *The use of potassium hydroxide (KOH) solution as a suitable approach to isolate plastics ingested by marine organisms*. Marine Pollution Bulletin, 2017. **115**(1): p. 86-90.
9. Enders, K., et al., *Extraction of microplastic from biota: recommended acidic digestion destroys common plastic polymers*. ICES Journal of Marine Science, 2017. **74**(1): p. 326-331.
10. Munno, K., et al., *Impacts of temperature and selected chemical digestion methods on microplastic particles*. Environmental Toxicology and Chemistry, 2018. **37**(1): p. 91-98.
11. Foekema, E.M., et al., *Plastic in North Sea fish*. Environmental Science & Technology, 2013. **47**(15): p. 8818–8824.
12. Li, F., et al., *Comparison of six digestion methods on fluorescent intensity and morphology of the fluorescent polystyrene beads*. Marine Pollution Bulletin, 2018. **131**: p. 515-524.
13. Al-Azzawi, M.S.M., et al., *Validation of Sample Preparation Methods for Microplastic Analysis in Wastewater Matrices—Reproducibility and Standardization*. Water, 2020. **12**(9): p. 2445.
14. Radford, F., et al., *Developing a systematic method for extraction of microplastics in soils*. Analytical Methods, 2021. **13**(14): p. 1695-1705.
15. Claessens, M., et al., *New techniques for the detection of microplastics in sediments and field collected organisms*. Marine Pollution Bulletin, 2013. **70**(1–2): p. 227-233.
16. Naidoo, T., K. Goordiyal, and D. Glassom, *Are Nitric Acid (HNO₃) Digestions Efficient in Isolating Microplastics from Juvenile Fish?* Water, Air, & Soil Pollution, 2017. **228**(12): p. 470.
17. Weisser, J., et al., *From the well to the bottle: Identifying sources of microplastics in mineral water*. Water, 2021. **13**(6).
18. Collard, F., et al., *Detection of anthropogenic particles in fish stomachs: An isolation method adapted to identification by Raman spectroscopy*. Archives of Environmental Contamination and Toxicology, 2015. **69**(3): p. 331.

19. Karlsson, T.M., et al., *Screening for microplastics in sediment, water, marine invertebrates and fish: Method development and microplastic accumulation*. Marine Pollution Bulletin, 2017. **122**(1): p. 403-408.
20. Courtene-Jones, W., et al., *Optimisation of enzymatic digestion and validation of specimen preservation methods for the analysis of ingested microplastics*. Analytical Methods, 2017. **9**(9): p. 1437-1445.
21. Möller, J.N., et al., *Tackling the challenge of extracting microplastics from soils: A protocol to purify soil samples for spectroscopic analysis*. Environmental Toxicology and Chemistry, 2021.
22. Zhao, S., et al., *An approach for extraction, characterization and quantitation of microplastic in natural marine snow using Raman microscopy*. Analytical Methods, 2017. **9**(9): p. 1470-1478.
23. Pfohl, P., et al., *Microplastic extraction protocols can impact the polymer structure*. Microplastics and Nanoplastics, 2021. **1**(1): p. 8.
24. Tagg, A.S., et al., *Fenton's reagent for the rapid and efficient isolation of microplastics from wastewater*. Chemical Communications, 2017. **53**(2): p. 372-375.
25. Roch, S. and A. Brinker, *Rapid and efficient method for the detection of microplastic in the gastrointestinal tract of fishes*. Environmental Science & Technology, 2017. **51**(8): p. 4522-4530.
26. Rodrigues, M.O., et al., *Effectiveness of a methodology of microplastics isolation for environmental monitoring in freshwater systems*. Ecological Indicators, 2018. **89**: p. 488-495.

Article 3



**Tackling the challenge of extracting microplastics from soils:
A protocol to purify soil samples for spectroscopic analysis**

Tackling the Challenge of Extracting Microplastics from Soils: A Protocol to Purify Soil Samples for Spectroscopic Analysis

Julia N. Möller,^{a,*} Ingrid Heisel,^a Anna Satzger,^a Eva C. Vizsolyi,^a S.D. Jakob Oster,^a Seema Agarwal,^b Christian Laforsch,^{a,*} and Martin G.J. Löder^{a,*}

^aDepartment of Animal Ecology I and BayCEER, University of Bayreuth, Bayreuth, Germany

^bDepartment of Macromolecular Chemistry II, University of Bayreuth, Bayreuth, Germany

Abstract: Microplastic pollution in soils is an emerging topic in the scientific community, with researchers striving to determine the occurrence and the impact of microplastics on soil health, ecology, and functionality. However, information on the microplastic contamination of soils is limited because of a lack of suitable analytical methods. Because micro-Fourier-transform infrared spectroscopy (μ -FTIR), next to Raman spectroscopy, is one of the few methods that allows the determination of the number, polymer type, shape, and size of microplastic particles, the present study addresses the challenge of purifying soil samples sufficiently to allow a subsequent μ -FTIR analysis. A combination of freeze-drying, sieving, density separation, and a sequential enzymatic-oxidative digestion protocol enables removal of the mineral mass (>99.9% dry wt) and an average reduction of 77% dry weight of the remaining organic fraction. In addition to visual integrity, attenuated total reflectance FTIR, gel permeation chromatography, and differential scanning calorimetry showed that polyamide, polyethylene, polyethylene terephthalate, and polyvinyl chloride in the size range of 100 to 400 μ m were not affected by the approach. However, biodegradable polylactic acid showed visible signs of degradation and reduced molecular weight distribution after protease treatment. Nevertheless, the presented purification protocol is a reliable and robust method to purify relatively large soil samples of approximately 250 g dry weight for spectroscopic analysis in microplastic research and has been shown to recover various microplastic fibers and fragments down to a size of 10 μ m from natural soil samples. *Environ Toxicol Chem* 2022;41:844–857. © 2021 The Authors. *Environmental Toxicology and Chemistry* published by Wiley Periodicals LLC on behalf of SETAC.

Keywords: Microplastics; Soil contamination; Analytical chemistry; Purification protocol; Enzymatic-oxidative digestion; μ -FTIR

INTRODUCTION

Introduction of macro- as well as microplastics into soils is estimated to exceed the numbers emitted into water bodies by far (Kawecki and Nowack 2019). Hence, a substantial proportion of plastic pollution is expected to enter and remain permanently in the soil column (Rillig et al. 2017; Hurley and Nizzetto 2018; Rochman 2018). One entryway for microplastics into soils is mismanagement of waste (Lebreton and Andrady 2019), but also common agricultural practices are known to

introduce microplastics directly into soil systems, such as using treated wastewater for irrigation (He et al. 2018), applying sewage sludge and certain compost types as fertilizers (Weithmann et al. 2018; Corradini et al. 2019; Van den Berg et al. 2020), or practicing plastic-film mulching (Zhou et al. 2019). However, nonagricultural soils have also been shown to contain microplastics, such as floodplain soils (Scheurer and Bigalke 2018), soils on industrial sites (Fuller and Gautam 2016), and soils in home gardens (Huerta Lwanga et al. 2017).

Ongoing research indicates that different types of microplastics may potentially influence a soil's health and functionality in different ways. For instance, De Souza Machado et al. (2019) conducted a study in which soils and spring onions were exposed to 6 microplastic types, including beads, fibers, and fragments. The exposure experiments resulted in altered physical soil parameters as well as changes in plant performance. Treatments with polyamide (PA) beads and polyester fibers elicited the largest differences from the control treatments,

This article contains online-only Supplemental Data.

This is an open access article under the terms of the Creative Commons Attribution License, which permits use, distribution and reproduction in any medium, provided the original work is properly cited.

* Address correspondence to julia.moeller@uni-bayreuth.de, christian.laforsch@uni-bayreuth.de, martin.loeder@uni-bayreuth.de

Published online 23 February 2021 in Wiley Online Library (wileyonlinelibrary.com).

DOI: 10.1002/etc.5024

allowing the tentative assumption that the microplastic's shape and size may also be relevant to the impact on soil properties. To better assess the impact of plastics on soil functionality, it is indispensable to accurately evaluate the microplastic contamination with regard to polymer type, shape, and size. Therefore, appropriate analytical tools and methods are necessary.

To date, there is no established standard method for the sampling, extraction, purification, and identification/quantification of microplastic particles in soil samples (Möller et al. 2020). However, methods developed for analyzing aquatic sediments, which have been the focus of research for a comparatively longer time than soils, can potentially be adapted and the lessons learned from them considered for the processing of soil samples for microplastic analysis. The following paragraph describes several methods mentioned in the literature to extract microplastics from sediment and soil samples.

One of the simplest methods used to extract microplastic particles from soil samples is manual sorting, which is often applied for particles >1 mm (Piehl et al. 2018, soil). Other methods used are oil extraction (Scopetani et al. 2020, compost and soil) and density separation with highly dense salt solutions using NaI, ZnCl₂, NaBr, or Na₆[H₂W₁₂O₆] (Möller et al. 2020, diverse matrices) to remove the mineral matrix. These extraction procedures are often found in combination with one or several purification steps to remove the organic components. These can include an oxidization step with hydrogen peroxide (H₂O₂; Nuelle et al. 2014, marine sediment) or Fenton's reagent (Tagg et al. 2017, wastewater; Hurley et al. 2018, sludge and soil) or alternatively an enzymatic digestion procedure (Löder et al. 2017, marine sediment and water). The methodologies used to identify the microplastic particles also vary between microplastic research groups. Some methods are based on visual identification, for example, by staining the microplastic particles with the fluorescent Nile red (Maes et al. 2017, marine sediment), while others rely on a combination of gas chromatography and mass spectrometry (GC-MS) to identify the polymer type and mass of the microplastics in a sample. Examples of this type of approach include pyrolysis GC-MS used for marine sediments (Nuelle et al. 2014) and thermal extraction desorption (TED) GC-MS developed by Dümichen et al. (2017) and used for digestate. These methods, however, only allow the analysis of very small sample sizes (0.5 mg for pyrolysis GC-MS and 20 mg for TED GC-MS), and therefore require a high degree of sample purification if a larger amount of sample is targeted (Dümichen et al. 2017). It is also important to note the loss of information on particle numbers, sizes, and shapes when using these methods. In comparison, focal plane array (FPA)-based micro-Fourier-transform infrared spectroscopy (μ -FTIR) and Raman microspectroscopy are established methods that can identify the polymer type, number, shape, and size of small (<500 μ m) microplastic particles within environmental samples (Löder et al. 2015; Kumar et al. 2021). A precondition for the identification of microplastic particles via these methods is that microplastic particles are extracted and ideally isolated from the environmental matrix (Löder et al. 2017).

Opposed to aquatic sediments, soils are rich in terrestrial plant debris and humus, which are difficult to break down. Although harsh purification steps with, for example, strong acidic solutions are able to destroy the organic soil content, they also alter the original plastic composition by destroying labile plastic types (Scheurer and Bigalke 2018). To our knowledge, no plastic-conserving approach has been published yet that explicitly addresses those issues related to the spectroscopic analysis of microplastics (10 μ m–5 mm) in soil samples. Therefore, we developed an effective sample purification protocol specifically for the extraction and purification of microplastics (10 μ m–5 mm) from soil samples that allows removal of the bulk mineral matter via density separation and removal of the organic matter by a plastic-friendly enzymatic-oxidative digestion protocol, thereby conserving the original plastic composition.

We investigated the purification efficiency of the protocol for an agriculturally used silt loam soil by analyzing the mass reduction of the total purification protocol. To validate the plastic-friendliness, potential destructive effects on microplastics sized 100 to 400 μ m of different plastic types—PA, polyethylene (PE), polyethylene terephthalate (PET), polyvinylchloride (PVC), and polylactic acid (PLA)—were analyzed. We investigated visual integrity and changes in the functional groups on the polymer surfaces via attenuated total reflectance (ATR)-FTIR spectroscopy, mean molar mass distribution via gel permeation chromatography (GPC), as well as changes in the thermal transition characteristics via differential scanning calorimetry (DSC).

MATERIALS AND METHODS

The protocol is designed to allow the extraction and identification of microplastics from 10 μ m to 5 mm. Because the process of manual extraction and ATR-FTIR analysis of particles >500 μ m is not new as such, the focus will mainly lie on the purification procedure for particles <500 μ m. Empirical experiments concerning the purification efficiency were conducted using three 250-g subsamples of a composite sample of silt-loam soil obtained from the first 10 cm of an experimental agricultural field near Stuttgart, southwest Germany, on 4 December 2019. Another 250-g aliquot of the same soil was used to verify the purification method for analysis of a natural sample.

Prevention of sample contamination

Sample contamination with microplastic particles from the ambient air, clothing, chemicals, or laboratory tools is a significant concern in microplastic analysis of environmental samples. Thus, precautionary measures were applied. Samples were always covered with a glass lid or aluminum foil unless direct handling was necessary. In this case samples were handled under a laminar-flow box. The tools used were made of glass, metal, or polytetrafluorethylene (PTFE), which is excluded from analysis. All required reagents and deionized

water were filtered through 0.2- μm -pore membranes (0.2- μm mixed cellulose ester membrane, diameter 47 mm, Whatman ME 24; Merck) before use, and enzymes were filtered through 0.45- μm membranes (0.45- μm regenerated cellulose membrane, diameter 100 mm, Whatman RC 55; Merck). All laboratory equipment was thoroughly rinsed with prefiltered deionized water, 35% ethanol, and again water before use and in between steps. Screw caps made of plastics were replaced by glass caps. Cotton laboratory coats were worn at all times. Blank samples undergoing the same procedures as the environmental samples were used to monitor possible contamination.

Detailed description of the purification procedure

Following is a description of the purification procedure in a step-by-step manual. Figure 1 shows a flowchart of the entire process.

Sampling and subsampling. Depending on the research question, different soil sampling techniques may be required (Möller et al. 2020), but often the field-sample amount exceeds the 250 g that can be processed with this protocol. Therefore, homogenized (thoroughly mixed but not ground) soil samples (~2 kg) are divided into subsamples of 250 g by

the cone-and-quarter method described by Schumacher et al. (1990).

Freeze drying. Subsamples are freeze-dried under vacuum for 24 h to reduce the soil's aggregate stability (Staricka and Benoit 1995).

Sieving. Subsamples are wet-sieved with prefiltered (0.2 μm) deionized water through a sieve cascade with mesh sizes of 5 mm, 1 mm, and 500 μm (50 mm height, 203 mm diameter; Retsch).

Proceedings for particles >500 μm . The residues on the larger sieves (>500 μm) are manually sorted under a stereomicroscope with forceps, photographed, and stored for a subsequent ATR-FTIR measurement and spectral analysis of all potential microplastic particles (Löder et al. 2017).

Density separation for particles <500 μm . The suspension containing the <500- μm soil fraction is transferred into a pre-cleaned, 2-L-volume glass beaker; covered with a glass lid; and left to settle overnight. This greatly facilitates decanting and filtering the supernatant water over stainless steel mesh filters (47 mm diameter, mesh size 10 μm ; Rolf Körner; filtration unit 3-branch stainless steel vacuum manifold with 500-mL funnels and lids; Sartorius) to remove the water in preparation for a density separation step with a highly dense aqueous zinc chloride (ZnCl_2) solution ($\rho = 1.8 \text{ g cm}^{-3}$; Th. Geyer; Imhof et al. 2012). The filter is kept, and the retained particles are washed back into the beaker with the prefiltered (with a 1- μm polypropylene (PP) absolute filter cartridge, followed by a 2- μm stainless steel mesh filter) ZnCl_2 solution. If necessary, the particles may be scraped off the filter gently using a small metal spatula. The sludge remaining at the bottom of the beaker is then mixed with approximately 1 L of the prefiltered ZnCl_2 solution

and stirred with a stir bar for 20 to 30 min to disperse any remaining aggregates. Subsequently, a custom-made straight-walled glass separation funnel ($\varnothing = 15 \text{ cm}$, $H = 45 \text{ cm}$) with a volume capacity of approximately 4 L is filled with approximately 1 L ZnCl_2 solution, and an overhead stirrer (LLG-uniSTIRRER OH2, 3-hole paddle stirrer, $\varnothing = 67 \text{ mm}$) is inserted and set to 50 rpm. Under continuous stirring, the homogenized soil- ZnCl_2 mixture is transferred into the separation funnel, and another 1 L of the ZnCl_2 solution is used to rinse all remaining particles from the beaker into the funnel, resulting in a final volume of approximately 3 L. The filled separation funnel is then covered with aluminum foil and stirred for 2 h before being left to settle overnight. After a minimum of 12 h of sedimentation, the bottom sediment and ZnCl_2 solution are slowly drained from the funnel, collected, and stored in a clean glass beaker, leaving the low-density fraction (i.e., organic and plastic) floating in the supernatant (0.6 L) in the separation funnel. This fraction is then discharged into a second clean glass beaker via the tap at the bottom and rinsed out of the separation funnel with a fresh ZnCl_2 solution. The collected supernatant is then filtered over 10- μm stainless steel mesh

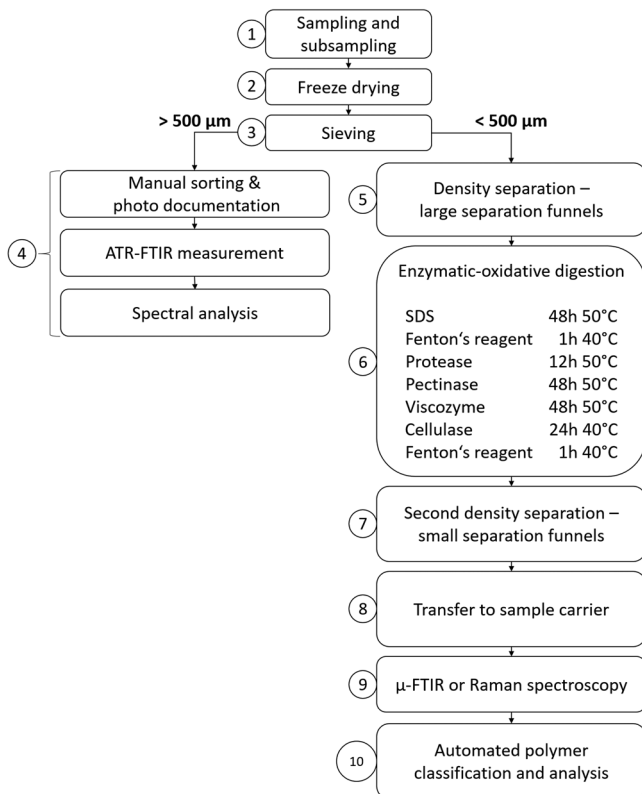


FIGURE 1: Flowchart of the soil purification protocol for microplastic analysis (10 μm –5 mm). ATR-FTIR = attenuated total reflectance Fourier-transform infrared spectroscopy; SDS = sodium dodecyl sulfate; μ -FTIR = micro-Fourier-transform infrared spectroscopy.

filters. The filter cake is then briefly washed with 98% filtered (0.2 μm) ethanol and then with filtered deionized water to remove residual ZnCl_2 . This filter cake is then placed, along with the filter, into a 290 mL precleaned mason jar with a glass lid (WECK) to be further processed with the sequential enzymatic-oxidative digestion protocol (see section *Enzymatic-oxidative digestion*).

The density separation procedure is then conducted a second time with the drained sediment, to increase recovery. The supernatant is collected and filtered, and the filter cake and second filter are added to the same mason jar as the supernatant collected from the first density separation because it is part of the same sample. The ZnCl_2 solution used during the density separation process is collected and regenerated by filtration for future use. The density of the ZnCl_2 solution is checked during regeneration, if the solution reaches a density of 1.7 g cm^{-3} as a result of the dilution with the moist sample, more ZnCl_2 is added to increase the density back to 1.8 g cm^{-3} .

Enzymatic-oxidative digestion. The present enzymatic purification protocol for soil samples is an optimized adaptation of the universal enzymatic purification protocol published by Löder et al. (2017).

The filter cake containing the low-density fraction of the density separation step is consecutively washed off the stainless steel filters into a reaction jar with a small amount of water or buffer using a self-designed high-pressure spray bottle with a needle nozzle, to which the respective chemical reagent or enzyme is added (see Table 1). The filters are also placed into the reaction jar. The mixture is then incubated at the respective temperature (see Table 1), under gentle agitation in an incubation cabinet. Subsequently, the filters, which are continuously used in every procedural step, are taken out of the jar and thoroughly rinsed with filtered, deionized water, washing any adhering particles back into the reaction jar. The cleaned filters are then placed into the stainless steel vacuum filtration unit funnels, through which the sample is then filtered. The jar is thoroughly rinsed onto the filters, and the filter cake on the stainless steel filters is washed with filtered deionized water to avoid reagents from the previous step interfering with subsequent reactions. Thereafter, any residual particles sticking to the filtration funnel are washed into the reaction jar with water or the appropriate buffer to avoid further dilution. The filters and filter cake are also added for the consecutive step.

Step a. Sodium dodecyl sulfate (SDS) is an anionic detergent capable of solubilizing lipids and proteins from cell walls (Cicolini et al. 1998). We used 50 mL of a 10% (w/v) SDS solution per reaction jar, incubated for 48 h at 50°C .

Step b. Fenton's reagent is a strong oxidizing agent composed of H_2O_2 and a ferrous ion (Fe^{2+}) catalyst, proposed in several previous publications as purification protocols for complex environmental samples because it is more effective at removing organic compounds than H_2O_2 alone (Tagg et al. 2017; Hurley et al. 2018). In the present protocol, 25 mL of 30% H_2O_2 is added to the sample and continuously stirred with a magnetic stir bar, before adding 25 mL of a 0.05 M Fe(II) solution (composed of 7.5 g iron[III] sulfate heptahydrate [$\text{FeSO}_4 \times 7\text{H}_2\text{O}$] in 500 mL ultrapure water and 3 mL concentrated sulfuric acid). The reaction with organic compounds is strongly exothermic; thus, an ice bath should be made ready beforehand and used when the reaction temperature reaches 38 to 39°C to keep the reaction temperature below 40°C because too high temperatures may adversely affect some microplastic particle types (Munno et al. 2018).

Step c. Protease hydrolyzes insoluble protein structures into soluble peptides. In the present study, 5 mL of Protease A-01 (subtilisin, EC 3.4.21.62, enzymatic activity 1.100 U mL^{-1} ; ASA Spezialenzyme) are used in 25 mL of 0.1 M Tris-HCl buffer, set to pH 9.0 with concentrated HCl. The samples are then incubated at 50°C for 12 h.

Step d. Dead plant matter containing lignin and cellulose structures are extremely stable, making their removal from environmental samples difficult without resorting to chemically harsh procedures that would also damage plastic particles (Löder et al. 2017). However, specific types of fungi are capable of degrading lignocellulosic structures. Ramos et al. (2016) explored the in vitro production of plant cell wall-degrading enzymes by *Macrophomina phaseolina* (a fungal plant pathogen). They established, that a sequence of pectinases followed by hemicellulases and cellulases “promote initial tissue maceration followed by cell wall degradation” (Ramos et al. 2016). To emulate the fungal plant degradation, commercially available technical enzymes were used: pectinase degrades pectin, which can be found in the primary cell walls of all land plants as well as in the middle lamellae between cell walls (Willats et al. 2001). In our protocol we use 5 mL of Pektinase L-40 (polygalacturonase, pectin depolymerase, EC

TABLE 1: Enzymatic-oxidative digestion protocol for soil samples^a

Step	Volume	Reagents	Incubation time	Incubation temperature
a	50 mL	10% sodium dodecyl sulfate	48 h	50°C
b	50 mL	Fenton's reagent	1 h	40°C
c	25 + 5 mL	Tris HCl 0.1 M buffer, pH 9, protease	12 h	50°C
d	25 + 5 mL	NaAc 0.1 M buffer, pH 5, pectinase	48 h	50°C
e	25 + 1 mL	NaAc 0.1 M buffer, pH 5, viscozyme L	48 h	50°C
f	25 + 5 mL	NaAc 0.1 M buffer, pH 5, cellulase	24 h	40°C
g	50 mL	Fenton's reagent	1 h	40°C

^aThis protocol enables the removal of soil organic matter and cellulosic plant residue.

3.2.1.15; ASA Spezialenzyme) in 25 mL of 0.1 M NaAc buffer set to pH 5 with concentrated acetic acid and incubated for 48 h at 50 °C.

Step e. Viscozyme L (endo-beta-glucanase, V2010; Novozymes) is a cellulolytic enzyme mix extracted from *Aspergillus aculeatus*, with the key enzyme being endo-1,3(4)-beta glucanase, splitting the β -(1,3) linkages of the molecules. The product also contains activity of arabanase, xylanase, cellulase, and hemicellulose. Viscozyme L (1 mL) is added to the sample with 25 mL of 0.1 M NaAc buffer set to pH 5 and incubated at 50 °C for 48 h.

Step f. Cellulase TXL (endo-1,4-beta-glucanase, EC3.2.1.4; ASA Spezialenzyme) is a very similar cellulolytic enzymatic mix (cellulase, hemicellulase, xylanase) extracted from *Trichoderma longibrachiatum*, splitting the β -(1,4) linkages of the molecules. Cellulase TXL (5 mL) is added to the samples with 25 mL of 0.1 M NaAc buffer set to pH 5 and incubated at 50 °C for 24 h.

Step g. A second Fenton's reagent step is conducted, as described in step b, to remove any residual organic matter.

Second density separation. After the second Fenton's reagent step, the sample is filtered with 10- μ m stainless steel filters and washed clean of any residual H₂O₂. The sample (filter cake) is then washed off the filter with a 1.8 g cm⁻³ ZnCl₂ solution into a precleaned glass beaker, using a stainless steel spatula to ensure the complete transfer of particles. The filter is then checked under a stereomicroscope to verify that no particles remain on the filter surface and then discarded. The ZnCl₂ solution-sample mixture is then transferred into a small, straight-walled separation funnel with a volume capacity of approximately 400 mL and stirred with a glass rod, which is then rinsed back into the separation funnel with ZnCl₂ solution to ensure that no particles are extracted accidentally. After stirring, the separation funnels are immediately covered with a glass lid and left to settle overnight (at least 12 h). This step is necessary to remove any silt or clay particles that were not removed in the first density separation step. The sediment is then released from the separation funnel and discarded, whereas the upper lightweight fraction containing floating microplastic particles is filtered onto a 10- μ m stainless steel mesh filter. This is then rinsed with 98% ethanol and deionized water to remove residual ZnCl₂.

Transfer to sample carrier. The filter is taken out and rinsed off thoroughly with deionized water into a small glass beaker and transferred, with a small custom-made glass funnel ($\varnothing = 10$ mm), onto one or more aluminum oxide filters (0.2 μ m, Anodisc; Whatman GE Healthcare), depending on the amount of particulate content in the purified sample. In this context it is important to avoid thicker layers of material because overlapping particles will obstruct the proper identification of microplastic particles in the sample.

μ -FTIR spectroscopy. The aluminum oxide filters are then measured using a Bruker Hyperion 3000 FTIR microscope (Bruker Optik), equipped with a 64 \times 64-pixel FPA detector in conjunction with a Tensor 27 spectrometer. The samples are measured in transmission mode with a 3.8 \times infrared objective (spatial resolution 11.05 μ m) and a wavelength range of 3600 to 1250 cm⁻¹ with a resolution of 8 cm⁻¹ and a coaddition of 6 scans. Data processing is conducted using the Bruker OPUS software, Ver 7.5 (Bruker Optik).

Polymer classification. Automated spectral analysis is performed with the "BayreuthParticleFinder" module in ImageLab, Ver 4.1 (EPINA). This software tool allows a fast and reliable automated identification of currently 22 common plastic polymers based on the principle of random decision forest classifiers (Hufnagl et al. 2019). Alternatively, other spectroscopic analysis tools, such as the free software siMPle (Primpke et al. 2020), may be used. In principle, the purified samples may also be analyzed using Raman microspectroscopy, which potentially would allow a pixel resolution of down to 500 nm (Käppler et al. 2015). In this case smaller mesh sizes of the filters used during the whole density separation and purification procedure would be necessary.

Determination of purification efficiency

Purification efficiency was determined by gravimetric analysis. A sample of approximately 2 kg silt loam obtained from the first 10 cm of an experimental agricultural field near Stuttgart, southwest Germany, was thoroughly mixed in an aluminum pan with a spoon and then freeze-dried. Three subsamples of 250 g each were taken by the cone-and-quarter method and underwent the density separation procedure described in the section *Density separation for particles <500 μ m*. Before filtering the supernatant containing the lightweight fraction, the 10- μ m stainless steel mesh filters were oven-dried at 105 °C and weighed with a laboratory precision scale ($d = 0.01$ mg, OHAUS Explorer), with the respective weights noted. The filtered lightweight fraction was then oven-dried on the filter at 40 °C for approximately 48 h and weighed until mass consistency (± 0.2 mg). The previously determined weight of the filters was subtracted to obtain the mass of the lightweight fraction.

After undergoing the enzymatic-oxidative digestion protocol as well as the second density separation step (see sections *Enzymatic-oxidative digestion* and *Second density separation*), the purified sample was again transferred onto the same stainless steel filter and washed off thoroughly with 98% ethanol and water to remove any residual ZnCl₂. The purified sample and filter were then dried at 40 °C and weighed until mass consistency. The mass difference of the sample matter before and after treatment was recorded and the mean purification efficiency calculated. In addition, the organic matter reduction after each purification step was photo-documented (see Figure 2) using a stereomicroscope (Leica M50; Leica

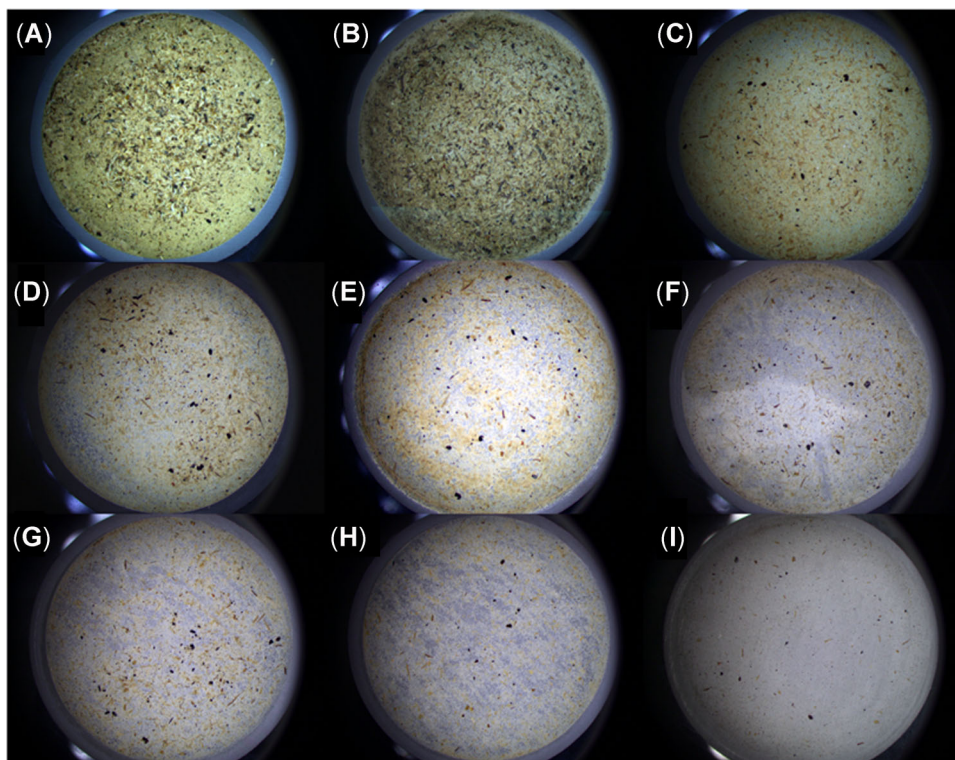


FIGURE 2: Sequential organic matter removal in the course of enzymatic-oxidative digestion—sample 3. Visual documentation of the removal efficiency of the single steps in the purification protocol. (A) Organic matter after density separation. (B) After 48-h sodium dodecyl sulfate. (C) After 1-h Fenton's reagent. (D) After 12-h protease. (E) After 48-h pectinase. (F) After 48-h viscozyme L. (G) After 24-h cellulase. (H) After 1-h Fenton's reagent. (I) After 24-h density separation in zinc chloride solution.

Microsystems; Olympus DP 26 camera; Olympus) and the imaging software cellSens (Olympus).

Determination of effects of the enzymatic-oxidative digestion procedure on microplastic particles

Seven different microplastic particle types were chosen to assess if the enzymatic-oxidative digestion protocol causes any damage on a visible or molecular level. Next to polymer types commonly found in environmental samples, such as the chemically resistant PE as well as polymers more vulnerable to chemical degradation such as PA, PET, and PVC, the biodegradable PLA was also tested. Polylactic acid is an increasingly popular plastic material used, for example, in 3D printing, food packaging, and bin liners for organic waste. Thus, PLA may also be among the synthetic polymers found in soils, especially agricultural soils amended with compost derived from biowaste-treatment plants.

The PLA fragments ($\varnothing = 200\ \mu\text{m}$ –1 mm) were obtained by cryo-milling virgin PLA pellets (Ingeo Biopolymer 7001D; Nature Works) and sieving the ground product. The milling and sieving were conducted by the Institute for Plastics Technology in Stuttgart. The fragments of PA ($\varnothing = 150$ –300 μm , Schaetti fix 5230) and PE ($\varnothing = 100$ –400 μm , Schaetti fix 140) were obtained from Schaetti. The fragments of PET ($\varnothing = 200$ –400 μm) and PVC

($\varnothing = 150$ –200 μm) were obtained by cryo-milling and sieving virgin pellets at the University of Bayreuth. Green fluorescent PE beads ($\varnothing = 150$ –180 μm , UVPMS-BG-1.00) were obtained from Cospheric, and yellow fluorescent PET fibers ($\varnothing = 16\ \mu\text{m}$, $l = 1\ \text{mm}$) were obtained from a high-visibility raincoat and cut to a length of 1 mm using a pair of microscissors.

Using needle and fine-point high-precision forceps, 25 particles of each microplastic type were counted out, photographed, and fixed on a gelatin platelet (1 × 1 cm) cut from a sheet of gelatine leaf (Dr. Oetker Blatt Gelatine) under a stereomicroscope (Leica M50) equipped with an Olympus DP 26 camera. The gelatin is used to ensure that all particles can be transferred from under the stereomicroscope into the reaction containers without losing them (e.g., from static forces). The gelatin was then dissolved in water at 40 °C and filtered off, with the particles remaining on the 10- μm stainless steel mesh filter. All particles then underwent the complete enzymatic-oxidative digestion protocol including the second ZnCl_2 solution treatment.

Visual analysis

After every step, once the reagents were filtered off, the filter containing the microplastic particles was carefully laid under the stereomicroscope and screened for the microplastic particles, which were then photographed. Despite rinsing the filtration funnels thoroughly with water in an attempt to transfer

any adhering particles onto the filter, some particles stuck to the bottom of the funnel when extracting the filter; these particles were then directly washed back into the reaction jar with the subsequent reagent and were not photographed at the respective point in time. After the final step (ZnCl₂ solution), all particles were extracted from the filter with a needle and photographed without the filter as background to better compare the particles' appearance before and after the treatments. Because of static forces causing the particles to "jump," some particles were lost during transfer with the needle. The extracted particles were then kept safe for later μ -FTIR and ATR-FTIR analyses.

ATR-FTIR analysis

Because the quality of the μ -FTIR spectra in transmittance mode is dependent on the particle shape and size (e.g., very thick particles may result in the total absorption of the infrared radiation, whereas spherical particles and fibers often show disrupted spectra as a result of radiation scattering), ATR-FTIR spectroscopy was chosen as a method to compare pristine particles and the particles that underwent the enzymatic-oxidative digestion protocol. For each polymer type, respectively, 5 of the particles that underwent the enzymatic-oxidative digestion protocol were selected randomly and measured via ATR-FTIR spectroscopy (Alpha ATR-FTIR equipped with diamond crystal; Bruker Optik). For the measurement of each particle, 8 background scans were pooled, followed by 8 sample scans with a spectral resolution of 8 cm⁻¹ in a wavenumber range of 4000 to 400 cm⁻¹. Using the software OPUS 7.5, the resulting spectra were compared to the spectra of untreated control particles, to determine if any changes to the functional groups in the polymer had occurred.

GPC analysis

To determine changes in the molar mass distribution of the pristine particles and particles that underwent the purification treatment, a GPC analysis was conducted.

For PLA, the GPC measurement was performed on an instrument with 4 styrene divinylbenzene (SDV) gel columns (particle size = 5 μ m) with porosity range from 10² to 10⁵ Å (Polymer Standards Service GmbH [PSS]) together with a refractive index detector (1200 Series, Agilent). Tetrahydrofuran (HPLC grade) was used as a solvent (for dissolving the polymer and as an eluting solvent) with a flow rate of 1.0 mL min⁻¹. As internal standard toluene (HPLC grade) was used. The calibration was done with narrowly distributed polystyrene (PS) homopolymers (PSS calibration kit). An injection volume of 20 μ L was used for the measurements. The sample was dissolved in tetrahydrofuran and filtered through a 0.22- μ m PTFE filter before analysis.

The molar mass of the rest of the polymers with the exception of PE was measured using hexafluoroisopropanol (HFIP; HPLC grade) as the eluting solvent. The GPC measurement was performed on an instrument with a perfluorinated gel

(PFG) precolumn and 2 PSS-PFG columns (particle size = 7 μ m) with porosity range from 100 to 300 Å (PSS) together with a refractive index detector (Agilent 1200 Series). Hexafluoroisopropanol with potassium trifluoroacetate (4.8 g in 600 mL HFIP) was used as a solvent (to dissolve the polymer and as an eluting solvent) with a flow rate of 0.5 mL min⁻¹. As an internal standard, toluene (HPLC grade) was used. The calibration was done with narrowly distributed polymethyl methacrylate (PMMA) homopolymers (PSS calibration kit). The sample was dissolved in HFIP with potassium trifluoroacetate and filtered through a 0.22- μ m PTFE filter before analysis. An injection volume of 20 μ L was used for the measurement, and the GPC columns were maintained at room temperature. The molar masses reported are in reference to PMMA standards.

The average mass of PE can only be analyzed by high-temperature GPC and could therefore not be analyzed in the scope of the present study.

DSC analysis

The DSC measurements were carried out on NETZSCH DSC 204F1 Phoenix instrument under a nitrogen atmosphere with a gas flow rate of 20 mL min⁻¹. A sample size of approximately 5 mg was used for each measurement. The samples were heated with a heating rate of 10 K min⁻¹.

The degree of crystallinity was calculated using the following formula:

$$X_c = \frac{\Delta H_m - \Delta H_c}{\Delta H_m^0} 100\%$$

In this equation, ΔH_m is the enthalpy of melting, ΔH_c is the enthalpy of crystallization, and ΔH_m^0 is the enthalpy of melting for 100% crystalline polymer. Values for the enthalpy of melting for 100% crystalline PLA, low-density PE, and PET were taken as 93.6 J g⁻¹ (Turner et al. 2004), 293 J g⁻¹ (Atkinson and Richardson 1969), and 130 J g⁻¹ (Müller et al. 2005), respectively. The actual chemical structure of PA is not known. Therefore, the percentage of crystallinity was not calculated.

RESULTS

Purification efficiency

The vast majority of the soil mass is already removed in the density separation step: of a 250-g soil sample, 52, 38, and 160 mg solid particulate matter (>10 μ m) remained in the supernatant phase of the ZnCl₂ solution for samples 1, 2, and 3, respectively. Thus, the removal of the mineral fraction results in a mass removal of >99.9%. Nevertheless, the low-density fraction remaining in the supernatant still contains too much matter for a comprehensive μ -FTIR analysis. For the sake of simplicity, the particulate matter extracted from the supernatant will henceforth be described as the "lightweight fraction."

After the lightweight fraction was extracted, dried, and weighed, it underwent the digestion protocol, as described in the sections *Enzymatic-oxidative digestion* and *Second density*

separation. As can be seen in Figure 2, each digestion step contributes slightly to the overall high purification efficiency. Figure 2A shows the lightweight fraction collected on a 10- μm stainless steel mesh filter ($\varnothing = 47\text{ mm}$) after undergoing density separation. Although the SDS step (Figure 2B) only shows a slight discoloration of the material, the subsequent step with Fenton's reagent already shows a visible decrease of organic matter (Figure 2C). The enzymes protease, pectinase, viscozyme, and cellulase (Figure 2D–G) show a slight but significant reduction in the mostly plant-derived organic matter, which is almost completely removed by the second Fenton's reagent step (Figure 2H). The small granular structures visible in Figure 2H, which are most likely of mineral origin, are removed in the second density separation step, leaving a manageable amount of seeds, black carbon particles, and some plant-based fragments on the filter to be analyzed for the presence of microplastics. In terms of mass loss, the enzymatic-oxidative digestion protocol and second density separation protocol allowed a mass reduction of 73.9, 73.0, and 84.8% for samples 1, 2, and 3, respectively (see Figure 3). An average purification efficiency of $77.2 \pm 6.6\%$ (standard deviation) can be achieved for the lightweight fraction of soil samples. The mass losses in between the single steps of the enzymatic-oxidative digestion steps were not recorded.

Effects of the enzymatic-oxidative digestion procedure on microplastic particles

For investigation of any obvious destructive effects on the added microplastic particles caused by the purification

TABLE 2: Number of spiked particles, number of recovered particles, and number of optical matches

	No. spiked particles	Recovery after enzymatic digestion protocol	Optical matches
PET fibers	25	23	23
PET fragments	25	23	23
PE spheres	25	23	21
PVC fragments	25	24	22
PE fragments	25	22	21
PA fragments	25	10	9
PLA fragments	25	30	0

PET = polyethylene terephthalate; PE = polyethylene; PVC = polyvinylchloride; PA = polyamide; PLA = polylactic acid.

protocol, the microplastic particles were photographed under a stereomicroscope before, during, and after the enzymatic-oxidative digestion protocol. The number of spiked and recovered particles as well as the number of optical matches per microplastic type are given in Table 2. Optical matches are to be understood as particles that do not show any visual differences in shape and size when comparing the photographs from before and after the enzymatic-oxidative digestion protocol (see Supplemental Data, Figure S1). With the exception of PA and PLA, the recovery rates for the investigated polymers were 88 to 96%. The reduced recovery in those polymers was most probably due to losses during the manual transfer from the filter. All of the recovered PET fibers and PET fragments were optical matches, whereas 2 of the recovered PE spheres

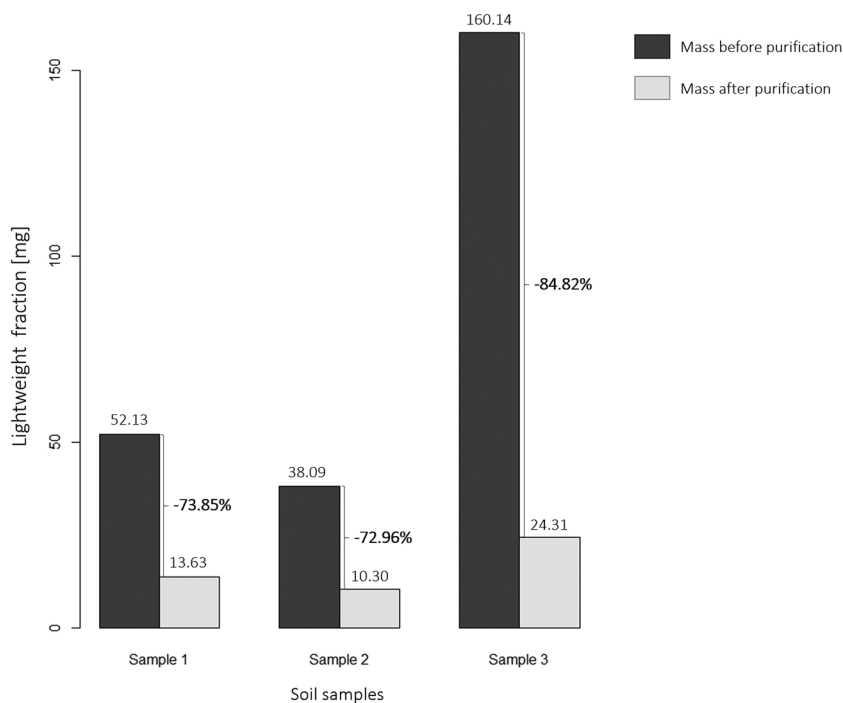


FIGURE 3: Lightweight fraction purification efficiency. The dark column represents the mass of the lightweight fraction (i.e., particulate matter remaining in the supernatant after density separation) before the enzymatic purification procedure. The light column represents the remaining mass after the purification procedure. The percentages given in bold next to the braces respectively represent the percentual mass loss.

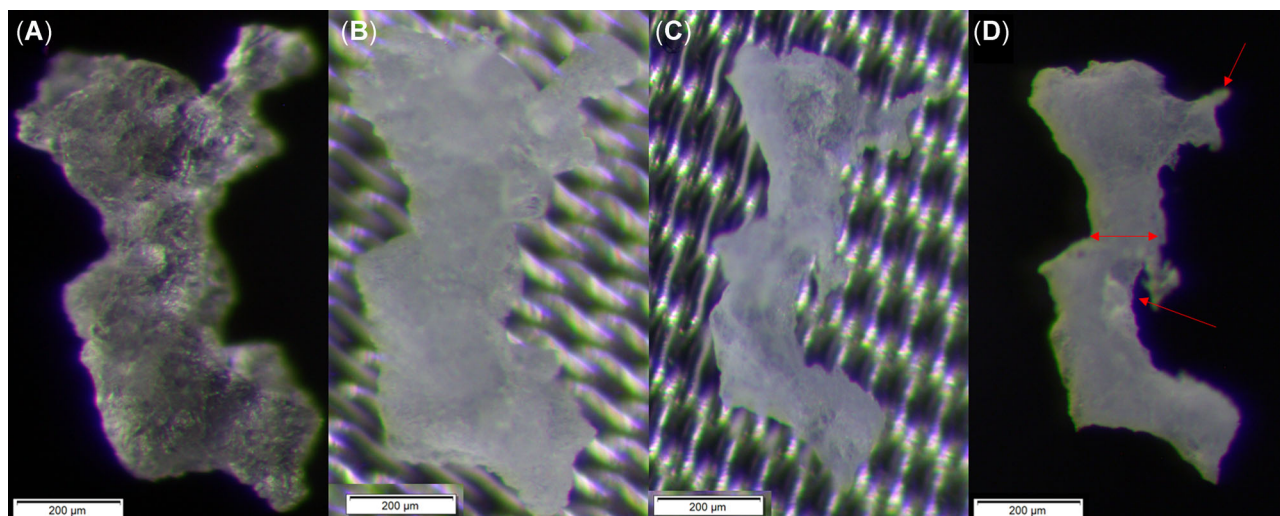


FIGURE 4: Degradation of a poly(lactic acid) particle during the enzymatic-oxidative digestion protocol. (A) Particle before enzymatic-oxidative digestion protocol. (B) Particle after 48 h in sodium dodecyl sulfate and 1 h in Fenton's reagent. (C) Particle after 12-h protease. (D) Particle after the 5 subsequent steps (i.e., 48-h pectinase, 48-h viscozyme L, 24-h cellulase, 1-h Fenton's reagent, and 24-h $ZnCl_2$ solution).

were sharp-edged fragments, indicating that at least one of the spheres had been broken mechanically. Two of the PVC particles and one of the PE particles seemed to have become slightly smaller and rounder, possibly due to mechanical abrasion when the particles are washed against the 10- μm stainless steel mesh filter with a high-pressure water jet. Polyamide showed very low recovery rates but high optical match rates, indicating losses as a consequence of the handling and filtration steps, rather than degradation processes. One exception is PLA, where >25 particles were recovered, because of fragmentation of the particles. All PLA particles showed a notable degradation in size and shape. When comparing the particles after each step of the enzymatic-oxidative digestion protocol, it became apparent that the particles only showed

signs of degradation after the 12-h protease step. The particles showed signs of surface erosion, becoming smaller and partially fragmented. No further degradation could be observed after the 5 following steps (Figure 4), indicating that the protease step was indeed the cause of the PLA particle degradation.

ATR analysis

Because of the shapes (spheres) and often relatively large thickness of the particles, ATR-FTIR analysis (instead of μ -FTIR analysis) was conducted to determine any changes in the functional groups of the particles' surface. The PET fibers, PET fragments, PE spheres, PVC fragments, low-density PE

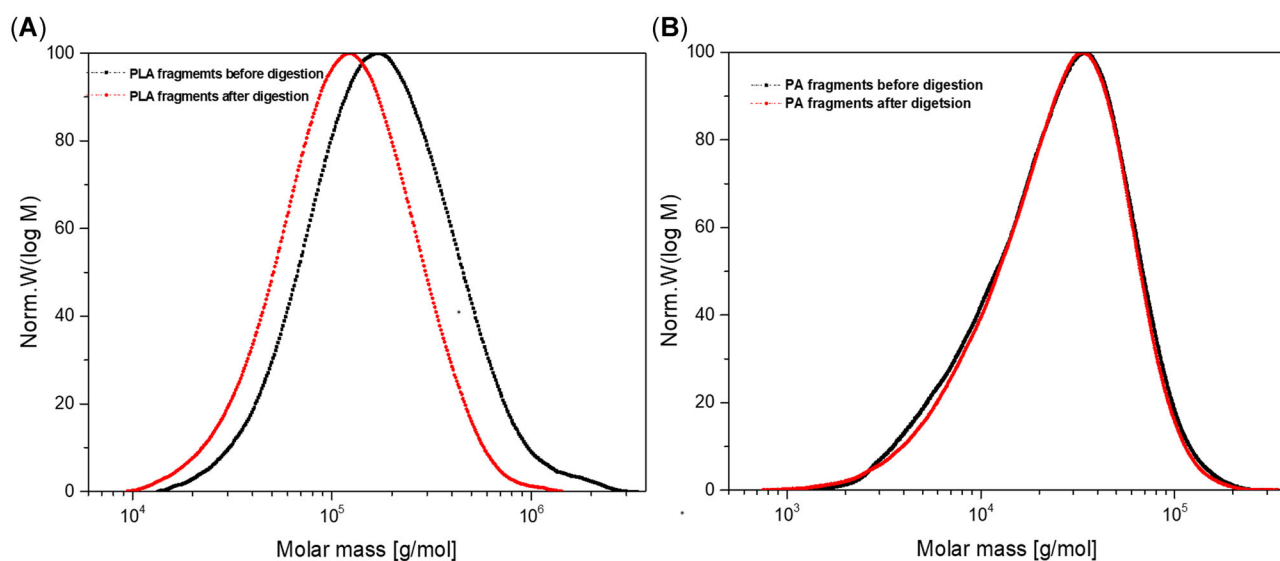


FIGURE 5: Molar mass curves of poly(lactic acid) (A) and polyamide (B) fragments before and after digestion using hexafluoro-2-propanol eluent in gel permeation chromatography. The black curve represents the pristine polymer and the red curve, the polymer after undergoing the digestion protocol. PLA = poly(lactic acid); PA = polyamide; Norm. W = normalised molecular weight.

fragments, and PA fragments showed no changes in the spectral bands compared to the control particles, whereas 3 of the 5 PLA fragments showed a broad band in the region of 3300 to 3650 cm^{-1} , indicating $-\text{OH}$ stretching, possibly as a result of degradation processes.

GPC analysis

Figure 5A shows the molar mass comparison of PLA before and after treatment, as determined by GPC using PS as the calibration standard. There was a change in the average molar mass, M_n (number average molar mass), after treatment from approximately 128.000 g mol^{-1} to approximately 89.000 g mol^{-1} , with a slight shift in molar mass dispersity from 1.93 to 1.75. The GPC curve remained unimodal. Proteolytic enzymes, such as proteases, are well known to catalyze the hydrolysis of ester bonds in aliphatic polyesters (PLA). Although, slight degradation of PLA with macromolecular chain scission was observed, PLA was not completely degraded under the conditions used in the present study based on the slow rate of hydrolysis. Other enzymes used for the treatment are not specific for polyester hydrolysis.

There was no change in the molar mass of the other polymers studied in the present study (see Figure 5B; Supplemental Data, Figures S2–S5), showing the tolerance to the steps used for sample preparation. These polymers have either a strong C–C backbone (PE, PVC) or a not easily hydrolyzable C-heteroatom backbone (PA, PET).

DSC analysis

DSC measurements were carried out to study the effect of the digestion procedure on thermal transitions of polymers. Polyvinylchloride was amorphous with a glass transition temperature (T_g) $85 \pm 2^\circ\text{C}$, which remained unchanged on digestion. Pristine PLA showed a very low degree of crystallinity ($\sim 1\%$). It showed a T_g of $64 \pm 2^\circ\text{C}$, broad crystallization, and melting peaks centered at 110 and 151°C , respectively. After digestion, PLA had almost the same thermal behavior in DSC measurements concerning crystallization and melting with a degree of crystallinity of approximately 2%. The significant difference was in the enthalpy of crystallization, which was significantly higher (20.8 J g^{-1}) than that of pristine PLA (2.26 J g^{-1}). This might be due to the decrease in molar mass, as evident by GPC measurement, providing better crystallization tendency during heating. Low-density PE, PET, and PA showed semicrystalline behavior. Melting transitions were seen as broad peaks without significant change in thermal transition behavior, degree of crystallinity, and enthalpy of melting after digestion (see Supplemental Data, Figure S6 and Table S1).

Application to an environmental sample

In an exemplary 250-g subsample from the same silt-loam experimental agricultural field near Stuttgart, which was fully digested and analyzed via μ -FTIR spectroscopy, a total of

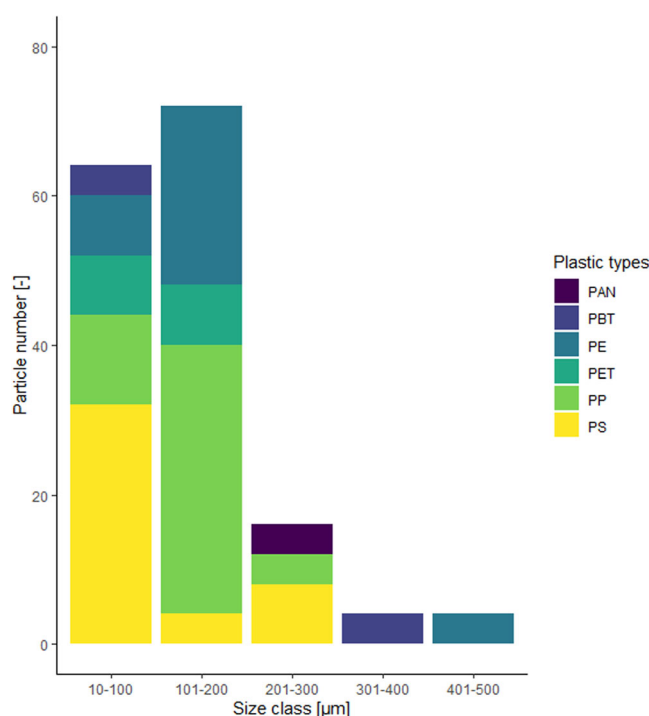


FIGURE 6: Distribution of microplastic types within different size classes in an exemplary environmental sample. PAN = polyacrylonitrile; PBT = polybutylene terephthalate; PE = polyethylene; PET = polyethylene terephthalate; PP = polypropylene; PS = polystyrene.

160 microplastic particles were found, of which 85% were fragments and 15% were fibers. The plastic types that were identified were, in decreasing abundance, PP (32.5%), PS (27.5%), PE (22.5%), PET (10%), polybutylene terephthalate (5%), and polyacrylonitrile (2.5%). Of the identified particles, 85% were $<201 \mu\text{m}$: 10 to $100 \mu\text{m}$ (40%), 101 to $200 \mu\text{m}$ (45%), 201 to $300 \mu\text{m}$ (10%), 301 to $400 \mu\text{m}$ (2.5%), 401 to $500 \mu\text{m}$ (2.5%; see Figure 6).

DISCUSSION AND CONCLUSION

The aim of the present study was to develop a soil sample purification method that 1) allows the identification microplastics in general but with a special focus on small ($<500 \mu\text{m}$) microplastic particles, 2) does not destroy conventional plastic types, and 3) enables the analysis of a relatively large sample volume of 250 g dry weight.

In this section, the differences of the soil purification protocol from previously published protocols (see Table 3) will be discussed.

Scheurer and Bigalke (2018) were among the first to publish a microplastic analysis protocol for soils that allows assessment of the size and number of microplastic particles using μ -FTIR analysis. However, the use of NaCl solution (1.2 g cm^{-3}) for density separation and hot nitric acid digestion to remove the organic matter may lead to underestimation of polymers with a density $>1.2 \text{ g cm}^{-3}$ and to an acid-induced destruction of PA, PET, and acrylonitrile butadiene styrene.

TABLE 3: Comparison between the present study and previously published purification protocols for soil samples

Reference	Density separation	Purification	Analytical method	Sample Size	Spiked MP size range	Purification efficiency	Polymer destruction/loss
Present study	ZnCl ₂ solution (1.8 g cm ⁻³) in separation funnel	Enzymatic-oxidative digestion; duration: 8 d	ATR-FTIR and μ -FTIR spectroscopy	250 g	100–400 μ m	Mineral matter >99.9%; organic matter 77.2 \pm 6.6%	Destruction: PLA Tested polymers: PET, PE, PVC, PA, PLA
Scheurer and Bigalke (2018)	NaCl solution (1.2 g cm ⁻³) with centrifugation	Hot nitric acid digestion; duration: 2 d	μ -FTIR spectroscopy	50 mL	500 μ m–1 mm	Mineral matter >99.9%; organic matter >99%	Destruction: ABS, PA, PET Tested polymers: PVC, PP, PE, PC, PS, PU, ABS, PA, PET
Hurley et al. (2018)	Water (1.0 g cm ⁻³) and NaI solution (1.8 g cm ⁻³) in settling tubes	Fenton's oxidation; duration: <2 h	n.a.	10 g	425 μ m–1 mm	Mineral matter n.a.; organic matter 106 \pm 13.8%	Destruction: none Tested polymers: PP, PE, PS, PET, PA, PC, PMMA
Han et al. (2019)	NaCl-NaI solution (1.5 g cm ⁻³) flotation	H ₂ O ₂ (35%) oxidation; duration: 7 d	Visual sorting and ATR-FTIR spectroscopy	200 g	<1 mm	n.a.	n.d. ^a
Scopetani et al. (2020)	RO water and olive oil separation in PTFE tubes	Protocatechuic acid promoted Fenton's oxidation; duration: 1 d	ATR-FTIR and μ -FTIR spectroscopy	25 g	200 μ m–2 mm	Mineral matter n.a.; organic matter 95%	Loss: PTFE ^b

^aNuelle et al. (2014) observed changes in PE and PP after treatment in 35% H₂O₂ for 7 d.

^bBecause of its inert properties, PTFE cannot be extracted by oil.

MP = microplastic particle; ATR-FTIR = attenuated total reflectance Fourier transform infrared; μ -FTIR = micro-Fourier-transform infrared spectroscopy; PLA = polylactic acid; PET = polyethylene terephthalate; PE = polyethylene; PVC = polyvinylchloride; PA = polyamide; ABS = acrylonitrile butadiene styrene; PP = polypropylene; PS = polystyrene; PU = polyurethane; n.a. = not available; PMMA = polymethyl methacrylate; n.d. = not determined; RO = reverse osmosis; PTFE = polytetrafluoroethylene.

Han et al. (2019) later developed a flotation device, using a NaCl-NaI solution (1.5 g cm^{-3}), which can separate even high-density polymers from the mineral matrix. As a measure to reduce the organic matter, they propose oxidizing the lightweight organic matter with 35% H_2O_2 for a duration of 7 d, as described by Nuelle et al. (2014). In this context Nuelle et al. (2014) stated that PE and PP particles showed a reduction in size of approximately 10% after the long treatment with H_2O_2 . This decrease in size may therefore bias any analytical results that include the assessment of microplastic size ranges and gives cause to assume that particles in the lower micrometer range may not be detected at all because they may have been dissolved completely.

By comparison, in the present study, visual analysis confirmed by the molecular assays (ATR-FTIR, GPC, and DSC analyses) showed that even relatively small particles (100–400 μm) made of PE, PVC, PET, and the relatively sensitive PA are not degraded during the applied purification protocol. Therefore, the present protocol is more suitable than other chemical digestion protocols using strong acids, strong bases, high temperatures, or long oxidation periods that may destroy common microplastic particles occurring in environmental samples (Löder et al. 2017; Hurley et al. 2018; Munno et al. 2018). Nevertheless, the biodegradable PLA particles showed signs of degradation and fragmentation after the protease digestion step, which needs to be considered when choosing a method for the desired analysis.

A possible alternative to the present protocol was devised by Hurley et al. (2018), in which they used NaI (1.8 g cm^{-3}) as a density separation medium and Fenton's reagent to remove the organic residue (removal efficiency $106 \pm 13.8\%$ by weight). At this point it is important to note that the organic matter removal efficiencies between Hurley's study and our study cannot be compared directly: whereas we measured the mass loss of the lightweight (organic) fraction before and after treatment, Hurley et al. (2018) determined the total organic matter content by loss-on-ignition ($5.79 \pm 0.19\%$ of the sample mass) and assumed the mass loss after Fenton's oxidation to directly reflect the loss of organic matter. Potentially, also inorganic matter such as CaCO_3 can be oxidized, which may explain the $>100\%$ removal efficiency. This is important because the Fenton's oxidation procedure used in our study is similar to the one used by Hurley et al. (2018), but, as can be seen in Figure 2C, the organic matter removal was not complete and therefore might hamper $\mu\text{-FTIR}$ measurements. Nevertheless, because the method presented by Hurley et al. (2018) is time- and resource-efficient, application of their protocol is advisable as a first step. If, however, the residual organic matter is still too much to allow a spectroscopic analysis, the enzymatic-oxidative digestion protocol may be used to increase organic matter removal.

All of the above-mentioned protocols use a salt solution for separation of the mineral fraction from the lightweight fraction. High-density salt solutions using NaI or ZnCl_2 are expensive and hazardous, and therefore require an internal recycling process. Scopetani et al. (2020) presented an olive oil-based

separation which is density-independent and relies on the oleophilic properties of most plastics. The method showed good recovery rates for PE, polyurethane (PU), PS, polycarbonate, PVC, and PET. But less oleophilic polymers, such as PTFE, will not be recovered and tests should be conducted if dirt and biofilms will change the extraction efficiency of aged polymers.

In comparison to previously published methods, our soil purification protocol is more elaborate but also allows processing of higher sample volumes and is very effective at removing stabilized soil organic matter. A current drawback of the purification protocol is the necessity of regularly filtering the samples over a vacuum filtration unit. This can be time- and labor-consuming and may make the system susceptible to losses and/or contamination. However, this could be avoided by applying capsuled methods like the single-pot method described by Scircle et al. (2020). The costs for each 250-g sample are, on average, 2.11 euros for the reagents of the enzymatic-oxidative digestion (see Supplemental Data, Table S2; not including costs for laboratory equipment and ZnCl_2 solution, which is internally regenerated and reused).

In conclusion, the present soil purification protocol has a high purification efficiency without affecting the commonly tested polymer types but does affect the biodegradable PLA. Experiments with an environmental soil sample have shown that a wide range of polymers in the shapes of fibers and fragments down to a minimum size of 10 μm can be identified with the presented method. Identifying the abundance, types, shapes, and sizes of the microplastic pollution is important for any microplastic-related risk assessment because these are relevant parameters for changes in the soil's biophysical properties as well as for the potential uptake of microplastics by soil-dwelling organisms (Wang et al. 2019). To fill the knowledge gap on the actual extent of microplastic pollution in soils, this purification protocol in combination with an automated $\mu\text{-FTIR}$ analysis could be an asset in future microplastic-monitoring schemes relying on a qualitative and quantitative microplastic assessment.

Supplemental Data—The Supplemental Data are available on the Wiley Online Library at <https://doi.org/10.1002/etc.5024>.

Acknowledgment—The authors especially thank the colleagues of the Department of Animal Ecology I and the Department of Macromolecular Chemistry II, with special thanks to A. Kumar, for their support in the revision and completion of the present study. The present study was conducted with the support of the Ministry for Environment, Climate Protection and Energy of Baden Württemberg, funding J.N. Möller in the scope of the German research program MiKoBo (Mikrokunststoffe in Komposten und Gärprodukten aus Bioabfallverwertungsanlagen und deren Eintrag in landwirtschaftlich genutzte Böden—Erfassen, Bewerten, Vermeiden; BMWK18007). Furthermore, the authors gratefully acknowledge the support of the German Research Foundation (391977956-SFB 1357) and the Federal Ministry of Education and Research (03F0789A) for funding the microplastic research projects "SFB Mikroplastik" and "PLAWES,"

respectively. The authors also acknowledge the support of the Institute for Plastics Technology for supplying the reference PLA fragments.

Author Contributions Statement—Study conception and design: J.N. Möller, S.D.J. Oster, S. Agarwal, M.G.J. Löder, and C. Laforsch conceived and designed the study; J.N. Möller, I. Heisel, A. Satzger, S. Agarwal, and E.C. Vizsolyi acquired the data; J.N. Möller, S. Agarwal, and E.C. Vizsolyi analyzed and interpreted the data; J.N. Möller drafted the manuscript; and J.N. Möller, I. Heisel, A. Satzger, S.D.J. Oster, S. Agarwal, M.G.J. Löder, C. Laforsch, and E.C. Vizsolyi critically revised the manuscript.

Data Availability Statement—Data, associated metadata, and calculation tools are available from the corresponding authors (julia.moeller@uni-bayreuth.de, christian.laforsch@uni-bayreuth.de, martin.loeder@uni-bayreuth.de).

REFERENCES

- Atkinson CML, Richardson MJ. 1969. Thermodynamic properties of ideally crystalline polyethylene. *Transactions of the Faraday Society* 65:1764–1773.
- Ciccolini LAS, Shamlou PA, Ward JM, Dunnill P. 1998. Time course of SDS-alkaline lysis of recombinant bacterial cells for plasmid release. *Biotechnol Bioeng* 60:3–5.
- Corradini F, Meza P, Eguiluz R, Casado F, Huerta-Lwanga E, Geissen V. 2019. Evidence of microplastic accumulation in agricultural soils from sewage sludge disposal. *Sci Total Environ* 671:411–420.
- De Souza Machado AA, Lau CW, Kloas W, Bergmann J, Bachelier JB, Faltin E, Becker R, Görlich AS, Rillig MC. 2019. Microplastics can change soil properties and affect plant performance. *Environ Sci Technol* 53:6044–6052.
- Dümichen E, Eisentraut P, Bannick CG, Barthel AK, Senz R, Braun U. 2017. Fast identification of microplastics in complex environmental samples by a thermal degradation method. *Chemosphere* 174:572–584.
- Fuller S, Gautam A. 2016. A procedure for measuring microplastics using pressurized fluid extraction. *Environ Sci Technol* 50:5774–5780.
- Han X, Lu X, Vogt RD. 2019. An optimized density-based approach for extracting microplastics from soil and sediment samples. *Environ Pollut* 254:113009.
- He D, Luo Y, Lu S, Liu M, Song Y, Lei L. 2018. Microplastics in soils: Analytical methods, pollution characteristics and ecological risks. *Trends Anal Chem* 109:163–172.
- Huerta Lwanga E, Mendoza Vega J, Ku Quej V, Chi J de los A, Sanchez del Cid L, Chi C, Escalona Segura G, Gertsen H, Salánki T, van der Ploeg M, Koelmans AA, Geissen V. 2017. Field evidence for transfer of plastic debris along a terrestrial food chain. *Sci Rep* 7:14071.
- Hufnagl B, Steiner D, Renner E, Löder MGJ, Laforsch C, Lohninger H. 2019. A methodology for the fast identification and monitoring of microplastics in environmental samples using random decision forest classifiers. *Analytical Methods* 11:2277–2285.
- Hurley RR, Lusher AL, Olsen M, Nizzetto L. 2018. Validation of a method for extracting microplastics from complex, organic-rich, environmental matrices. *Environ Sci Technol* 52:7409–7417.
- Hurley RR, Nizzetto L. 2018. Fate and occurrence of micro(nano)plastics in soils: Knowledge gaps and possible risks. *Curr Opin Environ Sci Health* 1:6–11.
- Imhof HK, Schmid J, Niessner R, Ivleva NP, Laforsch C. 2012. A novel, highly efficient method for the separation and quantification of plastic particles in sediments of aquatic environments. *Limnol Oceanogr Methods* 10:524–537.
- Käppler A, Windrich F, Löder MGJ, Malanin M, Fischer D, Labrenz M, Eichhorn K, Voit B. 2015. Identification of microplastics by FTIR and Raman microscopy: A novel silicon filter substrate opens the important spectral range below 1300 cm⁻¹ for FTIR transmission measurements. *Anal Bioanal Chem* 407:6791–6801.
- Kawecki D, Nowack B. 2019. Polymer-specific modeling of the environmental emissions of seven commodity plastics as macro- and microplastics. *Environ Sci Technol* 53:9664–9676.
- Kumar VBN, Löscher LA, Imhof HK, Löder MGJ, Laforsch C. 2021. Analysis of microplastics of a broad size range in commercially important mussels by combining FTIR and Raman spectroscopy approaches. *Environ Pollut* 269:116147.
- Lebreton L, Andrady A. 2019. Future scenarios of global plastic waste generation and disposal. *Palgrave Commun* 5:6.
- Löder MGJ, Imhof HK, Ladehoff M, Löscher LA, Lorenz C, Mintenig S, Piehl S, Primpke S, Schrank I, Laforsch C, Gerdts G. 2017. Enzymatic purification of microplastics in environmental samples. *Environ Sci Technol* 51:14283–14292.
- Löder MGJ, Kuczera M, Mintenig S, Lorenz C, Gerdts G. 2015. Focal plane array detector-based micro-Fourier-transform infrared imaging for the analysis of microplastics in environmental samples. *Environ Chem* 12:563–581.
- Maes T, Jessop R, Wellner N, Haupt K, Mayes AG. 2017. A rapid-screening approach to detect and quantify microplastics based on fluorescent tagging with Nile red. *Sci Rep* 7:44501.
- Möller JN, Löder MGJ, Laforsch C. 2020. Finding microplastics in soils: A review of analytical methods. *Environ Sci Technol* 54:2078–2090.
- Müller RJ, Schrader H, Profe J, Dresler K, Deckwer WD. 2005. Enzymatic degradation of poly(ethylene terephthalate): Rapid hydrolyse using a hydrolase from *T. fusca*. *Macromol Rapid Commun* 26:1400–1405.
- Munno K, Helm PA, Jackson DA, Rochman C, Sims A. 2018. Impacts of temperature and selected chemical digestion methods on microplastic particles. *Environ Toxicol Chem* 37:91–98.
- Nuelle MT, Dekiff JH, Remy D, Fries E. 2014. A new analytical approach for monitoring microplastics in marine sediments. *Environ Pollut* 184:161–169.
- Piehl S, Leibner A, Löder MGJ, Dris R, Bogner C, Laforsch C. 2018. Identification and quantification of macro- and microplastics on an agricultural farmland. *Sci Rep* 8:17950.
- Primpke S, Cross RK, Mintenig SM, Simon M, Vianello A, Gerdts G, Vollertsen J. 2020. Toward the systematic identification of microplastics in the environment: Evaluation of a new independent software tool (siMPle) for spectroscopic analysis. *Appl Spectrosc* 74:1127–1138.
- Ramos AM, Gally M, Szapiro G, Itzcovich T, Carabajal M, Levin L. 2016. In vitro growth and cell wall degrading enzyme production by Argentinean isolates of *Macrophomina phaseolina*, the causative agent of charcoal rot in corn. *Rev Argent Microbiol* 48:267–273.
- Rillig MC, Ziersch L, Hempel S. 2017. Microplastic transport in soil by earthworms. *Sci Rep* 7:1362.
- Rochman CM. 2018. Microplastics research—From sink to source. *Science* 360:28–29.
- Scheurer M, Bigalke M. 2018. Microplastics in Swiss floodplain soils. *Environ Sci Technol* 52:3591–3598.
- Schumacher BA, Shines KC, Burton JV, Papp ML. 1990. A comparison of soil homogenization techniques. In Simmons MS, ed, *Hazardous Waste Measurements*. Lewis, Chelsea, MI, USA, pp 1–40.
- Scircle A, Cizdziel JV, Missling K, Li L, Vianello A. 2020. Single-pot method for the collection and preparation of natural water for microplastic analyses: Microplastics in the Mississippi River system during and after historic flooding. *Environ Toxicol Chem* 39:986–995.
- Scopetani C, Chelazzi D, Mikola J, Leiniö V, Heikkinen R, Cincinelli A, Pellinen J. 2020. Olive oil-based method for the extraction, quantification and identification of microplastics in soil and compost samples. *Sci Total Environ* 733:139338.
- Staricka JA, Benoit GR. 1995. Freeze-drying effects on wet and dry soil aggregate stability. *Soil Sci Soc Am J* 59:218–223.
- Tagg AS, Harrison JP, Ju-Nam Y, Sapp M, Bradley EL, Sinclair CJ, Ojeda JJ. 2017. Fenton's reagent for the rapid and efficient isolation of microplastics from wastewater. *Chem Commun* 53:372–375.

- Turner JF, Riga A, O'Connor A, Zhang J, Collis J. 2004. Characterization of drawn and undrawn poly-L-lactide films by differential scanning calorimetry. *J Therm Anal Calorim* 75:257–268.
- Van den Berg P, Huerta-Lwanga E, Corradini F, Geissen V. 2020. Sewage sludge application as a vehicle for microplastics in eastern Spanish agricultural soils. *Environ Pollut* 261:114198.
- Wang J, Liu X, Li Y, Powell T, Wang X, Wang G, Zhang P. 2019. Microplastics as contaminants in the soil environment: A mini-review. *Sci Total Environ* 691:848–857.
- Weithmann N, Möller JN, Löder MGJ, Piehl S, Laforsch C, Freitag R. 2018. Organic fertilizer as a vehicle for the entry of microplastic into the environment. *Sci Adv* 4:eaap8060.
- Willats WGT, Mccartney L, Mackie W, Knox JP. 2001. Pectin: Cell biology and prospects for functional analysis. *Plant Mol Biol* 47:9–27.
- Zhou B, Wang J, Zhang H, Shi H, Fei Y, Huang S, Tong Y, Wen D, Luo Y, Barceló D. 2019. Microplastics in agricultural soils on the coastal plain of Hangzhou Bay, east China: Multiple sources other than plastic mulching film. *J Hazard Mater* 388:121814.

Supporting Information:

Title: Tackling the challenge of extracting microplastics from soils: A protocol to purify soil samples for spectroscopic analysis

Authors: Julia N. Möller^a, Ingrid Heisel^a, Anna Satzger^a, Eva C. Vizsolyi,^a Jakob Oster^a, Seema Agarwal^b, Martin G.J. Löder^a Christian Laforsch^a

Visual Effects of the enzymatic digestion procedure on microplastic particles

Figure S1 depicts exemplary particles photographed under a stereomicroscope (Leica M50, Leica Microsystems, coupled with an Olympus DP 26 camera, Olympus Corporation) before and after they underwent the digestion protocol. None of the tested particles with the exception of PLA (S1 Panel G) showed any obvious signs of degradation.

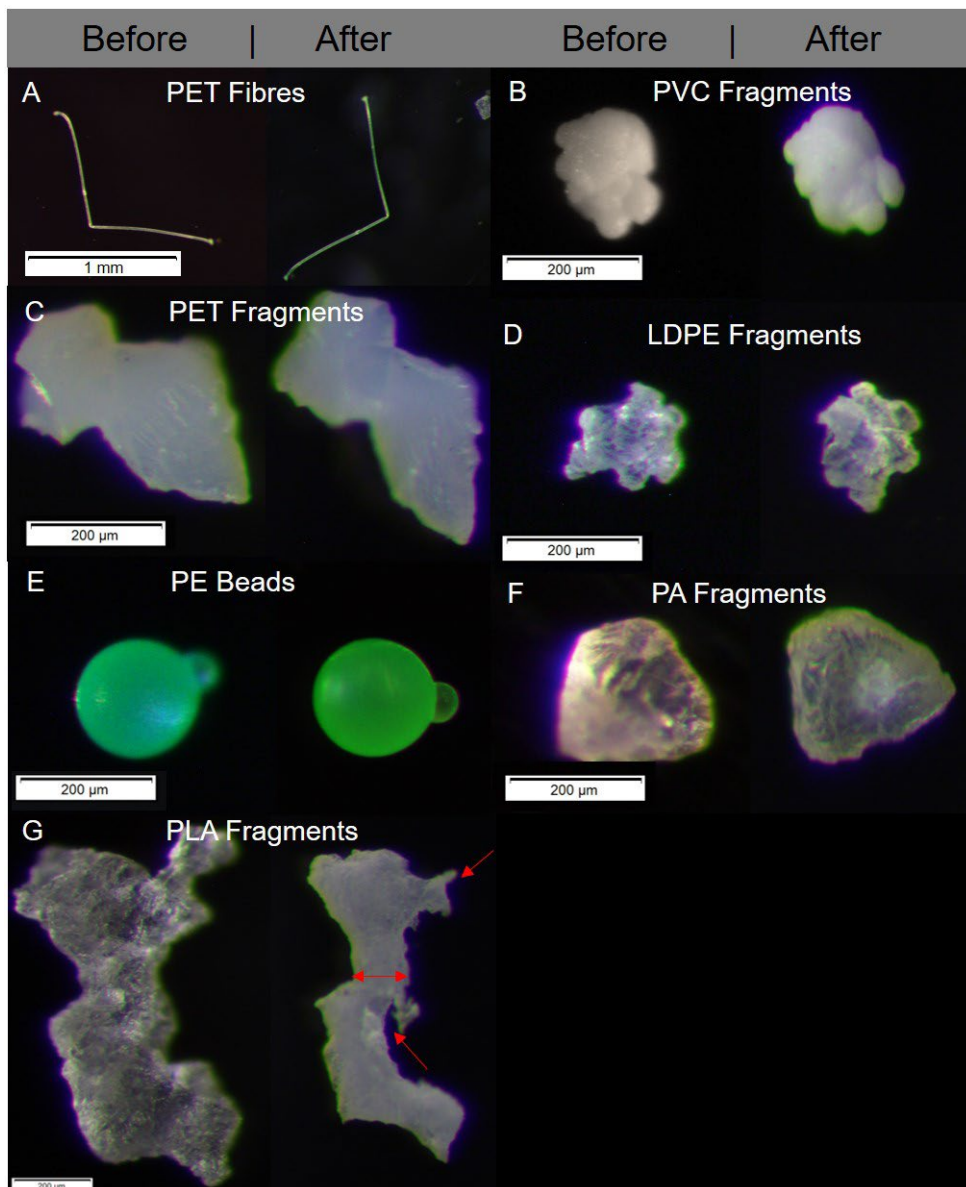


Figure S1: Overview over the effects of the purification protocol on microplastics. No obvious effects for PET Fibers (A), PVC fragments (B), PET fragments (C), LDPE Fragments (D), PE beads (E), PA fragments (F). The PLA fragments became smaller, thinner and show signs of corrosion (G).

Effects of the enzymatic digestion procedure on molar mass distribution of microplastic particles

GPC plots

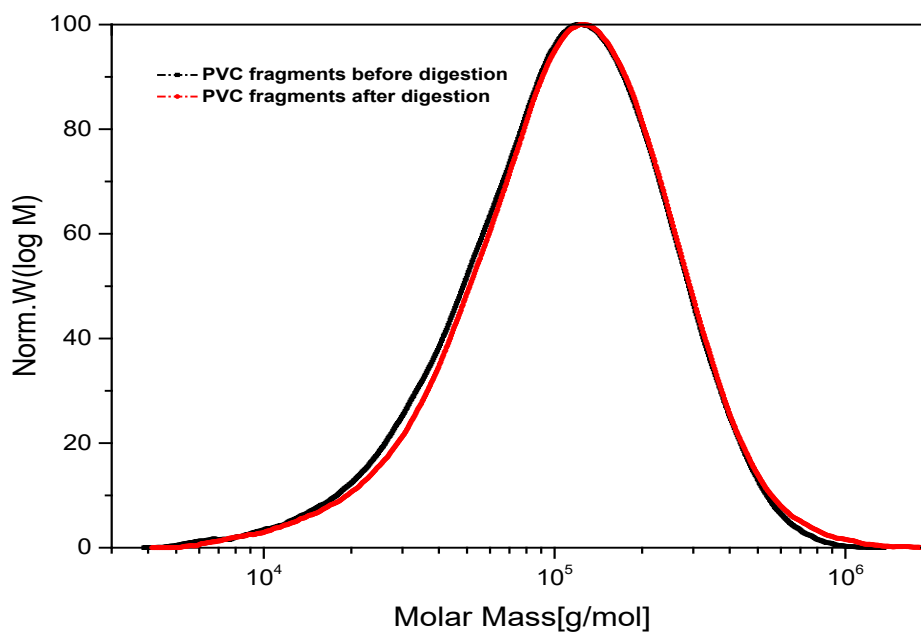


Figure S2: Molar Mass curves of PVC fragments before and after digestion using Hexafluoro-2-propanol (HFIP) eluent in Gel Permeation Chromatography.

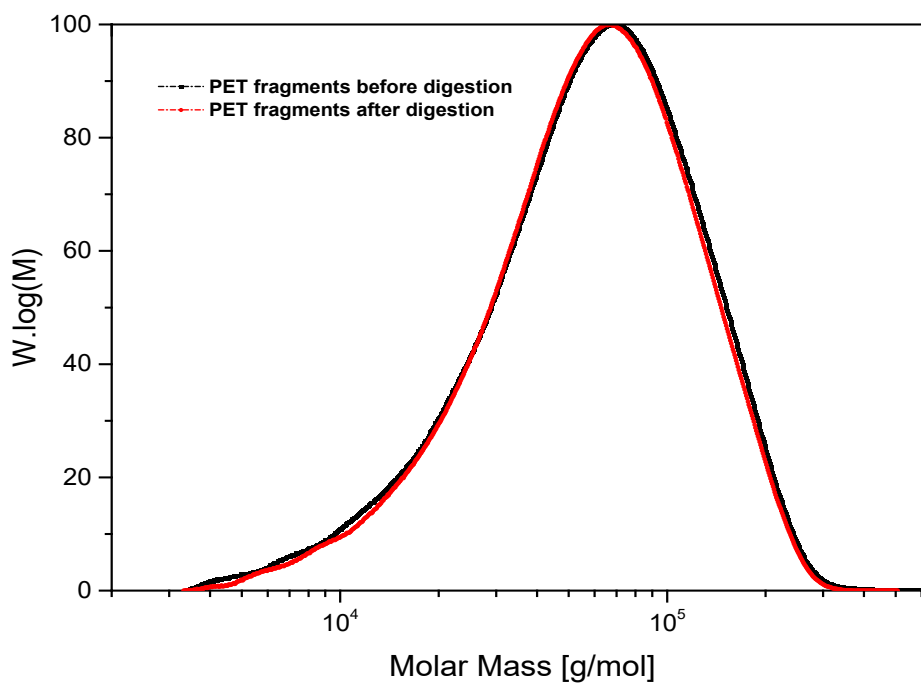


Figure S3 Molar Mass curves of PET fragments before and after digestion using Hexafluoro-2-propanol (HFIP) eluent in Gel Permeation Chromatography.

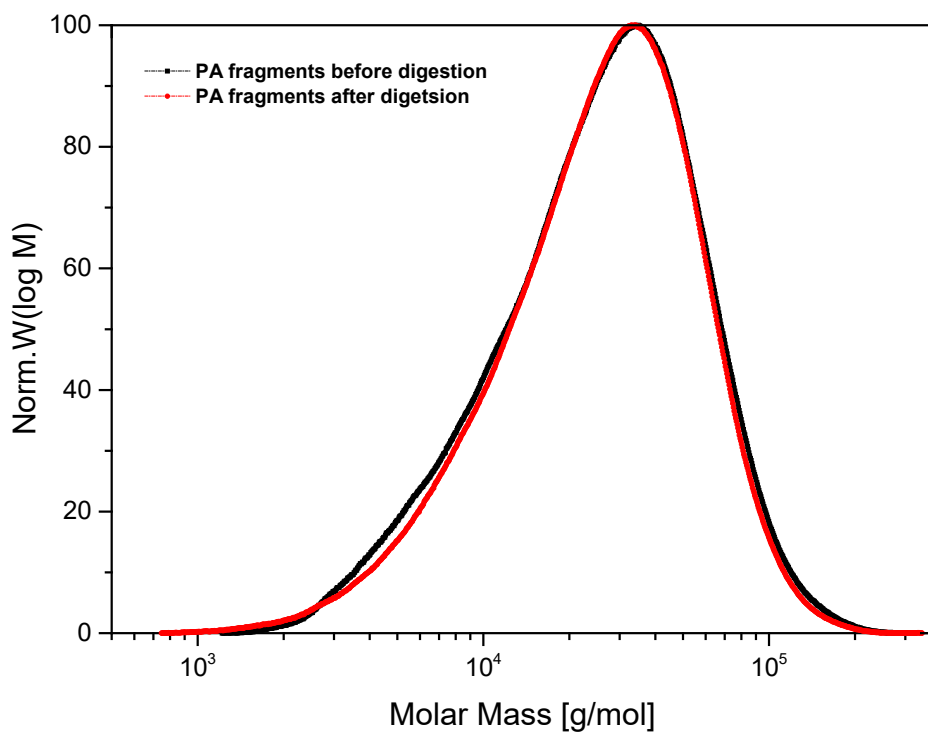


Figure S4: Molar Mass curves of PA fragments before and after digestion using Hexafluoro-2-propanol (HFIP) eluent in Gel Permeation Chromatography.

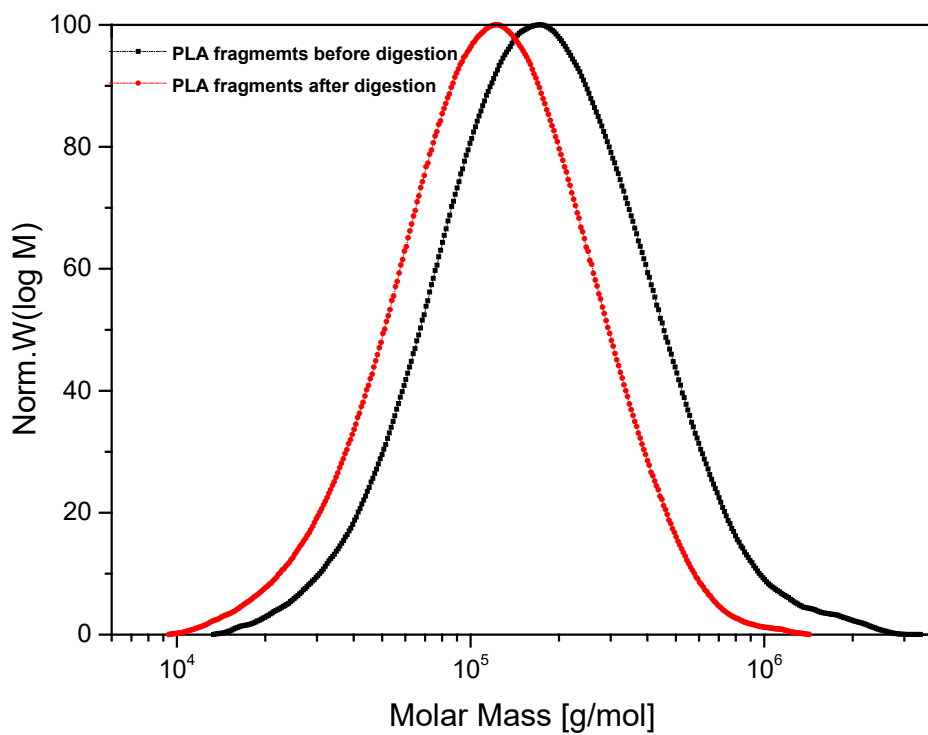


Figure S5 Molar Mass curves of PLA fragments before and after digestion using Hexafluoro-2-propanol (HFIP) eluent in Gel Permeation Chromatography.

Effects of the enzymatic digestion procedure on the thermal transition characteristics of microplastic particles

DSC first heating curves before and after digestion of different polymers

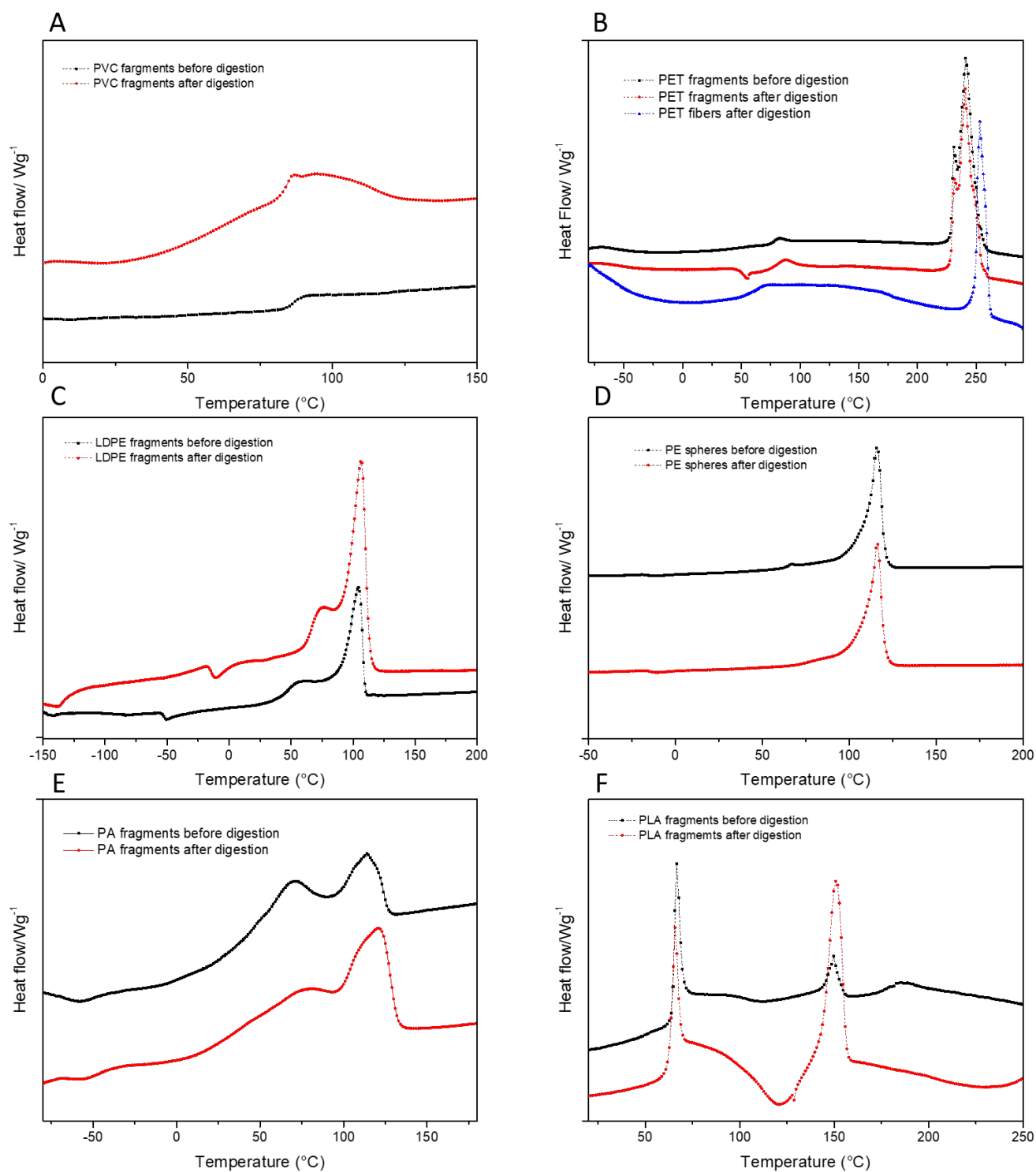


Figure S6: Heat Flow curves microplastic particles before and after digestion measured by Differential scanning calorimetry (DSC).

Table S1: Thermal transition and crystallinity characteristics of polymers before and after treatment

Sample Name	Melting enthalpy (ΔH_m), J/g	Enthalpy of crystallisation (ΔH_c), J/g	% Crystallinity (X_c)	T_{m1} (°C)	T_{m2} (°C)
PA fragments before digestion	89	--	Not determined as type of PA is not known	114	71
PA fragments after digestion	104	--	--	121	Broad shoulder
LDPE fragments before digestion	123	--	42	106	Broad shoulder
LDPE fragments after digestion	130	---	45	106	Broad shoulder
PE spheres before digestion	253	--	86	115	66
PE spheres after digestion	248	---	85	116	-
PET fragments before digestion	71	--	55	241	231
PET fragments after digestion	69	--	53	241	232
PET fibres after digestion	40	--	31	252	--
PLA fragments before digestion	4	2	2	149	--
PLA fragments after digestion	22	21	1	151	--

Table S2: List of reagents used in enzymatic-oxidative purification and respective costs needed per 250 g sample

Reagent	Bulk Cost	Amount needed for solution	Amount used	cost of used amount / sample	
10% SDS	32,4 €/ kg	100 g / l	50 ml	0.162	€
FeSO4	36,50 €/ kg	15 g / l	25 ml	0.0136875	€
30% H2O2	18,50 €/kg	n.a.	25 ml	0.4625	€
Protease	44 €/l	n.a.	5 ml	0.22	€
Pectinase	42 €/l	n.a.	5 ml	0.21	€
Viscozyme L	816 €/l	n.a.	1 ml	0.816	€
Cellulase	40 €/l	n.a.	5 ml	0.2	€
Tris/HCL 10 %	37,2 € / Kg	(121 g / l) *0,1	25 ml	0.011	€
NaAc 10 %	25,50 €/kg	(82 g/ l)*0,1	75 ml	0.015	€

Article 4

Microplastics persist in an arable soil but do not affect soil microbial biomass, enzyme activities, and crop yield



RESEARCH ARTICLE

Microplastics persist in an arable soil but do not affect soil microbial biomass, enzyme activities, and crop yield

Lion Schöpfer¹ | Julia N. Möller² | Thomas Steiner³ | Uwe Schnepf⁴ |
 Sven Marhan¹ | Julia Resch⁵ | Ansilla Bayha⁷ | Martin G. J. Löder² | Ruth Freitag³ |
 Franz Brümmer⁴ | Christian Laforsch² | Thilo Streck⁶ | Jens Forberger⁷ |
 Martin Kranert⁸ | Ellen Kandeler¹ | Holger Pagel⁶

¹Department of Soil Biology, Institute of Soil Science and Land Evaluation, University of Hohenheim, Stuttgart, Germany

²Department of Animal Ecology I and BayCEER, University of Bayreuth, Bayreuth, Germany

³Process Biotechnology and Centre for Energy Technology, University of Bayreuth, Bayreuth, Germany

⁴Research Unit Biodiversity and Scientific Diving, Institute of Biomaterials and Biomolecular Systems, University of Stuttgart, Stuttgart, Germany

⁵Department of Material Engineering, Institut für Kunststofftechnik, University of Stuttgart, Stuttgart, Germany

⁶Department of Biogeophysics, Institute of Soil Science and Land Evaluation, University of Hohenheim, Stuttgart, Germany

⁷Environmental Engineering Department, Fraunhofer Institute for Chemical Technology, Pfinztal, Germany

⁸Chair of Waste Management and Emissions, Institute for Sanitary Engineering, Water Quality and Solid Waste Management, University of Stuttgart, Stuttgart, Germany

Correspondence

Lion Schöpfer, Department of Soil Biology, Institute of Soil Science and Land Evaluation, University of Hohenheim, Emil-Wolff-Str. 27, 70599 Stuttgart, Germany.
 Email: l.schoepfer@uni-hohenheim.de

This article has been edited by Inigo Virto.

Abstract

Background: Microplastics (MP, plastic particles <5 mm) are ubiquitous in arable soils due to significant inputs via organic fertilizers, sewage sludges, and plastic mulches. However, knowledge of typical MP loadings, their fate, and ecological impacts on arable soils is limited.

Aims: We studied (1) MP background concentrations, (2) the fate of added conventional and biodegradable MP, and (3) effects of MP in combination with organic fertilizers on microbial abundance and activity associated with carbon (C) cycling, and crop yields in an arable soil.

Methods: On a conventionally managed soil (Luvisol, silt loam), we arranged plots in a randomized complete block design with the following MP treatments (none, low-density polyethylene [LDPE], a blend of poly(lactic acid) and poly(butylene adipate-co-terephthalate) [PLA/PBAT]) and organic fertilizers (none, compost, digestate). We added 20 kg MP ha⁻¹ and 10 t organic fertilizers ha⁻¹. We measured concentrations of MP in the soil, microbiological indicators of C cycling (microbial biomass and enzyme activities), and crop yields over 1.5 years.

Results: Background concentration of MP in the top 10 cm was 296 ± 110 (mean ± standard error) particles <0.5 mm per kg soil, with polypropylene, polystyrene, and polyethylene as the main polymers. Added LDPE and PLA/PBAT particles showed no changes in number and particle size over time. MP did not affect the soil microbiological indicators of C cycling or crop yields.

Conclusions: Numerous MP occur in arable soils, suggesting diffuse MP entry into soils. In addition to conventional MP, biodegradable MP may persist under field conditions. However, MP at current concentrations are not expected to affect C turnover and crop yield.

KEYWORDS

field experiment, LDPE, microbial biomass, organic fertilizers, PLA/PBAT, plastics contamination, soil enzyme activity

This is an open access article under the terms of the [Creative Commons Attribution-NonCommercial](https://creativecommons.org/licenses/by-nc/4.0/) License, which permits use, distribution and reproduction in any medium, provided the original work is properly cited and is not used for commercial purposes.

© 2022 The Authors. Journal of Plant Nutrition and Soil Science published by Wiley-VCH GmbH

1 | INTRODUCTION

Microplastics (MP) are commonly defined as plastic particles of various shapes and sizes between 100 nm and 5 mm (Okoffo et al., 2021; de Souza Machado et al., 2018). MP are suspected threats to soil organisms and functions (Helmberger et al., 2020; Pathan et al., 2020; Rillig et al., 2021; Q. Wang et al., 2022). Arable soils receive MP primarily due to amendment with sewage sludge, organic fertilizers, and plastic mulch (Corradini et al., 2019; Gui et al., 2021; van Schothorst et al., 2021; Vithanage et al., 2021; J. Wang et al., 2021; Weithmann et al., 2018; Yang et al., 2021). In addition, MP can enter soils through both wet and dry atmospheric deposition (Allen et al., 2019; Brahney et al., 2020; Kernchen et al., 2022). Soils receiving MP via sewage sludge application and plastic mulching have a global median background concentration of 1200 particles kg^{-1} soil (Büks & Kaupenjohann, 2020). Similarly, van Schothorst et al. (2021) found on average 888 particles kg^{-1} in soils that received annual compost inputs of 10 t ha^{-1} in the past 7–20 years. However, the reported uncertainties are large; robust estimates of MP loadings in soils due to organic fertilizer application are therefore not available (Büks & Kaupenjohann, 2020; Gui et al., 2021).

Biowastes well as the composts and digestates derived thereof have been found to contain plastics and there is some evidence that plastic pieces can break down and form MP during biowaste processing (Judy et al., 2019; Gui et al., 2021; Rodrigues et al., 2020; Watteau et al., 2018; Weithmann et al., 2018). Composts contain plastics mainly from packaging and plastic bag residues, which are usually made up of low-density polyethylene (LDPE) (Bandini et al., 2020; Gui et al., 2021; Rodrigues et al., 2020; Weithmann et al., 2018). There have been attempts to tackle plastic contamination of composts and soils by replacing conventional plastics such as LDPE with biodegradable polymers (Agarwal, 2020; Liao & Chen, 2021; Qin et al., 2021). Polymer blends with poly(lactic acid) (PLA) and poly(butylene adipate-co-terephthalate) (PBAT) are biodegradable alternatives to LDPE (Agarwal, 2020; Liao & Chen, 2021; Musioł et al., 2018). LDPE is resistant to microbial degradation due to its stable carbon (C) backbone (Kumar Sen & Raut, 2015; Krueger et al., 2015). In contrast, PLA/PBAT blends are hydrolyzable through enzymes such as lipases, cutinases, and esterases, and thus potentially biodegradable in soil or compost (Freitas et al., 2017; Jia et al., 2021; Palsikowski et al., 2018; Tabasi & Aji, 2015; Weng et al., 2013; Zumstein et al., 2018). However, there is significant uncertainty about the fate of biodegradable MP fragments originating from composts in arable soils. Indeed, there is some evidence for incomplete biodegradation of some biodegradable plastics, rapid fragmentation of biodegradable MP and thus more rapid *in situ* formation of MP in composts and soils compared with conventional polymers (Liao & Chen, 2021; Meng et al., 2022; Qin et al., 2021; Steiner et al., 2022). Biodegradable polymers could thus pose a greater risk of adverse effects on soil organisms and functions if they are not readily mineralized.

MP have many modes of action in soils. They can induce physicochemical changes in habitats by affecting soil porosity, bulk density, water holding capacity, and soil water repellence (X. Zhang et al., 2021), and form specific habitats for soil microorganisms, referred to as the

plastisphere (Bandopadhyay et al., 2020; Rüthi et al., 2020; M. Zhang et al., 2019; Zhou et al., 2021). Less is known about the influence of MP on C cycling, but MP are C-rich substrates and have the potential to change soil organic C and thus C cycling (Meng et al., 2022; Rillig et al., 2021; X. Zhang et al., 2021). Soil C cycling involves the decomposition of organic compounds originating from plant, microbial, and animal residues. The degradation of different complex compounds (cellulose, chitin < xylan < lignin) is catalyzed by microbially produced enzymes (Burns et al., 2013). For example, β -glucosidase and N-acetyl-glucosaminidase catalyze the final hydrolytic cleavage of cellobiose and chitobiose di- and oligomers after depolymerization of cellulose and chitin (Kandeler, 2015; Maillard et al., 2018), whereas β -xylosidase hydrolyzes cleavage products, for example, xylobioses and other short xylooligosaccharides, from different hemicelluloses such as xylan (Dodd et al., 2011; Uffen, 1997). Phenoloxidasases oxidize redox mediators initiating the depolymerization of lignin (Burns et al., 2013).

In a recent study under field conditions, increases of C cycling enzymes (α - and β -glucosidase) were observed in response to LDPE-MP addition (Lin et al., 2020). A meta-analysis identified multiple negative impacts on plant growth including crop yield and plant height, resulting from pollution of croplands with plastic residues from mulch films (D. Zhang et al., 2020). Given the importance of agricultural soils for food production, understanding the loadings and the extent to which MP, and especially biodegradable MP, affect C cycling and crop yields in agroecosystems is crucial (Rillig et al., 2017; G. S. Zhang & Liu, 2018; X. Zhang et al., 2021).

This study aimed to better understand the fate of MP and effects of MP on microbial abundance and activity related to C cycling, as well as crop yields in arable soils. We established a field experiment (1) to investigate MP background concentrations, (2) to quantify concentrations of added conventional and biodegradable MP after one and 17 months of addition, and (3) to identify potential effects of MP and of MP-containing organic fertilizers on soil microbial abundance, activities of selected C cycling enzymes, and crop yields. We expected that (1) the arable soil shows a low but significant background MP loading (before setup), (2) biodegradable MP (PLA/PBAT) fragment in soil, (3) conventional MP (LDPE) persist and are not altered, (4) biodegradation of PLA/PBAT leads to increased activity of lipase in soil as this enzyme catalyzes ester bond cleavage, but microbial abundance, activities of enzymes catalyzing other reactions, and crop yields are not affected because breakdown of PLA/PBAT is slow and direct toxic effects MP on plants are unlikely, and (5) due to its persistence, LDPE has no impact on soil microbiological indicators of C cycling or crop yields.

2 | MATERIAL AND METHODS

2.1 | Microplastics

As biodegradable plastics, we used a blend of PLA (Ingeo™ Biopolymer 7001D; NatureWorks LLC, Minnetonka, MN, USA) and PBAT (Ecoflex F Blend C1200; BASF SE, Ludwigshafen, Germany) in a mixing ratio of 80/20% w/w, which was compounded at the Institut für

Kunststofftechnik (University of Stuttgart, Stuttgart, Germany). LDPE (Lupolen 2420H; LyondellBasell Industries N.V., Rotterdam, Netherlands) served as the representative conventional MP. Polymer pellets were cryomilled (-196°C) with a speed rotor mill (Pulverisette, Fritsch GmbH, Idar-Oberstein, Germany) to obtain MP and subsequently fractionated using stainless-steel sieves to obtain two MP particle size fractions of <0.5 and $0.5\text{--}2$ mm. Both fractions were then mixed in a 1:1 ratio (mass based).

2.2 | Organic fertilizers

Solid digestate (C/N: 11, dry mass: 22.2%, substrate: 48.8% plant residues such as silage, 51.2% animal by-products such as manure) was provided by the research station Unterer Lindenhof of the University of Hohenheim. Compost (C/N:17, dry mass: 61.8%, substrate: green cuttings) originated from Häckselplatz Möhringen in Stuttgart, Germany.

Since there were no detection methods for MP particles <1 mm in composts and digestates at the initiation of the experiment (Weithmann et al., 2018), we used the plastic loading of the fractions $1\text{--}5$ and >5 mm in the compost and digestate as indicators of MP loading. The plastic loading of digestates and composts was determined after sieving and detection via attenuated total reflection Fourier-transform infrared (ATR-FTIR) spectroscopy (cf. Section 2.4). The compost (one batch) contained three polypropylene (PP) particles in the fractions $1\text{--}5$ mm per kg and three particles (50% were PP and 50% polystyrene [PS]) in the fraction >5 mm per kg. The digestate (mean of two batches) contained 11 particles in the fraction >5 mm per kg (25% were PE and 75% PP) and no particles in the $1\text{--}5$ mm fraction.

2.3 | Study site characteristics, experimental setup, and soil sampling

The experiment was established on a conventionally managed agricultural field at the research station Heidfeldhof (University of Hohenheim, central point of the field: $9^{\circ}11'22.984''$ longitude, $48^{\circ}43'11.137''$ latitude, EPSG: 4326, WGS 1984). In the past, neither plastic mulch nor compost had been applied. In addition to the mineral fertilizers commonly used in conventional management, the field was sporadically fertilized with manure from the research station Meiereihof (University of Hohenheim). The soil is a Luvisol with texture silt loam (3.4% sand, 76.2% silt, 20.5% clay), total soil C and nitrogen (N) content of 1.19 and 0.13%, respectively (C/N ratio: 9), and pH of 6.3 (measured in 0.01 M CaCl_2). Weather conditions at the study site and farm management during the experiment are shown in Figure 1.

The experimental design included the factors MP (none, LDPE, PLA/PBAT) and organic fertilizer (none, compost, digestate) arranged in a complete randomized block design with four blocks (Figure 2). The area of one plot was 32 m^2 (length: 8 m, width: 4 m). To avoid carry-over effects from one plot to another by tillage, a 5 m-wide buffer area between the plots was established in the direction of machine travel. In

consideration of German biowaste regulations that permits an application of $30\text{ t compost ha}^{-1}$ (note that all mass data are given on dry matter basis) over 3 years (BioAbfV, 2017), we applied 10 t ha^{-1} of compost and digestate. MP were applied at a concentration of 2 g m^{-2} . To homogeneously apply the MP, we weighted 10 kg soil randomly taken from the field per plot and added 68 g MP, then homogenized these MP-soil mixtures using a drilling machine with a stirring unit for 2 min in metal buckets (35 L). From these MP-soil mixtures, we took the amount required for two square meters, that is, 0.59 kg, added these to the plots (treatments without fertilizer) or mixed these with the amount of compost for two square meters, that is, 2 kg, using a drilling machine (treatments with compost). We chose these MP-soil mixtures and compost because they could be mixed, transported, and distributed well in the field. Due to the low bulk density of the digestate, it could not be mixed in the metal buckets with the MP-soil mixtures. Therefore, we applied the digestate and MP-soil mixtures (treatments with digestate and MP) separately to the field.

To investigate MP background contamination and determine soil properties, we took 15 randomly selected soil subsamples (Ap horizon, depth: 0–10 cm) on 32 m^2 ($n = 4$) from the plots without fertilizer and without MP using a soil core sampler (cross-sectional area: 9.53 cm^2) before the start of the experiment. To analyze MP particles added to the field and soil biological variables, before setup and 1 month (M1), 5 months (M5), and 17 months (M17) after setup, eight subsamples were taken from a 4 m^2 sampling square in the center of each plot (Ap horizon, depth: 0–10 cm) and pooled into composite samples of approximately 1 kg for each timepoint. Since the soil sampled in this way contained very few MP particles >0.5 mm at M1 and M5, we additionally sampled an area of 900 cm^2 per plot using a spade at the end of the experiment (M17).

Soil samples for soil biological analyses were stored at -20°C until analysis.

2.4 | MP analyses

To characterize the background contamination of the arable soil with MP and to investigate the fate of added MP particles, MP were extracted and measured according to Möller et al. (2022). In brief, soil samples were freeze-dried and sieved to 0.5 mm. All further analyses were done with aliquots of 250 g soil.

MP >0.5 mm were collected with tweezers and analyzed by ATR-FTIR spectrometry (spectrometer: Alpha ATR unit, Bruker 27; equipped with a diamond crystal for measurements). Spectra were taken from 4000 to 400 cm^{-1} (resolution 8 cm^{-1} , 16 accumulated scans; Software OPUS 7.5). Particles were identified by comparing the measured spectra against standard spectra from an in-house database described previously (Löder et al., 2015) and the database provided by the manufacturer of the instrument (Bruker Optik GmbH, Leipzig, Germany). An incident light microscope (microscope, Nikon SMZ 754T; digital camera, DS-Fi2; camera control unit, DS-U3; software, NIS Elements D) was used for visual documentation and size estimation of all synthetic plastic particles identified by ATR-FTIR.

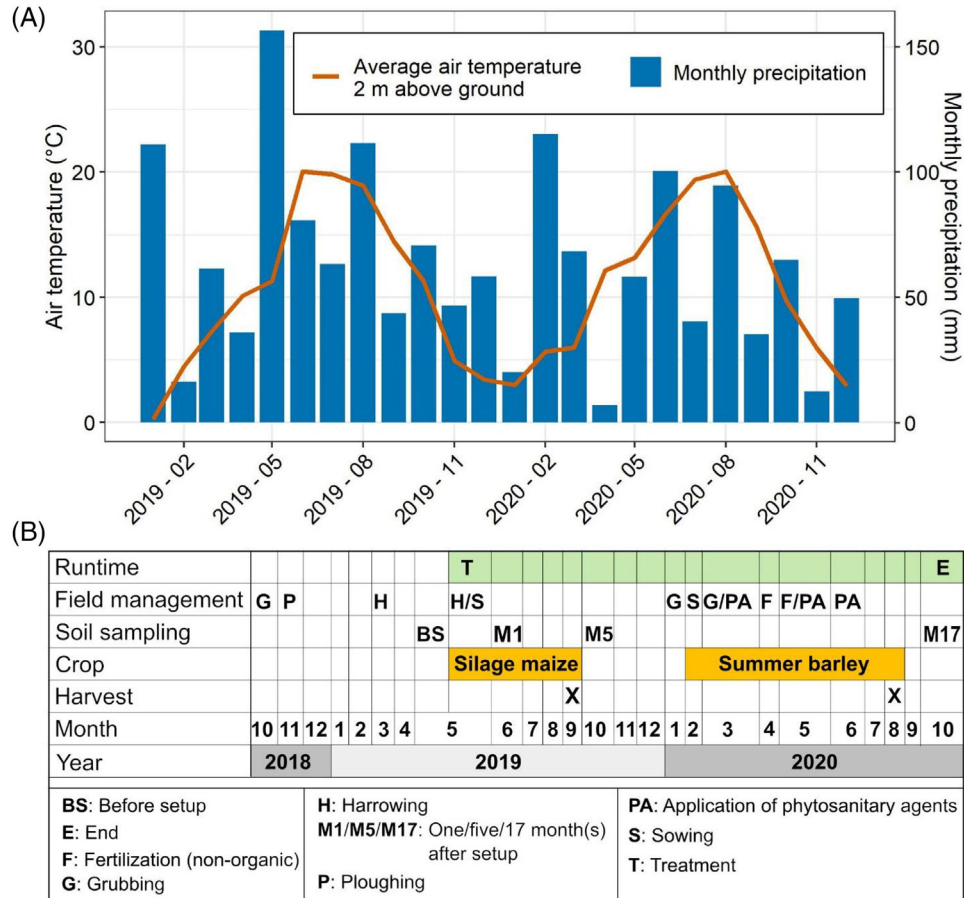


FIGURE 1 (A) Monthly average air temperature measured in 2 m above ground and monthly precipitation from nearby meteorological station and (B) overview of field management, soil sampling, and harvest. Meteorological data were obtained from LTZ (2021).

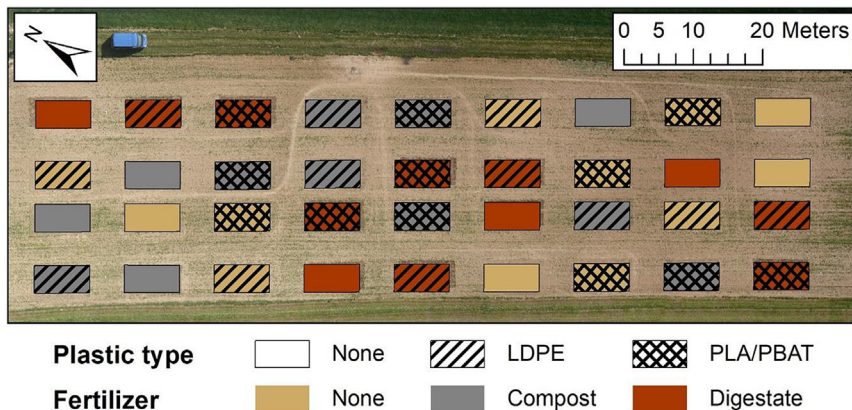


FIGURE 2 Experimental design of the field experiment. Plots were arranged in a complete randomized block design ($n = 4$).

Soil samples taken from the 900 cm² areas at M17 (corresponding to approximately 10 L soil) were analyzed in their entirety to detect large particles >0.5 mm. To this end, the soil samples were partitioned into 20 Fido jars (Bormioli Rocco, Fidenza, Italy; capacity 3 L each) and suspended with 2.5 L of water. The diluted samples were sieved at 2 mm and the retained particles were collected with tweezers (fraction >2 mm). All material <2 mm was sieved at 0.5 mm mesh size,

and the retained particles were again collected with tweezers (fraction 0.5–2 mm).

According to Möller et al. (2022), MP <0.5 mm were extracted via density separation with a zinc chloride brine ($\rho = 1.8 \text{ g cm}^{-3}$) and an enzymatic-oxidative purification step (Löder et al., 2017). Particles were then transferred onto an aluminum oxide sample carrier and analyzed by chemical imaging via Focal Plane Array-based μ -FTIR

spectroscopy (Löder et al., 2015). Identification of MP in the large chemical imaging data sets was performed with the help of an automated software solution based on Random Decision Forest Classifiers (Hufnagl et al., 2022). For quality control, the results of the automated MP classification was checked by trained experts. We only analyzed the samples from plots without organic fertilizers, that is, the samples from 12 out of 36 plots (see Figure 2), at M1 and M17 as well as the MP–soil mixtures that were added to the plots with MP treatment (in total: $12 + 12 + 8 = 32$ samples). We had to limit the number of analyzed samples due to the extensive and time-consuming extraction and purification procedure (Möller et al., 2022). In addition, the high organic matter content of compost and digestate interferes with the treatment of the samples. Thus, these samples could not be analyzed. Due to high numbers of MP particles, deviating from the above-mentioned protocol, for the initial MP–soil mixtures that were added to the field, four subsamples of 5 g each were analyzed.

We calculated the initial MP concentrations in soil at the start of the field experiment (MP_{start}), assuming that the applied MP–soil mixtures were homogeneously mixed within the top 10 cm of soil (Equation 1):

$$c_{MP,i} = \frac{m_{mix} \times c_{mix}}{(d \times \rho_B)}, \quad (1)$$

where $c_{MP,i}$ is the initial MP concentration in the soil of the field experiment (particles kg^{-1}), m_{mix} is the mass of applied MP–soil mixtures per area (0.294 kg m^{-2}), c_{mix} is the measured MP concentration of the MP–soil mixtures (particles kg^{-1}), d is the depth of the soil layer (10 cm), and ρ_B is the bulk density of top soil (1400 kg m^{-3}).

Since soil samples were separated into two fractions due to sieving of 0.5 mm and these two fractions were analyzed differently as described above, we excluded particles >0.5 mm in the small fraction (5.1–38.5%) and particles <0.5 mm in the large fraction (0–2.1%), respectively (Table S1). Due to sieving of MP to 2 mm before use in our study, particles >2 mm were filtered from datasets (this applied only to MP–soil mixtures).

We derived particle size distributions of LDPE and PLA/PBAT particles as initially added to the soil based on MP particles detected in MP–soil mixtures (Figure S1). The median size of LDPE particles in the small and large fractions were 186 and 1092 μm , respectively (Figure S1). The median size of PLA/PBAT particles in the small and large fractions were 200 and 1013 μm , respectively (Figure S1).

2.5 | Soil microbiological indicators of carbon cycling

To assess effects of MP and organic fertilizers on the soil microbial abundance and activity, we used microbial biomass C and activities of enzymes involved in C cycling as soil microbiological indicators. These were measured before as well as 1 month (M1), 5 months (M5), and 17 months (M17) after the setup of the experiment.

Microbial biomass C (C_{mic}) and nitrogen (N_{mic}) were quantified via chloroform fumigation extraction according to Vance et al. (1987). For a description of the method, we refer to Blöcker et al. (2020).

We analyzed the activity of enzymes that catalyze the degradation of organic substrates of different complexities: we considered β -glucosidase, N-acetyl-glucosaminidase, β -xylosidase, and phenoloxidase as indicators of the degradation of the polymers cellulose, chitin, xylan (hemicellulose), and lignin. In addition, we analyzed the activity of lipase because of its possible involvement in the depolymerization of PLA/PBAT. The activities of β -glucosidase, β -xylosidase, N-acetyl-glucosaminidase, and lipase were measured using microplate assays with fluorogenic substrates (Cooper & Morgan, 1981; German et al., 2011; Marx et al., 2001). Lipase activity was determined based on an adapted protocol from Cooper and Morgan (1981). Substrates and standards were purchased from Sigma–Aldrich (St. Louis, MO, USA). Standard stock solutions of 5 mM 4-methylumbelliferyl (MUF, M1381) were obtained by dissolving MUF in methanol and deionized water (1:1). Standard working solutions (10 μM MUF) were prepared in 0.1 M Tris–HCl buffer pH 6.8 (lipases) or MES buffer pH 6.1 (β -glucosidase, β -xylosidase, N-acetyl-glucosaminidase). For each soil sample, we prepared a standard curve with concentrations of 0, 0.5, 1, 2.5, 4, 6 μM MUF in soil suspension aliquots and buffer. Lipase substrate stock solutions (10 mM) were obtained by dissolving the substrates MUF heptanoate (M2514) in dimethyl sulfoxide (D8418). Working solutions (1 mM) were prepared by adding sterile 0.1 M Tris–HCl buffer pH 6.8. Substrate solutions of β -glucosidase, β -xylosidase, and N-acetyl-glucosaminidase were prepared and analyzed as outlined in Kramer et al. (2013).

Phenoloxidase activity was photometrically measured as described in Ali et al. (2015) with the following slight modifications. Before the measurement, we preincubated the microplates at 30°C and measured absorbance of the soil suspensions at a wavelength of 414 nm.

2.6 | Crop yields

Silage maize and summer barley were harvested in September of the first year (4 months after setup) and in August of the second year of the experiment (15 months after setup), respectively (Figure 1(B)).

To determine the biomass of the silage maize (*Zea mays*), we removed every second plant by cutting it 1 cm above its root system. We determined maize plant dry matter biomass (including cobs) after chopping the plants and drying them at 60°C and 110°C (for 3 days each). Two-step drying is common practice at the research station to accelerate drying to mass constancy at 110°C. We then multiplied mean silage maize biomass per plot by the number of plants per plot to obtain silage maize biomass yield per plot. Grain yield of summer barley (*Hordeum vulgare*) was determined from an area of 12 m^2 (1.5 m \times 8 m) per plot and grains were sampled using a plot threshing machine. Crop yields were converted to t ha^{-1} .

2.7 | Data analyses

All data analyses and figures were carried out using the statistical software R 4.0.2 (R Core Team, 2020). In addition to the packages

explicitly mentioned in this section, we used: *broom.mixed* 0.2.6 (Bolker & Robinson, 2020), *broom* 0.7.0 (Robinson et al., 2020), *flextable* 0.5.10 (Gohel, 2020), *patchwork* 1.0.1 (Pedersen, 2020), *scales* 1.1.1 (Wickham & Seidel, 2020), and *tidyverse* 1.3.0 (Wickham et al., 2019).

The MP background concentrations (before setup) and concentrations of MP particles >0.5 mm were evaluated only descriptively because there were too few data for inferential statistical analysis. For particles <0.5 mm, differences in particle number between MP_{start}, M1, and M17 were tested using a linear mixed effects model with particle number as dependent variable, and timepoint (MP_{start}, M1, and M17) as the explanatory variable, while accounting for a random effect for plot (ID). Tukey contrasts were computed using functions from the *emmeans* 1.5.0 package (Lenth, 2020). Particle size distributions of particles <0.5 mm were compared by plotting empirical cumulative density functions and using the Kolmogorov–Smirnov test (*ks.test*), to test whether the MP particles in MP_{start}, M1, and M17, originated from the same distribution (van Schothorst et al., 2021). Empirical cumulative density functions were calculated based on pooled samples per treatment group ($n = 4$).

Crop yields were evaluated using a linear model with the crossed factors plastic type and fertilizer and accounting for a block effect. Soil enzyme activities, C_{mic} , and N_{mic} data were analyzed by means of linear mixed effects models. Therefore, the linear model used for crop yield data was extended by the initial state of the variable of interest as covariate to account for the field variability (Value_TMinus1). We integrated the repeated measures factor timepoint (*i.e.*, M1, M5, and M17) by crossing it with the treatment structure, accounted for a block and block–timepoint interaction effect, and a random effect for the randomization unit (*i.e.*, plot) (Piepho et al., 2004). The models were fitted to the data using functions from base R and the package *lme4* 1.1–23 (Bates et al., 2015). We used ANOVAs in the case of linear mixed effects models with the Kenward–Rogers approximation for the degrees of freedom using functions from the *lmerTest* 3.1–2 package (Kenward & Roger, 1997; Kuznetsova et al., 2017) to identify significant effects ($p < 0.05$) and subsequently compared estimated marginal means. If an interaction with timepoint was significant, we evaluated simple contrasts per timepoint level.

Model assumptions, that is, variance homogeneity and normal distribution of the residuals, were checked visually and met for all variables except for N-acetyl-glucosaminidase activity, for which the model assumptions were met after log-transformation.

3 | RESULTS

3.1 | Background loading of MP in the arable soil

The arable soil had a MP loading with nine different polymer types at a background concentration of 296 ± 110 (mean \pm standard error) particles kg^{-1} . PP (108 ± 36 particles kg^{-1}), PS (76 ± 34 particles kg^{-1}), and polyethylene (PE, 60 ± 25 particles kg^{-1}) were the most abundant polymers and were found in all analyzed samples (Figure 3(A)). Other MP were polyacrylonitrile, PE terephthalate, polyvinyl

chloride, polybutylene terephthalate, ethylene-vinyl acetate, and polysulfone.

PS particles were smallest with a median particle size of $60 \mu m$ (Figure 3(B)). PP and PE particles had median sizes of 156 and $146 \mu m$, respectively. While the particle size distribution of PS MP was significantly shifted to lower particle lengths compared with PP ($p = 0.014$), the particle size distribution of PE MP was similar to that of PP and PS MP ($p = 0.187$ and $p = 0.188$).

3.2 | Fate of added MP <0.5 mm in soil

At the start, soil amended with LDPE and PLA/PBAT contained 1003 LDPE kg^{-1} and 134 PLA/PBAT particles kg^{-1} of MP <0.5 mm (MP_{start}; Figure 4(A)). After 1 month (M1), we detected on average 419 fewer LDPE particles kg^{-1} than at MP_{start} (not significant, $t_6 = -2.7$, $p = 0.082$). The mean number of LDPE particles 17 months after MP addition (M17) and PLA/PBAT particles at M1 and M17 did not differ significantly from MP_{start} (Table S2 and Figure 4(A)). The particle size distribution of LDPE and PLA/PBAT MP at M1 and M17 did not differ from MP_{start} (Figure 4(B)).

3.3 | Fate of added MP >0.5 mm in soil

We found a total of 57 particles >0.5 mm (27 varnish, 13 PE, 16 PLA/PBAT, and one PP) at the final sampling (M17), in all soil samples taken together ($n = 36$). PLA/PBAT and LDPE particles (up to 2) were detected in soil samples from only two (PLA/PBAT) and three plots (LDPE) without fertilizer treatment, respectively. Due to this low recovery, a quantitative comparison of particles >0.5 mm with MP_{start} was not possible. PLA/PBAT particles occurred only in soil samples from plots where PLA/PBAT had been added (Figures 5(A)–5(C)). All PLA/PBAT particles found looked similar (white and irregularly shaped) (Figures 5(A)–5(C)) and like the originally added particles (Figure S2).

However, PE particles (Figures 5(D)–5(F)) occurred not only in soil samples of plots, where PE had been added. They also had different shapes including plastic film residues (Figure 5(D)), fibers (Figure 5(E)), or irregularly shaped pieces (Figure 5(F)). PE particles found were distinct from the initially added PE particles (Figures S2(D)–S2(F)). All varnish particles were of the same type (Figures 5(G)–5(I)).

3.4 | Soil microbiological indicators of carbon cycling and crop yields

We investigated the effects of adding 2 g MP m^{-2} on soil microbial abundance and activity related to C cycling and crop yields based on soil microbiological indicators (C_{mic} , N_{mic} , and activities of C cycling enzymes), biomass of silage maize, and grain yield of summer barley. Overall, MP from LDPE and PLA/PBAT did not cause changes of the soil microbiological indicators at 1, 5, and 17 months after MP addition, or

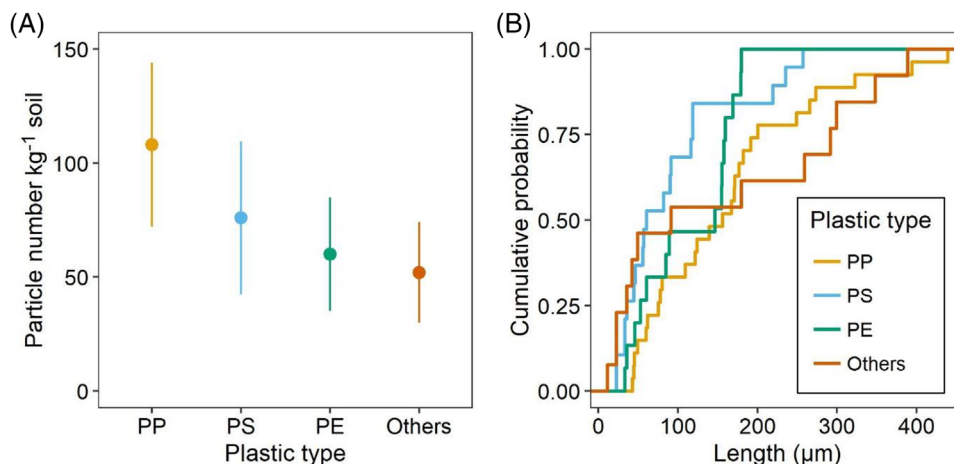


FIGURE 3 (A) Particle numbers of PP, PS, PE, and other polymers $<0.5\text{ mm}$. Data are presented as means and standard errors (error bars) ($n = 4$). (B) Empirical cumulative distribution function of pooled samples for PE (15 particles), PS (19 particles), PP (27 particles), and others (13 particles). Other MP were polyacrylonitrile, polyethylene terephthalate, polyvinyl chloride, polybutylene terephthalate, ethylene-vinyl acetate, and polysulfone.

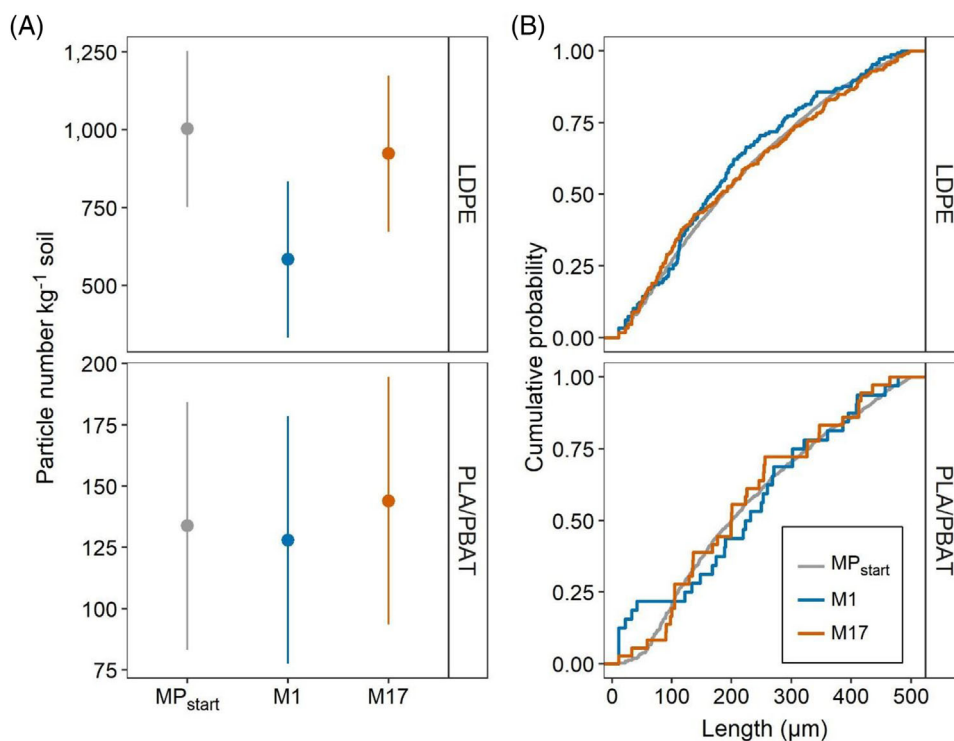


FIGURE 4 (A) Particle numbers of LDPE and PLA/PBAT particles after application of MP-soil mixtures as initially added to the plots (MP_{start}), after 1 month (M1), and after 17 months (M17). Data are presented as estimated marginal means with lower and upper 95% confidence intervals (error bars) ($n = 4$). Note that y-axis scales for LDPE and PLA/PBAT differ from one another. (B) Empirical cumulative density functions of number of LDPE and PLA/PBAT particles in MP mixtures as initially added to the plots (MP_{start}), at M1, and at M17, pooled by plastic type.

in crop yields compared with MP-free soil (Figures 6, S3, and S4 and Tables S3 and S4). The exception was LDPE at M5, which reduced N_{mic} significantly by 36% compared with the MP-free soil (Figure S4(A) and Table S5).

No combined effects of MP with organic fertilizers were detected, but amendment of soil with composts and digestates affected the activity of C cycling enzymes in soil (Figures 6(B), S3 and Tables S3–S6).

Lipase activities responded to the addition of compost (M1 and M5) and digestate (M5) significantly increasing from 37 to 62% compared with fertilizer-free soil (Figure 6(B) and Table S5). β -Xylosidase showed significantly enhanced activity in soil amended with digestate in comparison with the fertilizer-free soil at M5 (+60%) and M17 (+23%) (Figure S3(B) and Table S5). Both β -xylosidase and β -glucosidase activities increased by 47% in response to compost addition at M5 compared

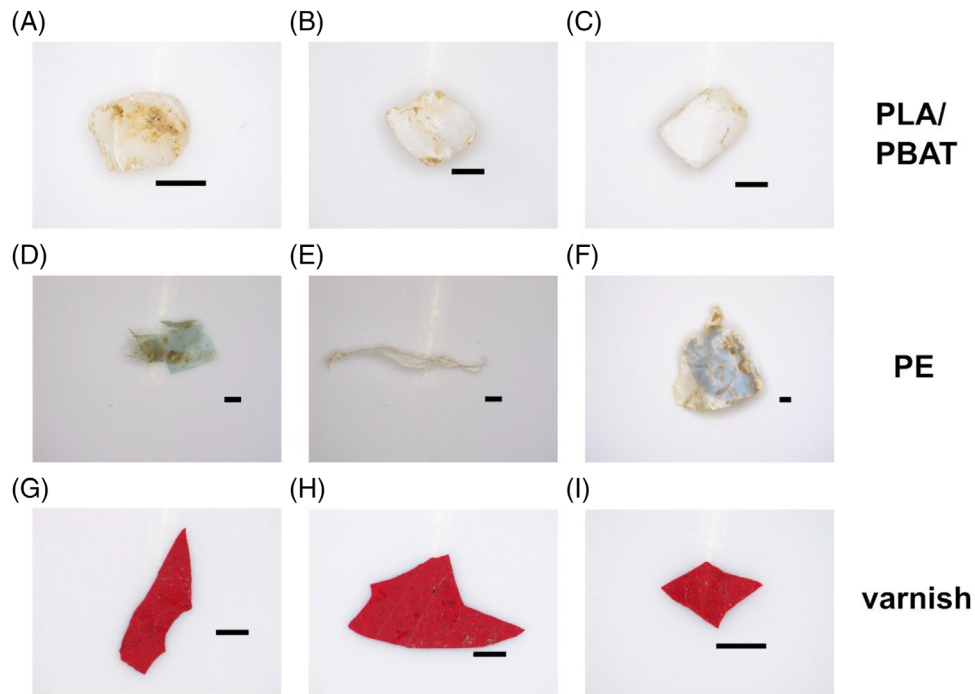


FIGURE 5 Representative microscopic images of MP >0.5 mm: (A–C) PLA/PBAT, (D–F) PE, and (G–I) varnish found after 17 months (M17). The scale bars indicate a length of 1 mm.

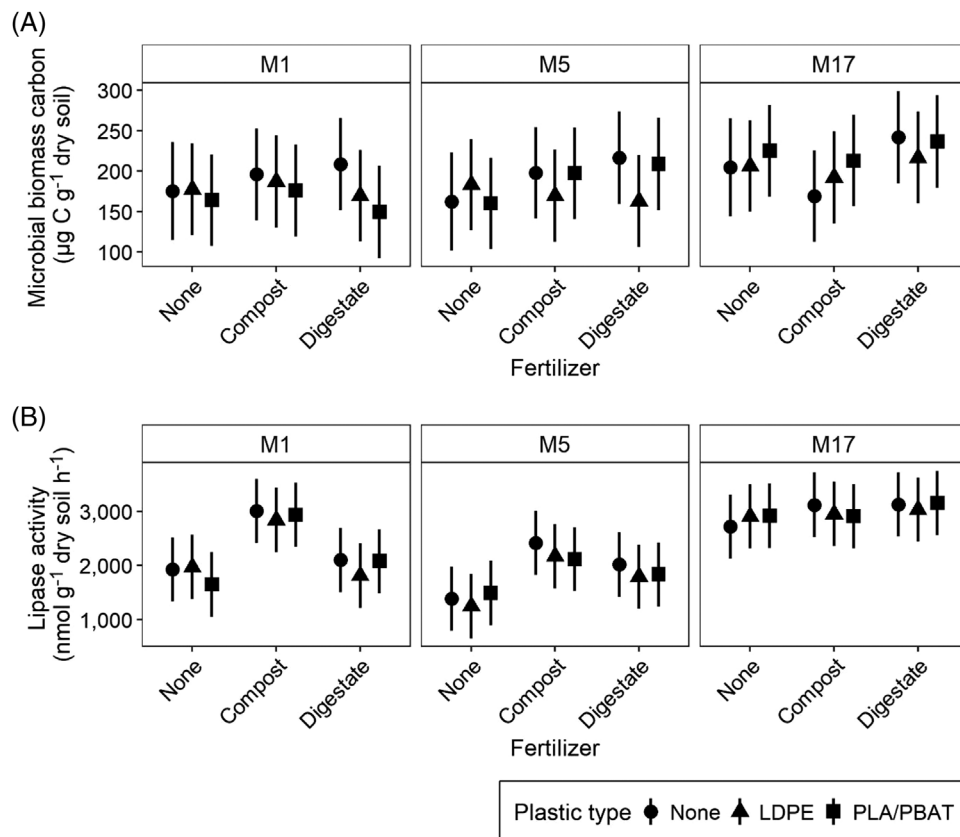


FIGURE 6 (A) Microbial biomass C and (B) lipase activity as a function of MP and organic fertilizers 1 month (M1), 5 months (M5), and 17 months (M17) after the addition of 2 g MP m^{-2} . Data are presented as estimated marginal means ($n = 4$) with lower and upper 95% confidence intervals (error bars).

with the fertilizer-free soil, but statistical uncertainties were large for β -xylosidase ($p = 0.061$) (Figures S3(A) and S3(B) and Table S5). Compared with nonfertilized soil, N-acetyl-glucosaminidase activities increased 59% (significant) after digestate addition at M5 (Figure S3(C) and Table S6).

After 17 months, the activities of β -xylosidase, N-acetyl-glucosaminidase, and β -glucosidase were significantly higher in the soil amended with digestate compared with compost (Figures S3(A)–S3(C) and Table S5). Strikingly, this coincided with increased N_{mic} in the soil enriched with digestate compared with compost at M17 (+22%, $p = 0.026$) (Figure S4(A) and Table S5).

Independent of timepoint, phenoloxidase activity was 16.6% higher in soil amended with digestate in comparison with fertilizer-free soil (Figure S3(D)). However, statistical uncertainties were large ($p = 0.069$) (Table S7).

Biomass yields of silage maize (mean and standard error: $19.70 \pm 0.48 \text{ t ha}^{-1}$) were not significantly higher on soil amended with compost and digestate in comparison with nonfertilized soil (Figure S4(B) and Table S4). However, grain yield of spring barley (estimated marginal mean: 6.95 t ha^{-1}) was larger (significantly) on soil amended with digestate compared with compost (6.31 t ha^{-1}) and larger (though not significantly) than on nonfertilized soil (6.46 t ha^{-1}) (Figure S4(C) and Table S7).

4 | DISCUSSION

4.1 | The arable soil was loaded with diverse MP types

The arable soil in our study contained 296 ± 110 (mean \pm standard error) MP particles $<0.5 \text{ mm kg}^{-1}$ as background concentration. This concentration was lower than estimates for arable soils amended with compost (888 ± 500 particles kg^{-1} soil; van Schothorst et al., 2021), sewage sludge (930 ± 740 particles kg^{-1} soil for low-density plastics and 1100 ± 570 particles kg^{-1} for high-density plastics; van den Berg et al., 2020), or plastic mulch ($18,760$ particles kg^{-1} soil; G. S. Zhang & Liu, 2018).

The most common plastic types found in our soil were $\text{PP} > \text{PS} > \text{PE}$. These are among the most economically important polymers and are also those that have previously been most frequently detected in soil (PlasticsEurope, 2019; X. Zhang et al., 2021). In accordance with our results, Piehl et al. (2018) identified PP, PS, and PE as the most abundant MP particles ($>1 \text{ mm}$) in a conventionally managed field that had not been amended with organic fertilizers or sewage sludges, and where no plastic mulches had been applied. Since the input of MP via the latter sources can be excluded in our study, the recovered MP presumably entered the soil by littering and atmospheric deposition (Allen et al., 2019; Dris et al., 2016; Kernchen et al., 2022; Scheurer & Bigalke, 2018). The relatively high number of extracted varnish particles (Figure 5) suggest that abrasion of protective coatings from agricultural machinery could be an important source of MP in arable soils (Figure S5).

We found that more than 75% of the PP, PS, and PE particles were smaller than 0.2 mm (PS: $<117 \mu\text{m}$, PE: $<159 \mu\text{m}$, PP: $<196 \mu\text{m}$), consistent with previous results from J. Wang et al. (2021). The current detection limit is $10 \mu\text{m}$ (Möller et al., 2020); we expect, therefore, that smaller particles occur even more frequently. This could have dramatic consequences for soil organisms because particles $<10 \mu\text{m}$ can be ingested by key member species of the soil food web such as nematodes, resulting in intestinal damage and neurotoxicity (Fueser et al., 2019; Lei et al., 2018; Schöpfer et al., 2020). PS particles in particular pose a risk to soil animals; these were the smallest in our study (median of $60 \mu\text{m}$). However, concentrations of small MP down to nanometer sizes are currently undetectable due to restrictions of analytical methods (Möller et al., 2020). Further progress in MP analytics is needed to better assess potential threats of small MP to soil organisms and their functions.

We can confidently state that the PLA/PBAT particles $>0.5 \text{ mm}$ we found at the last sampling of the experiment (M17) were the particles we had added. We found these exclusively in the PLA/PBAT treated plots but with no finds in the corresponding background loading. All PLA/PBAT particles looked similar and resembled the original particles. In contrast, we cannot rule out that a significant portion of the PE particles we found were part of the background loading. For one thing, LDPE particles also occurred in plots to which no LDPE had been added, and for another, the PE particles found had various shapes (Figure 5) and differed from the originally added LDPE particles (Figure S2).

At the last sampling, we found only very few particles $>0.5 \text{ mm}$. We can exclude the possibility that the particles had been fragmented (with the exception of the fragmentation $<0.01 \text{ mm}$, which we could not detect with our method) because this should have been detected via a clear shift in the size distribution of the particles $<0.5 \text{ mm}$. The low recovery, we suggest, could be due to the possibility that the amount of soil or area sampled was insufficient or that the methodology for analyzing these large particles needs further development. Methodological limitations apply especially to the LDPE particles, which had a more fibrous shape than the predominantly irregularly shaped PLA/PBAT particles. The LDPE particles may have been more prone to fall through the sieve during MP analysis in wet sieving. It is also possible that a significant proportion of large particles were transported vertically or horizontally. A recent study provides evidence for horizontal transport of MP (irregularly shaped polymethyl methacrylate particles with a mean length of $1215 \mu\text{m}$), which occurred along preferential pathways dictated by the micro- and macro-relief of the soil surface (Laermanns et al., 2021). However, more studies on the transport (including vertical transport) of particles in the field will be required to test our assumption.

4.2 | MP persisted in the arable soil

Both tested polymers persisted in the soil of the field experiment over 17 months. The number of added LDPE particles $<0.5 \text{ mm}$ ($584\text{--}1003$ particles kg^{-1} ; Figure 4) in our study roughly represents the LDPE accumulation that can be expected after 7–20 years of compost

accumulation (van Schothorst et al., 2021). PE is highly resistant to microbial degradation in soil due to its large molecular size, lack of functional groups, and high hydrophobicity (Albertsson, 1978; Krueger et al., 2015), which explains the unaltered particle size distribution compared with the initial particles, indicating a lack of fragmentation in the studied soil. Surprisingly, S. Zhang et al. (2020) found that fertilization with N and phosphorous stimulates the fragmentation of LDPE. According to the authors, LDPE fragmentation was triggered by increased soil microbial diversity and abundance. This behavior and its mechanisms need to be confirmed by further studies.

Contrary to our expectations, we recovered the same number of PLA/PBAT particles <0.5 mm as initially added to the soil, most likely due to the lack of biodegradation (Figure 4). The few existing studies on the persistence of films of PLA, PBAT, and PLA/PBAT blends in soil under field conditions demonstrate their low biodegradability within the time period of our field experiment (Liao & Chen, 2021; Rudnik & Briassoulis, 2011; Sintim et al., 2020). PLA exhibited changes in mechanical properties after 11 months in a Mediterranean soil but was visually poorly disintegrated (Rudnik & Briassoulis, 2011). In another study, mass loss of 1–8% and 1–7% were observed for PLA and PBAT, respectively, after 6 months, whereas a PBAT/PLA blend (90/10% w/w) showed no significant degradation (Liao & Chen, 2021). A lower degradability of PLA/PBAT (75/25% w/w) blend compared with the sole polymers was also observed in a laboratory study (Palsikowski et al., 2018). While 21% of the PBAT-C and 16% of PLA-C were mineralized, only 10% of PLA/PBAT-C were mineralized after 180 days in soil. Liao and Chen (2021) attributed the poor degradation of the blend in their study to the blending of PLA with PBAT; blending would change physical properties and increase hydrophobicity, thus impeding microbial colonization and microbial degradation. This could explain, why no fragmentation of PLA/PBAT was observed in our study.

Based on our results, nonbiologically pretreated PLA/PBAT particles are likely to accumulate in the soil under field conditions, given the highly variable climatic conditions with extremes such as cold and drought that may slow the biodegradation of PLA/PBAT.

4.3 | MP did not affect soil microbial biomass, enzyme activities, and crop yields

We did not find any effect of LDPE on soil microbiological indicators of C cycling, likely due to its inert nature (Restrepo-Flórez et al., 2014). However, we found an effect of LDPE on N_{mic} (Figure S4(A)), but this occurred only sporadically (at one timepoint) and the measurement uncertainties were large (Table S5). In line with our results, Lin et al. (2020) did not observe significant changes in soil microbial biomass C and microbial community composition due to the addition of LDPE at concentrations 5, 10, 15 g m⁻² (corresponding to 11,361, 23,789, and 39,172 particles kg⁻¹). In a recent field study, no effects of LDPE-MP on microbial abundance and composition were detected even at extremely high application rates up to 1000 g MP m⁻² (Brown et al., 2022). However, Lin et al. (2020) found substantial increases in C cycling enzymes such as α -glucosidase and β -glucosidase at all con-

centration levels between 36 and 86%, and an increase in L-leucine aminopeptidase, an N cycling enzyme, by 83–116%. They explained the enhanced enzyme activities by greater water availability due to a MP-induced increase of water holding capacity, which would positively influence enzyme activities. Compared with Lin et al. (2020), in our study, we used LDPE particles at a much lower concentration of 2 g m⁻² MP (584–1003 LDPE particles kg⁻¹) and larger LDPE particles (Figure S1; 90th percentile of particles <0.5 mm and >0.5 mm of 430 and 1619 μ m, respectively, compared with a 90th percentile of 68 μ m in their study). Accordingly, particles in our study had a lower specific surface area with less potential to affect soil physical properties including water holding capacity (Ng et al., 2018).

As expected, the addition of PLA/PBAT particles did not affect any of the soil microbiological indicators of C cycling. However, contrary to our expectation, PLA/PBAT also did not increase lipase activity in soil. This was likely due to the lack of biodegradation of PLA/PBAT particles (see Section 4.2) in soil and to the fact that soil microorganisms were apparently not able to use the added PLA/PBAT blend as a C source. In another study, PBAT/PLA MP affected soil C and N pools (Meng et al., 2022). For instance, there were significantly higher dissolved organic C and N due to addition of 2 and 2.5% PBAT/PLA MP additions in comparison with the control. Again, the lower concentration of PLA/PBAT particles in our study could explain why we did not detect changes in soil microbiological indicators of C cycling.

We verified previous studies in which compost and digestate led to a stimulation of enzyme activities (Albuquerque et al., 2012; Crecchio et al., 2004; Vinhal-Freitas et al., 2010). Depending on the quality of the organic fertilizers, we found slightly different temporal patterns of degradation of high molecular weight organic compounds. The increased lipase activities in fertilized soil after one and five months of addition reflected the rapid breakdown of fats and oils contained in compost and digestate into free fatty acids, diacylglycerols, monoglycerols, and glycerol (Hanc et al., 2021). The more pronounced increase due to compost compared with digestate addition indicates a higher lipid content in compost than in digestate. Breakdown of other compost- and digestate-derived polymers (hemicellulose, cellulose, and chitin) were induced at a later timepoint. For example, the degradation of chitins in soil fertilized with digestate as well as the degradation of cellulose in compost-amended soil were only evident five months after addition. The degradation of hemicellulose derived from amendments was still visible after 17 months. Since we did not find any differences in microbial biomass under the two organic amendments, the observed increase in activities was likely due to higher enzyme production of already present microorganisms.

Crop yield, that is, silage maize biomass and grain yield of summer barley, was not affected by MP addition in our study. Direct effects due to uptake and accumulation in plants have been observed for MP <2 μ m (Mateos-Cárdenas et al., 2021). Uptake by plants was unlikely in our study since MP were too large for uptake by plants. While additional mechanisms of MP effects on plant biomass remain unclear, changes in soil structure, bulk density, improved aeration, and microporosity, as well as rooting and nutrient immobilization, are discussed as possible results of both negative and positive effects of MP on plant

biomass (Boots et al., 2019; Lozano et al., 2021; Mateos-Cárdenas et al., 2021; Qi et al., 2018; Rillig et al., 2019). Such indirect effects are again likely to occur if MP concentrations exceed certain thresholds, which may be the case in fields with plastic mulch and sewage sludge application where MP loadings are particularly high (Büks & Kaupenjohann, 2020; G. S. Zhang & Liu, 2018; D. Zhang et al., 2020). However, Brown et al. (2022) did not observe growth and yield reductions of wheat plants even with loads of LDPE-MP >100 g m⁻². While these results, as in our case, indicate that MP might not pose a risk with respect to plant growth, this should be confirmed by investigations of other sites (with different soil types and climates) as well as plant species and MP types. Nevertheless, for fields with lower MP concentrations, such as in our study, no negative effects of MP on plant biomass can be expected.

5 | CONCLUSIONS

Our results highlight that diverse MP can be found in arable soils even without agricultural practices such as organic fertilization, sewage sludge addition, or plastic mulching. This indicates that there are significant diffuse MP inputs into soils through atmospheric deposition, littering, and, to our knowledge noted for the first time, due to the abrasion of coatings of agricultural machinery. In particular, small MP particles <0.2 mm were frequently found in the soil. Soil organisms can ingest such particles with to-date unknown long-term environmental risks. There remains much uncertainty regarding concentrations of small MP <0.01 mm and nanoparticles, and methods for their detection in soil are needed.

We provide evidence that conventional as well as biodegradable MP can persist and accumulate in soil under field conditions. Current MP loadings in arable soil under agricultural practices such as amendment with organic fertilizers have no detectable immediate negative consequences neither on soil microbial abundance and activity related to C cycling, nor on crop yields. However, due to regular MP inputs from diffuse sources and from organic fertilizers and sewage sludge contaminated with MP, as well as the high persistence of many polymers, long-term effects of MP on soil microbial abundance and activities related to C and nutrient cycling cannot be excluded. Additional long-term field studies examining different soil types and polymers will be crucial to assess the risks of environmental threats of MP to functions of agricultural soils.

ACKNOWLEDGMENTS

We thank all members of the soil biology and biogeophysics groups and especially Johannes Wirsching, Romina Schuster, Vinzent Leyrer, Adrian Lattacher, Philipp Mäder, Marie Uksa, Fabian Stache, and Rushan He, who helped setting up the field experiment and soil sampling. We also thank Sabine Rudolf, Heike Haslwimmer, Stefan Pilz, and Moritz Mainka for their assistance with soil physical and biological analyses. Thanks to the workers of the research station "Heidfeldhof" (Herbert Stelz, Christian Aigner, Christian Metzge, and Roger Lürig) for their support in logistics including the transport of digestate and composts and harvests of the crops. In addition, we would like to thank Stefan Knapp

who enabled the drone pictures. Thanks also goes to Alexander Hauser from the research station Untere Lindenhöfe for provision of the digestate. Furthermore, we would like to thank A. Schott, H. Schneider, and K. Thompson for excellent technical assistance. We also thank Kathleen Regan for English corrections. This study was funded by the Ministry of Environment, Climate and Energy of Baden-Württemberg in the framework of the research program MiKoBo (Mikrokunststoffe in Komposten und Gärprodukten aus Bioabfallverwertungsanlagen und deren Eintrag in landwirtschaftlich genutzte Böden-Erfassen, Bewerten, Vermeiden; reference numbers BWMK18001, BWMK18002, BWMK18003, BWMK18004, BWMK18005, BWMK18006, BWMK18007). Parts of the study were funded by the Deutsche Forschungsgemeinschaft (DFG, German Research Foundation), project number 391977956 - SFB 1357. Holger Pagel received financial support from Ellrichshausen Foundation. The funding agencies had no influence on the study design, collection of data or reporting of results. This was the sole work of the listed authors.

Open access funding enabled and organized by Projekt DEAL.

DATA AVAILABILITY STATEMENT

The data that support the findings of this study are openly available on Mendeley at <http://doi.org/10.17632/8chdw8vgnw9.2>.

REFERENCES

- Agarwal, S. (2020). Biodegradable polymers: Present opportunities and challenges in providing a microplastic-free environment. *Macromolecular Chemistry and Physics*, 221(6), 2000017. <https://doi.org/10.1002/macp.202000017>
- Albertsson, A. C. (1978). Biodegradation of synthetic polymers. II. A limited microbial conversion of ¹⁴C in polyethylene to ¹⁴CO₂ by some soil fungi. *Journal of Applied Polymer Science*, 22(12), 3419–3433.
- Albuquerque, J. A., de La Fuente, C., Campoy, M., Carrasco, L., Nájera, I., Baixauli, C., Caravaca, F., Roldán, A., Cegarra, J., & Bernal, M. P. (2012). Agricultural use of digestate for horticultural crop production and improvement of soil properties. *European Journal of Agronomy*, 43, 119–128.
- Ali, R. S., Ingwersen, J., Demyan, M. S., Funkuin, Y. N., Wizemann, H. D., Kandeler, E., & Poll, C. (2015). Modelling in situ activities of enzymes as a tool to explain seasonal variation of soil respiration from agroecosystems. *Soil Biology and Biochemistry*, 81, 291–303.
- Allen, S., Allen, D., Phoenix, V. R., Le Roux, G., Durántez Jiménez, P., Simonneau, A., Binet, S., & Galop, D. (2019). Atmospheric transport and deposition of microplastics in a remote mountain catchment. *Nature Geoscience*, 12(5), 339–344.
- Bandini, F., Frache, A., Ferrarini, A., Taskin, E., Cocconcelli, P. S., & Puglisi, E. (2020). Fate of biodegradable polymers under industrial conditions for anaerobic digestion and aerobic composting of food waste. *Journal of Polymers and the Environment*, 28(9), 2539–2550.
- Bandopadhyay, S., Liquet y González, J. E., Henderson, K. B., Anunciado, M. B., Hayes, D. G., & DeBruyn, J. M. (2020). Soil microbial communities associated with biodegradable plastic mulch films. *Frontiers in Microbiology*, 11, 587074. <https://doi.org/10.3389/fmicb.2020.587074>
- Bates, D., Mächler, M., Bolker, B., & Walker, S. (2015). Fitting linear mixed-effects models using lme4. *Journal of Statistical Software*, 67, 1–48.
- BioAbfV (2017). *Verordnung über die Verwertung von Bioabfällen auf landwirtschaftlich, forstwirtschaftlich und gärtnerisch genutzten Böden (Bioabfallverordnung - BioAbfV)*: BioAbfV.
- Blöcker, L., Watson, C., & Wichern, F. (2020). Living in the plastic age—Different short-term microbial response to microplastics addition to arable soils with contrasting soil organic matter content and farm

- management legacy. *Environmental Pollution*, 267, 115468. <https://doi.org/10.1016/j.envpol.2020.115468>
- Bolker, B., & Robinson, D. (2020). broom.mixed: Tidying methods for mixed models. <https://CRAN.R-project.org/package=broom.mixed>
- Boots, B., Russell, C. W., & Green, D. S. (2019). Effects of microplastics in soil ecosystems: Above and below ground. *Environmental Science & Technology*, 53(19), 11496–11506.
- Brahney, J., Hallerud, M., Heim, E., Hahnenberger, M., & Sukumaran, S. (2020). Plastic rain in protected areas of the United States. *Science*, 368(6496), 1257–1260.
- Brown, R. W., Chadwick, D. R., Thornton, H., Marshall, M. R., Bei, S., Distaso, M. A., Bargiela, R., Marsden, K. A., Clode, P. L., Murphy, D. V., Pagella, S., & Jones, D. L. (2022). Field application of pure polyethylene microplastic has no significant short-term effect on soil biological quality and function. *Soil Biology and Biochemistry*, 165, 108496. <https://doi.org/10.1016/j.soilbio.2021.108496>
- Büks, F., & Kaupenjohann, M. (2020). Global concentrations of microplastics in soils—A review. *SOIL*, 6(2), 649–662.
- Burns, R. G., DeForest, J. L., Marxsen, J., Sinsabaugh, R. L., Stromberger, M. E., Wallenstein, M. D., Weintraub, M. N., & Zoppini, A. (2013). Soil enzymes in a changing environment: Current knowledge and future directions. *Soil Biology and Biochemistry*, 58, 216–234.
- Cooper, A. B., & Morgan, H. W. (1981). Improved fluorometric method to assay for soil lipase activity. *Soil Biology and Biochemistry*, 13(4), 307–311.
- Corradini, F., Meza, P., Eguiluz, R., Casado, F., Huerta-Lwanga, E., & Geissen, V. (2019). Evidence of microplastic accumulation in agricultural soils from sewage sludge disposal. *Science of the Total Environment*, 671, 411–420.
- Crecchio, C., Curci, M., Pizzigallo, M. D., Ricciuti, P., & Ruggiero, P. (2004). Effects of municipal solid waste compost amendments on soil enzyme activities and bacterial genetic diversity. *Soil Biology and Biochemistry*, 36(10), 1595–1605.
- de Souza Machado, A. A., Kloas, W., Zarfl, C., Hempel, S., & Rillig, M. C. (2018). Microplastics as an emerging threat to terrestrial ecosystems. *Global Change Biology*, 24(4), 1405–1416.
- Dodd, D., Mackie, R. I., & Cann, I. K. (2011). Xylan degradation, a metabolic property shared by rumen and human colonic *Bacteroidetes*. *Molecular Microbiology*, 79(2), 292–304.
- Dris, R., Gasperi, J., Saad, M., Mirande, C., & Tassin, B. (2016). Synthetic fibers in atmospheric fallout: A source of microplastics in the environment? *Marine Pollution Bulletin*, 104(1–2), 290–293.
- Freitas, A. L. P. D. L., Tonini Filho, L. R., Calvão, P. S., & de Souza, A. M. C. (2017). Effect of montmorillonite and chain extender on rheological, morphological and biodegradation behavior of PLA/PBAT blends. *Polymer Testing*, 62, 189–195.
- Fueser, H., Mueller, M. T., Weiss, L., Höss, S., & Traunspurger, W. (2019). Ingestion of microplastics by nematodes depends on feeding strategy and buccal cavity size. *Environmental Pollution*, 255, 113227. <https://doi.org/10.1016/j.envpol.2019.113227>
- German, D. P., Weintraub, M. N., Grandy, A. S., Lauber, C. L., Rinkes, Z. L., & Allison, S. D. (2011). Optimization of hydrolytic and oxidative enzyme methods for ecosystem studies. *Soil Biology and Biochemistry*, 43(7), 1387–1397.
- Gohel, D. (2020). flextable: Functions for tabular reporting. <https://CRAN.R-project.org/package=flextable>
- Gui, J., Sun, Y., Wang, J., Chen, X., Zhang, S., & Wu, D. (2021). Microplastics in composting of rural domestic waste: Abundance, characteristics, and release from the surface of macroplastics. *Environmental Pollution*, 274, 116553.
- Hanc, A., Dume, B., & Hrebeckova, T. (2021). Differences of enzymatic activity during composting and vermicomposting of sewage sludge mixed with straw pellets. *Frontiers in Microbiology*, 12, <https://doi.org/10.3389/fmicb.2021.801107>
- Helmberger, M. S., Tiemann, L. K., & Grieshop, M. J. (2020). Towards an ecology of soil microplastics. *Functional Ecology*, 34(3), 550–560.
- Hufnagl, B., Stibi, M., Martirosyan, H., Wilczek, U., Möller, J. N., Löder, M. G. J., Laforsch, C., & Lohninger, H. (2022). Computer-assisted analysis of microplastics in environmental samples based on μ FTIR imaging in combination with machine learning. *Environmental Science & Technology Letters*, 9(1), 90–95. <https://doi.org/10.1021/acs.estlett.1c00851>
- Jia, H., Zhang, M., Weng, Y., & Li, C. (2021). Degradation of poly(lactic acid)/polybutylene adipate-co-terephthalate by coculture of *Pseudomonas mendocina* and *Actinomucor elegans*. *Journal of Hazardous Materials*, 403, 123679. <https://doi.org/10.1016/j.jhazmat.2020.123679>
- Judy, J. D., Williams, M., Gregg, A., Oliver, D., Kumar, A., Kookana, R., & Kirby, J. K. (2019). Microplastics in municipal mixed-waste organic outputs induce minimal short to long-term toxicity in key terrestrial biota. *Environmental Pollution*, 252, 522–531.
- Kandeler, E. (2015). Physiological and biochemical methods for studying soil biota and their functions, in E. A. Paul (Eds.), *Soil microbiology, ecology and biochemistry* (pp. 187–222). Elsevier.
- Kernchen, S., Löder, M. G., Fischer, F., Fischer, D., Moses, S. R., Georgi, C., Nölscher, A. C., Held, A., & Laforsch, C. (2022). Airborne microplastic concentrations and deposition across the Weser River catchment. *Science of the Total Environment*, 818, 151812.
- Kenward, M. G., & Roger, J. H. (1997). Small sample inference for fixed effects from restricted maximum likelihood. *Biometrics*, 983–997.
- Kramer, S., Marhan, S., Haslwimmer, H., Ruess, L., & Kandeler, E. (2013). Temporal variation in surface and subsoil abundance and function of the soil microbial community in an arable soil. *Soil Biology and Biochemistry*, 61, 76–85.
- Krueger, M. C., Harms, H., & Schlosser, D. (2015). Prospects for microbiological solutions to environmental pollution with plastics. *Applied Microbiology and Biotechnology*, 99(21), 8857–8874.
- Sen, S. K., & Raut, S. (2015). Microbial degradation of low density polyethylene (LDPE): A review. *Journal of Environmental Chemical Engineering*, 3(1), 462–473.
- Kuznetsova, A., Brockhoff, P. B., & Christensen, R. H. (2017). lmerTest package: Tests in linear mixed effects models. *Journal of Statistical Software*, 82, 1–26.
- Laermans, H., Lehmann, M., Klee, M., Löder, M. G., Gekle, S., & Bogner, C. (2021). Tracing the horizontal transport of microplastics on rough surfaces. *Microplastics and Nanoplastics*, 1(1), 1–12.
- Lei, L., Wu, S., Lu, S., Liu, M., Song, Y., Fu, Z., Shi, H., Raley-Susman, K. M., & He, D. (2018). Microplastic particles cause intestinal damage and other adverse effects in zebrafish *Danio rerio* and nematode *Caenorhabditis elegans*. *Science of the Total Environment*, 619, 1–8.
- Lenth, R. (2020). emmeans: Estimated marginal means, aka least-squares means. <https://CRAN.R-project.org/package=emmeans>
- Liao, J., & Chen, Q. (2021). Biodegradable plastics in the air and soil environment: Low degradation rate and high microplastics formation. *Journal of Hazardous Materials*, 418, 126329. <https://doi.org/10.1016/j.jhazmat.2021.126329>
- Lin, D., Yang, G., Dou, P., Qian, S., Zhao, L., Yang, Y., & Fanin, N. (2020). Microplastics negatively affect soil fauna but stimulate microbial activity: Insights from a field-based microplastic addition experiment. *Proceedings of the Royal Society B*, 287(1934), 20201268. <https://doi.org/10.1098/rspb.2020.1268>
- Löder, M. G. J., Imhof, H. K., Ladehoff, M., Löscher, L. A., Lorenz, C., Mintenig, S., Piehl, S., Primpke, S., Schrank, I., Laforsch, C., & Gerdtts, G. (2017). Enzymatic purification of microplastics in environmental samples. *Environmental Science & Technology*, 51(24), 14283–14292.
- Löder, M. G. J., Kuczera, M., Mintenig, S., Lorenz, C., & Gerdtts, G. (2015). Focal plane array detector-based micro-Fourier-transform infrared imaging for the analysis of microplastics in environmental samples. *Environmental Chemistry*, 12(5), 563–581.
- Lozano, Y. M., Lehnert, T., Linck, L. T., Lehmann, A., & Rillig, M. C. (2021). Microplastic shape, polymer type, and concentration affect soil

- properties and plant biomass. *Frontiers in Plant Science*, 12, 616645. <https://doi.org/10.3389/fpls.2021.616645>
- LTZ (2021): Landwirtschaftliches Technologiezentrum Augustenberg: Agrarmeteorologie BadenWürttemberg. <https://www.wetterbw.de/Internet/AM/NotesBwAM.nsf/bwweb/85f6baa2d299db4ac1257ca7003d9ab9?>
- Maillard, F., Didion, M., Fauchery, L., Bach, C., & Buée, M. (2018). N-Acetylglucosaminidase activity, a functional trait of chitin degradation, is regulated differentially within two orders of ectomycorrhizal fungi: Boletales and Agaricales. *Mycorrhiza*, 28(4), 391–397.
- Marx, M. C., Wood, M., & Jarvis, S. C. (2001). A microplate fluorimetric assay for the study of enzyme diversity in soils. *Soil Biology and Biochemistry*, 33(12–13), 1633–1640.
- Mateos-Cárdenas, A., van Pelt, F. N., O'Halloran, J., & Jansen, M. A. (2021). Adsorption, uptake and toxicity of micro-and nanoplastics: Effects on terrestrial plants and aquatic macrophytes. *Environmental Pollution*, 284, 117183. <https://doi.org/10.1016/j.envpol.2021.117183>
- Meng, F., Yang, X., Riksen, M., & Geissen, V. (2022). Effect of different polymers of microplastics on soil organic carbon and nitrogen—A mesocosm experiment. *Environmental Research*, 204, 111938. <https://doi.org/10.1016/j.envres.2021.111938>
- Möller, J. N., Heisel, I., Satzger, A., Vizsolyi, E. C., Oster, S. D. J., Agarwal, S., Laforsch, C., & Löder, M. G. (2022). Tackling the challenge of extracting microplastics from soils: A protocol to purify soil samples for spectroscopic analysis. *Environmental Toxicology and Chemistry*, 41(4), 844–857. <https://doi.org/10.1002/etc.5024>
- Möller, J. N., Löder, M. G. J., & Laforsch, C. (2020). Finding microplastics in soils: A review of analytical methods. *Environmental Science & Technology*, 54(4), 2078–2090.
- Musiół, M., Sikorska, W., Janeczek, H., Wałach, W., Hercog, A., Johnston, B., & Rydz, J. (2018). (Bio) degradable polymeric materials for a sustainable future—part 1. Organic recycling of PLA/PBAT blends in the form of prototype packages with long shelf-life. *Waste Management*, 77, 447–454.
- Ng, E. L., Lwanga, E. H., Eldridge, S. M., Johnston, P., Hu, H. W., Geissen, V., & Chen, D. (2018). An overview of microplastic and nanoplastic pollution in agroecosystems. *Science of the Total Environment*, 627, 1377–1388.
- Okoffo, E. D., O'Brien, S., Ribeiro, F., Burrows, S. D., Toapanta, T., Rauer, C., O'Brien, J. W., Tschärke, B. J., Wang, X., & Thomas, K. V. (2021). Plastic particles in soil: State of the knowledge on sources, occurrence and distribution, analytical methods and ecological impacts. *Environmental Science: Processes & Impacts*, 23(2), 240–274.
- Palsikowski, P. A., Kuchnier, C. N., Pinheiro, I. F., & Morales, A. R. (2018). Biodegradation in soil of PLA/PBAT blends compatibilized with chain extender. *Journal of Polymers and the Environment*, 26(1), 330–341.
- Pathan, S. I., Arfaio, P., Bardelli, T., Ceccherini, M. T., Nannipieri, P., & Pietramellara, G. (2020). Soil pollution from micro-and nanoplastic debris: A hidden and unknown biohazard. *Sustainability*, 12(18), 7255.
- Pedersen, T. L. (2020). patchwork: The composer of plots. <https://CRAN.R-project.org/package=patchwork>
- Piehl, S., Leibner, A., Löder, M. G., Dris, R., Bogner, C., & Laforsch, C. (2018). Identification and quantification of macro-and microplastics on an agricultural farmland. *Scientific Reports*, 8(1), 1–9.
- Piepho, H. P., Büchse, A., & Richter, C. (2004). A mixed modelling approach for randomized experiments with repeated measures. *Journal of Agronomy and Crop Science*, 190(4), 230–247.
- PlasticsEurope (2019). Plastics—the facts 2019: An analysis of European plastics production, demand and waste data. <https://plasticseurope.org/wp-content/uploads/2021/10/2019-Plastics-the-facts.pdf>
- Qi, Y., Yang, X., Pelaez, A. M., Huerta Lwanga, E., Beriot, N., Gertsen, H., Garbeva, P., & Geissen, V. (2018). Macro-and micro-plastics in soil-plant system: Effects of plastic mulch film residues on wheat (*Triticum aestivum*) growth. *Science of the Total Environment*, 645, 1048–1056.
- Qin, M., Chen, C., Song, B., Shen, M., Cao, W., Yang, H., ... & Gong, J. (2021). A review of biodegradable plastics to biodegradable microplastics: Another ecological threat to soil environments? *Journal of Cleaner Production*, 312, 127816. <https://doi.org/10.1016/j.jclepro.2021.127816>
- R Core Team (2020). *R: A Language and Environment for Statistical Computing*. R Foundation for Statistical Computing.
- Restrepo-Flórez, J. M., Bassi, A., & Thompson, M. R. (2014). Microbial degradation and deterioration of polyethylene—A review. *International Biodeterioration & Biodegradation*, 88, 83–90.
- Rillig, M. C., Ingrassia, R., & de Souza Machado, A. A. (2017). Microplastic incorporation into soil in agroecosystems. *Frontiers in Plant Science*, 8, 1805. <https://doi.org/10.3389/fpls.2017.01805>
- Rillig, M. C., Lehmann, A., de Souza Machado, A. A., & Yang, G. (2019). Microplastic effects on plants. *New Phytologist*, 223(3), 1066–1070.
- Rillig, M. C., Leifheit, E., & Lehmann, J. (2021). Microplastic effects on carbon cycling processes in soils. *PLoS Biology*, 19(3), e3001130. <https://doi.org/10.1371/journal.pbio.3001130>
- Robinson, D., Hayes, A., & Couch, S. (2020). broom: Convert statistical objects into tidy tibbles. <https://CRAN.R-project.org/package=broom>
- Rodrigues, L. C., Puig-Ventosa, I., López, M., Martínez, F. X., Ruiz, A. G., & Bertrán, T. G. (2020). The impact of improper materials in biowaste on the quality of compost. *Journal of Cleaner Production*, 251, 119601. <https://doi.org/10.1016/j.jclepro.2019.119601>
- Rudnik, E., & Briassoulis, D. (2011). Degradation behaviour of poly (lactic acid) films and fibres in soil under Mediterranean field conditions and laboratory simulations testing. *Industrial Crops and Products*, 33(3), 648–658.
- Rüthi, J., Bölsterli, D., Pardi-Comensoli, L., Brunner, I., & Frey, B. (2020). The “plastisphere” of biodegradable plastics is characterized by specific microbial taxa of alpine and arctic soils. *Frontiers in Environmental Science*, 8, 562263. <https://doi.org/10.3389/fenvs.2020.562263>
- Scheurer, M., & Bigalke, M. (2018). Microplastics in Swiss floodplain soils. *Environmental Science & Technology*, 52(6), 3591–3598.
- Schöpfer, L., Menzel, R., Schnepf, U., Ruess, L., Marhan, S., Brümmer, F., Pagel, H., & Kandeler, E. (2020). Microplastics effects on reproduction and body length of the soil-dwelling nematode *Caenorhabditis elegans*. *Frontiers in Environmental Science*, 8, 41. <https://doi.org/10.3389/fenvs.2020.00041>
- Sintim, H. Y., Bary, A. I., Hayes, D. G., Wadsworth, L. C., Anunciado, M. B., English, M. E., Bandopadhyay, S., Schaeffer, S. M., DeBruyn, J. M., Miles, C. A., Reganold, J. P., & Flury, M. (2020). In situ degradation of biodegradable plastic mulch films in compost and agricultural soils. *Science of The Total Environment*, 727, 138668. <https://doi.org/10.1016/j.scitotenv.2020.138668>
- Steiner, T., Zhang, Y., Möller, J. N., Agarwal, S., Löder, M. G. J., Greiner, A., Laforsch, C., & Freitag, R. (2022). Municipal biowaste treatment plants contribute to the contamination of the environment with residues of biodegradable plastics with putative higher persistence potential. *Scientific Reports*, 12(1), 1–14.
- Tabasi, R. Y., & Ajji, A. (2015). Selective degradation of biodegradable blends in simulated laboratory composting. *Polymer Degradation and Stability*, 120, 435–442.
- Uffen, R. L. (1997). Xylan degradation: A glimpse at microbial diversity. *Journal of Industrial Microbiology and Biotechnology*, 19(1), 1–6.
- van den Berg, P., Huerta-Lwanga, E., Corradini, F., & Geissen, V. (2020). Sewage sludge application as a vehicle for microplastics in eastern Spanish agricultural soils. *Environmental Pollution*, 261, 114198. <https://doi.org/10.1016/j.envpol.2020.114198>
- van Schothorst, B., Beriot, N., Huerta Lwanga, E., & Geissen, V. (2021). Sources of light density microplastic related to two agricultural practices: The use of compost and plastic mulch. *Environments*, 8(4), 36. <https://doi.org/10.3390/environments8040036>
- Vance, E. D., Brookes, P. C., & Jenkinson, D. S. (1987). An extraction method for measuring soil microbial biomass C. *Soil Biology and Biochemistry*, 19(6), 703–707.
- Vinhal-Freitas, I. C., Wangen, D. R. B., Ferreira, A. D. S., Corrêa, G. F., & Wendling, B. (2010). Microbial and enzymatic activity in soil after organic composting. *Revista Brasileira de Ciência do Solo*, 34, 757–764.

- Vithanage, M., Ramanayaka, S., Hasinthara, S., & Navaratne, A. (2021). Compost as a carrier for microplastics and plastic-bound toxic metals into agroecosystems. *Current Opinion in Environmental Science & Health*, 24, 100297. <https://doi.org/10.1016/j.coesh.2021.100297>
- Wang, Q., Adams, C. A., Wang, F., Sun, Y., & Zhang, S. (2022). Interactions between microplastics and soil fauna: A critical review. *Critical Reviews in Environmental Science and Technology*, 52(18), 3211–3243.
- Wang, J., Li, J., Liu, S., Li, H., Chen, X., Peng, C., Zhang, P., & Liu, X. (2021). Distinct microplastic distributions in soils of different land-use types: A case study of Chinese farmlands. *Environmental Pollution*, 269, 116199. <https://doi.org/10.1016/j.envpol.2020.116199>
- Watteau, F., Dignac, M. F., Bouchard, A., Revallier, A., & Houot, S. (2018). Microplastic detection in soil amended with municipal solid waste composts as revealed by transmission electronic microscopy and pyrolysis/GC/MS. *Frontiers in Sustainable Food Systems*, 2, <https://doi.org/10.3389/fsufs.2018.00081>
- Weithmann, N., Möller, J. N., Löder, M. G., Piehl, S., Laforsch, C., & Freitag, R. (2018). Organic fertilizer as a vehicle for the entry of microplastic into the environment. *Science Advances*, 4(4), eaap8060. <https://doi.org/10.1126/sciadv.aap80>
- Weng, Y. X., Jin, Y. J., Meng, Q. Y., Wang, L., Zhang, M., & Wang, Y. Z. (2013). Biodegradation behavior of poly (butylene adipate-co-terephthalate)(PBAT), poly (lactic acid)(PLA), and their blend under soil conditions. *Polymer Testing*, 32(5), 918–926.
- Wickham, H., Averick, M., Bryan, J., Chang, W., McGowan, L., François, R., Grolemund, G., Hayes, A., Henry, L., Hester, J., Kuhn, M., Pedersen, T., Miller, E., Bache, S., Müller, K., Ooms, J., Robinson, D., Seidel, D., Spinu, V., ... & Yutani, H. (2019). Welcome to the Tidyverse. *Journal of Open Source Software*, 4(43), 1686. <https://doi.org/10.21105/joss.01686>
- Wickham, H., & Seidel, D. (2020). scales: Scale functions for visualization. <https://CRAN.R-project.org/package=scales>
- Yang, J., Li, L., Li, R., Xu, L., Shen, Y., Li, S., Tu, C., Wu, L., Christie, P., & Luo, Y. (2021). Microplastics in an agricultural soil following repeated application of three types of sewage sludge: A field study. *Environmental Pollution*, 289, 117943. <https://doi.org/10.1016/j.envpol.2021.117943>
- Zhang, D., Ng, E. L., Hu, W., Wang, H., Galaviz, P., Yang, H., Sun, W., Li, C., Ma, X., Fu, B., Zhao, P., Zhang, F., Jin, S., Zhou, M., Du, L., Peng, C., Zhang, X., Xu, Z., Xi, B., ... & Liu, H. (2020). Plastic pollution in croplands threatens long-term food security. *Global Change Biology*, 26(6), 3356–3367.
- Zhang, G. S., & Liu, Y. F. (2018). The distribution of microplastics in soil aggregate fractions in southwestern China. *Science of the Total Environment*, 642, 12–20.
- Zhang, M., Zhao, Y., Qin, X., Jia, W., Chai, L., Huang, M., & Huang, Y. (2019). Microplastics from mulching film is a distinct habitat for bacteria in farmland soil. *Science of the Total Environment*, 688, 470–478.
- Zhang, S., Wang, J., & Hao, X. (2020). Fertilization accelerates the decomposition of microplastics in mollisols. *Science of the Total Environment*, 722, 137950. <https://doi.org/10.1016/j.scitotenv.2020.137950>
- Zhang, X., Li, Y., Ouyang, D., Lei, J., Tan, Q., Xie, L., Li, Z., Liu, T., Xiao, Y., Farooq, T. H., Wu, X., Chen, L., & Yan, W. (2021). Systematical review of interactions between microplastics and microorganisms in the soil environment. *Journal of Hazardous Materials*, 418, 126288. <https://doi.org/10.1016/j.jhazmat.2021.126288>
- Zhou, J., Gui, H., Banfield, C. C., Wen, Y., Zang, H., Dippold, M. A., Charlton, A., & Jones, D. L. (2021). The microplastisphere: Biodegradable microplastics addition alters soil microbial community structure and function. *Soil Biology and Biochemistry*, 156, 108211. <https://doi.org/10.1016/j.soilbio.2021.108211>
- Zumstein, M. T., Schintmeister, A., Nelson, T. F., Baumgartner, R., Woebken, D., Wagner, M., Kohler, H.-P. E., McNeill, K., & Sander, M. (2018). Biodegradation of synthetic polymers in soils: Tracking carbon into CO₂ and microbial biomass. *Science Advances*, 4(7), eaas9024. <https://doi.org/10.1126/sciadv.aas902>

SUPPORTING INFORMATION

Additional supporting information can be found online in the Supporting Information section at the end of this article.

How to cite this article: Schöpfer, L., Möller, J. N., Steiner, T., Schnepf, U., Marhan, S., Resch, J., Bayha, A., Löder, M. G. J., Freitag, R., Brümmer, F., Laforsch, C., Streck, T., Forberger, J., Kranert, M., Kandeler, E., & Pagel, H. (2022). Microplastics persist in an arable soil but do not affect soil microbial biomass, enzyme activities, and crop yield. *Journal of Plant Nutrition and Soil Science*, 1–14. <https://doi.org/10.1002/jpln.202200062>

Supporting Information

Microplastics persist in an arable soil but do not affect soil microbial biomass, enzyme activities, and crop yield

Lion Schöpfer, Julia N. Möller, Thomas Steiner, Uwe Schnepf, Sven Marhan, Julia Resch, Ansilla Bayha, Martin G. J. Löder, Ruth Freitag, Franz Brümmer, Christian Laforsch, Thilo Streck, Jens Forberger, Martin Kranert, Ellen Kandeler, Holger Pagel

10.002/jpln.202200062

Table S1. Number and proportion of particles <0.5 mm and >0.5 mm by sample type and analysis (μ FTIR, ATR-FTIR). Particles that were removed from the small fraction (μ FTIR analysis) and large fraction (ATR-FTIR analysis) datasets are shown in grey. M1 and M17 stand for one month and 17 months after setup of the experiment.

Analysis	Sample type	Particle numbers (absolute)		Proportion of particles (%)	
		< 0.5 mm	> 0.5 mm	< 0.5 mm	> 0.5 mm
small fraction (μ FTIR-ATR)	Background contamination (all MP types)	74	4	94.9	5.1
	LDPE-soil-mixture (only PE)	4774	1246	79.3	20.7
	Soil from LDPE plots at M1 (only PE)	146	34	81.1	18.9
	Soil from LDPE plots at M17 months (only PE)	231	36	86.5	13.5
	PLA/PBAT-soil-mixture (only PLA/PBAT)	1274	475	72.8	27.2
	Soil from PLA/PBAT plots at M1 (only PLA/PBAT)	32	20	61.5	38.5
	Soil from PLA/PBAT plots at M17 (only PLA/PBAT)	36	5	87.8	12.2
large fraction (ATR)	LDPE-soil-mixture (only PE)	27	1249	2.1	97.9
	PLA/PBAT-soil-mixture (only PLA/PBAT)	1	952	0.1	99.9
	Soil from all plots at M17 (all polymer types)	0	57	0	100

Table S2 Pairwise contrasts of LDPE and PLA/PBAT particle number of MP_{start} , M1 and M17 separate for MP type. Lower and upper 95 % confidence intervals (CI low, CI up), t statistics, df degrees of freedom and p values. Numbers in bold indicate p values < 0.05.

MP type	Contrast	Difference	CI low	CI up	t	df	p
LDPE	M1 – MP_{start}	-419	-900	62	-2.67	6	0.082
	M17 – MP_{start}	-79	-560	402	-0.50	6	0.872
	M17 – M1	340	-141	821	2.17	6	0.156
PLA/PBAT	M1 – MP_{start}	-6	-100	89	-0.19	6	0.981
	M17 – MP_{start}	10	-84	105	0.33	6	0.942
	M17 – M1	16	-78	110	0.52	6	0.865

Table S3 ANOVA tables with variable (Var.), numerator degrees of freedom (Num df), denominator degrees of freedom (Den df), sum of squares (sumsq), mean sum of squares (meansq), *F* and *p* values. Numbers in bold indicate *p* values < 0.05.

Var.	Factor	Num df	Den df	sumsq	meansq	<i>F</i>	<i>p</i>
lipase	Value_TMinus1	1	23	8.58e+05	8.58e+05	6.44	0.018
	Timepoint	2	48	2.44e+07	1.22e+07	91.41	< 0.001
	Fertilizer	2	23	8.34e+06	4.17e+06	31.32	< 0.001
	PlasticType	2	23	2.89e+05	1.44e+05	1.08	0.355
	Block	3	23	1.07e+06	3.57e+05	2.68	0.071
	Fertilizer:PlasticType	4	23	2.87e+05	7.18e+04	0.54	0.708
	Timepoint:Fertilizer	4	48	4.34e+06	1.09e+06	8.15	< 0.001
	Timepoint:PlasticType	4	48	1.18e+05	2.95e+04	0.22	0.925
	Timepoint:Block	6	48	8.5e+05	1.42e+05	1.06	0.397
	Timepoint:Fertilizer:PlasticType	8	48	4.92e+05	6.15e+04	0.46	0.877
β-glucosidase	Value_TMinus1	1	23	6.86e+02	6.86e+02	0.12	0.732
	Timepoint	2	48	6.18e+05	3.09e+05	54.38	< 0.001
	Fertilizer	2	23	3.37e+04	1.69e+04	2.97	0.071
	PlasticType	2	23	1.12e+04	5.59e+03	0.98	0.389
	Block	3	23	2.88e+04	9.61e+03	1.69	0.197
	Fertilizer:PlasticType	4	23	2.91e+04	7.28e+03	1.28	0.307
	Timepoint:Fertilizer	4	48	9.62e+04	2.4e+04	4.23	0.005
	Timepoint:PlasticType	4	48	2.8e+03	7.01e+02	0.12	0.973
	Timepoint:Block	6	48	1.95e+04	3.25e+03	0.57	0.75
	Timepoint:Fertilizer:PlasticType	8	48	9.02e+04	1.13e+04	1.98	0.069
β-xylosidase	Value_TMinus1	1	23	3.66e+02	3.66e+02	2.33	0.141
	Timepoint	2	48	2.53e+04	1.26e+04	80.23	< 0.001
	Fertilizer	2	23	1.9e+03	9.52e+02	6.05	0.008
	PlasticType	2	23	1.11e+02	5.55e+01	0.35	0.707
	Block	3	23	1.46e+03	4.88e+02	3.10	0.047
	Fertilizer:PlasticType	4	23	2.44e+02	6.11e+01	0.39	0.815
	Timepoint:Fertilizer	4	48	2.5e+03	6.24e+02	3.96	0.007
	Timepoint:PlasticType	4	48	2.58e+02	6.45e+01	0.41	0.801
	Timepoint:Block	6	48	1.16e+03	1.94e+02	1.23	0.307
	Timepoint:Fertilizer:PlasticType	8	48	1.6e+03	2e+02	1.27	0.282
phenoloxidase	Value_TMinus1	1	23	4.92e+06	4.92e+06	1.54	0.227
	Timepoint	2	48	1.27e+08	6.36e+07	19.88	< 0.001
	Fertilizer	2	23	2.27e+07	1.14e+07	3.55	0.045
	PlasticType	2	23	1.63e+06	8.14e+05	0.25	0.777
	Block	3	23	4.21e+07	1.4e+07	4.38	0.014
	Fertilizer:PlasticType	4	23	1.26e+07	3.14e+06	0.98	0.436
	Timepoint:Fertilizer	4	48	1.61e+07	4.03e+06	1.26	0.299
	Timepoint:PlasticType	4	48	5.05e+06	1.26e+06	0.40	0.811
	Timepoint:Block	6	48	1.87e+07	3.12e+06	0.98	0.452
	Timepoint:Fertilizer:PlasticType	8	48	1.27e+07	1.59e+06	0.50	0.852
C _{mi} _c	Value_TMinus1	1	23	5.43e+04	5.43e+04	44.60	< 0.001
	Timepoint	2	48	2.29e+04	1.14e+04	9.39	< 0.001

Var.	Factor	Num df	Den df	sumsq	meansq	F	p
	Fertilizer	2	23	4.17e+03	2.08e+03	1.71	0.203
	PlasticType	2	23	3.63e+03	1.82e+03	1.49	0.246
	Block	3	23	1.73e+04	5.75e+03	4.72	0.01
	Fertilizer:PlasticType	4	23	6.69e+03	1.67e+03	1.37	0.274
	Timepoint:Fertilizer	4	48	1.03e+04	2.58e+03	2.12	0.093
	Timepoint:PlasticType	4	48	8.77e+03	2.19e+03	1.80	0.144
	Timepoint:Block	6	48	2.17e+04	3.61e+03	2.97	0.015
	Timepoint:Fertilizer:PlasticType	8	48	5.25e+03	6.56e+02	0.54	0.821
N_{mic}	Value_TMinus1	1	23	4.9e+02	4.9e+02	17.38	< 0.001
	Timepoint	2	48	2.54e+03	1.27e+03	45.03	< 0.001
	Fertilizer	2	23	8.73e+00	4.36e+00	0.15	0.857
	PlasticType	2	23	2.18e+02	1.09e+02	3.87	0.036
	Block	3	23	8.44e+02	2.81e+02	9.98	< 0.001
	Fertilizer:PlasticType	4	23	3.22e+01	8.04e+00	0.29	0.884
	Timepoint:Fertilizer	4	48	4.48e+02	1.12e+02	3.97	0.007
	Timepoint:PlasticType	4	48	4.63e+02	1.16e+02	4.10	0.006
	Timepoint:Block	6	48	4.17e+02	6.94e+01	2.46	0.037
	Timepoint:Fertilizer:PlasticType	8	48	1.66e+02	2.08e+01	0.74	0.658
N-acetyl-glucosaminidase	Value_TMinus1	1	23	1.57e-04	1.57e-04	0.01	0.922
	Timepoint	2	48	3.46e+00	1.73e+00	107.80	< 0.001
	Fertilizer	2	23	8.42e-02	4.21e-02	2.63	0.094
	PlasticType	2	23	1.79e-02	8.97e-03	0.56	0.579
	Block	3	23	2.16e-02	7.2e-03	0.45	0.721
	Fertilizer:PlasticType	4	23	2.73e-02	6.83e-03	0.43	0.788
	Timepoint:Fertilizer	4	48	2.79e-01	6.98e-02	4.35	0.004
	Timepoint:PlasticType	4	48	1.78e-02	4.45e-03	0.28	0.891
	Timepoint:Block	6	48	2.09e-01	3.48e-02	2.17	0.062
	Timepoint:Fertilizer:PlasticType	8	48	1.2e-01	1.5e-02	0.93	0.498

Table S4 ANOVA table for silage maize biomass and grain yield of summer barley with variable (Var.), numerator degrees of freedom (df), sum of squares (sumsq), mean sum of squares (meansq), *F* and *p* values. Numbers in bold indicate *p* values < 0.05.

Variable	Factor	df	sumsq	meansq	F	p
Silage maize - biomass	Fertilizer	2	1.92e-01	9.58e-02	0.01	0.987
	PlasticType	2	3.95e+01	1.97e+01	2.69	0.089
	Block	3	5.71e+01	1.9e+01	2.59	0.076
	Fertilizer:PlasticType	4	1.13e+01	2.82e+00	0.38	0.818
	Residuals	24	1.76e+02	7.35e+00		
Summer barley - grain yield	Fertilizer	2	2.71e+00	1.35e+00	4.92	0.016
	PlasticType	2	1.17e+00	5.83e-01	2.12	0.142
	Block	3	1.27e+01	4.22e+00	15.37	< 0.001
	Fertilizer:PlasticType	4	9.58e-02	2.39e-02	0.09	0.986
	Residuals	24	6.6e+00	2.75e-01		

Table S5 Simple contrasts of *Fertilizer* or *PlasticType* within *Timepoint* levels. Absolute and relative differences (Diff.) between treatment groups with lower and upper 95 % confidence intervals (CI low, CI up), *t* statistics, *df* degrees of freedom and *p* values. Numbers in bold indicate *p* values < 0.05.

Var.	Contrast	Timepoint	Diff.	CI low	CI up	Diff. (%)	CI low (%)	CI up (%)	<i>t</i>	df	<i>p</i>
lipase	Compost - Control	M1	1077.59	718.33	1436.85	58.25	38.83	77.67	7.18	70.89	< 0.001
	Digestate - Control		147.24	-209.47	503.95	7.96	-11.32	27.24	0.99	70.97	0.587
	Digestate - Compost		-930.35	-1289.69	-571.00	-31.78	-44.05	-19.50	-6.20	70.88	< 0.001
	Compost - Control	M5	858.76	499.50	1218.02	62.46	36.33	88.59	5.72	70.89	< 0.001
	Digestate - Control		505.45	148.74	862.16	36.76	10.82	62.71	3.39	70.97	0.003
	Digestate - Compost		-353.31	-712.66	6.04	-15.82	-31.91	0.27	-2.35	70.88	0.055
	Compost - Control	M17	145.13	-214.12	504.39	5.10	-7.52	17.71	0.97	70.89	0.6
	Digestate - Control		254.27	-102.44	610.98	8.93	-3.60	21.46	1.71	70.97	0.21
	Digestate - Compost		109.14	-250.21	468.48	3.65	-8.36	15.66	0.73	70.88	0.748
β-xylosidase	Compost - Control	M1	2.83	-9.43	15.10	7.48	-24.92	39.87	0.55	70.97	0.845
	Digestate - Control		0.26	-12.01	12.52	0.68	-31.71	33.08	0.05	70.97	0.999
	Digestate - Compost		-2.57	-14.83	9.69	-6.32	-36.45	23.81	-0.50	70.97	0.87
	Compost - Control	M5	11.82	-0.44	24.09	47.32	-1.76	96.40	2.31	70.97	0.061
	Digestate - Control		14.98	2.71	27.24	59.94	10.86	109.02	2.92	70.97	0.013
	Digestate - Compost		3.15	-9.11	15.41	8.57	-24.74	41.87	0.62	70.97	0.812
	Compost - Control	M17	-6.48	-18.75	5.78	-9.86	-28.51	8.80	-1.27	70.97	0.42
	Digestate - Control		14.89	2.62	27.15	22.64	3.99	41.30	2.91	70.97	0.013
	Digestate - Compost		21.37	9.11	33.63	36.05	15.37	56.74	4.17	70.97	< 0.001
β-glucosidase	Compost - Control	M1	9.58	-64.53	83.69	3.95	-26.58	34.48	0.31	70.91	0.949
	Digestate - Control		3.23	-70.51	76.98	1.33	-29.05	31.71	0.10	70.97	0.994
	Digestate - Compost		-6.35	-80.80	68.10	-2.52	-32.02	26.99	-0.20	70.83	0.977
	Compost - Control	M5	80.62	6.51	154.73	46.77	3.78	89.76	2.60	70.91	0.03
	Digestate - Control		58.62	-15.13	132.36	34.00	-8.78	76.78	1.90	70.97	0.145
	Digestate - Compost		-22.01	-96.46	52.44	-8.70	-38.12	20.73	-0.71	70.83	0.76

Var.	Contrast	Timepoint	Diff.	CI low	CI up	Diff. (%)	CI low (%)	CI up (%)	t	df	p
	Compost - Control	M17	-53.90	-128.01	20.21	-13.94	-33.10	5.23	-1.74	70.91	0.197
	Digestate - Control		68.31	-5.43	142.06	17.66	-1.40	36.73	2.22	70.97	0.075
	Digestate - Compost		122.21	47.76	196.66	36.71	14.35	59.08	3.93	70.83	< 0.001
N _{mic}	LDPE - Control	M1	-0.62	-5.89	4.65	-3.02	-28.70	22.66	-0.28	70.70	0.957
	(PLA/PBAT) - Control		-3.16	-8.48	2.17	-15.37	-41.29	10.55	-1.42	70.42	0.336
	(PLA/PBAT) - LDPE		-2.54	-7.78	2.70	-12.74	-39.04	13.56	-1.16	70.85	0.481
	LDPE - Control	M5	-8.19	-13.47	-2.92	-36.56	-60.08	-13.03	-3.72	70.70	0.001
	(PLA/PBAT) - Control		-0.14	-5.46	5.19	-0.61	-24.36	23.13	-0.06	70.42	0.998
	(PLA/PBAT) - LDPE		8.06	2.82	13.30	56.65	19.82	93.48	3.68	70.85	0.001
	LDPE - Control	M17	-0.16	-5.44	5.11	-0.57	-18.88	17.74	-0.07	70.70	0.997
	(PLA/PBAT) - Control		2.97	-2.35	8.29	10.31	-8.17	28.79	1.34	70.42	0.38
	(PLA/PBAT) - LDPE		3.13	-2.10	8.37	10.94	-7.35	29.23	1.43	70.85	0.33
N _{mic}	Compost - Control	M1	0.76	-4.54	6.06	3.78	-22.40	29.95	0.35	70.56	0.936
	Digestate - Control		-3.68	-8.92	1.56	-18.16	-44.05	7.72	-1.68	70.84	0.22
	Digestate - Compost		-4.44	-9.70	0.81	-21.14	-46.14	3.86	-2.02	70.79	0.114
	Compost - Control	M5	4.58	-0.72	9.88	26.39	-4.13	56.91	2.07	70.56	0.103
	Digestate - Control		2.23	-3.01	7.47	12.86	-17.32	43.04	1.02	70.84	0.567
	Digestate - Compost		-2.35	-7.60	2.90	-10.70	-34.64	13.23	-1.07	70.79	0.535
	Compost - Control	M17	-2.12	-7.42	3.18	-7.25	-25.40	10.89	-0.96	70.56	0.606
	Digestate - Control		3.71	-1.54	8.95	12.69	-5.26	30.63	1.69	70.84	0.215
	Digestate - Compost		5.82	0.57	11.08	21.50	2.10	40.89	2.65	70.79	0.026

Table S6 Contrasts of N-acetyl-glucosaminidase activities by *Timepoint*. Statistical tests are performed on log-transformed data. The ratios of the contrasts and 95 % confidence intervals (CI low, CI up) are back-transformed to the original scale of the data. *t* statistics, df degrees of freedom and *p* values. Numbers in bold indicate *p* values < 0.05.

N-acetyl-glucosaminidase	Contrast	Timepoint	Ratio	CI low	CI up	<i>t</i>	df	<i>p</i>
	Compost / Control	M1	1.03	0.76	1.40	0.25	68	0.967
	Digestate / Control		0.92	0.68	1.24	-0.66	68	0.789
	Digestate / Compost		0.89	0.66	1.21	-0.90	68	0.642
	Compost / Control	M5	1.30	0.96	1.76	2.10	68	0.097
	Digestate / Control		1.59	1.18	2.16	3.71	68	0.001
	Digestate / Compost		1.22	0.90	1.66	1.59	68	0.255
	Compost / Control	M17	0.82	0.60	1.10	-1.61	68	0.249
	Digestate / Control		1.14	0.85	1.55	1.07	68	0.539
	Digestate / Compost		1.40	1.04	1.90	2.67	68	0.026

Table S7 Main effect contrasts of *Fertilizer* for grain yield of summer barley and phenoloxidase activity. Absolute and relative differences (Diff.) between treatment groups with lower and upper 95 % confidence intervals (CI low, CI up. *t* statistics, df degrees of freedom and *p* values. Numbers in bold indicate *p* values < 0.05.

Var.	Contrast	Diff.	CI low	CI up	Diff. (%)	CI low (%)	CI up (%)	<i>t</i>	df	<i>p</i>
Grain yield – summer barley	Compost - Control	-0.14	-0.68	0.39	-2.21	-10.49	6.07	-0.67	24	0.785
	Digestate - Control	0.50	-0.04	1.03	7.70	-0.58	15.98	2.32	24	0.072
	Digestate - Compost	0.64	0.11	1.17	10.13	1.67	18.60	2.99	24	0.017
Phenol-oxidase	Compost - Control	-25.07	-1283.02	1232.89	-0.35	-17.95	17.25	-0.05	23	0.999
	Digestate - Control	1185.34	-80.72	2451.40	16.58	-1.13	34.30	2.34	23	0.069
	Digestate - Compost	1210.40	-57.11	2477.91	16.99	-0.80	34.79	2.39	23	0.063

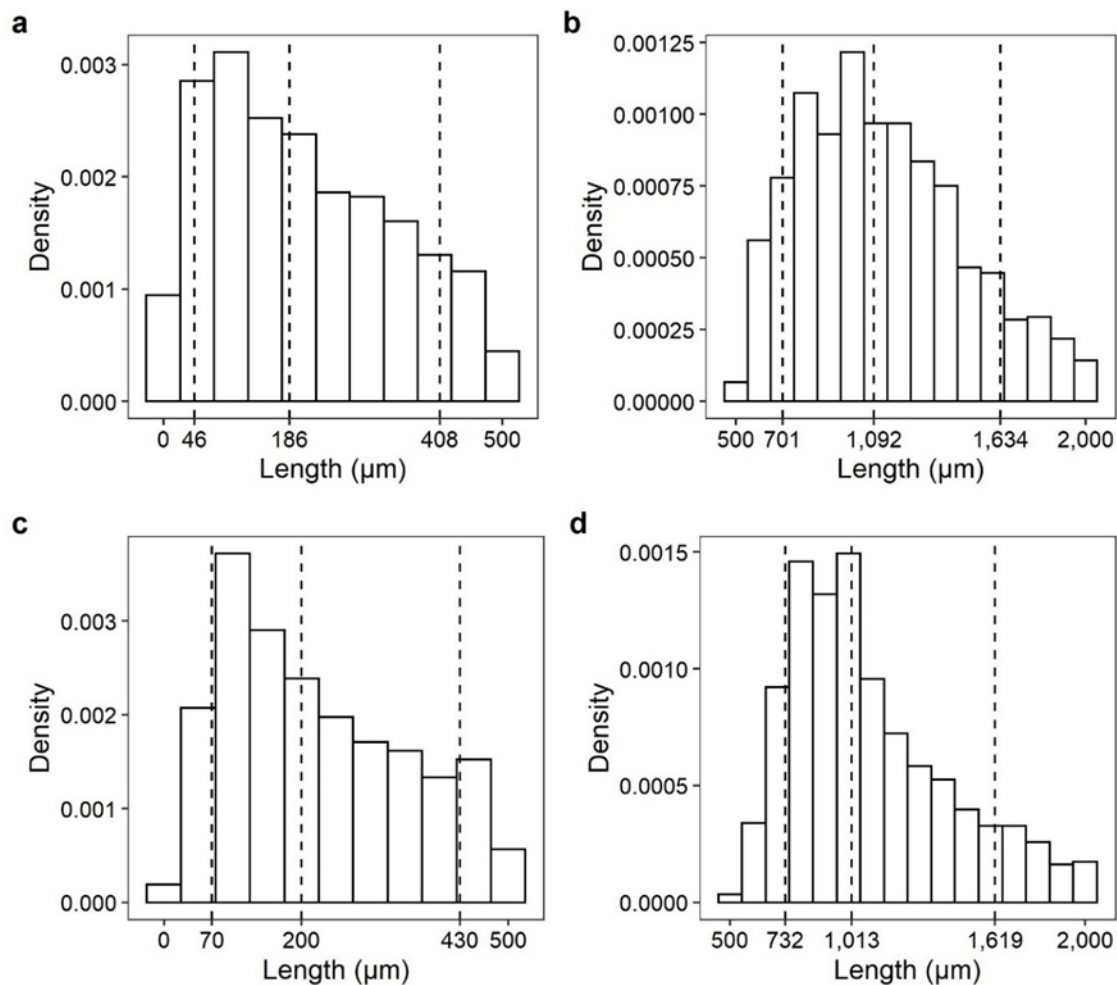


Figure S1 Particle size distributions of MP particles in MP-soil-mixtures of **a** LDPE < 0.5 mm (n = 4,774), **b** LDPE 0.5 – 2 mm (n = 1,053), **c** PLA/PBAT < 0.5 mm (n = 1,274), and **d** PLA/PBAT 0.5 – 2 mm (n = 857). The dashed lines show the 10th, 50th (median), and 90th percentiles from left to right.

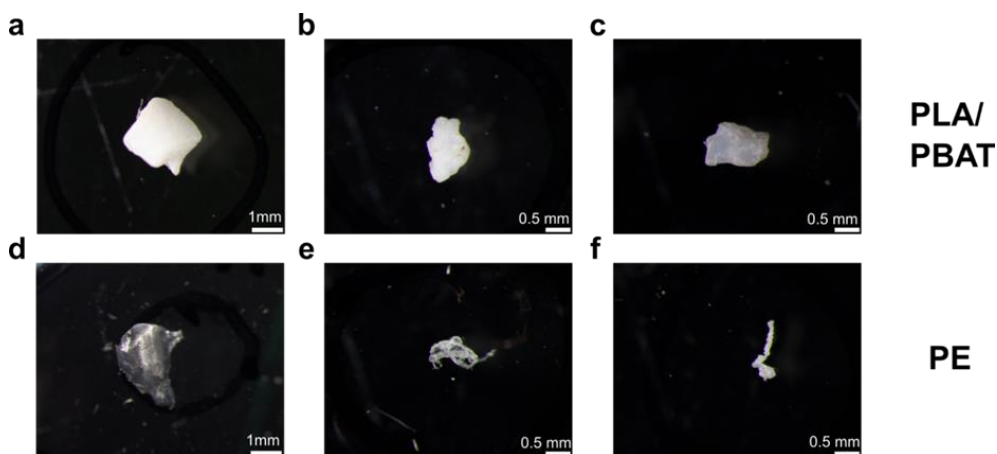


Figure S2 Representative microscopic images of MP > 0.5 mm as initially added to the field detected in the MP-soil-mixtures. **a – c** PLA/PBAT, **d – f** PE.

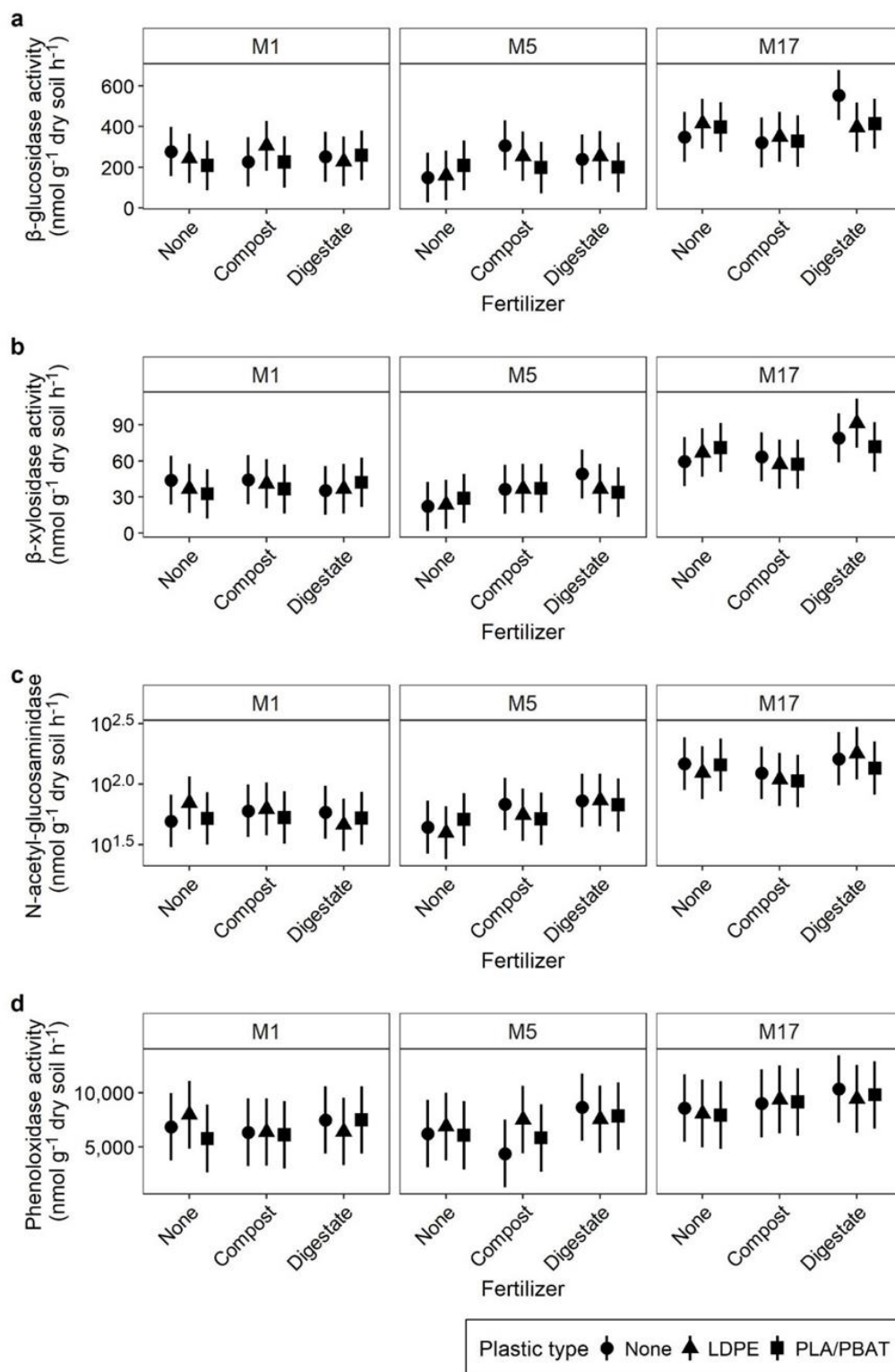


Figure S3 **a** β -glucosidase **b** β -xylosidase **c** N-acetyl-glucosaminidase, and **d** phenoloxidase activity as a function of MP and organic fertilizers one month (M1), five (M5), and 17 months (M17) after the addition of 2 g m^{-2} MP. Data are presented as estimated marginal means ($n = 4$) with lower and upper 95 % confidence intervals (error bars). Note that data of N-acetyl-glucosaminidase are log-transformed.

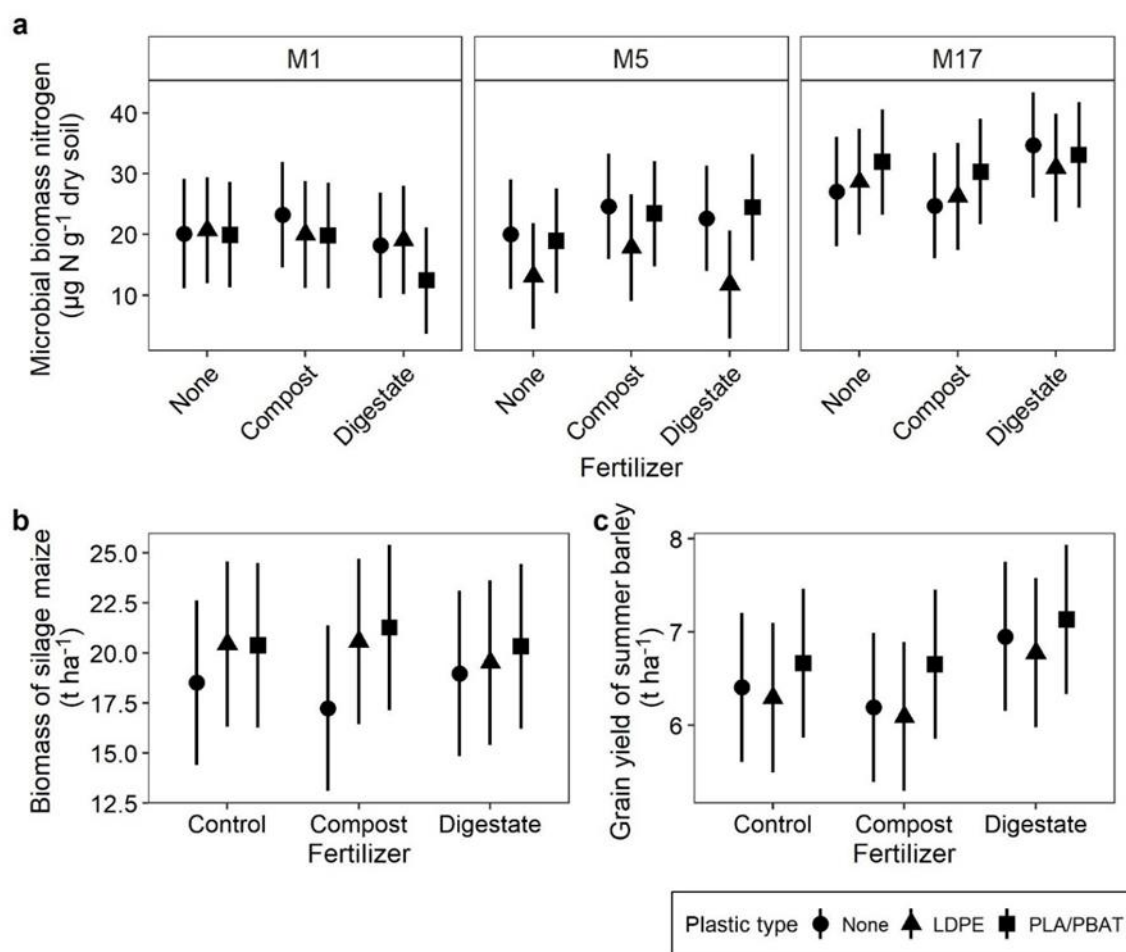


Figure S4 **a** Microbial biomass nitrogen, **b** biomass of silage maize, and **c** grain yield of summer barley as a function of MP and organic fertilizers after one month (M1), five (M5) and 17 months (M17) after the addition of 2 g m^{-2} MP. Data are presented as estimated marginal means ($n = 4$) with lower and upper 95 % confidence intervals (error bars).



Figure S5 Land machine harvesting summer barley on the site of the field experiment. Possible entry of red varnish particles due to abrasion of the red protective coating.

Article 5

**Flooding frequency and floodplain topography
determine abundance of microplastics in an
alluvial Rhine soil**



Flooding frequency and floodplain topography determine abundance of microplastics in an alluvial Rhine soil



Markus Rolf^a, Hannes Laermans^a, Lukas Kienzler^a, Christian Pohl^b, Julia N. Möller^c, Christian Laforsch^c, Martin G.J. Löder^{c,*}, Christina Bogner^{a,*}¹

^a Ecosystem Research Group, Institute of Geography, Faculty of Mathematics and Natural Sciences, University of Cologne, 50923 Cologne, Germany

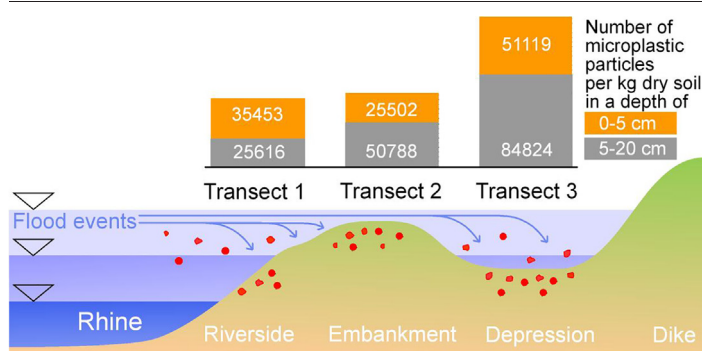
^b DHI WASY GmbH Büro Bremen, 28195 Bremen, Germany

^c Animal Ecology I, BayCEER, University of Bayreuth, 95440 Bayreuth, Germany

HIGHLIGHTS

- Microplastics in a Rhine floodplain originate mainly from fluvial input.
- Spatial distribution of microplastics seems to be a consequence of local topography and flooding frequency.
- Up to 75% of the found microplastics in the Rhine floodplain are smaller than 150 μm .
- The investigated floodplain accumulates microplastics in deeper soil.

GRAPHICAL ABSTRACT



ARTICLE INFO

Editor: Dimitra A Lambropoulou

Keywords:
 Microplastic
 Floodplain soil
 Riverine microplastics
 Microplastics contamination
 Rhine
 Flood modelling
 FTIR spectroscopy

ABSTRACT

Rivers are major pathways for the transport of microplastics towards the oceans, and many studies focus on microplastic abundance in fluvial ecosystems. Although flooding strongly affects transport of microplastics, knowledge about the potential input via floodwaters, spatial distribution, and fate of microplastics in adjacent floodplains remains very limited. In this study, we suggest that local topography and flood frequency could influence the abundance of microplastics in floodplains. Based on this concept, we took soil samples in a Rhine River floodplain in two different depths (0–5 cm and 5–20 cm) along three transects with increasing distance to the river and analysed the abundance of microplastics via FTIR spectroscopy. Flood frequency of the transects was estimated by a combination of hydrodynamic modelling with MIKE 21 (DHI, Hørsholm Denmark) and analysis of time series of water levels. Microplastic abundance per kg dry soil varied between 25,502 to 51,119 particles in the top 5 cm and 25,616 to 84,824 particles in the deeper soil (5–20 cm). The results of our study indicate that local topography and resulting flooding patterns are responsible for the amount of microplastics found at the respective transect. Differences in soil properties, vegetation cover and signs of earthworm activity in the soil profile seem to be related to microplastic migration and accumulation in the deeper soil. The interdisciplinary approach we used in our work can be applied to other floodplains to elucidate the respective processes. This information is essentially important both for locating potential microplastic sinks for process-informed sampling designs and to identify areas of increased bioavailability of microplastics for proper ecological risk assessment.

* Corresponding authors.

E-mail addresses: martin.loeder@uni-bayreuth.de (M.G.J. Löder), christina.bogner@uni-koeln.de (C. Bogner).

¹ Joint senior authorship.

1. Introduction

The occurrence of microplastics (plastic particles smaller than 5 mm) in our environment is a global challenge (Dris et al., 2020). Microplastics is an umbrella term for a heterogeneous pot-pourri of particles with different intrinsic properties affecting their transport, including i.e., diverse polymer types, sizes, shapes, densities, environmental ageing or biofouling (Rochman et al., 2019; Laforsch et al., 2021; Millican and Agarwal, 2021). Those particles have been found in literally all environmental compartments, even in remote areas such as coral islands (Imhof et al., 2017) or the Arctic (Bergmann et al., 2019). Research on microplastics started in the marine environment (Thompson et al., 2004) and shifted its focus to terrestrial and freshwater systems only recently (Frei et al., 2019; Horton et al., 2017; Dris et al., 2018), since it became clear that fluvial ecosystems act as a major transport route for microplastics towards the oceans (Napper et al., 2021; Lebreton et al., 2017; Meijer et al., 2021). Most plastic products are used and disposed of on land. Therefore, the large majority of microplastics originates from land-based sources (Jambeck et al., 2015) and could enter rivers through, e.g., runoff from urban, industrial and agricultural areas, effluents from industrial and waste water treatment plants, atmospheric deposition or littering (Liu et al., 2019; Bläsing and Amelung, 2018; van den Berg et al., 2020; Mintenig et al., 2017; Klein and Fischer, 2019; Dris et al., 2015; Geyer et al., 2017).

Rivers are not only pathways for microplastics, they are dynamic ecosystems which reach beyond the river channel into the adjacent floodplains and should consequently receive autonomous attention in microplastic research. Most of the studies which investigated microplastics in rivers focused on river water and sediments separately from the floodplains. These studies showed that fluvial sediments can serve as temporal and long-term sinks for microplastics (Ding et al., 2019; Scherer et al., 2020; Scheurer and Bigalke, 2018; Hurley et al., 2018; Roebroek et al., 2021; Woodward et al., 2021; Laermans et al., 2021). However, floodplains are an important interface between terrestrial and fluvial ecosystems, and might therefore also play an important role in the “plastic cycle” (Horton and Dixon, 2018).

The concept of plastic cycle emphasizes the connection between different environmental compartments when studying the transport, retention, and fate of microplastics (Horton and Dixon, 2018). Floods seem to be one of the driving forces in this plastic cycle (Lechthaler et al., 2021; Hurley et al., 2018). They intensify the erosion of riverbeds and riverbanks, which strongly affects re-mobilisation and subsequent deposition of microplastics (Hurley et al., 2018; Woodward et al., 2021). In this context, erosion experiments showed that microplastics are more mobile than natural river sediments (Waldschläger and Schüttrumpf, 2019). Only recently, the impact of floods on the transport of microplastics into floodplains and their subsequent entry into floodplain soils have gained more scientific attention (Lechthaler et al., 2021; Weber et al., 2021). Based on the available literature and our considerations, we suggest that floodplains may act as sinks for microplastics, when hydraulic conditions during flooding favour sedimentation. On the other hand, floodplains may act as a reservoir and a source of microplastics via potential re-mobilisation of particles during erosive conditions. Local topography of alluvial floodplains affects the above-mentioned hydraulic conditions, and should thus also determine the quantity and spatial distribution of microplastics in the floodplain introduced during flooding. Once deposited in the floodplain, microplastics can migrate down the soil profile with infiltrating water depending on soil properties or be transported to the deeper soil by bioturbation (Maaß et al., 2017; Rillig et al., 2017; Weber et al., 2021). Floodplain soils may thus act as a long-term sink for microplastics if sedimentation and subsequent migration into the soil column dominates over re-mobilisation by erosive forces during flooding (Lechthaler et al., 2021). Permanent vegetation cover is most probably the main factor that reduces or prevents erosion and thus re-mobilisation of particles. However, whether this sketched concept holds true under natural conditions has not been in the focus of microplastic research so far. Moreover, the current research on microplastics within floodplains completely overlooked the interactions

of topography and hydrology as a factor for the spatial distribution of riverine microplastics in floodplains.

The Rhine as one of the largest and highly anthropogenically modified rivers in Europe has been of a particular interest for microplastic research (Mani et al., 2016, 2019b, 2019a; Klein et al., 2015; Heß et al., 2018). It crosses six European countries, and nearly 60 million people live in its catchment (Belz, 2010). The land use in its surroundings is diverse and potential sources of microplastics are numerous (Mani et al., 2019b). Several studies reported microplastics concentrations of 1.6–14.7 particles m^{-3} in its surface waters and of $0.26\text{--}11.07 \times 10^3$ particles kg^{-1} in its benthic sediments (Heß et al., 2018; Mani et al., 2016, 2019b). The shoreline sediments of the Rhine contain 228–3763 microplastic particles kg^{-1} (Klein et al., 2015). Weber and Opp (2020) reported that deposition of microplastics in a floodplain was the largest close to the river channel and declined with distance from the river. However, the relationship between the abundance of microplastics in the Rhine floodplains and local topography, flooding frequency and soil properties as potential factors for migration and transport of microplastics into the deeper soil have not been addressed so far.

In this study, we aim to analyse the abundance and vertical distribution of microplastics in a Rhine floodplain soil. To elucidate our concept of how local topography and flood frequency could influence the abundance of microplastics in floodplains, we relate the amount of microplastics to differences in flooding frequency driven by the water level in the Rhine and the local topography, soil properties, vegetation cover, and signs of earthworm-related bioturbation. Therefore, we collected soil samples in three transects in an agriculturally undisturbed Rhine floodplain at the soil surface and in the deeper soil column for microplastic analysis. To determine the interplay between local topography and frequency of floods, we modelled different flooding scenarios at the three investigated transects.

2. Materials and methods

2.1. Study site

The study site is located at the left shore of the Lower Rhine, in a floodplain at the Rhine kilometre 704.7–704.8 in the nature reserve ‘Rheinaue Langel-Merkenich’ in Cologne (51°03′01.5″N 6°55′13.1″E, North-Rhine Westphalia, Germany) opposite the city of Leverkusen. We chose this site based on its land cover (permanent grassland) and its spatial isolation from the built-up areas by a dike and natural topography. On the floodplain, intensive agriculture, including ploughing, is prohibited since at least 1991 (protected nature reserve). The grass at the study site is mowed once a year. Additionally, we evaluated aerial photographs from 1945 (HES-NCAP, ncap.org.uk/NCAP-000-001-102-801, accessed on 2022-02-14) and 1988–1994 (provided by Land NRW, dl-de/by-2-0, <https://www.govdata.de/dl-de/zero-2-0>, <https://www.tim-online.nrw.de>, accessed on 2021-02-14, Supplementary Fig. S1). They also suggested the absence of intensive agriculture in this area and showed no major changes in topography (e.g., no buildings). Thus, potential sources of microplastics should be mainly limited to the fluvial inputs during flooding (originating from e.g., industrial and municipal sewage effluents, Supplementary Fig. S9) and, to a lower extent, to atmospheric deposition (Kernchen et al., 2021). Airborne microplastic inputs were not part of our study and should be addressed in the future. The Lower Rhine has a pluvio-nival regime along its course in the state of North-Rhine Westphalia (Belz, 2010). Therefore, at the study site, the highest runoffs and floods usually occur in winter and lowest runoffs in summer.

2.2. Soil sampling

We took soil samples in October and November 2019 in three transects. They followed different contour lines (i.e., elevations) parallel to the Rhine with increasing distance to the river shore (Fig. 1). The contour lines were identified by monocular levelling. Transect 1 (T1, length 35 m, patchy grass cover) was situated close to the river shore in-between of two groyes.

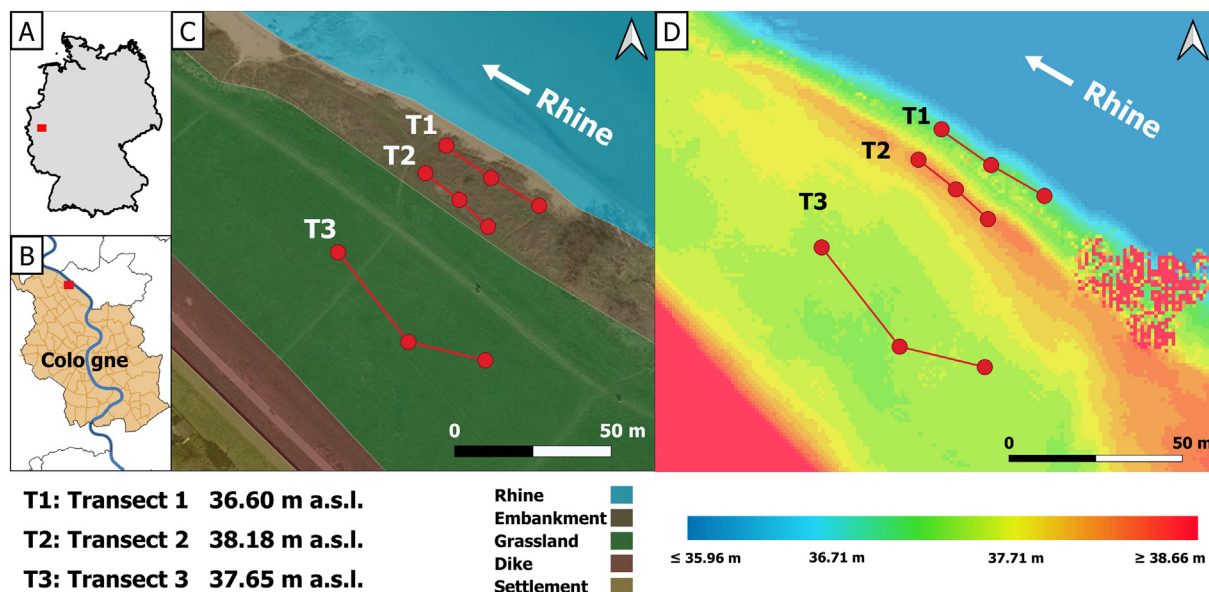


Fig. 1. A and B: location of the sampling area. C: land cover of the floodplain in the nature reserve ‘Rheinaue Langel-Merkenich’ with the sampled transects T1, T2 and T3, red points mark the soil sampling locations. D: digital elevation model of the study area. The elevation is given in meters above sea level (m a.s.l.). The fringing feature at the shore shows shrubs. Data sources: A: ©GeoBasis-DE / BKG 2019 (data changed); B: waterways shape file: <https://mapcruzin.com/free-germany-arcgis-maps-shapefiles.htm>, last accessed 2022-04-14, data derived from <https://www.openstreetmap.org/> licensed under the Open Data Commons Open Database License (ODbL) <https://opendatacommons.org/licenses/odbl/> and districts of the City of Cologne: <https://opendata-esri-de.opendata.arcgis.com/datasets/esri-de-content::stadtteile-k%C3%B6ln/about> ©Stadt Köln; C: accessed via Google Earth satellite, GeoBasis-DE/BKG (©2009); D: dl-zero-de/2.0, Datenlizenz Deutschland – Zero – Version 2.0, <https://www.govdata.de/dl-de/zero-2-0>, www.geoportal.nrw.

Transect 2 (T2, length 26 m, homogeneous grass cover) lay approximately 11 m further inland on an embankment and about 1.6 m higher than T1. Transect 3 (T3, length 61.5 m, homogeneous grass cover) was located in a depression the farthest inland in approximately 57 m distance to T1 and about 0.5 m lower than T2.

We took three soil cores in each transect for the analysis of microplastics. Therefore, we hammered three stainless-steel cylinders (diameter: 50 mm, length: 200 mm) per transect into the soil. The sampling points of the three soil cores were spaced roughly equidistantly within the transects. After excavating the sampling cylinders, we divided each core in two samples, namely the topsoil (0–5 cm) and the deeper soil (5–20 cm) samples. All three samples from one depth were pooled per transect, transferred to the same glass container (Weck GmbH, 1500 ml) and capped with a glass lid. Sample pooling allowed to obtain one representative sample per depth and transect.

Additionally, we dug a pit and prepared a soil profile with a spade in each transect. These profiles varied in depth between 45 cm and 85 cm. Preparing soil profiles beyond the sampling depth of 20 cm is necessary for their correct description. The soil profiles were described, and the soil color was classified with a Munsell soil color chart (Munsell Color (Firm), 2010) according to the World Reference Base classification (WRB) released by the Food and Agriculture Organization of the United Nations (FAO) (FAO, 2014). This information is provided in the Supplementary Figs. S2, S3 and S4 along with the photographs of the soil profiles. According to the FAO (2006, their Tables 79 to 81), we classified the size and abundance of roots, and examples and abundance of biological activity. The categories for the root diameter range from “very fine” to “coarse”, and abundance from “none”, “very few”, “few”, “common” to “many”. The abundance of biological activity can vary from “none”, “few”, “common” to “many”. Subsequently, we took bulk soil samples with a spatula from the soil surface to the maximum depth of the profiles in roughly 5 cm increments to determine the physico-chemical soil properties in the laboratory.

To account for microplastic contamination during sampling, we placed three clean sampling glass containers next to our sampling spot and left them open until the sampling ended. These glass containers served as

blank samples and were processed together with the samples later in the laboratory.

2.3. Soil properties

Bulk soil samples were dried in glass beakers for 48 h at 40 °C and sieved to < 2 mm. For soil texture analysis (i.e., percentage of sand, silt, and clay particles), we treated the samples with hydrogen peroxide (H₂O₂, 15%) until organic matter was destroyed completely. Then, we added sodium pyrophosphate (Na₄P₂O₇, 46 g L⁻¹) to avoid coagulation during the measurement. Each sample was measured three times by laser diffraction (LS 13320 Beckmann Coulter™ Laser Diffraction Particle Size Analyzer) in 116 channels using the optical Fraunhofer model. The measurements cover a particle size range from 0.4 to 2000 μm. The data were processed with GRADISTAT software version 8 (Blott and Pye, 2001) based on Folk and Ward (1957). Additionally, we analysed soil C and N contents and provide the results in the Supplementary Information (Supplementary Figs. S2, S3 and S4).

2.4. Prevention of microplastic contamination

To prevent contamination in the laboratory, the soil samples were handled under a laminar flow box whenever possible (Laminar Flow Box FBS, Spetec GmbH). Furthermore, the laboratory was equipped with an air purifier (DustBox with HEPA H14 filter, Möcklinghoff Lufttechnik GmbH) to reduce air-borne contamination. All tools and devices were cleaned twice before and after each usage by rinsing with filtered deionized water and filtered 35% ethanol (2 and 0.2 μm, respectively). All chemicals, solutions, and liquids were filtered before use. Cotton lab coats were worn during the sample preparation and analysis.

To account for and quantify potential contamination in the laboratory, the blank samples taken in the field underwent the same sample preparation procedures as the original soil samples. After analysis of the blank samples, the mean values of microplastic particles per polymer, shape and size class were calculated and rounded to the next larger integer. Subsequently, those values were subtracted from the respective polymer types, shapes,

and size classes in the sample results to correct the concentrations in the soil samples.

2.5. Extraction and purification of microplastics from soil samples

To extract microplastics from soil samples and prepare the samples for the subsequent Fourier-transform Infrared Spectroscopy (FTIR) analysis, we followed the protocol by Möller et al. (2021). The protocol was modified to account for the separation of black carbon particles by an additional density separation with a CaCl_2 brine. The supporting information contains a flow chart of the procedure (Supplementary Fig. S5). In this section, we describe the procedure briefly.

To destroy soil aggregates, we freeze-dried all soil samples in the glass containers covered with ash-free paper filters to allow evaporation (mesh size: 2 μm). From the dry samples taken in 5–20 cm depth, we took a subsample of 250 g after thorough homogenization. The dry topsoil samples (0–5 cm) were shaken in filtered deionized water (< 0.2 μm) on a laboratory shaker for 24 h to separate the soil components from vegetation. After this procedure, we picked the plant rests manually and washed the remaining particles off and back into the sample. The dry mass of the resulting topsoil samples varied between 388 g and 567 g and was processed completely. Subsequently, all samples were wet-sieved in a metal sieve cascade with stainless-steel meshes in a size of 5 mm, 1 mm and 500 μm and thoroughly rinsed during the whole sieving process. Putative microplastic particles on the 5 mm, 1 mm and 500 μm sieves were sorted under a binocular stereo microscope (Olympus SZ61), photographed, and their size was measured. Subsequently, they were stored until the attenuated total reflection (ATR) FTIR analysis. The fraction < 500 μm was density-separated with a ZnCl_2 brine (density 1.7–1.8 g cm^{-3}) to remove mineral particles and the organic matter was destroyed in an enzymatic-oxidative digestion including a second density separation with a ZnCl_2 brine after the purification process (Löder et al., 2017).

Because our samples contained a high amount of black carbon particles (verified by FTIR) after the purification and ZnCl_2 density separation, we performed an additional density separation with a CaCl_2 brine (1.23–1.40 g cm^{-3}) in small glass beakers (200 ml). During this separation process, the particles in the sample separated into two layers, namely a less dense layer free of black carbon particles at the surface and a layer enriched with black carbon at the bottom. After the separation process has finished, we froze the samples at -80°C and separated the frozen layers, namely top and bottom layer, into two glass beakers. Subsequently, we filtered them on stainless-steel filters (mesh size 5 μm) and took representative aliquots from each layer (procedure described in the Supplementary Information). We used 1/8–1/64 of the sample material from the surface layer, and from the bottom layer 1/74–1/249 respectively. These aliquots were filtered with an in-house made glass funnel with 10 mm diameter on aluminium oxide filters (mesh size 0.2 μm , 25 mm diameter Anodisc, Whatman GE Healthcare, 2–9 filters per sample) for subsequent measurement with micro-Focal Plane Array-based FTIR spectroscopy ($\mu\text{-FPA-FTIR}$) (Löder et al., 2015).

2.6. FTIR spectroscopy

2.6.1. Particles > 500 μm

We analysed every putative microplastic particle > 500 μm with an ATR-FTIR spectrometer (Bruker Alpha FTIR spectrometer with platinum ATR) equipped with a diamond ATR crystal. The measurements were performed in the wave number range from 4000 to 400 cm^{-1} with a resolution of 8 cm^{-1} and an accumulation of 8 scans. We measured the background against the ambient air with the same settings before particle analysis started. All spectra were checked against reference spectra from an in-house developed plastic polymer spectral library (Löder et al., 2017).

2.6.2. Particles < 500 μm

The Anodisc filters with the particles < 500 μm were measured with $\mu\text{-FPA-FTIR}$ microscope (Hyperion 3000, Bruker) connected to a spectrometer (Tensor 27, Bruker). We measured the whole sample filters in transmission mode with a $3.5\times$ IR objective in a wave number range from 3600 to

1250 cm^{-1} with a resolution of 8 cm^{-1} and an accumulation of 32 scans. The background was measured 32 times on the pure Anodisc filter. The focal plane array detector combined with the IR objective results in a spatial resolution of 11.05 μm per pixel. The data was converted to the ENVI file format in the Bruker OPUS Software (version 7.5) imported in the Epina ImageLab software (version 3.47) and the polymer type of each particle identified by a random forest decision classifier software tool for microplastics (BayreuthParticleFinder) (Hufnagl et al., 2022). This classifier can identify 22 different polymers automatically and enables an extremely rapid analysis within 0.5 h per filter. Each automatically identified microplastic particle was manually double-checked against reference spectra according to a four-eye principle by experienced staff for quality assurance. Subsequently, the particle sizes were measured and shapes recorded from the photographs of the Anodisc filters. We used the largest dimension of the particle as its size.

2.6.3. Microplastic size and shape classification

We classified the microplastic particles into eight size classes, namely 11–50 μm , 51–100 μm , 101–150 μm , 151–300 μm , 301–500 μm , 501–1000 μm , 1001–5000 μm and > 5000 μm (Fig. 3). Additionally, we assigned the particles to three shape categories, namely fragments, beads, and fibres (Fig. 4). The shape of less than 1% of microplastic particles remained undetermined due to their small size (e.g., only one pixel in the chemical image) or overlap with other particles. Those particles were recorded as unidentified shape. However, their IR spectra clearly confirmed that they were microplastics.

2.7. Hydrodynamic modelling and analysis of flood frequencies

To determine the frequency of flooding of the three transects and thus possible input of microplastics, we used the Rhine water levels between 1950 and 2020 from the gauging station in Cologne “Kölner Pegel”. The station is situated at the Rhine kilometre 688 (16.7 km upstream of the sampling site) and the data were provided by the Federal Waterways and Shipping Agency (WSV) and the German Federal Institute of Hydrology (BfG). To use the data, we corrected the water level data based on the decreasing elevation gradient in northern direction from gauging station to our sampling site (3.09 m bed level difference). To avoid confusions, in this research all water levels reference to the Amsterdam Ordinance level (NAP) and are given in meters above sea level (m a.s.l.). We used the dataset from Geobasis NRW (©Land NRW, dl-de/by-2-0, <https://www.govdata.de/dl-de/zero-2-0>, accessed 2021-07-24) for the digital elevation model (DEM) at our sampling site.

We simulated the flooding with the MIKE 21 software (DHI, Hørsholm Denmark), a model for the simulation of a 2D free-surface flow. In the model, the rising water levels of the Rhine flooded the DEM of our study site. The goal of the flood simulation was to determine the respective threshold of the Rhine level at which each of the transects is flooded. In our simulations, we excluded the impact of wind turbulences, infiltration into the soil, interactions with groundwater and the riverbed.

These thresholds were used for the analysis of frequency of floods in each transect. We determined the number of flooding days between January 1950 and April 2020, defined as days at which the Rhine exceeded the threshold levels in the time series of water levels provided by the “Kölner Pegel”. Additionally, we calculated the frequency and duration of flooding events. An event is defined as consecutive days at which the Rhine level exceeded the respective threshold. The analysis was done in R (R Core Team, 2021) using the packages tidyverse (Wickham et al., 2019) and lubridate (Grolemund and Wickham, 2011).

3. Results and discussion

3.1. Soil characteristics of the transects

Erosion and deposition processes within floodplains influence the development of the soil (Supplementary Fig. S6) (Asselman and

Middelkoop, 1995). Accordingly, we found typical floodplain soils, so-called fluvisols at our study site. In the riverside transect T1, the fluvisol was young and shallow (Supplementary Fig. S2) because the flooding periodically interrupts the soil development (Graf-Rosenfellner et al., 2016). In T2 and T3, we found deeper soils with horizons which are typical for the pedogenesis (i.e., soil development) of fluvisols located farther landwards (Supplementary Figs. S3 and S4).

All samples which we analysed for microplastic came from the humic topsoil, labelled Ah, and the underlying weathered horizon, denoted Bw (Ah and Bw are standard denominations for soil horizons, cf. Supplementary Information). These horizons reflect the sedimentation and erosion dynamics in the floodplain in their texture (i.e., proportions of clay, silt, and sand) (Graf-Rosenfellner et al., 2016). We found the largest sand content (up to 70%) and intercalated layers of sand within the first 20 cm of soil at the riverside in T1 (Supplementary Fig. S2). The deposition of coarse sediments indicates a high flow velocity, which can hold fine-grained particles in suspension. The larger the sand content, the larger the proportion of macropores in the soil and consequently also the saturated hydraulic conductivity, i.e., the ability of the saturated soil to conduct water. The proportion of sand declined to roughly 45% on embankment T2 and further to approximately 20% in the depression T3 (Fig. 2). In contrast, the proportions of clay and silt increased from T1 to T3 and indicate slower flow velocities farther landwards and more favourable sedimentation conditions behind the embankment T2 and in the depression T3. According to FAO's categories (FAO, 2006), the abundance of fine roots (root diameter < 2 mm) could be classified as "common" (second most frequent category with 50–200 roots) in T2 and T3. The abundance of biological activity is categorized as "common" (second most frequent category) with a high share of "earthworm channels". In contrast, in T1, we noticed "few" (20–50) fine roots and "few" signs of biological activity only.

3.2. Detected microplastics in the floodplain soil

3.2.1. Abundance of particles and polymers

We are aware that for our study we analysed two pooled depth-specific samples per transect only. However, we aimed at producing representative samples for each of the three transects and ensured this by our sampling design, sample pooling and homogenization. Furthermore, the processing of comparatively large samples (minimum of 250 g), the analysis of the whole surface of the sample filter via μ -FPA-FTIR and a maximum control of contamination ensured robust data. We detected microplastics in all samples, and our results indicate that a large amount of microplastic particles was deposited in the floodplain we studied. After subtraction of the blank values (in total 21 particles made of 13 polymers in the size range of 11–1000 μm in the three blanks), the number of microplastics within the

transects of the floodplain varied between 25,502–51,119 microplastics kg^{-1} in 0–5 cm depth and 25,616–84,824 microplastics kg^{-1} in 5–20 cm depth, respectively.

The lack of standardization in microplastic analysis seriously hampers the comparability between studies (Möller et al., 2020) because published research differs in sampling, sample preparation, and analysis. Nevertheless, we compare our data with the available literature on microplastic abundance and simultaneously point out the size ranges reported there and our results in the comparable size range. Klein et al. (2015), for example, found 228–3763 microplastics kg^{-1} at the Rhine shore (their size range: 63–5000 μm ; our results in the range 51–5000 μm : 20,844–75,084 microplastics kg^{-1}). Weber and Opp (2020) found up to 8.57 microplastics kg^{-1} in floodplain soils of the Lahn (Hesse, Germany), a tributary of the Rhine (their size range: 2000–5000 μm ; our results in the range 1001–5000 μm : 82–1044 microplastics kg^{-1}). In a follow-up study, Weber et al. (2021) reported on the average 3.33 microplastic particles kg^{-1} in the topsoils of several Lahn floodplains (their size range: 500–5000 μm ; our results in the range 501–5000 μm : 955–3540 microplastics kg^{-1}). However, the data of Weber et al. are based on 158 meso- and microplastic particles only (Weber et al., 2021). In another floodplain study at the Inde river (North Rhine-Westphalia, Germany), Lechthaler et al. (2021) identified 176 putative microplastics kg^{-1} by microscopy (their size range: 500–5000 μm). However, only 28 out of 88 tested particles were finally identified as microplastics by FTIR. In Swiss floodplains, Scheurer and Bigalke (2018) reported up to 598 microplastics kg^{-1} (their size range: 125–5000 μm ; our results in the range 150–5000 μm : 7619–21,048 microplastics kg^{-1}). Furthermore, Lenaker et al. (2019) reported up to 6229 microplastics kg^{-1} (size range: 125–5000 μm) in the sediments at the Menomonee river (USA). Although the published results differ widely both in the analysed size ranges and the numbers of detected microplastics, the amount of microplastic which we found at our study site is consistently larger, even when excluding the size ranges from our data that are not covered by the other publications. In addition, our analysis covered a size range from 11 to 5000 μm , and we provide a more comprehensive inventory of microplastics than reported in the available literature. The large numbers of microplastics that we found have to be considered as an alarming sign of microplastic contamination.

The investigated floodplain soil samples contained microplastics and macroplastics made of 16 different polymer types, namely in alphabetic order acrylonitrile butadiene styrene (ABS), ethylene vinyl acetate (EVAc), polyamide (PA), polyacrylonitrile (PAN), polybutylene terephthalate (PBT), polycarbonate (PC), polyethylene (PE), polyethylene terephthalate (PET), polylactic acid (PLA), polymethyl methacrylate (PMMA), polyoxymethylene (POM), polypropylene (PP), polystyrene (PS), polyurethane (PU), polyvinyl chloride (PVC) and silicone. In detail, we found 12

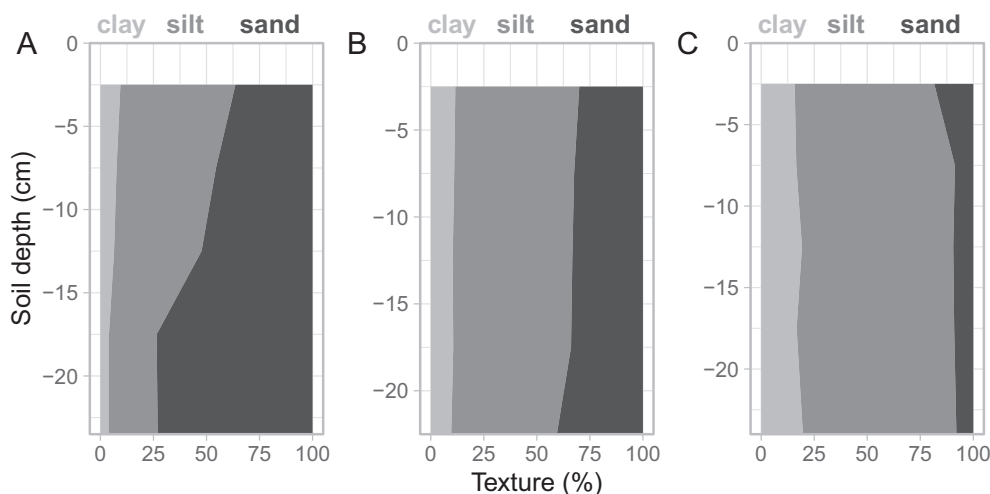


Fig. 2. Soil texture (percentage of clay, silt, and sand) in the soil profiles of transects T1 (A), T2 (B) and T3 (C).

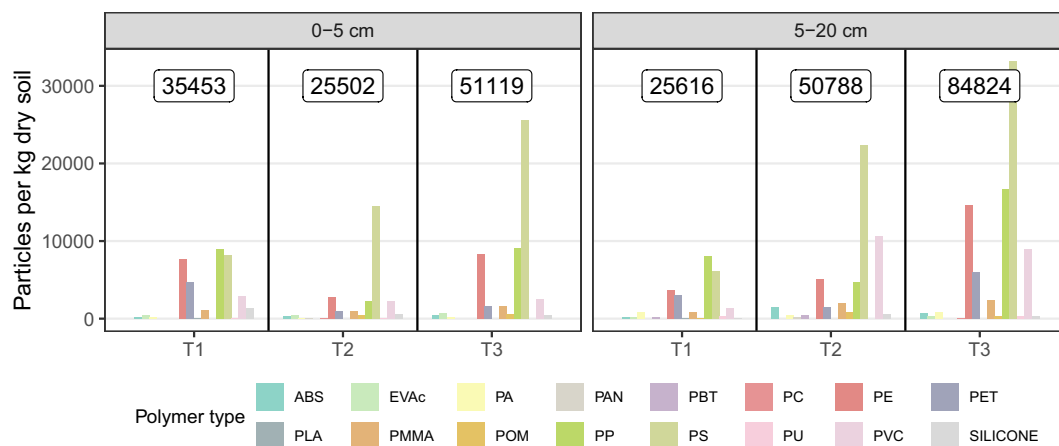


Fig. 3. Distribution of microplastic particles by polymer type in different soil depths (0–5 and 5–20 cm) and transects. T1 (36.6 m a.s.l.), T2 (38.18 m a.s.l.) and T3 (37.65 m a.s.l.) indicate the transects 1, 2 and 3, respectively. The distance from the Rhine increases from T1 to T3. Numbers on top of each transect show total particle numbers.

polymer types in 0–5 cm and 14 polymer types in 5–20 cm soil depths in the riverside transect T1 (Fig. 3). On the embankment T2, we found 15 polymer types in 0–5 cm and 12 polymer types in 5–20 cm soil depth. Finally, in the depression T3, we detected 11 polymer types in 0–5 cm and 13 polymer types in 5–20 cm soil depth. The distribution of polymers was unrelated to their densities. The most abundant microplastics in the floodplain (0–5 cm and 5–20 cm) consisted of PS (40.3%), PP (18.2%) and PE (15.4%) (Fig. 3). They are also among the six most demanded polymers in Europe (PE: 29.8%, PP: 19.4%, and PS: 6.2%) and utilized mostly as single-use products (Plastics Europe, 2020). In other studies in floodplains, Scheurer and Bigalke (2018) identified seven, Lechthaler et al. (2021) six and Weber et al. (2021) 12 different polymers, respectively. However, they found mainly microplastics made of PE. Weber and Opp (2020) reported five different polymers and characterized most of their particles as strongly degraded, without further polymer identification. We have to emphasize that the number of reported polymers depends on the one hand on the sources of microplastics in the respective study areas and on the other hand on the applied methods for identification.

3.2.2. Particle sizes and shapes

Macroplastic particles (> 5000 μm) were sparse and present in five of six samples only. In all transects, we found microplastic particles (up to 75% share) in the size range of 11–150 μm. In contrast, microplastic particles in the size range of 150–5000 μm accounted for up to 25% of particles only. In general, the number of microplastic particles increased with decreasing particle size, which is in accordance with other microplastic studies in floodplain soils and river sediments (Klein et al., 2015; Scheurer and Bigalke, 2018; Weber and Opp, 2020; Lechthaler et al., 2021; Lenaker et al., 2019). One exception to this ‘increasing number with decreasing size’ relationship was the size range between 11 and 50 μm. There, we found fewer particles than in the range of 101–150 μm. This could be due to a stronger vertical displacement of smaller particles (i.e., beyond the analysed depth of 20 cm).

Most particles present in our samples were fragments, beads and only a few were fibres (Fig. 4, Supplementary Figs. S7 and S8). Fragments and films seem to dominate in floodplain soils of the Lahn and Inde rivers (Lechthaler et al., 2021; Weber and Opp, 2020; Weber et al., 2021).

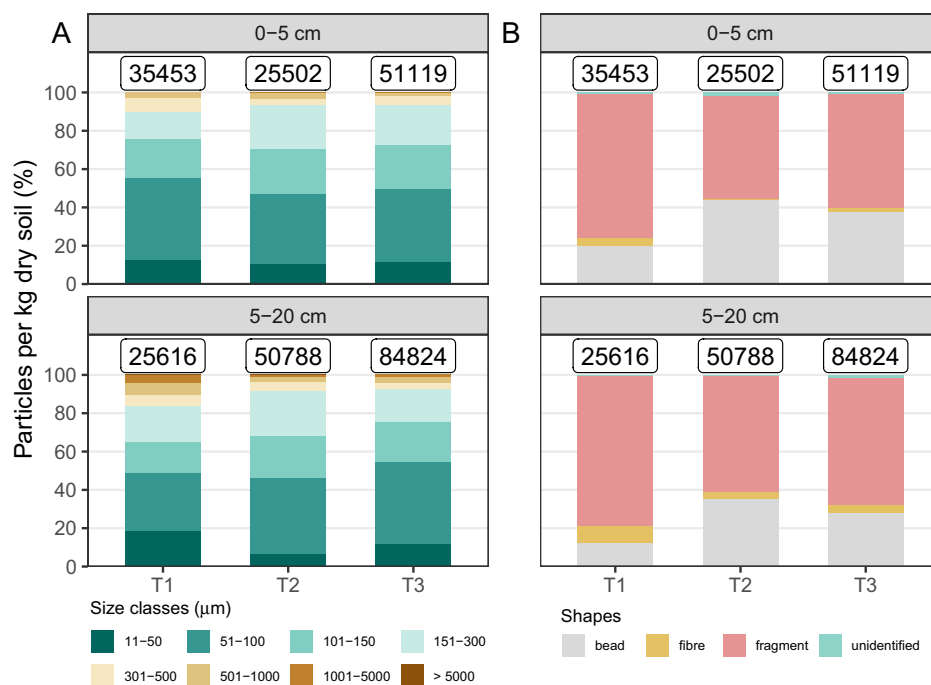


Fig. 4. A: Size distribution and B: Shape distribution of microplastic particles by soil depth. T1 (36.6 m a.s.l.), T2 (38.18 m a.s.l.) and T3 (37.65 m a.s.l.) indicate the transects 1, 2 and 3, respectively. The distance from the Rhine increases from T1 to T3. Numbers on top of each bar show total particle numbers.

However, Christensen et al. (2020) found mainly fragments (80%), but no films in three river floodplains in Virginia (USA). In our study, 65% of all detected particles were fragments, two times more than reported by Weber and Opp (2020) (32%), Weber et al. (2021) (32%) or Lechthaler et al. (2021) (30%). They could have entered the floodplain soil by atmospheric and fluvial depositions, or developed locally by fragmentation of larger plastic particles (Kernchen et al., 2021; Hurley et al., 2018; Chamas et al., 2020). None of the particles we analysed were films.

We found a considerable share of beads in T2 and T3 (up to roughly 40% in T2, 0–5 cm depth, Fig. 4). Most of the beads were made of PS (Supplementary Fig. S7), and approximately 70% were smaller than 100 μm (Supplementary Fig. S8). The occurrence of beads in the studied floodplain could be related to the detection of beads in the Rhine's surface water. In particular, Mani et al. (2019a) found 0.5 spheres m^{-3} (analysed size range: 300–> 5000 μm) in the surface water at the Rhine kilometre 705, close to our sampling site. Mani et al. (2019a) reported that PS beads were usually used as ion exchanger and attributed their sources to various effluents into the Rhine such as the nearby wastewater treatment plants and diverse polymer industries. In contrast, Weber and Opp (2020) and Weber et al. (2021) found no beads in floodplains of the Lahn river. Lechthaler et al. (2021) detected a small share of beads of 8.9% only in the Inde catchment. However, the sampling areas in those studies were surrounded by different land-uses in the respective catchments, and microplastic sources might therefore differ compared to our study area. Additionally, their studies focused on macroplastic and coarse microplastics only (size range: 2000–> 5000 μm in Weber and Opp (2020), 500–> 5000 μm in Weber et al. (2021); Lechthaler et al. (2021), respectively) and thus, small beads could have remained undetected.

We found the largest share of fibres (9%) in riverside transect T1 in 5–20 cm soil depth (Fig. 4). They were made of PET, PP, PBT, PE, PVC and PA. However, fibres accounted for 3.7% of all detected microplastics only. Similarly, the number of fibres in the sediments of the Elbe, the Rhine, and the Main reported in the literature were small (Laermanns et al., 2021; Klein et al., 2015). Weber and Opp (2020) and Weber et al. (2021) found up to 19–24.2% fibres in the floodplain soils of the Lahn and Lechthaler et al. (2021) detected 8.9% fibres in the Inde floodplains. These findings accord well with our results and indicate that fibres are less frequent than fragments in floodplain soils. However, we are aware that fibres with a small diameter are at the lower detection limit (10 μm) of $\mu\text{-FPA-FTIR}$ used in our study and could thus be underestimated (Pripke et al., 2019). Analogous to the identification of polymers and particle numbers, the applied method also affects the characterization of particle shapes.

3.2.3. Possible sources of microplastics in floodplain soils

The floodplain we studied is isolated from potential microplastic entry pathways from built-up areas by a dike. Therefore, inputs of microplastics are limited to fluvial and aeolian deposition and littering. In general, floodplains could receive microplastics from different sources during flooding (Woodward et al., 2021). Our study site is located close to many potential microplastic point sources such as wastewater treatment plants and several large plants of plastic producing chemical industry that have effluents into the Rhine (Supplementary Fig. S9) (Mintinig et al., 2017; Lechner and Ramler, 2015). In addition to those point-sources, diffuse sources such as atmospheric deposition, littering and runoff from agricultural, urban and industrial areas might contribute microplastics to the Rhine and subsequently to the study site during flooding (Bergmann et al., 2019; Dris et al., 2015; Kernchen et al., 2021; Rehm et al., 2021). One has to keep in mind that the Rhine traversed roughly 705 km before reaching our study site. Along its long course, it may have collected microplastics from a large variety of different sources, including inputs from its tributaries (Klein et al., 2015; Laermanns et al., 2021). Therefore, tracing the origin of riverine microplastics at our study site is hardly possible. Additionally, during flooding, microplastic particles can be re-mobilized from riverbed sediments. Hurley et al. (2018) and Woodward et al. (2021) studied several

urban, suburban and rural river catchments in northwest England and reported that up to 70% of microplastics stored in riverbed sediments could be flushed during large flood events. This implicates that additionally to microplastics present in the water during normal flow conditions, the microplastic load in the river could increase during high water by microplastics re-suspended from the riverbed sediment. That is precisely the point of time when high numbers of microplastics may enter floodplains by flooding.

The atmospheric deposition of microplastics is also a potential source at our study site. Kernchen et al. (2021), for example, reported a mean daily deposition of around 100 fibrous and fragment-shaped microplastic particles per m^2 in the Weser catchment and calculated an annual deposition of 232 tons of microplastics for the whole catchment area. Obviously, particles in atmospheric deposition were small, and Kernchen et al. (2021) reported that 90% of the microplastics were in a size range below 100 μm and 64% even below 50 μm . In contrast, we found a different size distribution of microplastics, namely roughly 50% below 100 μm and only roughly 13% below 50 μm , respectively. This indicates that the aeolian deposition of microplastics is probably a minor input pathway for the floodplain site we investigated.

3.3. Influence of flood events and local topography on distribution of microplastics

Our flood simulations (Fig. 5) show that the Rhine floods the transect T1 (modelled threshold 36.56 m a.s.l.) at the shore first. Subsequently, if the water level rises, T3 (modelled threshold 37.61 m a.s.l.) is flooded from the Northwest by the Rhine water flowing into the depression. And finally, the embankment T2 (modelled threshold 38.14 m a.s.l.) is flooded by the highest Rhine level. The studied floodplain has a connection to the Rhine in the Northeast (Fig. 5A). Therefore, all transects are flooded at roughly the same Rhine level as their elevation. In the period between 1950 and 2020, T1 was flooded most often (on average 47.88 days per year) and the flood events lasted longer (Fig. 6 and Supplementary Fig. S10). In contrast, T3 and T2 were flooded considerably less frequently (T3: on average 20.28 days per year; T2: on average 12.71 days per year) (Fig. 6 and Supplementary Fig. S10) and the flood events were shorter.

The distribution of microplastics in the studied transects could be the result of the interplay of flooding, local topography and vegetation cover and thus of the dynamics of erosion and deposition processes. Obviously, flooding also affects the vegetation cover, which in turn can prevent erosion, and the soil formation (Graf-Rosenfellner et al., 2016). The transect T1 is the most affected by erosion processes during flood events due to the longer inundation period and a faster, and thus more erosive, flow directly at the riverside (c.f. the erosion break-off edge in Supplementary Fig. S6) (Magilligan et al., 2015). Accordingly, it has a young and shallow soil with a coarse soil texture (Supplementary Fig. S2) and a patchy grass vegetation. Therefore, although this transect is flooded most frequently and the flooding events last longer than in other transects, we found the smallest total number of microplastics there (Fig. 6). Landwards, the number of microplastics increased from T2 to T3, although the flooding frequency decreased. This finding clearly shows that the influence of flooding frequency is modulated by topography (Asselman and Middelkoop, 1995). Transect 3 has the highest overall microplastic concentration. It is located the farthest from the Rhine in a depression and has the deepest soil with a dense grass cover preventing erosion. When the water level decreases with the falling flood, the depression could be cut off from the Rhine and become a sink for sediments and microplastics, which seems to lead to an accumulation of particles over time. Similarly to T3, T2 has a well-developed soil profile and a dense grass cover which prevents erosion (Graf-Rosenfellner et al., 2016). However, T2 is situated on an embankment. This transect has the largest altitude and thus the lowest flooding frequency and duration. However, although we found fewer particles in T2 than in T1 in 0–5 cm soil, the overall number of particles is larger and microplastics seem to accumulate in the deeper soil similarly to T3.

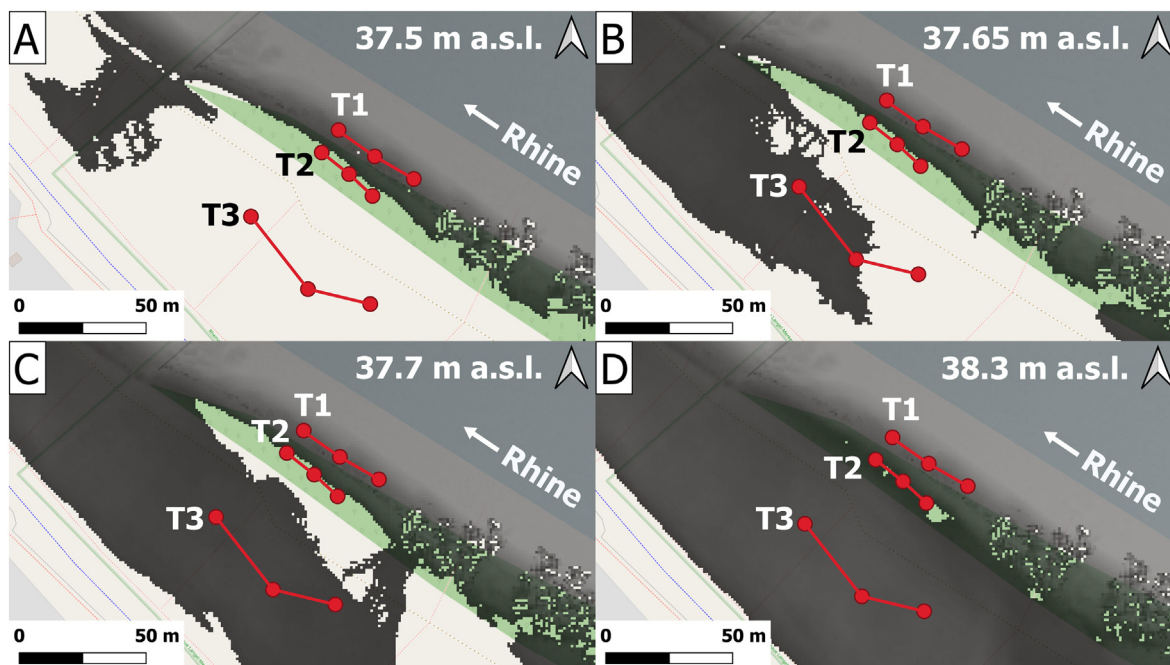


Fig. 5. Flood scenarios at the study site Langel-Merkenich in Cologne, Germany. A: Rhine level 37.5 m a.s.l., T1 is flooded, and Rhine water starts to flood the alluvial floodplain. B: Rhine level 37.65 m a.s.l., flooding of T3. C: Rhine level 37.7 m a.s.l. T1 and T3 are flooded, the Rhine floods the site also from the South. D: Rhine level 38.3 m a.s.l. all transects are flooded. Background by OpenStreetMap 2021, <https://www.openstreetmap.org/> licensed under the Open Data Commons Open Database License (ODbL) <https://opendatacommons.org/licenses/odbl/>.

3.4. Vertical distribution of microplastics in the soil

The interplay between flooding frequency, local topography and vegetation cover also affects the vertical distribution of microplastics in the studied transects. Additionally, soil texture and bioturbation can affect the vertical migration of microplastics. Once deposited on the soil surface in

the floodplain, microplastics might migrate vertically into deeper soil with infiltrating flood or precipitation water, by preferential flow due to soil cracks and macropores (e.g., along plant roots or in earthworm burrows) or be transported by bioturbation (O'Connor et al., 2019; Rillig et al., 2017; Mohanty et al., 2015; Frei et al., 2019). Similarly, Weber and Opp (2020) found mesoplastic and coarse microplastics in floodplain soils

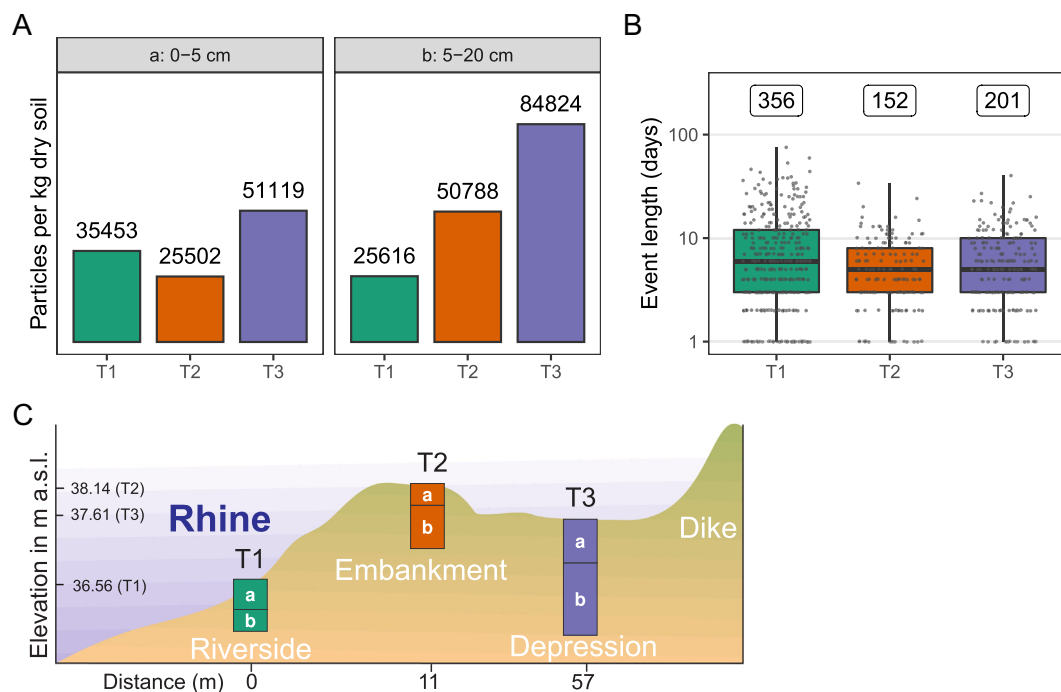


Fig. 6. A: Number of particles in different depths and transects. B: Duration of flooding events between January 1950 and April 2020. Numbers above the boxes show the total numbers of events. Note the logarithmic scale of the y axis. C: Scheme of the location of transects in the studied floodplain. The bar plots show the number of detected microplastics. The labels a and b refer to subfigure A. The elevations indicate the modelled flooding thresholds. T1, T2 and T3 indicate the transects 1, 2 and 3, respectively.

deeper than predicted by sedimentation rates. They explained this by the interplay of sedimentation and vertical displacement. Therefore, care should be taken when using microplastics as markers for sedimentation time as suggested by e.g., [Lechthaler et al. \(2021\)](#). For our study site, sedimentation rates of the Rhine are unavailable, and we cannot address this issue here.

To investigate patterns of migration, we sampled two depth intervals, namely the soil surface (0–5 cm) and the deeper soil (5–20 cm). The distribution of microplastics between the two depths shows different patterns of vertical migration of microplastics in the investigated floodplain. In T2 and T3, the transects which are located farther from the river, we consistently found more microplastics in the respective 5–20 cm depth than in the upper 0–5 cm soil ([Figs. 3 and 6](#)). We suppose that microplastic particles accumulated in deeper soil due to vertical transport from the surface to the deeper soil. Because the permanent grass cover in T2 and T3 protects the soil surface from erosion, sediments, and microplastic particles could be re-mobilized less easily by wind, runoff or the next flooding event once deposited at the soil surface. In contrast, in the riverside T1, we found a higher microplastic abundance in the upper 0–5 cm than in the deeper soil and the overall lowest concentration in 5–20 cm compared to the other transects. There, the vegetation cover is sparser and the interplay between deposition and erosion at the soil surface seems to be more dynamic ([Sections 3.1 and 3.3](#)).

We further compared the distribution of microplastic particle sizes between soil depths, and plotted the cumulative proportion of microplastic particles over the eight size classes ([Fig. 7B](#)). The distributions are similar in T2 and T3 and differ from T1. In the riverside transect T1 in the soil depth 5–20 cm, the proportion of small microplastics (size: 11–50 μm) is larger and simultaneously the proportion of particles in the size range 151–1000 μm is smaller. This coincides with the increasing sand content within the first 20 cm in the soil profile at T1, and could therefore indicate a translocation of smaller microplastics via macropore flow ([Section 3.1](#)). Due to the larger pore sizes in the soil and larger saturated hydraulic conductivity in T1, microplastics might infiltrate directly into the water-saturated sediment during flooding. [Frei et al. \(2019\)](#), for example, reported an infiltration of pore-scale microplastics (20–50 μm) into the

hyporheic zone of river sediments. Similarly, [Boos et al. \(2021\)](#) monitored the infiltration of smaller particles (1–10 μm) across the streambed interface directly. However, it remains unclear whether microplastics larger than 10 μm migrate vertically in soils more than a few centimetres deep via soil pores only. [Yu and Flury \(2021\)](#), for example, mentioned an exclusion of microplastics particles > 10 μm in soil based on their size and shape ([Yu and Flury, 2021](#)). In contrast, [O'Connor et al. \(2019\)](#) measured vertical infiltration of relatively large microplastics (21–535 μm) in sandy sediment columns.

In addition to translocation in pores, the vertical transport of microplastics could be enhanced by bioturbation. As mentioned in [Section 3.1](#), we observed more earthworm burrows in T2 and T3 compared to T1. Thus, we suggest that bioturbation might be an important factor for transport of microplastics to deeper soil in T2 and T3 and co-responsible for the accumulation of particles. However, the abundance of microplastics at our study site reflects the overall dynamics of transport processes, and it remains impossible to disentangle the contribution of bioturbation and purely physical transport in soil pores.

4. Conclusions

Floodplains are important ecosystems at the interface between terrestrial and aquatic environments. We report the analysis of microplastics and macroplastics in three transects in a floodplain in the size range accessible by $\mu\text{-FPA-FTIR}$ and ATR-FTIR , namely 11–> 5000 μm . Our results are based on pooled samples to ensure robustness. However, because the number of samples is limited, our conclusions must be backed up by more comparable studies in the future. In addition to the chemical analysis of particles, we provide an explanation for their distribution and accumulation by hydrological modelling, time series analysis and analysis of soil properties. This interdisciplinary approach indicates that floodplains may act as a sink and are dynamic systems concerning microplastic contamination. Our findings suggest that local topography and resulting flooding patterns are responsible for the amount of microplastics found at the respective transect and for their spatial distribution. Furthermore, vegetation cover, soil properties and earthworm activity seem to affect the migration and accumulation of microplastics in the deeper soil. Today, we ignore how long microplastics can be retained in a floodplain. To understand the role of floodplains in the plastic cycle, we must consider process-informed sampling based on flooding frequency, topography, and soil cover in future research. This information is essential for the evaluation of the representativeness of data on microplastics in floodplains, for locating potential microplastic accumulation sites and hotspots and to identify areas of increased bioavailability of microplastics for proper ecological risk assessment.

Funding sources

This study was funded by the Deutsche Forschungsgemeinschaft (DFG, German Research Foundation) – SFB 1357 – 391977956.

Data availability

Data on microplastics and soil properties and code to analyse them can be found on Zenodo (DOI: [10.5281/zenodo.6487653](https://doi.org/10.5281/zenodo.6487653)). Raw spectra of microplastic particles can be obtained from the authors upon reasonable request. The time series of the Rhine water levels was requested and obtained from the Municipal Sewage Works of the City of Cologne (Stadtentwässerungsbetriebe Köln, AöR) and is courtesy of the Federal Waterways and Shipping Agency (WSV) and the German Federal Institute of Hydrology (BfG). The data can be requested at datenstelle-M1@bafg.de.

CRediT authorship contribution statement

Conceptualization and Methodology: CB, MGJL, HL and MR; Software and Data Curation: CB, MR and MGJL; Formal analysis: MR, MGJL, LK,

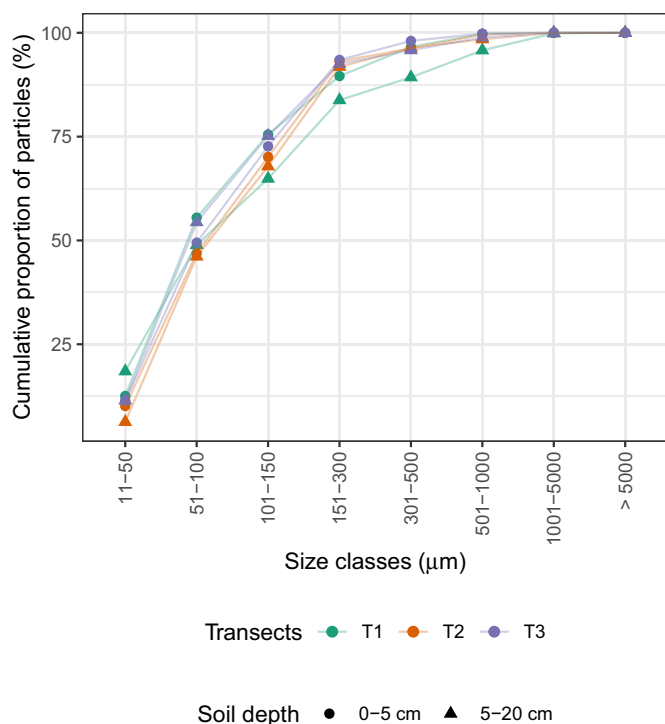


Fig. 7. Cumulative distribution of microplastic sizes by soil depth and transect. T1, T2 and T3 indicate the transects 1, 2 and 3, respectively.

CP and CB; Investigation: MR, HL and JNM; Visualization: CB, MR, HL and LK; Writing – Original Draft: MR, HL, MGJL, CL and CB; Writing – Review and Editing: all authors; Supervision: CB, MGJL, CL and HL; Project administration and Funding acquisition: CB, MGJL and CL.

Declaration of competing interest

The authors declare that they have no known competing financial interests or personal relationships that could have appeared to influence the work reported in this paper.

Acknowledgements

The authors thank Ursula Wilczek, Heghnar Martirosyan and student assistants for their help in measuring the μ -FPA-FTIR and ATR-FTIR spectra. Julia Horn analysed soil physico-chemical parameters. Florian Steininger, Katharina Müller and Dirk Hoffmeister have substantially supported the field work. DHI has provided the software MIKE21 for hydrodynamic modelling for Lukas Kienzler's bachelor thesis. This study was funded by the Deutsche Forschungsgemeinschaft (DFG, German Research Foundation) – SFB 1357 – 391977956.

Appendix A. Supplementary data

Supplementary data to this article can be found online at <https://doi.org/10.1016/j.scitotenv.2022.155141>.

References

- Asselman, N.E.M., Middelkoop, H., 1995. Floodplain sedimentation: quantities, patterns and processes. *Earth Surf. Process. Landf.* 20, 481–499. <https://doi.org/10.1002/esp.3290200602>.
- Belz, J.U., 2010. Das abflussregime des rheins und seiner nebenflüsse im 20. Jahrhundert – analyse, veränderungen, trends. *Hydrol. Wasserbewirtsch.* 54, 18.
- Bergmann, M., Mützel, S., Primpke, S., Tekman, M.B., Trachsel, J., Gerdts, G., 2019. White and wonderful? Microplastics prevail in snow from the alps to the arctic. *Sci. Adv.* 5, eaax1157. <https://doi.org/10.1126/sciadv.aax1157>.
- Bläsing, M., Amelung, W., 2018. Plastics in soil: analytical methods and possible sources. *Sci. Total Environ.* 612, 422–435. <https://doi.org/10.1016/j.scitotenv.2017.08.086>.
- Blott, S.J., Pye, K., 2001. GRADISTAT: a grain size distribution and statistics package for the analysis of unconsolidated sediments. *Earth Surf. Process. Landf.* 26, 1237–1248. <https://doi.org/10.1002/esp.261>.
- Boos, J.P., Gilfedder, B.S., Frei, S., 2021. Tracking microplastics across the streambed Interface: using laser-induced-fluorescence to quantitatively analyze microplastic transport in an experimental flume. *Water Resour. Res.* 57, e2021WR031064. <https://doi.org/10.1029/2021WR031064>.
- Chamas, A., Moon, H., Zheng, J., Qiu, Y., Tabassum, T., Jang, J.H., Abu-Omar, M., Scott, S.L., Suh, S., 2020. Degradation rates of plastics in the environment. *ACS Sustain. Chem. Eng.* 8, 3494–3511. <https://doi.org/10.1021/acssuschemeng.9b06635>.
- Christensen, N.D., Wisinger, C.E., Maynard, L.A., Chauhan, N., Schubert, J.T., Czuba, J.A., Barone, J.R., 2020. Transport and characterization of microplastics in inland waterways. *J. Water Process Eng.* 38, 101640. <https://doi.org/10.1016/j.jwpe.2020.101640>.
- Ding, L., Mao, R.F., Guo, X., Yang, X., Zhang, Q., Yang, C., 2019. Microplastics in surface waters and sediments of the Wei river, in the northwest of China. *Sci. Total Environ.* 667, 427–434. <https://doi.org/10.1016/j.scitotenv.2019.02.332>.
- Dris, R., Gasperi, J., Rocher, V., Saad, M., Renault, N., Tassin, B., 2015. Microplastic contamination in an urban area: a case study in greater Paris. *Environ. Chem.* 12, 592. <https://doi.org/10.1071/EN14167>.
- Dris, R., Imhof, H.K., Löder, M.G.J., Gasperi, J., Laforsch, C., Tassin, B., 2018. Chapter 3 - microplastic contamination in freshwater systems: methodological challenges, occurrence and sources. In: Zeng, E.Y. (Ed.), *Microplastic Contamination in Aquatic Environments*. Elsevier, pp. 51–93. <https://doi.org/10.1016/B978-0-12-813747-5.00003-5>.
- Dris, R., Agarwal, S., Laforsch, C., 2020. Plastics: from a success story to an environmental problem and a global challenge. *Global Chall.* 4, 2000026. <https://doi.org/10.1002/gch2.202000026>.
- FAO, 2006. *Guidelines for Soil Description*. 4th ed. Food and Agriculture Organization of the United Nations, Rome.
- FAO, 2014. *World Reference Base for Soil Resources 2014: International Soil Classification System for Naming Soils and Creating Legends for Soil Maps*. FAO, Rome.
- Folk, R.L., Ward, W.C., 1957. Brazos River Bar: a study in the significance of grain size parameters. *J. Sediment. Petrol.* 27, 3–26.
- Frei, S., Piehl, S., Gilfedder, B.S., Löder, M.G.J., Krutzke, J., Wilhelm, L., Laforsch, C., 2019. Occurrence of microplastics in the hyporheic zone of rivers. *Sci. Rep.* 9, 15256. <https://doi.org/10.1038/s41598-019-51741-5>.
- Geyer, R., Jambeck, J.R., Law, K.L., 2017. Production, use, and fate of all plastics ever made. *Sci. Adv.* 3, e1700782. <https://doi.org/10.1126/sciadv.1700782>.
- Graf-Rosenfellner, M., Cierjacks, A., Kleinschmit, B., Lang, F., 2016. Soil formation and its implications for stabilization of soil organic matter in the riparian zone. *Catena* 139, 9–18. <https://doi.org/10.1016/j.catena.2015.11.010>.
- Grolemund, G., Wickham, H., 2011. Dates and times made easy with lubridate. *URLJ. Stat. Softw.* 40, 1–25. <https://www.jstatsoft.org/v40/i03/>.
- Heß, M., Diehl, P., Mayer, J., Rahm, H., Reifenhäuser, W., Stark, J., Schwaiger, J., 2018. *Mikroplastik in Binnengewässern Süd- und Westdeutschlands. Teil 1: Kunststoffpartikel in der oberflächennahen Wasserphase*. Technical Report. LUBW, LfU, HLNUG, LANUV, LfU RLP.
- Horton, A.A., Dixon, S.J., 2018. Microplastics: an introduction to environmental transport processes. *Wiley Interdiscip. Rev. Water* 5, e1268. <https://doi.org/10.1002/wat2.1268>.
- Horton, A.A., Walton, A., Spurgeon, D.J., Lahive, E., Svendsen, C., 2017. Microplastics in freshwater and terrestrial environments: evaluating the current understanding to identify the knowledge gaps and future research priorities. *Sci. Total Environ.* 586, 127–141. <https://doi.org/10.1016/j.scitotenv.2017.01.190>.
- Hufnagl, B., Stibi, M., Martirosyan, H., Wilczek, U., Möller, J.N., Löder, M.G.J., Laforsch, C., Löhninger, H., 2022. Computer-assisted analysis of microplastics in environmental samples based on μ FTIR imaging in combination with machine learning. *Environ. Sci. Technol. Lett.* 9, 90–95. <https://doi.org/10.1021/acs.estlett.1c00851>.
- Hurley, R., Woodward, J., Rothwell, J.J., 2018. Microplastic contamination of river beds significantly reduced by catchment-wide flooding. *Nat. Geosci.* 11, 251–257. <https://doi.org/10.1038/s41561-018-0080-1>.
- Imhof, H.K., Sigl, R., Brauer, E., Feyl, S., Giesemann, P., Klink, S., Leupolz, K., Löder, M.G., Lösschel, L.A., Missun, J., Muszynski, S., Ramsperger, A.F., Schrank, I., Speck, S., Steibl, S., Trotter, B., Winter, I., Laforsch, C., 2017. Spatial and temporal variation of macro-, meso- and microplastic abundance on a remote coral island of the Maldives, Indian Ocean. *Mar. Pollut. Bull.* 116, 340–347. <https://doi.org/10.1016/j.marpolbul.2017.01.010>.
- Jambeck, J.R., Geyer, R., Wilcox, C., Siegler, T.R., Perryman, M., Andrady, A., Narayan, R., Law, K.L., 2015. Plastic waste inputs from land into the ocean. *Science* 347, 768–771. <https://doi.org/10.1126/science.1260352>.
- Kernchen, S., Löder, M.G., Fischer, F., Fischer, D., Moses, S.R., Georgi, C., Nölscher, A.C., Held, A., Laforsch, C., 2021. Airborne microplastic concentrations and deposition across the Weser River catchment. *Sci. Total Environ.* 151812. <https://doi.org/10.1016/j.scitotenv.2021.151812>.
- Klein, M., Fischer, E.K., 2019. Microplastic abundance in atmospheric deposition within the metropolitan area of Hamburg, Germany. *Sci. Total Environ.* 685, 96–103. <https://doi.org/10.1016/j.scitotenv.2019.05.405>.
- Klein, S., Worch, E., Knepper, T.P., 2015. Occurrence and spatial distribution of microplastics in river shore sediments of the Rhine-main area in Germany. *Environ. Sci. Technol.* 49, 6070–6076. <https://doi.org/10.1021/acs.est.5b00492>.
- Laermanns, H., Reifferscheid, G., Kruse, J., Dierkes, G., Schaefer, D., Scherer, C., Bogner, C., Stock, F., 2021. Microplastics in water and sediments at the confluence of elbe and mulde rivers in Germany. *Front. Environ. Sci.* 17. <https://doi.org/10.3389/fenvs.2021.794895>.
- Laforsch, C., Ramsperger, A.F.R.M., Mondellini, S., Galloway, T.S., 2021. Microplastics: a novel suite of environmental contaminants but present for decades. In: Reichl, F.X., Schwenk, M. (Eds.), *Regulatory Toxicology*. Springer Berlin Heidelberg, Berlin, Heidelberg, pp. 1–26. https://doi.org/10.1007/978-3-642-36206-4_138-1.
- Lebreton, L.C.M., van der Zwet, J., Damsteeg, J.W., Slat, B., Andrady, A., Reisser, J., 2017. River plastic emissions to the world's oceans. *Nat. Commun.* 8, 15611. <https://doi.org/10.1038/ncomms15611>.
- Lechner, A., Ramler, D., 2015. The discharge of certain amounts of industrial microplastic from a production plant into the river Danube is permitted by the austrian legislation. *Environ. Pollut.* 200. <https://doi.org/10.1016/j.envpol.2015.02.019>.
- Lechthaler, S., Esser, V., Schüttrumpf, H., Stauch, G., 2021. Why analysing microplastics in floodplains matters: application in a sedimentary context. *Environ Sci Process Impacts* 23, 117–131. <https://doi.org/10.1039/D0EM00431F>.
- Lenaker, P.L., Baldwin, A.K., Corsi, S.R., Mason, S.A., Reneau, P.C., Scott, J.W., 2019. Vertical distribution of microplastics in the water column and surficial sediment from the Milwaukee river basin to Lake Michigan. *Environ. Sci. Technol.* 53, 12227–12237. <https://doi.org/10.1021/acs.est.9b03850>.
- Liu, F., Olesen, K.B., Borregaard, A.R., Vollertsen, J., 2019. Microplastics in urban and high-way stormwater retention ponds. *Sci. Total Environ.* 671, 992–1000. <https://doi.org/10.1016/j.scitotenv.2019.03.416>.
- Löder, M.G.J., Kuczera, M., Mintenig, S., Lorenz, C., Gerdts, G., 2015. Focal plane array detector-based micro-fourier-transform infrared imaging for the analysis of microplastics in environmental samples. *Environ. Chem.* 12, 563–581. <https://doi.org/10.1071/EN14205>.
- Löder, M.G.J., Imhof, H.K., Ladehoff, M., Lösschel, L.A., Lorenz, C., Mintenig, S., Piehl, S., Primpke, S., Schrank, I., Laforsch, C., Gerdts, G., 2017. Enzymatic purification of microplastics in environmental samples. *Environ. Sci. Technol.* 51, 14283–14292. <https://doi.org/10.1021/acs.est.7b03055>.
- Maaß, S., Daphi, D., Lehmann, A., Rillig, M.C., 2017. Transport of microplastics by two collembolan species. *Environ. Pollut.* 225, 456–459. <https://doi.org/10.1016/j.envpol.2017.03.009>.
- Magilligan, F., Buraas, E., Renshaw, C., 2015. The efficacy of stream power and flow duration on geomorphic responses to catastrophic flooding. *Geomorphology* 228, 175–188. <https://doi.org/10.1016/j.geomorph.2014.08.016>.
- Mani, T., Hauk, A., Walter, U., Burkhardt-Holm, P., 2016. Microplastics profile along the Rhine river. *Sci. Rep.* 5, 17988. <https://doi.org/10.1038/srep17988>.
- Mani, T., Blarer, P., Storck, F.R., Pittroff, M., Wernicke, T., Burkhardt-Holm, P., 2019. a. Repeated detection of polystyrene microbeads in the lower Rhine river. *Environ. Pollut.* 245, 634–641. <https://doi.org/10.1016/j.envpol.2018.11.036>.
- Mani, T., Primpke, S., Lorenz, C., Gerdts, G., Burkhardt-Holm, P., 2019. b. Microplastic pollution in benthic midstream sediments of the Rhine River. *Environ. Sci. Technol.* 53, 6053–6062. <https://doi.org/10.1021/acs.est.9b01363>.

- Meijer, L.J.J., van Emmerik, T., van der Ent, R., Schmidt, C., Lebreton, L., 2021. More than 1000 rivers account for 80% of global riverine plastic emissions into the ocean. *Sci. Adv.* 7, eaaz5803. <https://doi.org/10.1126/sciadv.aaz5803>.
- Millican, J.M., Agarwal, S., 2021. Plastic pollution: a material problem? *Macromolecules* <https://doi.org/10.1021/acs.macromol.0c02814>.
- Mintenig, S., Int-Veen, I., Löder, M., Primpke, S., Gerdt, G., 2017. Identification of microplastic in effluents of waste water treatment plants using focal plane array-based micro-fourier-transform infrared imaging. *Water Res.* 108, 365–372. <https://doi.org/10.1016/j.watres.2016.11.015>.
- Mohanty, S.K., Bulicek, M.C.D., Metge, D.W., Harvey, R.W., Ryan, J.N., Boehm, A.B., 2015. Mobilization of microspheres from a fractured soil during intermittent infiltration events. *Vadose Zone J.* 14. <https://doi.org/10.2136/vzj2014.05.0058>.
- Möller, J.N., Löder, M.G.J., Laforsch, C., 2020. Finding microplastics in soils: a review of analytical methods. *Environ. Sci. Technol.* 54, 2078–2090. <https://doi.org/10.1021/acs.est.9b04618>.
- Möller, J.N., Heisel, I., Satzger, A., Vizolyi, E.C., Oster, J., Agarwal, S., Laforsch, C., Löder, M.G.J., 2021. Tackling the challenge of extracting microplastics from soils: a protocol to purify soil samples for spectroscopic analysis. *Environ. Toxicol. Chem.* <https://doi.org/10.1002/etc.5024> n/a.
- Munsell Color (Firm), 2010. *Munsell Soil Color Charts: With Genuine Munsell Color Chips. Munsell Color, Grand Rapids, MI.*
- Napper, I.E., Baroth, A., Barrett, A.C., Bhola, S., Chowdhury, G.W., Davies, B.F.R., Duncan, E.M., Kumar, S., Nelms, S.E., Hasan Niloy, M.N., Nishat, B., Maddalene, T., Thompson, R.C., Koldewey, H., 2021. The abundance and characteristics of microplastics in surface water in the transboundary ganges river. *Environ. Pollut.* 116348. <https://doi.org/10.1016/j.envpol.2020.116348>.
- O'Connor, D., Pan, S., Shen, Z., Song, Y., Jin, Y., Wu, W.M., Hou, D., 2019. Microplastics undergo accelerated vertical migration in sand soil due to small size and wet-dry cycles. *Environ. Pollut.* 249, 527–534. <https://doi.org/10.1016/j.envpol.2019.03.092>.
- Plastics Europe, 2020. *Plastics – the facts 2020*. Technical report. URL:Plastics Europe – Association of Plastics Manufacturers. https://plasticseurope.org/wp-content/uploads/2021/09/Plastics_the_facts-WEB-2020_versionJun21_final.pdf.
- Primpke, S., Dias, P.A., Gerdt, G., 2019. Automated identification and quantification of microfibrils and microplastics. *Anal. Methods* 11, 2138–2147. <https://doi.org/10.1039/C9AY00126C>.
- R Core Team, 2021. *R: a language and environment for statistical computing*. URL:R Foundation for Statistical Computing, Vienna, Austria. <https://www.R-project.org/>.
- Rehm, R., Zeyer, T., Schmidt, A., Fiener, P., 2021. Soil erosion as transport pathway of microplastic from agriculture soils to aquatic ecosystems. *Sci. Total Environ.* 795, 148774. <https://doi.org/10.1016/j.scitotenv.2021.148774>.
- Rillig, M.C., Ziersch, L., Hempel, S., 2017. Microplastic transport in soil by earthworms. *Sci. Rep.* 7, 1362. <https://doi.org/10.1038/s41598-017-01594-7>.
- Rochman, C.M., Brookson, C., Bikker, J., Djuric, N., Earn, A., Bucci, K., Athey, S., Huntington, A., McIlwraith, H., Munno, K., Frond, H.D., Kolomijeca, A., Erdle, L., Grbic, J., Bayoumi, M., Borrelle, S.B., Wu, T., Santoro, S., Werbowski, L.M., Zhu, X., Giles, R.K., Hamilton, B.M., Thaysen, C., Kaura, A., Klasios, N., Ead, L., Kim, J., Sherlock, C., Ho, A., Hung, C., 2019. Rethinking microplastics as a diverse contaminant suite. *Environ. Toxicol. Chem.* 38, 703–711. <https://doi.org/10.1002/etc.4371>.
- Roebroek, C.T.J., Harrigan, S., van Emmerik, T.H.M., Baugh, C., Eilander, D., Prudhomme, C., Pappenberger, F., 2021. Plastic in global rivers: are floods making it worse? *Environ. Res. Lett.* 16, 025003. <https://doi.org/10.1088/1748-9326/abd5df>.
- Scherer, C., Weber, A., Stock, F., Vurusic, S., Egerci, H., Kochleus, C., Arendt, N., Foeldi, C., Dierkes, G., Wagner, M., Brennholt, N., Reifferscheid, G., 2020. Comparative assessment of microplastics in water and sediment of a large European river. *Sci. Total Environ.* 738, 139866. <https://doi.org/10.1016/j.scitotenv.2020.139866>.
- Scheurer, M., Bigalke, M., 2018. Microplastics in Swiss floodplain soils. *Environ. Sci. Technol.* 52, 3591–3598. <https://doi.org/10.1021/acs.est.7b06003>.
- Thompson, R.C., Olsen, Y., Mitchell, R.P., Davis, A., Rowland, S.J., John, A.W.G., McGonigle, D., Russell, A.E., 2004. Lost at sea: where is all the plastic? *Science* 304. <https://doi.org/10.1126/science.1094559> 838–838.
- van den Berg, P., Huerta-Lwanga, E., Corradini, F., Geissen, V., 2020. Sewage sludge application as a vehicle for microplastics in eastern Spanish agricultural soils. *Environ. Pollut.* 261, 114198. <https://doi.org/10.1016/j.envpol.2020.114198>.
- Waldschläger, K., Schüttrumpf, H., 2019. Erosion behavior of different microplastic particles in comparison to natural sediments. *Environ. Sci. Technol.* 53, 13219–13227. <https://doi.org/10.1021/acs.est.9b05394>.
- Weber, C.J., Opp, C., 2020. Spatial patterns of mesoplastics and coarse microplastics in floodplain soils as resulting from land use and fluvial processes. *Environ. Pollut.* 267, 115390. <https://doi.org/10.1016/j.envpol.2020.115390>.
- Weber, C., Opp, C., Prume, J., Koch, M., Andersen, T., Chiffard, P., 2021. Deposition and in-situ translocation of microplastics in floodplain soils. *Sci. Total Environ.*, 152039 <https://doi.org/10.1016/j.scitotenv.2021.152039>.
- Wickham, H., Averick, M., Bryan, J., Chang, W., McGowan, L.D., François, R., Grolemund, G., Hayes, A., Henry, L., Hester, J., Kuhn, M., Pedersen, T.L., Miller, E., Bache, S.M., Müller, K., Ooms, J., Robinson, D., Seidel, D.P., Spinu, V., Takahashi, K., Vaughan, D., Wilke, C., Woo, K., Yutani, H., 2019. Welcome to the tidyverse. *J. Open Source Softw.* 4, 1686. <https://doi.org/10.21105/joss.01686>.
- Woodward, J., Li, J., Rothwell, J., Hurley, R., 2021. Acute riverine microplastic contamination due to avoidable releases of untreated wastewater. *Nat. Sustain.* <https://doi.org/10.1038/s41893-021-00718-2>.
- Yu, Y., Flury, M., 2021. Current understanding of subsurface transport of micro- and nanoplastics in soil. *Vadose Zone J.*, e20108 <https://doi.org/10.1002/vzj2.20108> n/a.

Flooding frequency and floodplain topography determine abundance of microplastics in an alluvial Rhine soil

Supplementary Information

Markus Rolf^a, Hannes Laermanns^a, Lukas Kienzler^a, Christian Pohl^b, Julia Möller^c, Christian Laforsch^c, Martin G.J. Löder^{c,*}, and Christina Bogner^{a,*}

^aEcosystem Research Group, Institute of Geography, University of Cologne, 50923 Cologne, Germany

^bDHI WASY GmbH, 12489 Berlin, Germany

^cAnimal Ecology I, BayCEER, University of Bayreuth, 95440 Bayreuth, Germany

*christina.bogner@uni-koeln.de, martin.loeder@uni-bayreuth.de, Joint senior and corresponding authorship

Contents

Supplementary figures 2

List of Figures

S1	Aerial photograph of sampling site	2
S2	Soil in T1	3
S3	Soil in T2	3
S4	Soil in T3	3
S5	Extraction of microplastics	4
S6	Erosion edge at T1	5
S7	Distribution of shapes and polymers	6
S8	Distribution of shapes and sizes	7
S9	Land use and effluents	8
S10	Number of flood days	9

Supplementary figures

Study site



Figure S1: Aerial ortho photograph of the floodplain of Langel-Merkenich from 1988 to 1994 (exact date not available). ©Land NRW, dl-de/by-2-0 (<https://www.govdata.de/dl-de/zero-2-0>) <https://www.tim-online.nrw.de>, accessed on 2022-02-14)

Soil chemical analysis

Total carbon (C), soil organic carbon (SOC) and total nitrogen (N) contents were measured with a Vario EL cube (Elementar Analysensysteme GmbH, Hanau, Germany). After homogenization, we transferred a weighed aliquot of a soil sample into a tin boat. For the determination of the SOC content, a second aliquot of each sample was dissolved with 10% HCl before measurement.

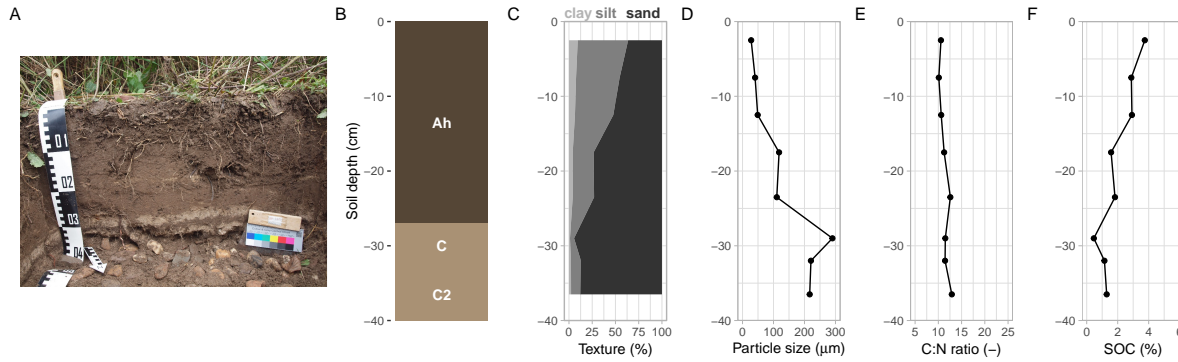


Figure S2: Photograph and soil properties of the soil profile in Transect 1. With its characteristic Ah and C horizons, it can be classified as a haplic fluvisol.

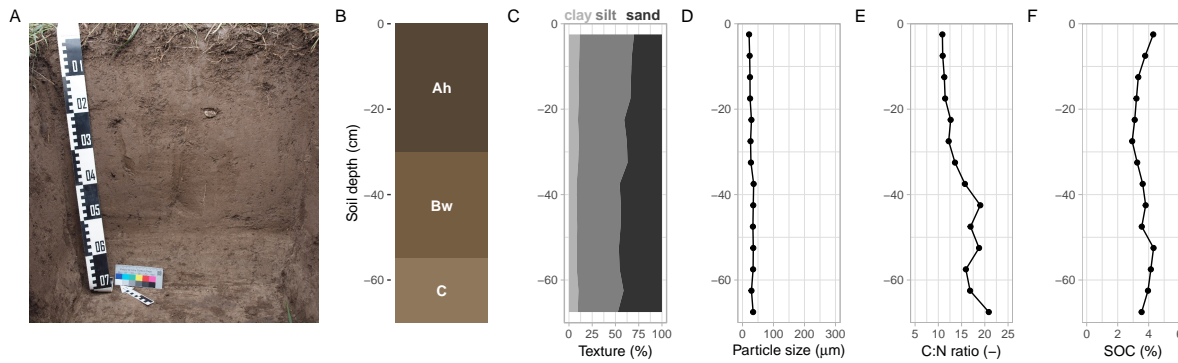


Figure S3: Photograph and soil properties of the soil profile in Transect 2. The formation of an initial subsoil indicates a more continuous soil formation than at in T2. The soil is classified as mollic fluvisol.

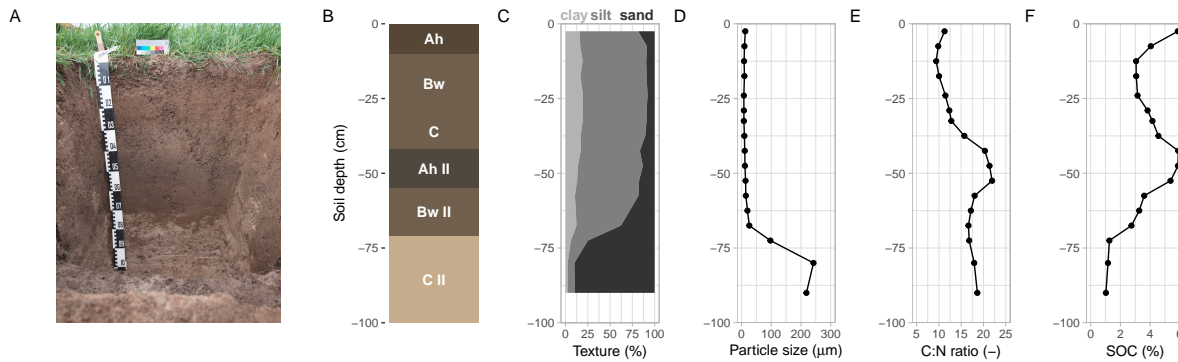


Figure S4: Photograph and soil properties of the soil profile in Transect 3. The soil is classified as mollic fluvisol. The horizons Ah II, BwII, CII indicate an older soil that was buried by fluvial deposits.

Extraction and purification of microplastics from soil samples Workflow

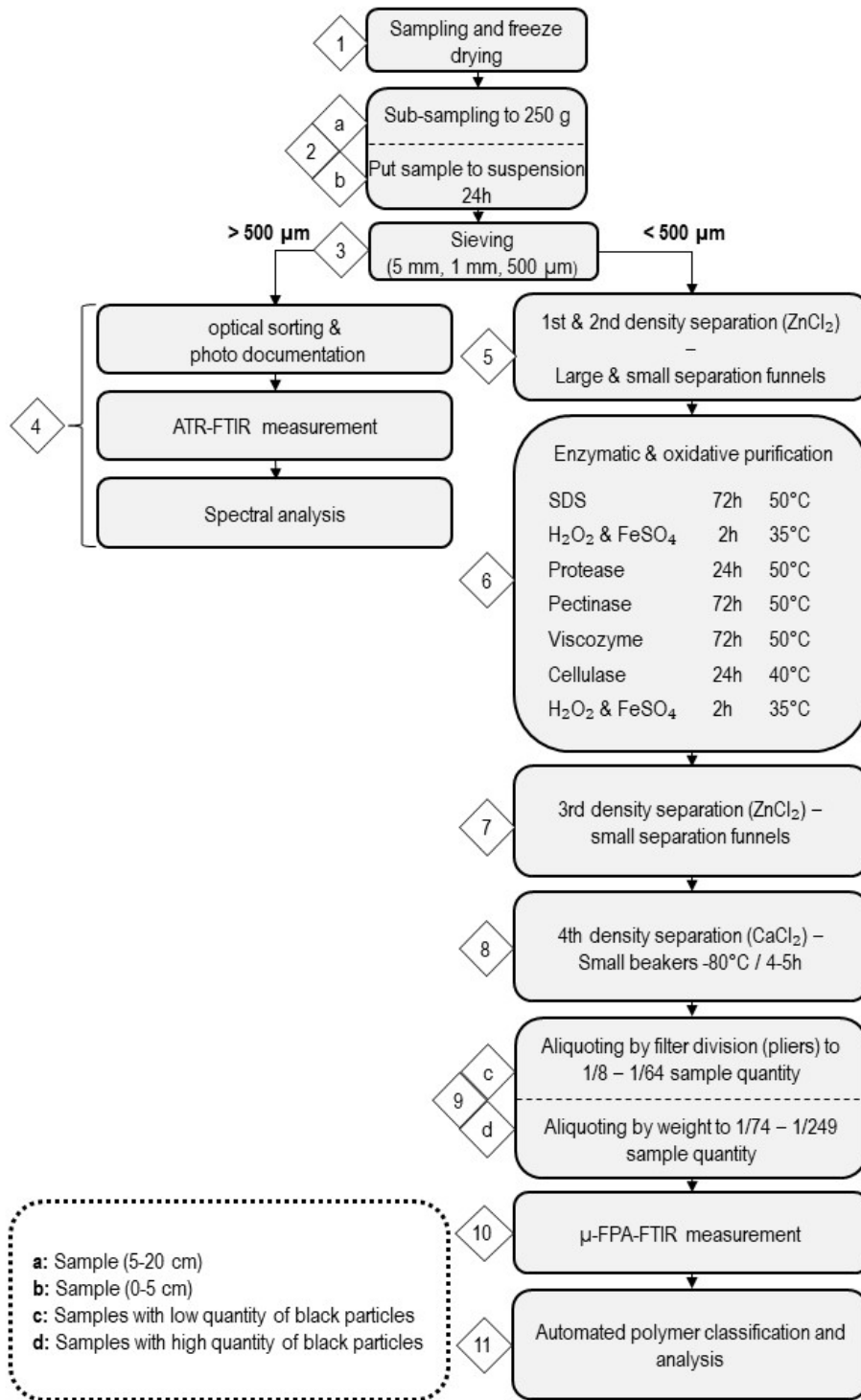


Figure S5: Purification workflow to extract microplastics from soil samples. Protocol adapted from Möller et al., 2021.

Sample aliquoting procedure

After the fourth density separation, the purification procedure was completed (step 8 in Supplementary Figure S5) and two fractions were obtained, namely a lower dense sample fraction free of black carbon particles and a fraction of denser particles enriched with black carbon. Due to the remaining sample quantity, aliquoting was needed to produce filters suitable for μ -FTIR imaging and analysis. Therefore, each of the two fractions was filtered on a stainless-steel filter (mesh size 5 μm) for aliquoting. The filter of the lower dense fraction was divided into two halves by an in-house made sample division pliers. One half was rinsed off from the filter and suspended in a pre-cleaned beaker, and the other half was kept as backup sample. Then the rinsed half was filtered again on a stainless-steel filter (mesh size 5 μm) for the next halving step as described before. This procedure was repeated until 1/8–1/64 of the sample material was obtained as a final aliquot (step 9c in Supplementary Figure S5). The fraction of the denser particles was aliquoted by weight after drying, resulting in aliquot amounts between 1/74–1/249 (step 9d in Supplementary Figure S5).

Signs of erosion at the study site



Figure S6: Erosion break-off edge adjacent to transect T1 at the study area in the nature reserve 'Rheinaue Langel-Merkenich' in Cologne.

Additional information on shapes, polymers, and size classes of microplastics

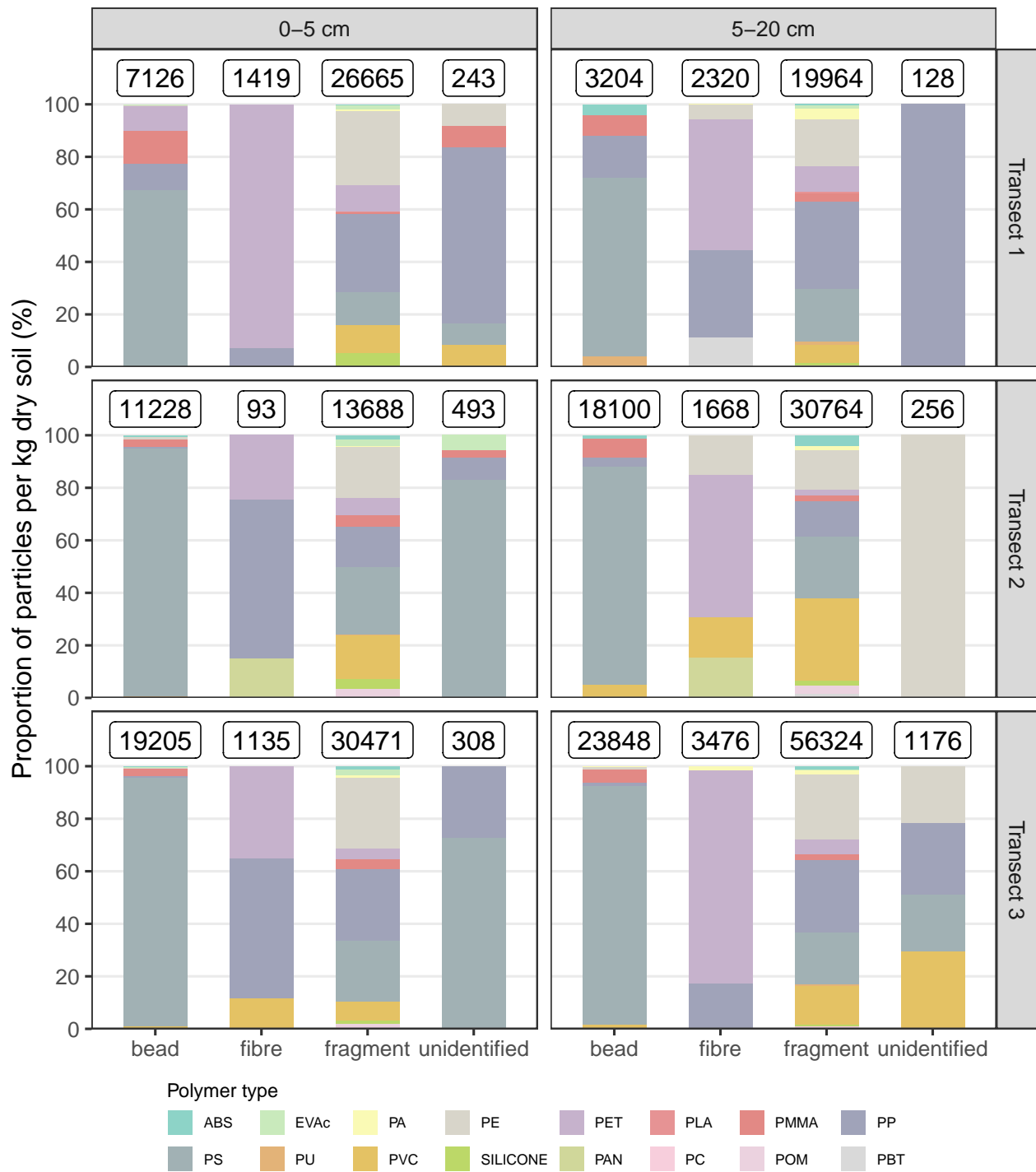


Figure S7: Distribution of shapes by polymer type in the transects and the soil depths. Numbers on top of each bar show total particle numbers.

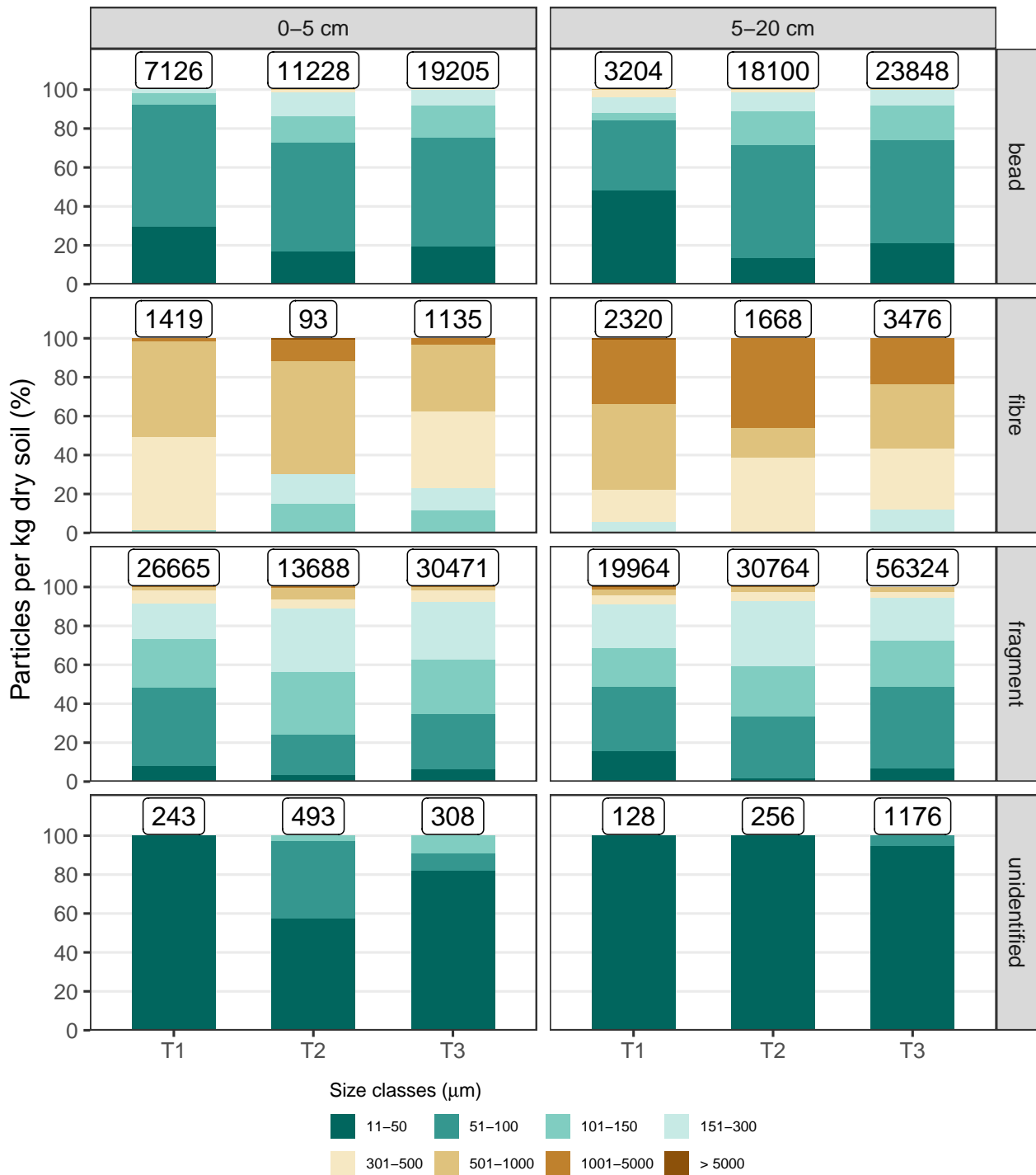


Figure S8: Distribution of size classes by shape in the transects and the soil depths. Numbers on top of each bar show total particle numbers.

Additional information on possible sources of microplastics

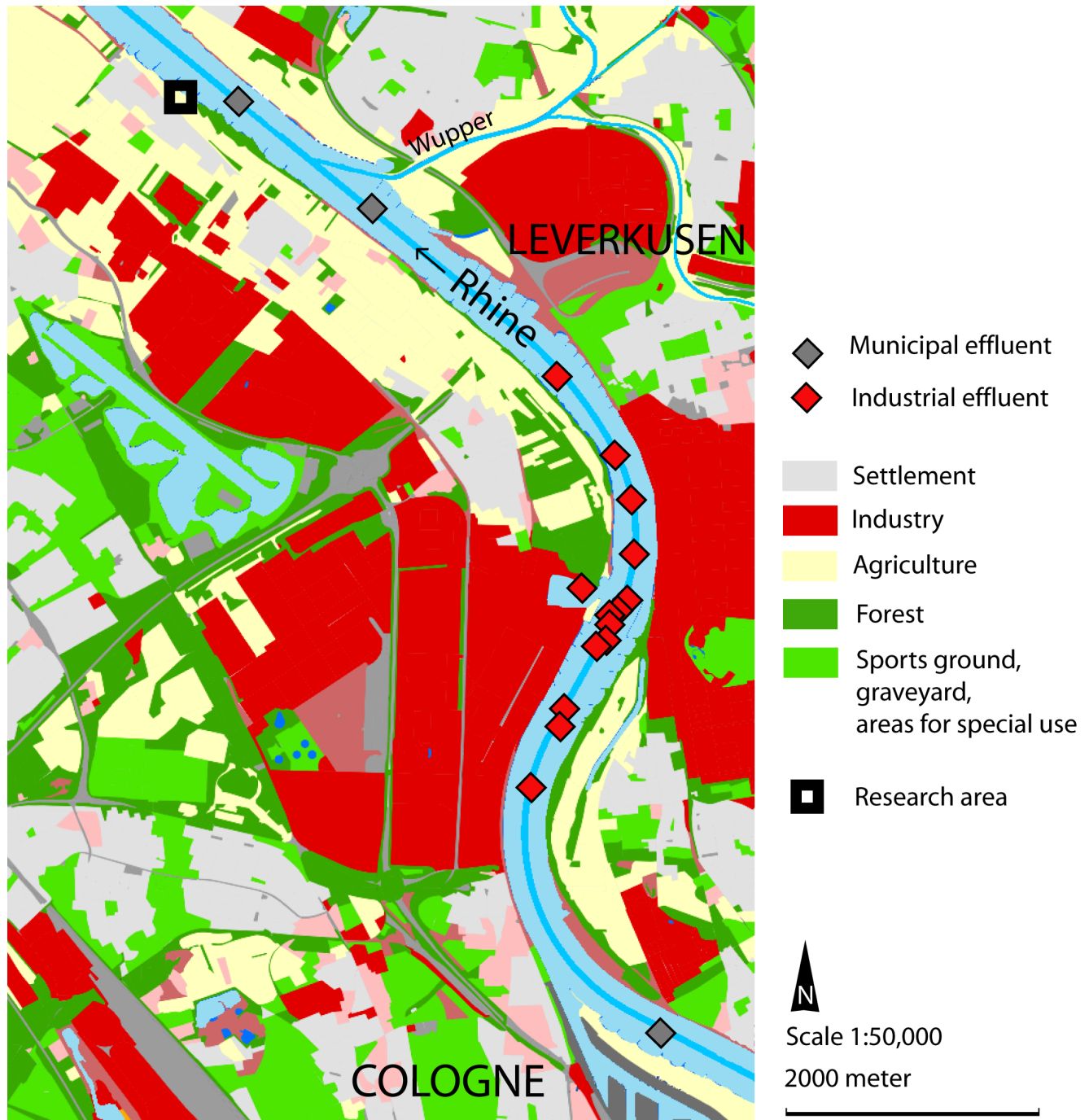


Figure S9: Land use forms and industrial & municipal effluents in northern Cologne and Leverkusen. Figure modified by the authors and data provided by ©Land NRW, dl-de/by-2-0 (www.govdata.de/dl-de/by-2-0) <https://www.elwasweb.nrw.de>, 2022-02-16

Additional information on flooding

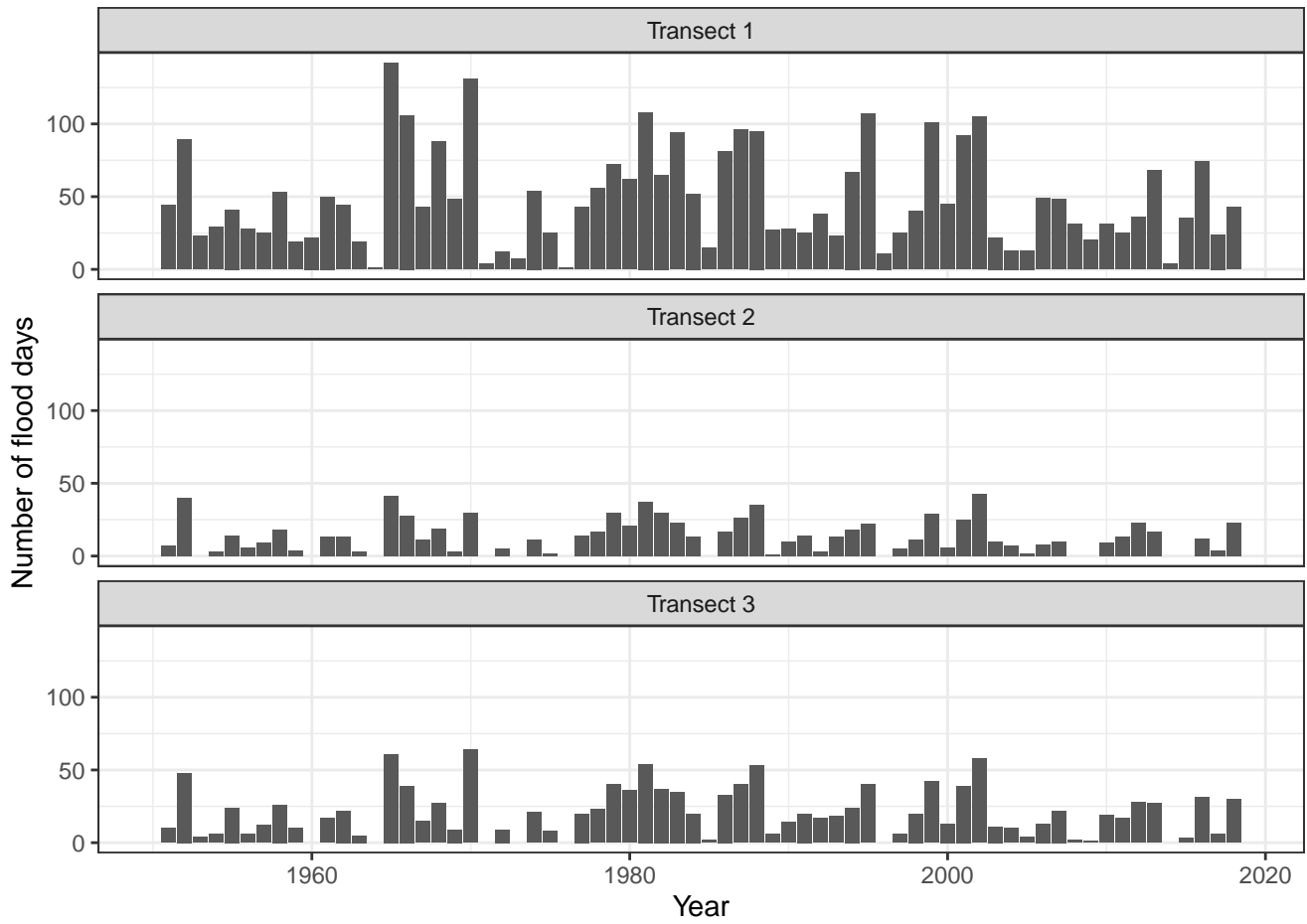


Figure S10: Number of flood days per year between January 1950 and April 2020. We define a day as a flood day if the Rhine level exceeds a transect-specific threshold, namely 35.46 m a.s.l. at T1, 38.14 m a.s.l. at T2 and 37.61 m.a.s.l. at T3, respectively.

Article 6

**Organic fertilizer as a vehicle for the entry of
microplastic into the environment**

ENVIRONMENTAL STUDIES

Organic fertilizer as a vehicle for the entry of microplastic into the environment

Nicolas Weithmann,¹ Julia N. Möller,² Martin G. J. Löder,² Sarah Piehl,² Christian Laforsch,^{2*} Ruth Freitag¹

The contamination of the environment with microplastic, defined as particles smaller than 5 mm, has emerged as a global challenge because it may pose risks to biota and public health. Current research focuses predominantly on aquatic systems, whereas comparatively little is known regarding the sources, pathways, and possible accumulation of plastic particles in terrestrial ecosystems. We investigated the potential of organic fertilizers from biowaste fermentation and composting as an entry path for microplastic particles into the environment. Particles were classified by size and identified by attenuated total reflection-Fourier transform infrared spectroscopy. All fertilizer samples from plants converting biowaste contained plastic particles, but amounts differed significantly with substrate pretreatment, plant, and waste (for example, household versus commerce) type. In contrast, digestates from agricultural energy crop digesters tested for comparison contained only isolated particles, if any. Among the most abundant synthetic polymers observed were those used for common consumer products. Our results indicate that depending on pretreatment, organic fertilizers from biowaste fermentation and composting, as applied in agriculture and gardening worldwide, are a neglected source of microplastic in the environment.

INTRODUCTION

Plastics are an integral part of everyday life. They fulfill a wide variety of functions, primarily packaging (39.9% of the total plastics used in Europe in 2016) (1). Additional applications are in building and construction; the electrical, electronic, automotive, and agriculture sectors; and, to a lesser extent, consumer and household appliances, furniture, sport, health, and safety (1). Despite its varied applications, approximately 80% of the produced plastic falls into six categories: polyethylene (PE), polypropylene (PP), polyvinyl chloride (PVC), polyurethane (PUR), PE terephthalate (PET), and polystyrene (PS). Worldwide plastic production has increased steadily since 1950, reaching an annual production of 322 million metric tons worldwide in 2015, of which approximately 40% was used in one-way products (1). Not surprisingly, because of inadequate end-of-life treatment, plastics are increasingly found as contaminants in the environment (2). Recently, the World Economic Forum estimated that 32% of plastic packaging is leaking into the environment (3), and models suggest that up to 12.7 million metric tons of plastic litter enters the oceans from land-based sources each year (4). Therefore, the G7 has acknowledged that “plastic litter poses a global challenge” (5). Accordingly, scientists have suggested to “classify plastic waste as hazardous” because it may have “significant ecological impacts, causing welfare and conservation concerns” (6). Among the plastic materials found in the aquatic environment, so-called microplastic particles (MPPs; <5 mm)—mainly fragments, fibers, and spheres—have attracted particular attention (7, 8) because harmful effects of MPPs on various aquatic organisms have been proposed (6, 8–11), linked either to the presence of MPPs per se, to toxic additives, or to potentially harmful microorganisms or chemicals enriched onto them. However, theoretical predictions based on models and empirical studies are often contradictory, and it is not known how effects reported for individual organisms may affect ecosystems (12).

Because of their small size, MPPs may presumably also enter the food web (10) and thus potentially end up in human food (13). There, they pose a risk that is not yet predictable, because the interaction of MPPs with tissue and cells is poorly understood. Investigation of the interaction is further complicated by the fact that MPPs are not single compounds but constitute mixtures of different plastic types, each often consisting of a blend of synthetic polymers, residual monomers, and chemical additives. Furthermore, their morphology (for example, fragments, fibers, or spheres) may influence their effects. In this context, a distinction is typically made between industrially manufactured primary MPPs, originating from cosmetics, household cleaners and other products to which they were purposely added, and secondary MPPs that originate from the disintegration of larger plastics caused by ultraviolet (UV) radiation, mechanical abrasion, and biological degradation (14, 15).

MPPs are detected ubiquitously in aquatic environments across the globe (16–19), reaching values of up to 100,000 particles per cubic meter, with predominantly secondary origin (8). Little is known about the exact origin of this significant contamination, although several pathways through which MPPs may enter surface water have been discussed. Most studies assume a transfer from land, including, but not restricted to, improper disposal of plastic waste, wind distribution, and municipal, as well as industrial wastewater and sewage sludge (10, 18, 20). However, detailed studies regarding MPP production and initial entry into terrestrial ecosystems are currently lacking.

Here, we investigated organic fertilizers (composts, digestates, and percolate-leachates from digestion, which is used as liquid fertilizer) from recycled biowaste as possible vehicles for the entry of MPPs >1 mm into the environment. According to best current practice, after separate collection, organic waste from households and industry is either directly composted or partially digested for biogas/energy production in an anaerobic biogas fermenter, typically followed by composting of the remaining digestates. The recycling of organic waste through composting or fermentation and subsequent application on agricultural land is, in principle, an environmentally sound practice to return nutrients, trace elements, and humus to the soil. However,

Copyright © 2018
The Authors, some
rights reserved;
exclusive licensee
American Association
for the Advancement
of Science. No claim to
original U.S. Government
Works. Distributed
under a Creative
Commons Attribution
NonCommercial
License 4.0 (CC BY-NC).

Downloaded from <http://advances.sciencemag.org/> on April 4, 2018

¹Process Biotechnology and Centre for Energy Technology, University of Bayreuth, 95440 Bayreuth, Germany. ²Animal Ecology I and BayCEER, University of Bayreuth, 95440 Bayreuth, Germany.

*Corresponding author. Email: christian.laforsch@uni-bayreuth.de

most household and municipal biowaste is contaminated by plastic material. Sieving and sifting procedures can significantly reduce, but never completely remove, these contaminants. Moreover, most countries allow a certain amount of foreign matter such as plastics in fertilizers; for example, Germany, which has one of the strictest regulations on fertilizer quality worldwide, allows up to 0.1 weight % (wt %) of plastics. In this regulation, particles smaller than 2 mm are not even considered (21). Thus, organic fertilizers may be a source of environmental MPPs that should not be overlooked. Our study is a first attempt to estimate the significance of this entry pathway to the terrestrial environment.

RESULTS

In this investigation, one biowaste composting plant (plant A; aerobic treatment) and one biowaste digester (plant B, “biogas plant”; anaerobic treatment) were studied in detail. The biowaste composting plant (plant A) processes the biowaste from households with a nearly equal amount of green clippings from the area. The plant removes potential nonbiodegradable material, including plastics, as thoroughly as possible by a series of sieving (80 mm), metal separation, and manual sorting steps. The remaining material is subsequently transferred into a box composter for rotting. The plant offers two types of commercial, quality-controlled, certified compost [composting plant (CP) 8 and CP 15 mm], sieved through 8- and 15-mm meshes, respectively. Both composts were sampled. The batch biowaste digester (parallel boxes, plant B) mainly processed biowaste from households with the addition of some green clippings and occasionally energy crops. The mixture is introduced directly into the digester without pretreatment. Instead, the operators remove contaminating materials from the final compost using one or two sieving steps (see Materials and Methods). From plant B, two mature composts (“Digest A” and “Digest B”), a nonmatured fertilizer (“Digest C”), and the pooled percolate (“Digest D”) from the parallel boxes were analyzed.

An agricultural energy crop digester (plant C) processing only energy crops and no biowaste served as a reference. In plant C, the sample (“Energycrop”) was taken from the postdigester outlet, corresponding to an end-of-process sample. This agricultural biogas plant processes energy crops such as corn/grass silage and, to a lesser extent, ground wheat. Ground wheat and silage arrive in plastic encasings, but these are removed before the substrate is passed through the shredder and entered into the fermenter. In addition, a commercially available fertilizer from a second biowaste digester (plant D, processing solely waste from commerce) located in the same area, as well as end-of-process digestate samples from 10 additional agricultural biogas plants (plants E to N), processing feeds such as dung/manure, sunflowers, or waste from fruit processing, together with the regular energy crops, were screened for MPPs.

Quantity of MPPs

With only 20 (CP 8 mm) and 24 (CP 15 mm) particles per kilogram dry weight (Table 1), the MPP load of the certified composts from the biowaste composting plant (plant A) was almost an order of magnitude lower than that determined in the samples from the biowaste digester (plant B), where up to 146 particles per kilogram dry weight were found in the fresh digestate-fertilizer (Digest C). Mature compost from the same biowaste digester (Digest A and Digest B) contained similar amounts of MPPs (70 and 122 particles per kilogram dry weight, respectively), whereas the pooled percolate sample (Digest D) was somewhat

less contaminated, containing only 14 particles per kilogram dry weight. In the agricultural energy crop digester (plant C), which served as a “blank” fermenter, no plastic particles were found in the end-of-process digestate (sample Energycrop) (Table 1). The end-of-process samples of digestates from the additional 10 agricultural biogas plants (plants E to N) included in the screening contained only negligible numbers of particles: The samples from eight plants contained no particle, whereas the samples from the other two plants contained one particle each, resembling a maximum of 11 MPPs per kilogram dry weight. In contrast, with 895 MPPs per kilogram dry weight, the sample from the second biowaste digester (plant D) included in the screening contained even higher numbers of MPPs than found in composts (Digests A to C) from the biowaste digester (plant B), despite the fact that plant B processed biowaste collected from households, whereas plant D processed biowaste directly supplied by commerce.

Polymer size, type, and morphology

Before further analysis, samples were gently fractionated using sieves with mesh sizes of 5, 2, 1, and exceptionally also 0.5 mm. Analysis of MPP size showed that most of the particles collected from the various samples were between 2 and 5 mm (Fig. 1). Only the pooled percolate sample (Digest D) from the biowaste digester (plant B) contained MPPs mostly from 1 to 2 mm. In some samples, we also found MPPs as small as 250 μm . However, because these data are not fully quantitative, we only present data in the size range of 1 to 5 mm. All MPPs were categorized by shape into three subgroups: fragments, fibers, and spheres. Examples are shown in Fig. 2. Most of the MPPs (75 to 100%) were fragments, followed by fibers (0 to 8%) and spheres (0 to 8%).

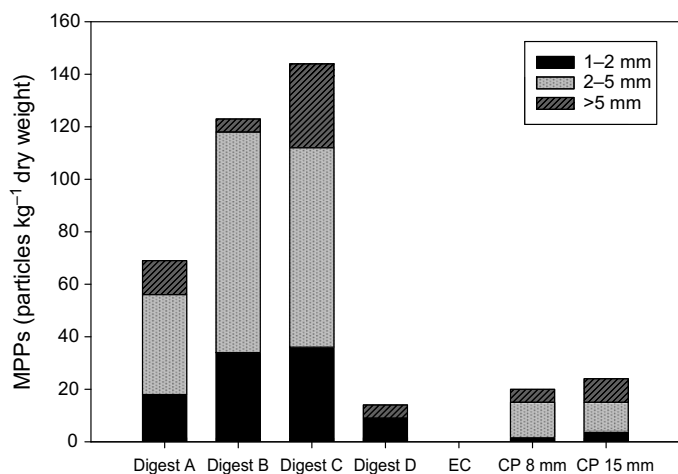
Attenuated total reflection (ATR)–Fourier transform infrared (FTIR) spectroscopy analysis identified 11 polymer types in the samples: styrene-based polymers (PS, acrylonitrile butadiene styrene, and styrene acrylonitrile), polyester (PES), PE, PP, PET, PVC, PUR, polyvinylidene chloride (PVDC), polyamide (PA), and latex- and cellulose-based polymers (Table 2). Most of the particles found in the high-quality composts from the biowaste composting plant (plant A) were styrene-based polymers (60%; 42%), followed by PE (30%; 33%) for the CP 8- and CP 15-mm samples, respectively. The most abundant polymer types in Digest A (73%) and Digest B (80%) from the biowaste digester (plant B) were also styrene-based polymers, whereas most of the MPPs found in the Digest C from this digester were PES with 38% and PE with 21%. The few polymers found in the additional energy crop digesters (plant E to N) were PP and PVC.

DISCUSSION

Organic waste from private households and industry is increasingly seen as a valuable source of both fertilizer and energy. Processing organic waste by fermentation and/or composting is a sustainable means of producing organic fertilizer for agriculture and private gardening, thereby reducing the need for chemical fertilizers. An initial anaerobic fermentation step (production of biogas) before composting is often proposed because this produces energy in a sustainable manner and helps to economically run a plant (production of electricity and heat) while avoiding the drawbacks of conventional biogas production from energy crops (monocropping, rivalry to esculents). Moreover, an initial fermentation step reduces the amount of methane—a more potent greenhouse gas than carbon dioxide—released into the atmosphere, as compared to composting alone.

Table 1. Overview of plants and compartments. The total number of particles is shown as particles >1 mm per kilogram of dry weight.

	Plant A		Plant B				Plant C	Plant D	Plants E to N
Type	Biowaste composting		Biowaste digestion				Energycrop digestion	Biowaste digestion	Agricultural digestion
Sampled	CP 8 mm	CP 15 mm	Digest A	Digest B	Digest C	Digest D	End-of-process	Commercial binding	End-of-process
Particles per kilogram	20	24	70	122	146	14	0	895	0 to 11

**Fig. 1. Size fractions of MPPs in different fertilizers.** Digests A/B/C/D, biowaste digester; EC, energy crop digester; CP 8 mm/15 mm, biowaste composting plant.

Current practice for collecting organic waste fractions from private households calls for separate collecting bins. Theoretically, a pure organic fraction very suitable to composting/biogas fermentation should be obtained. However, in practice, most biowaste contains contaminants, often including plastics. Organic materials from commercial sources, such as the food and drink industries, tend to be less contaminated by plastics, but in particular, unsold food items often arrive in packaged form, some parts of which may then also enter the respective biowaste processing plant. The fact that all the samples from biowaste processing plants investigated in this study contained a certain number of MPPs is therefore not surprising, although a detailed quantitative analysis has been lacking so far. Most of the MPPs were “fragments,” most likely secondary MPPs produced through breakdown of larger plastic materials, such as bags and containers, used for packaging. This hypothesis is corroborated by the fact that styrene-based polymers and PE tended to predominate among the identified materials (that is, materials used mainly for packaging and wrapping). In contrast, none of the samples from the investigated agricultural energy crop digesters contained significant amounts of MPPs, indicating that agricultural crops are only rarely contaminated with plastic items.

However, the relative distribution of MPPs among the different polymer types was not necessarily consistent for all samples from a given plant. For example, although polymer distribution was similar in Digests A and B from the biowaste digester (plant B), a different distribution was found in Digest C from the same plant. The three composts/fertilizers (Digests A to C) from plant B were sampled simultaneously. Because they had matured for differing lengths of time, the observed differences in MPP composition may very well reflect seasonal changes in

biowaste composition. However, because no samples of the original feed substrate were available, this aspect could not be further investigated.

The final processing step for compost is typically sieving using 8-, 10-, or even 15-mm mesh sizes. MPPs, defined as particles smaller than 5 mm, will therefore pass through these sieves and enter the compost. Here, samples were gently fractionated using sieves with mesh sizes of 5, 2, 1, and exemplarily 0.5 mm before the analysis. In most samples, MPP sizes ranged between 2 and 5 mm. The only exception was the percolate sample (Digest D) from plant B, which mainly contained particles between 1 and 2 mm. This may be because the percolate is filtrated because it passes through the fermenter content, and retention increases with particle size. This may also explain why the percolate sample contained a comparatively low number of MPPs compared to the other samples from plant B.

Although particles as small as 250 μm were found in some of the fractions, most likely because they had attached to larger fragments and were therefore retained, the smallest MPP size that could be examined with certainty in this study was 1 mm. At present, quantitative evaluation of smaller particles via the existing methodology is very difficult because the removal of the high organic load is extremely challenging and hampers reliable analysis (22). Hence, quantitative results are presented in this study only for the size range of 1 to 5 mm. Studies focusing on aquatic environments have reported that sites contaminated by MPPs in the range of 1 to 5 mm typically also contain an even higher amount of particles <1 mm, presumably created through further fragmentation of larger MPPs (23). However, fragmentation into a size <1 mm is perhaps more likely in the natural environment, where mechanical forces act (for example, wave action at a beach), than in biowaste treatment plants. Nevertheless, it cannot be excluded at present writing that MPPs <1 mm are produced during biowaste treatment as well (for example, due to the mechanical forces present during the various sieving steps), indicating that actual MPP numbers in fertilizer originating from biowaste may be much higher. This needs further study, particularly in view of the intended use of the material as organic fertilizer.

Although all samples from the biowaste treatment plants contained MPPs, significant differences in the level of contamination were observed. High-quality compost (“quality seal” label) from the biowaste composting plant (plant A) contained less than 25 MPPs per kilogram dry weight, whereas the contamination of the composts/digestates from the biowaste digester (plant B) was nearly an order of magnitude higher. Several factors may have contributed to this result. Although aerobic rotting (composting) reduces the dry mass of the material by approximately 50%, anaerobic conversion to biogas, followed by composting, will often achieve a reduction of more than 80%. Nondigested material, such as MPPs, is therefore enriched by a factor of 5 during anaerobic biowaste digestion but by only a factor of 2 during simple composting.

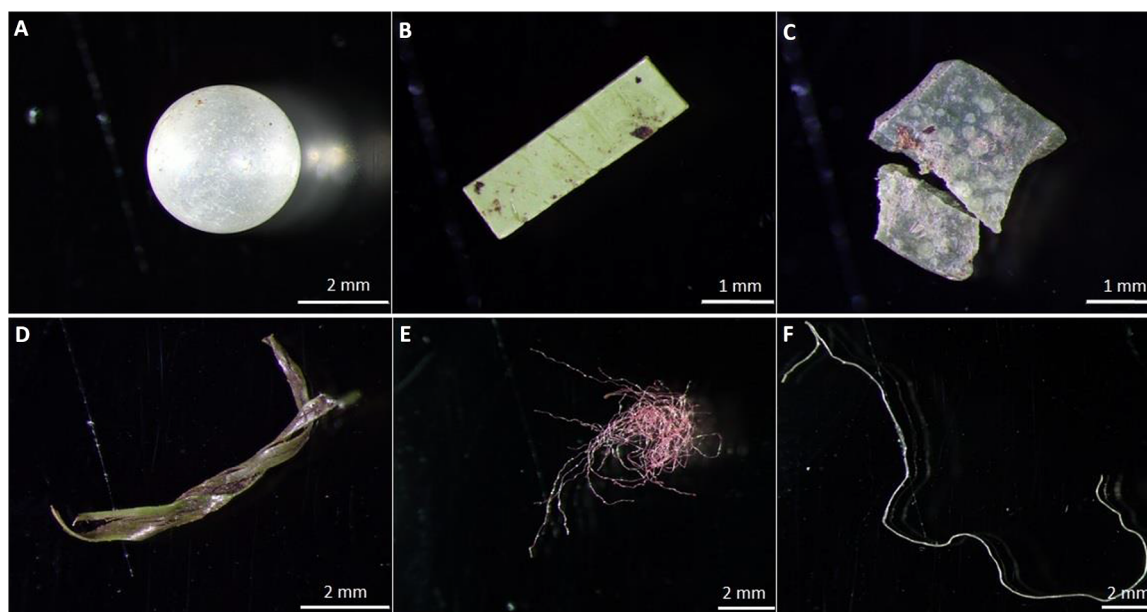


Fig. 2. Examples of MPPs of various shapes found in samples. (A) PE sphere. (B) PVC fragment. (C and D) PE fragments. (E) PES fiber. (F) PP fiber.

Table 2. MPP abundances in different samples. Digests A/B/C/D, biowaste digester; EC, energy crop digester, CP 8 mm/15 mm, biowaste composting plant; MPP per kilogram of dry weight; A, proportion of polymer type in specific sample.

	CP 8 mm		CP 15 mm		Digest A		Digest B		Digest C		Digest D		EC	
	MPP per kilogram	A (%)	MPP per kilogram	A (%)	MPP per kilogram	A (%)	MPP per kilogram	A (%)	MPP per kilogram	A (%)	MPP per kilogram	A (%)	MPP per kilogram	A (%)
Styrene-based polymer	12	60	10	42	51	73	97	80	10	7	0	0	0	0
PES	1	5	0	0	2	3	2	2	56	38	14	100	0	0
PE	6	30	8	33	6	9	3	2	31	21	0	0	0	0
PP	0	0	4	17	3	4	2	2	24	16	0	0	0	0
PET	0	0	1	4	0	0	0	0	16	11	0	0	0	0
Cellulose-based polymer	0	0	0	0	6	9	11	9	5	3	0	0	0	0
PVDC	0	0	0	0	2	3	0	0	0	0	0	0	0	0
PVC	1	5	1	4	0	0	5	4	2	1	0	0	0	0
Latex	0	0	0	0	0	0	0	0	1	1	0	0	0	0
PUR	0	0	0	0	0	0	0	0	1	1	0	0	0	0
PA	0	0	0	0	0	0	2	2	0	0	0	0	0	0
Σ MPP	20		24		70		122		146		14		0	

Concomitantly, in the biowaste composting plant (plant A), biowaste from private households was mixed with at least equal amounts of green clippings. The latter is typically much less contaminated with plastics and thus dilutes the MPP contamination. In addition, an elaborate substrate preparation protocol is in place at the biowaste composting plant (plant A), which attempts to remove contaminating materials as thoroughly as possible before the substrate enters the composter. Finally,

temperatures of up to 75°C are reached during aerobic rotting (composting as in plant A), whereas most anaerobic biowaste digesters, such as plant B, are operated between 45° and 55°C. This will directly influence, for example, the fraction of cellulose-based MPPs found in the final compost, which, in consequence, was nondetectable in the samples from the composting plant (plant A). In addition to the lower temperature, a lack of oxygen and UV radiation will also block potential MPP

degradation pathways in the anaerobic biowaste digesters, such as plant B, compared to aerobic composting, as in plant A. A recent study testing the degradability of PE and PET in an active anaerobic environment at 50°C showed no appreciable degradation of polymers over the investigation period of 500 days (24). In particular, PE and PS, which were detected in all samples from the biowaste treatment plants, are known to be highly persistent in the environment. It is therefore likely that these particles, once released, will accumulate in nature over time.

In Germany alone, which has one of the strictest regulations on fertilizer quality worldwide, more than 12 million metric tons of biowaste were either composted or passed through municipal biogas plants in 2013 (25). This quantity of biowaste translates into more than 5 million metric tons of compost from these plants, most of which is used in traditional agriculture and gardening. We recorded particle counts varying from 14 to 895 particles per kilogram dry weight (when conservatively calculated, 1-kg compost contains approximately 50% dry weight content) for MPPs larger than 1 mm, together with a yet unquantified number of smaller particles. Although our data may not be representative of all biowaste treatment plants, an extrapolation based on our results suggests that, in Germany alone, although counting only particles >1 mm, between 35 billion and 2.2 trillion MPPs are potentially introduced via this pathway into the environment each year.

An evaluation of our data is difficult because there is no other quantitative study on MPPs in compost available. However, our data can at least be compared with similar potential sources of MPPs such as sewage sludge, which is also used for fertilization of agricultural land. When considering only MPPs >1 mm, recent studies on the MPP contamination of sewage sludge have found concentrations ranging between 0 and 300 particles per kilogram dry weight in the analyzed samples (26, 27). The highest concentration found for sewage sludge in the latter study is by a factor of 3 lower than the highest concentration found in the compost samples in our study. However, as stated above, sewage sludge may be contaminated with an even higher amount of smaller MPPs (<1 mm) indicated by recent studies, which have found between 1000 and 24,000 particles per kilogram dry weight (26, 27). For various reasons, sewage sludge is in the public opinion increasingly seen as problematic waste inappropriate for redistribution into the environment, probably not least because of the contamination with heavy metals, residual pharmaceuticals, and also artificial fibers. The latter was detectable in agricultural soils up to 15 years after application of sewage sludge (28). This abandonment is not the case for composts and digestates from biowaste processing plants, which, in principle, do constitute valuable organic fertilizers.

However, compared to sewage sludge, which, in Germany, is routinely incinerated, fertilizer contaminated with MPPs from biowaste processing plants inevitably enters the environment. Because Germany has one of the strictest regulations on fertilizer quality worldwide, we here report only on the “best case scenario,” whereas the MPP contamination in countries with less strict regulations may be even higher.

However, advantages and disadvantages of the continuation of using biowaste for fertilizer production need to be carefully balanced, particularly because studies on the impact of MPPs on terrestrial life forms are still inconclusive. It cannot be excluded that, analogous to aquatic systems, MPPs can accumulate in the soil detrital food web (29). At least one study has shown that (pristine) PE particles mixed with litter and offered to earthworms for uptake led to higher mortality and a reduced growth rate (30). Another study showed that polybrominated diphenyl ether, a substance mixed into polymers as a flame retardant, is bioacces-

sible and can enter soils after volatilization or polymer deterioration. Accumulation in earthworms was shown, and transfer to higher trophic levels is likely (31). However, it is unknown whether these additives are still present in secondary MPPs after fermentation and/or composting. In addition, it cannot be excluded that MPPs in the investigated size range, or smaller, exert a direct influence on active microbiota in biowaste treatment plants or soils, which has not been considered yet in the literature. Hence, further studies on the possible consequences and impacts of MPP contamination of fertilizers originating from biowaste treatment plants for soil quality and soil life forms are necessary before any risk assessment can be undertaken.

MATERIALS AND METHODS

Biowaste composting plant (aerobic treatment), plant A

The biowaste composting plant (plant A) processes approximately 8000 metric tons per year (t/a) of biowaste solely from households, together with approximately 12,000 t/a of green clippings. The plant commercializes quality-controlled, certified composts of two compost qualities (sieving with 8- and 15-mm sieves), both of which were sampled. Arriving biowaste was initially sieved using an 80-mm mesh. The fraction <80 mm was passed through the metal separator and then directly placed into the rotting containers for fast initial decomposition. The fraction >80 mm was sorted manually to remove stones, metals, plastics, and glass. Afterward, the material was mechanically shredded and again added to the sieving drum. In the rotting container, temperatures >70°C were reached. After initial rotting, the compost was left to mature and stabilize in open piles for several months, followed by a final sieving step to reach the desired final corn sizes of below 8 and 15 mm, respectively.

Biowaste digester (anaerobic treatment), plants B and D

The investigated biowaste digester (plant B) was a nonstirred, discontinuous box fermentation system. The plant comprised several quadrangular box digesters, each with a volume of 945 m³ and a filling capacity of 500 m³, which corresponds to a mass of 350 metric tons of organic material. All boxes were equipped with a floor heating and operated at temperatures between 40° and 45°C. The substrate consisted of a pourable mixture of biowaste (11,000 t/a, solely from households) and green clippings (3000 t/a) with a water content below 15 wt %. The composition of the substrate follows seasonal changes. In the winter, the substrate is occasionally supplemented with energy crops.

To initiate the fermentation in the box, fresh substrate was predigested via aerobic digestion for several days and mixed with two volumes of fermenter content. The mixture was added into a fermenter box using an excavator. Afterward, the box was locked, assuring anaerobic conditions, and inoculated by sprinkling with percolate from other boxes. No mechanical treatment or manual presorting took place. After 28 days of fermentation, the box was emptied, 30 volume percent (volume %) of the digestate was removed, and the rest was mixed with 30 volume % of fresh substrate. Subsequently, the digestate was sieved (20-mm mesh) to remove impurities, such as stones, larger plastics, and metals, before it is processed to fertilizer and potting soil using an aerobic composting process. To produce high-quality compost, digestates were matured for 11 to 13 months and sieved using a 10-mm mesh. Lower-quality fertilizer was matured for only 8 to 9 months, and no additional sieving step was performed at 10 mm.

In addition, to expand the range and verify our findings, 1.5 liters of liquid fertilizer for private and agricultural use produced by another anaerobic plant (plant D) was screened for MPPs. This plant processes

16,000 t/a biowaste from commerce, particularly waste from the local market, as well as waste from food and drink industries.

Energy crop digester, plant C and plants E to N

The agricultural energy crop digester (plant C) serving as a presumably uncontaminated reference in this study was a standard two-stage “wet-digester” tank system consisting of a 30-m³ unit for feeding, a 400-m³ plug-flow fermenter with spool agitators, and a 1000-m³ agitated post-digester. The fermenter and postdigester were equipped with heating aggregates and operated between 42° and 45°C. The plant converts approximately 3200 t/a of corn silage and 200 t/a of ground wheat, together with varying amounts of grass silage, and produces approximately 950,000 Nm³ of biogas per year. Before feeding, the silage was removed from its plastic encasing and passed through a mechanical shredder. Enough water was added to ensure pumpability. In addition, similar end-of-process samples were taken from 10 additional agricultural biogas plants (plants E to N), with feeds ranging from dung/manure, sunflowers, or waste from fruit processing, together with regular energy crops; none of these plants processed any biowaste. Whatever material arrived in plastic encasings was taken from these foils before being either mechanically shredded or directly entered into the digester.

Sampling

All samples were stored in glass jars to avoid contamination by plastics. In the case of the energy crop digester (plant C), a 2-liter sample was taken from the outlet pipe of the postdigester after a certain amount of digestate was discharged to avoid clotted residues. The 10 additional agricultural biogas plants (plants E to N) included in the study were sampled in the same way as the agricultural biogas plant (plant C).

Four 0.75-liter subsamples were taken from the biowaste digester (plant B) and pooled from a compost (Digest A) matured for 11 months and a compost (Digest B) matured for 13 months. Both were sieved with a mesh size of 10 mm. In addition, one compost (Digest C) sample, which had not been matured beforehand, was sieved with a mesh size of 20 mm. For each compost sample, four subsamples were taken equidistantly at a constant height per heap according to the heap size (50 cm for heap A, 30 cm for heap B, and 1.5 m for heap C). The first subsample was always taken at a distance of 1 m from the wall, and every subsequent subsample was taken at an interval of 1 m from the previous subsample. Compost heap C was sampled from the rightmost end to the middle to maintain the greatest possible distance from the adjacent heap (which had not yet undergone sieving) to avoid contamination with objects that would not have passed the sieving process. In addition to the compost, 5.5-liter samples were taken from the percolate at the outlet of the pipeline pooling the percolate from all fermenter boxes (Digest D). In the second anaerobic biowaste digestion plant (plant D) in the study, a representative sample was drawn from commercially available 5-liter bindings.

In the case of the biowaste composting plant (plant A), two 40-liter batches of compost were purchased and subsampled to a 3-liter volume. One batch was sieved with a mesh size of 8 mm (“CP 8 mm”), and the other was sieved with a 15-mm mesh (“CP 15 mm”).

Isolation of MPPs

For MPP isolation, samples were wet-sieved through three stacked stainless steel sieves with mesh sizes of 5, 2, and 1 mm and exemplarily 500 μm (see below). Objects >5 mm were thoroughly rinsed over the sieves with filtered water and filtered ethanol (30%) to remove any attached MPPs. The material remaining on the sieves was

visually presorted under a Leica M50 stereomicroscope. Potential plastic particles were photographed, sized at a magnification of ×40 with a digital camera for microscopy (Olympus DP26), and stored for further analysis using ATR-FTIR spectroscopy (see below). Additional samples from 10 agricultural biogas plants and one liquid fertilizer were treated equally, with the exception of sieving with mesh sizes of 1 mm and 500 μm.

FTIR spectroscopy

A Bruker Tensor 27 FTIR spectrometer equipped with a germanium crystal for measurements in the ATR mode was used for spectral analysis of the putative MPPs. Following 16 background scans, 16 sample scans were performed with a spectral resolution of 8 cm⁻¹ within a range of 3940 to 800 cm⁻¹. The measured spectra were identified by comparison with reference spectra from a custom-made spectral polymer library. The library includes 131 records and contains not only the most common plastic polymers but also natural materials such as silicate, chitin, cotton, or keratin (32).

Determination of dry weight

For standardization, the dry weight of each pooled sample ($n = 5$) was determined by weighing before and after drying at 60°C to a constant weight.

REFERENCES AND NOTES

1. *Plastics - The facts 2016, An Analysis of European Plastics Production, Demand and Waste Data* (PlasticsEurope, 2016).
2. *Green Paper - On a European Strategy on Plastic Waste in the Environment* (European Commission, 2013).
3. L. Neufeld, F. Stassen, R. Sheppard, T. Gilman, Eds., *The New Plastics Economy: Rethinking the Future of Plastics* (World Economic Forum, 2016).
4. J. R. Jambeck, R. Geyer, C. Wilcox, T. R. Siegler, M. Perryman, A. Andrady, R. Narayan, K. L. Law, Plastic waste inputs from land into the ocean. *Science* **347**, 768–771 (2015).
5. G7 leaders, *Leaders' Declaration* (2015); www.g7germany.de/Content/EN/_Anlagen/G7/2015-06-08-g7-abschluss-eng_en.pdf?__blob=publicationFile&v=3.
6. C. M. Rochman, M. A. Browne, B. S. Halpern, B. T. Hentschel, E. Hoh, H. K. Karapanagioti, L. M. Rios-Mendoza, H. Takada, S. Teh, R. C. Thompson, Policy: Classify plastic waste as hazardous. *Nature* **494**, 169–171 (2013).
7. J. A. Ivar do Sul, M. Costa, The present and future of microplastic pollution in the marine environment. *Environ. Pollut.* **185**, 352–364 (2014).
8. S. L. Wright, R. C. Thompson, T. S. Galloway, The physical impacts of microplastics on marine organisms: A review. *Environ. Pollut.* **178**, 483–492 (2013).
9. A. McCormick, T. J. Hoellein, S. A. Mason, J. Schlupe, J. J. Kelly, Microplastic is an abundant and distinct microbial habitat in an urban river. *Environ. Sci. Technol.* **48**, 11863–11871 (2014).
10. M. A. Browne, P. Crump, S. J. Niven, E. Teuten, A. Tonkin, T. Galloway, R. Thompson, Accumulation of microplastic on shorelines worldwide: Sources and sinks. *Environ. Sci. Technol.* **45**, 9175–9179 (2011).
11. D. Lithner, Å. Larsson, G. Dave, Environmental and health hazard ranking and assessment of plastic polymers based on chemical composition. *Sci. Total Environ.* **409**, 3309–3324 (2011).
12. T. S. Galloway, M. Cole, C. Lewis, Interactions of microplastic debris throughout the marine ecosystem. *Nat. Ecol. Evol.* **1**, 0116 (2017).
13. L. van Cauwenberghe, C. R. Janssen, Microplastics in bivalves cultured for human consumption. *Environ. Pollut.* **193**, 65–70 (2014).
14. A. L. Andrady, Microplastics in the marine environment. *Mar. Pollut. Bull.* **62**, 1596–1605 (2011).
15. M. Cole, P. Lindeque, C. Halsband, T. S. Galloway, Microplastics as contaminants in the marine environment: A review. *Mar. Pollut. Bull.* **62**, 2588–2597 (2011).
16. H. K. Imhof, N. P. Ivleva, J. Schmid, R. Niessner, C. Laforsch, Contamination of beach sediments of a subalpine lake with microplastic particles. *Curr. Biol.* **23**, R867–R868 (2013).
17. M. Zbyszewski, P. Corcoran, Distribution and degradation of fresh water plastic particles along the beaches of Lake Huron, Canada. *Water Air Soil Pollut.* **220**, 365–372 (2011).
18. M. Wagner, C. Scherer, D. Alvarez-Muñoz, N. Brennholt, X. Bourrain, S. Buchinger, E. Fries, C. Grosbois, J. Klasmeier, T. Marti, S. Rodriguez-Mozaz, R. Urbatzka, A. Dick Vethaak,

- M. Winther-Nielsen, G. Reifferscheid, Microplastics in freshwater ecosystems: What we know and what we need to know. *Environ. Sci. Eur.* **26**, 12 (2014).
19. D. Eerkes-Medrano, R. C. Thompson, D. C. Aldridge, Microplastics in freshwater systems: A review of the emerging threats, identification of knowledge gaps and prioritisation of research needs. *Water Res.* **75**, 63–82 (2015).
 20. K. Duis, A. Coors, Microplastics in the aquatic and terrestrial environment: Sources (with a specific focus on personal care products), fate and effects. *Environ. Sci. Eur.* **28**, 2 (2016).
 21. B. Kehres, *H&K Aktuell, Änderung der Düngemittelordnung* (BGK e.V., 2015).
 22. M. G. J. Löder, H. K. Imhof, M. Ladehoff, L. A. Löschel, C. Lorenz, S. Mintenig, S. Piehl, S. Primpke, I. Schrank, C. Laforsch, G. Gerdts, Enzymatic purification of microplastics in environmental samples. *Environ. Sci. Technol.* **51**, 14283–14292 (2017).
 23. H. K. Imhof, C. Laforsch, A. C. Wiesheu, J. Schmid, P. M. Anger, R. Niessner, N. P. Ivleva, Pigments and plastic in limnetic ecosystems: A qualitative and quantitative study on microparticles of different size classes. *Water Res.* **98**, 64–74 (2016).
 24. S. Selke, R. Auras, T. A. Nguyen, E. Castro Aguirre, R. Cheruvathur, Y. Liu, Evaluation of biodegradation-promoting additives for plastics. *Environ. Sci. Technol.* **49**, 3769–3777 (2015).
 25. Federal Statistical Office (2017); www.destatis.de/EN/Homepage.html.
 26. S. M. Mintenig, I. Int-Veen, M. G. J. Löder, S. Primpke, G. Gerdts, Identification of microplastic in effluents of waste water treatment plants using focal plane array-based micro-Fourier-transform infrared imaging. *Water Res.* **108**, 365–372 (2017).
 27. A. M. Mahon, B. O'Connell, M. G. Healy, I. O'Connor, R. Officer, R. Nash, L. Morrison, Microplastics in sewage sludge: Effects of treatment. *Environ. Sci. Technol.* **51**, 810–818 (2017).
 28. K. A. V. Zubris, B. K. Richards, Synthetic fibers as an indicator of land application of sludge. *Environ. Pollut.* **138**, 201–211 (2005).
 29. M. C. Rillig, Microplastic in terrestrial ecosystems and the soil? *Environ. Sci. Technol.* **46**, 6453–6454 (2012).
 30. E. Huerta Lwanga, H. Gertsen, H. Gooren, P. Peters, T. Salánki, M. van der Ploeg, E. Besseling, A. A. Koelmans, V. Geissen, Microplastics in the terrestrial ecosystem: Implications for *Lumbricus terrestris* (Oligochaeta, Lumbricidae). *Environ. Sci. Technol.* **50**, 2685–2691 (2016).
 31. M. O. Gaylor, E. Harvey, R. C. Hale, Polybrominated diphenyl ether (PBDE) accumulation by earthworms (*Eisenia fetida*) exposed to biosolids-, polyurethane foam microparticle-, and Penta-BDE-amended soils. *Environ. Sci. Technol.* **47**, 13831–13839 (2013).
 32. M. G. J. Löder, M. Kuczera, S. Mintenig, C. Lorenz, G. Gerdts, Focal plane array detector-based micro-Fourier-transform infrared imaging for the analysis of microplastics in environmental samples. *Environ. Chem.* **12**, 563–581 (2015).

Acknowledgments: We want to thank U. Wilczek, H. Martirosyan, and M. Preiss for help with the experiments. Furthermore, we want to thank the editor and the anonymous reviewers for valuable and helpful comments on the manuscript and B. Trotter for linguistic improvements. Institutional Review Board and/or Institutional Animal Care and Use Committee guidelines were followed with human or animal subjects. **Funding:** The authors acknowledge that they received no funding in support of this research.

Author contributions: C.L. and R.F. designed the study. N.W., J.N.M., M.G.J.L., and S.P. performed the experiments. N.W., M.G.J.L., S.P., C.L., and R.F. wrote and revised the manuscript.

Competing interests: The authors declare that they have no competing interests.

Data and materials availability: All data needed to evaluate the conclusions in the paper are present in the paper. Additional data related to this paper may be requested from the authors.

Submitted 28 August 2017

Accepted 14 February 2018

Published 4 April 2018

10.1126/sciadv.aap8060

Citation: N. Weithmann, J. N. Möller, M. G. J. Löder, S. Piehl, C. Laforsch, R. Freitag, Organic fertilizer as a vehicle for the entry of microplastic into the environment. *Sci. Adv.* **4**, eaap8060 (2018).

Article 7

**Microplastic contamination of composts and liquid fertilizers from municipal biowaste treatment plants
- effects of the operating conditions**



Microplastic Contamination of Composts and Liquid Fertilizers from Municipal Biowaste Treatment Plants: Effects of the Operating Conditions

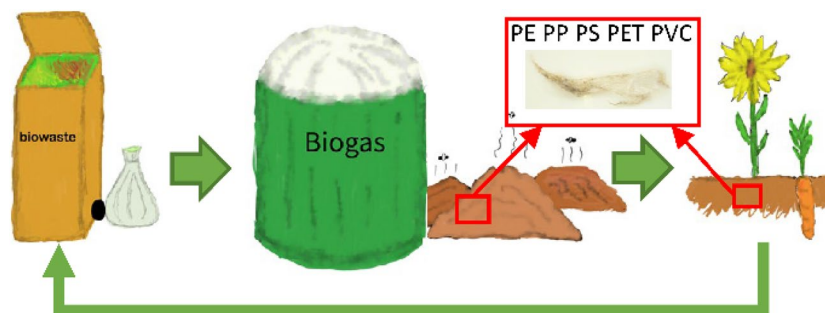
Thomas Steiner¹ · Julia N. Möller² · Martin G. J. Löder² · Frank Hilbrig¹ · Christian Laforsch² · Ruth Freitag¹

Received: 16 February 2022 / Accepted: 1 July 2022
© The Author(s) 2022

Abstract

High-caloric-value household biowaste is an attractive substrate for the production of biogas and fertilizer. Most household biowaste is contaminated by plastics, typically in the form of bags and foils from packaging. Operators of municipal biowaste treatment plants take great care to remove these contaminants, often at the cost of reducing the organic material entering the process. This study compares the residual plastic contamination of fertilizer (composts, digestates) from biowaste treatment plants with compost produced from greenery and digestates produced by agricultural biogas plants processing manure and energy crops. While the fertilizers from the agricultural biogas plants and greenery composts were minimally contaminated by plastic, we found considerable numbers of plastic fragments in the composts/fertilizers from the biowaste treatment plants. Moreover, while certainly being influenced by the quality of the incoming biowaste, this residual contamination appeared to depend largely on the operating conditions. In particular, shredding of the incoming material increased the degree of contamination. Sieving was an efficient method for the removal of fragments > 5 mm but was less efficient for the removal of smaller fragments. In view of the number of the recovered fragments in that size range, it is likely that still none of the finished composts surpassed the current dry weight limits imposed for the plastic contamination of high-quality composts with fragments > 1 mm in Europe (0.3% of dry weight) nor even in Germany (0.1% of dry weight). The contamination of the liquid fertilizer produced via anaerobic digestion by three of the investigated biowaste treatment plants (up to 10,000 particles with a size between 10 and 1000 μm^{-1}) may pose a more serious concern.

Graphical Abstract



Keywords Biogas · Biowaste · Compost · Fertilizer · Microplastic · Nanoplastic

✉ Ruth Freitag
ruth.freitag@uni-bayreuth.de

¹ Process Biotechnology, University of Bayreuth,
Universitätsstrasse 30, 95447 Bayreuth, Germany

² Animal Ecology I, University of Bayreuth, Bayreuth,
Germany

Statement of Novelty

The topic of our manuscript is the residual contamination by (micro-)plastic fragments of quality composts and liquid fertilizer produced by state-of-the-art biowaste treatment plants.

Composts from such plants have been suspected to release significant numbers of plastic fragments into the environment, yet this has never been systematically studied and correlated with plant operation and process conditions. Concomitantly, high-caloric household biowaste is an attractive substrate for biogas and fertilizer. Most household biowaste is contaminated by plastics, typically in the form of bags and foils from packaging. Operators of municipal biowaste treatment plants take great care to remove these contaminants, often at the cost of reducing the organic material entering the process. This study compares the residual plastic contamination of fertilizer (composts, digestates) from biowaste treatment plants with compost produced from greenery and digestates produced by agricultural biogas plants processing manure and energy crops. Our results can contribute to the ongoing discussion of the significance of plastic in the environment and are expected to be of interest to readers from a wider range of communities.

Introduction

The increasing contamination of the environment by macro- and microplastics, the latter defined as particles < 5 mm, has been the subject of intensive study in recent years [1–3]. Most studies to date have focused on aquatic systems, but the contamination of terrestrial compartments may also be significant [4]. Possible entry pathways for plastics into terrestrial systems are thus of interest and also have implications in the development of future containment strategies. Various entry pathways have been identified, including illegal waste deposits, common agricultural practices such as the use of foils for mulching, the transfer of airborne particles (e.g., rubber particles from tires) to the ground by natural precipitation (snow, rain) [5–7] and the utilization of organic fertilizer [8].

Organic fertilizer is produced at a large scale in technical biogas and composting plants from various organic substrates, including household biowaste. These plants play an important role in recycling organic material (biomass). Plants that deal with high-caloric household biowastes tend to process incoming material with a two-step combination of (1) anaerobic fermentation (biogas production) followed by (2) composting of the solid digestate. The production of biogas, which can be transformed into electricity and heat, improves the economic balance of such waste treatment plants [9]. In addition, biogas represents a possible contribution to the ongoing transition from fossil fuels to renewable energies.

Quality composts, including those from biowaste treatment plants, are strictly regulated in regard to allowable residual contaminants, including plastics. For the European Union regulation is found in EU document 2019/1009 [10]

specifying limits for metals, glass and plastic in composts and digestates from biowaste (0.3% dry weight for each impurity type with a particles size > 2 mm, 0.5% dry weight for the total sum of these impurities). Regulations for Germany are somewhat stricter (limit of 0.1% dry weight for particles > 1 mm) and can be found in the DüMV (Düngemittelverordnung). For details see, e.g., § 3, 4b, DüMV and § 3, 4c, DüMV. A positive identification of the chemical nature of recovered plastic particles is typically not required, even though such identification, e.g., by IR spectroscopy, is possible [11].

Collected household biowaste nearly always contains plastics, mainly bags and foils, but increasingly also coffee and tea capsules. Consequently, stringent removal steps, typically involving sieving, are implemented to reduce such contamination, a practice that incidentally also reduces the amount of organic material entering the digester/composter. Despite these measures, even quality biowaste composts may still contain a significant number of microplastic (MP) fragments, as recently shown by Weithmann et al. [8]. However, in their paper, Weithman et al. included only one biowaste composting plant and one biowaste digesting plant and thus could not establish general conclusions. As far as we could ascertain, no one has to date studied whether MP contamination of fertilizers from biowaste treatment plants is typical and to what extent the operating conditions contribute or not to the final contamination. Moreover, two-stage digester–composter plants often produce liquid fertilizer (LF) in addition to compost. This fertilizer is directly applied to the soil and has, to the best of our knowledge, never been studied regarding possible contamination by MP.

Given the acknowledged need to recycle organic waste in a suitable manner together with the relevance of organic fertilizer as an attractive substitute for artificial fertilizer, the present study systematically studies operational conditions and their influence on the production of MP fragments during biowaste treatment. To the best of our knowledge, this is the first study of its kind.

Materials and Methods

Materials

If not otherwise indicated, the suppliers for chemicals were Th. Geyer (Renningen, Germany) and SigmaAldrich (Taufkirchen, Germany). Ultrapure water was produced with an Elga-Veolia-Purelab (Flex2) unit, while ‘Millipore water’ came from a Millipore-Synergy-UV-system (Type 1). Protease A-01 (activity: > 1100 U mL⁻¹), Pektinase L-40 (exo-PGA activity: > 900 U mL⁻¹, endo-PGA activity, > 3000 U mL⁻¹, pectinesterase activity: > 300 U mL⁻¹), and Cellulase TXL (activity: > 30 U mL⁻¹) were from ASA

Spezialenzyme GmbH (Wolfenbüttel, Germany). Viscozyme L (activity: > 100 FBG U g⁻¹) was obtained from Novozymes A/S (Bagvaerd, Denmark).

Selection of Biowaste Treatment Plants and Sample Denomination

Plants representing three basic types were included in this study, namely, simple composting plants (aerobic treatment, six plants), simple anaerobic digesters (“biogas plants”, three plants) and two-stage plants comprising (1) anaerobic digestion and (2) aerobic composting (five plants). The selection included plants treating biowaste, green cuttings and/or energy crops; for details, see Table 1. Plants in category 1 included both plants that convert household biowaste and some that convert other organic materials, including greenery. Plants in category 2 were all agricultural biogas plants, converting mainly agricultural waste (manure) and/or energy crops. Household biowaste was not used. However, one of these plants, plant #2.1, processed organic waste from local markets and landscape conservation material alongside the typical mix of agricultural waste and energy crops. The plants from category 3 were all current state-of-the-art biowaste treatment plants, processing high-caloric household biowaste and recovering part of the energy in the form of biogas via anaerobic digestion during the first.

treatment stage. Three of these plants separated the digestate obtained during the fermentation step by press filtration into a solid digestate going into the composting stage and into LF intended for direct application to agricultural soil. Most of the category 3 plants added a certain percentage of green cuttings to their solid digestate prior to composting; for details, see Table 1. Plants processing biowaste are indicated by bold print in Table 1.

Depending on the plant type, samples were taken of the precomposts (before final sieving), the finished composts (after final sieving), and the solid and liquid fertilizers obtained after anaerobic digestion. Samples are coded according to plant number and source (P, F, and L for precompost, finished compost, and liquid fertilizer, respectively). In the case of the agricultural biogas plants, the indicator “S” is used for the solid digestate. When several samples were taken from a given plant/source, each sample is indicated by a number following the plant number. Sample P_3.3-2 would thus correspond to the second sample of precompost taken from plant #3.3.

Sampling of Composts and Liquid Fertilizers

Bulk samples were taken from the composts according to the guidelines of the German Association for Quality Compost [12]. A slight modification to the standard procedure was introduced to avoid additional contamination of the compost

samples with plastics, particularly via the plastic foil recommended in the standard protocol for sample mixing. Instead, the individual aliquots obtained from a given compost heap were pooled, mixed and stratified directly on the concrete floor (after a ‘washing’ step with compost from the same heap). To obtain a representative sample, the interior of the heap was made accessible using a wheel loader. Then, individual samples were taken at evenly dispersed points. The number and volume of individual samples depended on the volume and grain size of the compost pile; the current procedural guidelines were followed. For example, in the case of 100 m³ of compost with grain sizes of 2–20 mm (typical finished compost), 16 individual samples (1 L each) were taken, and a minimum of 4 mixed samples (2 L each) were created. For the coarser precomposts, the number of samples taken was identical to the number of samples taken for the corresponding finished composts.

In most cases, the precomposts and finished composts for a given plant were sampled at the same visit and consequently stemmed from different processing batches. In one case (plant 3.3), one processing batch was sampled before (precompost) and again several days after (finished compost) the final sieving step. In all cases, sample aliquots were transferred to 3 L Fido jars (Bormioli Rocco, Fidenza, Italy) for transport. If immediate analysis was not possible, samples were stored at 4 °C in the glass vessels. Solid digestates from the agricultural biogas plants were sampled analogously to the compost. Solid digestates from the biowaste digester composters were not accessible to sampling for technical reasons. Samples of the liquid digestates (liquid fertilizer, LF) (~6 L) were collected from the outlet of the storage tanks into glass vessels. The first few liters of LF were discarded to rinse the outlet pipe before the sample was taken. If necessary, LF samples were also stored at 4 °C. Backup samples of approximately 1 L were taken for all samples and stored at –20 °C. Glass vessels intended for transport, for storage or for backup samples were washed in advance with Millipore water.

Analysis of Plastic Fragments in Solid Digestates and composts

A significant concern during the analysis of MP in environmental samples is possible contamination with MP from the ambient air, clothing, laboratory tools, or reagents used during sample processing. To avoid any such contamination, precautionary measures were taken. Cotton lab coats were worn throughout. Unless direct handling was necessary, samples were covered with a glass or aluminum foil lid. Sample processing took place in a laminar-flow box to prevent airborne particles from falling into the samples. All laboratory tools used were made of glass, metal or polytetrafluorethylene (PTFE), a polymer that is rarely found in

Table 1 Technical details of the investigated plants (plants handling biowaste are indicated by bold print)

	Plant 1.1_I	Plant 1.1_II	Plant 1.2	Plant 1.3	Plant 1.4	Plant 1.5	Plant 1.6	Plant 2.1	Plant 2.2	Plant 2.3	Plant 3.1	Plant 3.2	Plant 3.3	Plant 3.4	Plant 3.5
Substrate preparation	Cuttings	Biowaste	Cuttings	cuttings: 25,000 t year ⁻¹	Biowaste, 32,000 t year⁻¹, cuttings 3000 t year⁻¹	Cuttings: 9500 t year ⁻¹	Biowaste 60,000 t year⁻¹	Agricultural waste; energy crops; grapes, organic waste from local markets; landscape conservation material; 18,000 t year ⁻¹	Agricultural waste; energy crops	Agricultural waste; energy crops; 15,000 t year ⁻¹	Biowaste (88% and cuttings (12%); 44,000 t year⁻¹	Biowaste; 18,000 t year⁻¹	Biowaste with a small fraction of added cuttings	Biowaste (75%) and cuttings (25%); 35,000 t year⁻¹	Biowaste (85%) and cuttings (15%); 20,000 t year⁻¹
Substrate preparation	Shredder, magnetic separator	Bag slicer, sieving (80 mm); magnetic separator; mixing with shredded cuttings; sieving (80 mm)	Shredder	Shredder	Biowaste sieving (80 mm); mixing with shredded cuttings	Shredder	Bag slicer, sieving; mixing with up to 5% shredded cuttings, sieving (80 mm)	Shredding of solid material; mixing with liquid substrate	No data available	Shredding of solid material; mixing with liquid manure	Shredder, sieving (80 mm)	None	Shredder	Biowaste: cross-flow shredder, sieving (60 mm), cuttings: sieving > 80 mm, shredder, sieving, fraction 15–80 mm is used for fermentation and < 15 mm for composting	Shredder; sieving (100 mm)
Fermentation	-	-	-	-	-	-	-	Main fermenter: 50 days, 53 °C Secondary fermenter: 25 days, 54 °C;	No data available	Main fermenter: 150–160 days Secondary fermenter: no data available	Plug flow; 55 °C, ca. 17 days	Box fermenter, 40 °C, ca. 40 days	Plug flow, 55 °C, ca. 21 days	Plug flow, ca. 21 days^a	Plug flow (20 days, 52–55 °C)
Composting	10–12 month movement every 2 weeks	12 weeks; movement every 2 weeks	Composting to a degree of rotting of 3–5	3–4 months, plate-like stacks, movement every 4 weeks	1 week intensive rotting; weekly movement (10 weeks)	4 weeks covered floor aeration; 2 weeks maturation	9 movements every 5 days, then drying	-	-	-	Up to 5 weeks	> 5.5 weeks	Up to 9 weeks	6 weeks	5 weeks
Product preparation	-	-	-	-	-	-	-	Solid-liquid separation	No data available	Solid-liquid separation	Solid-liquid separation	-	Solid-liquid separation	-	Solid-liquid separation

Table 1 (continued)

	Plant 1.1_I	Plant 1.1_II	Plant 1.2	Plant 1.3	Plant 1.4	Plant 1.5	Plant 1.6	Plant 2.1	Plant 2.2	Plant 2.3	Plant 3.1	Plant 3.2	Plant 3.3	Plant 3.4	Plant 3.5
Final sieving	12 mm	10–15 mm	10 mm	15 mm	12 mm	20 mm	25 mm, 12 mm and 10 mm	-	-	-	12 mm	20 mm	10 or 12 mm	12 mm	10 mm
Products	Compost	Compost	Compost	15,000 t year ⁻¹ compost	12,000 t year ⁻¹ compost	3000 t year ⁻¹ compost	14,000 t year ⁻¹ compost	Solid digestate, liquid fertilizer	Solid digestate, liquid fertilizer	Solid digestate, liquid fertilizer	Compost/liquid fertilizer ^{a,b}	Only compost	Compost/liquid fertilizer ^{a,b}	Only compost	Compost/liquid fertilizer ^{a,b}

^aOne part of the digestate was dried and composted, and another part was mixed with fresh substrate and returned to the fermenter

^bPart of the liquid fraction was returned to the fermenter to mash the substrate; separation was performed with dewatering press

environmental samples and was excluded here from the analysis. All required solutions and the deionized water used to prepare them were filtered through 0.2 μm pore membranes (mixed cellulose ester membrane, diameter 47 mm, Whatman ME 24, Merck KGaA) before use. Enzyme solutions were filtered through 0.45 μm pore membranes (regenerated cellulose membrane, diameter 100 mm, Whatman RC 55, Merck KGaA) and stored in glass bottles with glass caps before use. All laboratory equipment was thoroughly rinsed with filtered deionized water, 35% ethanol, and again with filtered water before use and between steps to avoid cross contamination. Blanks subjected to the same treatment as the environmental samples were used to detect possible contamination in the laboratory.

In preparation for analysis, the digestate or compost samples were filled into a rectangular metal form (790 mm × 510 mm × 150), thoroughly mixed with a metal shovel and quartered. Sample aliquots for analysis of the plastic content were taken from two quarters (bottom right and top left). Sample aliquots for the determination of the dry weight (DW) were taken from the bottom left quarter, while sample backups (1 L) were taken from the top right quarter. For the determination of the DW, 100 mL sample aliquots were weighed into 250 mL Schott-Duran beakers and dried at 105 °C (oven: Memmert UM 500, Memmert, Schwabach, Germany) for at least 24 h. Afterward, the beakers were allowed to cool to room temperature in a desiccator, and the DW was determined by reweighing the beakers.

For the recovery of individual plastic fragments, approximately 3 L of material were used. The wet weight was measured and correlated to the dry weight determined from another aliquot of the sample, see above. Then the material was evenly distributed into six glass vessels (capacity 3 L each). The material was suspended in 2.5 L of water and first sieved with a mesh size of 5 mm. All retained particles (fraction > 5 mm) were collected with tweezers, while the material passing the sieve was sieved again at 1 mm, followed by collection of the retained particles (fraction 1–5 mm). The sieves were obtained from Retsch GmbH (Haan, Germany; test sieve, IS 3310-1; body/mesh, S-steel; body, 200 mm × 50 mm).

For the analysis of the chemical nature of the particles, attenuated total reflection-Fourier transform infrared (ATR-FTIR) spectrometry (spectrometer: Alpha ATR unit, Bruker Optik GmbH, Ettlingen, Germany; equipped with a diamond crystal for measurements) was used. Spectra were taken from 4000 to 400 cm⁻¹ (resolution 8 cm⁻¹, 16 accumulated scans, OPUS 7.5 software) and compared with entries from an in-house database described previously [11] or the database provided by the manufacturer of the instrument (Bruker Optik GmbH). An incident light microscope (microscope, Nikon SMZ 754T; digital camera, DS-Fi2; camera control unit, DS-U3; software, NIS Elements D) was used for visual

documentation and dimensional analysis of all particles identified by ATR-FTIR as synthetic plastics.

Analysis of Plastic Fragments in the Liquid Fertilizers

The LF samples were also sieved with 5 mm and 1 mm sieves to obtain all fragments > 1 mm. In addition, fragments with sizes ranging between 10 and 1000 μm were treated and analyzed as described previously [13, 14]. Briefly, the LF sample was mixed well with a metal rod, and 50 mL were quickly poured into a 300 mL glass beaker (Schott-Duran). The metal rod and the glass beakers were washed in advance with Millipore water. Subsequently, the samples were purified using an enzymatic-oxidative digestion sequence, as summarized in Table 2 below. Blank samples were processed in parallel in the same way.

Between steps, the sample was filtered through a 10 μm stainless steel mesh filter (47 mm diameter, Rolf Körner GmbH, Niederzier, Germany) with a vacuum filtration unit (3-branch stainless steel vacuum manifold with 500 mL funnels and lids, Sartorius AG, Göttingen, Germany) and rinsed with filtered deionized water to remove residues from the reagents of the previous step. Then, the sample was rinsed back into the reaction vessel with either 20 mL of filtered deionized water or the amount of buffer specified in Table 2, and the filter was placed in the reaction jar to be used again in the subsequent step. All filtrations were conducted under a laminar flow hood to minimize contamination with MP from the surrounding air.

For the final density separation step, the retained matter was transferred from the filter into a clean glass beaker using a metal spatula, and an aqueous ZnCl_2 solution (50 mL; $\rho = 1.8 \text{ g cm}^{-3}$) was added. The mixture was stirred with a magnetic stir bar until all aggregates had been dispersed. Then, the mixture was transferred into a straight-walled separation funnel (400 mL). The mixture was stirred for several minutes with a glass rod and left to settle overnight (at least 12 h). The plastic fragments separated from any mineral matter by rising to the top. After separating the sediment, this less-dense fraction was filtered onto a new 10 μm stainless steel mesh filter, which was then rinsed with 98% filtered ethanol and filtered deionized water to remove residual ZnCl_2 .

Depending on the initial amount and the quality of the matrix, the amount of plastic recovered by the outlined purification procedure can vary. To avoid matrix interference, which would make FTIR analysis difficult, overloading of the aluminum oxide sample carrier filters (0.2 μm , Anodisc, Whatman GE Healthcare) must be avoided. Therefore, samples with a high amount of material were suspended in filtered deionized water, evenly filtered through a 5 μm stainless steel mesh filter (diameter: 47 mm), and then halved

using custom-made pliers. One half was washed into a clean 100 mL beaker, while the other was kept as a backup sample. This process was repeated as often as necessary to achieve a subsample that could be transferred onto 3–5 aluminum oxide filters for spectroscopic measurement. The filters were analyzed with focal plane array-based $\mu\text{-FTIR}$ spectroscopy (10), which allows the determination of the fragment shape, size, color and polymer type, using a Bruker Hyperion 3000 FTIR microscope (Bruker Optik GmbH) equipped with a 64×64 pixel FPA detector in conjunction with a Tensor 27 spectrometer. The samples were measured in transmission mode with a $3.5 \times$ IR objective (spatial resolution 11.05 μm per pixel) and a wavelength range of $3600\text{--}1250 \text{ cm}^{-1}$ (resolution 8 cm^{-1} , 6 accumulated scans). Data processing was conducted using Bruker OPUS software version 7.5 (Bruker Optik GmbH), and automated spectral analysis was performed with the “BayreuthParticleFinder” module in ImageLab version 4.1 (EPINA GmbH, Retz, Austria) based on random forest decision classifiers [15, 16] for 22 different polymer types. The results of the automated spectral analysis were checked by experienced personnel for quality assurance and finally corrected with the blank values.

Results

Plastic Contamination of the Sampled Composts and Solid Digestates

When choosing the biowaste treatment plants for our study, we attempted to cover the current technical range of such plants, i.e. both simple composting plants and two stage digester–composters. Simple composting plants processing greenery and agricultural biomass digesters (biogas plants) processing mostly manure and energy crops were included for comparison. Table 3 summarizes the number of plastic fragments found per kilogram dry weight (DW) in the investigated composts and solid digestates. Composts sampled from plants processing biowaste are indicated by bold print. Note that solid digestates could only be sampled from the biogas plants, for technical reasons they were not available from the biowaste treatment plants.

Plastic fragment were collected in two size categories, > 5 mm and 1–5 mm. Consequently, we were able to distinguish between larger particles (> 5 mm) and those constituting MP (< 5 mm). The lower limit of 1 mm in the 1–5 mm category is of interest, since the current German regulations of compost quality in regard to contamination by plastic fragments consider only particles > 1 mm, the EU is expected to soon follow (current limit > 2 mm). Fragment numbers were normalized to the DW of the samples since the water content of the samples varied significantly; for details, see Table 3.

Table 2 Enzymatic-oxidative digestion sequence for analysis of microplastics (10–1000 µm) from liquid fertilizer samples

Step	Volume	Reagents	Function of reagents	Incubation time	Incubation temperature
1	50 mL	10% sodium dodecyl sulfate*	Anionic detergent to solubilize lipids and proteins	72 h	50 °C
2	50 mL in 2 × 25 mL batches	30% H ₂ O ₂ **	Oxidizing agent to degrade organic material	2 h	35–40 °C temperature controlled in an ice bath
3	50 mL & 10 mL	0.1 M Tris HCl buffer (pH 9)*** & protease A-01	Hydrolyzation of proteins into soluble peptides	12 h	50 °C
4	25 mL & 5 mL	0.1 M NaAc buffer**** (pH 5) & Pektinase L-40	Degradation of any pectin in the primary cell wall and middle lamella of plants	72 h	50 °C
5	25 mL & 1 mL	0.1 M NaAc buffer (pH 5) & Viscozyme L	Splitting of the β(1,3) linkages of cellulose	48 h	50 °C
6	25 mL & 5 mL	0.1 M NaAc buffer (pH 5) & Cellulase TXL	Splitting of the β(1,3) linkages of cellulose	24 h	40 °C
7	40 mL	Fenton's reagent**	Oxidation of degradation products and remaining organic material	2 h	40 °C

*≥ 95% SDS; Karl Roth; **30% H₂O₂; Fischer Scientific; ***≥ 99.3%, buffer grade; Karl Roth; ****≥ 98.5%, sodium acetate; Karl Roth

In three of the plants (#1.6, #3.1, and #3.3), we were also able to sample the precomposts. However, only in the case of plant #3.3 did we have access to material from a particular batch of compost before and after the final sieving step. In all other cases, precomposts and finished composts were sampled at the same time; i.e., the samples originated from different batches/initial loadings and thus cannot be compared directly. In plant #1.6, samples were taken of finished compost, material after an intermediate sieving step, and precompost. In the case of biogas plant #2.1, we had access to digestate pellets made from dried and pressed digestate, as well as to fresh digestate.

A comparison of the precomposts and finished composts shows that the final sieving step (typically using a 10 or 12 mm mesh size, Table 1) reduces the contamination of fragments > 5 mm, while sieving is less efficient in regard to the removal of fragments in the 1–5 mm range. In case of plant #3.3 were pre- and final composts were available for a given compost batch and hence directly comparable, the final sieving reduced the number of particles > 5 mm from 194 in the precompost to 53 in the finished compost while having little to no effect on particles in the range of 1–5 mm (46 and 48 particles, respectively).

With values between 10 and 15 particles kg_{DW}⁻¹, finished biowaste composts from simple composting plants (category 1) showed only slightly higher plastic contamination than did finished greenery composts, which was not anticipated, given that incoming biowaste is much more contaminated by plastics than is greenery (Fig. 1). The data for plant # 1.6, i.e., the only simple biowaste composter where precompost data were also available, particularly demonstrates the

efficiency of the final sieving step in terms of reducing the number of fragments.

In comparison, the finished composts from the digester–composters contained a significantly higher number of particles in both the > 5 mm and 1–5 mm categories despite the use of similar final sieving mesh sizes. The digester–composters included in our study tended to use shredders to process incoming biowaste, whereas the simple biowaste composters mainly used bag slicers. While shredding is effective in making material accessible for digestion and biogas production, it presumably increases plastic and MP contamination. By comparison, digester–composter #3.2, which used an initial box fermentation step (no initial substrate preparation/shredding), had significantly lower plastic contamination in its finished compost, particularly from the difficult-to-remove 1–5 mm size fraction. Moreover, the content of particles in the > 5 mm fraction could presumably be further reduced by using a 10/12 mm mesh for final sieving instead of the currently used 20 mm mesh.

In general, the final sieving had a significant effect on the particle dimensions. Most retained particles had a longish shape. Whereas the range of particle length was nearly identical for particles sieved with a 10, 12, or 15 mm mesh size, the average width of the particles passing the final sieve nearly doubled from 10/12 to 15 mm. Particles capable of passing the 20 mm mesh were considerably larger in both length and width, for details see Fig. S1. Average values and standard deviations for the fragment sizes (length × width) are given in Table S1.

Finally, the production of LF (by press filtration) seems to increase the contamination of composts prepared from the

Table 3 Number of plastic fragments in two size categories (> 5 mm and 1–5 mm) found in compost and solid fertilizer samples

Sample	Number of plastic fragments $\text{kg}_{\text{DW}}^{-1}$		DW content [%]
	> 5 mm	1–5 mm	
F_1.1_I	1.58	1.58	64.46
F_1.1_II	11.07	2.46	74.9
F_1.2-1	13.27	4.82	80.15
F_1.2-2	7.55	–	76.62
F_1.2-3	3.44	3.44	62.46
F_1.3-1	6.35	1.27	58.25
F_1.3-2	5.13	–	72.53
F_1.4-1	10.69	–	60.52
F_1.5-1	42.14	7.80	61.83
P_1.6-1	34.78	–	86.50
P_1.6-2^a	90.00	6.67	73.31
F_1.6-1	11.53	4.60	68.71
S_2.1-1 ^b	13.04	15.66	86.13
S_2.1-2 ^b	4.90	1.84	88.27
S_2.1-3	18.99	22.79	31.73
S_2.2-1	13.60	–	18.57
S_2.2-2	7.79	–	19.9
S_2.3-1	0.00	–	21.93
F_3.1-1	67.41	23.68	45.86
F_3.2-1	28.65	4.77	64.88
P_3.3-1	193.95	46.31	57.49
F_3.3-1	53.14	48.53	57.41
P_3.4-1	53.62	7.94	39.66
F_3.4-1	15.41	5.60	51.57
F_3.5-1	97.88	16.04	70.22

Samples from plants processing biowaste are indicated by bold print

^aSample taken after an intermediate sieving step

^bSample of digestate pellets

corresponding pressed solid digestate, since the composts from plants #3.1, #3.3, and #3.5 were the most contaminated ones found in this investigation. Incidentally, the addition of cuttings as structuring material to the digestate for the composting step, which presumably would dilute the particle contamination (such added cuttings contain little to no plastic) is not able to compensate for this effect. All three plants in question, #3.1, #3.3, and #3.5, add cuttings in varied amounts, yet there is no correlation between the added amount and the residual plastic contamination of the finished composts. Moreover, composts from plant #3.2 (no press filtration, *no addition* of cuttings) were less contaminated than composts from plant #3.4 (no press filtration, *addition* of cuttings). Of course, other process conditions also contribute to the final results, while the number of sampled plants is at present too small for a statistically significant analysis of this contribution.

Chemical Signatures of the Plastic Fragments Found in the samples

Figures 2, 3 and 4 summarize the chemical signatures of the plastic fragments found in the investigated compost and solid digestate samples according to relative percentage. In Fig. 2 arrows indicate samples from plants processing biowaste. Only plastic types accounting for > 5% of the total number of fragments are specified. All other types are grouped as “others”.

According to these data, polyethylene (PE)-based fragments tend to dominate in the compost samples prepared from biowastes. This is independent on whether the compost is prepared by simple biowaste composting or via the more intensive two-stage process of digestion–composting. In all cases the domination of PE is more pronounced in the sieving fraction > 5 mm. The polymer type distribution



Fig. 1 Left: incoming greenery waste, right: incoming biowaste, both at plant #1.1

found in the greenery compost seems to be more diverse, with a stronger tendency towards polypropylene (PP) over PE. However, in particular in case of the simple composts, the samples typically contained only a small total number of fragments, a statistically relevant analysis is therefore not possible.

Of some concern is the category “other plastics”, which tended to accumulate in the 1–5 mm size fraction. Among the “other plastics”, we found mainly polyethylene terephthalate (PET), Platilon T (a thermoplastic adherent polyurethane film) and other polyurethanes, as well as polyvinyl chloride (PVC), acrylonitrile compounds such as acrylonitrile butadiene styrene and styrene–acrylonitrile, and Teflon compounds. Polymers such as poly(lactic acid) (PLA) or poly(butylene adipate-co-terephthalate) (PBAT) were occasionally also found, but were not considered in this study due to their presumed biodegradable nature. Notably, fragments with PBAT and PLA signatures were found only in the composts from the two-stage digester–composters, never in those from the simple biowaste composters.

In the case of the digestates from the agricultural biogas plants (Fig. 3), no sieving took place. Nevertheless, no plastic fragments were found in the case of plant #2.3, which corroborates previous findings (8) that fertilizers (digestates) from such plants are minimally contaminated with plastic. In case of plant #2.2, two samples were investigated. Both contained some plastic fragments > 5 mm, but no smaller fragments. Moreover, the contamination was very uniform. In the case of digestate sample S-2.2-1, 100% of the few fragments found in the size fraction > 5 mm were PP, while in the case of sample S-2.2-2, 50% were PE, and 50% PP (Fig. 3a). It is thus possible that the contamination was caused by a single piece of plastic entering the digester by accident. Both plants #2.2 and #2.3 exclusively processed agricultural waste and energy crops.

Plant #2.1 processed a wider selection of organic material, including organic waste from local markets and landscape conservation material (see Table 1 for details). In addition to fresh digestate, plant 2.1 produced digestate pellets as fertilizer. Two charges of pellets were sampled in addition to the fresh digestate. The contamination in terms of fragments > 5 mm was similar to that of the digestate from plant 2.2. For the first time, however, we also found significant numbers of fragments in the 1–5 mm size category in a fertilizer from an agricultural biogas plant. The diversity of the particle chemical signatures detected in the fertilizers from plant #2.1 (Fig. 3) is also much broader than that for the other two plants in category 2 and similar to the variability found for the biowaste processing plants.

Contamination of Liquid Fertilizer by Plastic Particles

Plants #3.1, #3.3, and #3.5 produce LF in addition to biowaste compost. LF has a low solid content and is produced by press filtration of the digestate obtained at the end of the anaerobic step. While the solids from the press filtration step thus enter the composting stage, LF is typically directly distributed on agricultural soil. Since LF is essentially a liquid, plastic particles down to a size of 10 µm could be isolated and identified in the LF samples using environmental techniques developed for water analysis (10), which was not possible in the case of the solid digestates and composts. The LF samples were also analyzed for fragments > 1 mm, but none were found. Presumably, these fragments were retained in the solid digestate during press filtration and went into the composting stage. As discussed before, this effect is most likely also responsible for the fact that the composts from plants #3.1, #3.3 and #3.5 contain a higher number of plastic particles than do the composts of plants #3.2 and #3.4. Table 4 summarizes the particle numbers and plastic types found in the LF samples.

LF from the biowaste treatment plants contained between 6000 and 12,000 MP fragments per liter. Most of these fragments had sizes between 22 and 300 µm. PP, PE, and PET were detected in all samples, while PS, silicone and PVC were found occasionally. In certain cases, e.g., in sample L3.5-1, we again observed large numbers of MP with IR signatures corresponding to biodegradable materials, mainly PBAT; however, these particles were not considered here for reasons already given.

In the case of the agricultural biogas plants (category 2), only the LFs produced by plants #2.1 and #2.3 were sampled since for technical reasons, LF from plant #2.2 was not available. In the case of plant #2.3, which produced a particularly clean solid digestate, the number of contaminating particles found in the LF was also negligible. Moreover, all particles had the chemical signature of silicone. Silicone is used in biogas plants for various purposes, including as an antifoaming agent, for the sealing of concrete floors and walls, and as an antimicrobial barrier layer [17, 18]. Finding silicone residues in LF is therefore not necessarily a surprise. By comparison, plant #2.1, which used a wider range of possibly pre-contaminated substrates and had no pre-sorting and/or sieving system installed, showed a higher contamination level in the case of LF. Most MPs found were in the range of 22–100 µm, and some were also in the range of 100–300 µm. PE, PP, and PS were again observed, but surprisingly large numbers of PET fragments were also observed. This is surprising since PET fragments > 1 mm were not found in the corresponding compost samples.

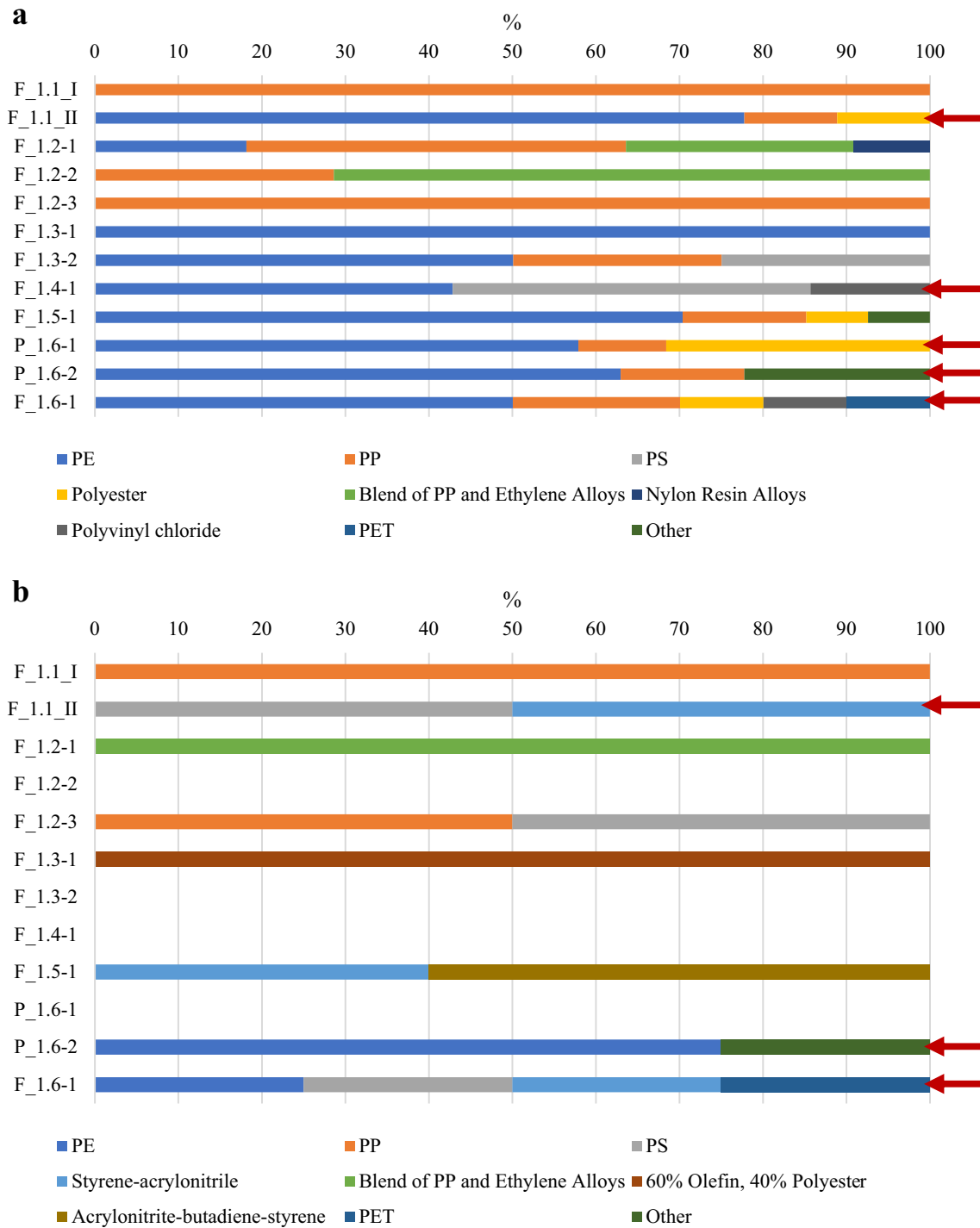


Fig. 2 Distribution over the material classes for plastic fragments found in plants from category 1 (simple composters). Arrows indicate samples from biowaste treatment plants. For the total number of

particles found in each sample, see Table 3. **a** >5 mm size category; **b** 1–5 mm size category. P_1.6-2: sample taken after the 12 mm sieving step but before the final 10 mm sieving step

Discussion

Our study focuses on current practices for the recycling of household biowaste into fertilizer using either simple

composting or the more economic two-stage digestion–composting approach. Three agricultural biogas plants (simple digesters) and several composting plants producing greenery compost were included in our study for comparison. As

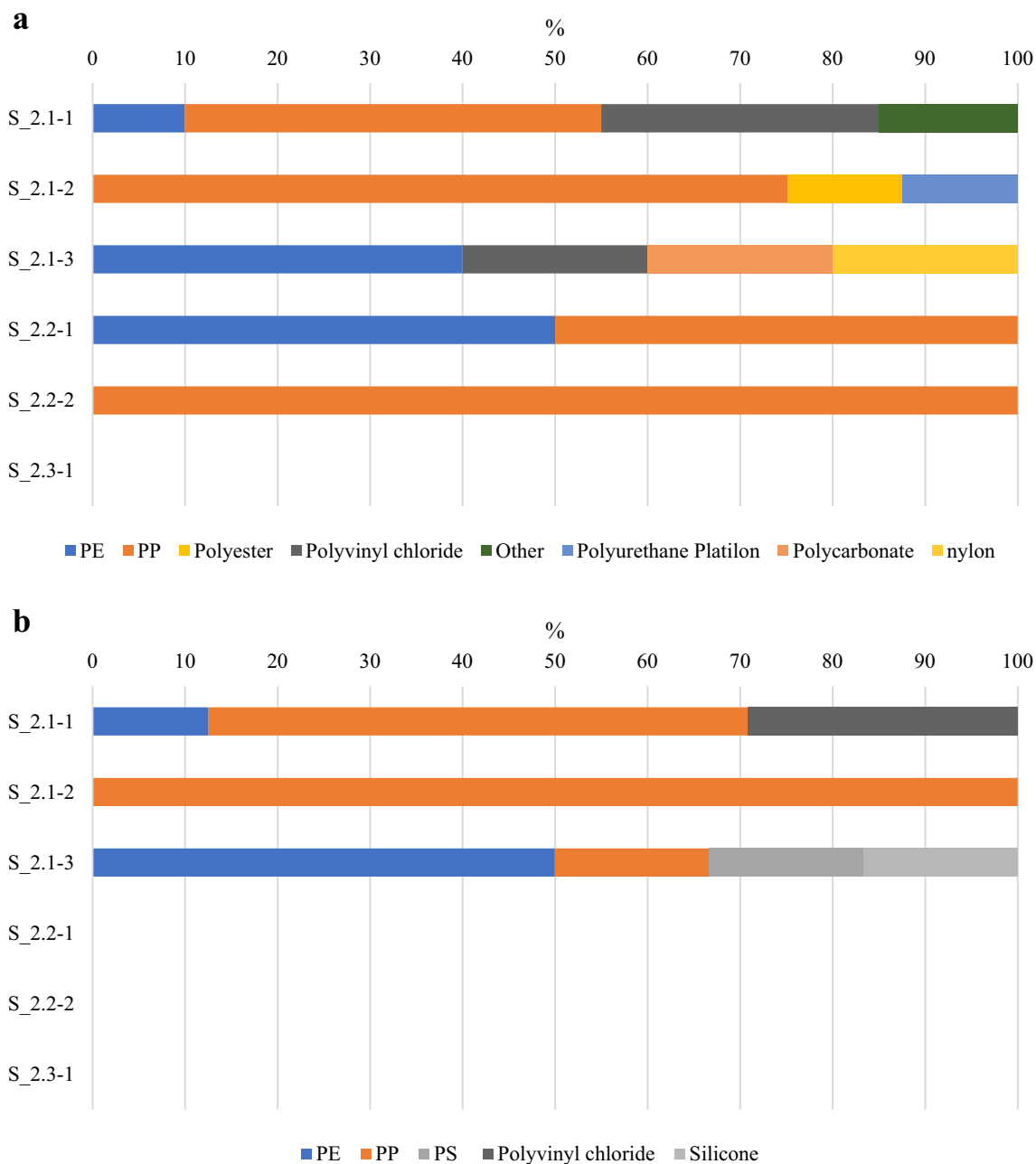


Fig. 3 Distribution over the material classes for plastic fragments found in plants from category 2 (agricultural biogas plants). For the total number of particles found in each sample, see Table 3. **a** > 5 mm

size category; **b** 1–5 mm size category. S_2.1-1 and S_2.1-2: digestate pellets made from dried and pressed digestate.

observed before [8], the liquid and solid fertilizers from the agricultural biogas plants exhibited unremarkable residual plastic contamination. Only the digestate from plant #2.1, i.e., the only agricultural biogas plant in our study that added a wider variety of organic material to its substrate mix, showed increased levels of contamination.

Greenery composts also showed only a low level of plastic contamination compared to the biowaste composts (Table 3). Plant #1.1 is of particular relevance in this regard,

since it comprises two composting lines operated in parallel, one for greenery waste (1.1_I) and the other for biowaste (1.1_II), under otherwise similar conditions. One exception in our data set is the greenery compost from plant #1.5, which, despite stemming from cuttings, contained an average of 50 plastic particles $\text{kg}_{\text{DW}}^{-1}$. With only 9500 t year⁻¹, plant #1.5 was by far the smallest in our study, and more stringent quality control of the input material together with a final sieving using a mesh size below the currently used

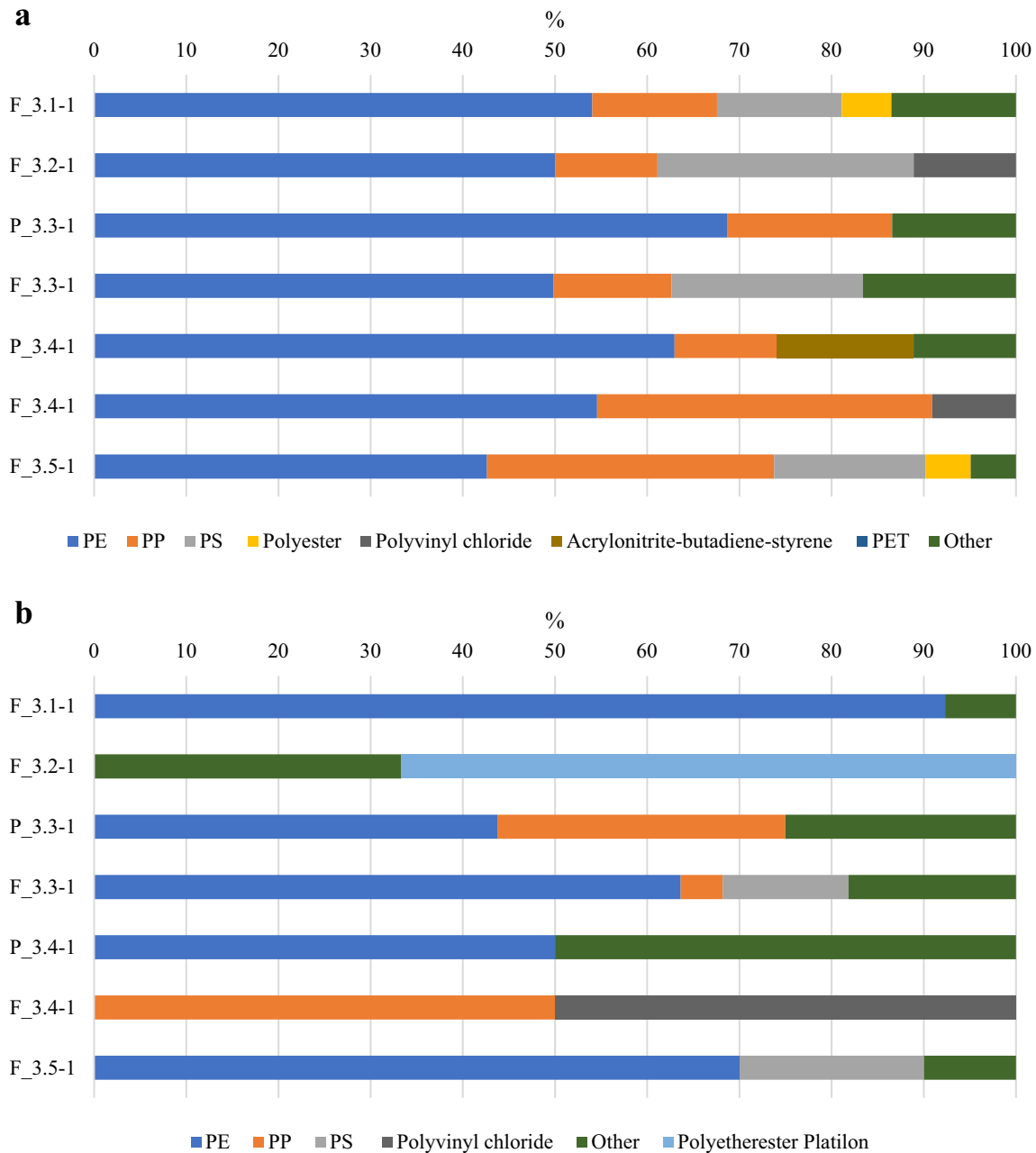


Fig. 4 Distribution over the material classes for plastic fragments found in plants from category 3 (digester-composters of biowaste). For the total number of particles found in each sample, see Table 3. **a** > 5 mm size category; **b** 1–5 mm size category

20 mm might help to improve the quality of the compost from that plant.

While biowaste compost in general tended to contain more plastic fragments than greenery compost, there was a consistent and significant difference in the level of contamination between the composts from the simple biowaste composters and those produced by the two-stage biowaste digester-composters. The composts from the digester-composters were significantly more contaminated by plastic fragments, even when the higher mass reduction achieved by the

two-stage process during biogas production or a possible enrichment of plastic fragments > 1 mm during press filtration in some of these plants is taken into account (Table 3). Simple biowaste composters often use bag slicers to gain access to organic material, whereas two-stage plants tend to use shredders. It seems that the latter approach, as beneficial as it is for efficient biogas production, aids in the formation of plastic fragments. This would explain why the composts produced in digester-composter plant #3.2 were among the least contaminated composts ($33 \text{ particles kg}_{\text{DW}}^{-1}$) found in

Table 4 Plastic particles per liter of liquid fertilizer and percentages according to size and type; biowaste treatment plants: L_3.1-1, L_3.3-1, L_3.5-1; agricultural biogas plants: L_2.1-1, L_2.3-1

Sample	Fragment number and type	11–22 μm	22–100 μm	100–300 μm	300–500 μm	500–1000 μm
L_3.1-1	Number	–	5120	2560	1280	1280
	PET		25.0%	50.0%		
	PE		25.0%			100%
	PP			50.0%		
	PS				100.0%	
L_3.3-1	Number	640	3840	2240	–	–
	PET	50.0%	33.3%	14.3%		
	PVC			14.3%		
	PE	50.0%	33.3%	28.6%		
	PP		16.7%	14.3%		
	PS		16.7%	28.6%		
L_3.5-1	Number	–	5120	6400	–	–
	PET			40.0%		
	PE		75.0%	40.0%		
	PP		25.0%	20.0%		
L_2.1-1	Number	–	1280	320	–	–
	PET	–	25.0%	100.0%	–	–
	PE	–	25.0%	–	–	–
	PP	–	25.0%	–	–	–
	PS	–	25.0%	–	–	–
L_2.3-1	Number	320	320	–	–	–
	Silicone	100.0%	100.0%	–	–	–

category 3. In contrast to all other plants in that category, plant #3.2 did not use a shredder to process the incoming material. Furthermore, the data from this plant suggest that using an anaerobic digestion step does not necessarily increase the plastic fragment content. Otherwise, one would expect the composts from plant #3.2 to show a higher content of residual plastic fragments.

While the anaerobic treatment and shorter composting times applied in two-stage plants are unlikely to influence the contamination of the finished composts with fragments of conventional plastics, these differences in operating conditions could explain why we found residues of biodegradable plastics in the composts (and LF, see below) from the two-stage plants but not in any of the composts from the single composting plants. The digester–composters included in our study typically only used composting times of 5–6 weeks (after digestion), in contrast to at least 12 weeks in the case of the simple composters. Anaerobic digestion is not expected to contribute to the degradation of biodegradable plastics, and the length of the subsequent composting stage may thus not be sufficient for the full degradation of such biodegradable materials. The pertinent literature suggests that once biodegradable plastics enter the environment, they can persist there for quite some time [19–21].

For all investigated compost samples (both biowaste and greenery), the final sieving step used to prepare the finished composts was effective in reducing the number of contaminating plastic fragments. However, sieving is much more efficient for fragments > 5 mm than for smaller fragments. Any processing step that increases the number of fragments, particularly that of smaller fragments, is therefore problematic. The bias for removing larger fragments in the final sieving step can be seen in Fig. S1. Whereas the lengths of the particles sieved with 10, 12, or 15 mm mesh sizes cover a very similar range, the widths of the retained particles tend to increase with the mesh size used during sieving, see also Table S1. If we presume the fragments pass a given hole “head on”, it makes sense that the fragment width determines the likelihood of passage. In terms of the types of plastics found in the most contaminated (> 30 particles $\text{kg}_{\text{DW}}^{-1}$) and hence most statistically relevant compost samples, PE was the most common type of plastic found in the biowaste composts. PP and PS, as well as some “other polymers” (individually representing > 5% of the total), were also found in the composts made from biowaste and/or cuttings. In the greenery composts, PP was the dominant polymer, along with PE.

Due to the restrictions of the analytical methods, mainly the need to isolate and clean fragments for spectroscopy, the

study of the composts was restricted to fragments retained by the 1 mm sieve. Given the especially high load of > 1 mm fragments in the composts from the digester–composters, the additional presence of yet smaller particles in the composts cannot be excluded. Three of the digester–composters produced LFs, recovered via press filtration after anaerobic digestion, which could be analyzed for plastic fragments down to 10 µm using techniques originally developed for water samples. According to the results, the LFs contained up to 10,000 MP particles with sizes of 10–1000 µm⁻¹, while no fragments > 1000 µm were found. According to common agricultural practices, LF is applied several times a year at a concentration of 2–3 L m⁻².

Most fragments/particles found in the LFs were in the range of 22–300 µm and smaller. The mechanical stress exerted on fermented plastics during the press filtration step can presumably lead to fragmentation and in consequence the formation of small MP particles, especially since the materials presumably become more brittle during anaerobic digestion due to the extraction of additives such as plasticizers [22]. It does not take many large fragments to result in a significant number of small ones. For instance, a single 4 mm × 4 mm fragment could break down in more than 100,000 fragments of 100 µm². Recently, it has been shown that PE and PS macroparticles (> 25 mm) can release 4–63 MP particles during the composting process [23]. While we thus still assume that most larger fragments present in a given digestate end up in the solid fraction after press filtration and thus in the composter, some fragmentation under the mechanical stress of press filtration may result in the heavily contaminated liquid fertilizer. The LFs produced by the agricultural biogas plants contained significant numbers of MPs from commodity plastics only in the case of plant #2.1, i.e., the plant where the solid digestate also contained unusually high plastic contamination. While significant, the MP content of the LF from plant #2.1 was still an order of magnitude less than that of the LFs from the biowaste treatment plants.

Chemically speaking, the MPs found in the LFs stemmed mostly from commodity plastics such as PE, PP and PS, all of which have been shown to be toxic or harmful to the environment [24–26]. Moreover, in all investigated LFs, fragments of PET were found in 22–40% of the detected particles (Table 4), even in those cases where PET was not found in larger fragments in the corresponding composts or digestates (Figs. 3, 4). This could be an indication that PET is easily fragmented into MPs under anaerobic/aerobic treatment of organic material. It has been shown that PET in soil can be highly toxic to nematodes [25].

Conclusions

Plant type and operating conditions have a major influence on the residual contamination of composts and organic fertilizers with plastic fragments. The removal of such fragments would cause a further reduction in process yield and efficiency. Reducing the plastic content in the incoming biowaste is thus still the most important measure for reducing the release of plastics and MPs into the environment via such composts and LF. Whether biodegradable materials may present a solution in this context was not part of our study. The fact that we did find residues of biodegradable material in some of the composts shows that the behavior of such materials during biowaste treatment may have to be reevaluated in the future.

Supplementary Information The online version contains supplementary material available at <https://doi.org/10.1007/s12649-022-01870-2>.

Acknowledgements We would like to thank the operators of the biowaste treatment plants for their cooperation and support. Furthermore, we would like to thank A. Schott, H. Schneider and K. Thompson for excellent technical assistance.

Author Contributions Conceptualization: TS, JNM, MGJL, FH, CL, RF. Methodology: TS, JNM, MJGL, FH, CL, RF. Validation: TS, JNM, MJGL, FH, CL, RF. Investigation: TS, JNM, FH, RF. Visualization: TS. Supervision: MGJL, CL, RF. Writing—original draft: TS, RF. Writing—review & editing: TS, JNM, MJGL, CL, RF.

Funding Open Access funding enabled and organized by Projekt DEAL. This study was funded by the Deutsche Forschungsgemeinschaft (DFG, German Research Foundation)—SFB 1357–391977956. We also gratefully acknowledge the financial support of the Ministry of the Environment, Climate Protection and Energy, Baden-Württemberg, Germany (Project: MiKoBo, Reference Numbers BMWK18001 and BMWK18007). German Research Foundation, CRC 1357—“Mikroplastik” 391977956 (TS, MGJL, CL, RF). Ministry of the Environment, Climate Protection and Energy, Baden-Württemberg, Germany BMWK18001 (TS, FH, CL, RF). Ministry of the Environment, Climate Protection and Energy, Baden-Württemberg, Germany BMWK18007 (JNM, MGJL, CL).

Data Availability All data are available in the main text or the supplementary materials.

Declarations

Competing Interests Authors declare that they have no competing interests.

Open Access This article is licensed under a Creative Commons Attribution 4.0 International License, which permits use, sharing, adaptation, distribution and reproduction in any medium or format, as long as you give appropriate credit to the original author(s) and the source, provide a link to the Creative Commons licence, and indicate if changes were made. The images or other third party material in this article are included in the article's Creative Commons licence, unless indicated otherwise in a credit line to the material. If material is not included in the article's Creative Commons licence and your intended use is not permitted by statutory regulation or exceeds the permitted use, you will need to obtain permission directly from the copyright holder. To view a copy of this licence, visit <http://creativecommons.org/licenses/by/4.0/>.

References

- Lassen, C., Hansen, S.F., Magnusson, K., Norén, F., Hartmann, N.I., Jensen, P.R., Nielsen, T.G., Brinch, A.: Microplastics—occurrence, effects and sources of releases to the environment in Denmark. (2012). <https://mst.dk/service/publikationer/publikationsarkiv/2015/nov/rapport-om-mikroplast/>
- Lehmphul, K.: Sources of Microplastics Relevant to Marine Protection in Germany. Umweltbundesamt, Dessau-Roßlau (2015)
- Stolte, A., Forster, S., Gerdts, G., Schubert, H.: Microplastic concentrations in beach sediments along the German Baltic coast. *Mar. Pollut. Bull.* **99**, 216–229 (2015). <https://doi.org/10.1016/j.marpolbul.2015.07.022>
- Kawecki, D., Nowack, B.: Polymer-specific modeling of the environmental emissions of seven commodity plastics as macro- and microplastics. *Environ. Sci. Technol.* **53**, 9664–9676 (2019). <https://doi.org/10.1021/acs.est.9b02900>
- Allen, S., Allen, D., Phoenix, V.R., Le Roux, G., Durántez Jiménez, P., Simonneau, A., Binet, S., Galop, D.: Atmospheric transport and deposition of microplastics in a remote mountain catchment. *Nat. Geosci.* **12**, 339–344 (2019). <https://doi.org/10.1038/s41561-019-0335-5>
- Baensch-Baltruschat, B., Kocher, B., Stock, F., Reifferscheid, G.: Tyre and road wear particles (TRWP)—a review of generation, properties, emissions, human health risk, ecotoxicity, and fate in the environment. *Sci. Total Environ.* **733**, 137823 (2020). <https://doi.org/10.1016/j.scitotenv.2020.137823>
- Steinmetz, Z., Wollmann, C., Schaefer, M., Buchmann, C., David, J., Tröger, J., Muñoz, K., Frör, O., Schaumann, G.E.: Plastic mulching in agriculture. Trading short-term agronomic benefits for long-term soil degradation? *Sci. Total Environ.* **550**, 690–705 (2016). <https://doi.org/10.1016/j.scitotenv.2016.01.153>
- Weithmann, N., Möller, J.N., Löder, M.G.J., Piehl, S., Laforsch, C., Freitag, R.: Organic fertilizer as a vehicle for the entry of microplastic into the environment. *Sci. Adv.* **4**, eaap8060 (2018). <https://doi.org/10.1126/sciadv.aap8060>
- Jędrzak, A.: Composting and fermentation of biowaste—advantages and disadvantages of processes. *Civ. Environ. Eng. Rep.* **28**, 71–87 (2018). <https://doi.org/10.2478/ceer-2018-0052>
- Regulation, E.U.: 2019/1009 of the European Parliament and of the Council of 5 June 2019 laying down rules on the making available on the market of EU fertilizing products and amending Regulations (EC) No 1069/2009 and (EC) No 1107/2009 and repealing Regulation (EC) No 2003/2003
- Löder, M.G.J., Kuczera, M., Mintenig, S., Lorenz, C., Gerdts, G., Löder, M.G.J., Kuczera, M., Mintenig, S., Lorenz, C., Gerdts, G.: Focal plane array detector-based micro-Fourier-transform infrared imaging for the analysis of microplastics in environmental samples. *Environ. Chem.* **12**, 563–581 (2015). <https://doi.org/10.1071/EN14205>
- Kehres, B., Bundesgütegemeinschaft Kompost: Methodenbuch zur Analyse organischer Düngemittel, Bodenverbesserungsmittel und Substrate. Selbstverlag, Köln (2006)
- Löder, M.G.J., Imhof, H.K., Ladehoff, M., Löschel, L.A., Lorenz, C., Mintenig, S., Piehl, S., Primpke, S., Schrank, I., Laforsch, C., Gerdts, G.: Enzymatic purification of microplastics in environmental samples. *Environ. Sci. Technol.* **51**, 14283–14292 (2017). <https://doi.org/10.1021/acs.est.7b03055>
- Möller, J.N., Heisel, I., Satzger, A., Vizsolyi, E.C., Oster, S.D.J., Agarwal, S., Laforsch, C., Löder, M.G.J.: Tackling the challenge of extracting microplastics from soils: a protocol to purify soil samples for spectroscopic analysis. *Environ. Toxicol. Chem.* **41**, 844–857 (2022). <https://doi.org/10.1002/etc.5024>
- Hufnagl, B., Steiner, D., Renner, E., Löder, J., Laforsch, M.G., Lohninger, C.: A methodology for the fast identification and monitoring of microplastics in environmental samples using random decision forest classifiers. *Anal. Methods* **11**, 2277–2285 (2019). <https://doi.org/10.1039/C9AY00252A>
- Hufnagl, B., Stibi, M., Martirosyan, H., Wilczek, U., Möller, J.N., Löder, M.G.J., Laforsch, C., Lohninger, H.: Computer-assisted analysis of microplastics in environmental samples based on μ FTIR imaging in combination with machine learning. *Environ. Sci. Technol. Lett.* **9**, 90–95 (2022). <https://doi.org/10.1021/acs.estlett.1c00851>
- Surita, S.C., Tansel, B.: Emergence and fate of cyclic volatile polydimethylsiloxanes (D4, D5) in municipal waste streams: release mechanisms, partitioning and persistence in air, water, soil and sediments. *Sci. Total Environ.* **468–469**, 46–52 (2014). <https://doi.org/10.1016/j.scitotenv.2013.08.006>
- Tansel, B., Surita, S.C.: Differences in volatile methyl siloxane (VMS) profiles in biogas from landfills and anaerobic digesters and energetics of VMS transformations. *Waste Manag.* **34**, 2271–2277 (2014). <https://doi.org/10.1016/j.wasman.2014.07.025>
- Helmberger, M.S., Tiemann, L.K., Grieshop, M.J.: Towards an ecology of soil microplastics. *Funct. Ecol.* **34**, 550–560 (2020). <https://doi.org/10.1111/1365-2435.13495>
- Ng, E.-L., Huerta Lwanga, E., Eldridge, S.M., Johnston, P., Hu, H.-W., Geissen, V., Chen, D.: An overview of microplastic and nanoplastic pollution in agroecosystems. *Sci. Total Environ.* **627**, 1377–1388 (2018). <https://doi.org/10.1016/j.scitotenv.2018.01.341>
- Palsikowski, P.A., Kuchnier, C.N., Pinheiro, I.F., Morales, A.R.: Biodegradation in soil of PLA/PBAT blends compatibilized with chain extender. *J. Polym. Environ.* **26**, 330–341 (2018). <https://doi.org/10.1007/s10924-017-0951-3>
- Boll, M., Geiger, R., Junghare, M., Schink, B.: Microbial degradation of phthalates: biochemistry and environmental implications. *Environ. Microbiol. Rep.* **12**, 3–15 (2020). <https://doi.org/10.1111/1758-2229.12787>
- Gui, J., Sun, Y., Wang, J., Chen, X., Zhang, S., Wu, D.: Microplastics in composting of rural domestic waste: abundance, characteristics, and release from the surface of macroplastics. *Environ. Pollution.* **274**, 116553 (2021). <https://doi.org/10.1016/j.envpol.2021.116553>
- Hüffer, T., Metzelder, F., Sigmund, G., Slawek, S., Schmidt, T.C., Hofmann, T.: Polyethylene microplastics influence the transport of organic contaminants in soil. *Sci. Total Environ.* **657**, 242–247 (2019). <https://doi.org/10.1016/j.scitotenv.2018.12.047>
- Kim, S.W., Waldman, W.R., Kim, T.-Y., Rillig, M.C.: Effects of different microplastics on nematodes in the soil environment: tracking the extractable additives using an ecotoxicological approach. *Environ. Sci. Technol.* **54**, 13868–13878 (2020). <https://doi.org/10.1021/acs.est.0c04641>
- Zhu, K., Jia, H., Zhao, S., Xia, T., Guo, X., Wang, T., Zhu, L.: Formation of environmentally persistent free radicals on microplastics under light irradiation. *Environ. Sci. Technol.* **53**, 8177–8186 (2019). <https://doi.org/10.1021/acs.est.9b01474>

Publisher's Note Springer Nature remains neutral with regard to jurisdictional claims in published maps and institutional affiliations.

Supplementary Materials

Title

Microplastic contamination of composts and liquid fertilizers from municipal biowaste treatment plants — effects of the operating conditions

Journal:

Waste and Biomass Valorization

Authors

Thomas Steiner¹, Julia N. Möller², Martin G.J. Löder², Frank Hilbrig^{1†}, Christian Laforsch², Ruth Freitag^{1*}

Affiliations

¹ Process Biotechnology, University of Bayreuth

² Animal Ecology I, University of Bayreuth

* Corresponding author address: Process Biotechnology, University of Bayreuth,

Universitätsstrasse 30, 95440 Bayreuth, Germany, phone: +49 921 557371, Fax: 0049 921

557375, e-mail ruth.freitag@uni-bayreuth.de

Table S1: Type or paste caption here. Create a page break and paste in the Table above the caption.

Sample	Size				Size				Size			
	> 5 mm				1–5 mm				total			
	length [mm]	SD	width [mm]	SD	length [mm]	SD	width [mm]	SD	length [mm]	SD	width [mm]	SD
F_1.1_I	16.06	-	2.16	-	4.35	-	1.22	-	10.21	5.86	1.69	0.47
F_1.1_II	13.55	5.38	2.79	1.81	3.39	0.24	1.45	0.08	11.70	6.24	2.54	1.72
F_1.2-1	18.68	14.81	4.48	4.06	5.78	3.11	1.88	1.04	15.24	14.00	3.79	3.70
F_1.2-2	22.06	8.94	10.05	0.96	6.75	2.05	0.92	0.29	11.12	8.58	3.53	4.16
F_1.2-3	14.83	5.31	3.00	2.32	4.02	0.45	3.64	0.56	9.43	6.59	3.32	1.72
F_1.3-1	20.34	11.84	9.04	9.22	5.11	-	4.15	-	17.81	12.21	8.22	8.61
F_1.3-2	9.46	8.02	8.19	6.93	-	-	-	-	9.46	8.02	8.19	6.93
F_1.4-1	11.96	9.25	7.47	6.82	-	-	-	-	11.96	9.25	7.47	6.82
F_1.5-1	61.12	36.95	18.13	24.22	7.42	2.21	2.28	0.34	52.73	39.15	15.66	22.98
P_1.6-1¹⁾	35.79	17.17	20.81	14.75	-	-	-	-	35.79	17.17	20.81	14.75
P_1.6-2¹⁾	23.93	12.00	9.22	7.01	15.34	5.21	2.93	1.56	23.47	11.80	8.91	6.92
F_1.6-1	13.82	9.72	5.01	4.55	6.91	2.37	2.95	0.97	11.85	8.88	4.43	3.99
S_2.1-1 ²⁾	6.78	3.69	2.68	1.63	5.39	2.24	1.92	1.13	6.02	3.07	2.27	1.43
S_2.1-2 ²⁾	6.18	3.00	2.86	1.64	6.31	2.48	1.91	1.01	6.21	2.87	2.60	1.55
S_2.1-3	16.50	10.65	8.47	8.56	6.08	5.23	2.10	1.77	10.82	9.67	5.00	6.71
S_2.2-1	19.72	9.17	5.08	4.55	-	-	-	-	19.72	9.17	5.08	4.55
S_2.2-2	47.87	0.98	0.53	0.04	-	-	-	-	47.87	0.98	0.53	0.04
S_2.3-1	-	-	-	-	-	-	-	-	-	-	-	-
F_3.1-1	19.15	10.39	6.99	5.70	8.19	3.45	3.73	2.72	16.30	10.30	6.14	5.29
F_3.2-1	30.65	37.01	16.79	24.98	1.66	0.39	1.19	0.12	26.50	35.73	14.56	23.76
P_3.3-1	69.67	80.93	26.72	35.71	10.89	6.75	4.41	1.93	58.73	76.57	22.57	33.38
F_3.3-1	12.41	6.51	4.41	2.46	10.30	5.32	3.92	2.32	11.23	6.15	4.11	2.42
P_3.4-1	45.67	36.72	22.43	27.29	7.03	3.22	3.39	2.59	40.69	36.66	19.97	36.66
F_3.4-1	17.07	7.77	7.96	4.96	6.24	2.37	2.74	1.16	14.22	8.29	6.58	4.87
F_3.5-1	15.35	8.82	5.17	3.76	10.18	4.15	3.64	1.31	14.62	8.52	4.96	3.56

1) The samples from P_1.6–1 and P_1.6–2 were from two different precompost batches, P1.6–1 was a sample before the fine sieving steps, and P_1.6–2 was a sample after the fine sieving step (12 mm mesh size). 2) The samples from S_2.1–1 and S_2.1–2 were taken from digestate pellets made from dried and pressed digestate. Samples printed in bold use biowaste as the substrate and the other cuttings.

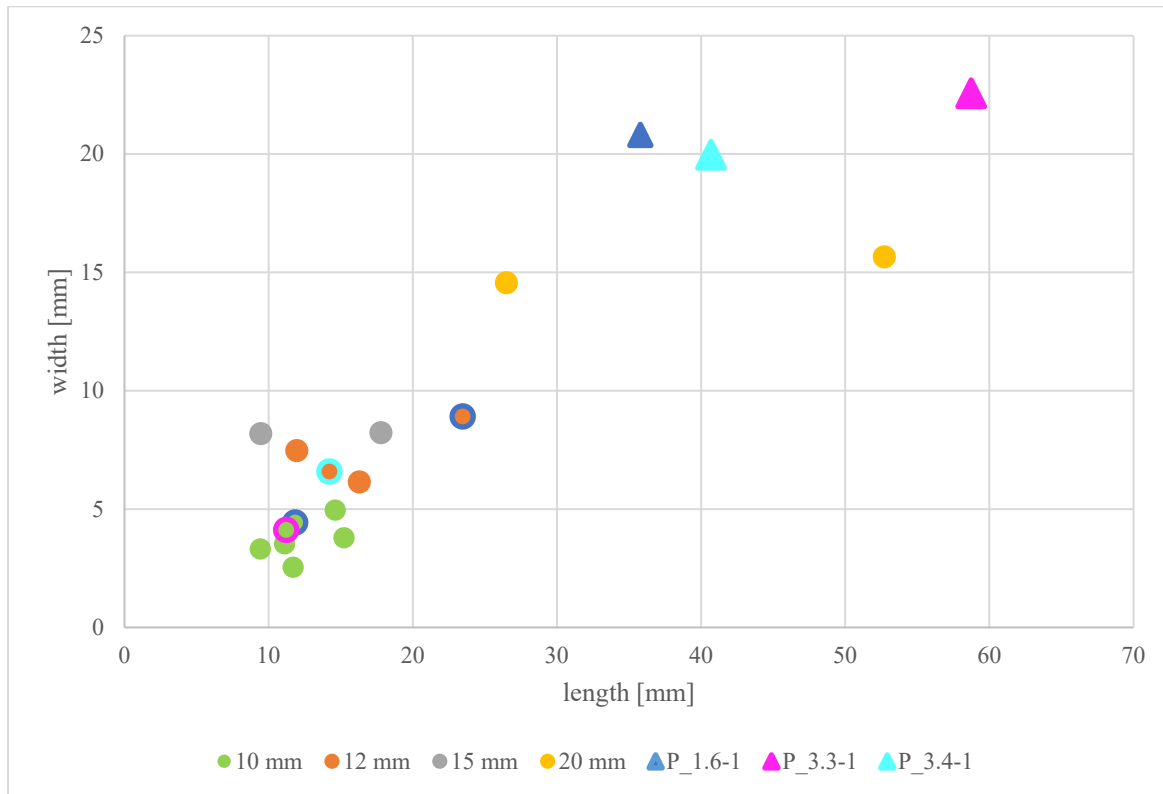


Figure S1: Average sizes (length x width) of particles recovered from individual samples (circles) as a function of the final sieving mesh size; the sizes of sampled precomposts (triangles) are given for comparison.

Figure S1 shows the size of the recovered particles (average length x average width) from individual compost samples (circles) as a function of the final sieving step. Data for the particles found in the available precomposts are given for comparison (triangles). To facilitate the direct comparison of the data for precomposts to that of the corresponding finished composts, the data points for finished composts are coded with a ring matching the color of the corresponding precompost data point where available. Samples from the agricultural biogas plants were not included since they were not sieved. Compost sample F-1.1_I-1 was also not included since the number of particles in this sample was too small for statistical consideration. Average values and standard deviations for the fragment sizes (length x width) are given in Table S1.

Article 8

Municipal biowaste treatment plants contribute to the contamination of the environment with residues of biodegradable plastics with putative higher persistence potential



OPEN

Municipal biowaste treatment plants contribute to the contamination of the environment with residues of biodegradable plastics with putative higher persistence potential

Thomas Steiner^{1,4}, Yuanhu Zhang^{2,4}, Julia N. Möller^{3,4}, Seema Agarwal², Martin G. J. Löder³, Andreas Greiner^{2,5}, Christian Laforsch^{3,5} & Ruth Freitag^{1,5}✉

Biodegradable plastics (BDP) are expected to mineralize easily, in particular under conditions of technical composting. However, the complexity of the sample matrix has largely prevented degradation studies under realistic conditions. Here composts and fertilizers from state-of-the-art municipal combined anaerobic/aerobic biowaste treatment plants were investigated for residues of BDP. We found BDP fragments > 1 mm in significant numbers in the final composts intended as fertilizer for agriculture and gardening. Compared to pristine compostable bags, the recovered BDP fragments showed differences in their material properties, which potentially renders them less prone to further biodegradation. BDP fragments < 1 mm were extracted in bulk and came up to 0.43 wt% of compost dry weight. Finally, the liquid fertilizer produced during the anaerobic treatment contained several thousand BDP fragments < 500 µm per liter. Hence, our study questions, if currently available BDP are compatible with applications in areas of environmental relevance, such as fertilizer production.

Biodegradable plastics (BDP) are increasingly proposed as eco-friendly alternatives to commodity plastics for foils, wrappings and bags. One area where the utilization of BDP could be of significant benefit is the collection of organic household waste. Currently most collected household biowaste is contaminated by conventional plastic bags, presumably because a significant fraction of the population prefers, if at all, to collect its biowaste in such bags. However, conventional plastics are not supposed to enter a biowaste treatment plant, since they will not degrade. In consequence they have to be removed as completely as possible from the incoming biowaste by elaborate sorting procedures, which incidentally also leads to significant losses of degradable organic material. Since the biogas (electricity, heat) and fertilizer produced from that material create the revenues, while the refuse has to be disposed at considerably costs, any such loss is not in the interest of the plant operators. In spite of the elaborate preparation, the entry of plastics into biowaste treatment plants cannot be completely prevented and strict regulation have been introduced inter alia in regard to the maximum amount of plastic allowed, e.g. in certified compost of high quality, such as < 0.1 wt% according to §3, 4b, DüMV and §3, 4c, DüMV. For reasons of practicability, only plastic fragments > 2 mm are counted for the quantification of the contamination, a limit which is expected to be lowered to fragments > 1 mm in the near future. In this situation, compostable plastic

¹Process Biotechnology, University of Bayreuth, Universitätsstrasse 30, 95440 Bayreuth, Germany. ²Macromolecular Chemistry II, University of Bayreuth, Bayreuth, Germany. ³Animal Ecology I & BayCEER, University of Bayreuth, Bayreuth, Germany. ⁴These authors contributed equally: Thomas Steiner, Yuanhu Zhang and Julia N. Möller. ⁵These authors jointly supervised this work: Andreas Greiner, Christian Laforsch, and Ruth Freitag. ✉email: ruth.freitag@uni-bayreuth.de

bags are seen as an attractive option, in particular since the conditions during technical biowaste treatment by composting should be ideal for their breakdown and dedicated bags for the purpose of household biowaste collection have appeared in supermarkets. Admittedly, not all adverse effects of foils and bags in biowaste treatment plants would automatically be resolved through the introduction of biodegradable bags. Operators have been known to fear for their machinery, in particular during anaerobic digestion, where biodegradable materials are not expected to disintegrate to a significant degree. However, much in this regard depends on the actual operation conditions. Plants with active mixing may face more difficulties than box plants.

A typical definition for biodegradability is given in European Norm EN 13432 (Requirements for packaging recoverable through composting and biodegradation—Test scheme and evaluation criteria for the final acceptance of packaging¹), which states that a material is biodegradable, if it is converted (‘mineralized’) by microbial activity in the presence of oxygen into CO₂, water, mineral salts, and biomass or in the absence of oxygen into methane, CO₂, water, mineral salts, and biomass. While the definition is clear, actual biodegradation is typically estimated in a non-specific manner through a comparison of the CO₂ produced by an aerobic standard culture in the presence of the test material compared to a culture without as well as a culture containing similar amounts of a natural biodegradable material such as cellulose. Under these circumstances nothing is learned about the mechanism of breakdown of the biodegradable material, in particular, if a significant part of it remains as micro- and nanoplastics, i.e. particles, which are considered to have considerable impact on environmental and human health². Moreover, current biodegradable/compostable materials are not certified for disintegration under anaerobic conditions. In addition, the term compostable is used in the context of biodegradable plastics. EN 13432 defines a material as compostable, if 90 wt% of the material is fragmented (disintegrated) into particles < 2 mm, i.e. below the limit at which particles “count”, after twelve weeks of standardized composting and fully mineralized by 90 wt% within 6 months. The remaining 10 wt% may be transformed into biomass or simply be fragmented into microplastic. In addition, a compostable material may not bring heavy metals or introduce ecotoxic effects in the final compost.

Studies investigating the fate of BDP under realistic conditions, i.e., in technical systems for organic waste management (composting and biogas plants), are still rare, in particular in regard to fragments < 2 mm. A recent study by members of our group found that composts and fertilizers from biowaste treatment plants are a path of entry into the environment for microplastic³, but BDP was not considered in this case. Since then, a few studies on BDP in technical biowaste treatment and composting plants have appeared in trade journals^{4–6}. However, these considered only residual fragments > 2 mm, which, according to these studies, were no longer in evidence after the composts had been conditioned by the customary sieving steps. In one case, foils certified as biodegradable were purposely introduced in controlled amounts into the digestion/composting process, and again no plastic fragments were visible in the finished—sieved—compost⁶. The size fraction < 2 mm was not considered in any of these studies.

Finally, the degradation of BDP in the environment has been studied. Admittedly, the certification of a material as biodegradable/compostable concerns the behavior of said material under composting conditions rather than a possible environmental impact, e.g. after littering. However, these environmental studies are highly relevant in regard to any residual BDP released into the environment with the composts. For instance, degradation in fresh and salt water, has for some BDP been less efficient than one would expect for a truly biodegradable material⁷. Physical properties seem to play a role, as some studies have shown a significant impact of a BDP’s crystallinity on its susceptibility to enzymatic depolymerization^{8,9}. For microbial digestion under both aerobic¹⁰ and anaerobic⁹ conditions, the polyester PHBV (poly(hydroxybutyrate-cohydroxyvalerate) in the semicrystalline state was found to degrade more slowly than the corresponding amorphous material. Studies on the use of biodegradable foils for agricultural purposes^{11–13} show that BDP can persist for several years in the environment, while the question of whether they are indeed finally mineralized or merely disintegrated into yet smaller fragments under environmental conditions is not fully resolved.

Compostable materials are designed for disintegration/mineralization through composting. Technical composting plants provide optimal conditions for biodegradation, both in terms of the process conditions (temperature, intensive aeration) and the metabolic activity of the specialized microbial communities found therein. If mineralization is incomplete under these circumstances, the remaining material is released into the environment, where it may persist for an unknown time, with putatively all the negative consequences already known for commodity plastics^{14,15}. The aim of this study was therefore, to determine to what extent residues of BDP can be found in the fertilizers (compost, liquid fertilizer) produced by organic waste treatment plants and thereby contribute to an ongoing discussion of whether the currently available BDP are already suited to replace conventional plastics in environmentally sensitive areas.

Results and discussion

Choice of biowaste treatment plants and sample identifiers. Compost samples were collected from four central municipal biowaste treatment plants (denominated as #1 to #4) in Baden-Württemberg, Germany (Table 1). All plants used a state-of-the-art two-stage biowaste treatment process comprising of (a) anaerobic digestion/biogas production and (b) subsequent composting of the solid digestate to produce a high-quality mature compost sold for direct use as fertilizer in agriculture. The composts were regularly analyzed by an independent laboratory for quality and residual contamination and consistently fulfilled the quality requirements of the label RAL-GZ 251 Gütezeichen Kompost of the German Bundesgütegemeinschaft Kompost e.V. (www.gz-kompost.de). Plants #1 and #3 produce in addition a liquid fertilizer, which is separated from the solid digestate at the end of stage a) by press filtration and which is also intended for direct use on agricultural soil (replacement of liquid manure). In case of plants #1, #3, and #4 up to 25 wt% of shrub/tree cuttings were added to the solid digestate for composting. All plants used sieving (typically with a 12 or a 20 mm mesh) at the end of

	Plant #1		Plant #2		Plant #3				Plant #4			
Compost sample type	Finished		Finished		Pre		Finished		Pre		Finished	
Biowaste preparation	Shredder, sieving (80 mm)		None		Shredder				Cross-flow shredder, sieving (2 lines: biowaste 60 mm, shrub/tree cuttings 80 mm)			
Anaerobic digestion	Plug flow 55 °C average 21 days		Box fermenter 40 °C average 40 days		Plug flow 55 °C average 21 days				Plug flow average 21 days [†]			
Composting	Up to 5 weeks		At least 5.5 weeks		Up to 9 weeks				6 weeks			
Final sieving step	12 mm		20 mm				Yes ^b				12 mm	
Products	Compost and liquid fertilizer ^a		Only compost		Compost and liquid fertilizer ^a				Only compost			
Fragment size (mm)	>5	1–5	>5	1–5	>5	1–5	>5	1–5	>5	1–5	>5	1–5
Number of BDP fragments per kg of compost ^c	16	18	–	19	29	3	–	–	2	4	–	–

Table 1. Technical data of the investigated plants and incidence of BDP fragments in the sampled composts.

^aPart of the liquid fraction was returned into the fermenter for mashing the substrate. [†]One part of the digestate is dried and composted, another part is mixed with fresh substrate and returned to the fermenter. ^bNo details available. ^cDry weight.

the process to assure the necessary purity of their finished composts. Whenever technically possible, we as well took samples of the pre-compost immediately before this final sieving step to evaluate its contribution to the removal of residual BDP fragments. For analysis, composts were passed consecutively through two sieves with mesh sizes of 5 mm and 1 mm, yielding two fragment preparations for IR-analysis namely a >5 mm fraction corresponding to the contamination by residual “macroplastic” (5 mm is a commonly used upper size limit for “microplastic”, anything larger is macroplastic) and a 1–5 mm fraction corresponding to the regulatory relevant residual contamination by microplastic. The lower limit of 1 mm rather than 2 mm was chosen in anticipation of the expected changes in regulation, where the replacement of the 2 mm limit by a 1 mm limit is imminent.

Occurrence of plastic fragments >1 mm in the sampled composts. Composting times of 5–9 weeks were used in the investigated plants (Table 1), which is shorter than the 12 weeks indicated in EN 13432 for the 90% disintegration of a compostable plastic material, but a realistic time span for state-of-the-art technical waste treatment. Since we were not in a position to estimate the quantity of BDP entering the plants, since for technical reasons we were unable to obtain a representative sample, we cannot say, whether any residual BDP detected by us in the finished composts was due to a yet incomplete disintegration process or whether it corresponds to the 10% material still permissible by EN 13432 even after the full composting step. However, in 7 out of the 12 sampled composts and pre-composts fragments with chemical signatures corresponding to the BDPs poly (lactic acid) (PLA) and poly (butylene-adipate-co-terephthalate) (PBAT) were identified in the >5 mm and/or the 1–5 mm sieving fractions using FTIR analysis³ (Fig. 1; Table 1). All recovered fragments appeared to stem from foils, bags or packaging, since they were thin compared to their length and width (see Suppl Figure S1 for typical examples). Fragments with overlapping signatures, most likely PBAT/PLA mixtures or blends, were also found (see Suppl Figure S2 for the interpretation of the spectra). In addition, the recorded BDP fragment spectra (Fig. 1A) showed high similarity to the FTIR spectra of commercial compostable bags sold in the vicinity of the biowaste treatment plants (Fig. 1B), which together with the geometry of the recovered fragments led us to assuming that the majority of the BDP entered the biowaste in the form of such bags.

The BDP fragments were found alongside fragments of commodity plastics (mostly PE) in all cases. Finished composts tended to contain fewer and smaller fragments than the corresponding pre-composts. The final sieving of the pre-composts to prepare the finished composts hence appears to be quite effective in removing such fragments, in particular those from the >5 mm size fraction (Table 1) and for that reason has become state-of-the-art in preparing quality composts (contamination by plastic fragments >2 mm of less than 0.1 wt%). Given that the size of the fragments is a crucial factor regarding ecological risk, we analyzed the sizes (length \times width) of the BDP fragments in comparison to that of the plastic fragments with signatures of commodity plastics such as PE (Fig. 2). BDP fragments found in a given compost sample tended to be smaller than the fragments stemming from non-BDP materials, which may indicate that BDPs degrade faster or tend to disintegrate into tinier particles than commodity plastics. This may also explain why in the compost from plant #2, no BDP fragments were found in the particle fraction retained by the 5 mm sieve (>5 mm fraction), while 19 such particles were found in the fraction then retained by the 1 mm sieve (1–5 mm fraction). Interestingly, plant #2 is the only one included in our study that uses no mechanical breakdown of the incoming biowaste. This reduces the mechanical stress on the incoming material. Mechanical stress can alter the properties of plastic foils such as the crystallinity whereby crystallinity has been shown to influence the biological degradation of BDP such as PLA⁷.

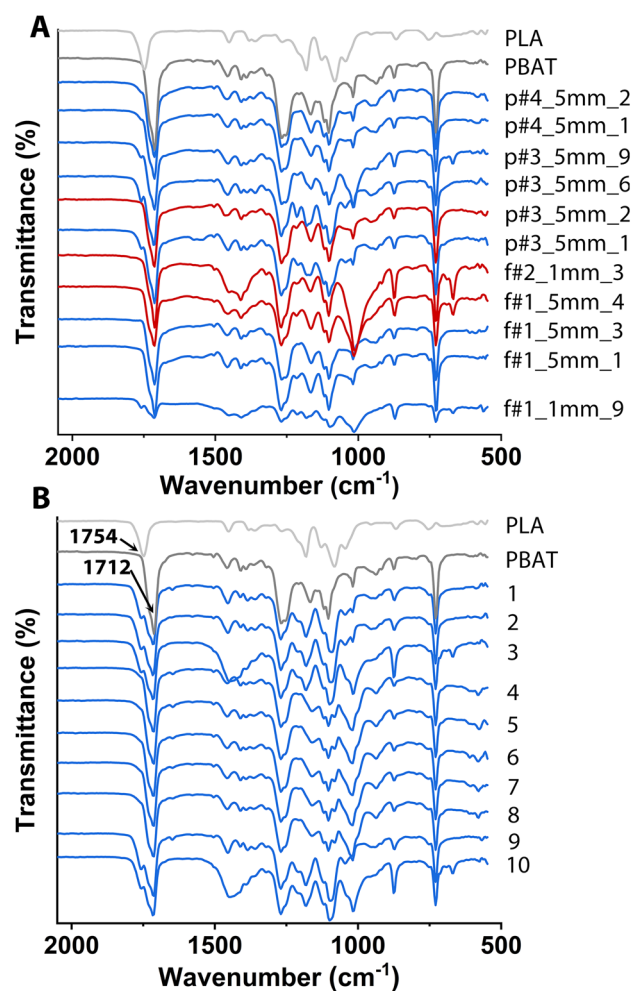


Figure 1. FTIR spectra of BDP fragments from composts and commercial bags. **(A)** BDP fragments recovered from the composts and **(B)** the commercial compostable bags. Fragments were coded as follows: p or f for pre-compost or finished compost, followed by the plant number (#1 to #4), an indication of the size fraction (>5 mm or 1–5 mm) in which the fragment was found, and finally, the fragment number. Fragment F#1_5mm_4 therefore represents the 4th fragment collected in the >5 mm size fraction from the finished compost of plant number 1. Bags were arbitrarily numbered 1–10, see Suppl Table S1 for supplier information. The spectra (in grey) of the reference materials for PLA and PBAT are given as basis for the interpretation. Spectra in red refer to test samples consisting only of PBAT, while those in blue indicate samples composed of PBAT/PLA mixtures.

Material characteristics of BDP fragments in comparison to those of commercial biodegradable bags.

In order to verify whether the BDP fragments recovered from the composts differed from the compostable bags in any parameter with possible relevance for biodegradation and environmental impact¹⁶, the physico-chemical properties of bags and fragments were studied in detail. Since we wanted to have a maximum of information of the BDP fragments, size/weight was a limiting factor in selecting fragments for analysis. Fragments of at least 1 mg were required for the FT-IR analysis. 5 mg-fragments could be analyzed in addition by ¹H-NMR, while the full set of analytics (FT-IR, ¹H-NMR, and DSC) required at least 10 mg of sample.

For insight into the chemical composition, ¹H-NMR spectra of the commercial bags and all suitable BDP fragments were compared (Fig. 3). In case of material mixtures and blends, the ¹H-NMR analysis allows quantification of the PBAT/PLA weight ratio in the materials and also of the ratio of the butylene terephthalate (BT) and butylene adipate (BA) units in the involved PBAT polyesters.

The ¹H-NMR spectra corroborate the FTIR measurements in that all investigated commercial bags were made from PBAT/PLA mixtures of varied composition (Table 2). By comparison, some of the fragments, for instance, f#1_5mm_4, appeared to consist of only PBAT. Other fragments, e.g., f#1_1mm_9, were mixtures of PLA and PBAT (Table 2). However, even in the case of PBAT/PLA mixtures, the average PBAT content tended to be higher in the fragments than in the bags, while the BT/BA monomer ratio in the respective PBATs, was also significantly higher in the fragments than in the bags. If we assume the fragments to stem from similar compostable bags as the ones included in our comparison, this would mean that during composting of such a bag, the PLA degrades

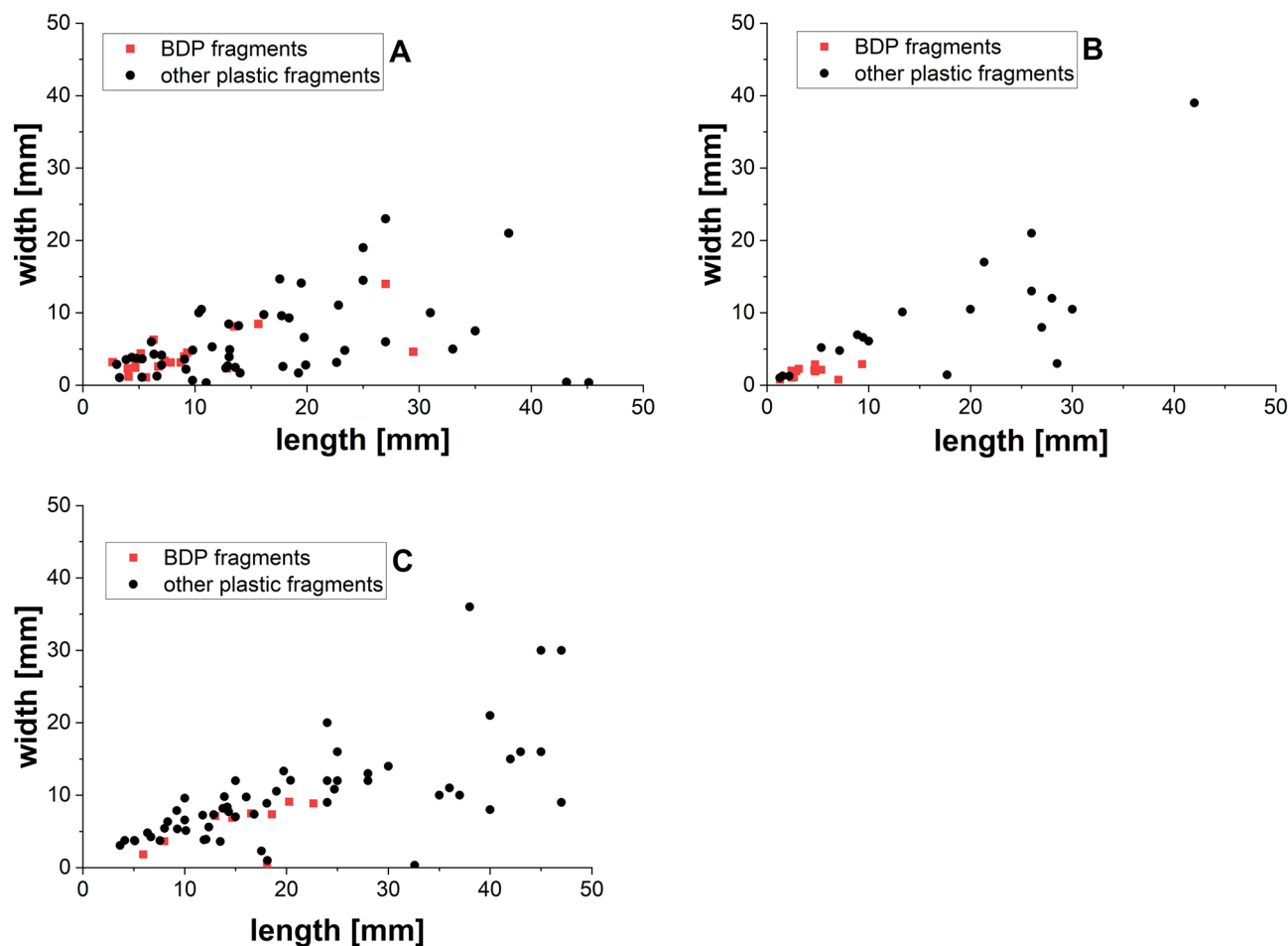


Figure 2. Size distribution of plastic fragments > 1 mm. (A) Fragments found in the finished compost from plant #1, (B) in the finished compost from plant #2, and (C) in the pre-compost from plant #3. For reasons of statistical relevance, only samples containing more than 20 BDP fragments per kg of compost were included in the analysis.

more quickly than the PBAT, whereas within a given PBAT polyester, the BA unit is more easily degraded than the BT unit. Evidence can indeed be found in the pertinent literature that PLA has faster biodegradation kinetics than PBAT, while BT is more resistant to mineralization than BA^{17,18}.

Next, differential scanning calorimetry (DSC) was used to analyze fragments compared to commercial bags in regard to the presence of amorphous vs. crystalline domains, a parameter expected to affect biodegradation kinetics and therefore the putative environmental impact of the produced microplastic¹⁶ upon release into the environment with the composts. Whereas amorphous domains show glass transition, crystalline domains show melting, both of which can be discerned by the respective phase transition enthalpy in the DSC curves (Fig. 4).

The curve for the reference PBAT shows a glass transition temperature (T_g) of $-29\text{ }^\circ\text{C}$ and a broad melting range between 100 and $140\text{ }^\circ\text{C}$ for the crystalline domains, while that of the PLA reference shows a glass transition temperature of $58\text{ }^\circ\text{C}$ and a narrower melting peak between $144\text{ }^\circ\text{C}$ and $162\text{ }^\circ\text{C}$. The curve for commercial bag #1, which had a comparatively high PLA content, shows a pronounced melting peak in the expected range; the same is the case for fragment p#3_5mm_1 and to a lesser extent for fragment p#3_5mm_9, two fragments, which also have high PLA contents. The DSC curves of the other fragments and bag #1 are undefined in comparison, which is due to their high PBAT content. According to the DSC curves, most of the investigated materials are semicrystalline, i.e., contain both amorphous (glass transition) and crystalline (melting) domains. However, the DCS data alone allow only a qualitative discussion of the differences between fragments and bags.

To obtain quantitative data on the crystallinity differences, wide angle X-ray scattering (WAXS) spectra were recorded. WAXS requires fragments at least 3 cm long, which restricted the number of fragment samples to three, all of which were found in pre-compost samples. The corresponding curves are shown in Fig. 5A–C. The spectra of the commercial biodegradable bags are shown in Suppl Figure S3. Foils were in addition prepared by heat pressing from the reference materials for PLA and PBAT in order to include them into the WAXS measurements (Fig. 5D). While the foils produced from the PBAT reference material produced crystallinity peaks at 16.2° , 17.3° , 20.4° , 23.2° , and 24.8° , the foil prepared from the PLA reference material showed only an amorphous halo at 15.5° and 31.5° , which is in accordance with values published in the literature¹⁹. A more pronounced crystallinity peak was obtained in the case of an additionally annealed PLA foil.

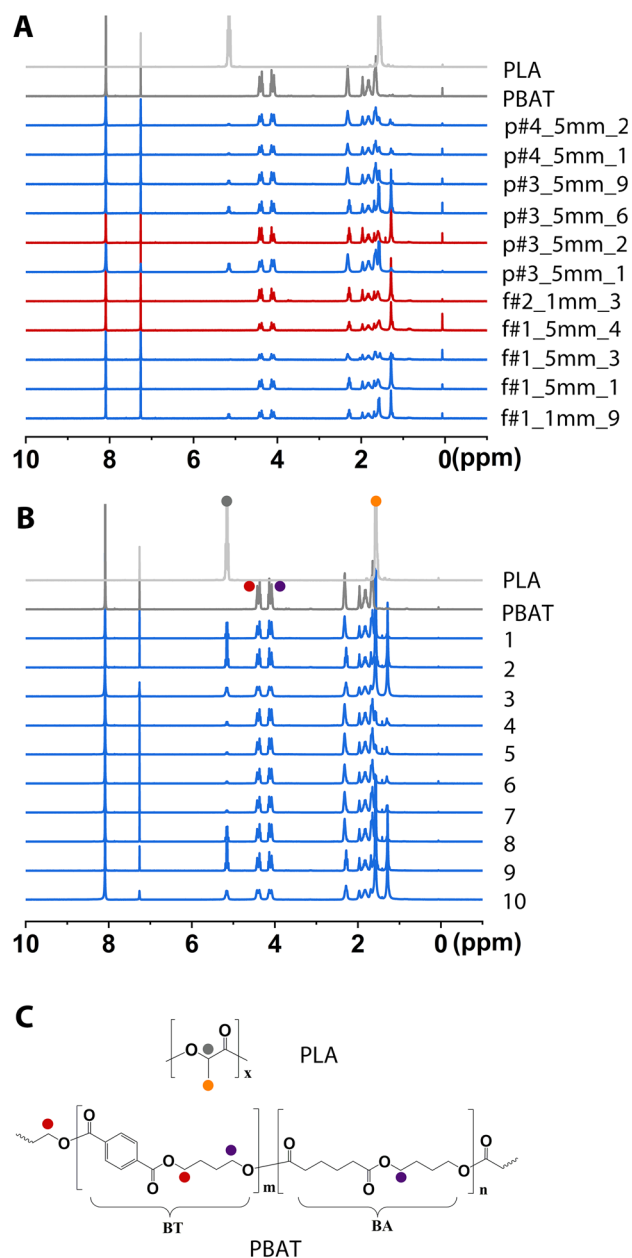


Figure 3. ^1H NMR spectra of BDP fragments from composts and commercial bags. (A) BDP fragments recovered from the composts and (B) the commercial compostable bags. Fragments were coded as follows: p or f for pre-compost or finished compost, followed by the plant number (#1 to #4), an indication of the size fraction (>5 mm or 1–5 mm) in which the fragment was found, and finally, the fragment number. Bags were arbitrarily numbered 1–10, see Suppl Table S1 for supplier information. The spectra (in grey) of the reference materials for PLA and PBAT are given as basis for the interpretation. Spectra in red refer to test samples consisting only of PBAT, while those in blue indicate samples composed of PBAT/PLA mixtures. (C) Chemical structures of PLA and PBAT, chemical shifts of the protons are assigned as indicated in the reference spectra in (B).

In case of the fragments and bags, the peaks of PLA and PBAT overlapped to some extent in the WAXS spectra, but by conducting Lorenz fitting using Origin software, the overall crystallinity could be calculated as follows:

$$\chi = 100\% * Aa / (Aa + Ac)$$

where χ is the crystallinity and Aa and Ac represent the areas of the amorphous and crystalline peaks.

Using this equation, crystallinities of 55% (fragments p#3_5mm_1), 34% (p#3_5mm_9), and 34% (p#4_5mm_2) were calculated for the fragments. The foils prepared in house for the reference materials had similar crystallinities (43% in case of the annealed PLA foil and 26% of the PBAT foil), while the simple PLA

Sample	PBAT (wt%)	PLA (wt%)	BT/BA-ratio in the PBAT	
Bag No.1	79.3	20.7	0.86	Average PBAT (wt%): 80.8 ± 12.1 Average BT/BA ratios: 0.91 ± 0.06
Bag No.2	66.1	33.9	0.96	
Bag No.3	68.8	31.2	1.01	
Bag No.4	92.0	8.0	0.87	
Bag No.5	95.4	4.6	0.87	
Bag No.6	95.4	4.6	0.86	
Bag No.7	95.6	4.5	0.88	
Bag No.8	79.3	20.7	0.85	
Bag No.9	66.1	33.9	0.94	
Bag No.10	70.2	29.8	1.01	
f#1_1mm_9	82.5	17.5	0.99	Average PBAT (wt%): 92.8 ± 7.9 Average BT/BA ratios: 1.02 ± 0.12
f#1_5mm_1	99.2	0.8	1.00	
f#1_5mm_3	97.4	2.6	1.02	
f#1_5mm_4	100	–	1.02	
f#2_1mm_3	100	–	1.15	
p#3_5mm_1	77.9	22.1	0.93	
p#3_5mm_2	100	–	1.33	
p#3_5mm_6	82.1	17.9	0.99	
p#3_5mm_9	89.9	10.1	0.95	
p#4_5mm_1	96.2	3.8	0.94	
p#4_5mm_2	95.6	4.4	0.90	

Table 2. Composition of commercial compostable bags and BDP fragments recovered from the composts as analyzed by $^1\text{H-NMR}$. BT/BA-ratio in the PBAT: BT, butylene terephthalate; BA, butylene adipate, molar ratio of the two monomeric units found in the co-polyester PBAT. Fragments were coded as follows: p or f for pre-compost or finished compost, followed by the plant number (#1 to #4), an indication of the size fraction (> 5 mm or 1–5 mm) in which the fragment was found, and finally, the fragment number.

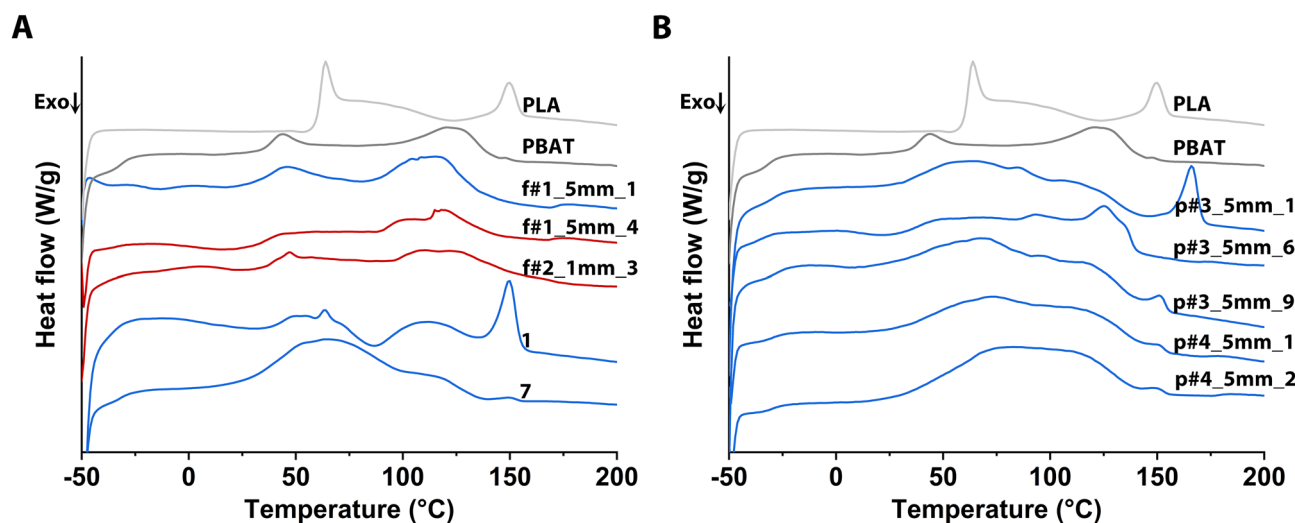


Figure 4. DSC curves of BDP fragments and compostable bags #1 and #7. Curves for the reference materials (in grey) for PLA and PBAT are given for comparison. Curves were recorded during the first heating run (temperature range: $-50\text{ }^{\circ}\text{C}$ to $200\text{ }^{\circ}\text{C}$, heating rate: $10\text{ }^{\circ}\text{C min}^{-1}$). (A) and (B) curves in red refer to test samples consisting only of PBAT, while those in blue indicate samples composed of PBAT/PLA mixtures. Fragments were coded as follows: p or f for pre-compost or finished compost, followed by the plant number (#1 to #4), an indication of the size fraction (> 5 mm or 1–5 mm) in which the fragment was found, and finally, the fragment number.

foil was amorphous. By comparison, for eight of the commercial bags, crystallinities in the range from 1% to 7% were calculated, whereas these values were 14% and 15% for the remaining two bag types (Suppl Figure S3).

The high crystallinity of the larger fragments recovered from the pre-compost samples suggests that crystalline domains of BDP materials may indeed disintegrate more slowly than the amorphous ones, as prior studies on microbial biodegradation have suggested^{7,8}. Admittedly, such large fragments *per se* would not enter the

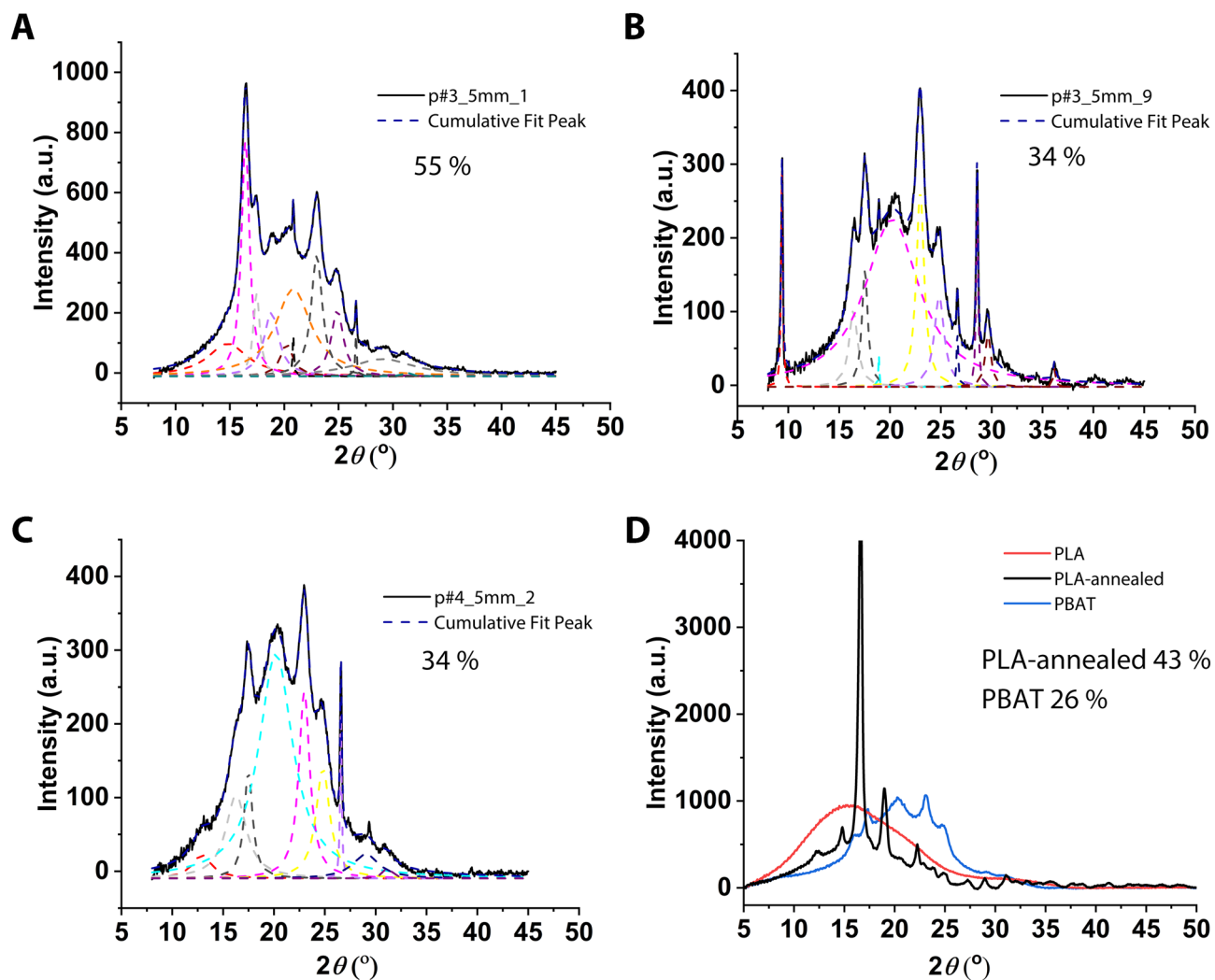


Figure 5. WAXS curves with Lorenz fitting for (A) fragment p#3_5mm_1, (B) fragment p#3_5mm_9, and (C) fragment p#4_5mm_2. (D) WAXS curves for foils produced from the PBAT and PLA reference materials; the percent values indicate the crystallinity. The dash lines are the fitting peak curves for the XRD spectrum. Crystallinity can be obtained by dividing the integration area of the fitted peaks by the integration area of the entire spectrum. Fragments were coded as follows: p or f for pre-compost or finished compost, followed by the plant number (#1 to #4), an indication of the size fraction (>5 mm or 1–5 mm) in which the fragment was found, and finally, the fragment number.

environment, since the final sieving step used to prepare the finished composts is quite efficient at removing them. However, it is tempting to extrapolate that residual BDP in general are remnants of the more crystal domains of the original material, even though experimental proof of this assumption is at present not possible. 10 wt% of a BDP bag is allowed to remain after standard composting. It is usually assumed that any such residues continue to degrade with comparable speed. However, should these residues correspond to the more crystalline domains, rather than degrading with similar speed as the bulk material, the more crystalline fragments can be expected to persist for a much longer and at present unpredictable length of time in the environment, e.g. when applied to the soil with the composts; in particular, when they are also enriched in PBAT and BT units as suggested by our analysis of the chemical composition. Data from the use of biodegradable foils in agriculture show that the degradation in the environment may take years²⁰. Altogether this may have unforeseen economic and environmental consequences, especially when considering the high fraction of BDP fragments < 5 mm. Putative consequences include changes in soil properties, the soil microbiome and therefore in plant performance²¹, a factor indispensable for worldwide nutrition.

Residues of BDP fragments <1 mm in liquid fertilizer and in composts. In addition to the composts, plants #1 and #3 produce a so-called liquid fertilizer (LF). LF is applied directly to agricultural soil without further treatment. No plastic fragments > 1 mm were found in the collected LF samples. This is hardly surprising, given that the LF is produced by press filtration of the digestate after the anaerobic stage. Such a filtration step can be expected to retain fragments > 1 mm in the produced filter cake, which goes into the composting step, leaving the filtrate, i.e. the LF, essentially free of such particles. Anaerobic digestion is currently not assumed to

Plant	11–22 μm	22–100 μm	100–300 μm	300–500 μm	500–1000 μm	%
#1	0/0	3840/8960	6400/8960	1280/2560	0/1280	53
#3	1280/1920	7040/10,880	3840/6080	320/320	0/0	65

Table 3. Microplastic fragments (BDP/all) found per liter of liquid fertilizer. %: Percentage of BDP fragments within all recovered plastic fragments.

	f#1	f#2	p#3	f#3	p#4	f#4
Dry weight [%]	45.9	64.9	57.5	57.4	39.7	51.6
M_c [g]	100	100	65	54	100	100
M_e [g]	0.78	1.41	0.51	0.45	1.14	0.68
M_0 [mg]	14.0	14.8	14.8	12.2	15.3	13.5
M_{STD} [mg]	9.1	8.9	9.5	12.0	8.6	15.2
M_{PLA} [mg]	1.488	1.259	1.300	0.369	2.645	1.788
M_{PBAT} [mg]	1.228	3.283	1.102	0.381	0.370	0.148
P_{PLA} [%]	10.6	8.5	8.8	3.0	17.3	13.2
P_{PBAT} [%]	8.8	22.2	7.4	3.1	2.4	1.1
C_{PLA} [ppm]	827	1199	690	250	1972	898
C_{PBAT} [ppm]	686	3130	581	258	274	75
A_{PLA} [m ²]	29.00	42.04	24.19	8.77	69.14	31.49
A_{PBAT} [m ²]	23.67	108.01	20.05	8.90	9.45	2.59

Table 4. Evidence of PBAT and PLA residues caused by fragments < 1 mm in the composts. M_c : mass of dry compost subjected to extraction; M_e : mass extracted from compost sample; M_0 : mass of material used for ¹H NMR; M_{STD} : mass internal standard used for ¹H NMR; M_{PLA} , M_{PBAT} : masses of PLA and PBAT in M_0 ; P_{PLA} , P_{PBAT} : wt% of PLA and PBAT in M_e ; C_{PLA} , C_{PBAT} : mass concentration of PLA and PBAT in M_e ; A_{PLA} and A_{PBAT} : calculate surface area covered by PLA and PBAT in 1 ton of drycompost.

contribute significantly to the degradation of BDP^{17,22}, but the process conditions (mixing, pumping) may promote breakdown of larger fragments, particularly when additives such as plasticizers²³ leach out of the material.

Since the residual solids content of the LF is low (plant #1: 8.6 wt%, plant #3: 5.8 wt%), a combination of enzymatic-oxidative treatment and μ FTIR imaging originally developed for environmental samples from aqueous systems^{24,25} could be adapted for the analysis (size and chemical signature) of particles in the LF down to a size of 10 μm . The corresponding data are compiled in Table 3. In all cases, residual fragments from PBAT-based polymers represented the dominant plastic fraction in the investigated samples; i.e. approximately 53% of all plastic particles in the LF from plant #1 (11,520 BDP particles per liter) and 65% in the case of plant #3 (12,480 BDP particles per liter). Liquid manure is applied several times a year to fields at a concentration of 2–3 L m⁻². According to our analysis > 20,000 BDP microparticles of a size ranging from 10 μm to 500 μm enter each m² of agricultural soil whenever LF is applied on agricultural surfaces.

Due to the complexity of the matrix, a similar analysis of individual plastic fragments < 1 mm was not possible in case of the composts. These were instead subjected to an organic solvent extraction after removal of all fragments > 1 mm. Six compost samples representing the more contaminated ones based on the content of fragments > 1 mm, namely, f#1, f#2, p#3, f#3, p#4 and f#4 (nomenclature: f or p for finished or pre-compost, followed by plant number), were extracted with a 90/10 vol% chloroform/methanol mixture. The amounts of PBAT and PLA in the obtained extracts were then quantified via ¹H-NMR (Table 4). Briefly, the intensity of characteristic signals in the extract spectra of the compost samples (see Suppl Figure S4) were compared to peak intensities produced by calibration standards of the pure polymer dissolved at a known concentration in the chloroform/methanol. All samples and standards were normalized using the 1,2-dichloroethan signal at 3.73 ppm as internal standard. See also Suppl Figure S5 for an exemplification of the quantification of the PBAT/PLA ratios. Based on the amounts of PBAT and PLA extracted from a known amount of compost, the total mass concentration (wt% dry weight) of these polymers in the composts was calculated.

Compost samples contained between 0.5 and 1.5 wt% extractable material out of which between 6 wt% and 30 wt% were made up of the biodegradable polymers PLA and PBAT. In consequence, the compost samples contained between 0.05 and 0.43 wt% PLA and/or PBAT < 1mm per unit dry weight. This is in the same order of magnitude and even above the current limit (0.1 wt%) for certified composts in regard to the contamination with plastic fragments²⁶ > 2 mm. Moreover, residues of PBAT and PLA were found in all investigated compost samples, including the finished compost from plant #4, which had shown no contamination by larger BPD fragments (Table 1). The pre-compost from that plant had shown a few contaminating BDP fragments in the > 5 mm fraction. However, in regard to the fragments < 1 mm, the composts from plant #4 showed a similar incidence, at least for PLA, as the finished compost samples from the other plants (Table 4).

Since the material was extracted and quantified in solution, no direct information regarding the original dimension of the fragments < 1 mm could be derived. However, if we assume a similar thickness as for the larger fragments or commercial bags (17–25 μm) together with densities of 1240 kg m^{-3} (PLA) and 1260 kg m^{-3} (PBAT) as measured for the corresponding reference materials, the particles < 1 mm found in one ton of these composts would, when placed side by side, cover an area between 17 and 150 m^2 (see values A_{PLA} and A_{PBAT} in Table 4). Therefore, if 10 tons of such compost were to be distributed over 1 ha (10,000 m^2) of agricultural surface, which is not unreasonable²⁷, the added plastic particles < 1 mm combined would theoretically cover up to 15% of this area. Taken together with the data on larger BDP fragments and on commodity plastics, environmental contamination via composts may be much higher than previously thought³.

Given that our results show that predominantly tiny BDP fragments (microplastic) enter the environment via compost and LF, a possible impact on environmental and finally human health and nutrition is indicated. Polymer particles in the micron- and nanometer range have already been shown to be more toxic than larger ones^{2,28,29}. In addition, the coverage with an ecocorona³⁰, that will certainly take place during digestion/composting, facilitates the internalization into cells³¹ and therefore increases the risk associated with the ingestion of microplastic, e.g. by soil macrofauna³². Finally, the higher crystallinity and therefore higher resistance to further biodegradation extends the period of bioavailability of BDP microparticles with all the above-mentioned consequences. Whether BDP fragments with higher crystallinity or a higher BA unit within the PBAT co-polyester also induce stronger toxic effects remains to be investigated. In this view, the mechanisms and kinetics of BDP breakdown under conditions of industrial biowaste treatment, but also in soils used for food and feed production, should be investigated in more detail, before the widespread use of the currently available biodegradable materials as presumably environmentally friendly alternatives to conventional plastics is advocated.

Materials and methods

Materials. If not otherwise indicated, suppliers for chemicals were Th. Geyer (Renningen, Germany) and Sigma-Aldrich (Taufkirchen, Germany). Ultrapure water was produced with an Elga-Veolia-Purelab (Flex2) unit, while ‘Millipore-water’ came from a Millipore-Synergy-UV-system (Type 1). Compostable bags (10 different brands) designated for the collection of organic waste by the supplier were bought from different local supermarkets (Table S1). Polymer reference materials for BDP were: PLA (batch no.: GH0728B133, commercial name: Ingeo Biopolymer 4043D, supplier: NatureWork, Minnetonka, MN) and PBAT (batch no.: 95010016KO, commercial name: Ecoflex F Blend C1200, supplier: BASF). Protease A-01 (activity: > 1.100 U mL^{-1}), Pektinase L-40 (activity: > 900 U mL^{-1} , Exo PGA, > 300 U mL^{-1} Endo PGA, > 300 U mL^{-1} Pektinesterase), and Cellulase TXL (activity: > 30 U mL^{-1}) were from ASA Spezialenzyme GmbH (Wolfenbüttel, Germany), Viscozyme L (activity: > 100 FBG U g^{-1}) was from Novozymes A/S (Bagsværd, Denmark).

Sampling of composts and liquid fertilizer. Bulk samples were taken from composts according to the guidelines of the German Association for Quality Compost²⁶. A slight modification to the standard procedure was introduced to avoid contacts of the compost samples with the plastic foil recommended in the standard protocol for sample mixing. Instead, the individual aliquots obtained from a given compost heap were pooled, mixed and stratified directly on the concrete floor (after a ‘washing’ step with compost from the same heap). To obtain a representative sample, the interior of the heap was made accessible using a wheel loader. Then, individual samples were taken at evenly dispersed points. The number and volume of the individual samples depended on the volume and grain size of the compost pile. For example, in the case of 100 m^3 of a compost with grain sizes of 2–20 mm, 16 individual samples (1 L each) were taken, and 4 mixed samples (2 L each) were created at minimum. Whenever possible, samples of both the pre-compost (before the final sieving step) and the finished compost were taken. Pre-compost sample volumes were determined based on the volume required for the corresponding finished compost samples. Pre-compost and finished compost were sampled at the same time. Consequently, they represented different processing batches. Sample aliquots were transferred to 3 L Fido jars (Bormioli Rocco, Fidenza, Italy) for transport. If immediate analysis was not possible, samples were stored at 4 °C in the glass vessels. Samples of liquid fertilizer (~ 6 L) were collected from the outlet of the storage tanks also into glass vessels. The first few liters of liquid fertilizer were discarded to rinse the outlet pipe and ensure that representative samples were obtained. If necessary, liquid fertilizer samples were also stored at 4 °C. Backup samples of approximately 1 L were taken for all samples and stored at –20 °C. Glass vessels for transport, storage or backup samples were rinsed in advance with Millipore water.

Analysis of plastic fragments in the composts. A significant concern during the analysis in particular of microplastic particles in environmental samples is the possible contamination of samples with microplastic particles from the ambient air, clothing, laboratory tools or reagents used during sample preparation. In order to avoid contamination, precautionary measures were taken. Cotton lab coats were worn throughout. Unless direct handling was necessary, samples were covered with a glass or aluminum foil lid. Sample processing took place in a laminar-flow-box to prevent airborne particles from falling into the sample. All laboratory tools used were made of glass, metal or polytetrafluorethylene (PTFE), a polymer which is rare in environmental samples and is excluded from the analysis. All required solutions and the deionized water used to prepare them were filtered through 0.2 μm pore membranes (mixed cellulose ester membrane, diameter 47 mm, Whatman ME 24, Merck KGaA) before use. Enzyme solutions were filtered through 0.45 μm membranes (regenerated cellulose membrane, diameter 100 mm, Whatman RC 55, Merck KGaA) and stored in glass bottles with glass caps, ready for use. All laboratory equipment was thoroughly rinsed with filtered deionized water, 35% ethanol, and again filtered water before use and in between steps to avoid cross contamination. Blanks undergoing the same treatment as the environmental samples were used in order to detect possible contamination in the laboratory.

Prior to analysis, compost samples were filled into a rectangular metal form (790 mm × 510 mm × 150 mm), homogenized with a metal shovel and quartered. From two quarters (bottom right, top left), samples were taken for the investigation of the plastic content. Samples for the determination of the dry weight (DW) were taken from the bottom left quarter, while backup samples (1 L) were taken from the top right quarter. For the determination of the DW 100 mL sample aliquots were weighed into 250 mL Schott-Duran beakers and dried at 105 °C (oven: Memmert UM 500, Memmert, Schwabach, Germany) for at least 24 h. Afterwards, the beakers were allowed to cool to room temperature in a desiccator and the DW determined by weighing the beakers again.

For the recovery of the fragments > 1 mm, approximately 3 L of the compost sample was weighed and evenly distributed into 6 glass vessels (capacity 3 L each). The material was suspended in 2.5 L of water and first sieved with a mesh size of 5 mm (yielding fraction > 5 mm). All particles retained by the sieve were collected with tweezers and transferred to the system for ATR-FTIR analysis, see below, while the material passing the sieve was sieved again at 1 mm, followed again by collection of the retained particles (yielding fraction 1–5 mm), which were subsequently also analyzed by ATR-FTIR. Sieves were from Retsch GmbH (Haan, Germany; test sieve, IS 3310-1; body/mesh, S-Steel; body, 200 mm × 50 mm). For the analysis of the chemical nature of the collected particles Attenuated total reflection—Fourier transform infrared (ATR-FTIR) spectrometry (spectrometer: Alpha ATR unit, Bruker 27; equipped with a diamond crystal for measurements) was used. Spectra were taken from 4000 to 400 cm⁻¹ (resolution 8 cm⁻¹, 16 accumulated scans, Software OPUS 7.5) and compared with entries from an in-house database described previously²⁴ or the database provided by the manufacturer of the instrument (Bruker Optik GmbH, Leipzig, Germany). This comparison of the IR-spectra allowed to distinguish biodegradable from conventional plastic fragments, but also from residues of other materials including unknowns. An incident light microscope (microscope, Nikon SMZ 754T; digital camera, DS-Fi2; camera control unit, DS-U3; software, NIS Elements D) was used for visual documentation of all particles identified by ATR-FTIR as synthetic plastics (biodegradable or otherwise).

Analysis of plastic fragments in the liquid fertilizers. The liquid fertilizer samples were also sieved with 5 mm and 1 mm sieves to obtain possibly present fragments > 1 mm. For the preparation of the plastic fragments < 1 mm (down to 10 μm) an adjusted enzymatic-oxidative digestion method based on a method suggested by Löder et al. 2017 was adapted²⁵. For this, the liquid fertilizer sample was mixed well with a metal rod and 50 mL were quickly poured into a 300 mL glass beaker (Schott-Duran). The metal rod and the glass beakers were washed in advance with Millipore water. Then 50 mL of a 10 wt% sodium dodecyl sulfate (SDS) solution (≥ 95 % SDS; Karl Roth) was added and the mixture incubated at 50 °C for 72 h under gentle agitation (Universal Shaker SM 30 B, Edmund Bühler GmbH, Bodelshausen, Germany). Subsequently, 2 × 25 mL of 30% hydrogen peroxide was slowly added under a fume hood. Since the reaction of hydrogen peroxide with organic matter is highly exothermic, an ice bath was used to keep the reaction temperature below 40 °C. Once the reaction had subsided and the mixture had again reached room temperature, the solution was filtered over a 10 μm stainless-steel-mesh filter (47 mm diameter, Rolf Körner GmbH, Niederzier, Germany) with a vacuum filtration unit (3-branch stainless-steel vacuum manifold with 500 mL funnels and lids, Sartorius AG, Göttingen, Germany). All filtrations were conducted under a laminar flow hood to minimize contamination with microplastics from the surrounding air. All matter retained by the filter was rinsed with filtered (0.2 μm) deionized water to remove residual chemicals. Afterwards, the retained matter was rinsed into a fresh 300 mL glass beaker with approximately 50 mL of 0.1 M Tris-HCl buffer (pH 9.0). As particles tended to adhere to the stainless-steel filter, the filter was also placed into the beaker. Ten milliliters of Protease A-01 solution were added and the beaker was incubated at 50 °C for 12 h with gentle agitation. Afterwards, the filter was thoroughly rinsed off into the beaker with filtered deionized water to recover any adhering particles and then used to filter the incubated solution. The retained matter was rinsed into a fresh glass beaker with 25 mL of 0.1 M NaAc buffer (pH 5). The filter was again placed in the jar as well, 5 mL of the Pektinase L-40 solution was added, and the beaker was incubated for 72 h at 50 °C. The filter was rinsed and used to filter the sample as before. Any matter retained by this filtration step was again rinsed into a fresh glass beaker with 25 mL of 0.1 M NaAc buffer (pH 5). The filter was again placed in the beaker, 1 mL of a Viscozyme L solution was added, and the jar was incubated at 50 °C for 48 h. The sample was filtered and the retained matter was transferred into 25 mL of a 0.1 M NaAc buffer (pH 5). Five mL of Cellulase TXL solution was added and the jar was incubated at 40 °C for 24 h.

Only after the enzymatic digestion were the preparations oxidized with Fenton's reagent. This combination of enzymatic digestion and Fenton oxidation was necessary since for these types of samples Fenton treatment alone was not sufficient to remove enough of the organic material to allow μ-FTIR imaging. A detailed analysis of the challenge of sample preparation for μ-FTIR in case of complex samples has recently been published by some members of our group³³, where further details can be found.

For this purpose, the mixture was filtered and the matter retained by the filter rinsed into a fresh glass beaker with ca. 20 mL filtered deionized water. Then, 20 mL of 30% H₂O₂ solution was added, and the mixture continuously stirred with a magnetic stir bar under the fume hood while adding 20 mL of 0.05 M Fe(II) solution (7.5 g of iron(II) sulfate heptahydrate (FeSO₄ · 7 H₂O) in 500 mL ultrapure water and 3 mL of concentrated sulfuric acid). An ice bath was again used to keep the reaction temperature below 40 °C. After approximately 2 h, the reaction had subsided, and the reagents were filtered off over a 10 μm stainless-steel-mesh filter. Residual Fenton's reagent was removed by rinsing the filter retentate with filtered deionized water.

This treatment was followed by a density separation step with an aqueous zinc chloride solution. For this, the retained matter was transferred from the filter into a clean glass beaker using a metal spatula and approximately 50 mL ZnCl₂ solution (ρ = 1.8 g cm⁻³) was added. The mixture was stirred with a magnetic stir bar until all aggregates were dispersed. Then, the mixture was transferred into a straight-walled separation funnel with a capacity of 400 mL. The mixture was stirred for several minutes with a glass rod and left to settle overnight (at

least 12 h). Any plastic fragments present in the sample separate from any mineral matter by rising to the top. After release of the sediment, the low density particle fraction was filtered onto a new 10 µm stainless-steel-mesh filter, which was then rinsed with 98% filtered ethanol and filtered deionized water to remove residual ZnCl₂.

Depending on the initial amount and the quality of its matrix, the number of particles recovered by the purification can vary. In order to avoid matrix interference, which would make FTIR analysis impossible, the aluminum oxide sample carrier filters (0.2 µm, Anodisc, Whatman GE Healthcare) must not be overloaded. Therefore, samples with a high amount of matter were suspended in filtered deionized water, evenly filtered over a 5 µm pore stainless steel-mesh filter (diameter: 47 mm), and then halved using custom made pliers that divide the circular filter in half. One half was washed into a clean 100 mL beaker, while the other was kept as backup sample. This process was repeated as often as necessary to achieve a subsample that could be transferred onto 3–5 aluminum oxide filters for spectroscopic measurement. The filters were analyzed with focal plane array-based µ-FTIR spectroscopy²⁴, which allows the determination of the fragment shape, size, color and polymer type (again via the IR spectrum), using a Bruker Hyperion 3000 FTIR microscope (Bruker Optik GmbH) equipped with a 64 × 64 pixel FPA detector in conjunction with a Tensor 27 spectrometer. The samples were measured in transmission mode with a 3.8 × IR objective (spatial resolution 11.05 µm per pixel) and a wavelength range of 3600–1250 cm⁻¹ (resolution 8 cm⁻¹, 6 accumulated scans). Data processing was conducted using Bruker OPUS software version 7.5 (Bruker Optik GmbH) and automated spectral analysis was performed with the “Bayreuth-ParticleFinder” module in ImageLab version 4.1 (EPINA GmbH, Güttersloh, Germany) based on Random Forest Decision Classifiers³⁴ for 22 different polymer types.

Analysis of the material properties of the various plastic materials. FTIR spectroscopy was used to directly compare the material properties of the BDP fragments, the commercial biodegradable bags, and the reference materials. The measurement was performed on either a Digilab Excalibur Series FTIR spectrometer (range 4000 to 550 cm⁻¹, resolution ~4 cm⁻¹, 16 accumulative scans) or a PerkinElmer Spectrum 100 FTIR spectrometer (range 4000 to 450 cm⁻¹, resolution 4 cm⁻¹, 4 accumulative scans).

The polymer content and composition of bags and fragments were quantified by ¹H NMR in CDCl₃ with 64 scans using a 300 MHz Bruker Ultrashield 300 spectrometer. MestreNova software was used for evaluation. 1,2-dichloroethane (DCE), which shows a single peak at 3.73 ppm, served as an internal standard. Proton peak integration of the areas at chemical shifts of 4.37–4.43 ppm (abbreviated as A_T, methylene in BT units), 4.08–4.14 ppm (abbreviated as A_A, methylene in BA units), 5.12 ppm (abbreviated as A_L, methine in lactide units), and 3.73 ppm (abbreviated as A_{STD}, methylene in the internal standard DCE) were used to calculate the respective masses of PBAT and PLA in the residue according to:

$$m_{\text{PBAT}} = n_{\text{BT}} * M_{\text{BT}} + n_{\text{BA}} * M_{\text{BA}}$$

$$m_{\text{PBAT}} = (A_{\text{T}} * M_{\text{BT}} + A_{\text{A}} * M_{\text{BA}}) * \frac{m_{\text{STD}}}{M_{\text{STD}} * A_{\text{STD}}}$$

$$m_{\text{PLA}} = n_{\text{LA}} * M_{\text{LA}} = 4 * A_{\text{L}} * M_{\text{LA}} * \frac{m_{\text{STD}}}{M_{\text{STD}} * A_{\text{STD}}}$$

where m_{PBAT} is the mass of PBAT; n_{BT} and n_{BA} correspond to the moles of the BT and BA units of PBAT, respectively; M_{BT} and M_{BA} are their molar masses; m_{PLA} is the mass of PLA; n_{LA} corresponds to the moles of the lactic acid unit; M_{L} is the corresponding molar mass; M_{STD} is the molar mass of the internal standard; and m_{STD} is the mass (amount) used in the measurement. In addition, the ratios of the BT and BA units within the PBAT fraction of a given sample were calculated from the ¹H-NMR data.

DSC was performed using a DSC 204 F1 Phoenix from Netzsch Instruments from –50 to 200 °C with a heating rate of 10 °C min⁻¹ under nitrogen atmosphere with a flow rate of 20 mL min⁻¹. Each measurement consisted of two full heating and cooling runs.

WAXS was performed on a Bruker D8 Advance diffractometer within 2θ ranges of 5°–60° (for reference PLA and PBAT) and 8°–45° (for BDP fragments from compost and the commercial bags) in transmission mode (step size = 0.05°, scanning rate 40 s step⁻¹), and Cu Kα (λ = 1.54 Å) X-rays were used. Foils from the reference materials PBAT and PLA were prepared by heat pressing at 150 °C and 160 °C, respectively. The heat-pressed PLA was further annealed at 80 °C for 3 days to increase crystallinity.

Extraction and quantification of residual plastic as bulk from compost samples. Residual PBAT and PLA matter corresponding to fragments < 1 mm were extracted in bulk from compost samples using a previously published method³⁵ in modified form. Compost aliquots were first sieved through a 1 mm mesh to remove the larger fragments, and then dried at 60 °C for 48 h prior to extraction. One hundred grams of material was placed in 500 mL glass bottles and 250 mL of a 90/10 vol% chloroform/methanol mixture was added. The glass bottles were sealed, placed on a horizontal shaker for 10 min and subsequently sonicated in a water bath at room temperature for 10 min. Afterwards, the containers were placed overnight in a fume hood. The next day, the contents were passed through a Büchner funnel under vacuum, and the retained residues were washed with excess chloroform to remove any remaining dissolved material. The solvents were removed from the filtrate by rotary evaporation under vacuum and the obtained residue was dried overnight in an oven at 45 °C under vacuum. To quantify polymer content and composition, ¹H-NMR spectra were recorded for each extract. 1,2-dichloroethane was chosen as inner standard since it has a single peak at δ = 3.74 ppm and thus does not interfere with the peaks of PLA and PBAT (see Suppl Figure S4). The peaks assigned to PLA or PBAT in a spectrum were integrated. As

the peak intensity of $^1\text{H-NMR}$ is proportional to the number of protons in a molecule, the integration values of peaks can be used for quantification purpose. The amounts of PBAT and PLA calculated for the extracts were then correlated to the dry weight of the extracted compost sample and used for the calculation of the total mass concentration (wt%) of PBAT and PLA per unit of dried compost.

Data availability

All data are available in the main text or the supplementary materials.

Received: 3 January 2022; Accepted: 16 May 2022

Published online: 30 May 2022

References

1. "DIN EN 13432:2000-12, Verpackung - Anforderungen an die Verwertung von Verpackungen durch Kompostierung und biologischen Abbau - Prüfschema und Bewertungskriterien für die Einstufung von Verpackungen; Deutsche Fassung EN_13432:2000" (Beuth Verlag GmbH). <https://doi.org/10.31030/9010637>.
2. Anbumani, S. & Kakkar, P. Ecotoxicological effects of microplastics on biota: A review. *Environ. Sci. Pollut. Res.* **25**, 14373–14396 (2018).
3. Weithmann, N. *et al.* Organic fertilizer as a vehicle for the entry of microplastic into the environment. *Sci. Adv.* **4**, eaap8060 (2018).
4. Reißfeste Biomülltüten für den Kompost. <https://www.basf.com/at/de/media/science-around-us/tear-resistant-waste-bags-for-compost.html>.
5. Kern, M., Neumann, F., Siepenkothen, H.-J., Turk, T. & Löder, M. Kunststoffe im Kompost. *Müll Abfall* **5**, 1 (2020).
6. Kern, M., Turk, T., Hüttner, A. & Koj, U. BAW-Beuteleinsatz in Biogutvergärungsanlagen. *Müll Abfall* **4**, 1 (2017).
7. Bagheri, A. R., Laforsch, C., Greiner, A. & Agarwal, S. Fate of so-called biodegradable polymers in seawater and freshwater. *Global Chall.* **1**, 1700048 (2017).
8. Mochizuki, M. & Hirami, M. Structural effects on the biodegradation of aliphatic polyesters. *Polym. Adv. Technol.* **8**, 203–209 (1997).
9. Abou-Zeid, D. Anaerobic biodegradation of natural and synthetic polyesters. *Vegetatio* <https://doi.org/10.24355/dbbs.084-200511080100-81> (2000).
10. Wang, S. *et al.* Characteristics and biodegradation properties of poly(3-hydroxybutyrate-co-3-hydroxyvalerate)/organophilic montmorillonite (PHBV/OMMT) nanocomposite. *Polym. Degrad. Stab.* **87**, 69–76 (2005).
11. Helmberger, M. S., Tiemann, L. K. & Grieshop, M. J. Towards an ecology of soil microplastics. *Funct. Ecol.* **34**, 550–560 (2020).
12. Ng, E. L. *et al.* An overview of microplastic and nanoplastic pollution in agroecosystems. *Sci. Total Environ.* **627**, 1377–1388 (2018).
13. Palsikowski, P. A., Kuchnier, C. N., Pinheiro, I. F. & Morales, A. R. Biodegradation in soil of PLA/PBAT blends compatibilized with chain extender. *J. Polym. Environ.* **26**, 330–341 (2018).
14. Wang, J. *et al.* Microplastics as contaminants in the soil environment: A mini-review. *Sci. Total Environ.* **691**, 848–857 (2019).
15. Boots, B., Russell, C. & Green, D. Effects of microplastics in soil ecosystems: Above and below ground. *Environ. Sci. Technol.* <https://doi.org/10.1021/acs.est.9b03304> (2019).
16. Lambert, S., Scherer, C. & Wagner, M. Ecotoxicity testing of microplastics: Considering the heterogeneity of physicochemical properties. *Integr. Environ. Assess. Manag.* **13**, 470–475 (2017).
17. Ren, Y., Hu, J., Yang, M. & Weng, Y. Biodegradation behavior of poly (lactic acid) (PLA), poly (butylene adipate-co-terephthalate) (PBAT), and their blends under digested sludge conditions. *J. Polym. Environ.* **27**, 2784–2792 (2019).
18. Kijchavengkul, T. *et al.* Biodegradation and hydrolysis rate of aliphatic aromatic polyester. *Polym. Degrad. Stab.* **95**, 2641–2647 (2010).
19. Pan, H. *et al.* The effect of MDI on the structure and mechanical properties of poly(lactic acid) and poly(butylene adipate-co-butylene terephthalate) blends. *RSC Adv.* **8**, 4610–4623 (2018).
20. Napper, I. E. & Thompson, R. C. Environmental deterioration of biodegradable, oxo-biodegradable, compostable, and conventional plastic carrier bags in the sea, soil, and open-air over a 3-year period. *Environ. Sci. Technol.* **53**, 4775–4783 (2019).
21. de Souza Machado, A. A. *et al.* Microplastics can change soil properties and affect plant performance. *Environ. Sci. Technol.* **53**, 6044–6052 (2019).
22. Zhang, W., Heaven, S. & Banks, C. J. Degradation of some EN13432 compliant plastics in simulated mesophilic anaerobic digestion of food waste. *Polym. Degrad. Stab.* **147**, 76–88 (2018).
23. Correa-Pacheco, Z. N. *et al.* Preparation and characterization of bio-based PLA/PBAT and cinnamon essential oil polymer fibers and life-cycle assessment from hydrolytic degradation. *Polymers (Basel)*. <https://doi.org/10.3390/polym12010038> (2019).
24. Löder, M. G. J. *et al.* Focal plane array detector-based micro-Fourier-transform infrared imaging for the analysis of microplastics in environmental samples. *Environ. Chem.* **12**, 563–581 (2015).
25. Löder, M. G. J. *et al.* Enzymatic purification of microplastics in environmental samples. *Environ. Sci. Technol.* **51**, 14283–14292 (2017).
26. Kehres, B. Bundesgütegemeinschaft Kompost, Eds., *Methodenbuch zur Analyse Organischer Düngemittel, Bodenverbesserungsmittel und Substrate* (Selbstverlag, Köln, 5. Aufl., 2006).
27. Watteau, F., Dignac, M.-F., Bouchard, A., Revallier, A. & Houot, S. Microplastic detection in soil amended with municipal solid waste composts as revealed by transmission electronic microscopy and pyrolysis/GC/MS. *Front. Sustain. Food Syst.* <https://doi.org/10.3389/fsufs.2018.00081> (2018).
28. Jeong, C.-B. *et al.* Microplastic size-dependent toxicity, oxidative stress induction, and p-JNK and p-p38 activation in the monogonont rotifer (*Brachionus koreanus*). *Environ. Sci. Technol.* **50**, 8849–8857 (2016).
29. Hwang, J. *et al.* Potential toxicity of polystyrene microplastic particles. *Sci. Rep.* **10**, 7391 (2020).
30. Galloway, T. S., Cole, M. & Lewis, C. Interactions of microplastic debris throughout the marine ecosystem. *Nat. Ecol. Evol.* **1**, 1–8 (2017).
31. Ramsperger, A. F. R. M. *et al.* Environmental exposure enhances the internalization of microplastic particles into cells. *Sci. Adv.* **6**, eabd1211 (2020).
32. Riedl, S. A. B. *et al.* In vitro cultivation of primary intestinal cells from *Eisenia fetida* as basis for ecotoxicological studies. *Ecotoxicology* <https://doi.org/10.1007/s10646-021-02495-2> (2021).
33. Möller, J. N. *et al.* Tackling the challenge of extracting microplastics from soils: A protocol to purify soil samples for spectroscopic analysis. *Environ. Toxicol. Chem.* **41**, 844 (2021).
34. Hufnagl, B. *et al.* A methodology for the fast identification and monitoring of microplastics in environmental samples using random decision forest classifiers. *Anal. Methods* **11**, 2277–2285 (2019).
35. Nelson, T. F., Remke, S. C., Kohler, H.-P.E., McNeill, K. & Sander, M. Quantification of synthetic polyesters from biodegradable mulch films in soils. *Environ. Sci. Technol.* **54**, 266–275 (2020).

Acknowledgements

We would like to thank the operators of the biowaste treatment plants for their cooperation and support. Furthermore, we would like to thank A. Schott, H. Schneider and K. Thompson for excellent technical assistance. This study was funded by the Deutsche Forschungsgemeinschaft (DFG, German Research Foundation) – SFB 1357 – 391977956. We also gratefully acknowledge the financial support of the Ministry of the Environment, Climate Protection and Energy, Baden-Württemberg, Germany (Project: MiKoBo, reference number BWMK18001 and BWMK18007). Open Access Publishing was funded by the German Research Foundation – 491183248 and the Open Access Publishing Fund of the University of Bayreuth. Yuanhu Zhang would like to thank the CSC (China Scholarship Council) for scholarship support.

Author contributions

Conceptualization: T.S., S.A., A.G., M.G.J.L., C.L., R.F. Methodology: T.S., Y.H.Z., J.N.M., M.J.G.L., S.A., A.G., C.L., R.F. Validation: T.S., Y.H.Z., J.N.M., M.J.G.L., S.A., A.G., C.L., R.F. Investigation: T.S., Y.H.Z., J.N.M., R.F. Visualization: T.S., Y.H.Z. Supervision: S.A., A.G., M.G.J.L., C.L., R.F. Writing—original draft: T.S., R.F. Writing—review and editing: T.S., Y.H.Z., J.N.M., M.J.G.L., S.A., A.G., C.L., R.F.

Funding

Open Access funding enabled and organized by Projekt DEAL. German Research Foundation, CRC 1357-“Mikroplastik” 391977956 (TS, YHZ, MJGL, SA, AG, CL, RF). Ministry of the Environment, Climate Protection and Energy, Baden-Württemberg, Germany BWMK18001 and BWMK18007 (TS, JNM, MJGL, CL, RF).

Competing interests

The authors declare no competing interests.

Additional information

Supplementary Information The online version contains supplementary material available at <https://doi.org/10.1038/s41598-022-12912-z>.

Correspondence and requests for materials should be addressed to R.F.

Reprints and permissions information is available at www.nature.com/reprints.

Publisher's note Springer Nature remains neutral with regard to jurisdictional claims in published maps and institutional affiliations.



Open Access This article is licensed under a Creative Commons Attribution 4.0 International License, which permits use, sharing, adaptation, distribution and reproduction in any medium or format, as long as you give appropriate credit to the original author(s) and the source, provide a link to the Creative Commons licence, and indicate if changes were made. The images or other third party material in this article are included in the article's Creative Commons licence, unless indicated otherwise in a credit line to the material. If material is not included in the article's Creative Commons licence and your intended use is not permitted by statutory regulation or exceeds the permitted use, you will need to obtain permission directly from the copyright holder. To view a copy of this licence, visit <http://creativecommons.org/licenses/by/4.0/>.

© The Author(s) 2022

Supplementary materials

BIODEGRADABLE PLASTICS IN MUNICIPAL BIOWASTE TREATMENT PLANTS: PATHWAY INTO THE ENVIRONMENT FOR MICROPLASTICS WITH PUTATIVE HIGHER PERSISTENCE POTENTIAL

Authors

Thomas Steiner^{1†}, Yuanhu Zhang^{2†}, Julia N. Möller^{3†}, Seema Agarwal², Martin G.J. Löder³, Andreas Greiner^{2‡}, Christian Laforsch^{3‡}, Ruth Freitag^{1‡*}

¹Process Biotechnology, University of Bayreuth

²Macromolecular Chemistry II, University of Bayreuth

³Animal Ecology I & BayCEER, University of Bayreuth

Affiliations

† These authors contributed equally to the experimental part of the described work

‡ Shared senior authorship

* Corresponding author address: Process Biotechnology, University of Bayreuth, Universitätsstrasse 30, 95440 Bayreuth, Germany, phone: +49 921 557371, Fax: +49 921 557375, e-mail: ruth.freitag@uni-bayreuth.de

Content

5 supplementary figures

1 supplementary table

2 supplementary references

Supplementary figures



Fig. S1. Examples for plastic fragments found in composts.

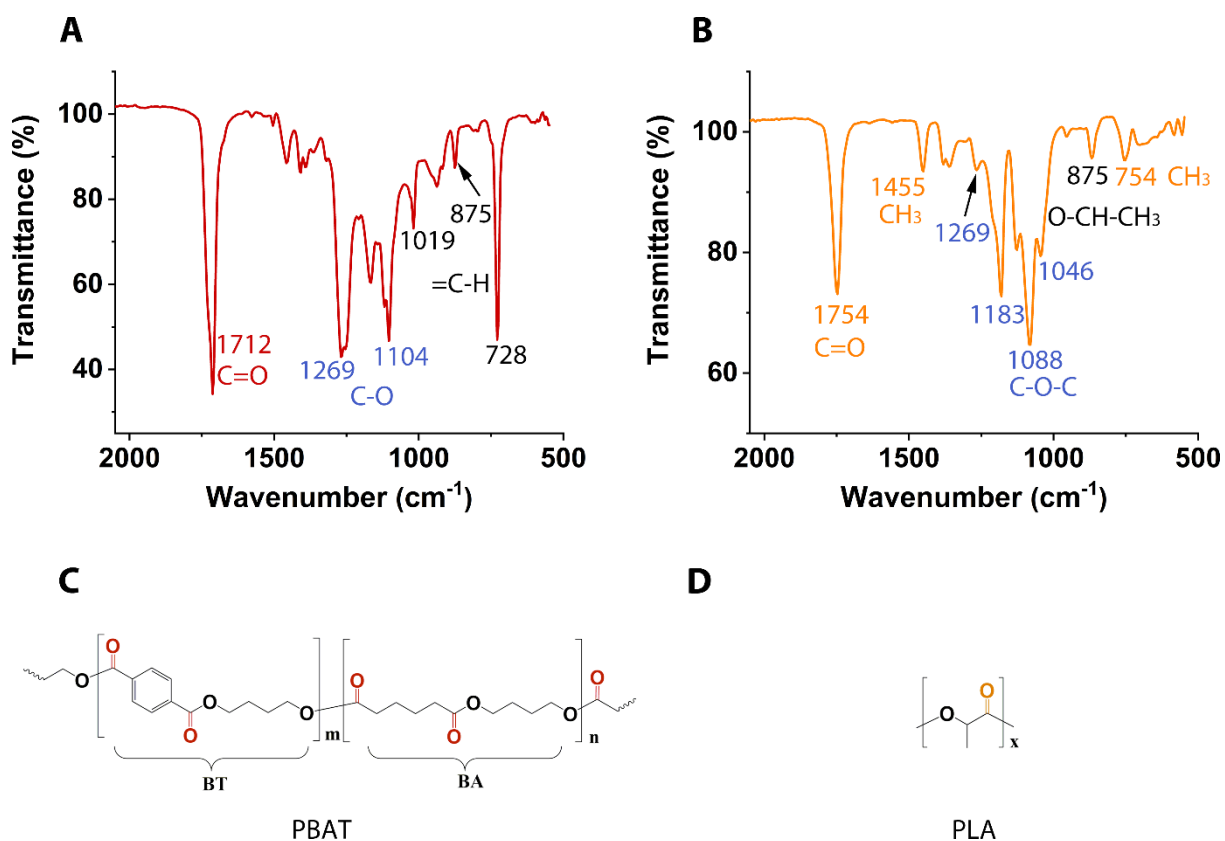


Fig. S2. FT-IR of references **(A)** PBAT and **(B)** PLA, and the chemical structures of **(C)** PBAT and **(D)** PLA. Representative functional groups of PBAT and PLA are indicated in their spectra in the same color. Peaks at 1754 cm^{-1} for the C=O group of PLA and at 1712 cm^{-1} for the C=O group of PBAT can easily differentiate these two polymers.

In these spectra, specific peaks at 1754, 1455, 1390, 1364, 1183, 1088, 1046, 952, 875, and 754 cm^{-1} were assigned to PLA. Among them, the peaks at 1754 cm^{-1} and 754 cm^{-1} , representing C = O stretching and wagging of $\alpha\text{-CH}_3$, respectively, can also be used to identify PLA in mixtures. The peaks at 1269, 1183, 1088, and 1046 cm^{-1} correspond to C–O–C stretching. The peak at 1455 cm^{-1} was assigned to the asymmetric bending of CH_3 , while the peaks at 1390 cm^{-1} and 1364 cm^{-1} correspond to the symmetric bending of CH_3 and CH. The peak at 875 cm^{-1} is related to the absorption of O–CH– CH_3 . PBAT shows peaks at 2960, 2874, 1712, 1580, 1506, 1455, 1411, 1364, 1269, 1104, 1019, 875, and 728 cm^{-1} , with the peaks at 2960 cm^{-1} and 2874 cm^{-1} corresponding to the stretching of CH_3 and CH_2 , the peak at 1712 cm^{-1} to the C = O stretching, that at 1455 cm^{-1} to the in-plane bending of CH_2 , that at 1364 cm^{-1} to the out-of-plane bending of CH_2 , that at 1411 cm^{-1} to the O– CH_2 bending, those at 1269 and 1104 cm^{-1} to the C–O stretching, those at 1580 and 1506 cm^{-1} to the skeleton vibration of benzene, that at 1019 cm^{-1} to the =C–H in-plane bending in the benzene ring, and those at 875 and 728 cm^{-1} to the =C–H-out-of-plane bending of benzene (S1, S2).

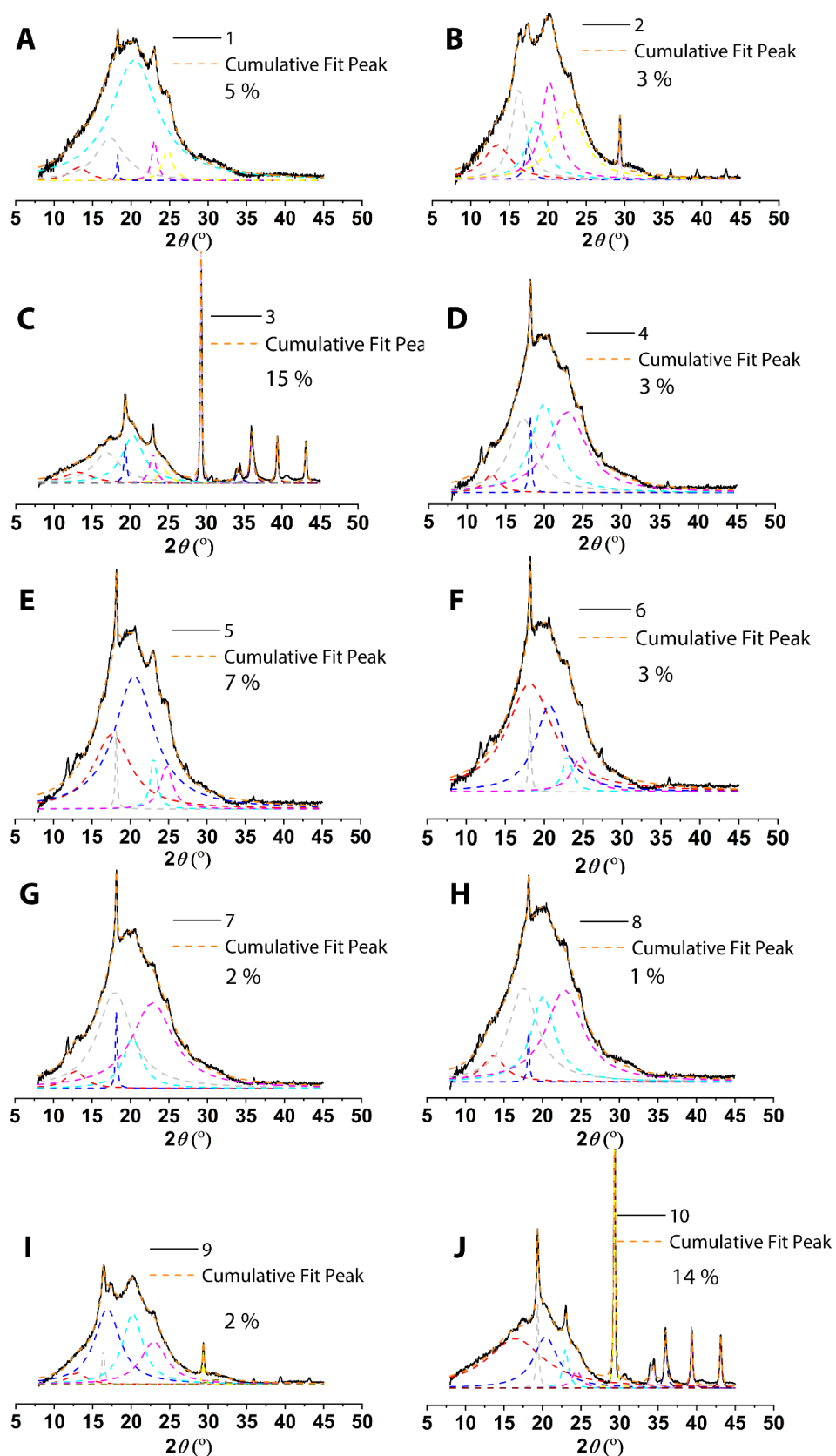


Fig. S3. WAXS curves and Lorenz fitting of commercial bags No. 1 (A) to No. 10 (J); the percent value indicates the degree of crystallinity. The dash lines are the fitting peak curves for the XRD spectrum. Crystallinity can be obtained by dividing the integration area of the fitted peaks by the integration area of the entire spectrum.

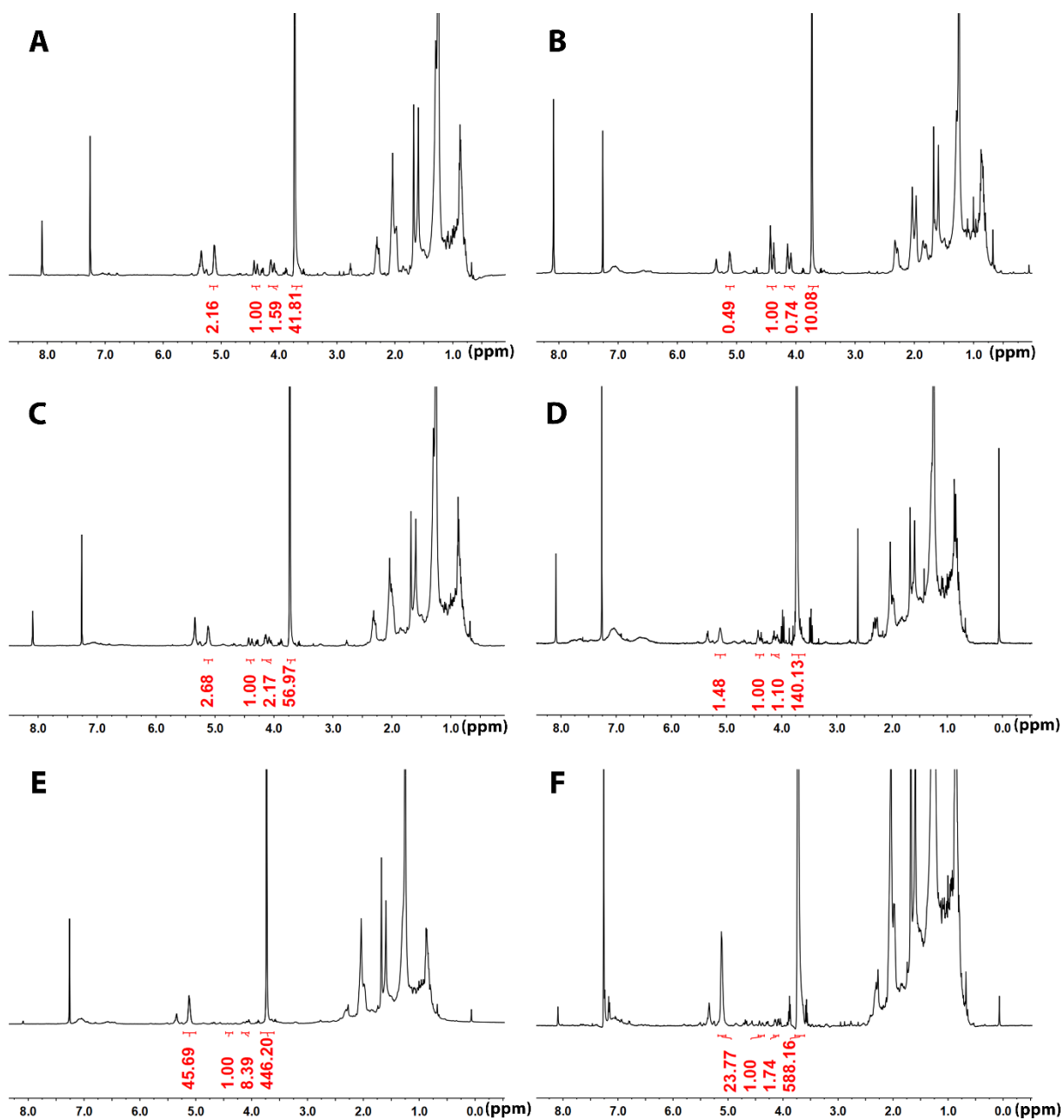


Fig. S4. ^1H NMR of the extracted PLA and PBAT from f#1 (A), f#2 (B), p#3 (C), f#3 (D), p#4 (E), and f#4 (F); 1,2-dichloroethane was used as the internal standard (chemical shift, 3.73 ppm).

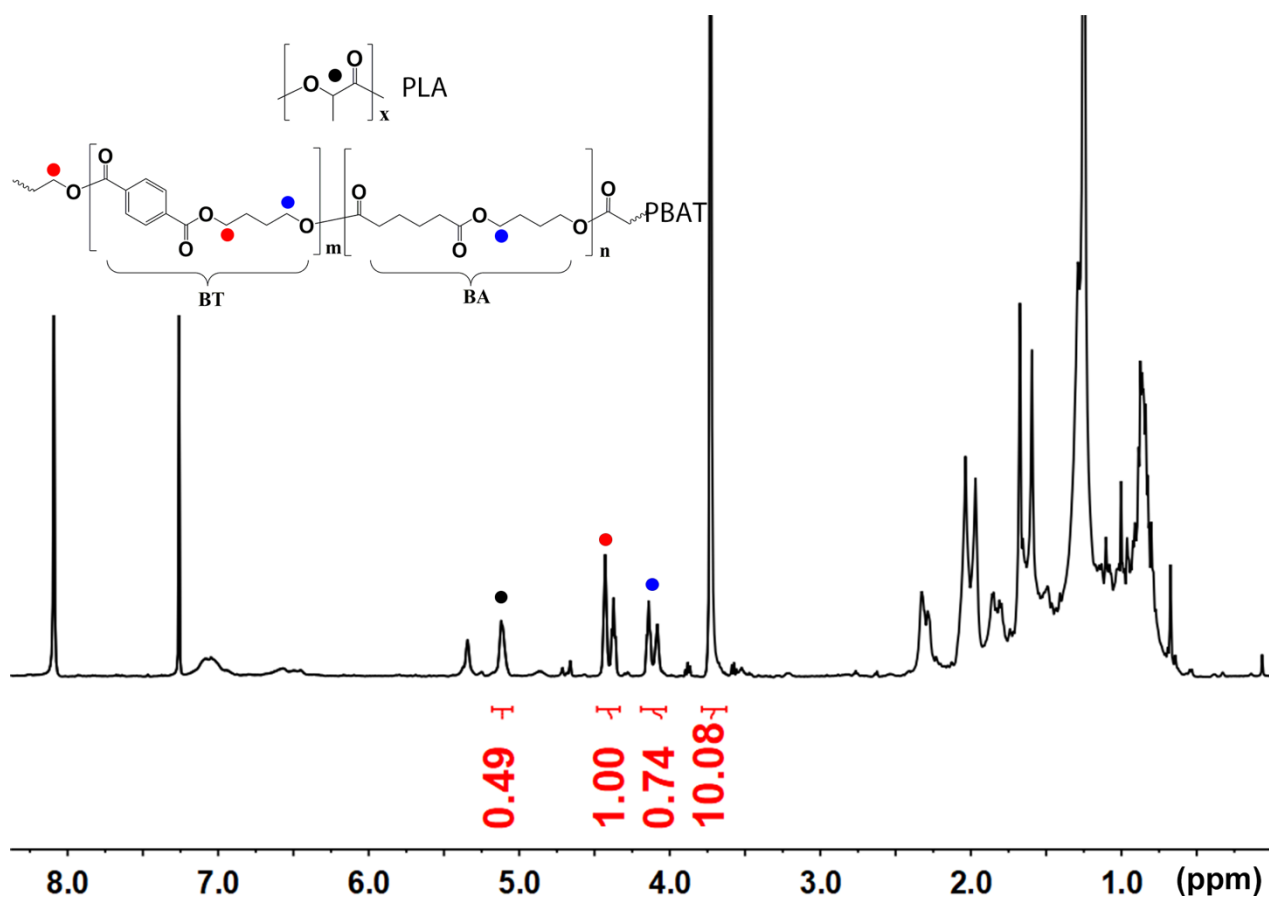


Fig. S5. Example of quantification of extracted PBAT and PLA from #2 compost.

Supplementary Tables

Table S1. Bags certified as compostable, bought from local supermarkets for our investigation

Nr.	Supermarket chain	Brand of Bag
1	Real	Pely
2	Real	real Bio
3	ALDI	alio
4	Netto	Priva
5	Edeka	swirl
6	Edeka	Gut & Günstig
7	REWE	REWE
8	LIDL	purio
9	DM	Profissimo (dm)
10	Kaufland	Classic

Supplementary references

- S1 J. Coates, Interpretation of Infrared Spectra, A Practical Approach in *Meyers, R.A. (ed.) Encyclopedia of analytical chemistry*, pp. 10815 – 10837 (Wiley, Chichester, 2000).
- S2 Y. Cai, J. Lv, J. Feng, Spectral Characterization of Four Kinds of Biodegradable Plastics: Poly (Lactic Acid), Poly (Butylenes Adipate-Co-Terephthalate), Poly (Hydroxybutyrate-Co-Hydroxyvalerate) and Poly (Butylenes Succinate) with FTIR and Raman Spectroscopy. *J. Polym. Environ.* 21, 108–114 (2013). doi: 10.1007/s10924-012-0534-2

9. Author contributions

Article 1

Authors: Julia N. Möller, Martin G. J. Löder, Christian Laforsch

Title: Finding Microplastics in Soils - A Review of Analytical Methods.

Journal and Status: Published in *Environmental Science and Technology*, 54(4), 2078-2090

Own contribution: Concept and study design: 100%, Data acquisition: 100%, Interpretation of results: 90%, Manuscript writing: 90%.

JNM conceived the idea and designed the review structure, JNM carried out the literature review and JNM, MGJL and CL interpreted the results and wrote the manuscript.

Article 2

Authors: Isabella Schrank*, Julia N. Möller*, Hannes K. Imhof, Oliver Hauenstein, Franziska Zielke, Seema Agarwal, Martin G.J. Löder, Andreas Greiner, Christian Laforsch.

*Shared first authorship

Title: Microplastic sample purification methods - assessing detrimental effects of purification procedures on specific plastic types

Journal and Status: Published in *Science of the Total Environment*, 833, 154824

Own contribution: Concept and study design: 0%, data acquisition: 15%, sample analysis: 15%, data analysis and figures: 15%, interpretation of results: 30%, manuscript writing: 80%.

IS, HKI and CL conceived the idea and designed the experiments. FZ, and JNM carried out the experiments. OH, SA, MGJL, HI and JNM performed the analytical measurements and interpreted the results. All authors were involved in the writing and revising process.

Article 3

Authors: Julia N. Möller, Ingrid Heisel, Anna Satzger, Eva C. Vizsolyi, S. D. Jakob Oster, Seema Agarwal, Christian Laforsch, Martin Löder

Title: Tackling the challenge of extracting microplastics from soils: A protocol to purify soil samples for spectroscopic analysis.

Journal and Status: Published in *Environmental Toxicology and Chemistry*, 00, 1–14.

Own contribution: Concept and study design: 90%, data acquisition: 50%, sample analysis: 80%, data analysis and figures: 80%, interpretation of results: 90%, manuscript writing: 80%.

JNM, CL and MGJL conceived the idea and the study design. JNM, IH, AS and ECV carried out the experiments. JNM and SA with the kind support of Anil Kumar (Macromolecular Chemistry II) performed the analytical measurements and interpretation of the results. JNM, SDJO, SA, CL and MGJL wrote the manuscript.

Article 4

Authors: Lion Schöpfer, Julia N. Möller, Thomas Steiner, Uwe Schnepf, Sven Marhan, Julia Resch, Ansilla Bayha, Martin G.J. Löder, Ruth Freitag, Franz Brümmer, Christian Laforsch, Thilo Streck, Jens Forberger, Martin Kranert, Ellen Kandeler, Holger Pagel

Title: Microplastics persist in an arable soil but do not affect soil microbial biomass, enzyme activities, and crop yield

Journal and Status: Published in *Journal of Plant Nutrition and Soil Science*, 2022, 1-14

Own contribution: Concept and study design: 5%, data acquisition: 30%, sample analysis: 50%, data analysis and figures: 30%, interpretation of results: 20%, manuscript writing: 20%

All authors conceived the idea and the study design. LS and HP set up and conducted the field experiment. LS analyzed the microbial carbon turnover and crop yield supervised by SM and HP. JNM and TSte analyzed the background contamination and microplastics concentrations supervised by ML and RF. LS performed the data analysis and interpretation, supported by JNM, TSte, SM and HP. JR, AB and JF were involved in the microplastics production. All authors were involved in the writing process, but LS is first author and contributed the most.

Article 5

Authors: Markus Rolf, Hannes Laermans, Lukas Kienzler, Christian Pohl, Julia N. Möller, Christian Laforsch, Martin G. J. Löder, Christina Bogner

Title: Flooding frequency and floodplain topography determine abundance of microplastics in an alluvial Rhine soil

Journal and Status: Published in *Science of the Total Environment*, 836, 155141

Own contribution: Concept and study design: 10%, data acquisition: 30%, sample analysis: 30%, data analysis and figures: 15%, interpretation of results: 20%, manuscript writing: 20%.

All authors conceived the idea and the study design. MR and HL conducted the field work. MR and JNM conducted the sample preparation and analysis. MR and MGJL conducted the spectral analysis. CB, MR and LK conducted the data analysis. LK and CP conducted the spatial and temporal analysis of flooding frequency. CB, MR, HL and LK provided the graphics, MR, HL, MGJL and CB wrote the manuscripts. All authors were involved in the writing process, but MR is first author and contributed the most.

Article 6

Authors: Nicolas Weithman, Julia N. Möller, Martin G. J. Löder, Sarah Piehl, Christian Laforsch, Ruth Freitag.

Title: Organic fertilizer as a vehicle for the entry of microplastic into the environment

Journal and Status: Published in *Science Advances*, 4(4), 1–7

Own contribution: Concept and study design: 0%, sampling design: 30%, data acquisition: 30%, sample analysis: 30%, data analysis and figures: 0%, interpretation of results: 0%, manuscript writing: 5%.

NW, RF and CL conceived the idea and the study design. Field sampling was conducted by NW, JNM and MGJL. Sample preparation and microplastics analysis was conducted by JNM and SP. MGJL and SP analyzed the data. NW, MGJL, SP, CL and RF interpreted the results. Figures and tables were created by

NW and SP. All authors contributed to the writing of the manuscript, NW is the first author and contributed the most.

Article 7

Authors: Thomas Steiner, Julia N. Möller, Martin G. J. Löder, Frank Hilbrig, Christian Laforsch, Ruth Freitag

Title: Microplastic contamination of composts and liquid fertilizers from municipal biowaste treatment plants — effects of the operating conditions

Journal and Status: Published in *Waste and Biomass Valorization*, 2022

Own contribution: Concept and study design: 0%, data acquisition: 20%, sample analysis: 35%, data analysis and figures: 20%, interpretation of results: 20%, manuscript writing: 20%

TS, FH, MGJL, CL and RF conceived the idea and study design. TS conducted the field sampling. Sample preparation and small microplastics (10µm-500µm) analysis was conducted by JNM. TS with the kind support of Andrea Schott and Helena Schneider conducted big microplastics (500µm-5mm) analysis. TS, JNM, MGJL, FH, CL and RF interpreted the results. All authors contributed to the writing of the manuscript, but TS is first author and contributed the most.

Article 8

Authors: Thomas Steiner*, Yuan-Hu Zhang*, Julia N. Möller*, Seema Agarwal, Martin G. J. Löder, Andreas Greiner, Christian Laforsch, Ruth Freitag

* Shared first authorship

Title: Municipal biowaste treatment plants contribute to the contamination of the environment with residues of biodegradable plastics with putative higher persistence potential

Journal and Status: Published in *Scientific Reports*, 12, 9021

Own contribution: Concept and study design: 0%, data acquisition: 33%, sample analysis: 33%, data analysis and figures: 33%, interpretation of results: 33%, manuscript writing: 25%

TS, MGJL, CL and RF conceived the idea and study design. TS conducted the sampling. TS with the kind support of Andrea Schott and Helena Schneider (Process Biotechnology) conducted big microplastics (500µm-5mm) analysis.

Author contributions

YHZ analyzed the material characteristics of composted fragments and pristine compostable plastics bags. YHZ conducted the ¹H-NMR analysis of compost. JNM adapted and conducted the particulate microplastics analysis of liquid digestate. TS, YHZ and JNM analyzed and interpreted the data. TS, YHZ and JNM wrote the first draft with the support of RF, MGJL and CL. The manuscript was discussed and reviewed by all authors.

10. List of publications

Published in peer reviewed journals

Möller, J. N., Löder, M. G. J., & Laforsch, C. (2020). Finding Microplastics in Soils: A Review of Analytical Methods. *Environmental Science and Technology*, 54(4), 2078–2090. <https://doi.org/10.1021/acs.est.9bo4618>

Möller, J. N., Heisel, I., Satzger, A., Vizsolyi, E. C., Oster, S. D. J., Agarwal, S., Laforsch, C., & Löder, M. G. J. (2021). Tackling the Challenge of Extracting Microplastics from Soils: A Protocol to Purify Soil Samples for Spectroscopic Analysis. *Environmental Toxicology and Chemistry*, 00, 1–14. <https://doi.org/10.1002/etc.5024>

Schrank, I.* , **Möller, J. N.*** , Imhof, H. K., Hauenstein, O., Zielke, F., Agarwal, S., Löder, M. G. J., Greiner, A., Laforsch, C. (2022). Microplastic sample purification methods – assessing detrimental effects of purification procedures on specific plastic types. *Science of the Total Environment*, 833, 154824. <https://doi.org/10.1016/j.scitotenv.2022.154824>

* Shared first authorship

Steiner, T*., Zhang, Y. H.* , **Möller, J. N.*** , Agarwal, S., Löder, M. G. J., Greiner, A., Laforsch, C., Freitag, R. (2022). Municipal biowaste treatment plants contribute to the contamination of the environment with residues of biodegradable plastics with putative higher persistence potential. *Scientific Reports*, 12, 9021. <https://doi.org/10.1038/s41598-022-12912-z>

* Shared first authorship

Schöpfer, L., **Möller, J. N.**, Steiner, T., Schnepf, U., Marhan, S., Resch, J., Bayha, A., Löder, M., Freitag, R., Brümmer, F., Laforsch, C., Streck, T., Forberger, J., Kranert, M., Kandeler, E., Pagel, H. (2022). Microplastics persist in an arable soil but do not affect carbon cycling and crop yield. *Journal of Plant Nutrition and Soil Science*, 1-14. <https://doi.org/10.1002/jpln.202200062>

Steiner, T., **Möller, J. N.**, Löder, M. G. J., Hilbrig, F.†, Laforsch, C., Freitag, R. (2022). Microplastic contamination of composts and liquid fertilizers from municipal biowaste treatment plants — effects of the operating conditions. *Waste and Biomass Valorization*, 2022. <https://doi.org/10.1007/s12649-022-01870-2>

Rolf, M., Laermans, H., Kienzler, L., Pohl, C., **Möller, J. N.**, Laforsch, C., Löder, M. G. J., Bogner, C. (2022) Flooding frequency and floodplain topography determine abundance of microplastics in an alluvial Rhine soil. *Science of the Total Environment*, 836, 155141. <https://doi.org/10.1016/j.scitotenv.2022.155141>

List of publications

- Weithmann, N., **Möller, J. N.**, Löder, M. G. J., Piehl, S., Laforsch, C., & Freitag, R. (2018). Organic fertilizer as a vehicle for the entry of microplastic into the environment. *Science Advances*, 4(4), 1–7. <https://doi.org/10.1126/sciadv.aap8060>
- Hufnagl, B., Stibi, M., Martirosyan, H., Wilczek, U., **Möller, J. N.**, Löder, M. G. J., Laforsch, C., & Lohninger, H. (2022). Computer-Assisted Analysis of Microplastics in Environmental Samples Based on μ FTIR Imaging in Combination with Machine Learning. *Environmental Science & Technology Letters*, 9(1), 90–95. <https://doi.org/10.1021/acs.estlett.1c00851>
- Ajonina, C., Buzie, C., **Möller, J. N.**, & Otterpohl, R. (2018). The detection of *Entamoeba histolytica* and *Toxoplasma gondii* in wastewater. *Journal of Toxicology and Environmental Health, Part A*, 81(1–3), 1–5. <https://doi.org/10.1080/15287394.2017.1392399>

Under Review

- Jakobs, A., Gürkal, E., **Möller, J. N.**, Löder, M. G. J., Laforsch, C., Lueders, T. (2022). A novel approach to extract, purify and fractionate microplastics from environmental matrices by isopycnic ultracentrifugation. *Science of the Total Environment*.

Non-peer-reviewed publications

Möller, J. N., Laforsch, C., Löder, M. G. J., Schrank, I., Piehl, S. (Oktober 2018). Von der Tonne auf den Acker. Entsorga – Das Fachmagazin für Abfall, Abwasser, Luft und Boden.

Möller, J. N., Laforsch, C. (April-Juni 2019). Verpackungen in der Biotonne – ein Problem für die nachhaltige Kreislaufwirtschaft. ASG Ländlicher Raum Ausgabe 2 2019. https://www.asg-goe.de/zeitschrift_archiv.shtml (27.02.2022)

Kreienhop N., **Möller, J. N.,** Laforsch, C., Beeken, M. (September 2020) Wissenschaft trifft Schule – Mikroplastik als Thema im naturwissenschaftlichen Unterricht. Unterricht Chemie 179: Mikroplastik. <https://www.friedrich-verlag.de/shop/mikroplastik-510179> (27.02.2022)

Möller, J. N., Löder, M., Freitag, R., Lehndorf E., Lüders T., Laforsch C. (May 2021) Growing Plastics – An effort to determine the extent and effects of microplastic pollution in agricultural soils. AWE International. <https://www.awemagazine.com/article/growing-plastics/> (27.02.2022)

11. Acknowledgements

First and foremost, I would like to thank Prof. Dr. Christian Laforsch for enabling this PhD thesis and his supervision and support throughout the years. I would also like to thank Dr. Martin Löder, who not only supported me in my work, but also kept on reminding me to worry less – these reminders were invaluable and kept me on track to achieve my goals.

I would also like to thank all the colleagues and co-authors of the projects Babba and MiKobo, and the CRC 1357 with whom I had the privilege to work with and to publish amazing results.

My special thanks also go to Ursula Wilczek, who was my greatest support in the lab and has become a true friend. I sincerely thank Heghnar Martirosyan, Marion Preiß, Mechthild Kredler and Eva Möller, for the cheerful discussions and genuine helpfulness in day-to-day life. Thanks also go to Martina Karsch, the good soul in administration without whom many of us would have been lost.

I would also like to thank my fellow PhD students and colleagues, Simona Mondellini, Jens Diller, Sven Ritschar, Frederic Hüftlein, Hendrik Eck, Anja Ramsperger, Eva Vizsolyi, Julian Brehm, Patricia Diel, Marvin Kiene, Jakob Oster, Dimitri Seidenath, Michael Schwarzer and Sebastian Steibl – you were the ones I turned to, to process failures and celebrate successes.

Thanks also go to my students: Ingrid Heisel, Anna Satzger, Magdalena Bittel, Markus Rolf, Luise Weber and Nora Voigt, who were an essential part of my growth as a PhD candidate.

Last but not least I want to say thank you to my family: My parents, Ursula Reif and Wilhelm Möller - you have been pillars of support throughout my life and you are the reason I found my passion in science; and my sister, Ina Möller, who has been my life-coach and inspiration for as long as I can remember. Without you I would not be the person I have become.

Statutory Declaration and Statement

(Eidesstattliche) Versicherungen und Erklärungen

(§ 9 Satz 2 Nr. 3 PromO BayNAT)

Hiermit versichere ich eidesstattlich, dass ich die Arbeit selbstständig verfasst und keine anderen als die von mir angegebenen Quellen und Hilfsmittel benutzt habe (vgl. Art. 64 Abs.1 Satz 6 BayHSchG).

(§ 9 Satz 2 Nr. 3 PromO BayNAT)

Hiermit erkläre ich, dass ich die Dissertation nicht bereits zur Erlangung eines akademischen Grades eingereicht habe und dass ich nicht bereits diese oder eine gleichartige Doktorprüfung endgültig nicht bestanden habe.

(§ 9 Satz 2 Nr. 4 PromO BayNAT)

Hiermit erkläre ich, dass ich Hilfe von gewerblichen Promotionsberatern bzw. -vermittlern oder ähnlichen Dienstleistern weder bisher in Anspruch genommen habe noch künftig in Anspruch nehmen werde.

(§ 9 Satz 2 Nr. 7 PromO BayNAT)

Hiermit erkläre ich mein Einverständnis, dass die elektronische Fassung meiner Dissertation unter Wahrung meiner Urheberrechte und des Datenschutzes einer gesonderten Überprüfung unterzogen werden kann.

(§ 9 Satz 2 Nr. 8 PromO BayNAT)

Hiermit erkläre ich mein Einverständnis, dass bei Verdacht wissenschaftlichen Fehlverhaltens Ermittlungen durch universitätsinterne Organe der wissenschaftlichen Selbstkontrolle stattfinden können.

Bayreuth,

Ort, Datum, Unterschrift